Methods in Molecular Biology 1535

Springer Protocols

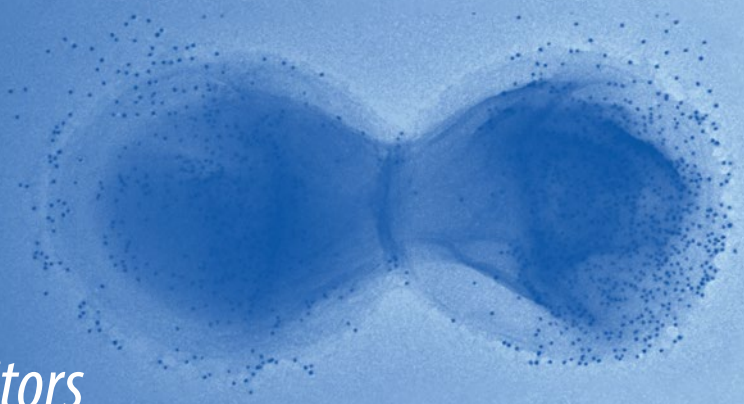

Pontus Nordenfelt
Mattias Collin *Editors*

Bacterial Pathogenesis

Methods and Protocols

Humana Press

METHODS IN MOLECULAR BIOLOGY

Series Editor
John M. Walker
School of Life and Medical Sciences
University of Hertfordshire
Hatfield, Hertfordshire, AL10 9AB, UK

For further volumes:
http://www.springer.com/series/7651

Bacterial Pathogenesis

Methods and Protocols

Edited by

Pontus Nordenfelt

Department of Clinical Sciences, Lund University, Division of Infection Medicine, Lund, Sweden

Mattias Collin

Department of Clinical Sciences, Lund University, Division of Infection Medicine, Lund, Sweden

Humana Press

Editors
Pontus Nordenfelt
Department of Clinical Sciences
Lund University, Division of Infection Medicine
Lund, Sweden

Mattias Collin
Department of Clinical Sciences
Lund University, Division of Infection Medicine
Lund, Sweden

ISSN 1064-3745 ISSN 1940-6029 (electronic)
Methods in Molecular Biology
ISBN 978-1-4939-6671-4 ISBN 978-1-4939-6673-8 (eBook)
DOI 10.1007/978-1-4939-6673-8

Library of Congress Control Number: 2016959981

Printed on acid-free paper

This Humana Press imprint is published by Springer Nature
The registered company is Springer Science+Business Media LLC
The registered company address is: 233 Spring Street, New York, NY 10013, U.S.A.

Preface

Understanding bacterial infections is more important than ever. Despite the development of antibacterial agents during the last century, bacterial infections are still one of the leading causes to worldwide morbidity and mortality. What is especially alarming is that we are entering a postantibiotic era where we have no, or very limited, treatment options to several bacterial infections previously not considered as threats (CDC. Antibiotic resistance: threat report 2013). A fundamental issue in infection biology has been, and still is: What is virulence and how does it relate to pathogenesis? There is no simple answer to this and the theoretical framework is continuously developing. The molecular dissection of Koch's postulates made possible by the molecular genetics revolution has been instrumental in understanding bacterial-host interactions at the molecular level, but this somewhat bacteria-centered view has had its limitations in describing the whole process ranging all the way from commensalism to severe infections. Here, more recent frameworks taking both the bacterial properties and the host responses into account have gained recognition. However, theoretical frameworks will remain theoretical until they can be experimentally tested. Therefore, methodologies assessing many different aspects of bacterial infections are absolutely crucial in moving our understanding forward, for the sake of knowledge itself, and for developing novel means of controlling bacterial infections.

In this volume, *Bacterial Pathogenesis*: *Methods and Protocols*, we have had the privilege of recruiting researchers with very different methodological approaches, with the common goal of understanding bacterial pathogenesis from molecules to whole organisms. The methods describe experimentation of a wide range bacterial species, such as *Streptococcus pyogenes*, *Streptococcus dysgalactiae*, *Staphylococcus aureus*, *Helicobacter pylori*, *Propionibacterium acnes*, *Streptococcus pneumoniae*, *Enterococcus faecalis*, *Listeria monocytogenes*, *Pseudomonas aeruginosa*, *Escherichia coli*, *Salmonella typhimurium*, and *Mycobacterium marinum*. However, many of the protocols can be modified and generalized to study any bacterial pathogen of choice. Part I details very different approaches to identifying and characterizing bacterial effector molecules, from high-throughput gene-based methods, via advanced proteomics, to classical protein chemistry methods. Part II deals with structural biology of bacterial pathogenesis and how to overcome folding and stability problems with recombinantly expressed proteins. Part III describes methodology that with precision can identify bacteria in complex communities and develop our understanding of how genomes of bacterial pathogens have evolved. Part IV, the largest section, reflects the rapid development of advanced imaging techniques that can help us answer questions about molecular properties of individual live bacteria, ultrastructure of surfaces, subcellular localization of bacterial proteins, motility of bacteria within cells, and localization of bacteria within live hosts. Part V describes methods from in vitro and in vivo modeling of bacterial infections, including using zebra fish as a surrogate host, bacterial platelet activation, antimicrobial activity of host proteases, assessment of biofilms in vitro and in vivo, and using a fish pathogen as a surrogate infectious agent in a mouse model of infection. Finally, Part VI is based on the notion that bacterial pathogens are the true experts of our immune system. Therefore, immune evasion bacterial factors can, when taken out of their infectious context, be used as

powerful tools or therapeutics against immunological disorders. This is exemplified by the use of proteases from pathogenic bacteria for characterization of therapeutic antibodies, measurements of antibody orientation on bacterial surfaces, and finally the potential use of immunoglobulin active enzymes as therapy against antibody-mediated diseases.

We are indebted to John M. Walker, the series editor, for the opportunity to put this volume together and for the continuous encouragement during the whole process. Above all, we are extremely grateful to all the authors who have taken time from their busy schedules and provided us with the outstanding chapters that make up this volume. Finally, we would like to acknowledge our research environment, the Division of Infection Medicine, Department of Clinical Sciences, Lund University. This environment has fostered generations of outstanding researchers within infection biology, and we are truly standing on the shoulders of giants (no one mentioned, no one forgotten).

Lund, Sweden

Mattias Collin
Pontus Nordenfelt

Contents

Contributors

Linda Andersson • *Genovis, AB, Lund, Sweden*

Nathalie Aulner • *Institut Pasteur, Imagopole-CITech, Paris, France*

Ali Azhdarinia • *Center for Molecular Imaging, Brown Foundation Institute of Molecular Medicine for the Prevention of Human Diseases, The University of Texas Health Science Center at Houston, Houston, TX, USA*

Damien Balestrino • *Institut Pasteur, Unité des Interactions Bactéries-Cellules, Paris, France; INSERM, Paris, France; INRA, Paris, France; UMR CNRS, Laboratoire Microorganismes: Génome Environnement, Université d'Auvergne, Clermont-Ferrand, France*

Caroline Bergenfelz • *Division of Experimental Infection Medicine, Department of Translational Medicine, Lund University, Malmö, Sweden*

Lars Björck • *Division of Infection Medicine, Department of Clinical Sciences, Lund University, Lund, Sweden*

Daniel A. Bonsor • *Institute of Human Virology, University of Maryland School of Medicine, Baltimore, MD, USA*

Amy L. Bottomley • *The iThree Institute, University of Technology Sydney, Sydney, NSW, Australia*

Fredric Carlsson • *Section for Immunology, Department of Experimental Medical Science, Lund University, Lund, Sweden*

Yashuan Chao • *Division of Experimental Infection Medicine, Department of Translational Medicine, Lund University, Malmö, Sweden*

Mattias Collin • *Division of Infection Medicine, Department of Clinical Sciences, Lund University, Lund, Sweden*

Caitlin Collins • *Department of Infectious Disease Epidemiology, Imperial College London, London, UK*

Pascale Cossart • *Institut Pasteur, Unité des Interactions Bactéries-Cellules, Paris, France; INSERM, Paris, France; INRA, Paris, France*

Anne Danckaert • *Institut Pasteur, Imagopole-CITech, Paris, France*

Jonas Danielsen • *Division of Infection Medicine, Department of Clinical Sciences, Lund University, Lund, Sweden*

Xavier Didelot • *Department of Infectious Disease Epidemiology, Imperial College London, London, UK*

Jost Enninga • *Institut Pasteur, Unité Dynamique des Interactions Hôte-Pathogène, Paris, France*

Isabelle Fellay • *Unit of Anatomy, Department of Medicine, University of Fribourg, Fribourg, Switzerland*

Cindy Fevre • *Department of Medical Microbiology, University Medical Center, Utrecht, The Netherlands*

Jennifer Fredlund • *Institut Pasteur, Unité Dynamique des Interactions Hôte-Pathogène, Paris, France*

Inga-Maria Frick • *Division of Infection Medicine, Department of Clinical Science, Lund University, Lund, Sweden*
Peng Gao • *Center for Molecular Imaging, Brown Foundation Institute of Molecular Medicine for the Prevention of Human Diseases, The University of Texas Health Science Center at Houston, Houston, TX, USA*
Théodore Grenier • *Institut Pasteur, Unité des Interactions Bactéries-Cellules, Paris, France; INSERM, Paris, France; INRA, Paris, France*
Pieter-Jan Haas • *Department of Medical Microbiology, University Medical Center, Utrecht, The Netherlands*
Elizabeth J. Harry • *The iThree Institute, University of Technology Sydney, Sydney, NSW, Australia*
Barrett R. Harvey • *Center for Molecular Imaging, Brown Foundation Institute of Molecular Medicine for the Prevention of Human Diseases, The University of Texas Science Center at Houston, Houston, TX, USA; Division of Infectious Diseases, Department of Internal Medicine, The University of Texas Health Science Center at Houston, Houston, TX, USA; Department of Microbiology and Molecular Genetics, The University of Texas Health Science Center at Houston, Houston, TX, USA*
Anders P. Håkansson • *Division of Experimental Infection Medicine, Department of Translational Medicine, Lund University, Malmö, Sweden*
Anders Jensen • *Department of Biomedicine, Aarhus University, Aarhus, Denmark*
Christofer Karlsson • *Division of Infection Medicine, Department of Clinical Sciences, Lund University, Lund, Sweden*
Vincent T. Lee • *Department of Cell Biology and Molecular Genetics, University of Maryland, College Park, MD, USA; Maryland Pathogen Research Institute, University of Maryland, College Park, MD, USA*
Diego López León • *Unit of Anatomy, Department of Medicine, University of Fribourg, Fribourg, Switzerland*
Julia Lienard • *Section for Immunology, Department of Experimental Medical Science, Lund University, Lund, Sweden*
Rolf Lood • *Division of Infection Medicine, Department of Clinical Science, Lund University, Lund, Sweden*
Johan Malmström • *Division of Infection Medicine, Department of Clinical Sciences, Lund University, Lund, Sweden*
Pierre-Yves Mantel • *Unit of Anatomy, Department of Medicine, University of Fribourg, Fribourg, Switzerland*
Malin Mejàre • *Genovis AB, Lund, Sweden*
Barbara E. Murray • *Division of Infectious Diseases, Department of Internal Medicine, The University of Texas Health Science Center at Houston, Houston, TX, USA; Department of Microbiology and Molecular Genetics, The University of Texas Health Science Center at Houston, Houston, TX, USA*
Matthias Mörgelin • *Division of Infection Medicine, Department of Clinical Science, Lund University, Lund, Sweden*
Melody N. Neely • *Department of Biology, Texas Woman's University, Denton, TX, USA*
Pontus Nordenfelt • *Division of Infection Medicine, Department of Clinical Sciences, Lund University, Lund, Sweden*
Fredrik Olsson • *Genovis AB, Lund, Sweden*

Mona W. Orr • *Department of Cell Biology and Molecular Genetics, University of Maryland, College Park, MD, USA; Biological Sciences Graduate Program, University of Maryland, College Park, MD, USA*
Kenneth L. Pinkston • *Center for Molecular Imaging, Brown Foundation Institute of Molecular Medicine for the Prevention of Human Diseases, The University of Texas Health Science Center at Houston, Houston, TX, USA*
Javier Pizarro-Cerdá • *Institute Pasteur, Unité des Interactions Bactéries-Cellules, Paris, France; INSERM, Paris, France; INRA, Paris, France*
Juan J. Quereda • *Institute Pasteur, Unité des Interactions Bactéries-Cellules, Paris, France; INSERM, Paris, France; INRA, Paris, France*
Assaf Raz • *Laboratory of Bacterial Pathogenesis and Immunology, The Rockefeller University, New York, NY, USA*
Martin Sachse • *Institut Pasteur, Ultrapole-CITech, Paris, France*
Lisette Scheepmaker • *Department of Medical Microbiology, University Medical Center, Utrecht, The Netherlands*
Christian F.P. Scholz • *Department of Biomedicine, Aarhus University, Aarhus, Denmark*
Eva M. Sevick-Muraca • *Center for Molecular Imaging, Brown Foundation Institute of Molecular Medicine for the Prevention of Human Diseases, The University of Texas Health Science Center at Houston, Houston, TX, USA*
Sarah Shabayek • *Institute of Medical Microbiology and Hygiene, University of Ulm, Ulm, Germany; Faculty of Pharmacy, Department of Microbiology and Immunology, Suez Canal University, Ismailia, Egypt*
Oonagh Shannon • *Division of Infection Medicine, Department of Clinical Science, Lund University, Lund, Sweden*
Spencer Shorte • *Institut Pasteur, Imagopole-CITech, Paris, France*
Kavindra V. Singh • *Division of Infectious Diseases, Department of Internal Medicine, The University of Texas Health Science Center at Houston, Houston, TX, USA*
Jonathan Sjögren • *Genovis AB, Lund, Sweden*
Barbara Spellerberg • *Institute of Medical Microbiology and Hygiene, University of Ulm, Ulm, Germany*
Eric J. Sundberg • *Institute of Human Virology, University of Maryland School of Medicine, Baltimore, MD, USA; Department of Medicine, University of Maryland School of Medicine, Baltimore, MD, USA; Department of Microbiology and Immunology, University of Maryland School of Medicine, Baltimore, MD, USA*
Johan Teleman • *Division of Infection Medicine, Department of Clinical Sciences, Lund University, Lund, Sweden; Department of Immunotechnology, Lund University, Lund, Sweden*
Lynne Turnbull • *The iThree Institute, University of Technology Sydney, Sydney, NSW, Australia*
Michael Walch • *Unit of Anatomy, Department of Medicine, University of Fribourg, Fribourg, Switzerland*
Cynthia B. Whitchurch • *The iThree Institute, University of Technology Sydney, Sydney, NSW, Australia*
Wei Xia • *MOE Key Laboratory of Bioinorganic and Synthetic Chemistry, School of Chemistry, Sun Yat-sen University, Guangzhou, China*

Part I

Identification and Characterization of Bacterial Effector Molecules

Chapter 1

Protein-Based Strategies to Identify and Isolate Bacterial Virulence Factors

Rolf Lood and Inga-Maria Frick

Abstract

Protein–protein interactions play important roles in bacterial pathogenesis. Surface-bound or secreted bacterial proteins are key in mediating bacterial virulence. Thus, these factors are of high importance to study in order to elucidate the molecular mechanisms behind bacterial pathogenesis. Here, we present a protein-based strategy that can be used to identify and isolate bacterial proteins of importance for bacterial virulence, and allow for identification of both unknown host and bacterial factors. The methods described have among others successfully been used to identify and characterize several IgG-binding proteins, including protein G, protein H, and protein L.

Key words Plasma adsorption, Affinity purification, Virulence factors, Bacteria, Release of bacterial surface proteins

1 Introduction

Bacterial species express proteins, surface-bound or secreted, that play important roles in pathogenesis by interacting with host-specific molecules or defense systems. In order to understand and study the molecular mechanisms whereby bacteria infect their host and cause disease it is fundamental to identify and isolate bacterial proteins and their interacting partners of importance for bacterial virulence. Here, we describe a protein-based strategy that successfully has been used for isolation of several proteins from Gram-positive bacteria, interacting with plasma components [1–8]. Due to the complexity of bacterium–host interactions, a flowchart is supplied to facilitate the understanding and design of experiments (Fig. 1), allowing for identification of both unknown host and bacterial factors. The specific identification of bacterial and host proteins using mass spectrometry related methods is discussed elsewhere in this volume (Karlsson et al.). In this chapter, we in detail demonstrate the feasibility and advantageous nature of using the following methods in order to identify bacterial virulence factors interacting with human plasma.

Pontus Nordenfelt and Mattias Collin (eds.), *Bacterial Pathogenesis: Methods and Protocols*, Methods in Molecular Biology, vol. 1535, DOI 10.1007/978-1-4939-6673-8_1,

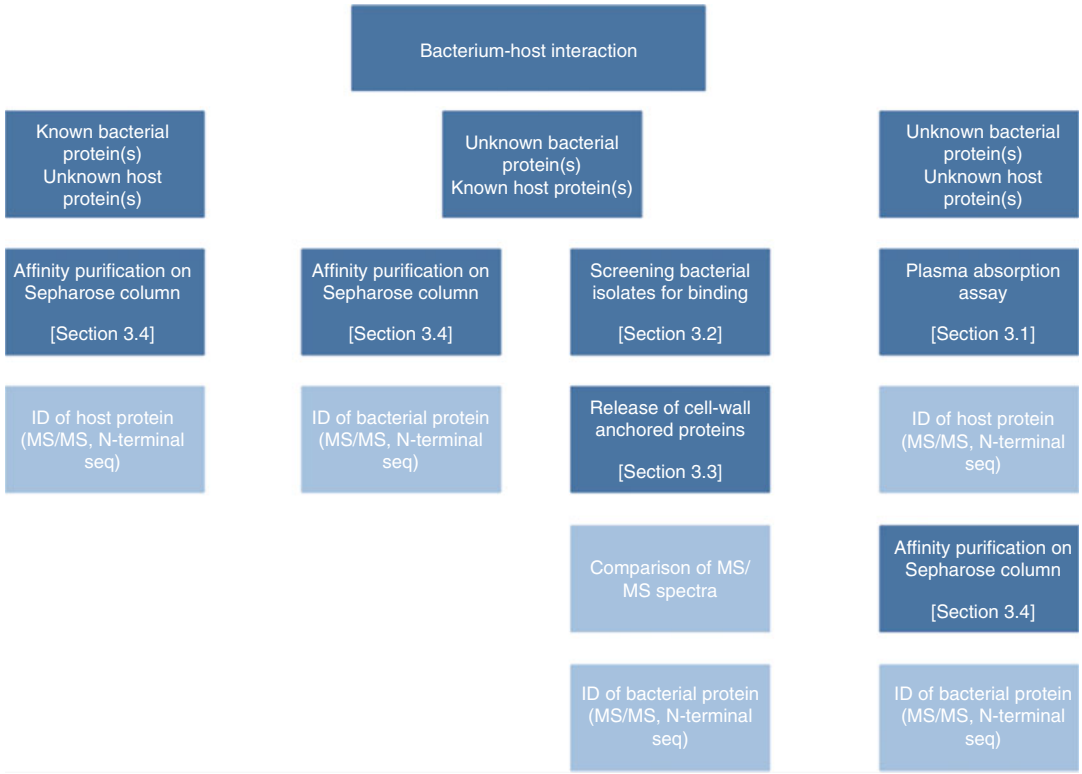

Fig. 1 Schematic overview of the identification process of proteins involved in bacterium–host interactions. Different strategies for identifying unknown bacterial proteins, plasma-interacting partners, or a combination of both, are outlined. Sections marked with *dark blue* will be covered in this chapter, while *light blue* sections can be found elsewhere. Their respective methodological part in this chapter is implied in brackets

1. In plasma adsorption assays, bacterial cells are incubated with plasma and bound proteins are released, separated by SDS-PAGE and identified by N-terminal sequencing or MS/MS.
2. Population-wide screening of bacterial isolates for binding to specific host proteins, based on ^{125}-Iodine-labeled (or fluorescently labeled) plasma proteins will demonstrate the conserved phenotype amongst other isolates/species.
3. Identification of bacterial surface proteins, interacting with plasma proteins, using cyanogen bromide (CNBr) cleavage at methionine residues in proteins or proteolytic release of surface proteins. The efficiency of treatment is followed by analysis of binding of the radiolabeled probe. Following choice of cleavage procedure, a large-scale release of proteins is performed. The protein of interest is purified using chromatographic methods, binding of ligand confirmed with slot-binding and Western blot, and the bacterial protein is identified using N-terminal sequencing or MS/MS.

4. Sepharose-coupled host protein can be used for affinity purification of bacterial protein released from the bacterial surface. Sepharose-coupled bacterial protein, natively or recombinantly produced, can be used as a tool for identification of human proteins from plasma or other extracellular secretions [9].

2 Materials

All solutions should be prepared using ultrapure water (deionized water filtrated to attain a sensitivity of 18 M Ω cm at 25 °C). Buffers are stored at room temperature (or as indicated). Waste materials are disposed of according to the regulations of the laboratory.

2.1 Plasma Adsorption Assay

1. Wash buffer (PBS): 0.12 M NaCl, 0.03 M phosphate, pH 7.4.
2. Elution buffer: 0.1 M glycine–HCl, pH 2.0, (store at +4 °C).
3. 1 M Tris solution (*see* **Note 1**).
4. Citrate-treated plasma from healthy donors, stored at –80 °C (*see* **Note 2**).
5. Eppendorf tubes.
6. Sterile syringe filters 0.2 μm (Acrodisc 13 mm filters).

2.2 Screening Bacterial Isolates for Binding

1. PD-10 desalting column (Sephadex G-25; GE Healthcare).
2. IODO-BEAD® iodination reagent (Pierce) (*see* **Note 3**).
3. Filter paper (Whatman).
4. ^{125}Iodine (0.1 m Curie/μl) (*see* **Note 4**).
5. PBS.
6. PBST: PBS + 0.05 % Tween 20.
7. Eppendorf tubes.
8. Ellerman tubes (3.2 ml plastic tubes; Sarstedt) and lids.

2.3 Release of Cell-Wall Anchored Proteins

2.3.1 With CNBr

1. 0.2 M HCl and 0.1 M HCl: Dilute concentrated HCl with water (*see* **Note 5**).
2. 1.5 M Tris–HCl pH 8.8.
3. 1 M NaOH.
4. 30 mg/ml cyanogen bromide (CNBr) (*see* **Note 6**).
5. Sterile syringe filters 0.2 μm (Acrodisc 13 mm filters).
6. Dialysis tubing (MWCO: 3500 Da) (*see* **Note 7**).

2.3.2 With Proteolytic Enzymes

1. Papain buffer: 0.01 M Tris–HCl pH 8.0.
2. 1 M L-cysteine.
3. 1 M iodoacetic acid.

4. Pepsin buffer: 0.05 M KH_2PO_4 pH 5.8.
5. 7.5% $NaHCO_3$.
6. Trypsin buffer: 0.05 M KH_2PO_4, 0.005 M EDTA pH 6.1.
7. 1 M benzamidine hydrochloride hydrate (*see* **Note 8**).
8. Mutanolysin buffer: 0.01 M KH_2PO_4 pH 6.8.
9. 4 mg/ml DNase solution.
10. 2 mg/ml papain solution.
11. 1 mg/ml pepsin solution.
12. 10 mg/ml trypsin solution.
13. 1000 U/ml mutanolysin solution.

2.4 Affinity Purification on Sepharose Column

1. CNBr-activated Sepharose (Amersham Bioscience).
2. Coupling buffer: 0.1 M $NaHCO_3$, 0.5 M NaCl, pH 8.3.
3. Dialysis tubing (MWCO: 3500 Da) (*see* **Note 7**).
4. Poly-Prep Chromatography Columns (10 ml).
5. PBS.
6. Elution buffer: 0.1 M glycine-HCl, pH 2.0.
7. 1 M Tris solution (*see* **Note 1**).
8. Tris buffer: 20 mM pH 7.5, 0.15 M NaCl.

3 Methods

3.1 Plasma Adsorption Assay

1. Grow bacteria in suitable broth overnight at 37 °C to stationary phase or to mid-logarithmic growth phase (*see* **Note 9**).
2. Spin down the bacteria at 2000 × *g* for 10 min. Wash the bacterial cells twice with PBS. Adjust the concentration to 2×10^{10} cells/ml (*see* **Note 10**).
3. Incubate 100 µl bacterial solution with 100 µl human citrate treated plasma or PBS, for 60 min, end-over-end rotation at room temperature (*see* **Note 11**). Use eppendorf tubes.
4. Spin down the cells in an eppendorf centrifuge 13,000 × *g* for 1 min. Remove the supernatant and resuspend the bacteria with 1 ml PBS (*see* **Note 12**) and spin down cells as above. Repeat this step twice. The washing steps will remove all unbound proteins.
5. After the last washing step resuspend the bacterial cells in 100 µl elution buffer. Incubate for 15–30 min at room temperature, end-over-end rotation (*see* **Note 13**).
6. Spin down the bacterial cells as above and transfer the supernatant to a new eppendorf tube. Sterile filter the supernatant using a 0.2 µm syringe filter. Adjust the pH to approximately 7.5 by adding 5 µl 1 M Tris.

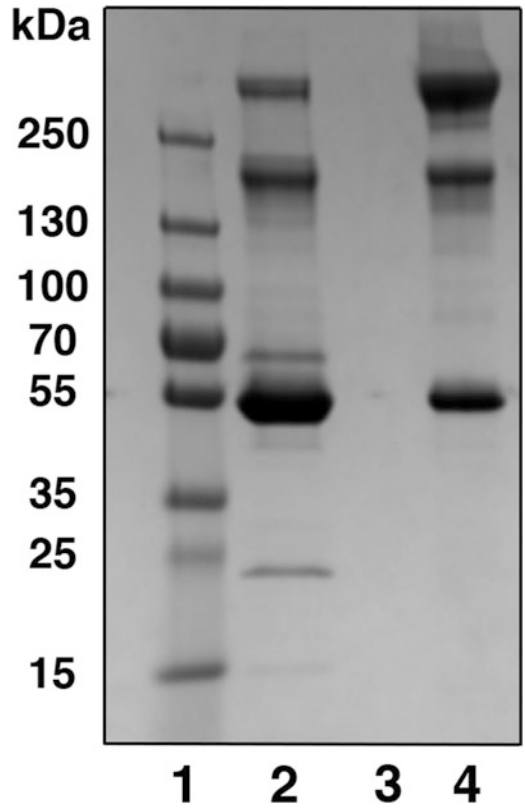

Fig. 2 SDS-PAGE analysis of plasma proteins eluted from group G streptococci. A measure of 100 µl G45 bacterial suspension (2×10^{10} cells/ml) was incubated with 100 µl human citrate-treated plasma or PBS (as a background control), respectively for 1 h at 37 °C. Proteins bound to the bacterial surface were eluted with 0.1 M glycine buffer pH 2.0. The material was separated by SDS-PAGE (4–20 % gradient gel) under reducing conditions and the gel was stained with Coomassie Blue. *Lane 1*: molecular marker; *lane 2*: human plasma diluted 1:25; *lane 3*: proteins eluted from G45 incubated with PBS; *lane 4*: proteins eluted from G45 incubated with plasma

7. Analyze the supernatant by SDS-PAGE (*see* Fig. 2 for a representative result). The protein fragments eluted from the bacteria (Fig. 2, lane 4) can be cut out and identified by N-terminal sequencing or MS/MS.

3.2 Screening Bacterial Isolates for Binding

In order to screen bacteria for binding of a specific host protein, the protein of interest is first labeled with ^{125}Iodine (*see* **Note 14**).

1. Wash a PD-10 desalting column with 5 column volumes of PBST.
2. Take one IODO-BEAD and put it on a piece of filter paper. Wash the bead with four times 1 ml PBS to remove loose particles and reagent from the bead.
3. Transfer the bead to an eppendorf tube and add 100 µl PBS.

4. Add 2 µl ^{125}Iodine (0.2 mCi) and incubate for 5 min at room temperature (*see* **Note 15**).
5. Add 20 µl protein (1 mg/ml) and 80 µl PBS, and incubate for 10 min at room temperature.
6. Separate free iodine from iodine bound to the protein using the PD-10 column. Add the sample to the column and collect the flow-through, using Ellerman tubes (Fraction 1).
7. Wash the bead with 300 µl PBST and transfer to the column, collect the flow-through in fraction 1.
8. Elute the radiolabeled protein with PBST, nine times 0.5 ml fractions, in total 10 fractions. The free iodine will remain on the column (*see* **Note 16**).
9. Transfer 10 µl from each fraction to new Ellerman tubes and close the tubes with a lid. Count them in a gamma counter.
10. Pool fractions containing the protein (*see* **Note 17**) and calculate the amount of counts per minute (cpm)/ml. Store the radiolabeled protein at +4 °C in a lead container.
11. Bacteria from overnight cultures are collected at 2000*g* for 10 min. The cells are washed twice with PBST and resuspended in PBST to a 1% solution (2×10^9 cfu/ml).
12. Dilute the ^{125}I-labeled protein in PBST to approximately 400 cpm/µl (*see* **Note 18**). Transfer 25 µl of this solution into Ellerman tubes (*see* **Note 19**). Close the tubes with a lid and count them in a gamma counter (value 1).
13. Remove the lids from the tubes and add 200 µl of the bacterial solutions to the tubes and 200 µl PBST as a control for non-specific binding of the ^{125}I-labeled protein to the plastic tubes.
14. Incubate at room temperature for 30 min (*see* **Note 20**).
15. Add 2 ml PBST to each tube and spin down the cells at 1600 × *g* for 15 min.
16. Carefully transfer the supernatant to a disposable container (*see* **Note 21**).
17. Put lid on the tubes and count the bacterial pellets in the gamma counter (value 2).
18. Calculate the binding of the radiolabeled protein to the bacteria: value 2/value 1, given in percent (Fig. 3).

3.3 Release of Cell-Wall Anchored Proteins

A small-scale treatment of bacteria with CNBr [10] or the hydrolytic enzymes papain, pepsin, trypsin, and mutanolysin [2], is initially performed. Following treatment the cells are analyzed for binding of the radiolabeled probe of interest, *see* Subheading 3.2, in order to estimate the efficiency of the treatment (*see* **Note 22**). The released material is also analyzed by SDS-PAGE (*see* Fig. 4 for a representative result). Once the

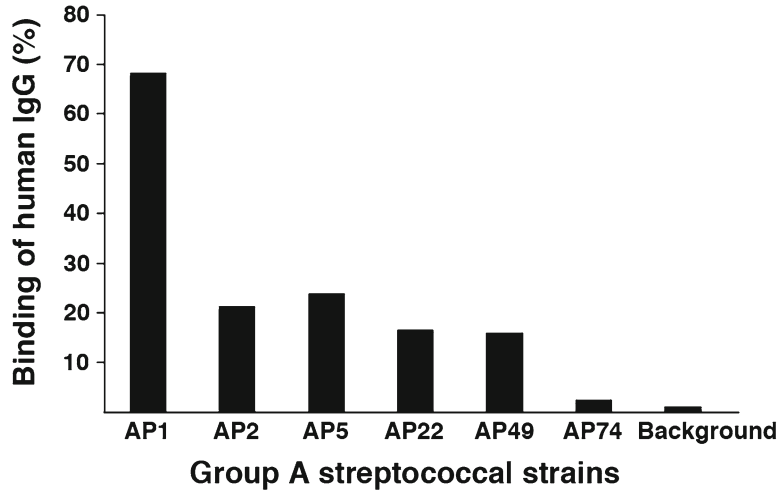

Fig. 3 Analysis of IgG-binding to group A streptococcal strains. Various strains of group A streptococci, at a concentration of 2 x 10^9 cfu/ml, were incubated with ^{125}I-labeled human IgG for 30 min at room temperature. Binding of IgG is expressed in percent. The streptococcal strains are from the World Health Organization Collaborating Centre for Reference and Research on Streptococci, Prague, Czech Republic

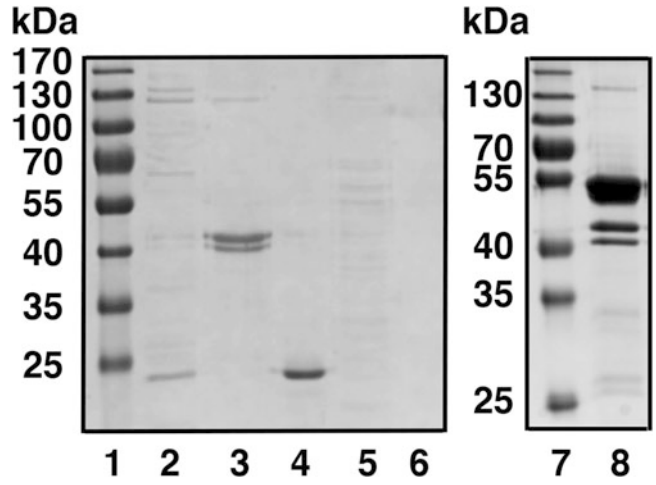

Fig. 4 SDS-PAGE analysis of proteins released from the surface of *Finegoldia magna. F. magna* bacteria (strain 23.75) was treated with papain, pepsin, trypsin, mutanolysin, and CNBr. The released material was separated by SDS-PAGE (12 % gel) under reducing conditions and the gel was stained with Coomassie *Blue. Lane 1*: molecular marker; lane 2–5: proteins released with (2) trypsin, (3) pepsin, (4) papain, (5) mutanolysin; *lane 6*: bacteria treated with glycine buffer as control; *lane 7*: molecular marker; *lane 8*: proteins released with CNBr

optimal releasing agent has been decided a large-scale release of cell-wall anchored proteins can be performed and the protein of interest is purified using chromatographic methods. Binding of the ligand is confirmed with slot-binding and Western blot, and the protein is identified using N-terminal sequencing or MS/MS.

3.3.1 Using CNBr

1. Grow bacteria to stationary phase in appropriate broth. Spin down the bacterial cells and wash twice with PBS.
2. Weigh the bacterial cells (wet weight) and resuspend the cells in PBS to a concentration of 0.4 g/ml.
3. Add an equal volume of CNBr solution, 30 mg/ml, to the bacterial solution.
4. Incubate under rotation 8–16 h (overnight) at room temperature (in a fume hood).
5. Spin down the bacteria at 10,000 × *g* for 15 min.
6. Sterile filter the supernatant using a 0.2 μm syringe filter.
7. Dialyze the supernatant against 0.1 M HCl (over day or overnight, in the fume hood) with 4–5 changes of HCl (*see* **Note 23**).
8. Raise the pH in the supernatant to 7.4 by adding 1.5 M Tris–HCl pH 8.8 (approximately 1 ml/g wet bacteria).

3.3.2 Using Papain

1. Grow bacteria to stationary phase in appropriate broth. Spin down the bacterial cells at 2000 × *g* for 10 min and wash twice with papain buffer and resuspend the bacterial cells in the same buffer to a 10% solution (2×10^{10} cfu/ml).
2. Add to 1 ml 10% bacterial solution 55 μl 1 M L-cysteine (*see* **Note 24**) and 100 μl 2 mg/ml papain solution.
3. Incubate for 60 min at 37 °C end-over-end rotation.
4. Terminate the reaction by adding 12 μl 1 M iodoacetic acid (final concentration 10 mM) (*see* **Note 25**).
5. Spin down the bacterial cells at 2000 × *g* for 15 min.
6. Sterile filter the supernatant using a 0.2 μm syringe filter. Store the supernatant at −20 °C.

3.3.3 Using Pepsin

1. Grow bacteria to stationary phase in appropriate broth. Spin down the bacterial cells at 2000 × *g* for 10 min and wash twice with pepsin buffer and resuspend the bacterial cells in the same buffer to a 10% solution (2×10^{10} cfu/ml).
2. Add to 1 ml 10% bacterial solution 200 μl pepsin solution 1 mg/ml.
3. Incubate for 60 min at 37 °C end-over-end rotation.
4. Terminate the reaction by adjusting the pH to approximately 7.5 with 7.5% $NaHCO_3$ (*see* **Note 26**).

5. Spin down the bacterial cells at 2000 × *g* for 15 min.
6. Sterile filter the supernatant using a 0.2 μm syringe filter. Store the supernatant at –20 °C.

3.3.4 Using Trypsin

1. Grow bacteria to stationary phase in appropriate broth. Spin down the bacterial cells at 2000 × *g* for 10 min and wash twice with trypsin buffer and resuspend the bacterial cells in the same buffer to a 10% solution (2×10^{10} cfu/ml).
2. Add to 1 ml 10% bacterial solution 20 μl trypsin solution 10 mg/ml.
3. Incubate for 60 min at 37 °C end-over-end rotation.
4. Terminate the reaction by adding 5 μl 1 M Benzamidine (final concentration 5 mM) (*see* **Note 27**).
5. Spin down the bacterial cells at 2000 × *g* for 15 min.
6. Sterile filter the supernatant using a 0.2 μm syringe filter. Store the supernatant at –20 °C.

3.3.5 Using Mutanolysin (See Note 28)

1. Grow bacteria to stationary phase in appropriate broth. Spin down the bacterial cells at 2000 × *g* for 10 min and wash twice with mutanolysin buffer and resuspend the bacterial cells in the same buffer to a 10% solution (2×10^{10} cfu/ml).
2. Add to 1 ml 10% bacterial solution 10 μl mutanolysin 1000 U/ml and 2 μl DNase 4 mg/ml.
3. Incubate for 2 h at 37 °C end-over-end rotation.
4. Terminate the reaction by adjusting the pH to approximately 7.5 with 7.5% $NaHCO_3$ (*see* **Note 26**).
5. Spin down the bacterial cells at 2000 × *g* for 15 min.
6. Sterile filter the supernatant using a 0.2 μm syringe filter. Store the supernatant at –20 °C.

3.4 Affinity Purification on Sepharose Column

1. Pack a column with the protein of interest (bacterial or host protein) coupled to CNBr-activated Sepharose, according to the manufacturer's protocol.
2. Wash the column with PBS.
3. Apply the sample containing the protein to be purified (a bacterial lysate or plasma). Collect the flow-through.
4. Wash the column with at least 10 column volumes of PBS. The Sepharose should be washed until the absorbance at 280 nm of the washing solution is close to zero.
5. Elute the bound protein(s) with 0.1 M glycine–HCl, pH 2.0. Collect fractions of 0.5 μl, add 1 M Tris to raise the pH to approximately 7.5 (*see* **Note 29**).
6. Measure the absorbance at 280 nm of the fractions and combine fractions containing the protein(s) of interest.

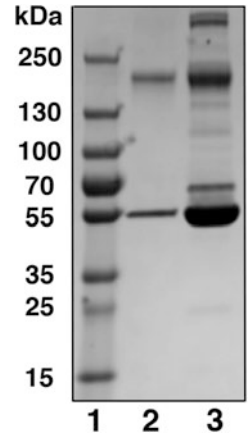

Fig. 5 SDS-PAGE analysis of plasma proteins eluted from protein H-Sepharose. Human citrate-treated plasma was applied to a column with streptococcal protein H-Sepharose. Proteins bound to the Sepharose were eluted with 0.1 M glycine buffer pH 2.0. The material was separated by SDS-PAGE (4–20 % gradient gel) under reducing conditions and the gel was stained with Coomassie Blue. *Lane 1*: molecular marker; *lane 2*: proteins eluted from protein H-Sepharose; *lane 4*: human plasma diluted 1:25

7. Dialyze the sample against PBS or Tris buffer (20 mM pH 7.5, 0.15 M NaCl) and if necessary concentrate the sample using micro-spin columns.
8. Analyze the sample by SDS-PAGE (Fig. 5). The eluted protein fragments are cut out and identified by N-terminal sequencing or mass spectrometry.

4 Notes

1. 1 M Tris solution is used to neutralize the low pH glycine–HCl buffer (pH 2.0) in order to minimize denaturation of eluted protein(s).
2. Citrate treated plasma is used for analysis of interactions with coagulation factors. Other plasmas or other host extracellular secretions can of course also be used depending on the question at issue.
3. IODO-BEAD® iodination reagent is a mild oxidizing agent, which does not require a reduction step. This is an advantage for maintaining biological activity of the protein to be labeled.
4. Labeling of proteins is not restricted to the usage of ^{125}I, and can be performed with any easy detectable label of choice (e.g., fluorescent probes such as FITC, and Alexa).
5. Concentrated HCl is 12.0 M. Dilute to 0.1 and 0.2 M by adding 8.33 ml and 16.66 ml concentrated acid to a final volume of 1000 ml water.

6. CNBr is toxic and thus it is important that all work with this chemical reagent is performed in a fume hood. Weigh an empty glass tube with a lid. Add CNBr to the test tube, close the lid and weigh the tube again. Calculate the volume of 0.2 M HCl that should be added to get a solution of 30 mg/ml. Spoon, tips, and beakers that have been in contact with CNBr solution should be neutralized with NaOH solution, approximately 1–2 M for 3 h. Then the solution can be thrown out in the fume hood sink.
7. In general, dialysis tubing with a MWCO of 3500 Da is used. Depending on the size and structure of the protein dialysis tubing with other MWCO can be chosen.
8. Benzamidine hydrochloride hydrate is a reversible inhibitor of trypsin.
9. Bacterial proteins can be expressed during different growth phases, and thus binding results might vary depending on which growth phase that is used.
10. Lower/higher concentrations of bacteria can be used as well, but if the protein of interest is expressed in low numbers at the bacterial surface higher concentrations of bacteria would be preferred.
11. Incubation at other temperatures, for instance 37 °C, can be used as well. Protein binding may differ between various temperatures.
12. The bacterial pellet is easier to dissolve in a small volume, 100–200 μl of PBS. Then add PBS to a final volume of 1000 μl.
13. The incubation time is not that important, but a minimum of 15 min is recommended to allow the change in ionization of groups involved in binding between the bacterial protein and the host ligand to occur.
14. This lab has good experience working with ^{125}I, but any label that is easy to detect in screening systems will work, including FITC and Alexa.
15. The labeling procedure using ^{125}I should be performed in a fume hood with a protection shield of lead. All waste material (tubes, pipette tips, etc.) should be put in a plastic bag for disposal of radioactive waste according to the regulations of the laboratory.
16. A volume size of 0.5 ml per fraction is generally used. PD-10 desalting columns contain Sephadex G25 and allow rapid separation of high molecular weight substances (>5000 Da) from low molecular weight compounds, such as free Iodine. The bed volume of these columns is 8.3 ml. Due to the larger size of proteins as compared to free iodine, labeled proteins will be eluted first (in or just after the void volume) and the free iodine will elute just before one column volume of buffer has passed through. With a fraction size of 0.5 ml and 10 fractions the free iodine will remain bound to the column, which can be disposed (*see* **Note 15**).

17. In general the radiolabeled protein will be eluted in fractions 7–8 with a fraction size of 0.5 ml. Fractions not containing the protein are disposed (*see* **Note 15**).
18. Once the protein is labeled with ^{125}I all work can be performed at the lab bench, but a protective bench paper is required. All waste material should be put in a plastic bag for later disposal (*see* **Note 15**).
19. Make duplicates for each bacterial strain to be analyzed for binding of the protein and for the PBST control.
20. Longer incubation times or incubation at 37 °C can be performed.
21. The supernatant is carefully removed by using a vacuum suction device connected to a Fluid Management System for liquid waste (Medela), working in a fume hood. Alternatively the supernatant can be removed to a plastic bag by pipetting and the liquid solidified by adding Swell (Abra Tech).
22. By screening bacteria before and after treatment for binding of radiolabeled ligand the efficiency of the treatment can be determined. The released material can also be analyzed by SDS-PAGE.
23. The purpose of the HCl dialyses is to remove the CNBr from the protein solution.
24. Papain is a cysteine protease having a sulfhydryl (SH) group necessary for its activity. Addition of L-cysteine is essential for enzyme activity.
25. Iodoacetic acid is an SH-blocking reagent modifying cysteine residues.
26. Approximately 5 µl 7.5 % $NaHCO_3$ to 1 ml solution is needed. Check the pH of the solution by adding 1 µl to a pH-indicator paper.
27. Alternatively, trypsin inhibitor can be used. 1 mg trypsin inhibitor inactivates 1 mg trypsin.
28. Opposite to the other hydrolytic enzymes (papain, trypsin, pepsin), mutanolysin is a glycosidase hydrolyzing the bonds in the peptidoglycan, and will thus not degrade the proteins using prolonged incubations.
29. Approximately 30–50 µl 1 M Tris is needed. Check the pH of the solution by adding 1 µl to a pH-indicator paper.

Acknowledgment

This work was supported by the Swedish Research Council (project 7480) and The Crafoord Foundation.

References

1. Björck L, Kronvall G (1984) Purification and some properties of streptococcal protein G, a novel IgG-binding reagent. J Immunol 133:969–974
2. Björck L (1988) A novel bacterial cell wall protein with affinity for Ig L chains. J Immunol 140:1194–1197
3. Åkesson P, Cooney J, Kishimoto F, Björck L (1990) Protein H–a novel IgG binding bacterial protein. Mol Immunol 27:523–531
4. Otten RA, Raeder R, Heath DG, Lottenberg R, Cleary PP, Boyle MDP (1992) Identification of two type IIa IgG-binding proteins expressed by a single group A *Streptococcus*. J Immunol 148:3174–3182
5. Karlsson C, Andersson M-L, Collin M, Schmidtchen A, Björck L, Frick I-M (2007) SufA–a novel subtilisin-like serine proteinase of *Finegoldia magna*. Microbiology 153:4208–4218
6. Frick I-M, Karlsson C, Mörgelin M, Olin A, Janjusevic R, Hammarström C, Holst E, de Château M, Björck L (2008) Identification of a novel protein promoting the colonization and survival of *Finegoldia magna*, a bacterial commensal and opportunistic pathogen. Mol Microbiol 70:695–708
7. Janulczyk R, Pallon J, Björck L (1999) Identification and characterization of a *Streptococcus pyogenes* ABC transporter with multiple specificity for metal cations. Mol Microbiol 34:596–606
8. Areschoug T, Stålhammar-Carlemalm M, Larsson C, Lindahl G (1999) Group B streptococcal surface proteins as targets for protective antibodies: identification of two novel proteins in strains of serotype V. Infect Immun 67:6350–6357
9. Åkesson P, Sjöholm AG, Björck L (1996) Protein SIC, a novel extracellular protein of *Streptococcus pyogenes* interfering with complement function. J Biol Chem 271:1081–1088
10. Faulmann EL, Boyle MDP (1991) A simple preparative procedure to extract and purify protein G from group G streptococci. Prep Biochem 21:75–86

Chapter 2

Analysis of Bacterial Surface Interactions with Mass Spectrometry-Based Proteomics

Christofer Karlsson, Johan Teleman, and Johan Malmström

Abstract

Host–pathogen protein–protein interaction networks are highly complex and dynamic. In this experimental protocol we describe a method to isolate host proteins attached to the bacterial surface followed by quantitative mass spectrometry based proteomics analysis. This technique provides an overview of the host–pathogen interaction network, which can be used to guide directed perturbations of the system, and to select target of specific interest for further studies.

Key words Bacteria, Surface absorption, Mass spectrometry, Proteomics, Trypsin digestion, Peptide solid phase extraction, Bioinformatics

1 Introduction

Microbial pathogenesis is the result of complex molecular interactions between the host and a microbial pathogen. Nonspecific and specific pathogen recognition results in the coating of the pathogen surface by immune system proteins derived from several different biochemical processes such as complement deposition and antibody binding. These processes aid the pathogen killing and clearance. However, pathogens have evolved mechanisms to interfere with the host immune reactions by for example expressing surface proteins that specifically bind host proteins, to facilitate immune evasion and bacterial dissemination.

A specific example of a pathogen that can bind many different host proteins to the bacterial surface is *Streptococcus pyogenes*. The major virulence factor on the *S. pyogenes* surface is the cell wall anchored M-protein that can bind several human host proteins [1–4]. The M-protein, together with other streptococcal host binding surface proteins, forms a complex host–pathogen protein interaction network on the bacterial surface [5–11]. Investigating binary interactions between host and pathogen proteins is not sufficient to describe the topology of the protein interaction network.

Pontus Nordenfelt and Mattias Collin (eds.), *Bacterial Pathogenesis: Methods and Protocols*, Methods in Molecular Biology, vol. 1535, DOI 10.1007/978-1-4939-6673-8_2,

Steric hinders, degree of affinity, secondary binding, competitive interactions, and protein abundances are factors that affect which proteins adhere to the bacterial surface. The comprehensive measurement of these interactions requires analytical techniques capable of identifying and quantifying the majority of the proteins involved in the network.

In this protocol we provide a method for quantitative MS analysis of both surface bound host proteins and the complete bacterial protein content in one experimental setup. The protocol includes the use of whole bacteria as affinity probes to isolate host proteins that attach to the bacterial surface (Fig. 1). Whole bacteria and the proteins adhered to the bacterial surface are isolated using centrifugation followed by quantitative mass spectrometry analysis. The rapid development of mass spectrometry (MS) based proteomics has made MS an important technology within life science [12–14]. The prevailing bottom-up MS based techniques analyze digested proteins (peptides), separated based on hydrophobicity using online liquid chromatography, which are then eluted via electrospray to form gas-phase ions. The chromatographic separation reduces the sample complexity, but numerous peptide ions still enter the MS instrument simultaneously. These peptide ions are first mass analyzed (MS1), after which the most abundant peptide ions are selected for collision-induced dissociation (CID) followed by a second mass analysis (MS2) of the derived fragment ions. Subsequent data analysis strategies attempts to match all acquired MS2 spectra computationally to one of all theoretically derived peptide MS spectra from the organisms analyzed [15–20]. From the identified peptides, proteins are inferred using statistical

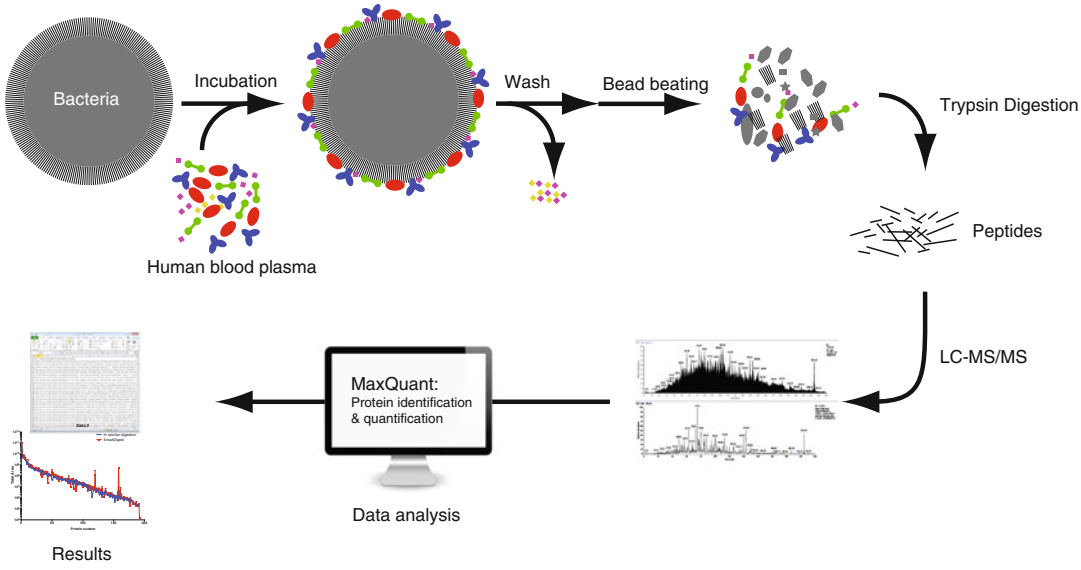

Fig. 1 Outline of the method to identify and quantify bacterial surface interacting host proteins

methods [21, 22]. The intensities of the individual MS1 features are integrated and the area under this curve is used to infer peptide and protein abundance using one of several published software programs [23–27]. In this protocol we use the MaxQuant software [26] as an example, which can be freely downloaded and installed on a standard Microsoft Windows computer.

The protocol outlines how bacterial cellular and surface proteins together with surface attached host proteins can be identified and quantified using MS and label-free quantification. The summed bacterial protein quantity can be utilized to normalize results for uneven sample loss during sample preparation, to remove confounding factors while comparing differential individual protein abundances between different strains or biological conditions. In addition, the quantification of the attached host proteins allows characterization of the host–pathogen protein interaction network topology.

2 Materials

2.1 Bacterial Plasma Adsorption and Sample Homogenization

1. Wash buffer (WB): 150 mM NaCl, 20 mM Tris–HCl pH 7.6.
2. Pooled Normal Human Blood Plasma (Innovative Research) (*see* **Note 1**).
3. LC-grade water.
4. 90 mg silica beads 0.1 μm ∅ (Biospec) in 0.5 ml tubes with an O-ring screw cap.
5. Beadbeater (Fastprep 96, MpBio).

2.2 Trypsin Digestion

1. Urea buffer (UB): 8 M Urea, 0.1 M NH_4HCO_3 in LC-grade water (*see* **Note 2**).
2. Sequence grade trypsin (Promega).
3. 100 mM NH_4HCO_3 (ABC) in LC-grade water (*see* **Note 2**).
4. 500 mM tris(2-carboxyethyl)phosphine) (TCEP).
5. 500 mM 2-iodoacetamide in LC-grade water (*see* **Note 2**).

2.3 Peptide C18 Solid Phase Extraction

1. 10% formic acid (FA) (*see* **Note 3**).
2. UltraMicro Spin Silica C18 300 Å columns (Harvard Apparatus).
3. LC-grade methanol.
4. LC-grade acetonitrile (ACN).
5. LC-grade water.
6. Buffer A: 2% ACN, 0.2% FA in LC-grade water.
7. Buffer B: 50% ACN, 0.2% FA in LC-grade water.
8. Vacuum concentrator.
9. Ultrasonic water bath.

2.4 Shotgun Mass Spectrometry

1. High-resolution, accurate-mass (HR/AM) mass spectrometer with nano-flow UHPLC.

2.5 Data Analysis

1. MaxQuant, http://www.coxdocs.org/doku.php?id = maxquant:start.
2. Protein database in FASTA format, describing the expected protein contents of the samples. This typically includes the proteome of both the bacterium and host/plasma (*see* **Note 4**).

3 Methods

3.1 Bacterial Plasma Adsorption

1. Grow the bacteria to desired growth phase for the interaction analysis.
2. Harvest the bacteria by centrifugation and wash by resuspending the pellet in the wash buffer.
3. Wash the bacteria for a second time and dissolve the pellet in WB to a concentration of 1% w/v.
4. Mix 150 µl of 1% bacteria solution with 450 µl plasma, vortex bacteria briefly just before adding to plasma.
5. Incubate for 30 min at 37 °C on thermal block with 500 rpm shaking.
6. Wash three times with 1 ml WB (5000 × *g*, 5 min, swing-out, soft).
7. Transfer 100 µl of the solution to a 0.5 ml tube with an O-ring screw cap containing 90 mg silica beads.
8. Centrifuge for 5 min 5000 × *g*, remove the supernatant and add 100 µl LC-grade water.
9. Lyse the bacteria with a bead beater for 2 × 3 min at 1600 oscillations/min and 1.5-inch stroke speed.
10. Dry samples completely using a vacuum concentrator.

3.2 Sample Homogenization and Trypsin Digestion

1. Add 50 µl UB to the dried sample.
2. Incubate for 30 min on shaker.
3. Add 1 µl TCEP and incubate at 37 °C for 60 min.
4. Add 2 µl IAA and incubate for 30 min at room temperature in a dark environment.
5. Add 500 µl ABC to the sample.
6. Add 2 µg trypsin to the sample and Incubate for >6 h at 37 °C.
7. Add 100 µl 10% FA to stop the digestion.
8. Ensure that the pH is ≥3.

3.3 Peptide C18 Solid Phase Extraction

1. Place the C18 column in 2 ml collection tube. Add 300 µl methanol for column wash and centrifuge at 200 × *g* for 1 min. Discard the flow-through liquid.

2. Add 300 µl Buffer A to the column and centrifuge at 200 × *g* for 1 min, repeat three times. Discard the flow-through liquid after the second and third centrifugation.
3. Dry the column tip on a lint-free paper towel and place the column in a new collection tube. Add 450 µl digested sample to the column and centrifuge at 200 × *g* for 1.5 min. Reapply the flow-through liquid to the column and centrifuge as above. Repeat twice (totally three centrifugations). Discard the final flow-through liquid.
4. Add 300 µl Buffer A to the column and centrifuge at 200 × *g* for 1.5 min. Repeat three times. Discard the flow-through liquid after the second centrifugation.
5. Dry the column tip on a lint-free paper towel and place the column in a new collection tube.
6. Add 100 µl Buffer B to the column and centrifuge at 200 × *g* for 1 min. Do not discard the flow-through. Repeat three times. Then briefly centrifuge at 1000 × *g*. The final elution volume is 300 µl.
7. Dry the samples to complete dryness using a vacuum concentrator.
8. Add 50 µl Buffer A, resuspend the peptides by incubating for 5 min in a ultrasonic water bath.

For a recent detailed overview of sample preparations methods for MS, *see* ref. [28].

3.4 Shotgun Mass Spectrometry

1. This protocol is optimized for the LC-MS/MS analysis of 1 µl sample corresponding to ~1 µg protein (*see* **Note 5**).
2. Separate the peptides on a 2 h gradient and run the mass spectrometer in data dependent acquisition (DDA) mode according to the instrument vendor's recommendations.

3.5 Data Analysis

1. Launch MaxQuant by double-clicking on "MaxQuant.exe".
2. Click "load" and select the MS data files in the file dialog (*see* **Note 6**).
3. Under the "Group-specific parameters" tab:
   (a) Click "Label-free quantification". In the dropdown menu, select "LFQ".
   (b) Click "Digestion". Ensure that "Trypsin/P" is the only entry in the right list.
   (c) Click "Instrument". Ensure that the instrument type is matching the used instrument (*see* **Note 7**).
   (d) Click "Modifications". Ensure that the right-hand list consists of "Oxidation (M)" and "Acetyl (Protein N-term)".

4. Under the "Global parameters" tab:
   (a) Click "Sequences":
      - Click "Add file" and select the FASTA protein database.
      - Ensure that the right-hand list consists of "Carbamidomethyl (C)".
   (b) Click "Identification". Set the "PSM FDR" to 0.01, and "Protein FDR" to 0.01.
5. Under the "Configuration" tab:
   (a) Click "Sequence databases":
      - Click "Add". On the right hand side, click "Select" and choose the fasta protein database. Type in the fasta file source in the "Source" field. Replace "Homo sapiens" for the appropriate host and pathogen species. Finally click "Modify table" to save this entry.
      - Click "Save changes".
6. Under the "Raw files" tab:
   (a) Click "Start" to start the analysis. Depending on the number of sample and size of the protein database, the analysis might take several hours.
7. Results are found in the tab-separated file combined/proteinGroups.txt.
   (a) The measured relative quantity of each protein is given in the "Intensity" column. This is very precise for comparing the concentration of a given protein between samples, but should not be used to compare levels between different proteins.
   (b) Protein IDs starting with "CON__" or "REV__" are known contaminants and mock proteins respectively. This status is also shown in the "Potential contaminant" and "Reverse" columns. Such proteins should not be used in the following analysis.
   (c) Many proteomics scientists consider proteins with only one supporting peptide dubious, these proteins should be used with caution.

4 Notes

1. Other proteinous fluids can also be used, for example saliva.
2. These solutions should be made fresh and used the same day.
3. Prepare 10% working solution in LC-grade water. Do not use plastics (tips, beakers or bottles) when handling concentrated FA.
4. Translated bacterial genomes can be found both in Uniprot (http://uniprot.org), but also in the Human Microbiome Project

(http://hmpdacc.org/), PANTHER (http://pantherdb.org) and Patric (http://patricbrc.org) databases. For host-translated genomes (human, mouse, etc.) we suggest using the UniProt KB reference proteomes.

5. The injection volume is dependent on the amount of bacteria and absorbed proteins. The total protein concentration of the sample homogenate can be estimated with protein assays, for example bicinchoninic acid (BCA) assay kits.
6. MaxQuant support the native data formats of several vendors. If the used instrument vendor is not in this list. MSConvert [29] might be used to convert the data files to the generic format mzXML, that is also supported by MaxQuant.
7. To maximize mass spectrometry search results, the search parameters and especially precursor and fragment tolerances should be adapted to the used method and instrument. If unsure, please consult with the instrument operator on the appropriate settings.

Acknowledgments

This work was supported by the Swedish Research Council (project 621-2012-3559).

References

1. Macheboeuf P, Buffalo C, Fu C-Y et al (2011) Streptococcal M1 protein constructs a pathological host fibrinogen network. Nature 472:64–68. doi:10.1038/nature09967
2. Cunningham MW (2000) Pathogenesis of group A streptococcal infections. Clin Microbiol Rev 13:470–511
3. Herwald H, Cramer H, Mörgelin M et al (2004) M protein, a classical bacterial virulence determinant, forms complexes with fibrinogen that induce vascular leakage. Cell 116:367–379
4. Carlsson F, Berggård K, Stålhammar-Carlemalm M, Lindahl G (2003) Evasion of phagocytosis through cooperation between two ligand-binding regions in Streptococcus pyogenes M protein. J Exp Med 198:1057–1068. doi:10.1084/jem.20030543
5. Sjöholm K, Karlsson C, Linder A, Malmström JA (2014) A comprehensive analysis of the Streptococcus pyogenes and human plasma protein interaction network. Mol Biosyst 10:1698–1708. doi:10.1039/c3mb70555b
6. Cole JN, Barnett TC, Nizet V, Walker MJ (2011) Molecular insight into invasive group A streptococcal disease. Nat Rev Microbiol 9:724–736. doi:10.1038/nrmicro2648
7. Malmström JA, Karlsson C, Nordenfelt P et al (2011) Streptococcus pyogenes in human plasma: adaptive mechanisms analyzed by mass spectrometry based proteomics. J Biol Chem 287:1415–1425. doi:10.1074/jbc.M111.267674
8. Nyberg P, Rasmussen M, Bjorck L (2004) Alpha2-macroglobulin-proteinase complexes protect Streptococcus pyogenes from killing by the antimicrobial peptide LL-37. J Biol Chem 279:52820–52823. doi:10.1074/jbc.C400485200
9. Kronvall G, Simmons A, Myhre EB, Jonsson S (1979) Specific absorption of human serum albumin, immunoglobulin A, and immunoglobulin G with selected strains of group A and G streptococci. Infect Immun 25:1–10
10. Kahn F, Mörgelin M, Shannon O et al (2008) Antibodies against a surface protein of Streptococcus pyogenes promote a pathological inflammatory response. PLoS Pathog 4:e1000149. doi:10.1371/journal.ppat.1000149
11. Nordenfelt P, Waldemarson S, Linder A et al (2012) Antibody orientation at bacterial surfaces is related to invasive infection. J Exp Med 209:2367–2381. doi:10.1084/jem.20120325

12. Aebersold R, Mann M (2003) Mass spectrometry-based proteomics. Nature 422:198–207. doi:10.1038/nature01511
13. Gillette MA, Carr SA (2013) Quantitative analysis of peptides and proteins in biomedicine by targeted mass spectrometry. Nat Methods 10:28–34. doi:10.1038/nmeth.2309
14. Picotti P, Bodenmiller B, Aebersold R (2013) Proteomics meets the scientific method. Nat Methods 10:24–27. doi:10.1038/nmeth.2291
15. Xu C, Ma B (2006) Software for computational peptide identification from MS-MS data. Drug Discov Today 11:595–600. doi:10.1016/j.drudis.2006.05.011
16. Nesvizhskii AI, Vitek O, Aebersold R (2007) Analysis and validation of proteomic data generated by tandem mass spectrometry. Nat Methods 4:787–797. doi:10.1038/nmeth1088
17. Käll L, Storey JD, MacCoss MJ, Noble WS (2008) Assigning significance to peptides identified by tandem mass spectrometry using decoy databases. J Proteome Res 7:29–34. doi:10.1021/pr700600n
18. Elias JE, Gygi SP (2007) Target-decoy search strategy for increased confidence in large-scale protein identifications by mass spectrometry. Nat Methods 4:207–214. doi:10.1038/nmeth1019
19. Craig R, Beavis RC (2004) TANDEM: matching proteins with tandem mass spectra. Bioinformatics 20:1466–1467. doi:10.1093/bioinformatics/bth092
20. Perkins DN, Pappin DJ, Creasy DM, Cottrell JS (1999) Probability-based protein identification by searching sequence databases using mass spectrometry data. Electrophoresis 20:3551–3567. doi:10.1002/(SICI)1522-2683(19991201)20:18<3551::AID-ELPS3551>3.0.CO;2-2
21. Nesvizhskii AI, Keller A, Kolker E, Aebersold R (2003) A statistical model for identifying proteins by tandem mass spectrometry. Anal Chem 75:4646–4658
22. Reiter L, Claassen M, Schrimpf SP et al (2009) Protein identification false discovery rates for very large proteomics data sets generated by tandem mass spectrometry. Mol Cell Proteomics 8:2405–2417. doi:10.1074/mcp.M900317-MCP200
23. Häkkinen J, Vincic G, Månsson O et al (2009) The proteios software environment: an extensible multiuser platform for management and analysis of proteomics data. J Proteome Res 8:3037–3043. doi:10.1021/pr900189c
24. Weisser H, Nahnsen S, Grossmann J et al (2013) An automated pipeline for high-throughput label-free quantitative proteomics. J Proteome Res 12:1628–1644. doi:10.1021/pr300992u
25. Mueller LN, Rinner O, Schmidt A et al (2007) SuperHirn - a novel tool for high resolution LC-MS-based peptide/protein profiling. Proteomics 7:3470–3480. doi:10.1002/pmic.200700057
26. Cox J, Mann M (2008) MaxQuant enables high peptide identification rates, individualized p.p.b.-range mass accuracies and proteome-wide protein quantification. Nat Biotechnol 26:1367–1372. doi:10.1038/nbt.1511
27. Zhang R, Barton A, Brittenden J, Huang JT, Crowther D (2010) Evaluation for computational platforms of LC-MS based label-free quantitative proteomics: A global view. J Proteomics Bioinform 3:260–265. doi:10.4172/jpb.1000149
28. Vowinckel J, Capuano F, Campbell K et al (2013) The beauty of being (label)-free: sample preparation methods for SWATH-MS and next-generation targeted proteomics. F1000Res 2:272. doi:10.12688/f1000research.2-272.v2
29. Kessner D, Chambers M, Burke R et al (2008) ProteoWizard: open source software for rapid proteomics tools development. Bioinformatics 24:2534–2536. doi:10.1093/bioinformatics/btn323

Chapter 3

Differential Radial Capillary Action of Ligand Assay (DRaCALA) for High-Throughput Detection of Protein–Metabolite Interactions in Bacteria

Mona W. Orr and Vincent T. Lee

Abstract

Bacteria rely on numerous nucleotide second messengers for signal transduction such as cyclic AMP, cyclic-di-GMP, and cyclic-di-AMP. Although a number of receptors responsible for known regulated phenotypes have been established, the completeness of protein receptors in any given organism remains elusive. We have developed a method called differential radial capillary action of ligand assay (DRaCALA) that allows for an unbiased, systematic high-throughput screen for the detection of ligand binding proteins encoded by a genome. DRaCALA permits interrogation of ligand binding directly to an overexpressed protein in a cell lysate and bypasses the need of protein purification. Gateway-cloning-compatible open reading frame libraries are available for a diverse range of bacterial species and permits generation of the lysates overexpressing each open reading frame. These lysates can be assessed by DRaCALA in a 96-well format to allow rapid identification of protein–ligand interactions, including previously unknown proteins. Here, we present the protocols for generating the expression library, conducting the DRaCALA screen, data analysis, and hit validation.

Key words Protein–ligand interaction, DRaCALA, High-throughput screen, ORFeome, Nucleotide signals, Receptors

1 Introduction

Bacteria use many different nucleotide signaling molecules to regulate a variety of phenotypes. However, despite years of research dating back decades, identification of ligand binding proteins for many of these signaling molecules has been a challenge. For example, c-di-GMP is a well-studied ubiquitous bacterial second messenger that regulates a range of behaviors such as biofilm formation and motility [1]. Although c-di-GMP was first described in 1987 [2], novel receptors are still being identified nearly three decades later [3–6]. While some c-di-GMP receptors contain conserved predicted binding domains, additional proteins have been reported

Pontus Nordenfelt and Mattias Collin (eds.), *Bacterial Pathogenesis: Methods and Protocols*, Methods in Molecular Biology, vol. 1535, DOI 10.1007/978-1-4939-6673-8_3,

with unique and previously unknown binding sites. These include the PelD from *Pseudomonas aeruginosa* and DNA binding proteins, including FleQ from *P. aeruginosa* [7, 8], BldD from *Streptomyces coelicolor* [3], and the CRP-homolog Clp from *Xanthomonas* species [9–11]. Furthermore, new signaling molecules such as c-di-AMP and c-AMP-GMP are being identified [12, 13]. The protein receptors for these molecules still remain largely unknown. Since these signaling molecules govern a wide range of bacterial behaviors and their mechanism of action remains unclear, the identification of their cognate receptors will be immensely helpful in understanding their functions to regulate bacterial physiology.

Successful methods to identify the protein binding partners of bacterial metabolites include bioinformatics-based approaches, mass spectrometry analysis of proteins pulled down using affinity tagged ligands, and targeted approaches to test proteins regulated by the signaling molecule. For c-diGMP, in silico bioinformatics predictions based on known binding motifs, including PilZ [14], I-site of DGCs [15, 16], and catalytically inactive PDE-A [15, 17] have identified c-di-GMP receptors [1, 18, 19]. Affinity pull-down based methods such as those using the cyclic di-GMP analog 2-AHC-c-di-GMP covalently coupled to sepharose beads [20] and the c-di-GMP-specific Capture Compound [21] have been successful in identifying additional binding proteins. In addition to these methods, additional binding proteins for c-di-GMP have been identified through targeted approaches [22]. The high throughput DRaCALA open reading frame library (ORFeome) screen described here allows for another approach by permitting high-throughput screening of the individual open reading frames from an entire bacterial genome.

DRaCALA relies on differential movement of a radiolabeled nucleotide and protein on nitrocellulose [23]. For this assay, a small volume of protein mixed with radiolabeled ligand in a binding buffer is applied to dry nitrocellulose. The protein remains bound to the nitrocellulose at the point of application. While the free ligand will be mobilized by capillary action with the liquid phase, bound ligand will remain sequestered with the protein at the point of application. These DRaCALA spots can be quantified by calculating the fraction bound: the intensity of the radiation detected from protein-sequestered ligand over the total radiation of the spot [23]. DRaCALA can be used to detect interactions without the need to purify from *Escherichia coli* overexpression strain lysates under two conditions: first, the protein is expressed above the dissociation constant and second, the ligand is not naturally abundant in the overexpression strain to compete for radioactively labeled ligand binding.

The DRaCALA screen can take advantage of available Gateway-compatible ORFeome libraries to query each predicted ORF of an entire genome individually for ligand binding. The ORF is recombined into Gateway compatible destination expression plasmids and transformed into the *E. coli* T7Iq expression strain, which is then grown, induced for protein expression, and lysed all in a 96-well plate

format. Each well in the expression library contains a lysate overexpressing a single ORF. Radiolabeled ligand is then added via a liquid dispenser. This lysate-ligand mix are then transferred to a nitrocellulose sheet using a 96-pin tool and exposed for quantification. ORFs that increase binding above the average background binding seen for the expression library are considered positive hits. These candidate binding proteins can then be purified and assayed for confirmation of binding (*see* Fig. 1 for process overview). The DRaCALA screen has recently been successfully used to identify novel binding partners of c-di-AMP in *Staphylococcus aureus* [24], c-di-GMP in *Vibrio cholerae* [5] and *E. coli* [4], and pGpG in *V. cholerae* [25]. We anticipate that the DRaCALA ORFeome screen will be a powerful tool for identifying further protein–ligand interactions.

2 Materials

2.1 Gateway Cloning into Expression Plasmids

1. Autoclave-sterilized 96-well PCR plates and silicone sealing mats.
2. Thermocyclers.
3. TE buffer, pH 8.0: 10 mM Tris–HCl, pH 8.0, 1 mM EDTA. 10 mL 1 M Tris–HCl, pH 8.0, 2 mL 0.5 M EDTA, bring volume up to 1 L with double-distilled water (ddH_2O).
4. 2 μg/μL proteinase K: 2 mg proteinase K dissolved in 1 mL ddH_2O. Make 100 μM aliquots and store at −20 °C.
5. LR Clonase (Invitrogen).
6. Gateway compatible donor plasmid containing ORFs of interest in TE Buffer, pH 8.0 at 15–150 ng/μL, arrayed in 96-well plates.
7. Gateway compatible destination expression plasmid(s) in TE Buffer, pH 8.0 at 150 ng/μL (*see* **Note 1** for cloning into multiple destination plasmids and choice of tags in one LR Clonase reaction).

2.2 Transformation into E. coli T7Iq

1. Chemically competent *E. coli* T7Iq (NEB).
2. 96-well sterile flat-bottomed microtiter plates.
3. Foil adhesive plate sealers.
4. Incubator with plate shaker at 30 °C.
5. Selection antibiotic stocks. The antibiotics used will depend on the antibiotic resistance cassette present on the donor and destination plasmids. Prepare stocks at 1000× concentration and split into 1 mL aliquots. Store at the appropriate temperature for the antibiotic.
6. LB-M9: 7 g anhydrous Na_2HPO_4, 2 g KH_2PO_4, 0.5 g NaCl, 1 g NH_4Cl, 2 g glucose, 1 g Na succinate hexahydrate, 10 g tryptone, 5 g yeast extract, add 750 mL ddH_2O, bring pH to 7.2 with NaOH, add volume up to 1 L with ddH_2O, and

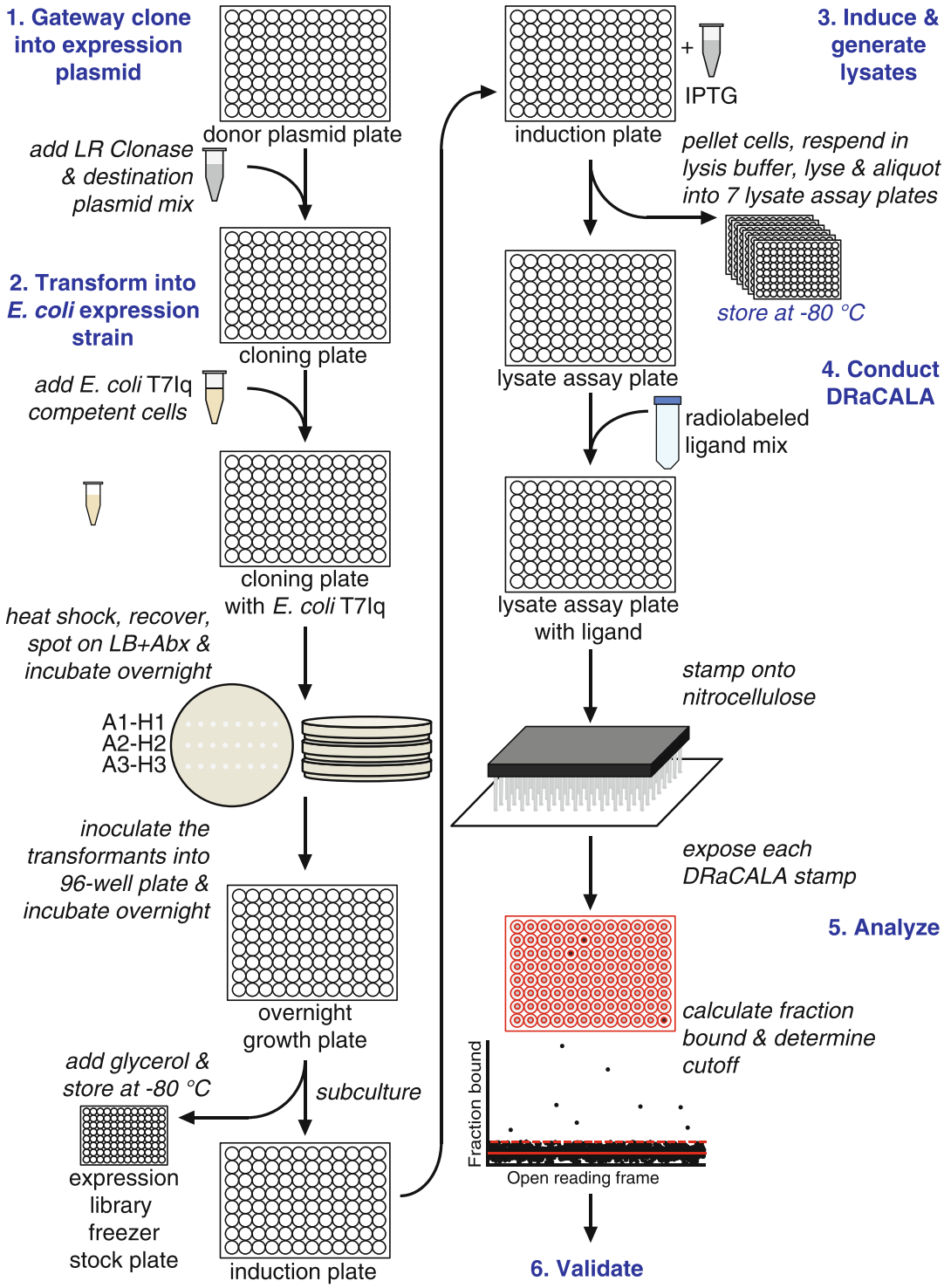

Fig. 1 Schematic of high-throughput DRaCALA ORFeome screen. Steps corresponding to each text section are *numbered* and in *bold*. Each of the plates has a designated name, shown below the plate, which is used in the accompanying text. The general procedural steps are indicated by text on the side of each *arrow*

autoclave to sterilize. Right before use, add 3 mL of autoclaved sterilized 1 M $MgSO_4$ and 1 mL 1000× selection antibiotic stock to each L of LB-M9 media. Expect to use ~160 mL of LB-M9 in the generation of every 96-well expression plate.

7. LB 1% agar plates with appropriate selection antibiotic: 10 g tryptone, 5 g yeast extract, 10 g NaCl, 10 g agar, dissolve in 1 L ddH_2O, autoclave to sterilize, let cool to ~50 °C, add 1 mL 1000× antibiotic stock, pour into petri dishes and let cool.
8. LB-M9 40% glycerol: 10 g tryptone, 5 g yeast extract, 10 g NaCl, dissolve in 600 mL ddH_2O, then mix in 400 mL glycerol and autoclave to sterilize.

2.3 Lysate Generation

1. 2 mL sterile 96-well plates with lids.
2. 96-well U-bottom microtiter plates.
3. LB-M9 (see above).
4. 0.1 M (100×) isopropyl β-D-1-thiogalactopyranoside (IPTG) stock: 238 mg IPTG, add ddH_2O to 10 mL, sterile filter through 0.45 nm filter, aliquot 1.5 mL into sterile microfuge tubes and store at −20 °C.
5. 10× binding buffer (100 mM Tris–HCl, pH 8.0, 1 M NaCl, 50 mM $MgCl_2$): 100 mL 1 M Tris–HCl, pH 8.0, 58.4 g NaCl, 10.2 g $MgCl_2$, dissolve salts, bring volume up to 1 L with ddH_2O, and autoclave to sterilize (*see* **Note 2** for buffer component considerations).
6. 1× binding buffer: dilute 10× binding buffer 1:10 into sterile ddH_2O.
7. 1× lysis buffer: 1× binding buffer with 10 μg/mL DNAse, 250 μg/mL lysozyme, and 1 μM PMS. Make the day of use.
8. 100× DNase (1 mg/mL): 10 mg DNase, add ddH_2O to 10 mL, aliquot 1 mL into sterile microfuge tubes and store at −20 °C.
9. 100× lysozyme (25 mg/mL): 250 mg lysozyme, add ddH_2O to 10 mL, aliquot 1 mL into sterile microfuge tubes and store at −20 °C.
10. 100× PMSF (0.1 M): 871 mg PMSF, add isopropanol to 50 mL in a 50 mL conical. Store at room temperature. Another protease inhibitor may be substituted.

2.4 DRaCALA Screen

1. Radiolabeled ligand in binding buffer: calculate the volume of radiolabeled ligand that will result in 150 μCi activity/50 mL of buffer (*see* **Note 3** regarding radiolabel mixture). To this volume add 5 mL 10× binding buffer and ddH_2O to 50 mL in a 50 mL conical. Store at −20 °C until use.
2. 0.01% (vol) Tween 20 in H_2O: mix 5 μL Tween 20 and 50 mL ddH_2O in a 50 mL conical. Make fresh each time.

3. 96-well pin tool with 2 μL slot (V&P Scientific).
4. 0.45 μm dry nitrocellulose membrane sheets cut to a size that permits duplicate stamps on one sheet (12 cm × 19 cm). Nitrocellulose MUST BE DRY.
5. MultiFlo liquid dispenser (BioTek) or other liquid handlers.
6. Phosphorimager screens and cassettes.

2.5 Quantification and Analysis

1. Phosphorimager and associated image analysis software (Our lab uses a Fujifilm FLA-7000 phosphorimager and Fujifilm Multi Gauge software v3).
2. Graphing program.

2.6 Validation

1. Expression library freezer stock plate generated in Subheading 3.2.
2. 96-well sterile flat-bottomed microtiter plates.
3. Materials listed in Subheading 2.3.

3 Methods

Before starting this protocol, the user needs to obtain or generate a library of Gateway compatible donor plasmids arrayed in 96-well plates that contain their ORFs of interest. This can be generated in house or ordered from a repository (*see* **Note 4**).

The methods are split into six sections: (1) Gateway cloning into the expression plasmid, (2) transformation into the expression strain, (3) protein expression and lysate library generation, (4) conducting the DRaCALA screen, (5) data analysis, and (6) validation (Fig. 1). All the wet lab steps take place in 96-well plate format. The use of multi-channel pipettes, multichannel stepper pipettes or robotic fluid dispensers is beneficial for expediting these high-throughput processes.

3.1 Gateway Cloning into Expression Plasmids

In this section, the Gateway cloning reaction is performed in 96-well format using PCR plates to introduce the ORFs of interest into the expression vectors.

1. Thaw LR Clonase, ORFeome donor library plate, and destination plasmid(s). Refreeze immediately after use (*see* **Note 1** for cloning into multiple destination plasmids in one LR Clonase reactions).
2. Make a master mix of destination plasmid and LR Clonase for each plate: 48 μL destination plasmid (150 ng/μL), 48 μL LR Clonase, 96 μL TE buffer, pH 8.0 (each individual reaction will have 0.5 μL destination plasmid, 0.5 μL LR Clonase, 1.5 μL TE buffer, pH 8.0). Pipette to mix and place on ice. If efficiency is low, increase LR Clonase to 1 μL and decrease TE buffer to 1 μL.

3. Aliquot 3 μL of master mix into each well of a sterilized 96-well PCR plate (cloning plate).
4. Transfer 2 μL of miniprepped donor plasmid from the plasmid library plate to the corresponding well in the cloning plate. Pipette to mix.
5. Cover the cloning plate with a sterile silicone sealing mat and incubate at 25 °C in thermocycler for 2 h.
6. Remove the cloning plates from the thermocycler. Change the temperature to 37 °C. Add 1 μL of 2 μg/μL proteinase K solution to each well and incubate at 37 °C in the thermocycler for 10 min to stop the Gateway reaction.

3.2 Transformation into E. coli T7Iq

In this section, the Gateway cloning product from Subheading 3.1 is transformed into the *E. coli* T7Iq expression strain (New England Biolabs). The cells are added to the Gateway product, heat shocked, and recovered in 96-well plates. The 96-well plate containing the Gateway reaction is referred to as the "cloning plate." They are then plated onto selective plates using an 8-channel multichannel pipette. The transformants are picked and inoculated into media in a 96-well plate for growth for frozen stocks and for subculture to induce protein expression (Subheading 3.3). This process can be staggered to increase throughput (*see* **Note 5**).

1. Thaw chemically competent *E. coli* T7Iq on ice during the proteinase K incubation step. After proteinase K incubation, remove the cloning plate from the thermocycler and place on ice and allow to cool.
2. Add 20 μL of thawed competent *E. coli* T7Iq to each well of the cloning plate and incubate on ice for 30 min.
3. During ice incubation, preheat a thermocycler to 42 °C. Transfer the cloning plate from ice to thermocycler and heat shock at 42 °C for 30 s.
4. Transfer the cloning plate from thermocycler to ice and recover for 2 min.
5. Add 50 μL of LB and incubate the cloning plate on a plate shaker at 30 °C for 30 min.
6. Use an 8-channel pipette to spot 5 μL from each column of the cloning plate onto 2 LB agar plates with the appropriate selection antibiotic with 3 columns per plate. If transforming into two destination vectors, pipette transformation onto two different selection plates.
7. Incubate LB agar plates overnight at 30 °C. Each transformation spot should generate at least one colony (*see* **Note 6**).
8. The following morning, thaw an aliquot of 1000× antibiotic stock and add to a bottle of LB-M9 media.

9. Transfer 150 μL of LB-M9 media supplemented with antibiotic into each well of a sterile 96-well microtiter plate (overnight growth plate). 150 μL is used to ensure enough culture is present for both creation of a freezer stock and subculture for expression.
10. To inoculate the overnight growth plate with the transformants, take an 8-channel pipette and drag the tips through the colonies and then place the tips into the corresponding column of the overnight growth plate.
11. Replace the lid and shake overnight at 30 °C (*see* **Note 7**).
12. Prepare an expression library freezer stock plate from the overnight growths. Transfer 100 μL of LB-M9 40% glycerol into each well of a sterile flat-bottomed 96-well microtiter plate (expression library freezer stock plate). Transfer 100 μL of the overnight growth plate cultures to the freezer stock plate, shake at room temperature for 5 min to mix, then seal with an adhesive foil. This stock is now in 20% glycerol and can be stored at −80 °C.

3.3 Lysate Generation

In this section, the expression strains are subcultured and induced for ORF expression, lysed, and aliquoted into the lysate assay plates.

1. Remove the lid of a sterilized 2 mL 96-well plate and transfer 1.5 mL of the LB-antibiotic media into each well (induction plate). Allow to warm to room temperature before use.
2. Dilute overnight growth cultures 1:50 (30 μL) from an overnight growth plate into the induction plate and grow with shaking at 30 °C for 4 h. Either use the remaining overnight growth cultures from Subheading 3.2, **step 11** or start 150 μL cultures from the expression library freezer stock (from Subheading 3.2, **step 12**) the night before.
3. After 4 h, add 15 μL of sterile 0.1 M IPTG into each well of the induction plate to induce and grow at 30 °C for an additional 4 h.
4. Centrifuge the subculture plate for 10 min at 2000 × *g* to pellet cells. As soon as the centrifugation is over, quickly invert the induction plate, hold for 5 s and shake sharply once to remove media without disrupting the pellet.
5. During centrifugation, thaw DNase and lysozyme to compose lysis buffer by mixing 30 mL of 1× binding buffer, 300 μL DNase, 300 μL lysozyme, and 300 μL of PMSF stocks to a pipetting reservoir (final concentration 10 μg/mL DNase, 250 μg/mL lysozyme, and 1 μM PMSF).
6. Transfer 150 μL of lysis buffer into each well of the induction plate and shake on a plate shaker for 10 min at RT to resuspend the pellet. If necessary, pipette up and down to fully resuspend.
7. Aliquot 20 μL of resuspended pellet into 96-well U-bottom plates (lysate library plates) and seal with a foil seal. Seven replicate lysate library plates can be made from each induction plate.

8. Subject each lysate library plate to three freeze–thaw cycles to lyse cells. Freeze at −80 °C for 30 min and thaw at RT for 30 min twice, then store −80 °C until use in the DRaCALA screen. This final thaw completes the third freeze–thaw cycle (*see* **Note 8**).
9. In most library plates, there is one well that is left empty that is used for the addition of a lysate expressing a known binding protein of the signaling nucleotide of interest. That well is typically empty. The buffer in the well is removed and the lysate of the positive control lysate is added.

3.4 DRaCALA Screen

In this section, the DRaCALA screen is performed in high-throughput manner. An automated liquid dispenser is used to add radiolabeled ligand into each well of the lysate plates and the mix is transferred to dry nitrocellose using a 96-well pin tool for the creation of the DRaCALA spots. The use of automation and the 96-well pin tool, while not strictly necessary, is what allows for the high-throughput processing of samples and rapid analysis. This section uses radiation and should be performed in an area certified for use of radioactivity.

1. Lay out a pre-cut nitrocellulose sheet on the radiation bench so that the 12 cm edge is parallel to the front edge of the bench (*see* **Note 9**).
2. Thaw the 50 mL conical containing radiolabeled ligand mix (Subheading 2.4, **item 1**) (*see* **Note 3**). This can be thawed in a beaker of warm water to speed the process. If all wells show positive binding, there may be nonspecific binding proteins in the lysates (*see* **Note 10**).
3. Prepare the wash bath for the 96-well pin tool by pouring the 50 mL 0.01% Tween 20 into a reservoir large enough to accommodate the pin tool. The tips (3–5 mm) of the pins should be immersed in the 0.01% Tween 20 wash solution when the pin tool is placed in the reservoir.
4. Turn on the MultiFlo liquid dispenser and wash the lines with 10 mL ddH_2O.
5. Empty the lines of ddH_2O. Place conical tube with thawed radiolabeled ligand in binding buffer into the MultiFlo liquid dispenser and fill the lines with radiolabeled ligand mix.
6. Thaw a lysate library plate at room temperature for 10 min. All plates should be used within ~15 min of thawing for consistency. Three plates can be thawed at once since completing the DRaCALA for each plate takes ~5 min/plate.
7. Set the MultiFlo liquid dispenser to dispense 20 μL in a 96-well plate format. Remove the foil seal from the thawed lysate library plate, place the plate onto the MultiFlo liquid dispenser tray and dispense the radiolabeled ligand.

8. Transfer the lysate library plate onto a plate shaker at room temperature and shake for 1 min to mix.
9. While the plate is shaking, wash the 96-well pin tool in the 0.01% Tween 20 by dipping it into the reservoir and then blotting on a paper towel. Repeat total of 3× to make sure the tips of the pins are cleaned and coated in 0.01% Tween 20.
10. As soon as the 1 min of mixing is over, move the lysate library plate from the shaker to the bench. Place the pin tool into the lysate library plate and make sure all the pins have dropped and made contact with the lysate.
11. Pick up the pin tool and transfer it to the top half of the nitrocellulose membrane. Let pin tool sit on the membrane for 5–10 s while tapping the top of the pintool to make sure all lysates in the pins have made contact with the nitrocellulose membrane (*see* **Note 11**).
12. After 10 s, carefully pick up the pin tool vertically away from the membrane to avoid dragging the tips sideways across the surface of the membrane. The liquid transferred by the pins onto the nitrocellulose should be visible as an array of 96 wet circles. Check that all of the 96 circles are present and of uniform size.
13. Wash in 0.01% Tween 20 again, then repeat **steps 9–12** for technical replicates using the same assay mixture.
14. Move membrane aside and process additional plates.
15. After membranes have fully dry (~15 min at room temperature), wrap in plastic cling wrap and expose to phosphorimager screen (exposure time depends on the activity of radioisotope) (*see* **Note 12**).
16. Image on phosphorimager. Figure 3a shows a representative DRaCALA 96-well stamp.

3.5 Quantification and Analysis

In this section, the fraction bounds for the DRaCALA spot are quantified using image analysis software in a 96-well plate format. Fraction bound is measured by drawing two circles: an outer circle that encloses the entire spot and an inner circle that encloses the inner spot (Fig. 2b). Most analysis software packages have a 96-well plate measuring tool, where the well size and distance between adjacent wells can be adjusted (Fig. 2c). While drawing individual circles for quantification is possible, this can be time-prohibitive for analyzing an entire ORFeome of thousands of spots. When the fraction bounds of the entire library have been determined, those ORFs that increase the fraction bound above a determined "cut-off" value above the background are considered positive hits.

1. Use the analysis software to draw the outer and inner circles and obtain the area and radiation intensities for each DRaCALA spot in the 96-well stamp (Figs. 2b and 3b) (*see* **Note 13**).

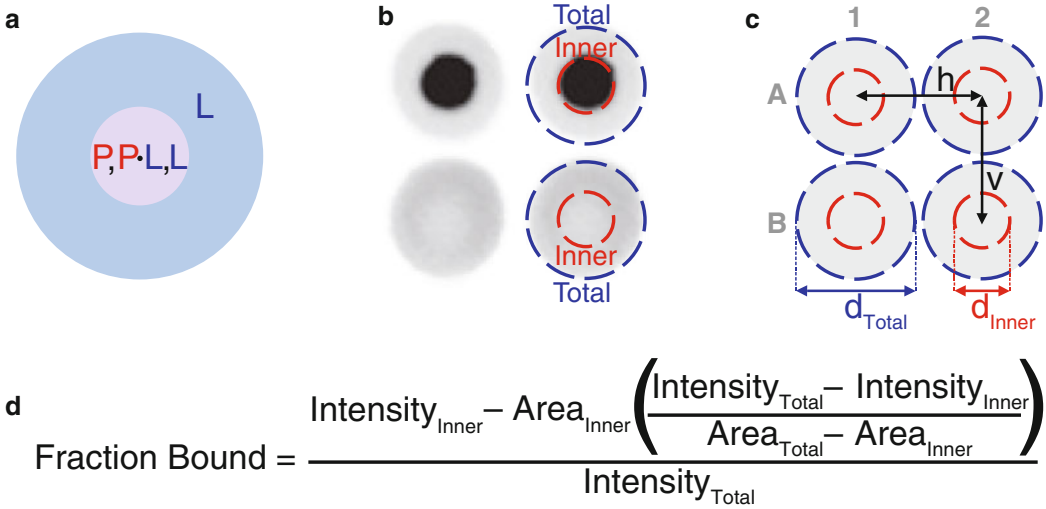

Fig. 2 Principle of DRaCALA and fraction bound calculations. (**a**) Shown is a cartoon representation of a DRaCALA spot and (**b**) two images of DRaCALA spots, one indicating binding (*top*) and another indicating no binding (*bottom*). The locations of protein (P), ligand (L), and ligand bound to protein (P·L), are indicated in the cartoon. The location of the quantification circles are shown in *red* (inner circle) and *blue* (total circle). (**c**) A schematic showing the three different parameters that can be adjusted to customize the 96-well measuring tool on the Fujifilm Multi Gauge software. Shown are the circles for quantification for four spots from a 96-well plate. The horizontal distance between wells of adjacent columns is *h* and the vertical distance between wells of adjacent rows is *v*. These two parameters should be the same for the inner and total circles. The diameter of the inner circle is d_{Inner} (in *red*) and the diameter of the total circle is d_{Total} (in *blue*). (**d**) The equation for calculation of fraction bound

2. Use these four measurements to calculate fraction bound. First determine the background intensity of unbound ligand (*see* **Note 14** for background explanation), subtract this background from the intensity of inner circle, and divide this value by the intensity of the total DRaCALA spot for the fraction bound (*see* Fig. 2d for equations). Excel or another processing spreadsheet can be set up to automate calculations if the measurements are taken and exported the same way each time.
3. After calculating the fraction bound for every ORF in the library, plot the data with the fraction bound on the *y*-axis and the ORF on the *x*-axis. Remove the values for the positive and negative control wells (*see* Fig. 3d for a representative plot).
4. Calculate the cutoff for positive hits. The cutoff for positive hits can be defined for the entire library or on a plate by plate basis. The use of these different definitions of positive hits will depend on the data (*see* **Note 15**).

3.6 Validation

1. To validate that the overexpressed protein increases binding in the lysate, restreak positive hits for single colonies from the expression library freezer stock plate, pick eight colonies from each putative

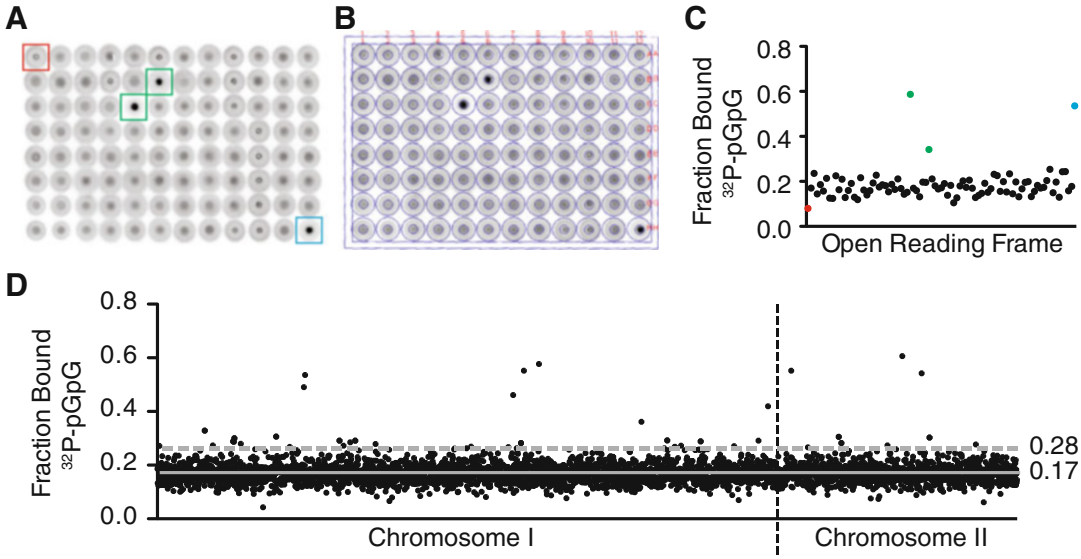

Fig. 3 Example of a DRaCALA screen result and sample quantification. (**a**) An image of a DRaCALA stamp from a pGpG screen against a His-MBP tagged *V. cholerae* ORFeome plate [25]. A1, *boxed in red*, is the negative control and contains a lysate of an empty vector strain. H1, *boxed in blue*, is the positive control and contains a lysate of a strain overexpressing the protein RocR. The two spots *boxed in green* are lysates that show increased binding of radiolabeled ligand. (**b**) A screen shot of the DRaCALA stamp with inner and total circles drawn using the 96-well plate measuring tool from the Fujifilm Multi Gauge software (in *blue*). (**c**) Quantification of fraction bound of each well from (**a**). The *red dot* is the fraction bound calculated for the negative control, the *blue dot* is the fraction bound for the positive control well, and the *two green dots* are two potential positive hits corresponding to the same *colored boxes* from (**a**). (**d**) Quantification of the fraction bound of the entire pGpG *V. cholerae* ORFeome binding screen [25]. The ORFs are arrayed by chromosome in ascending numerical order along the *x*-axis. The *vertical black dotted line* divides between chromosomes I and II in *V. cholerae*. The *horizontal solid gray line* is the average fraction bound of the entire library and the *horizontal dotted line* shows three standard deviations above the mean

binding protein to regenerate new lysates (as described in Subheading 3.3) and re-assay for binding. The reason for picking eight colonies is to ensure that the binding is not due to cross-contamination that can easily occur during high-throughput manipulations of the libraries. Binding by all eight colonies will confirm that the increased fraction bound seen in the original binding assay can be replicated. If only a subset of the eight colonies bind, that subset should be used for additional analysis below.

2. Specificity can be determined by competition assays. Mix radiolabeled ligand with an excess of unlabeled competitor (*see* **Note 16**) and add this mix to lysates of putative binding ORFs and check for binding by DRaCALA. Specific binding interaction should be only competed by the specific unlabeled competitor.
3. Purify the expression plasmid from colonies that bind and sequence the ORF encoded on the plasmid to validate the identity of the gene of interest.

4. Subsequent validation requires the candidate protein to be purified to ensure that the protein bind directly to the signaling nucleotide. False positives can arise from the screen because the binding assay occurs within the context of a cell lysate. For example, overexpression of a non-binding protein that drives the production of a binding protein encoded in the *E. coli* genome would result in a false positive. Purification techniques for individual proteins can vary widely and will not be discussed here.

4 Notes

1. This procedure can be modified to simultaneously clone into two different destination plasmids in one LR Clonase reaction by using destination plasmids containing two different antibiotic resistance cassettes. For example, in our studies we utilized two different destination plasmids: one with an N-terminal His-MBP tag and a gentamycin resistance cassette and a second with an N-terminal His tag and an ampicillin resistance cassette. By plating the same LR Clonase reaction on gentamycin containing plates (thus selecting for the transformants with the HisMBP tagged ORF) and carbenicillin containing plates (thus selecting for transformants with the His tagged ORF), we were able to construct two differently tagged expression libraries using a single LR Clonase reaction. To alter the procedure, use 75 ng of each destination plasmid and decrease TE buffer accordingly in the LR Clonase mix.
2. Choice of binding buffer is important. Some enzymes are active in certain conditions and may degrade the radiolabeled ligand. For example, one class of enzymes that cleaves c-di-GMP is active in Mg^{2+} but not Ca^{2+}. One can use a binding buffer without divalent cations during lysate production and provide it in 2× with the radiolabeled ligand mix, allowing use of different divalent cations for the same frozen lysate library. If necessary, an excess of unlabeled nonspecific competitor can also be included in the binding buffer to prevent nonspecific interactions.
3. Prepare radiolabeled ligand by adding sufficient counts of radioisotope to give >5000 counts for the total spot intensity when exposed for 15 min to a phosphorimager screen. Add that amount of radiolabeled ligand to 20 μL of 1× binding buffer. If screening a full library, make 50 mL of the radiolabeled mixture and freeze until use. For smaller screens, prepare ~2 mL of the radiolabeled ligand in 1× binding buffer per plate to be screened. If using an automated dispenser, account for the liquid required for priming the machine. This varies depending on the equipment and the inner diameter of the tubing.

4. The Gateway compatible donor plasmid library can either be generated in house by PCR and BP recombination based on manufacturer instructions, or obtained from already generated Gateway compatible ORFeome libraries. For example, BEI Resources stocks a repository of several prokaryotic Gateway compatible ORFeome libraries in *E. coli*. Each 96-well plate of the library should include one well containing a strain with the empty vector as a negative control and one well containing a strain with the plasmid encoding a known binding protein as a positive control. These libraries should first be miniprepped to yield donor plasmid using a 96-well plate miniprep kit.
5. Stagger the timing of the second set of LR Clonase reactions to begin just prior to the end of the 2 h incubation of the first set (Subheading 3.1, **step 6**).
6. It is possible that a few reactions will result in no transformants. These individual reactions should be repeated and the expression strain plate can be filled in later with successful transformants.
7. 150 μL cultures may evaporate in some incubators or warm rooms after overnight incubation. A "humidified chamber" may be used by placing the plate shaker in a container that contains 0.5–1 cm depth of water to increase humidity.
8. Having high quality lysates (defined as fully lysed with high protein overexpression levels) is crucial for the success of this assay. Thus, testing conditions for growth, induction, lysis, and DRaCALA spotting in small scale in lab prior to screening the full ORFeome library is highly recommended. Three common problems that result in low quality lysates for DRaCALA are poor protein expression, incomplete lysis, and high viscosity. Poor expression results in no detection of binding because the protein needs to be present in a concentration above the K_d. Assess the protein expression levels after generating a lysate library plate. Randomly select 16 out of 96 wells. Add 5 μL of lysates to 5 μL loading dye, boil 20 min, load 5 μL into a 12% acrylamide gel, separate by SDS-PAGE, stain with Coomassie, and check if there is a visible overexpression band present that is of the correct size for the ORF expressed in that well. If bands are weak, adjusting richness of the media or IPTG levels can improve expression. Incomplete lysis will result in reduced availability of the overexpressed protein for binding. Increasing the amount of lysozyme or adding additional freeze–thaw cycles may help improve lysis. A very viscous lysate will affect spreading of the spot on nitrocellulose. Increasing the DNase concentration can reduce viscosity.
9. Nitrocellulose membrane sheets come sandwiched between sheets of wax paper. When stamping, keep the bottom sheet of the sandwich below the nitrocellulose. The sheet of wax paper

helps keep the nitrocellulose membrane from sticking to the bench and prevents radiation from contaminating the bench. Pre-cut nitrocellulose sheets and keep them in the stamping area in case there is an error in stamping and another replicate is needed.

10. If binding is detected in all lysates, there is likely the presence of a nonspecific binding protein in the lysate. This can be tested by using a lysate containing the vector only. If the binding activity is present in negative control lysates of cells with vector alone, the addition of a related, but nonspecific competitor may prevent nonspecific binding to the signaling nucleotide of interest. For example, in the c-di-GMP screen, 100 μM of unlabeled GTP was added to prevent detection of nonspecific binding interactions.
11. There are three common problems with the stamping portion of this protocol. Firstly, the pins may drag on the nitrocellulose when placing the pin tool on the membrane or lifting the pin tool off the membrane, resulting in distorted spots. Place and lift the pin tool vertically and be sure that the nitrocellulose is laid flat on the bench. If the nitrocellulose curls, the corners of the membrane can be immobilized (by weights or tape) to ensure the membrane remains flat. Secondly, the pins sometimes become stuck and do not contact the membrane to allow for transfer of the liquid to the membrane. This is most likely due to dirty pins. If the pins are not dropping, wash the pin tool according to supplier instructions. Finally, the pin sometimes does not transfer the reaction mix to the nitrocellulose immediately. To address this issue, tap fingers vigorously along the back of pin tool to make sure lysate is transferred to the membrane. Alternatively, the teeth of the pin can be dirty and must be cleaned. The 40 μL reaction volume in a U-bottomed plate allows for up to four replicate stamps. If after lifting the pin tool, it is clear that volume from one or more wells has not been transferred to the nitrocellulose, wash the pin tool and re-stamp on another sheet.
12. Be careful when wrapping in plastic cling wrap to not have folds or creases in the wrap between the membrane and the screen. This will result in uneven exposure and lines on the radiograph of the DRaCALA image.
13. Properly centering and aligning the circles is important. Quantification circles that have too much white space or miss part of the spot will result in incorrect values. For our experiments, we made two sets of 96-well plates for each DRaCALA stamp (Fig. 3b): one for an outer circle with a $d = 8$ mm, $h = 8.97$ mm, $v = 8.95$ mm, and one of the inner circle with a $d = 3.5$, $h = 8.97$ mm, $v = 8.95$ mm (Fig. 2c).
14. Simply, the fraction bound is the intensity of the protein-bound ligand over the total intensity of all ligand in the spot. The radiation intensity detected from the inner circle contains

signal from the ligand bound to protein (L·P), but also has free ligand (L) (Fig. 2a). The background can be calculated to estimate the amount of signal that can be attributed to free ligand present in inner circle. The "donut" area between the total circle and the inner circle contains only unbound ligand (L), which is similarly distributed in the inner circle. By calculating the area of the donut ($Area_{Total} - Area_{Inner}$) and the radiation intensity present in the donut ($Intensity_{Total} - Intensity_{Inner}$) and dividing these two values, we get a value that is the intensity/area of the free ligand. Multiplying this value by $Area_{Inner}$ gives the intensity of the free ligand in an area the size of the inner circle. This value is an estimation of the radiation intensity in the inner circle that can be attributed to the unbound ligand.

15. There can be plate-to-plate variation in the fraction bound. As a consequence, the fraction bound cutoff to define positive hits need to account for this variation. Assuming that the majority of proteins do not bind the signaling nucleotide of interest, a rapid way to normalize the plate is to adjust the average fraction bound for the entire plate (excluding the positive control) such that they are the same [25]. For example, if plate 1 has an average fraction bound of 0.05 and plate 2 has 0.1, all of the fraction bound in plate 2 can be subtracted by 0.05 so that the average of plate 1 and plate 2 would both be 0.05. Note that this can lead to fraction bound of a few well to be below 0. These data points are typically plotted at 0 fraction bound. An alternative way is to analyze each plate for lysates that have a fraction bound that is three standard deviation above the mean of fraction bound of the entire plate. This analysis is repeated iteratively after removing the positive hits until no additional positive hits are found [5].
16. For competition assays, specific and nonspecific related nucleotides can be added to the radiolabeled signaling nucleotide prior to addition to the lysates expressing positive hits. For example, addition of unlabeled c-di-GMP in excess competes away the ability of lysates expressing positive hits to bind radiolabeled c-di-GMP, whereas addition of nucleotides, such as GTP, GDP, GMP, or cGMP, does not compete. Together, the panel of unlabeled competitors can demonstrate the binding interaction is specific to the signaling nucleotide of interest.

References

1. Römling U, Galperin MY, Gomelsky M (2013) Cyclic di-GMP: the first 25 years of a universal bacterial second messenger. Microbiol Mol Biol Rev 77(1):1–52
2. Ross P, Weinhouse H, Aloni Y, Michaeli D, Weinberger-Ohana P, Mayer R, Braun S, de Vroom E, van der Marel GA, van Boom JH, Benziman M (1987) Regulation of cellulose synthesis in *Acetobacter xylinum* by cyclic diguanylic acid. Nature 325(6101):279–281
3. Tschowri N, Schumacher MA, Schlimpert S, Chinnam NB, Findlay KC, Brennan RG, Buttner MJ (2014) Tetrameric c-di-GMP mediates effective transcription factor dimerization to control *Streptomyces* development. Cell 158(5):1136–1147

4. Fang X, Ahmad I, Blanka A, Schottkowski M, Cimdins A, Galperin MY, Römling U, Gomelsky M (2014) GIL, a new c-di-GMP-binding protein domain involved in regulation of cellulose synthesis in enterobacteria. Mol Microbiol 93(3):439–452
5. Roelofs KG, Jones CJ, Helman SR, Shang X, Orr MW, Goodson JR, Galperin MY, Yildiz FH, Lee VT (2015) Systematic identification of cyclic-di-GMP binding proteins in *Vibrio cholerae* reveals a novel class of cyclic-di-GMP-binding ATPases associated with Type II secretion systems. PLoS Pathog 11(10), e1005232
6. An SQ, Caly DL, McCarthy Y, Murdoch SL, Ward J, Febrer M, Dow JM, Ryan RP (2014) Novel cyclic di-GMP effectors of the YajQ protein family control bacterial virulence. PLoS Pathog 10(10), e1004429
7. Hickman JW, Harwood CS (2008) Identification of FleQ from *Pseudomonas aeruginosa* as a c-di-GMP-responsive transcription factor. Mol Microbiol 69(2):376–389
8. Baraquet C, Harwood CS (2013) Cyclic diguanosine monophosphate represses bacterial flagella synthesis by interacting with the Walker A motif of the enhancer-binding protein FleQ. Proc Natl Acad Sci U S A 110(46):18478–18483
9. Leduc JL, Roberts GP (2009) Cyclic di-GMP allosterically inhibits the CRP-like protein (Clp) of *Xanthomonas axonopodis* pv. citri. J Bacteriol 191(22):7121–7122
10. Chin KH, Lee YC, Tu ZL, Chen CH, Tseng YH, Yang JM, Ryan RP, McCarthy Y, Dow JM, Wang AH, Chou SH (2010) The cAMP receptor-like protein CLP is a novel c-di-GMP receptor linking cell-cell signaling to virulence gene expression in *Xanthomonas campestris*. J Mol Biol 396(3):646–662
11. Tao F, He YW, Wu DH, Swarup S, Zhang LH (2010) The cyclic nucleotide monophosphate domain of *Xanthomonas campestris* global regulator Clp defines a new class of cyclic di-GMP effectors. J Bacteriol 192(4):1020–1029
12. Witte G, Hartung S, Buttner K, Hopfner KP (2008) Structural biochemistry of a bacterial checkpoint protein reveals diadenylate cyclase activity regulated by DNA recombination intermediates. Mol Cell 30(2):167–178
13. Davies BW, Bogard RW, Young TS, Mekalanos JJ (2012) Coordinated regulation of accessory genetic elements produces cyclic di-nucleotides for *V. cholerae* virulence. Cell 149(2):358–370
14. Amikam D, Galperin MY (2006) PilZ domain is part of the bacterial c-di-GMP binding protein. Bioinformatics 22(1):3–6
15. Galperin MY, Nikolskaya AN, Koonin EV (2001) Novel domains of the prokaryotic two-component signal transduction systems. FEMS Microbiol Lett 203(1):11–21
16. Chan C, Paul R, Samoray D, Amiot NC, Giese B, Jenal U, Schirmer T (2004) Structural basis of activity and allosteric control of diguanylate cyclase. Proc Natl Acad Sci U S A 101(49):17084–17089
17. Schmidt AJ, Ryjenkov DA, Gomelsky M (2005) The ubiquitous protein domain EAL is a cyclic diguanylate-specific phosphodiesterase: enzymatically active and inactive EAL domains. J Bacteriol 187(14):4774–4781
18. Hengge R (2009) Principles of c-di-GMP signalling in bacteria. Nat Rev Microbiol 7(4):263–273
19. Schirmer T, Jenal U (2009) Structural and mechanistic determinants of c-di-GMP signalling. Nat Rev Microbiol 7(10):724–735
20. Duvel J, Bertinetti D, Moller S, Schwede F, Morr M, Wissing J, Radamm L, Zimmermann B, Genieser HG, Jansch L, Herberg FW, Häussler S (2012) A chemical proteomics approach to identify c-di-GMP binding proteins in *Pseudomonas aeruginosa*. J Microbiol Methods 88(2):229–236. doi:10.1016/j.mimet.2011.11.015
21. Nesper J, Reinders A, Glatter T, Schmidt A, Jenal U (2012) A novel capture compound for the identification and analysis of cyclic di-GMP binding proteins. J Proteome 75(15):4874–4878
22. Lee VT, Matewish JM, Kessler JL, Hyodo M, Hayakawa Y, Lory S (2007) A cyclic-di-GMP receptor required for bacterial exopolysaccharide production. Mol Microbiol 65(6):1474–1484
23. Roelofs KG, Wang J, Sintim HO, Lee VT (2011) Differential radial capillary action of ligand assay for high-throughput detection of protein-metabolite interactions. Proc Natl Acad Sci U S A 108(37):15528–15533
24. Corrigan RM, Campeotto I, Jeganathan T, Roelofs KG, Lee VT, Gründling A (2013) Systematic identification of conserved bacterial c-di-AMP receptor proteins. Proc Natl Acad Sci U S A 110(22):9084–9089
25. Orr MW, Donaldson GP, Severin GB, Wang J, Sintim HO, Waters CM, Lee VT (2015) Oligoribonuclease is the primary degradative enzyme for pGpG in *Pseudomonas aeruginosa* that is required for cyclic-di-GMP turnover. Proc Natl Acad Sci U S A 112(36):E5048–E5057

Chapter 4

Identifying Bacterial Immune Evasion Proteins Using Phage Display

Cindy Fevre, Lisette Scheepmaker, and Pieter-Jan Haas

Abstract

Methods aimed at identification of immune evasion proteins are mainly rely on in silico prediction of sequence, structural homology to known evasion proteins or use a proteomics driven approach. Although proven successful these methods are limited by a low efficiency and or lack of functional identification. Here we describe a high-throughput genomic strategy to functionally identify bacterial immune evasion proteins using phage display technology. Genomic bacterial DNA is randomly fragmented and ligated into a phage display vector that is used to create a phage display library expressing bacterial secreted and membrane bound proteins. This library is used to select displayed bacterial secretome proteins that interact with host immune components.

Key words Immune evasion, Phage display, Secretome, Functional identification, High-throughput

1 Introduction

In order to inhibit immune responses, immune evasion proteins need to reside outside the bacterial cell wall and thus are part of the bacterial secretome. Secretome proteins include membrane proteins, cell wall anchored proteins, and extracellular proteins. They are synthesized in the cytoplasm as protein precursors encoding various motifs such as signal sequences, cell wall-anchoring motifs and/or transmembrane domains. The type and combination of these motifs determine the ultimate location of the protein. Signal sequences address proteins to different secretion systems that will allow their translocation across the plasma membrane for further insertion in the membrane, binding to the membrane, retention in the cell wall, or secretion. Classical methods to identify immune modulatory secretome proteins are inefficient and time consuming. They are often based on genetic or structural homologies or proteomic identification in bacterial supernatant, and especially rely on laborious inefficient readouts [1, 2].

Pontus Nordenfelt and Mattias Collin (eds.), *Bacterial Pathogenesis: Methods and Protocols*, Methods in Molecular Biology, vol. 1535, DOI 10.1007/978-1-4939-6673-8_4,

Phage display technology provides an alternative strategy to functionally identify immune evasion proteins using a high throughput system [3]. Phage display technology is the process of expressing proteins fused to capsid proteins on the surface of a filamentous Ff-phage (viruses that specifically infect the Gram negative bacterium *Escherichia coli* carrying F-pili) and selecting the fraction of displayed proteins that exhibit a desired property. By far the most commonly used capsid protein for phage display is pIII that allows expression of large proteins [4].

A phage library contains a large amount of different phage clones displaying a different protein resulting in a heterogeneous mixture of phages. The expressed protein often retains the behavior of its free counterpart. This allows for affinity selection of phage displayed molecules [3, 5]. The selected phages are amplified and the phage and expressed protein are further characterized. The expression of the capsid protein (and thus the fusion protein) depends on the presence of a signal sequence that directs the protein to the inner membrane of the bacterial host where it is incorporated into the newly formed phage particle, an essential step for phage production and stability [3]. This allows for selective expression of a bacterial secretome since secretome proteins are characterized by the presence of a signal sequence that addresses the protein to the bacterial inner cell membrane (Fig. 1).

Secretome phage display, also called signal sequence phage display, is based on a genomic library and constitutes a very promising alternative to *in silico* analysis and to the classical functional characterization methods [6]. The strategy is derived from whole genome phage display where randomly sheared chromosomal DNA is inserted into a phagemid vector containing a signal sequence which addresses the encoded bacterial protein in fusion with a phage coat protein to the *E.coli* cytoplasmic membrane, where it is assembled into the phage particle. In a secretome phage display strategy, the signal sequence, or any other membrane-targeting signal, is absent

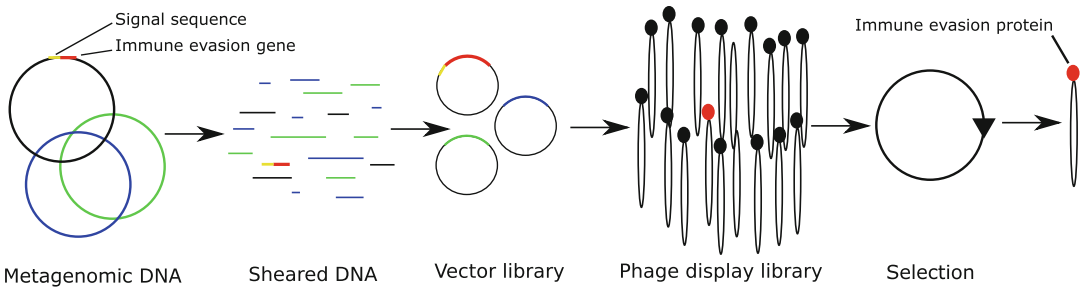

Fig. 1 In bacterial secretome phage display genomic DNA is randomly sheared into small fragments that are ligated into a phage display (phagemid) vector. These vectors are transformed into a *E.coli* and phage production is initiated by addition of helper phage. In secretome phage display only inserts encoding a gene containing a signal sequence are displayed including immune evasion proteins. The resulting phage library can than be selected for binding to a specific immunological target in order to identify interacting bacterial proteins

from the phagemid vector. Therefore, only phagemids containing an insert encoding a native membrane-targeting signal will give rise to phage particles displaying a fusion protein, which means that only secretome proteins will be displayed [7].

Here we describe the creation of a bacterial secretome phage display library and how it is used to identify bacterial immune evasion proteins.

2 Materials

Prepare all solutions using ultrapure water and analytical grade reagents. Prepare all reagents at room temperature and store at 4 °C unless indicated otherwise. To prevent phage contamination of the reagents aliquot the reagents in a volume sufficient for single use. Sterilize all glassware, solutions, and media in an autoclave that is never used to autoclave biological waste in order to keep the phage load to a minimum. Phages are known to survive standard autoclaving conditions but are heat-killed by dry heating to 105 °C for 4 h.

Decontaminate all surfaces and non-autoclavable materials like pipettes with phage active disinfectants like chlorine.

2.1 Preparing Library Insert DNA Fragments from Genomic DNA

1. Bacterial target strain and appropriate culture medium.
2. Phosphate buffered saline.
3. 20% sodium dodecyl sufate (SDS).
4. 0.1 mm zirconia beads.
5. TE: 10 mM Tris–HCl, 1 mM Na_2EDTA, pH 8.0. Autoclave and store at room temperature.
6. Phenol–chloroform–isoamyl alcohol (25:24:1).
7. Rnase A.
8. Ultra Pure agarose, DNA grade.
9. 3 M NaAc pH 5.2. Autoclave and store at room temperature.
10. 96% ethanol.
11. 70% ethanol: stored at –20 °C.
12. TE-200 and TE-1000 size exclusion spin columns.
13. T4 DNA polymerase.
14. dNTP mix: 10 mM of each dNTP in water.
15. T4 polynucleotide kinase.
16. PCR purification kit.

2.2 Preparing Vector DNA

1. pDJ01 phagemid vector: The pDJ01 vector was created by Jankovic at al. (Massey University, Palmerston North, New Zealand). The vector contains a chloramphenicol resistance

cassette and a multiple cloning site and myc-tag sequence in front of the gene encoding the C-terminal domain of the minor coat protein pIII [3].

2. DNA gel extraction kit.
3. Restriction buffer 10×: 330 mM Tris-acetate, 100 mM magnesium acetate, 660 mM potassium acetate, 1 mg/mL BSA, pH 7.9 at 37 °C.
4. SmaI endonuclease 10 U/μL.
5. Calf Intestinal alkaline phosphatase.
6. 0.5 M EDTA.
7. Shrimp alkaline phosphatase.

2.3 Ligation of Vector and Inserts

1. Ready to Go ligation Kit (GE Healthcare) or alternative.
2. Plasmid purification spin columns.

2.4 Electroporation of Bacterial Library

1. TG1 strain *E.coli*: [F′ *traD36 proAB lacIqZ ΔM15] supE thi-1 Δ(lac-proAB) Δ(mcrB-hsdSM)5(rK - mK -)*.
2. TG1 electrocompetent cells.
3. LB medium: Dissolve 10 g of tryptone, 5 g of yeast extract and 10 g of NaCl in 1 L H2O. Adjust pH to 7.00 with NaOH, autoclave and store at room temperature. When appropriate add antibiotics directly before use.
4. LB agar: add 11 g Bacto agar to 1 L LB medium, autoclave and allow to solidify. When appropriate add antibiotics to cooled agar just before solidification occurs.
5. 1 mm electroporation cuvettes.
6. SOC medium: to 950 mL deionized water add, 20 g of tryptone, 5 g of yeast extract, 0.5 g of NaCl, 186 mg of KCl. Mix thoroughly until completely dissolved and adjust pH to 7.0 with NaOH. Adjust the volume to 1 L. Sterilize by autoclaving for 20 min at 15 psi on liquid cycle. When cooled add 10 mL of sterile 1 M $MgCl_2$. Add 20 mL of 1 M glucose (filter sterilized). Store at room temperature.
7. 23 × 23 cm LB agar plates.
8. Chloramphenicol.
9. Sterile 85 % glycerol.

2.5 Phage Library Production

1. VCSM13 helper phage.
2. Kanamycin.
3. PEG/NaCl: 200 g PEG-8000, 116.9 g NaCl, dissolve in water to total volume of 600 mL. Brief heating to 65 °C may be necessary to dissolve solids, can be autoclaved, store at room temperature.

4. EDTA free protease inhibitor tablets.
5. TBS: 50 mM Tris–HCl, pH 7.5, 150 mM NaCl. Autoclave and store at room temperature.

2.6 Phage Selection on Immobilized Targets

1. 96 well ELISA plates.
2. Washing buffer: PBS–0.05% Tween 20.
3. Blocking buffer: PBS–0.05% Tween 20, 4% BSA.
4. Elution buffer: 0.2 M glycine, 0.15 M NaCl, pH2.
5. Neutralization buffer: 1 M Tris–HCl, pH 8.4.

2.7 Identification of Selected Fusion Proteins

Forward sequence primer: 5′-GGAAGAGCTGCAGCATGATGAAA-3′

Reversed sequence primer: 5′-CACCGTAATCAGTAGCGACAGAA-3′

3 Methods

Carry out all procedures at room temperature unless otherwise specified. To prevent phage contamination perform all procedures with phages in a laminar flow cabinet. Decontaminate all used equipment and all surfaces with a phage active disinfectant like chlorine (*see* **Note 1**). The secret of creating a high diversity phage library is in taking care to optimize every single step.

3.1 Preparing Library Insert DNA Fragments from Genomic DNA

1. Prepare a 200 mL overnight culture from one colony of the bacterium from which you want to create a secretome phage library, culture medium and conditions depend on the selected bacterial strain. Transfer the overnight culture to 4 × 50 mL tubes, spin at 2424 × *g* for 15 minutes. Discard the supernatant and dissolve the bacterial pellet in 1 mL PBS.
2. Add 500 µL of the bacterial suspension to 210 µL 20% SDS, 500 µL phenol–chloroform–isoamyl alcohol (1, 25, 24), (*see* **Note 2**) 500 µL 0.1 mm zirconia beads in a 2 mL tube with screw cap. Bead beat for 1 min at 2100 rpm. Spin at 18,626 × *g*, 5 min.
3. Transfer aqueous layer (top layer) to a new tube, add equal volume of chloroform, mix well and spin at 18,626 × *g* for 5 min. Transfer top layer to a new tube, add 15 µL 10 mg/mL RNase A. Incubate 30 min at 37 °C and centrifuge at 18,626 × *g* maximum speed for 5 min.
4. Transfer the top layer to a new tube, add 0.1 × 3 M NaAc pH 5.2 and 1× volume isopropanol. Incubate for 30 min at −20 °C. Spin at 18,626 × *g* for 30 min and at 4 °C.
5. Wash pellet with 1 mL 70% EtOH and centrifuge at 18,626 × *g* for 10 min at room temperature. Dry the pellet and dissolve in

150 µL EB. Quantify the isolated DNA and load the samples on an 0.8% agarose gel (*see* **Note 3**).

6. When multiple strains from a bacterial species are used to create a secretome library the isolated DNA is mixed in this step. Mix 150 µg of gDNA from each strain to create a combined library (*see* **Note 4**).
7. Use 20–50 µg purified genomic DNA. Adjust the volume to 250 µL with TE. Keep on ice.
8. Shear the gDNA by sonication for 3 s repeating this procedure three times. The exact sonication time needs to be determined experimentally, (*see* **Note 5**).
9. Run the sheared DNA on a 1.5 agarose gel to determine fragment size and distribution (Fig. 2). Add 0.1 volume 3 M NaAc pH 5.2 + 3 volumes 96% EtOH and precipitate the sheared DNA overnight at −20 °C. Centrifuge at 18,626 × *g* for 30 min at 4 °C.

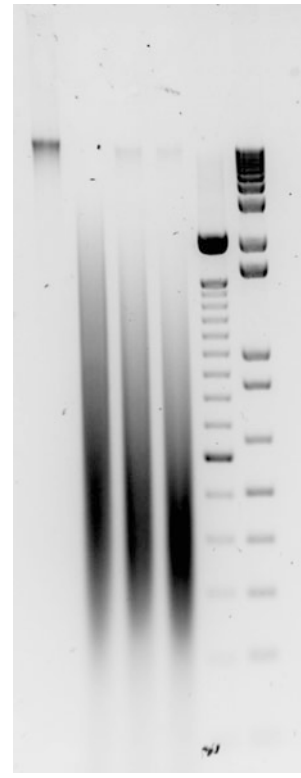

Fig. 2 Genomic bacterial DNA (*Staphylococcus aureus*) was sheared using different sonication protocols and run on 1.5% agarose gel to visualize fragment size. This experiment was aimed at fragment size of 300–500 base pairs. *Left lane* is isolated genomic DNA followed by different sonication protocols with sonication time of 3 s and 3–5 repeats. Aim at producing fragments with a median fragment size of 300 and 3000 base pairs by changing sonication time and repeats

10. Remove supernatant taking care not to disrupt the pellet. Wash the pellet with 1 mL 70% EtOH (stored at −20 °C) and centrifuge at 18,626 × *g* for 10 min at room temperature. Remove supernatant and dry the pellet. Dissolve the dried pellet in 50 µL H_2O.
11. Centrifuge the chromaspin TE-200 and TE-1000 size exclusion columns for 5 min at 700 × *g*. Load the sheared gDNA onto the column and spin for 5 min at 700 × *g*. Keep the flow-through and discard the column. Quantify the fragmented DNA (*see* **Note 6**).
12. Mix 1 µg sheared gDNA, 5× reaction buffer, 0.2 µL dNTP 10 mM, 0.2 µL T4 DNA polymerase, add H_2O to 20 µL. Incubate for 10 min at room temperature. Inactivate the DNA polymerase for 10 min at 75 °C (*see* **Note 7**).
13. Mix 1,5 µg fragmented DNA, 5 µL 10× reaction buffer, 2 µL T4 polynucleotide kinase, add H_2O to 50 µL. Incubate for 30 min at 37 °C. Inactivate for 20 min at 65 °C. Purify the fragmented DNA using PCR purification columns and quantify the DNA.

3.2 Preparing Vector DNA

Carry out all procedures at room temperature unless otherwise specified.

1. Mix 1 µg purified pDJ01 vector with 2.5 µL 10× restriction buffer, 1 U SmaI, add H_2O to 25 µL. Incubate at 25 °C for 4 h to digest the vector followed by incubation at 60 °C for 20 min to inactivate SmaI. Run the restricted vector on a 0.8% agarose gel along the uncut vector as a reference.
2. Excise the restricted vector from gel and extract the DNA, elute in 50 µL preheated elution buffer.
3. Perform a second SmaI digestion. Mix 1 µg purified pDJ01 vector with 2.5 µL 10× restriction buffer, 1 U SmaI, add H_2O to 25 µL. Incubate at 25 °C for 1 h and incubate at 65 °C for 20 min to inactivate SmaI and purify the digested DNA using a PCR purification column. Quantify the isolated DNA (*see* **Note 8**).
4. Following SmaI digestion dephosphorylate the digested DNA to prevent religation. Mix 1 µg digested pDJ01 vector, 4 µL 10× buffer, 1 U Calf Intestinal Alkaline Phosphatase (CIAP), add H_2O to 40 µL and incubate at 50 °C for 60 min followed by incubation at 65 °C for 15 min.
5. Add 1 U CIAP to the reaction mixture and incubate at 50 °C for 60 min followed by incubation at 65 °C for 15 min. To inactivate CIAP, add 0.5 µL, 0.5 M EDTA and incubate at 75 °C for 10 min. Purify the DNA using a PCR purification column, elute in 50 µL H_2O. Quantify the DNA.

6. Perform an additional dephosphorylation step using shrimp alkaline phosphatase (SAP). Mix 1 μg DNA, 2 μL 10× buffer, 1 U SAP, add H_2O to 20 μL. Incubate at 37 °C for 90 min and inactivate by incubation at 65 °C for 15 min. Purify the digested and dephosphorylated vector using a PCR purification column and quantify the DNA. The vector is now ready for ligation of DNA fragments (*see* **Note 9**).

3.3 Ligation of Vector and Insert

1. Estimate the mean fragment size from gel and calculate the mean molar mass of the fragments. Mix vector and fragment in a 1:3 M ratio (*see* **Note 10**).
2. Add 1 μg of the mixed DNA to the Ready to Go reaction tube and add sufficient water to bring the final volume to 20 μL. Incubate at room temperature for 3–5 min and then mix by gently pipetting up and down several times (*see* **Note 11**).
3. Centrifuge briefly to collect the contents at the bottom of the tube and remove any air bubbles.
4. Incubate 8 h at 16 °C. Purify the ligated DNA using plasmid purification columns. Elute the bound DNA by adding 50 μL water and spin for 1 min, add an additional 40 μL water to the filter and spin for 1 min (final volume is 90 μL).
5. Perform an ethanol precipitation to purify and concentrate the DNA. Add 0.1 volume 3 M NaAc pH 5.2 + 3 volumes 96% EtOH and incubate overnight at −20 °C. Centrifuge for 30 min at 18,626 × *g* and 4 °C. Gently remove supernatant and wash the pellet with 1 mL 70% EtOH (stored at −20 °C). Centrifuge for 10 min at 18,626 × *g* and 4 °C, remove supernatant and dry pellet. Dissolve the purified DNA in 5 μL H_2O and quantify. Dilute the DNA sample with H_2O to a final concentration of 600 ng/μL.

3.4 Electroporation of Bacterial Library

Electroporation is the most effective means of making libraries. By transforming *E.coli* with the ligated DNA construct 10^7–10^9 clones can be produced per μg DNA. To restrict the degree of growth competition the libraries are grown on large agar plates. For library production we use TG1 *E.coli*. This strain contains an amber suppression gene (*supE* - TAG stop codon is read as Glutamine) and is F′ (contains the F-episome necessary for phage infection). The number of electroporations performed needed depends on the transformation efficiency and the desired library size (*see* **Note 12**).

1. Have recovery SOC medium and 1.5 mL sterile culture tubes ready available at 37 °C. Make up samples of library DNA at 600 ng/μL (*see* **Note 13**). As a negative control, to check for contamination of the competent cells, include a sample of 5 μL H_2O that is being used to dilute the DNA.

2. Prechill the electroporation cuvettes and microcentrifuge tubes on ice (one cuvette and one microcentrifuge tube for each transformation reaction).
3. Take electrocompetent cells from the −80 °C freezer and place on wet ice until they thawed completely (10–15 min). Mix the thawed cells by gently tapping the tube. Aliquot 25 μL (*see* **Note 14**) into the chilled microcentrifuge tubes on ice. Add 1 μL of library DNA (600 ng), stir briefly with the pipet tip. Do not pipet up and down which can introduce air bubbles and warm the cells.
4. Carefully transfer the cell–DNA mixture to a chilled 1 mm electroporation cuvette taking care not to introduce air bubbles. Hold the cuvette by the plastic rim, wiping it down with a KimWipes and quickly flick the cuvette downward to deposit the cells across the bottom of the well. Immediately electroporate the cells at 1.8 kV, 10 μF, 600 Ω (*see* **Note 15**).
5. Immediately add 1 mL of warmed recovery medium and transfer to a 50 mL conical tube, cap it loosely. Transfer the 1 mL control electroporations to labeled 15 mL polypropylene tubes. Incubate the samples in a shaking incubator at 250 rpm for 1 h at 37 °C.
6. Optional: Collect 10 μL samples of the cell–DNA mixture before and after electroporation for titering. Make serial dilutions by diluting cells in LB medium and plating on LB-agar plates (containing no antibiotics); these titers can be used to calculate the percent cell death caused by the electroporation, an important number to follow when optimizing electroporation efficiency.
7. Collect a 10 μL sample of each electroporation, make serial dilutions in LB medium and plate on LB agar containing 10 μg/mL chloramphenicol. The number of chloramphenicol resistant clones/μg of DNA can be calculated and compared with a control plasmid. Also the total number of clones in the bacterial library can be calculated from the serial dilutions. This number reflects the complexity of the library. The minimal library complexity is 10^7 clones per library (*see* **Note 16**).
8. Spread the remainder of the cells onto large LB agar plates containing 10 μg/mL chloramphenicol (*see* **Note 17**) (1 mL per plate) Incubate overnight at 37 °C.
9. Pick 48 well separated single colonies (from the serial dilutions used to calculate the library complexity). Isolate the DNA and amplify the insert by PCR using the sequence primers and standard PCR protocols. Take along an empty pDJ01 vector as a control. Run the PCR products on gel and determine the ratio of empty vector and fragment diversity (*see* **Note 18**).

10. Pool all colonies from the big and titration plates. For the big plates, use a cell scraper to pool most of the bacteria and resuspend them in 5 mL LB. Then wash the plates twice with 5 mL LB.
11. Add 1/5 volume of sterile 85% glycerol and flash freeze the bacterial library for long term storage.
12. Optionally: sequence the 48 amplified inserts using method described in section "Identification of selected fusion proteins".

3.5 Phage Library Production

1. Inoculate at least 200/bacteria per clone in prewarmed LB medium containing 10 μg/mL chloramphenicol. Adjust volume until OD_{600} measures 0.4 (*see* **Note 19**). Incubate in a shaking incubator at 105 rpm for 2 h at 37 °C. Measure OD_{600} after 2 h of incubation and calculate the total number of bacteria in the culture. Infect the culture with VCSM13 helper phages at an MOI (Multiplicity of infection) of 10–100 (10–100 helper phages per bacterium) (*see* **Note 20**). Mix and incubate at room temperature for 30 min (no shaking).
2. Add LB-medium containing 10 μg/mL chloramphenicol to increase the culture volume to 600 mL. Add kanamycin at a final concentration of 0.4 μg/mL and incubate for 30 min at 37 °C. (induction of kanamycin resistance). Next add kanamycin to a final concentration of 25 μg/mL and incubate overnight at 37 °C at 140 rpm (*see* **Note 21**).
3. Transfer the culture into three centrifuge bottles and centrifuge at room temperature for 40 min at 4260 × *g* (200 mL per bottle). Keep the supernatant containing the phages and add six tablets of EDTA free protease inhibitor (*see* **Note 22**). Incubate at 120 rpm for 1 h at 37 °C. Transfer to centrifuge bottles and centrifuge at CE: 8340 × *g* for 40 min at 4 °C. Transfer the supernatant to a 1 L glass bottle and add 0.15 volume of PEG/NaCl (90 mL for 600 mL) incubate overnight at 4 °C or on ice for at least 1 h (see **Note 23**).
4. Split the mixture and transfer to three clean centrifuge tubes and centrifuge at 13,790 × *g* for 4 h at 4 °C.
5. Discard the supernatant and leave the bottles upside down on absorbent paper for 10 min to remove the maximum amount of supernatant (*see* **Note 24**). Dissolve 1 tablet of EDTA free protease inhibitor in 50 mL TBS. Resuspend each phage pellet in 1 mL TBS/Pinh and pool the tree pellets in a 50 mL tube. To recover the maximal amount of phages add an additional 1 mL TBS/Pinh to the centrifuge tubes and transfer into the same 50 mL tube. Leave at 4 °C at least overnight.
6. Clear the supernatant from any remaining debris by centrifuging at 14,462 × *g* for 10 min at 4 °C. Keep supernatant containing the phage library and store at 4 °C.

7. Prepare an overnight culture of TG1 *E.coli* on LB agar. Next day pick a single colony and inoculate 20 mL LB medium (without antibiotics) and grow until early log phase ($OD_{600} = 0.3$) shaking at 105 rpm.
8. Take 10 µL of the purified phage library and make 10 fold serial dilutions in TBS. Mix 10 µL of each phage dilution with 90 µL TG1 cells and incubate for 20 min at room temperature. (During this incubation infection of TG1 cells takes place conferring chloramphenicol resistance).
9. Spread 100 µL of the infected TG1 cells onto LB agar plates containing 10 µg/mL chloramphenicol and incubate overnight at 37 °C. Count the colony forming units and calculate the concentration of phages in the phage library. When the phage concentration exceeds 2×10^{13} cfu/mL add TBS to reduce the phage concentration (*see* **Note 25**).
10. For short term storage of the phage library (up to 3 months) add 0.02% sodium azide and keep at 4 °C (*see* **Note 26**). For long term storage mix 830 µL of the phage library with 170 µL sterile 85% glycerol and store at −80 °C (*see* **Note 27**).

3.6 Phage Selection on Immobilized Targets

Different selection strategies can be used to select phages binding to a specific target. The most frequently used is a selection strategy where the target is coated to 96-well ELISA plates. Using this selection protocol we successfully identified bacterial proteins that interact with various purified immunological targets including antibodies, components of the complement system and components involved in blood coagulation (*see* **Note 28**).

The pDJ01 vector encodes a Myc tag sequence between the cloning site and the pIII gene. This allows the election of all phages expressing a fusion protein using an anti-Myc-tag antibody (*see* **Note 29**).

1. Coat five wells of a 96 well ELISA plate with 100 µL/well of the target protein at 10 µg/mL in PBS and incubate overnight at 4 °C. Simultaneously prepare an overnight culture of TG1 *E.coli* on LB agar.
2. Next day wash the ELISA plates three times with washing buffer. Add 120 µL PBS/tween/BSA blocking buffer and incubate for 1 h at 37 °C. An additional specific blocking step can be performed (*see* **Note 30**).
3. Wash three times with washing buffer. Mix phage T200 and T1000 libraries in equal volumes (*see* **Note 31**). To prevent aspecific binding add BSA (*see* **Note 32**) to the phages at a final concentration of 10 mg/mL (1% w/v) and add Tween 20 (1:8,000).
4. Add 100 µL of the phage preparation to each well (thus a total of 500 µL of phages is used for each target). Incubate for 4 h at room temperature with gentle shaking.

5. Inoculate 4,5 mL/target LB medium with a few colonies from the overnight TG1 culture ($0.25 > OD_{600} > 0.3$) Incubate 2–2:30 h at 37 °C with slow shaking (120 rpm).
6. Remove the phage preparation from the wells and wash three times with washing buffer. Add 100 µL/well of elution buffer. Wait for 2–3 min and transfer the 500 µL of eluted phages to an eppendorf tube containing 62.5 µL of neutralization buffer.
7. Transfer eluted phages (500 µL) in 4.5 mL of the TG1 culture. Incubate for 20–30 min at room temperature without shaking for bacterial infection to take place (*see* **Note 33**).
8. To determine the amount of eluted phages (reflecting the amount of phages bound to the target), take 10 µL of the infected TG1 cells and make serial dilutions (10 µL culture and 90 µL LB medium). Plate the serial dilutions onto LB-agar plates containing 10 µg/mL chloramphenicol.
9. Spread the 5 mL infected TG1 cells onto large LB-agar plates containing 10 µg/mL chloramphenicol and incubate overnight at 37 °C. Next day, count the CFU on the serial dilution plates and calculate the total amount of eluted phages (*see* **Note 34**).
10. Pool all colonies from the big and titration plates. For the big plates, use a cell scraper to pool most of the bacteria and resuspend them in 5 mL LB. Then wash the plates twice with 5 mL LB.
11. Optionally store a sample of the selected library: add 1 mL 85% glycerol to 5 mL of the resuspended bacteria and flash-freeze in liquid nitrogen. Store at −80 °C.
12. Measure the OD_{600} nm of several dilutions usually 1/100 and 1/300 dilutions give good results and calculate the total amount of bacteria $1\ OD = 2.10^8$ bact/mL. Calculate the amount of bacteria per phage (total amount of bacteria / total amount of eluted phages). Calculate the volume of bacteria to resuspend in 50 mL LBCm10 to have >1000 bact/phage and $0.25 < OD600 < 0.4$. Grow for 2 h/2 h30 at 37 °C with gentle shaking.
13. Determine the bacterial concentration by measuring OD_{600} (1/3 and 1/10 dilutions and $1\ OD = 2.10^8$ bact/mL). Calculate the volume corresponding to 2.10^9 bacteria. Mix 2×10^9 bacteria with 100 µL of VCSM13 helper phage ($>1.10^{10}$ HP/mL, MOI ≈ 10). Incubate 20–30 min at room temperature. Fill up to 30 mL with LB containing chloramphenicol. Add kanamycin (final concentration 0.4 µg/mL) to induce kanamycin resistance. Incubate for 15 min at 37 °C and add kanamycin to a final concentration of 25 µg/mL. Incubate for 2 h at 37 °C with gentle agitation.
14. Transfer the culture to centrifuge tubes and centrifuge at $17{,}096 \times g$ for 10 min at room temperature.
15. Transfer the supernatant to clean centrifuge tubes and centrifuge at $23{,}269 \times g$ for 10 min at 4 °C. Transfer the supernatant

to clean tubes and add 0.15 volume of PEG/NaCl and mix thoroughly by inverting the tubes 100 times.

16. Incubate overnight at 4 °C. Centrifuge at 23,269 × *g* for 2 h at 4 °C. Resuspend the phages in 500 µL TBS. This phage preparation can be used for a next selection round. Optionally: before continuing to the next round determine phage titer (cfu/mL).
17. Perform two additional selection rounds reducing the binding time to 1 h and increasing the wash stringency in each round (*see* **Note 35**).

3.7 Identification of Selected Fusion Proteins

1. Pick 48 colonies from the serial dilution plates from phage selection.
2. Resuspend each clone in 100 µl LB.
3. Transfer 50 µl in a new plate add 10 µL 85 % glycerol and store it at −20 °C as a "clone stock".
4. Centrifuge the remaining 50 µL at 18,626 × *g* for 5 min. Discard the supernatant, resuspend the pellet in 50 µL H_2O and incubate at 96 °C for 10 min.
5. Centrifuge at 18,626 × *g* for 5 min and transfer the supernatant containing phage DNA into clean eppendorf tube.
6. Amplify the insert DNA using forward and reversed sequence primers and 3 µL of the DNA preparation in 25 µL PCR reaction mix.
7. After amplification run 4 µL on a 1 % agarose gel (*see* **Note 36**).
8. Sequence the amplified insert using the forward and reversed primers.

3.8 Data Analysis

The sequence data will include part of the pDJ01 vector before and after the insert as well as part of the insert. One should include a series of checks on the identified sequence.

1. Determine if the gene of interest encoded in the insert is in frame with the pIII protein (*see* **Note 37**).
2. Look for a stop codon (except TAG that is read as Gln by TG1) within the reading frame of pIII.
3. Look for the presence of a signal sequence in the translated gene using online prediction tools like Signal-P and Topcons (*see* **Note 38**).
4. The presence of different clones encoding a different fraction of the same gene is a strong indication of a positive selection (*see* **Note 39**).
5. Recombinant expression of the identified protein is required to confirm interaction and identify the protein as an immune evasion protein (*see* **Note 40**).

4 Notes

1. Phage selection is an extremely sensitive technique. Less than ten specific phages can be selected from a library containing 10^{13} phages/mL and a single phage is able to infect a bacterium and amplify. This creates a huge risk of contamination. The system used in this selection is a phagemid/helper phage system and phages are only amplified in the presence of helper phage. However, contaminating phages are infective and can ruin your experiment. We have occasional contaminations where we selected phages from earlier experiments (e.g., finding mycobacterial genes when performing a selection using a streptococcal library). The risk of contamination is reduced by following strict working and cleaning procedures. Always work with phages in a laminar flow cabinet and preferably in a separate lab. Phages can infect and confer antibiotic resistance to all *E. coli* carrying an F-pilus like Top10F′ a bacterial host widely used in cloning experiments. Decontaminate all used materials and surfaces using chlorine. Aliquot all reagents for single use. When dealing with a contamination structurally test all reagents for contamination and if necessary to contain the contamination clean the lab thoroughly! Wear a disposable lab coat.
2. Phenol acts as a denaturing agent and denatured proteins are readily dissolved in the organic phase as phenol is poorly soluble in water (max 7%). DNA and RNA remain in the aqueous phase unless the pH is to low and DNA is reduced and dissolve in phenol fraction. This is the basis of RNA purification. This protocol is for the isolation of gDNA and therefore the pH of phenol must be raised to 8. Water saturated phenol has a pH of approximately 4. Therefore the phenol needs to be buffer saturated. However, buffered phenol has limited shelf life (weeks) as it is more susceptible to oxidation turning it to a yellow color. Therefore buffered phenol needs to be prepared in advance buffering it with 0.5 M Tris–HCl.

   Mix an equal volume of water saturated phenol and 0.5 M tris pH 8. Mix thoroughly by shaking vigorously. Let stand for the fractions to separate. Move the phenol fraction to a new tube using a pipet (phenol fraction is the bottom fraction). Add one volume of 0.5 M tris pH 8 to the isolated phenol and mix vigorously. Let stand for the fractions to separate. Repeat steps an additional two times (total of 4). Move phenol fraction to a clean tube and measure pH using pH paper! pH should be 8. pH meter cannot be used since this is equilibrated for aqueous solutions. A pH meter can be used by taking a small amount of phenol and adding 45% methanol, but paper is much easier. Add a small volume 0.1 M tris pH 8 to the phenol fraction, just enough to give a separate layer on top of the phenol. Store at 4 °C protected from light (buffered

phenol can be stored for a couple of months, appearance of a yellow color indicates oxidation)

The mechanism of this isolation is to denature and extract proteins from the lysed bacteria using phenol and isolate DNA from the aqueous phase. Isoamyl alcohol is added as antifoaming agent. As trace amounts phenol can interfere with enzymatic reactions (phenol is an extremely powerful denaturing agent) the aqueous phase is thoroughly washed with chloroform. In this protocol only once but in case of low ligation efficiency consider repeating the chloroform washings.

3. We normally use a NanoDrop spectrophotometer to quantify DNA in micro-volumes of sample for high DNA concentrations. When measuring low DNA concentrations (below 100 ng/μL) we use Qubit™ fluorometric quantification (ThermoFisher).
4. We generally combine genomic DNA from different strains when making a secretome library of a certain bacterial species. An alternative approach would be to make separate libraries and combine them in the selection experiments. Although making separate libraries offers somewhat more flexibility it greatly increases the workload.
5. Many of the immune evasion proteins that were identified are relatively small proteins or are larger proteins containing multiple distinct domains. In order to restrict fragment length in the creation of a secretome phage display library for the detection of immune evasion molecules we aim at expressing fusion proteins between 100 and 1000 amino acids in length. Therefore the insert size ligated into the phagemid vector contains 300–3000 base pairs. Small fragments are easier ligated than large fragments. In order to prevent competition and skew the library to much towards small fragments the phage library is divided into two separate complementing libraries of 300–1000 base pairs and 1000–3000 base pairs. Therefore the sonication time and settings should be optimized experimentally to give to different smears of DNA comprising the preferred fragment length.
6. Size exclusion is performed to fully remove all small DNA fragments (that are not removed by the ethanol precipitation) that can interfere with ligation and to restrict fragment size.
7. The fragmentation creates 5′ and 3′ overhangs. To create blunt end fragments the sheared DNA is treated with T4 DNA polymerase and phosphorylated using T4 nucleotide kinase.
8. We found that a second SmaI digestion further reduced the amount of transformants containing an empty vector.
9. We found that a second dephosphorylation reaction further reduced background ligation.

10. The conditions in this protocol generally work for us. However, optimizing the ligation condition may be necessary when the number of transformants is low. Optimizations include changing the fragment to insert ratio, ligation temperature, and ligation time. Keep in mind that increasing the amount of insert may give rise to constructs with concatenating inserts because of the blunt end ligation. Especially when using high concentrations of both vector and insert. One solution to this is to start at high concentration to aid initial ligation of one side of the insert and after short incubation dilute the sample to prevent concatenating inserts. We used different ligation kits and protocols to optimize the blunt end ligation and found the RTG ligation performing optimal. The polyethylene glycol increases the blunt end ligation efficiency. However, extra care should be taken to remove the PEG from the reaction mixture before transformation as trace amounts of PEG negatively affect transformation efficiency especially in prolonged ligation times at low temperature.
11. As T4 ligase is sensitive to shearing extra care should be taking when handling the sample. Vortexing and centrifuging the ligation sample should be avoided.
12. We normally find that five electroporations, performed as described, per library is sufficient to obtain a library complexity of 10^7 unique clones.
13. We found that 600 ng of ligated library DNA per electroporation gave the highest yield. When library diversity is low, consider changing the amount of added DNA.
14. Although it is possible to electroporate a larger volume of electrocompetent cells (up to 100 μL in a 1 mm cuvette) we found that electroporation of 25 μL gave optimal results. When increasing the electroporation volume one should be aware to increase the amount of DNA added and also to split the sample after electroporation to prevent excessive competition between clones when plating on large agar plates.
15. The optimal settings for electroporation depend on bacterial strain, sample, and cuvette used. We found that these settings generally give optimal results; however, when transformation efficiency is low optimization may be required.
16. The minimal required library complexity is set at 10^7 different clones per library. This is an arbitrary number. Based on a genome size of around 3 M base and a fragment size between 300 and 3000 base-pairs, this library size theoretically sufficient to include all secretome proteins with >99 % probability. Of course a higher diversity may be better and a lower diversity may also work. To prevent ongoing discussions (and because there is no right answer) we have set the lower limit of diversity by convention at 10^7 unique clones/library.

17. To prevent competition between clones we plate the electroporated cells onto large LB-agar plates (23× 23 cm).
18. Amplification of the insert and running the PCR product on gel will give an indication of background (electroporation of empty vector). Normally we find empty vector in <2 % of clones (no empty vector in 48 picked clones). Make sure that library complexity is $>10^7$ unique clones omitting the background.
19. When producing phages from a bacterial library with a complexity of 10^7 unique clones start with 2×10^9 bacteria. An OD_{600} of $0.4\approx0.8\times10^8$ bacteria/mL. The start culture should therefore have a volume of at least 25 mL.
20. We normally add around 1 mL helper phage at a concentration of $>10^{10}$ /mL.
21. When culturing phages we found a reduced infection efficiency and phage production when cultures were shaken to vigorously especially just before infection. The suggested rpm is sufficient to prevent sedimentation of bacterial cells. Explanation could be that for efficient infection of TG1 cells a intact F-pilus is necessary that is disrupted upon vigorous shaking.
22. To prevent degradation of the displayed proteins by bacterial proteases we included this step.
23. PEG/NaCl is used for phage precipitation and purification. Although a 1 h incubation on ice may suffice we found a significant larger yield when performing an overnight precipitation step.
24. Make sure to properly clean all non disposable items and the work space thoroughly using chlorine.
25. 2×10^{13} phages/mL is the maximum amount of phages that can be stably suspended. A higher concentration of phages will lead to agglutination and precipitation giving the sample a gel like appearance.
26. We did not observe a decrease in phage titer up to 3 months. It is possible to store phages for longer period at 4 °C; however, one should be aware of a reduction in infectious phages. Therefore redetermine the cfu/mL of the phage stock upon prolonged storage.
27. When using a phage stock stored in glycerol perform a PEG/NaCl precipitation to remove glycerol. Add 1/5 volume of PEG/NaCl. Incubate on ice for 1 h. Centrifuge for 40 min at full speed (14,000×*g*) at 4 °C. A pellet should be visible. Remove the supernatant, respin briefly and remove residual PEG/NaCl. Resuspend the pellet in TBS.
28. This protocol is for phage selection on targets immobilized onto an ELISA plate. These targets can be purified components, mixtures of purified components, or complex mixtures.

We have performed successful phage selections on cell lysates and neutrophil degranulate. This protocol can easily be adapted to perform selections on isolated or cultured cells [7].

29. The pDJ01 vector encodes a Myc tag sequence in front of the pIII gene. There displayed proteins can be identified using an anti-Myc-antibody. The use of a wild type VCSM13 helper phage containing the wild type pIII will give a high proportion of phages not displaying a fusion protein because the insert is in the wrong orientation does not contain a signal sequence, is out of frame or contains a stop codon. Performing a selection using an immobilized anti-Myc-antibody will efficiently enrich for phages expressing a fusion protein.
30. When selecting for a specific target it may be necessary to specifically block to prevent selection of known immune evasion molecules. When we performed selections using a *S. aureus* secretome library on purified targets isolated from serum we consistently found Staphylococcal protein A (Spa) in our selections. Spa is known to bind to IgG, a protein that is abundantly present in serum. Even trace amounts of IgG present in the protein preparations were sufficient to select the high affinity interaction with Spa. Pre-incubation of the immobilized target with Spa prevented this selection.
31. We always mix phage libraries in equal volumes also when complexity between the libraries differ. It is also possible to combine libraries from different bacterial strains in this step.
32. Next to blocking with BSA we add BSA to the phage preparation in order to reduce background binding. When expecting selection towards the blocking agent consider changing the blocking agent in consecutive selection rounds.
33. We tested optimal incubation time for phage infection. Incubation times below 20 min dramatically reduced infection efficiency. There was no difference in infection efficiency between 20 and 40 min incubation times.
34. Only a small fraction of the phages will bind the target and therefore there will be a large reduction of phages after elution. Upon selection of a specific phage there will be an increase in phages after elution in consecutive selection rounds because a larger fraction of the selected libraries will bind the target. Although this is theoretically the case we did perform successful selections without seeing an evident rise in the amount of phages binding the target.
35. Wash stringency can be increased in several ways. We normally increase the amount of washing steps from three in the first round to ten in next rounds. An alternative strategy would be to increase salt concentration or the concentration Tween in the washing buffer. When performing selection on purified targets three selection rounds are usually sufficient to identify

proteins that interacts with the immobilized target. When using mixed targets or complex targets like cells four rounds of selection may be necessary.

36. Run the amplified sample on an agarose gel to determine if the sample quality is sufficient for sequencing. However, this also provides information on diversity of the selected library and fraction of empty vectors.
37. The gene encoded in the insert needs to be in frame with the gene for pIII in order to have expression of the fusion protein.
38. A signal sequence is necessary for efficient incorporation into the phage particle. Signal sequence predictions have their limitations. We have identified proteins where signal sequence prediction showed no evident signal sequence. The pDJ01 vector contains a phage specifc promoter, a ribosome binding site and a ATG start codon in front of the SmaI restriction site. We found that the presence of an additional promoter or ribosome binding site does not hamper phage production [7].
39. In majority of positive selections we find multiple clones encoding the same protein. Since there is also a selection for small gene size we found that the C-terminal end of the smallest insert correlated with the C-terminal position of the active site. In case of problems with recombinant protein expression and purification one could consider expressing the truncated form of the protein as it is displayed on the selected phage.
40. In theory it is possible to confirm interaction using purified phages expressing the protein of interest and performing a phage ELISA using an anti-M13-antibody for detection. We stopped performing this check as we found insufficient correlation between the phage ELISA and activity of the purified protein.

References

1. Jongerius I, Köhl J, Pandey MK, Ruyken M, van Kessel KPM, van Strijp JAG et al (2007) Staphylococcal complement evasion by various convertase-blocking molecules. J Exp Med 204:2461–2471. doi:10.1084/jem.20070818
2. de Haas CJ, Veldkamp KE, Peschel A, Weerkamp F, Van Wamel WJ, Heezius EC et al (2004) Chemotaxis inhibitory protein of Staphylococcus aureus, a bacterial antiinflammatory agent. J Exp Med 199:687–695
3. Jankovic D, Collett MA, Lubbers MW, Rakonjac J (2007) Direct selection and phage display of a Gram-positive secretome. Genome Biol 8:R266. doi:10.1186/gb-2007-8-12-r266
4. Carlos F, Barbas III, Burton DR, Scott JK, Silverman GJ (2001) Phage display: a laboratory manual. Cold Spring Harbor Laboratory Press, New York
5. Hoogenboom HR (2002) Overview of antibody phage-display technology and its applications. Methods Mol Biol 178:1–37, doi:11968478
6. Karlström Å, Jacobsson K, Flock M, Flock J-I, Guss B (2004) Identification of a novel collagen-like protein, SclC, in Streptococcus equi using signal sequence phage display. Vet Microbiol 104:179–188. doi:10.1016/j.vetmic.2004.09.014
7. Fevre C, Bestebroer J, Mebius MM, de Haas CJC, van Strijp JAG, Fitzgerald JR et al (2014) Staphylococcus aureus proteins SSL6 and SElX interact with neutrophil receptors as identified using secretome phage display. Cell Microbiol 16:1646–1665. doi:10.1111/cmi.12313

Part II

Structural Biology of Bacterial–Host Interactions

Chapter 5

Competition for Iron Between Host and Pathogen: A Structural Case Study on *Helicobacter pylori*

Wei Xia

Abstract

Helicobacter pylori (*H. pylori*) is a highly successful bacterial pathogen, which colonizes the stomach of more than half of the world's population. To colonize and survive in such an acidic and inhospitable niche, *H. pylori* cells have evolved complex mechanisms to acquire nutrients from human hosts, including iron, an essential nutrient for both the pathogens and host cells. However, human cells also utilize diverse strategies in withholding of irons to prevent the bacterial outgrowth. The competition for iron is the central battlefield between pathogen and host. This mini-review summarizes the updated scenarios of the battle for iron between *H. pylori* and human host from a structural biology perspective.

Key words Host–pathogen interactions, *Helicobacter pylori*, Nutritional immunology, Iron-binding protein

1 Iron Is Sequestered by Host Iron-Binding Proteins

In human stomach, ingested food provides the main source of iron. The digestive enzymes as well as the low pH value in stomach readily release iron from food into gastric lumen. Although substantial amount of iron is released from food, the availability of free iron at the gastric mucosa, where *H. pylori* colonizes, is relatively low since most free iron is readily sequestered by host iron-binding proteins such as lactoferrin (LTF) and human transferrin (hTF). Both LTF and hTF are glycoproteins that control the free iron level in biological fluids. They are associated with the human innate immune system, creating an environment low in free iron at the mucoses that impedes bacterial growth [1]. Belonging to the same protein family, hTF and LTF have quite similar sequences and structures and coordinate iron in the same manner. However, they differ in the affinities for iron, hTF tightly but reversibly binds iron with K_d of ~10^{-22} M [2], LTF exhibits 300 times higher binding affinity than that of hTF [3]. The crystal structures of hTF and LTF consist of two homologous lobes (termed the N- and C-lobes) connected by a short peptide linker.

Pontus Nordenfelt and Mattias Collin (eds.), *Bacterial Pathogenesis: Methods and Protocols*, Methods in Molecular Biology, vol. 1535, DOI 10.1007/978-1-4939-6673-8_5,

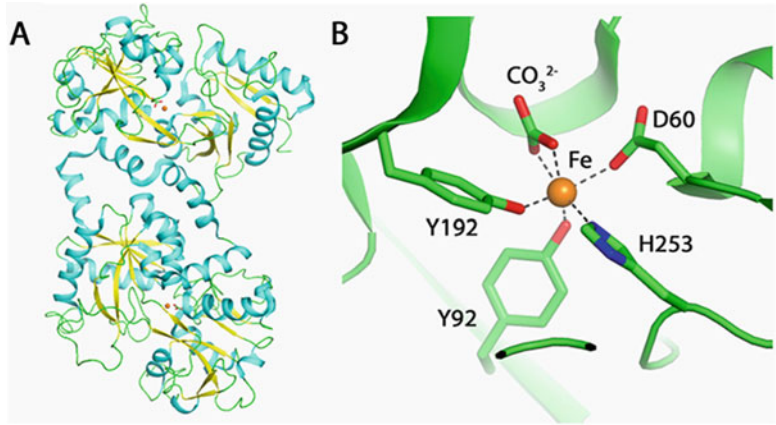

Fig. 1 Crystal structure of Fe-bound human lactoferrin (PDBID: 1B0I). (**a**) Overall structure of human lactoferrin. (**b**) The iron binding site of N-lobe of human lactoferrin. The coordination residues are shown in *sticks* and iron is shown as *orange sphere*

Each lobe can be further divided into two subdomains that form a cleft, which can adopt either fully open or fully closed conformations in the absence or presence of bound iron [4–7]. The amino acids that bind the iron are identical for both lobes, including two tyrosines, one histidine and one aspartic acid, one anion such as carbonate (CO_3^{2-}) is also required for iron binding (Fig. 1). A recently reported diferric bound hTF crystal structure captured the unique "partially open" conformations in the N-lobes, providing the last piece of puzzle for the dynamic motion of hTF subdomains upon iron binding [8]. Beside its ability to sequester environmental iron to impede bacterial growth, LTF exhibits bactericidal activity by direct interaction with bacterial surface moieties, such as lipopolysaccharide (LPS), porins [9, 10], although the detailed mechanism is unknown.

Calprotectin is a heterodimer protein complex consisting two non-covalently linked component proteins S100A8 and S100A9 [11]. It can comprise up to 60% of the soluble protein content of cytosol of neutrophil leukocyte and be secreted into extracellular space during inflammation. The calprotectin exhibits antimicrobial activity by sequestration of bacterial essential transition metals such as zinc and manganese [12, 13]. Calprotectin is currently the only identified antimicrobial agent that can act through manganese sequestration. Each calprotectin can only bind one manganese ion with nanomolar affinity at the interface between S100A8 and S100A9 through a unique hexa-histidine motif, which consists of two histidines from S100A8 and four histidines from S100A9 [14, 15] (Fig. 2). A recent study shows that calprotectin also coordinates Fe(II) at this hexahistidine site with unprecedented subpicomolar affinity in the presence of Ca(II). Therefore, calprotectin can efficiently inhibit bacterial growth by depriving

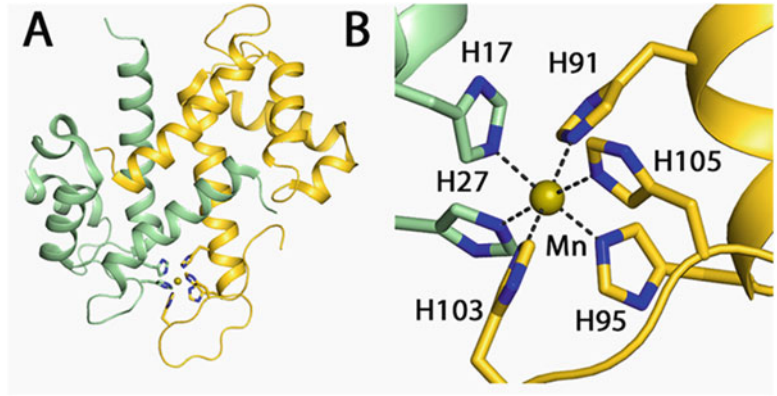

Fig. 2 Crystal structure of human calprotectin with manganese-bound (PDBID: 4GGF). (**a**) Overall structure of calprotectin, the S100A8 subunit is shown in *pale green* and S100A9 subunit is shown in *gold*. (**b**) The manganese binding site of calprotectin with six histidines. The coordination residues are shown in *sticks* and manganese is shown in *brown sphere*

bacteria of iron [16]. Withholding the essential iron by host is the first line of defense against pathogen infection and this process is termed nutritional immunity [17].

2 *H. pylori* Competes for Iron with High-Affinity Iron Transporter

In order to survive within the host, *H. pylori* has evolved different mechanism to evade host nutritional immunity. Direct competition with the host for Fe(II) or Fe(III) are facilitated by two types of high-affinity iron uptake systems. The Fe(II) can pass freely through the *H. pylori* outer membrane and acquired by a high-affinity Fe(II) transporter termed FeoB [18]. The FeoB family proteins are widely distributed prokaryotic transmembrane Fe(II) transporters, which contain an N-terminal cytoplasmic GTPase domain (G-domain) and a C-terminal transmembrane domain (TM). The G domain shares sequence homology with the eukaryotic small GTPase proteins and can slowly hydrolyzes GTP to regulate Fe(II) uptake [19]. The G domain structure of FeoB was reported for several prokaryotes including *E. coli*, the sequence of which is 29% identical to *H. pylori* [20]. The homo-trimer *Ec*FeoB protein can adopt a closed conformation in the apo-form, while it forms a central cytoplasmic pore with diameter of ~1.2 Å at the nearest point when bound to GTP analog, which probably facilitates the gating and transportation of non-hydrated Fe(II) ions (Fig. 3).

Ferric citrate is another important iron source for *H. pylori*. The complete genome sequence of *H. pylori* strains revealed that the pathogen possesses three *fecA*-like genes [21, 22], which are likely to encode ferric-dicitrate transporters as reported in *E. coli* [23].

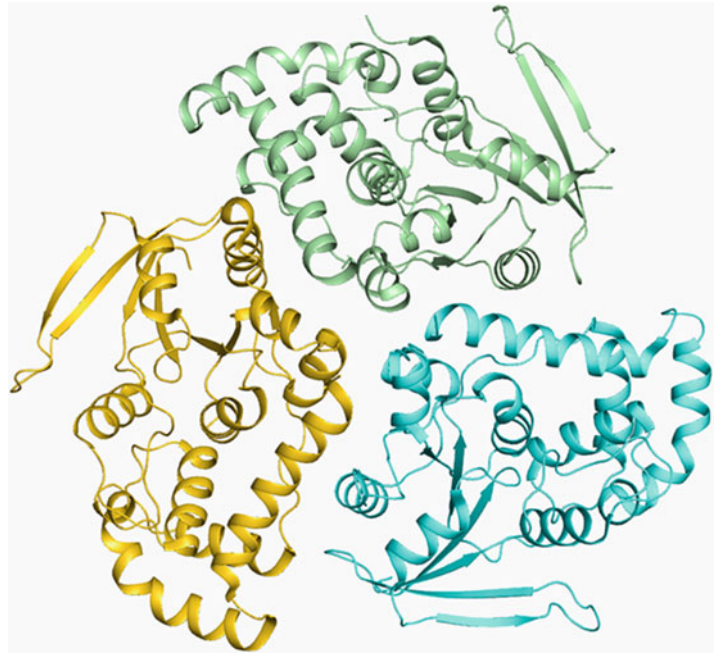

Fig. 3 Homo-trimer structure of the FeoB G-domain from *Escherichia coli* (PDBID: 3I8X). Three monomeric subunits are shown in different colors

The redundancy in iron transporter genes may result from the evolutionary adaptation to the iron-limited environment. The *Ec*FecA structure exhibited an overall β-barrel topology consisting of three distinct domains, the external barrel domain, the plug domain and a short N-terminal extension. The plug domain is located inside the barrel domain and blocks the direct passage of ferric citrate across the outer membrane. Binding of the ferric citrate ligand induces a conformational change of extracellular loops of the barrel domain, which close the external pocket of FecA barrel, favoring the following transportation of the bound ligand (Fig. 4) [23, 24]. The inner membrane protein complex TonB, ExbB, and ExbD provide energy for the iron citrate transportation [25, 26].

3 *H. pylori* Can Circumvent Iron Withholding from Host

Besides the direct competition for iron, *H. pylori* has evolved iron acquisition mechanisms by "stealing" iron from host iron-binding proteins to circumvent iron withholding [27–29]. Although lactoferrin is an important component of nutritional immunity, it was reported that iron-loaded lactoferrin (holo-lactoferrin) could support the growth of *H. pylori* in iron-deficient medium, indicating that the pathogen could take use of iron from holo-lactoferrin [28]. Furthermore, a 70-kDa outer membrane protein that can bind

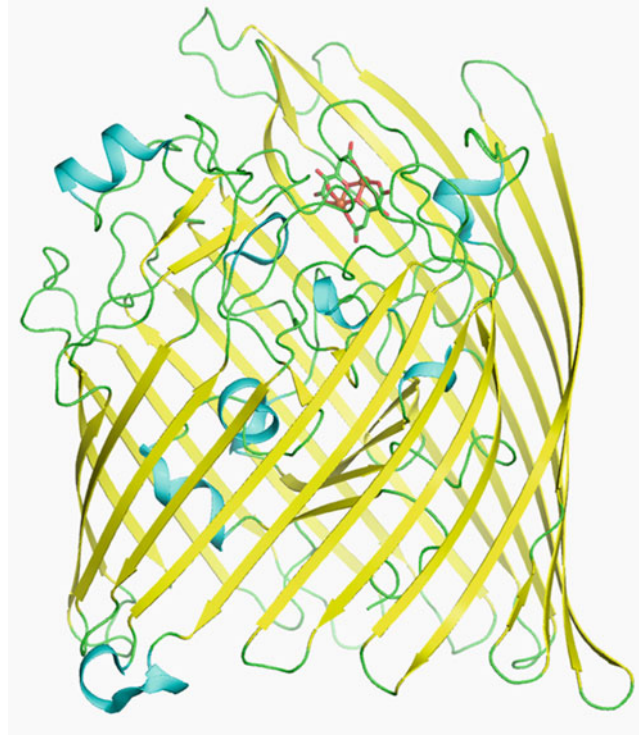

Fig. 4 Crystal structure of FecA from *Escherichia coli* (PDBID: 1KMP). Bound dicitrate ligands are shown in *sticks*, iron is shown in *orange sphere*

lactoferrin was discovered several years ago by affinity pull-down [30]. However, the identity of this protein remains unknown. A more recent study of *H. pylori* iron utilization mechanism using iron-deficient chemically defined media revealed that *H. pylori* can bind and extract iron from human hemoglobin, transferrin and even lactoferrin [27]. Intriguingly, data showed that *H. pylori* could bind apo-transferrin and apo-lactoferrin with higher affinity than the holo-form of the two proteins, indicating that iron saturation of transferrin (and lactoferrin) can influence the iron-acquisition of *H. pylori*.

Although the transferrin and lactoferrin receptors on *H. pylori* surface have not been identified, the capability of *H. pylori* to use hemoglobin as iron source and corresponding surface receptor are well documented. Two outer membrane proteins FrpB1 and FrpB2 are reported to be related to haem utilization by *H. pylori* [29, 31]. The mRNA level of *frpB1* and *frpB2* gene were repressed by iron and modulated by haem or hemoglobin. The overexpressed and purified FrpB1 protein possesses haem-binding property while *E. coli* expressing *frpB2* gene can utilize human hemoglobin as iron source. All current research data support the binding of haem or hemoglobin to FrpB protein. The FrpB family homologue from *Neisseria meningitidis* was solved recently. *Nm*FrpB1 adopts a classical TonB-dependent outer membrane transporters (TBDTs)

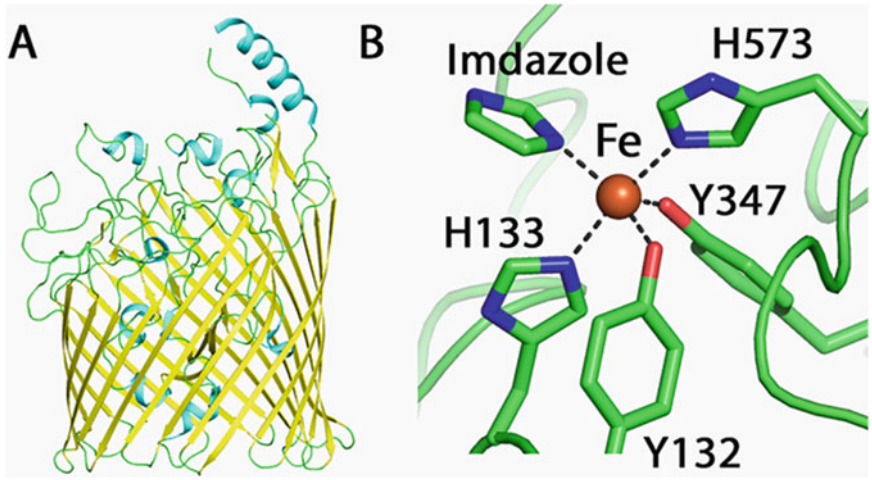

Fig. 5 Crystal structure of iron-bound FrpB from *Neisseria meningitides* (PDBID: 4AIQ). (**a**) Overall structure of FrpB protein. (**b**) Iron-binding site of FrpB. The coordination residues and imidazole ligand are shown in *sticks*, the iron are shown in *orange sphere*

structure with a 22-stranded β-barrel and a plug domain inside [32]. Intriguingly, *Nm*FrpB can directly bind ferric iron with two tyrosines and three histidines (Fig. 5). However, these residues are not conserved in *Hp*FrpB1 and *Hp*FrpB2, implying distinct ligand-binding property of *Hp*FrpB proteins.

4 Regulation of Iron Homeostasis in *H. pylori*

As an essential trace element, iron is required for the survival of *H. pylori*. However, excess amount of iron stimulates the formation of reactive oxygen species via Fenton reaction, causing DNA, proteins and membrane lipids damage [33]. Therefore, *H. pylori* has developed complex mechanisms to sense, response to and control iron level in vivo. Ferric uptake regulator (Fur) is one of the major gene regulators of *H. pylori*, which controls the expression of genes closely related to iron metabolism, including the previously mentioned iron transporters FeoB, FecA, and FrpB [34, 35]. Fur is an iron-binding protein that is unable to bind tightly to the Fur box DNA region when the intracellular iron concentration is low. Downstream genes are therefore de-repressed and iron-uptake capability of *H. pylori* increases significantly to acquire more extracellular iron. In addition to the genes related to iron metabolism, Fur also controls the expression of a category of genes with diverse functions, including biofalvin biosynthesis [36], cytotoxin-associated gene CagA expression [37]. The crystal structure of *Hp*Fur protein was reported recently, the overall fold of *Hp*Fur is a homodimer that is similar to other members in Fur family [38]. Each monomer consists of an N-terminal DNA-binding domain

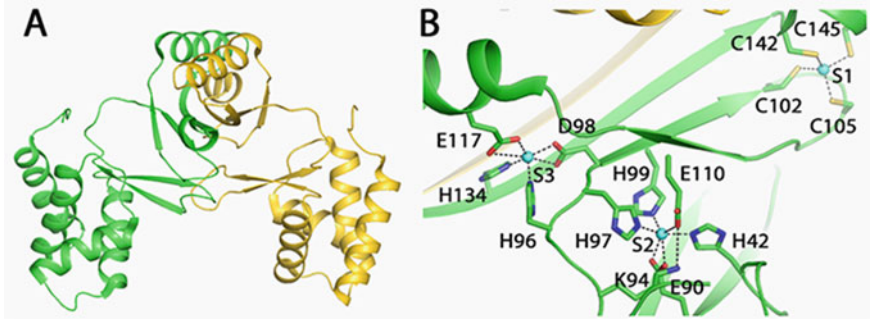

Fig. 6 Crystal structure of zinc-bound form Fur from *Helicobacter pylori* (PDBID: 2XIG). (**a**) Overall structure of dimeric Fur. (**b**) The three different zinc-binding sites of Fur, the coordination residues are shown in *sticks*, zinc are shown in *cyan spheres*

(DBD) and a C-terminal dimerization domain. Three zinc-binding sites are identified in *Hp*Fur structure termed S1, S2, and S3 (Fig. 6). The S1 site has four cysteines that are coordinated to zinc and stabilizes the dimeric form of *Hp*Fur while the S2 site is crucial for the regulatory function of *Hp*Fur. The S3 site is not conserved and site-directed mutagenesis data suggested it could strengthen the DNA-binding affinity of *Hp*Fur. The functionality of Fur is important for the colonization and survival of *H. pylori* in human stomach. It is reported that *Hp*Fur regulated more than 50 genes in response to iron-binding [39]. Intriguingly, *Hp*Fur is also able to regulate certain target genes even in its apo-form, probably through apo-form protein polymerization [40, 41]. Therefore, further investigation on the detailed regulation mechanism by apo- and holo-Fur is necessary.

5 Iron Storage in *H. pylori*

Excess uptake of iron requires removal or storage of the cytoplasmic iron by *H. pylori* to prevent the iron toxicity as well as providing a source of iron when the essential nutrient is scarce. Two different types of iron storage proteins have been identified in *H. pylori*, the prokaryotic ferritin protein (Pfr) and the neutrophil-activating protein (NAP). The Pfr resembles the structure of eukaryotic heavy-chain ferritin and other prokaryotic ferritin [42, 43]. The Pfr protein assembles into a hollow spherical protein oligomer with 24 monomeric units, where each monomer folds into a four-α-helix bundle (Fig. 7a) [44]. It is worth noting that the protective function of Pfr against metal toxicity may not be limited to iron, since *pfr*-negative strain of *H. pylori* also exhibited increased sensitivity to manganese, copper and cobalt ions [45]. The NAP of *H. pylori* belongs to the bacterioferritin family and was originally identified as a predominant antigen of *H. pylori* that can

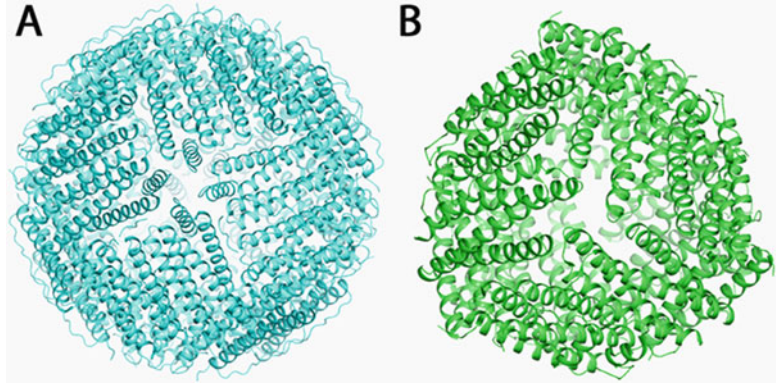

Fig. 7 Crystal structures of (**a**) Pfr (PDBID: 3BVE) and (**b**) NAP (PDBID: 1JI4) from *Helicobacter pylori*

activate neutrophils [46]. NAP is a dodecamer with 12 identical subunits, forming a nearly spherical protein shell with an internal hollow cavity for iron storage (Fig. 7b). Structural analysis showed that the internal surface of NAP was highly negatively charged, which is suitable for cation storage, while the outside surface of the protein is characterized by a large percentage of positively charged residues which may confer the neutrophil-activation ability [47].

H. pylori is one of the most widely spread human pathogens. Infection with this bacterium can lead to a series of human stomach diseases, including peptic ulcer, gastritis as well as stomach cancer. The bacterium has been classified as a type I carcinogen by WHO in 1994. The standard regimen to treat the bacterial infection is triple therapy, including a proton pump inhibitor (PPI) and two antibiotics, typically clarithromycin and amoxicillin or metronidazole. However, the therapy efficacy has dropped due to increased antibiotic resistance. Quadruple therapy regimens containing additional bismuth showed increased efficacy and are recommended for the bacterial infection treatment in areas of high clarithromycin resistance [48]. The antibacterial mechanisms of bismuth-containing drug are complex [49, 50]. Particularly, recent research data implicated that bismuth drug could inhibit *H. pylori* growth by interfering with bacterial iron uptake. As an essential nutrient for both host and pathogens, iron has become the most precious "treasury" pursued by both sides. Vertebrate hosts are devoid of free iron by high-affinity iron-binding proteins to ensure that all bacterial pathogens will face iron starvation upon entering the host cells. Meanwhile, pathogenic bacteria have likewise evolved diverse mechanisms to guarantee iron acquisition. For example, *Borrelia burgdorferi*, the pathogen responsible for Lyme disease, has evolved to require manganese rather than iron for growth [51]. Whereas *H. pylori* did not evolve this simple defense strategy, the bacteria has its own secret weapons to compete against

host iron-withholding through high-affinity iron uptake mechanism, including the multiple copies of ferric citrate transporters, transferrin/lactoferrin receptor, and heme acquisition system. Moreover, the pathogen also possesses a comprehensive feedback regulation system to maintain the proper cytoplasmic iron concentration, which can satisfy the iron requirement for metabolism and prevent iron toxicity. The major iron-responsive gene regulator Fur that regulates a battery of downstream genes responsible for iron uptake, storage and efflux controls the intact regulatory circuit. Undoubtedly, the complete arsenal of *H. pylori* in the battle for iron has not been unveiled. Further studies on the iron metabolism of *H. pylori* will help the development of efficient agents against this pathogen.

Acknowledgments

This work was supported by the National Natural Science Foundation of China (21501200) and a starting fund from Sun Yat-sen University.

References

1. Crichton RR, Charloteaux-Wauters M (1987) Iron transport and storage. Eur J Biochem 164(3):485–506
2. Aisen P, Leibman A, Zweier J (1978) Stoichiometric and site characteristics of the binding of iron to human transferrin. J Biol Chem 253(6):1930–1937
3. Mazurier J, Spik G (1980) Comparative study of the iron-binding properties of human transferrins. I. Complete and sequential iron saturation and desaturation of the lactotransferrin. Biochim Biophys Acta 629(2):399–408
4. Anderson BF, Baker HM, Norris GE, Rice DW, Baker EN (1989) Structure of human lactoferrin: crystallographic structure analysis and refinement at 2.8 A resolution. J Mol Biol 209(4):711–734
5. Jameson GB, Anderson BF, Norris GE, Thomas DH, Baker EN (1998) Structure of human apolactoferrin at 2.0 A resolution. Refinement and analysis of ligand-induced conformational change. Acta Crystallogr Sect D: Biol Crystallogr 54(Pt 6 Pt 2):1319–1335
6. Jeffrey PD et al (1998) Ligand-induced conformational change in transferrins: crystal structure of the open form of the N-terminal half-molecule of human transferrin. Biochemistry 37(40):13978–13986
7. Wally J et al (2006) The crystal structure of iron-free human serum transferrin provides insight into inter-lobe communication and receptor binding. J Biol Chem 281(34):24934–24944
8. Yang N, Zhang H, Wang M, Hao Q, Sun H (2012) Iron and bismuth bound human serum transferrin reveals a partially-opened conformation in the N-lobe. Sci Rep 2:999
9. Appelmelk BJ et al (1994) Lactoferrin is a lipid A-binding protein. Infect Immun 62(6):2628–2632
10. Naidu SS, Svensson U, Kishore AR, Naidu AS (1993) Relationship between antibacterial activity and porin binding of lactoferrin in *Escherichia coli* and *Salmonella typhimurium*. Antimicrob Agents Chemother 37(2):240–245
11. Stríz I, Trebichavský I (2004) Calprotectin—a pleiotropic molecule in acute and chronic inflammation. Physiol Res 53(3):245–253
12. Brophy MB, Nolan EM (2015) Manganese and microbial pathogenesis: sequestration by the Mammalian immune system and utilization by microorganisms. ACS Chem Biol 10(3):641–651
13. Lehmann FS, Burri E, Beglinger C (2015) The role and utility of faecal markers in inflammatory bowel disease. Therap Adv Gastroenterol 8(1):23–36
14. Damo SM et al (2013) Molecular basis for manganese sequestration by calprotectin and roles in the innate immune response to invading

bacterial pathogens. Proc Natl Acad Sci U S A 110(10):3841–3846

15. Hayden JA, Brophy MB, Cunden LS, Nolan EM (2013) High-affinity manganese coordination by human calprotectin is calcium-dependent and requires the histidine-rich site formed at the dimer interface. J Am Chem Soc 135(2):775–787
16. Nakashige TG, Zhang B, Krebs C, Nolan EM (2015) Human calprotectin is an iron-sequestering host-defense protein. Nat Chem Biol 11(10):765–771
17. Hood IM, Skaar EP (2012) Nutritional immunity: transition metals at the pathogen–host interface. Nat Rev Microbiol 10(8):525–537
18. Velayudhan J et al (2000) Iron acquisition and virulence in *Helicobacter pylori*: a major role for FeoB, a high-affinity ferrous iron transporter. Mol Microbiol 37(2):274–286
19. Hantke K (2003) Is the bacterial ferrous iron transporter FeoB a living fossil? Trends Microbiol 11(5):192–195
20. Guilfoyle A et al (2009) Structural basis of GDP release and gating in G protein coupled Fe^{2+} transport. EMBO J 28(17):2677–2685
21. Alm RA et al (1999) Genomic-sequence comparison of two unrelated isolates of the human gastric pathogen *Helicobacter pylori*. Nature 397(6715):176–180
22. Tomb JF et al (1997) The complete genome sequence of the gastric pathogen *Helicobacter pylori*. Nature 388(6642):539–547
23. Ferguson AD et al (2002) Structural basis of gating by the outer membrane transporter FecA. Science 295(5560):1715–1719
24. Yue WW, Grizot S, Buchanan SK (2003) Structural evidence for iron-free citrate and ferric citrate binding to the TonB-dependent outer membrane transporter FecA. J Mol Biol 332(2):353–368
25. Braun V, Braun M (2002) Active transport of iron and siderophore antibiotics. Curr Opin Microbiol 5(2):194–201
26. Ferguson AD, Deisenhofer J (2004) Metal import through microbial membranes. Cell 116(1):15–24
27. Senkovich O, Ceaser S, McGee DJ, Testerman TL (2010) Unique host iron utilization mechanisms of *Helicobacter pylori* revealed with iron-deficient chemically defined media. Infect Immun 78(5):1841–1849
28. Husson MO, Legrand D, Spik G, Leclerc H (1993) Iron acquisition by *Helicobacter pylori*: importance of human lactoferrin. Infect Immun 61(6):2694–2697
29. Worst DJ, Otto BR, de Graaff J (1995) Iron-repressible outer membrane proteins of *Helicobacter pylori* involved in heme uptake. Infect Immun 63(10):4161–4165
30. Dhaenens L, Szczebara F, Husson MO (1997) Identification, characterization, and immunogenicity of the lactoferrin-binding protein from *Helicobacter pylori*. Infect Immun 65(2):514–518
31. Carrizo-Chávez MA, Cruz-Castañeda A, Olivares-Trejo Jde J (2012) The frpB1 gene of *Helicobacter pylori* is regulated by iron and encodes a membrane protein capable of binding haem and haemoglobin. FEBS Lett 586(6):875–879
32. Saleem M et al (2013) Use of a molecular decoy to segregate transport from antigenicity in the FrpB iron transporter from *Neisseria meningitidis*. PLoS ONE 8(2)
33. Touati D (2000) Iron and oxidative stress in bacteria. Arch Biochem Biophys 373(1):1–6
34. Bijlsma JJ et al (2002) The *Helicobacter pylori* homologue of the ferric uptake regulator is involved in acid resistance. Infect Immun 70(2):606–611
35. van Vliet AH et al (2002) The role of the Ferric Uptake Regulator (Fur) in regulation of *Helicobacter pylori* iron uptake. Helicobacter 7(4):237–244
36. Fassbinder F et al (2000) Identification of iron-regulated genes of *Helicobacter pylori* by a modified fur titration assay (FURTA-Hp). FEMS Microbiol Lett 184(2):225–229
37. Pich OQ, Carpenter BM, Gilbreath JJ, Merrell DS (2012) Detailed analysis of *Helicobacter pylori* Fur-regulated promoters reveals a Fur box core sequence and novel Fur-regulated genes. Mol Microbiol 84(5):921–941
38. Dian C et al (2011) The structure of the *Helicobacter pylori* ferric uptake regulator Fur reveals three functional metal binding sites. Mol Microbiol 79(5):1260–1275
39. Danielli A et al (2006) In vivo dissection of the *Helicobacter pylori* Fur regulatory circuit by genome-wide location analysis. J Bacteriol 188(13):4654–4662
40. Delany I, Spohn G, Rappuoli R, Scarlato V (2001) The Fur repressor controls transcription of iron-activated and -repressed genes in *Helicobacter pylori*. Mol Microbiol 42(5):1297–1309
41. Delany I, Spohn G, Rappuoli R, Scarlato V (2003) An anti-repression Fur operator upstream of the promoter is required for iron-mediated transcriptional autoregulation in *Helicobacter pylori*. Mol Microbiol 50(4)
42. Frazier BA et al (1993) Paracrystalline inclusions of a novel ferritin containing

nonheme iron, produced by the human gastric pathogen *Helicobacter pylori*: evidence for a third class of ferritins. J Bacteriol 175(4):966–972

43. Doig P, Austin JW, Trust TJ (1993) The *Helicobacter pylori* 19.6-kilodalton protein is an iron-containing protein resembling ferritin. J Bacteriol 175(2):557–560
44. Cho K et al (2009) The crystal structure of Ferritin from *Helicobacter pylori* reveals unusual conformational changes for iron uptake. J Mol Biol 390(1):83–98
45. Bereswill S et al (1998) Structural, functional and mutational analysis of the pfr gene encoding a ferritin from *Helicobacter pylori*. Microbiology 144(Pt 9):2505–2516
46. Evans DJ et al (1995) Characterization of a *Helicobacter pylori* neutrophil-activating protein. Infect Immun 63(6):2213–2220
47. Zanotti G et al (2002) Structure of the neutrophil-activating protein from *Helicobacter pylori*. J Mol Biol 323(1):125–130
48. Luther J et al (2010) Empiric quadruple vs. triple therapy for primary treatment of *Helicobacter pylori* infection: Systematic review and meta-analysis of efficacy and tolerability. Am J Gastroenterol 105(1):65–73
49. Wang Y et al (2015) Bio-coordination of bismuth in *Helicobacter pylori* revealed by immobilized metal affinity chromatography. Chem Commun 51(92):16479–16482
50. Tsang C-N, Bianga J, Sun H, Szpunar J, Lobinski R (2012) Probing of bismuth antiulcer drug targets in H. pylori by laser ablation-inductively coupled plasma mass spectrometry. Metallomics 4(3):277–283
51. Posey JE (2000) Lack of a role for iron in the Lyme disease pathogen. Science 288(5471):1651–1653

Chapter 6

Common Challenges in Studying the Structure and Function of Bacterial Proteins: Case Studies from *Helicobacter pylori*

Daniel A. Bonsor and Eric J. Sundberg

Abstract

Employing biophysical and structural methods is a powerful way to elucidate mechanisms of molecular recognition in bacterial pathogenesis. Such studies invariably depend on the production of pure, folded and stable proteins. Many proteins that can be expressed recombinantly ultimately fail to meet one or more of these criteria. The *cag* proteins from *Helicobacter pylori* form a secretion system that delivers the oncoprotein, CagA, into human gastric epithelial cells through an interaction between CagL and host cell integrins, where it can cause gastric adenocarcinoma. Expression of full length CagA and CagL is problematic as CagA undergoes rapid degradation during purification and CagL is thermally unstable. Here, we describe a method for the purification of CagA that results in the production of the full length protein through coexpression with its endogenous chaperone, CagF, and its subsequent separation from its chaperone. Furthermore, we detail the production of CagL and the use of differential scanning fluorimetry to identify how CagL is thermally stabilized by reduced pH, which led to a new crystal form of CagL and novel insight to pathogenic mechanisms. The methods described here for the production of stable *cag* proteins can be applied to a wide range of proteins involved in bacterial pathogenesis.

Key words Chaperones, Coexpression, Protein purification, Differential scanning fluorimetry

1 Introduction

Helicobacter pylori infection is widespread. Approximately half of the world's population is infected [1]. Most infected individuals will remain asymptomatic for life; however, around 20% will develop complications during their lifetimes including gastritis, peptic ulcers, lymphomas involving the mucosa-associated lymphoid tissue (MALT lymphoma) and gastric adenocarcinomas [2]. Infection by *H. pylori* is believed to occur during childhood through ingestion. Once in the stomach, *H. pylori* utilizes several virulence factors to achieve colonization of the boundary between the mucosa and surface of the gastric epithelial cells including urease to neutralize the stomach acid, flagella to burrow into the

Pontus Nordenfelt and Mattias Collin (eds.), *Bacterial Pathogenesis: Methods and Protocols*, Methods in Molecular Biology, vol. 1535, DOI 10.1007/978-1-4939-6673-8_6,

mucosa and away from the stomach acid, modified O-antigens to mimic host cell Lewis antigens and adhesins to anchor *H. pylori* onto epithelial cells [3]. Once attached to the host gastric epithelial cell, several virulence factors are secreted. Vacuolating cytotoxin A (VacA) binds to the host cells where it is internalized and causes the formation of large vesicles and in certain cases cell death [4]. More importantly for gastritis, ulcers, lymphomas and adenocarcinomas, cytotoxic associated gene A (CagA), one of the few known oncogenic bacterial proteins, is injected into the host cell cytoplasm though a Type IV secretion system (T4SS) [5].

CagA is a large protein with a variable molecular weight ranging from 120 to 150 kDa due to different strains of *H. pylori* producing CagA with a diverse number and type of tyrosine phosphorylation motifs (TPMs) near the C-terminus [5, 6]. The number of TPMs present in CagA from a particular *H. pylori* strain correlates with gastric cancer risk [7]. CagA is a five domain protein that includes a stable and structured N-terminal 100 kDa region composed of three distinct domains [8–10], an intrinsically disordered domain containing a variable number of TPMs [8] and a C-terminal domain containing a signal peptide that is recognized by the T4SS [11]. CagA translocation through the T4SS is dependent on the recognition of the C-terminal signal peptide of CagA and, prior to that, its interaction with its chaperone protein CagF inside the bacterial cell [11, 12]. CagF is a 32 kDa protein, which contains a putative coiled-coil domain and dimerizes with an association constant of approximately 200 μM [12, 13]. It has been shown using peptide array assays and isothermal titration calorimetry measurements that monomeric CagF contacts all five domains of CagA [13]. The production of milligram quantities of full length CagA for biophysical and structural work has been problematic due to the rapid proteolytic degradation of CagA during expression and purification with the loss of the C-terminus resulting in a protein with a molecular weight of 100 kDa [14], consisting of only the N-terminal structured domains. A *cagA* library, from which ~18,000 expression constructs were screened, identified several constructs corresponding to proteins of approximately 100 kDa in molecular weight that resulted in milligram-level expression of purified CagA [9, 15] and eventually led to the high-resolution X-ray crystal structures of CagA [8, 9]. However, no construct greater than 110 kDa in molecular weight was identified in this screen [15]. As the extreme C-terminus contains both the TPMs, which are important for CagA-host protein interaction, and the secretion peptide that is recognized by the T4SS, production of full length CagA for both biophysical and structural characterization is essential for fully elucidating the function of this oncoprotein.

Upon CagA binding of CagF and recognition by the T4SS, CagF is removed and CagA shuttled into a pore than spans the

periplasm to the pilus [12]. The pilus is comprised of CagC with a diameter of ~70 nm with the surface decorated with at least three other *cag* proteins—CagH, CagI, and CagL [16, 17]. Each of these proteins are believed to attach to the pilus through a highly similar C-terminal hexapeptide sequence ([S/T]-K-[I/V]-I-V-K) [17]. Deletion of CagH, CagI, or CagL results in *H. pylori* that produce either no or stunted pili [17]. Integrins, which are presented on the surface of gastric epithelial cells, were identified as a receptor involved in the secretion of CagA. The $\alpha_5\beta_1$ integrin was initially found to be responsible for CagA translocation into host gastric epithelial cells, although further investigations have indicated that $\alpha_V\beta_3$, $\alpha_V\beta_5$, and $\alpha_V\beta_6$ integrins also permit CagA translocation [17–21]. Most integrins recognize ligands containing an arginine–glycine–aspartic acid (RGD) motif [22]. Sequence analysis of the *cag* pathogenicity island revealed a single RGD motif located within CagL and mutation of this RGD motif prevented CagL binding of integrins and the subsequent translocation of CagA into host cells [18]. Although CagL triggers the translocation of CagA across the host cell plasma membrane, the mechanism by which this is achieved remains unknown. Several X-ray crystal structures of CagL have been solved, revealing that the RGD motif is located in an α-helix, which is unique—all other proteins for which structures have been determined contain their RGD motifs in loop regions [23–25]. Furthermore, each CagL structure revealed both minor and gross conformational changes, such as the sliding of a neighboring α-helix relative to the α-helix in which the RGD motif resides, as well as a helix–turn–helix motif that rearranges to form a single elongated helix [24, 25]. These conformational changes have been shown to occur in response to a change in pH [25]. The relative sliding of neighboring α-helices has been proposed to bury the RGD motif in order to prevent CagL from binding to integrins from shedding cells that have been discarded in the stomach where the pH is acidic [25]. By regulating the CagL–integrin interaction through a pH-induced mechanism, the *H. pylori* T4SS could engage host gastric epithelial cells along the stomach lining where the pH is more accommodating [25].

This chapter describes the production of full length CagA by coexpression with the effector protein CagF, mimicking that which occurs in *H. pylori* cells. We describe the purification of the CagA–CagF complex and the removal of CagF through partial denaturation to yield highly purified milligram quantities of full length CagA. We also describe the refolding and purification of CagL and its crystallization using a differential scanning fluorimetry assay to identify a buffer system that increased the melting temperature (T_m) and led to a new crystal form and the discovery of the above mentioned conformational changes. These protocols are adaptable to other proteins and could aid in their production, purification and stabilization in order to make them more amendable to biochemical, biophysical and structural studies.

2 Materials

2.1 Bacterial Strains and Media

All strains are grown at 37 °C (unless otherwise stated) either on LB agar plates or in LB broth, supplemented with ampicillin and/or kanamycin at their stated concentrations below.

1. *E. coli* strains: *TOP10* (F- *mcrA* Δ(*mrr-hsd*RMS-*mcr*BC) Φ80*lac*ZΔM15 Δ *lac*X74 *rec*A1 *ara*D139 Δ(*araleu*)7697 *gal*U *gal*K *rps*L (StrR) *end*A1 *nup*G) and *BL21(DE3)* (F^- *ompT* *hsd*S_B(r_B^- m_B^-) *gal dcm* (DE3)).
2. Media: LB Broth is prepared by dissolving 10 g tryptone, 10 g NaCl, and 5 g yeast extract in a total volume of 1 L of deionized H_2O and sterilizing by autoclaving at 121 °C for 20 min. LB agar is prepared by adding 15 g of agar in 1 L of LB Broth before sterilization.
3. Ampicillin stock: 100 mg/mL ampicillin sodium salt in H_2O, filter-sterilized with 0.22 μm pore-size syringe filter and store at −20 °C. Use at a final concentration of either 100 μg/mL for single plasmids or 25 μg/mL for two plasmids.
4. Kanamycin stock: 30 mg/mL kanamycin sulfate in H_2O, filter-sterilized with 0.22 μm pore-size syringe filter and store at −20 °C. Use at a final concentration of 15 μg/mL.
5. Isopropylthiogalactoside stock (IPTG): IPTG is dissolved in deionized H_2O to a final concentration of 1 M, filter-sterilized with 0.22 μm pore-size syringe filter and stored at −20 °C.

2.2 Plasmids, Plasmid Construction, and Cloning

1. TBE buffer: Dissolve 10.8 g Tris base, 5.5 g boric acid in 900 mL H_2O, add 20 mL 0.5 M EDTA, pH 8.0 and adjust the pH to 8.4. Dilute to a final volume of 1 L.
2. Ethidium bromide stock: 10 mg/mL in H_2O kept at room temperature.
3. pRSFDuet™-1 (Novagen) is modified to remove the C-terminal S-tag in the second multiple cloning site and is replaced with a decahistidine (10×His) tag. This vector is subsequently used for the expression of CagA with an N-terminal hexahistidine (6×His) and a C-terminal 10×His.
4. pET21-d (Novagen) is used for expression of CagL with a C-terminal 6×His.
5. pGEX-5×-2 (GE Healthcare Life Sciences) is used for expression of CagF with an N-terminal GST tag.
6. DNA modifying enzymes: *BamHI*, *NcoI*, *PacI*, *SacI*, and *XhoI* restriction enzymes, Pfu Turbo, T4 Polynucleotide kinase, and Quick T4 DNA ligase with their respective buffers are commercially available.

7. Low-melt agarose gels (1% w/v): 0.5 g of low-melt agarose is added to 25 mL of TBE. The solution is heated in a microwave oven with occasional swirling until the agarose is dissolved. A further 25 mL of TBE is added followed by 2 μl of Ethidium Bromide and the gel is poured into a sealed gel mold with comb and left to set. The gel is placed in an electrophoresis tank and covered with TBE. The samples are loaded and the gel is run at a constant voltage of 100 V for 30 min.

2.3 Protein Expression and Purification

1. GST Binding Buffer (GSTBB): 1 mM KH_2PO_4, 10 mM Na_2HPO_4, 137 mM NaCl, 2.7 mM KCl, pH 7.4.
2. GST Elution Buffer (GSTEB): 20 mM Tris–HCl pH 7.5, 50 mM NaCl, 10 mM reduced glutathione.
3. Glutathione agarose (e.g., GE Healthcare Life Sciences).
4. Nickel Binding Buffer (NiBB): 20 mM Tris–HCl pH 7.5, 500 mM NaCl.
5. Nickel Elution Buffer (NiEB): 20 mM Tris–HCl pH 7.5, 500 mM NaCl, 400 mM imidazole.
6. Ni-NTA agarose (e.g., Thermo Scientific).
7. Partial Denaturation Wash (PDW): 20 mM Tris–HCl pH 7.5, 2.0 M urea.
8. Inclusion Bodies Lysis Buffer: 50 mM KH_2PO_4–K_2HPO_4 pH 7.5, 200 mM NaCl.
9. Inclusion Bodies Wash Buffer: 10 mM Tris–HCl, 1 M NaCl, pH 8.0.
10. Denaturation Buffer (DB): 50 mM KH_2PO_4–K_2HPO_4 pH 7.5, 200 mM NaCl, 6.0 M guanidine hydrochloride.
11. Refolding Buffer (RB): 50 mM Tris–HCl pH 8.3, 20 mM NaCl, 0.1 mM KCl, 1 mM EDTA, 2 mM reduced glutathione, 0.2 mM oxidized glutathione.
12. Gel Filtration Buffer (GFB): 20 mM Tris–HCl pH 7.5, 200 mM NaCl, 1 mM EDTA.

2.4 Differential Scanning Fluorimetry

1. SYPRO Orange 5000x Stock (Sigma).
2. 96-well White TempPlate with semi-skirt (USA Scientific).
3. Buffer Screen: A 24-well screen was devised to screen a pH range from 4.0 to 9.5 in intervals of 0.5 pH units according to Table 1 and aliquoted to positions A1-B12 of a 96-deep well block. The 24 conditions are repeated for positions C1-D12 with the addition of 500 mM NaCl. All 48 conditions are then duplicated for positions E1-H12.
4. Optical Sealing Tape.
5. iQ5 Multicolor Real Time PCR Detection System (Bio-Rad) or similar system.

Table 1
Composition of the 96 differential scanning fluorimetry screen solutions

Well	Buffer
A1/E1 (C1/G1)	Water (500 mM NaCl)
A2/E2 (C2/G2)	200 mM sodium acetate-HCl pH 4.0 (500 mM NaCl)
A3/E3 (C3/G3)	200 mM sodium citrate-HCl pH 4.0 (500 mM NaCl)
A4/E4 (C4/G4)	200 mM sodium acetate-HCl pH 4.5 (500 mM NaCl)
A5/E5 (C5/G5)	200 mM sodium citrate-HCl pH 5.0 (500 mM NaCl)
A6/E6 (C6/G6)	200 mM sodium acetate-HCl pH 5.0 (500 mM NaCl)
A7/E7 (C7/G7)	200 mM sodium citrate-HCl pH 5.5 (500 mM NaCl)
A8/E8 (C8/G8)	200 mM Bis-Tris-HCl pH 5.5 (500 mM NaCl)
A9/E9 (C9/G9)	200 mM K/Na phosphate pH 6.0 (500 mM NaCl)
A10/E10 (C10/G10)	200 mM Bis-Tris-HCl pH 6.0 (500 mM NaCl)
A11/E11 (C11/G11)	200 mM MES-NaOH pH 6.5 (500 mM NaCl)
A12/E12 (C12/G12)	200 mM sodium cacodylate-HCL pH 6.5 (500 mM NaCl)
B1/F1 (D1/H1)	200 mM Bis-Tris-HCL pH 6.5 (500 mM NaCl)
B2/F2 (D2/H2)	200 mM Bis-Tris propane-HCl pH 6.5 (500 mM NaCl)
B3/F3 (D3/H3)	200 mM K/Na phosphate pH 7.0 (500 mM NaCl)
B4/F4 (D4/H4)	200 mM Hepes-NaOH pH 7.0 (500 mM NaCl)
B5/F5 (D5/H5)	200 mM Hepes-NaOH pH 7.5 (500 mM NaCl)
B6/F6 (D6/H6)	200 mM Tris-HCl pH 7.5 (500 mM NaCl)
B7/F7 (D7/H7)	200 mM K/Na phosphate pH 8.0 (500 mM NaCl)
B8/F8 (D8/H8)	200 mM Hepes-NaOH pH 8.0 (500 mM NaCl)
B9/F9 (D9/H9)	200 mM Tris-HCl pH 8.0 (500 mM NaCl)
B10/F10 (D10/H10)	200 mM Tris-HCl pH 8.5 (500 mM NaCl)
B11/F11 (D11/H11)	200 mM Tris-HCl pH 9.0 (500 mM NaCl)
B12/F12 (D12/H12)	200 mM CHES-HCl pH 9.5 (500 mM NaCl)

The concentrations given are the stock solutions which are mixed 1:1 with the protein–SYPRO Orange mixture

3 Methods

The production of proteins that are pure, stable, and crystallizable can be problematic due to contamination and degradation of the protein sample, as well as the low success rate of protein crystallization. Below, we describe the production of the unstable full length

protein CagA through coexpression with CagF and stabilization of CagL by identifying buffer conditions that increase its melting temperature leading to the production of a new crystal form.

3.1 Protein Stabilization by Coexpression

Unstable proteins that display degradation during purification are common. Typically, alternative constructs are designed as the separation of degradation products from full length proteins is problematic and often produces low protein yields. CagA exhibits substantial degradation during expression, resulting in an approximately 100 kDa product [14, 15]. Expression of the target protein with known binding partners has often been used where proteins fail to express or are found in inclusion bodies. Other forms of coexpression involve the expression of chaperones (e.g., GroES-GroEL) or foldases (e.g., peptidyl prolyl *cis/trans* isomerases or disulfide isomerases) [26–29]. We have found that CagA coexpression with CagF, the binding partner and chaperone of CagA, suppresses CagA degradation during expression and purification [13]. However, a major problem with coexpression of known binding partners for the target protein is the separation of the protein of interest and the coexpressed proteins. We have modified the commercial pRSFDuet-1 vector (Fig. 1a) that contains two multiple cloning sites, one with

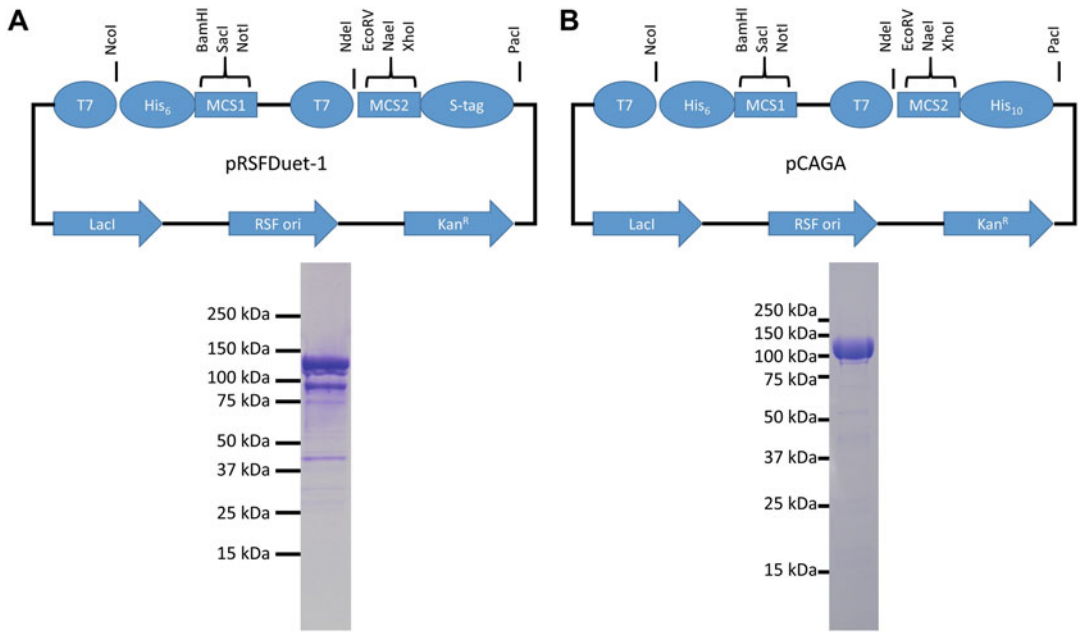

Fig. 1 Construction of a CagA expression vector and its purification. (**a**) Vector map of pRSFDuet. CagA was originally ligated into MCS1. (**b**) Purification of CagA from 6 L growth of BL21(DE3) coexpressing GST-CagF using pRSFDuet shows excessive degradation and low yields. (**c**) Removal of S-tag from MCS2 generated pCAGA. CagA was ligated into a SacI/XhoI cut pCAGA. (**d**) Expression and purification of CagA from 2 L of BL21(DE3) coexpressing GST-CagF using pCAGA show protein of high purity

an N-terminal 6×His tag and the other with a C-terminal S-tag, and replaced the S-tag with a 10×His tag (Fig. 1b). CagA is cloned through both cloning sites such that it contains both an N-terminal 6×His tag and a C-terminal 10×His tag. CagF is expressed as a GST fusion from the pGEX-5×-2 vector. Coexpression of both proteins in BL21(DE3) is permitted as the pRSFDuet and pGEX-5×-2 vectors have different origins of replication (RSF and BR322 origins, respectively) and antibiotic resistances (kanamycin and ampicillin, respectively), thereby preventing plasmid instability. As CagA degradation occurs close to the C-terminus [14], washing of the nickel affinity chromatography column with 150–200 mM imidazole removes the N-terminal 100 kDa degradation product, while the full length protein (~130 kDa) and the C-terminal degradation product (~30 kDa) is retained until a further more stringent elution step with 300–400 mM imidazole. The C-terminal degradation product is subsequently separated from full length CagA by size exclusion chromatography.

3.1.1 Preparation of the Modified pRSFDuet Vector (pCAGA)

1. The primers RSFfp (5′-TCGAGCATCACCACCATCAT CACCACCATCACCATTAAAT-3′) and RSFrp (5′-TTAAT G G T G A T G G T G G T G A T G A T G G T G G T G A TGC-3′) are diluted with deionized H_2O to a concentration of 25 μM) and are each phosphorylated using a reaction mix containing: 12 μl primer, 32 μl deionized H_2O, 5 μl 10× T4 Polynucleotide kinase buffer (NEB), and 1 μl T4 Polynucleotide kinase. The reaction is carried out for 30 min at 37 °C, the phosphorylated primers are then mixed and heated to 95 °C for 5 min by water bath or heating block. The power source is removed and the primers are cooled to room temperature gently (*see* **Note 1**).
2. 2 μg of pRSFDuet is double digested with *XhoI/PacI* for 2 h at 37 °C. The restriction enzyme digestion products are analyzed on a 1% w/v low melt agarose gel. The cut vector is visualized with UV-light and carefully excised using a clean razor blade and placed in a microfuge tube. The cut vector is purified using a commercial agarose gel purification kit (e.g., QIAgen).
3. The phosphorylated annealed primers are ligated into the gel purified *XhoI/PacI* pRSFDuet vector. Specifically, 1 μl of purified cut vector is mixed with 1 μl of annealed primers, 2 μl deionized H_2O, 5 μl 2×Quick Ligation Reaction Buffer, and 1 μl Quick T4 DNA Ligase are incubated at RT for 5 min before subsequent transformation into chemically competent *E. coli* Top10, plated on LB agar plates supplemented with kanamycin (30 μg/mL) and incubated overnight at 37 °C (*see* **Note 2**).
4. Single colonies are picked and grown overnight at 37 °C in 3–5 mL LB containing kanamycin (30 μg/mL) and plasmid DNA minipreps are conducted using a commercial kit (e.g., QIAgen).

5. Conformation of insert is verified by DNA sequencing using either the commercial available universal T7 Terminator primer or the ACYCDuetUP1 primer (Novagen, 5′-GGAT CTCGACGCTCTCCCT-3′).

3.1.2 Cloning and Ligation of CagA and CagF for Expression

1. Genomic DNA of the *H. pylori* strain 11637 was purchased from ATCC and used as a template for gene amplification of full length CagA and CagF using the following primers: CagAFP-SacI (5′-GCGCGCCTCGAGAGATTTTTGGAAAC CACCTTTTGTATTAACA-TTTTTG-3′), CagARP-XhoI (5′-GCGCGCGAGCTCGATGACTAACGAAACT ATTGACCAACAACCAC-3′), CagFFP-BamHI (5′-GCG G A T C C C G G A A A A C T T G T A T T T C C A G GGCATGAAACAAAATTTGCGTGAACAAAAATT-3′) and CagFRP-XhoI (5′-GCGCGCCTCGAGTCAATCGTTAC TTTTGTTTTGATTTTTTTGATCG-3′) (*see* **Note 3**). PCR reactions are carried out in a final volume of 50 μL, 10 ng of template, 5 μL 10× Cloned Pfu DNA Polymerase Reaction Buffer, 1 μL 10 mM dNTP mixture (final concentration of 200 μM of each dNTP), 1 μL of each 5 μM primer (100 nM final concentration), and 1 μL of Pfu Turbo. After an initial denaturation of 2 min at 95 °C, the PCR reactions proceed for 30 cycles of 30 s of denaturation at 95 °C, 30 s of annealing at 60 °C, and 3 min 45 s for CagA and 50 s for CagF extensions at 72 °C followed by 6 min at 72 °C.
2. Amplification of *cag* genes are analyzed on a 1 % w/v low melt agarose gel and confirmed by UV light. PCR products are purified (using a commercial kit, e.g., QIAgen) and digested with *SacI/XhoI* (CagA) or *BamHI/XhoI* (CagF) restriction enzymes for 2 h at 37 °C before purification.
3. The vectors pCAGA and pGEX-5x-2 are digested with *SacI/XhoI* and *BamHI/XhoI*, respectively at 37 °C for 2 h. The restriction enzyme digestion products are analyzed on a 1 % w/v low melt agarose gel, visualized with UV-light and extracted using a clean razor blade, placed in a microfuge tube and purified from the gel using a commercial agarose gel purification kit.
4. The digested inserts are ligated into their respective digested vectors. Specifically, 1 μl of purified digested vector is mixed with 1 μl of digested insert, 2 μl deionized H_2O, 5 μl 2×Quick Ligation Reaction Buffer, and 1 μl Quick T4 DNA Ligase and incubated at RT for 5 min before transformation into chemically competent *E. coli* Top10. Cells are plated on LB agar plates supplemented with either kanamycin (30 μg/mL) for the pCAGA-CagA ligation or ampicillin (100 μg/mL) for the pGEX-5×-2-CagF vector, and are incubated overnight at 37 °C.

5. Single colonies are plucked to inoculate 3–5 mL of LB containing either kanamycin (30 μg/mL) or ampicillin (100 μg/mL) and grown overnight at 37 °C.
6. DNA plasmid minipreps are performed and insertion of clones is confirmed by DNA sequencing. Specifically, CagA is sequenced using the T7 Terminator primer, the ACYCDuetUP1 primer (Novagen, 5′-GGATCTCGACGCTCTCCCT-3′) and three internal primers to completely cover the sequence (11637Int1 5′-CCGCCTGAATCTAGGGATTTGCTTG ATG-3′, 11637Int2 5′-GTCCTGATAAGGGTGTAG GCGTTACAAATG-3′, and 11637Int3 5′-GCGACC T T G A A A A T T C C G T T A A A G A T G T G A T C A TC-3′). CagF is sequenced using the commercial 5GEX and 3GEX universal primers.

3.1.3 Coexpression and Purification of Full Length CagA

1. 40 μg of pCAGA-CagA and pGEX-5×-2-CagF are combined into a sterile microfuge tube and is transformed into chemical competent *E. coli* BL21(DE3) (*see* **Note 4**). Cells are plated onto LB agar plates supplemented with both kanamycin and ampicillin (15 and 25 μg/mL, respectively) and incubated overnight at 37 °C (*see* **Note 5**). In a separate sterile microfuge tube, 40 μg of pGEX-5×-2-CagF is transformed into *E. coli* BL21 (DE3), plated onto LB agar plates containing ampicillin (100 μg/mL) and incubated overnight.
2. A single colony of each BL21 (DE3) transformant is used to inoculate 100 mL of LB broth containing appropriate concentrations of antibiotics and grown overnight on an orbital shaker at 37 °C.
3. A 1:100 dilution of BL21(DE3) + pCAGA-CagA/pGEX-5×-2-CagF is used to inoculate typically 4 × 1 L of LB broth containing ampicillin and kanamycin. A 1:100 dilution of BL21(DE3) + pGEX-5×-2-CagF is used to inoculate 0.5 L of LB containing ampicillin. Cells are grown at 37 °C until an A_{600nm} of ~ 0.4–0.5 is reached. The flasks are transferred to an orbital shaker set at 18 °C and left to grow for 20 min before induction with a final concentration of 1 mM IPTG. Cells are left to express the protein overnight.
4. Cells were harvested (5500*g*, 4 °C, 12 min) and the BL21(DE3) + pGEX-5×-2-CagF cells were resuspended in ~ 35 mL ice-cold GSTBB. They were disrupted by sonication on ice using a Branson Sonifier 450 with ½ in. stud probe and 60 × 0.7 s pulses at 70 W (0.3 s spacings between pulses). This cell extract is used to resuspend the BL21(DE3) + pCAGA-CagA/pGEX-5×-2-CagF cells and are diluted to ~ 70 mL with ice-cold GSTBB (*see* **Note 6**). The mixture is disrupted further by sonication (2 × 60 × 0.7 s at 70 W with 0.3 s spacings between pulses). Cell debris was removed by centrifugation (20,000 × *g*, 4 °C, 30 min) and the soluble cell extract was loaded onto

~5 mL of Glutathione agarose in a gravity column equilibrated with GSTBB. Unbound protein was washed out with 25 mL of GSTBB before elution with 20 mL of GSTEB.

5. The elution fraction is diluted 2-fold with NiBB and loaded at 2 mL/min onto a 5 mL Ni-NTA agarose column. The column is washed with 50 mL of NiBB before washing with 1.5 L of PDW at a rate of ~1–2 mL/min, which is typically left to run overnight at room temperature (*see* **Note 7**). The beads are washed with 50 mL of NiBB to remove the urea, 30 mL of 1:1 NiBB + NiEB (final imidazole concentration 200 mM) to remove degradation products and CagA is eluted with 15 mL of NiEB. The purified protein is concentrated to ~2–3 mL and can be used as is for biophysical characterization or further purified by size exclusion chromatography (*see* **Note 8**).

3.2 Protein Stabilization for Crystallization

Crystallization of purified protein for X-ray diffraction studies has a low success rate due to the vast number of variables that exist. Typically, after a target protein has either failed to crystallize or produces crystals with poor or no diffraction, several options are available that can be performed with a construct as is, prior to designing an altered construct for expression, purification and crystallization. These include, but are by no means limited to, matrix microseeding, limited proteolysis, lysine methylation, and molecular imprinted polymers which have all shown to have rescued "non-crystallizable" proteins [30–33]. An alternative method that we have had success with is to use differential scanning fluorimetry to identify buffers that stabilize the protein of interest, which may be unstable in the crystallization storage buffer (typically low buffer and salt concentrations) [25]. The differential scanning fluorimetry assay screens pH in the presence and absence of salt to identify a new crystallization storage buffer in which the protein is soluble, folded and exhibits an increased melting temperature (T_m) [34–36]. This is achieved by the addition of fluorescent dye, typically SYPRO Orange, which strongly fluoresces when the protein unfolds and exposes the hydrophobic core as the temperature increases. We present a method for the expression and purification of CagL, and the identification of a crystallization buffer through differential scanning fluorimetry that we used successful to crystallize CagL in a new crystal form.

3.2.1 Cloning and Ligation of CagL for Expression

1. Genomic DNA of the *H. pylori* strain 26695 was purchased from ATCC and used as a template for gene amplification of CagL residues 21-237 using the following primers: CagLFP-NcoI (5′-GCG-CGCCCATGGAAGATATAACAAGCGGTT TAAAGCAACTGG-3′) and CagLRP-XhoI (5′-GCGCGC CTCGAGTTTAA-CAATGATCTTACTTGATTGCCTTTCT TG-3′). The PRC reaction is carried out in a final volume of 50 μL, 10 ng of template, 5 μL 10× Cloned Pfu DNA

Polymerase Reaction Buffer, 1 μL 10 mM dNTP mixture (final concentration of 200 μM of each dNTP), 1 μL of each 5 μM primer (100 nM final concentration), and 1 μL of Pfu Turbo. After an initial denaturation of 2 min at 95 °C, the PCR reactions proceed for 30 cycles of 30 s of denaturation at 95 °C, 30 s of annealing at 60 °C, 40 s for CagL extensions at 72 °C, followed by 6 min at 72 °C.

2. Amplification of the CagL gene is analyzed on a 1% w/v low melt agarose gel and confirmed by UV light. The PCR product is purified (using a commercial kit, e.g., QIAgen) and digested with *NcoI* and *XhoI* restriction enzymes for 2 h at 37 °C before purification.
3. The pET21d vector is digested with *NcoI* and *XhoI* at 37 °C for 2 h. The restriction enzyme digestion products are analyzed on a 1% w/v low melt agarose gel, visualized with UV-light and extracted using a clean razor blade, placed in a microfuge tube and purified from the gel using a commercial agarose gel purification kit.
4. The CagL digested insert is ligated into the NcoI/XhoI digested pET21d vector using the method described above for CagA and CagF. The ligation reaction is transformed into chemically competent Top10 cells which are plated onto LB agar plates supplemented with ampicillin (100 μg/mL). Plates are incubated overnight at 37 °C.
5. Single colonies are plucked to inoculate 3–5 mL of LB containing ampicillin (100 μg/mL) and grown overnight at 37 °C.
6. DNA plasmid minipreps are performed and insertion of the clone is confirmed by DNA sequencing using the universal T7 Forward and T7 Termination primers.

3.2.2 Expression and Purification of CagL

1. 40 μg of pET21d-CagL is placed in a sterile microfuge tube and is transformed into chemical competent *E. coli* BL21 (DE3). Cells are plated out onto LB Agar containing ampicillin and are left to incubate overnight at 37 °C. A single colony is used to inoculate 100 mL of LB broth containing ampicillin and placed on an orbital shaker at 37 °C overnight.
2. A 1:100 dilution of the overnight is used to inoculate 2 × 1 L of LB containing ampicillin and left to shake on an orbital shaker until an A_{600nm} of ~ 0.6 is reached. Cells are induced with a final concentration of 1 mM IPTG and left to grow at 37 °C for 4 h. Cells are harvested by centrifugation (5500 × *g*, 12 min, 4 °C).
3. Cells are resuspended in ~35 mL of Inclusion Bodies Lysis Buffer and are lysed by sonication on ice using a Branson Sonifier 450 with ½ in. stud probe and 2 × 60 × 0.7 s pulses at 70 W (0.3 s spacings between pulses). Inclusion bodies are isolated by centrifugation (20,000 × *g*, 4 °C, 30 min). The supernatant is

discarded and the inclusion bodies are resuspended and broken up by pipette in Inclusion Bodies Wash Buffer. Inclusion bodies are isolated by centrifugation (20,000×*g*, 4 °C, 30 min), supernatant discarded and dissolved in ~5 mL of DB buffer (the inclusion bodies are broken up by pipette and the solution left at room temperature for 1 h). Undissolved cell debris is removed by microcentrifuge (20,000×*g*, 5 min, room temperature).

4. The dissolved inclusion body solution is refolded by manual injected into 400 mL of ice cold RB with stirring (kept at 4 °C) at a rate of ~100 μL/min. The solution is left stirring at 4 °C for 2.5 days before EDTA is quenched with an excess of $MgCl_2$ (final concentration 2 mM) (*see* **Note 9**). Precipitated protein is removed by centrifugation (10,000×*g*, 4 °C, 30 min) and the supernatant is loaded on a 5 mL bead volume of Ni-NTA agarose in a gravity column by a peristaltic pump. The beads are washed with 30 mL NiBB, 20 mL of 1:8 mixture of NiBB and NiEB (imidazole final concentration 50 mM), respectively and CagL is eluted with 10 mL of NiEB. CagL is dialyzed overnight at 4 °C against 2 L of gel filtration buffer. CagL is subjected to size exclusion chromatography on an S200 10/300 GL column (GE Healthcare) equilibrated with gel filtration buffer by 4–6×2mL injections. Folded CagL typically elutes around 16–17 mL. Protein purity is confirmed by SDS PAGE.

3.2.3 Differential Scanning Fluorimetry of CagL

1. CagL is diluted to 1 mg/mL with gel filtration buffer. In limited lighting, 1.375 mL of CagL is added to 2.75 μL of SYPRO Orange in a sterile microfuge tube. 12.5 μL of the CagL-SYPRO Orange mixture is added to each well of a 96-well White TempPlate. Carefully dispense 12.5 μL of the differential scanning fluorimetry solutions to the same plate, seal with Optical Sealing Tape and briefly centrifuge the plate at room temperature (500×*g*, 5 min) to remove any air bubble that may have occurred during the preparation of the plate (*see* **Note 10**).
2. Place the plate in an iQ5 Multicolor Real Time PCR Detection System or other appropriate Real Time PCR machine (e.g., ABi 7900). Run a program which scans the temperature from 25 to 95 °C, at 1 °C/min with a dwell time of 1 min at each temperature (*see* **Note 11**).
3. Export the Relative Fluorescence Units (RFUs) to an EXCEL spreadsheet. Download a copy of the "Transform" for the appropriated Real Time PCR machine and "DSF Analysis" EXCEL spreadsheet (ftp://ftp.sgc.ox.ac.uk/pub/biophysics/). Paste the raw RFUs from your experiment into the "RfU" tab of the Transform spreadsheet. Copy the output data from this and paste into the "Paste in transformed Data" tab of the DSF Analysis file. Visually inspect the graphs produced in the "All Graphs" tab for melting transitions (*see* **Note 12**). In the

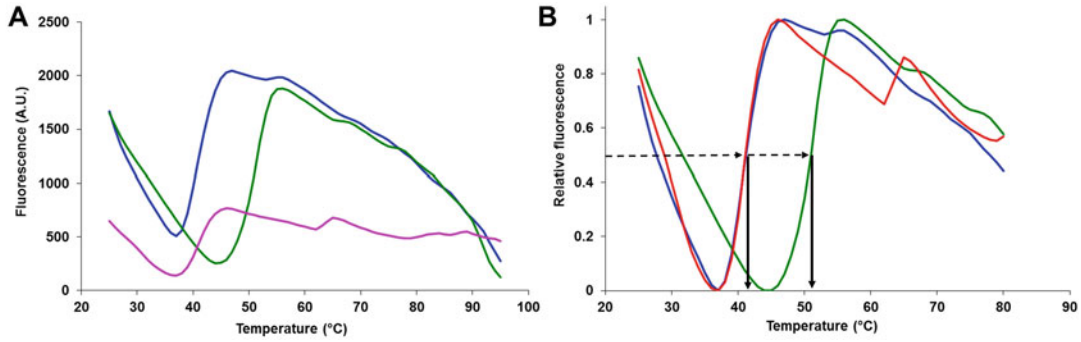

Fig. 2 Differential scanning fluorimetry assay of purified CagL. (**a**) Raw fluorescence of CagL-SYPRO Orange undergoing thermal melting in water (blue), 100 mM Tris, pH 8.0 (magenta) and 100 mM sodium acetate pH 4.0 (green). (**b**) Normalized thermal melt of the same condition. In water and 100 mM Tris, pH 8.0, a T_m of 41 °C is observed. Lowering of the pH (100 mM sodium acetate pH 4.0) causes the T_m to increase by 10 °C

"Custom Graphs" tab several graphs can be superimposed onto a single graph (Fig. 2a), whilst in the "Custom Normalized Graphs" tab, superimposed graphs can be normalized (Fig. 2b). Melting temperatures are calculated where the relative fluorescence is equal to 0.5. CagL should display melting temperatures of ~ 50 °C at low pH (Fig. 2b). As the pH is increased, CagL becomes thermally unstable and shifts to a melting temperature of ~ 40 °C (Fig. 2b).

4 Notes

1. The primers can potentially be purchased phosphorylated, annealed directly together and then ligated into the *XhoI/PacI* cut pRSFDuet vector.
2. Ligations can be carried out with T4 ligase, though reaction times are increased.
3. The forward primer for GST-CagF contains a Tobacco Etch Virus (TEV) protease site. We use this to cleave GST from CagF using TEV protease made in-house. pGEX-5×-2 contains a Factor X_A site, which is in reading frame with GST and CagF and can also be used to cleave CagF.
4. Coexpression of GST-CagF and CagA could be achieved by placing them in MCS1 and MCS2 of the modified pRSFDuet-1. However, expression in BL21(DE3) does not produce any protein. Replacing the T7 promoter controlling expression of GST-CagF with a *tac* promoter promotes GST-CagF expression, though no expression of CagA is observed. We only find expression of both CagA and CagF when they are expressed on different vectors. Expression of proteins either from the same

plasmid or on separate plasmids should be considered if no protein expression is observed for the method one chooses to follow.

5. Cells containing multiple plasmids are typically more sensitive to antibiotic selection and concentrations should be halved.
6. Lysing BL21(DE3)+pCAGA-CagA/pGEX-5×-2-CagF cells which have been suspended in a cell extract of lysed BL21(DE3)+pGEX-5×-2-CagF ensures an excess of GST-CagF to bind free CagA and suppress degradation.
7. We have tried several methods to remove CagF from CagA including lower concentrations of urea (1.0 and 1.5 M) and high concentrations of NaCl (3.0 M). However, CagF was not fully removed from CagA after 2 days of washing the Ni-NTA agarose.
8. Typically, we would use the protein that eluted from the Ni-NTA agarose in isothermal titration calorimetry after dialysis and not perform size exclusion chromatography. This is due without CagF present; CagA starts to degrade within 2 days. We note that for unknown reasons, CagA degradation is accelerated in phosphate buffers and should be avoided once CagF is removed.
9. We observed by leaving CagL to refold longer in the REDOX buffer suppresses dimerization though formation of intermolecular disulfides by allowing reshuffling of the disulfides to form intramolecular disulfides.
10. Centrifugation of the plate should be carried out at room temperature to prevent condensation forming on the optical film, which may affect the fluorescence readings in the RT PCR.
11. SYPRO Orange has both a broad excitation and emission. Select an emission filter that encompasses the 600–630 nm range, such as ROX (610 nm) or Cy3 (615 nm).
12. A protein melting curve should show a low initial fluorescence which increases with temperature as the dye binds to unfolding of the protein and begins to fluoresce, reaches a maximum when all the protein is unfolded, and then slowly decrease as the dye dissociates from the unfolded protein. However, several types of curves may present themselves; (1) No transition is observe due to the protein having a higher melting temperature than the experiment; (2) Several transitions may occur suggesting either oligomerization of multi-domain unfolding or; (3) A high fluorescent background with a small transition suggesting that the protein is not folded or hydrophobic patches occur on the surface. In these cases the protein should be either refolded using a different method if you suspect the protein is still unfolded or screen different ratios of protein to

SYPRO Orange. For instance 1 mg/mL of protein to 1× SYPRO Orange if the background is too high or 10× SYPRO Orange if the transition is not clear.

References

1. Peek RM Jr, Blaser MJ (2002) *Helicobacter pylori* and gastrointestinal tract adenocarcinomas. Nat Rev Cancer 2(1):28–37
2. Blaser MJ, Perez-Perez GI, Kleanthous H, Cover TL, Peek RM, Chyou PH, Stemmermann GN, Nomura A (1995) Infection with *Helicobacter pylori* strains possessing cagA is associated with an increased risk of developing adenocarcinoma of the stomach. Cancer Res 55(10):2111–2115
3. Wen S, Moss SF (2009) *Helicobacter pylori* virulence factors in gastric carcinogenesis. Cancer Lett 282(1):1–8
4. de Bernard M, Arico B, Papini E, Rizzuto R, Grandi G, Rappuoli R, Montecucco C (1997) *Helicobacter pylori* toxin VacA induces vacuole formation by acting in the cell cytosol. Mol Microbiol 26(4):665–674
5. Odenbreit S, Puls J, Sedlmaier B, Gerland E, Fischer W, Haas R (2000) Translocation of *Helicobacter pylori* CagA into gastric epithelial cells by type IV secretion. Science 287(5457):1497–1500
6. Fischer W, Puls J, Buhrdorf R, Gebert B, Odenbreit S, Haas R (2001) Systematic mutagenesis of the *Helicobacter pylori* cag pathogenicity island: essential genes for CagA translocation in host cells and induction of interleukin-8. Mol Microbiol 42(5):1337–1348
7. Yamaoka Y, El-Zimaity HM, Gutierrez O, Figura N, Kim JG, Kodama T, Kashima K, Graham DY (1999) Relationship between the cagA 3′ repeat region of *Helicobacter pylori*, gastric histology, and susceptibility to low pH. Gastroenterology 117(2):342–349
8. Hayashi T, Senda M, Morohashi H, Higashi H, Horio M, Kashiba Y, Nagase L, Sasaya D, Shimizu T, Venugopalan N, Kumeta H, Noda NN, Inagaki F, Senda T, Hatakeyama M (2012) Tertiary structure-function analysis reveals the pathogenic signaling potentiation mechanism of *Helicobacter pylori* oncogenic effector CagA. Cell Host Microbe 12(1):20–33
9. Kaplan-Turkoz B, Jimenez-Soto LF, Dian C, Ertl C, Remaut H, Louche A, Tosi T, Haas R, Terradot L (2012) Structural insights into *Helicobacter pylori* oncoprotein CagA interaction with β1 integrin. Proc Natl Acad Sci U S A 109(36):14640–14645
10. Backert S, Tegtmeyer N (2012) *Helicobacter pylori* CagA tertiary structure reveals functional insights. Cell Host Microbe 12(1):3–5
11. Hohlfeld S, Pattis I, Puls J, Plano GV, Haas R, Fischer W (2006) A C-terminal translocation signal is necessary, but not sufficient for type IV secretion of the *Helicobacter pylori* CagA protein. Mol Microbiol 59(5):1624–1637
12. Pattis I, Weiss E, Laugks R, Haas R, Fischer W (2007) The *Helicobacter pylori* CagF protein is a type IV secretion chaperone-like molecule that binds close to the C-terminal secretion signal of the CagA effector protein. Microbiology 153(Pt 9):2896–2909
13. Bonsor DA, Weiss E, Iosub-Amir A, Reingewertz TH, Chen TW, Haas R, Friedler A, Fischer W, Sundberg EJ (2013) Characterization of the translocation-competent complex between the *Helicobacter pylori* oncogenic protein CagA and the accessory protein CagF. J Biol Chem 288(46):32897–32909
14. Couturier MR, Tasca E, Montecucco C, Stein M (2006) Interaction with CagF is required for translocation of CagA into the host via the *Helicobacter pylori* type IV secretion system. Infect Immun 74(1):273–281
15. Angelini A, Tosi T, Mas P, Acajjaoui S, Zanotti G, Terradot L, Hart DJ (2009) Expression of *Helicobacter pylori* CagA domains by library-based construct screening. FEBS J 276(3):816–824
16. Rohde M, Puls J, Buhrdorf R, Fischer W, Haas R (2003) A novel sheathed surface organelle of the *Helicobacter pylori* cag type IV secretion system. Mol Microbiol 49(1):219–234
17. Shaffer CL, Gaddy JA, Loh JT, Johnson EM, Hill S, Hennig EE, McClain MS, McDonald WH, Cover TL (2011) *Helicobacter pylori* exploits a unique repertoire of type IV secretion system components for pilus assembly at the bacteria-host cell interface. PLoS Pathog 7(9):e1002237
18. Kwok T, Zabler D, Urman S, Rohde M, Hartig R, Wessler S, Misselwitz R, Berger J, Sewald N, Konig W, Backert S (2007) Helicobacter exploits integrin for type IV secretion and kinase activation. Nature 449(7164):862–866
19. Conradi J, Huber S, Gaus K, Mertink F, Royo Gracia S, Strijowski U, Backert S, Sewald N

(2012) Cyclic RGD peptides interfere with binding of the *Helicobacter pylori* protein CagL to integrins αVβ3 and α5β1. Amino Acids 43(1):219–232

20. Wiedemann T, Hofbaur S, Tegtmeyer N, Huber S, Sewald N, Wessler S, Backert S, Rieder G (2012) *Helicobacter pylori* CagL dependent induction of gastrin expression via a novel αVβ5-integrin-integrin linked kinase signalling complex. Gut 61(7):986–996
21. Barden S, Niemann HH (2015) Adhesion of several cell lines to *Helicobacter pylori* CagL Is mediated by integrin αVβ6 via an RGDLXXL motif. J Mol Biol 427(6 Pt B):1304–1315
22. Barczyk M, Carracedo S, Gullberg D (2010) Integrins. Cell Tissue Res 339(1):269–280
23. Barden S, Lange S, Tegtmeyer N, Conradi J, Sewald N, Backert S, Niemann HH (2013) A helical RGD motif promoting cell adhesion: crystal structures of the *Helicobacter pylori* type IV secretion system pilus protein CagL. Structure 21(11):1931–1941
24. Barden S, Schomburg B, Conradi J, Backert S, Sewald N, Niemann HH (2014) Structure of a three-dimensional domain-swapped dimer of the *Helicobacter pylori* type IV secretion system pilus protein CagL. Acta Crystallogr D Biol Crystallogr 70(Pt 5):1391–1400
25. Bonsor DA, Pham KT, Beadenkopf R, Diederichs K, Haas R, Beckett D, Fischer W, Sundberg EJ (2015) Integrin engagement by the helical RGD motif of the *Helicobacter pylori* CagL protein is regulated by pH-induced displacement of a neighboring helix. J Biol Chem 290(20):12929–12940
26. Bross P, Andresen BS, Winter V, Krautle F, Jensen TG, Nandy A, Kolvraa S, Ghisla S, Bolund L, Gregersen N (1993) Co-overexpression of bacterial GroESL chaperonins partly overcomes non-productive folding and tetramer assembly of E. coli-expressed human medium-chain acyl-CoA dehydrogenase (MCAD) carrying the prevalent disease-causing K304E mutation. Biochim Biophys Acta 1182(3):264–274
27. Maskos K, Huber-Wunderlich M, Glockshuber R (2003) DsbA and DsbC-catalyzed oxidative folding of proteins with complex disulfide bridge patterns in vitro and in vivo. J Mol Biol 325(3):495–513
28. Ramm K, Pluckthun A (2000) The periplasmic Escherichia coli peptidylprolyl cis,trans-isomerase FkpA. II. Isomerase-independent chaperone activity in vitro. J Biol Chem 275(22):17106–17113
29. Bothmann H, Pluckthun A (2000) The periplasmic Escherichia coli peptidylprolyl cis,trans-isomerase FkpA. I. Increased functional expression of antibody fragments with and without cis-prolines. J Biol Chem 275(22):17100–17105
30. Ireton GC, Stoddard BL (2004) Microseed matrix screening to improve crystals of yeast cytosine deaminase. Acta Crystallogr D Biol Crystallogr 60(Pt 3):601–605
31. Saridakis E, Khurshid S, Govada L, Phan Q, Hawkins D, Crichlow GV, Lolis E, Reddy SM, Chayen NE (2011) Protein crystallization facilitated by molecularly imprinted polymers. Proc Natl Acad Sci U S A 108(27):11081–11086
32. Rayment I, Rypniewski WR, Schmidt-Base K, Smith R, Tomchick DR, Benning MM, Winkelmann DA, Wesenberg G, Holden HM (1993) Three-dimensional structure of myosin subfragment-1: a molecular motor. Science 261(5117):50–58
33. Wernimont A, Edwards A (2009) In situ proteolysis to generate crystals for structure determination: an update. PLoS One 4(4):e5094
34. Ericsson UB, Hallberg BM, Detitta GT, Dekker N, Nordlund P (2006) Thermofluor-based high-throughput stability optimization of proteins for structural studies. Anal Biochem 357(2):289–298
35. Dupeux F, Rower M, Seroul G, Blot D, Marquez JA (2011) A thermal stability assay can help to estimate the crystallization likelihood of biological samples. Acta Crystallogr D Biol Crystallogr 67(Pt 11):915–919
36. Niesen FH, Berglund H, Vedadi M (2007) The use of differential scanning fluorimetry to detect ligand interactions that promote protein stability. Nat Protoc 2(9):2212–2221

Part III

Genetics and Phylogenetics of Bacterial Pathogens

Chapter 7

Development of a Single Locus Sequence Typing (SLST) Scheme for Typing Bacterial Species Directly from Complex Communities

Christian F.P. Scholz and Anders Jensen

Abstract

The protocol describes a computational method to develop a Single Locus Sequence Typing (SLST) scheme for typing bacterial species. The resulting scheme can be used to type bacterial isolates as well as bacterial species directly from complex communities using next-generation sequencing technologies.

Key words SLST, MLST, Core-genome, Bioinformatics, Genomics, Bacterial typing, Sequencing

1 Introduction

Bacteria are ubiquitous and found in every environment of the Earth's biosphere where they are responsible for numerous biological activities [1]. In addition, the microorganisms of the human body have been related to disease as well as health [2]. Recent research has shown that dysbiosis of the human microbiome may be responsible for many human disorders. For example, type 2 diabetes, obesity, and some immune related diseases are associated with specific groups of bacteria in the human gut microbiome [2–6]. Similarly, specific groups of bacteria in the oral microbiome are associated with oral/dental diseases like gingivitis and periodontitis [7–9]. While these are examples of diseases where groups of bacteria, at taxonomic ranks higher than species level, interact with the human body, there are also many examples of diseases that are related to a specific bacterial species or even specific strains/types within a bacterial species [10–12]. In addition, different strains/types of bacteria often possess distinctive virulence factors that are related to their potential to cause disease. Identification of bacterial isolates is mainly done using a few biochemical tests, MALDI-TOF, or sequencing of the 16S rRNA gene) [13], but for many bacterial species, e.g., *Streptococcus* species, biochemical analysis

Pontus Nordenfelt and Mattias Collin (eds.), *Bacterial Pathogenesis: Methods and Protocols*, Methods in Molecular Biology, vol. 1535, DOI 10.1007/978-1-4939-6673-8_7,

and 16S rRNA sequences lack discriminatory power to resolve bacterial species from each other [14, 15]. As an alternative to 16S rRNA, multilocus sequence typing/analysis (MLST/MLSA) has shown to be a suitable tool for identification and typing of bacterial isolates with superior resolution [16, 17]. Based on phylogenetic reconstructions based on several housekeeping genes, MLSA has been used to identify bacterial species from many different genera, which cannot be identified by biochemical test or 16S rRNA sequences [18–21].

While the identification and typing of bacterial isolates may be difficult, comprehensive identification and characterization of bacteria in vivo directly from complex microbial communities is even more difficult. However, recent advances in second-generation sequencing technologies like 454 pyrosequencing and Illumina sequencing have revolutionized the capability to characterize and identify the taxa in a complex microbial community with references to databases of 16S rRNA gene sequences [22]. Currently, the most commonly used approach to characterize and identify bacteria in complex environments is to partial sequence the 16S rRNA gene using universally conserved primers [23]. However, due to the high similarity of 16S rRNA gene sequences among different bacteria and the short read length produced by next generation methods such as 454 pyrosequencing and Illumina, this approach can only confidently identify bacteria at high taxonomic levels (e.g., genus and family) [24]. Few studies have tried to develop different methods to retrieve species-level information from 16S rRNA sequences derived from complex communities using next-generation sequencing technologies. Eren et al. [25] used Shannon entropy to identify information-rich nucleotide positions in V1-V3- and V3-V5 data from Human Microbiome Project. The resulting oligotypes could be associated with species taxon names by using the curated Human Oral Microbiome Database [26]. Other studies have also shown that species-level information is present in the partial 16S rRNA gene sequences, but is most applicable in well-described communities [27, 28]. Shotgun metagenome sequencing using next-generation sequencing technologies has also proven capable of describing bacterial communities at species—or even type/strain level in several occasions. Tu et al. [29] used a novel k-mer approach to identify genome specific markers from metagenome sequencing, allowing them to identify specific strains in the gastrointestinal tract associated with type 2 diabetes patients and obese/lean individuals. Recently, Joseph et al. [30] developed a method to type *Staphylococcus aureus* directly from shotgun metagenomic data. While typing from metagenomic data seems very promising it is applicable only to taxa that are relatively abundant in the samples, which also limits the number of samples) that can be multiplexed and sequenced simultaneously. These limitations can be overcome by amplifying

species/strain specific genes directly from samples of complex communities before sequencing. Drevinek et al. [31] were able to type strains of the *Burkholderia cepacia* Complex from sputum samples of cystic fibrosis patients by MLST. However, as MLST uses several loci for typing, MLST schemes can only be applied to complex samples if a single type of the bacterial species of interest is present in the sample. Alternatively, a single locus may be used for typing of bacteria in complex communities where several different types of the same species are present simultaneously.

Here, we describe a computational method to identify single loci within the genome, which may have comparable typing resolution to MLST. The method, called single locus sequence typing (SLST), is designed for bacterial species with a nearly clonal population structure and has previously been described for the human skin bacterium *Propionibacterium acnes* [32], for which specific types have been associated with disease [33].

2 Materials

2.1 Prerequisites

It is a prerequisite for this protocol that:

1. The target species should be clonal with minimum degree of genetic recombination.
2. The number of available whole genome sequences should cover the known genetic diversity.

2.2 Genome Sequences

The method described here is basically a genome-wide search for a single locus that best describes the phylogenetic diversity of a given species represented by the core-genome. Therefore, to perform this analysis it is a prerequisite that whole-genome sequences covering the known phylogenetic variation of the species are available. Genome sequences can be downloaded from NCBI or other similar databases) (*see* **Note 1**).

2.3 Software

Python [34] will be used to demonstrate implementation of the methods used. However, most scripting/programming language can be used. The NCBI Blast+suite [35] is used for extraction of locus sequences from genomes. Multiple alignments of FASTA files are performed using Muscle [36].

3 Methods

3.1 Designing a Single Locus Typing Scheme

Whether the SLST scheme has to reflect an existing MLST scheme or the phylogenetic relationship between strains, a good reference tree is essential. For this protocol we describe a method to generate a reference core genome tree using whole genome sequences.

3.1.1 Establishing a Reference Tree

The following method generates a core-genome tree from unannotated whole genome sequences without any knowledge of the specific genes within the genomes. To make a tree based on all shared sequences of the included genomes choose any genome and slice it into segments of 200 bp. *See* python Code 1 for a slicing script example. Store the fragments in a multi FASTA-file using unique headers for all fragments (e.g., ">strain_start_end"). This file will be used to extract homologous sequences from the other genomes. For this task blastn of the BLAST+ suite will be used [35]. Code 2 demonstrates how Python can interact with blastn to automate a repetitive blasting process) (*see* **Note 2**). Store all homologous sequences from the included genomes in a multi-FASTA-file, where each genome should be given the exact same header, e.g., strain name, across the different fragment files (this step is important for later concatenation of the fragments). Align the resulting multi-FASTA files separately using muscle from the command-line (e.g., "muscle-in fragment0_200.fas-out fragment0_200.fas"). Note, Python has several libraries for multi-threading, blast searches and alignments may be run in parallel on a multi-core computer to speed up the process. Following the alignment, the fragments need to be concatenated into a single sequence for each genome (*see* Code 3). The concatenated sequences can now be used to generate a phylogenetic tree in a bioinformatic software package like Mega [37] or Ugene [38].

3.1.2 Deciding on Target Locus Size

The locus size is very important, as it dictates which sequencing technology and experimental designs can be used. Locus size is also directly linked to the theoretical maximum resolution of the scheme. Using a size around 500 bp, the typing scheme can both be used for typing of isolates with the Sanger sequencing

```
>>> def slice(sequence, jump=200, size=200):
...     start = 0
...     end = size
...     while len(sequence) >= end:
...         yield sequence[start:end]
...         start += jump
...         end += jump
...
>>> genome = 'ATGGTAGTAGTACCTCAGCTG'
>>> for seq in slice(genome, jump=6, size=6):
...     print(seq)
...
ATGGTA
      GTAGTA
            CCTCAG
```

Code 1 Note that the variable "genome" is an exemplified genome sequence. The variable should point to an already opened and parsed FASTA-file)

```
>>> def blast_extraction(fragments_fasta_path, genome_fasta_path):
...     from subprocess import check_output
...     cmd = ('blastn -query "' + candidate_fasta_path +
...     '" -outfmt "6 std" -subject "' + genome_fasta_path + '"')
...     p = check_output(cmd, shell=True).decode('ascii')
...     lasthit = 'None'
...     for hit in p.split('\n'):
...         value = hit.split('\t')
...         if len(value)>1 and value[0] != lasthit:
...             print('Candidate %s found in %s between nt %s and %s'
...                   % (value[0], value[1], value[8], value[9],))
...             lasthit = value[0]
...
>>> blast_extraction('./fragments.fasta', './strain06.fasta')
```

Code 2 A simplified blast script. Note, the script will only print the first hit for each query sequence

```
>>> def concat(fragments):
...     out = {}
...     count = 0
...     for frag in fragments:
...         for f in frag:
...             try:
...                 out[f] += frag[f]
...             except KeyError:
...                 out[f] = count*'-' + frag[f]
...         count = max([len(out[i]) for i in out])
...         for n in out:
...             while len(out[n]) < count:
...                 out[n] += '-'
...     return out
...
>>> fragA = {'strain7':'AT', 'strain9':'ATC'}
>>> fragB = {'strain7':'TTT', 'strain9':'TTA'}
>>> concat([fragA, fragB,])
```

Code 3 Note that the variables "fragA" and "fragB" are examples of aligned fragment files (of two strains each) that have been opened and parsed into dictionaries, so that the headers are keys to the corresponding sequences. The "concat" function is given a list of dictionaries and returns the concatenated sequences as a single dictionary

technology as well as for typing of the species in vivo in complex communities using 454 pyrosequencing or Illumina paired-end sequencing. While discriminatory sequence variation within the locus is necessary for typing, a conserved region upstream and downstream is important for designing specific primers. Furthermore, one should design the primers having in mind that the first 20–40 nucleotides in Sanger sequencing are of low quality. To optimize for price per sequence/sample, a locus of around 400 bp may be preferred, as this allows the use of Illumina sequencing technology, which generates more short-read sequences and at

a lower cost compared to the longer reads of 454 pyrosequencing. However, in the interest of keeping a high resolution comparable to the core-genome tree, 400 bp was not sufficient for the SLST scheme of *P. acnes* [32].

3.1.3 Fragmenting the Genomes)

To locate all candidates spanning the defined locus size (x) a reference genome will be used. The sequence will serve as query sequence for blastn (*see* **Note 3**). To test all possible windows of x nucleotides throughout the genome a "sliding window" approach is used. This means the first candidate will start at nucleotide one and end after x nucleotides, the next will start at the second nucleotide and end at $x+1$. This will result in a large number of candidates for evaluation (*see* **Note 4**). For a closed genome this number will be "genome size in bases minus x" candidates. Here, the slice function defined in Subheading 3.1.1 above can be reused by changing the variables (*see* Code 4). The resulting candidates should be named uniquely (e.g., ">strain_name_start_end") and stored in a multi-FASTA-file. This file will then be used to extract homologous sequences from the other genomes using blastn from the BLAST+ suite [35]. A simple script for retrieving hit-results from blastn is demonstrated above in Code 2. Generate one multi-FASTA-file for each candidate containing homologous sequences from the other genomes. Sequence within the files should be labeled with the corresponding genome name.

3.1.4 Filtering Out Candidates

To reduce the number of candidate FASTA-files to a few candidates that mirror the phylogeny of the reference tree, a set of different filters is applied. Firstly, all candidate files, which do not contain sequences from all genomes, should be removed (*see* **Note 5**). Secondly, all candidates with variation in number of gaps beyond a certain threshold should be removed (e.g., 6 nt). Thirdly, implement a "blacklist" (*see* Code 5). From the reference tree pairs of two strains that are located in phylogenetically distinct clusters can be identified (Fig. 1). Note that a type in the SLST scheme is defined by a unique sequence that differs by one or more bases from other sequence types. The candidates are filtered out if the "blacklisted" pairs have identical sequence-types (*see* Code 5). Start with a few pairs, and gradually include more pairs to decrease the number of

```
>>> for window in slice(genome, jump=1, size=19):
...     print(seq)
...
ATGGTAGTAGTACCTCAGC
 TGGTAGTAGTACCTCAGCT
  GGTAGTAGTACCTCAGCTG
```

Code 4 The "slice" function defined in Code 3 is reused, and to implement the sliding window approach the "jump" variable is lower than the "size" variable. Note that the locus size is set to 19 bp for simplification of the example

```
>>> def filter(cand):
...     blacklist = [('strain1', 'strain9'),
...                  ('strain4', 'strain5'),]
...     for pair in blacklist:
...         if cand[pair[0]] == cand[pair[1]]:
...             return False
...     return True
...
>>> cand1 = {'strain1':'ATG',
...          'strain9':'ATC',
...          'strain4':'ATT',
...          'strain5':'ATG',}
>>> filter(cand1)
True
```

Code 5 The function "filter" takes a candidate locus in the form of a dictionary where the keys are strain names for their corresponding sequences and returns a boolean "True" if the candidate is able to discriminate between all the pairs defined in the variable "blacklist." Sequences are 3 bp long for simplification of the example)

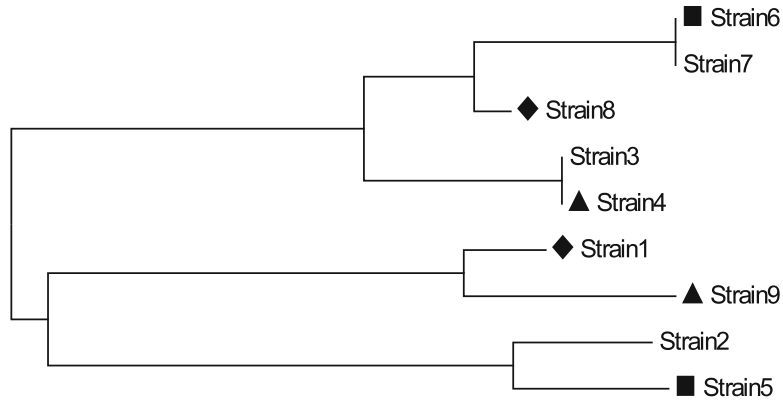

Fig. 1 An exemplified core-genome tree of nine strains demonstrating the selection of blacklist pairs. In this example, strains 5 and 6 (indicated by *black squares*) should have different sequence types. Similarly, the pairs 4/9 and 1/8 should at least be separated by one nucleotide

candidates. You may find that some pairs eliminate all candidates. However, this is expected, as an ideal typing scheme may not exist, but you may find an applicable scheme by removing that pair. By adding new pairs in iterations, the candidate-list will be reduced and should ideally return less than ten candidates) (*see* **Note 6**).

3.1.5 Choosing the Best Candidate for Validation

There is no exact method to select the best candidate after the filtering process. One way is, by manual inspection, to determine whether the remaining candidates reflect the phylogenetic tree

structure as found in the reference tree. Potential conflicts may be resolved by shifting the locus right or left, or by increasing/decreasing the locus size. The sequence integrity (indels) should also be taken into account before deciding on the final candidate/locus. Finally, the feasibility of finding a conserved region for primers in the near vicinity of the chosen locus is important (*see* **Note 7**). There are many tools available for designing PCR primers. However, using primer-blast [39] from NCBI you will have the option to check if your primers are specific for the intended group of strains/bacteria, which is essential if used on a complex sample.

3.1.6 Validation of the SLST Scheme

Searching the whole genome introduces the risk that the resulting SLST scheme achieved the wanted separation by chance. Therefore, it is advisable to verify the new SLST scheme including the selected primer pair using a set of strains, where the phylogeny and sequence type from MLST is known. This could be performed by Sanger sequencing the new locus from strains previously typed by MLST or genome sequenced).

3.2 Applications of SLST Schemes

An SLST scheme provides a unique and simple method to type isolates as well as to determine the clonal diversity of a species in a complex sample. Typing of bacterial isolates using the developed SLST scheme by PCR and Sanger sequencing is simple, cheap, and straightforward compared to, e.g., MLST where normally seven genes have to be amplified and sequenced. The most important use of a well-designed SLST scheme is that it can be used to type the species directly from samples. Samples taken from an environment with a complex bacterial community, like the skin, can directly be analyzed for the presence of different SLST types using the SLST scheme after DNA extraction, PCR amplification, and finally sequencing in a high-throughput sequencer like 454 pyrosequencing. We have previously used an SLST scheme for the skin bacteria *P. acnes* to demonstrate how it can be used to provide "unbiased" typing of *P. acnes* across different skin sites where different SLST types of *P. acnes* are present simultaneously [32].

3.2.1 Establishing a Database

Finally, for optimal utilization of the developed SLST)scheme a public database has to be established and maintained by dedicated curators. New types will be found and need to be screened for sequencing errors or ambiguous base calling (*see* **Note 8**). The curator should validate raw data files (e.g., forward and reverse Sanger reads in AB1 files) before inclusion of new types. Furthermore, it is increasingly imperative to establish a policy of how to handle new types acquired from whole-genome sequencing or single reads of next-generation sequencers. Strain isolation and bidirectional Sanger sequencing will often be considered the gold standard for new types. However, it can be difficult to uphold such strict criteria in the light of better quality in whole-genome sequencing or in the case of a large number of identical reads in one sample.

4 Notes

1. At the NCBI databases species names of sequences are provided by the submitter to the best of their knowledge. This means that it is possible to find genomes identified only at the genus level (e.g., "*Propionibacterium* sp.") or genomes that have been incorrectly identified. This is an important realization. Firstly, including an incorrectly identified strain in the analysis will significantly reduce the number of candidate loci and secondly, there is a risk of excluding an important strain that conflict with the SLST scheme. A simple yet effective way to check this is to find few genes from a known strain and blast them against all genomes of the genus by NCBI blast. Remember to use both the "Genomes" and the "WGS" databases!
2. Blastn may return alignments missing one or two nucleotides at the edges if these do not match the query sequence. Therefore, it is advisable to check this in the script, and include missing nucleotides using the hit coordinates from the subject sequence, e.g., the genome.
3. With the described method a locus overlapping with contig breaks in the reference genome will not be evaluated. To avoid missing potential good candidates use a genome with fewest possible breaks (e.g., closed genomes).
4. This step can greatly affect the computation time of the subsequent analysis. If this is a concern, the "jump" of the sliding window can be increased to two or more nucleotides. This will dramatically reduce the number of candidates under assumption that a few nucleotides at the edges will not change the final choice of typing scheme).
5. It may be more appropriate to filter out candidates with less than 50–80% of the included strains, especially if unclosed genomes are used.
6. Remember to inspect the remaining candidates as they are reduced in numbers. A list of 100–200 candidates may actually represent just a few loci overlapped by many candidates (*see*, e.g., Fig. 2 in ref. 32). In an exemplified case, two remaining candidates could be the same candidate, except for a single nucleotide shift at both edges. The overlapping candidates should be merged into one candidate, when the reduction of candidates has progressed sufficiently.
7. To some degree a less conserved region can be used by adding a few wobble bases, which corresponds to two or more bases, to encompass all strains in your PCR primers.
8. Only new types verified from bidirectional Sanger sequencing of isolates should be included in the database. New types found

in complex communities by next-generation sequencing should in most cases be dismissed, due to the number of sequencing errors introduced by new sequencing technologies.

References

1. Gruber N, Galloway JN (2008) An Earth-system perspective of the global nitrogen cycle. Nature 451:293–296
2. Cho I, Blaser MJ (2012) The human microbiome: at the interface of health and disease. Nat Rev Genet 13:260–270
3. Hartstra AV, Bouter KEC, Bäckhed F, Nieuwdorp M (2015) Insights into the role of the microbiome in obesity and type 2 diabetes. Diabetes Care 38:159–165
4. Ley RE (2010) Obesity and the human microbiome. Curr Opin Gastroenterol 26:5–11
5. Proal AD, Albert PJ, Marshall TG (2013) The human microbiome and autoimmunity. Curr Opin Rheumatol 25:234–240
6. Round JL, Mazmanian SK (2009) The gut microbiota shapes intestinal immune responses during health and disease. Nat Rev Immunol 9:313–323
7. Liu B, Faller LL, Klitgord N et al (2012) Deep sequencing of the oral microbiome reveals signatures of periodontal disease. PLoS ONE 7:e37919
8. Peterson SN, Snesrud E, Liu J et al (2013) The dental plaque microbiome in health and disease. PLoS ONE 8:e58487
9. Wade WG (2013) The oral microbiome in health and disease. Pharmacol Res 69:137–143
10. Haubek D, Ennibi O-K, Poulsen K et al (2008) Risk of aggressive periodontitis in adolescent carriers of the JP2 clone of *Aggregatibacter* (*Actinobacillus*) *actinomycetemcomitans* in Morocco: a prospective longitudinal cohort study. Lancet 371:237–242
11. Kazakova SV, Hageman JC, Matava M et al (2005) A clone of methicillin-resistant *Staphylococcus aureus* among professional football players. N Engl J Med 352:468–475
12. Karch H, Tarr PI, Bielaszewska M (2005) Enterohaemorrhagic *Escherichia coli* in human medicine. Int J Med Microbiol 295:405–418
13. Sabat AJ, Budimir A, Nashev D et al (2013) Overview of molecular typing methods for outbreak detection and epidemiological surveillance. Euro Surveill 18:20380
14. Richter M, Rosselló-Móra R (2009) Shifting the genomic gold standard for the prokaryotic species definition. Proc Natl Acad Sci 106:19126–19131
15. Scholz CFP, Poulsen K, Kilian M (2012) Novel molecular method for identification of *Streptococcus pneumoniae* applicable to clinical microbiology and 16S rRNA sequence-based microbiome studies. J Clin Microbiol 50:1968–1973
16. Maiden MCJ (2006) Multilocus sequence typing of bacteria. Annu Rev Microbiol 60:561–588
17. Maiden MCJ, Bygraves JA, Feil E et al (1998) Multilocus sequence typing: a portable approach to the identification of clones within populations of pathogenic microorganisms. Proc Natl Acad Sci U S A 95:3140–3145
18. Bishop CJ, Aanensen DM, Jordan GE et al (2009) Assigning strains to bacterial species via the internet. BMC Biol 7:3
19. Gevers D, Cohan FM, Lawrence JG et al (2005) Re-evaluating prokaryotic species. Nat Rev Microbiol 3:733–739
20. Glaeser SP, Kämpfer P (2015) Multilocus sequence analysis (MLSA) in prokaryotic taxonomy. Syst Appl Microbiol 38:237–245
21. Sawabe T, Kita-Tsukamoto K, Thompson FL (2007) Inferring the evolutionary history of vibrios by means of multilocus sequence analysis. J Bacteriol 189:7932–7936
22. Shendure J, Ji H (2008) Next-generation DNA sequencing. Nat Biotechnol 26:1135–1145
23. Wang Y, Qian P-Y (2009) Conservative fragments in bacterial 16S rRNA genes and primer design for 16S ribosomal DNA amplicons in metagenomic studies. PLoS ONE 4:e7401
24. Schloss PD, Westcott SL (2011) Assessing and improving methods used in operational taxonomic unit-based approaches for 16S rRNA gene sequence analysis. Appl Environ Microbiol 77:3219–3226
25. Eren AM, Borisy GG, Huse SM, Mark Welch JL (2014) Oligotyping analysis of the human oral microbiome. Proc Natl Acad Sci U S A 111:E2875–E2884
26. Chen T, Yu W-H, Izard J et al (2010) The human oral microbiome database: a web accessible resource for investigating oral microbe taxonomic and genomic information. Database 2010:baq013.
27. Conlan S, Kong HH, Segre JA (2012) Species-level analysis of DNA sequence data from the

NIH human microbiome project. PLoS ONE 7:e47075

28. Jensen A, Fagö-Olsen H, Sørensen CH, Kilian M (2013) Molecular mapping to species level of the tonsillar crypt microbiota associated with health and recurrent tonsillitis. PLoS ONE 8:e56418
29. Tu Q, He Z, Zhou J (2014) Strain/species identification in metagenomes using genome-specific markers. Nucleic Acids Res 42:e67
30. Joseph SJ, Li B, Petit RA et al (2015) The single-species metagenome: subtyping *Staphylococcus aureus* core genome sequences from shotgun metagenomic data. bioRxiv 030692
31. Drevinek P, Vosahlikova S, Dedeckova K et al (2010) Direct culture-independent strain typing of *Burkholderia cepacia* complex in sputum samples from patients with cystic fibrosis. J Clin Microbiol 48:1888–1891
32. Scholz CFP, Jensen A, Lomholt HB et al (2014) A novel high-resolution single locus sequence typing scheme for mixed populations of *Propionibacterium acnes* in vivo. PLoS ONE 9:e104199
33. Lomholt HB, Kilian M (2010) Population genetic analysis of *Propionibacterium acnes* identifies a subpopulation and epidemic clones associated with acne. PLoS ONE 5:e12277
34. Welcome to Python.org. In: Python.org. https://www.python.org/. Accessed 28 Nov 2015
35. Camacho C, Coulouris G, Avagyan V et al (2009) BLAST+: architecture and applications. BMC Bioinformatics 10:421
36. Edgar RC (2004) MUSCLE: multiple sequence alignment with high accuracy and high throughput. Nucleic Acids Res 32:1792–1797
37. Tamura K, Stecher G, Peterson D et al (2013) MEGA6: molecular evolutionary genetics analysis version 6.0. Mol Biol Evol 30:2725–2729
38. Okonechnikov K, Golosova O, Fursov M, UGENE Team (2012) Unipro UGENE: a unified bioinformatics toolkit. Bioinformatics 28:1166–1167
39. Ye J, Coulouris G, Zaretskaya I et al (2012) Primer-BLAST: a tool to design target-specific primers for polymerase chain reaction. BMC Bioinformatics 13:134

Chapter 8

Reconstructing the Ancestral Relationships Between Bacterial Pathogen Genomes

Caitlin Collins and Xavier Didelot

Abstract

Following recent developments in DNA sequencing technology, it is now possible to sequence hundreds of whole genomes from bacterial isolates at relatively low cost. Analyzing this growing wealth of genomic data in terms of ancestral relationships can reveal many interesting aspects of the evolution, ecology, and epidemiology of bacterial pathogens. However, reconstructing the ancestry of a sample of bacteria remains challenging, especially for the majority of species where recombination is frequent. Here, we review and describe the computational techniques currently available to infer ancestral relationships, including phylogenetic methods that either ignore or account for the effect of recombination, as well as model-based and model-free phylogeny-independent approaches.

Key words Pathogen genomics, Population structure, Bacterial recombination, Phylogenetics, Ancestral inference, Comparative genomics

1 Introduction

Owing to rapid progress in DNA sequencing technologies, bacterial whole genome sequence data is becoming increasingly available [1, 2]. The genomes of many of the world's infectious pathogens are already available; yet, infectious diseases remain accountable for 23% of worldwide annual mortality [3]. Moreover, as globalization continues to increase the rate and scope of human interaction, with each other, and with animals, the evidence suggests this process will be accompanied by parallel change in the spread and evolution of infectious pathogens [4–7].

Reconstructing the ancestral relationships between bacterial isolates can help in answering a wide range of questions, such as:

1. What historical processes gave rise to the patterns of antibiotic resistance and serotype dynamics observed in *Streptococcus pneumoniae*? [8].

Pontus Nordenfelt and Mattias Collin (eds.), *Bacterial Pathogenesis: Methods and Protocols*, Methods in Molecular Biology, vol. 1535, DOI 10.1007/978-1-4939-6673-8_8,

2. What is the effective population size of *Escherichia coli*? [9] And what impact does this have on its evolution? [10].
3. How old are bacterial pathogens, for example *Yersinia pestis*? [11].
4. Does host association in *Campylobacter coli* have an evolutionary basis or can the observed genetic association be attributed to identity by descent? [12].
5. What genetic and phenotypic state most likely characterized the common ancestor of divergent *Staphylococcus aureus* lineages? [13].
6. Can transmission events be reconstructed from one individual to another, for example in *Mycobacterium tuberculosis*? [14].

As these questions make evident, a better picture of the genetic ancestry of bacterial isolates can greatly improve our understanding of infectious pathogens and their evolution as agents of disease. We define "genetic ancestry" quite broadly in the context of bacteria. In human genetics, a distinction is drawn between "ancestral" relationships (deep-rooted in the evolutionary past) and "familial" relationships (occurring at present or in the recent past) [15]. This distinction is sensibly enforced in sexually recombining, outbreeding human populations as different methods may be needed to elucidate genealogies (at the individual level) and phylogenies (at the population level) [16]. Clonal inheritance in bacterial populations, by contrast, allows us to consider genetic relatedness at all levels and on any timescale to be a suitable target for methods attempting to reconstruct "ancestral relationships" between genomes.

At present, a wide array of analytical methods can be applied to bacterial genomes for the purpose of reconstructing the ancestral relationships between bacterial isolates. Furthermore, the parallel advancement in computational efficiency and the increasing accessibility of relevant software platforms means that these methods can be applied by a greater number of users to more sequences in less time. Here, we present the most persistent, popular, and promising methods used to elucidate the ancestral relationships between bacterial genomes.

2 Materials

2.1 Software

Table 1 contains a list of computer software that can be used to reconstruct ancestral relationships between bacterial isolates based on whole-genome sequence alignments**.** Details of how these software work are given in Subheading 3.

Table 1
List of software for inferring ancestral relationships

Description	Name	Class	Reference	Documentation
Phylogenetic methods ignoring recombination	FastME	D	[17]	http://www.ncbi.nlm.nih.gov/CBBresearch/Desper/FastME.html
	R: *hclust*	D	[18]	https://stat.ethz.ch/R-manual/R-devel/library/stats/html/hclust.html
	R: *pvclust*	D	[19]	https://cran.r-project.org/web/packages/pvclust/pvclust.pdf
	R: *ape*	D	[20]	http://ape-package.ird.fr/
	R: *phangorn*	D, P, ML	[21]	https://cran.r-project.org/web/packages/phangorn/
	BIONJ	D	[22]	http://www.atgc-montpellier.fr/bionj/
	MEGA	D, P, ML	[23]	http://www.megasoftware.net
	PHYLIP	D, P, ML	[24]	http://evolution.genetics.washington.edu/phylip.html
	PAUP	D, P, ML	[25]	http://paup.csit.fsu.edu/
	PhyML	ML	[26]	http://www.atgc-montpellier.fr/phyml/binaries.php
	RAxML	ML	[27]	http://sco.h-its.org/exelixis/web/software/raxml/index.html
	GARLI	ML	[28]	http://www.bio.utexas.edu/faculty/antisense/garli/garli.html
	FastTree	ML	[29, 30]	http://microbesonline.org/fasttree/
	FastTree2	ML	[30]	http://microbesonline.org/fasttree/
	FastML	D, ML	[31]	http://fastml.tau.ac.il/
	MrBayes	B	[32]	http://www.molecularevolution.org/software/phylogenetics/mrbayes
	BEAST	B	[33]	http://beast.bio.ed.ac.uk/
	BEAST2	B	[34]	http://beast2.org/

(continued)

Table 1 (continued)

Description	Name	Class	Reference	Documentation
Phylogenetic methods accounting for recombination	ClonalFrame	M(B)	[35]	http://www.stats.ox.ac.uk/~didelot/files/clonalframe-userguide.pdf
	ClonalFrameML	M(ML)	[36]	http://clonalframeml.googlecode.com/
	Gubbins	M(ML)	[37]	https://github.com/sanger-pathogens/gubbins
Model-based non-phylogenetic methods	STRUCTURE	M(B)	[38, 39]	http://pritchardlab.stanford.edu/structure.html
	BAPS	M(B)	[40]	http://www.helsinki.fi/bsg/software/BAPS/
	BratNextGen	M(B)	[41]	http://www.helsinki.fi/bsg/software/BRAT-NextGen/
	ADMIXTURE	M(ML)	[42]	https://www.genetics.ucla.edu/software/admixture/
	FineStructure	M(B)	[43]	http://www.maths.bris.ac.uk/~madjl/finestructure/finestructure.html
	orderedPainting	M(B)	[44]	https://github.com/bioprojects/orderedPainting
Model-free non-phylogenetic methods	R: *ade4*	DR(PCA)	[45]	http://pbil.univ-lyon1.fr/ade4/home.php?lang=eng
	R: *adegenet*	DR(DAPC)	[46]	http://adegenet.r-forge.r-project.org/

A list of relevant software, including programs from each class of method described in Subheadings 3.1–3.4. A column named "Class" contains the following sets of abbreviations:

- D (Distance-based), P (Parsimony), ML (Maximum-likelihood), B (Bayesian)
- M( ) = Model-based (e.g., M(B) = Model-based Bayesian); DR( ) = Dimension reduction

A reference is given and a URL is provided to link the reader to relevant documentation for each item

3 Methods

3.1 Procedure Overview

While the purpose and scope of analyses that involve the reconstruction of ancestral relationships between bacterial isolates vary considerably, the following steps are usually followed:

1. Collect bacterial isolates from a pathogenic lineage or species of interest.
2. Sequence the genomes.
3. Construct an alignment of the genomes.
4. Select and run computer software that implements a method of ancestry reconstruction.
5. Estimate the reliability and uncertainty in the results.
6. Visualize the results and draw conclusions.

The aim of this chapter is to describe how genomes can be used to make inferences about ancestry in samples of bacteria. We therefore focus primarily on the second half of this procedure, though the essential elements of genome sequence alignment are introduced briefly below.

3.2 Genome Sequence Alignment

For a complete overview of the workflow involved in generating a genome sequence alignment, starting from the collection of isolates, *see* ref. [47]. The fundamental element enabling this process is the whole-genome sequencing of bacterial DNA, which has in the last few years become a much cheaper and faster than ever before, owing to the emergence of new techniques [2].The raw output of most DNA sequencing techniques is a large volume of short reads from the genome, which have to be assembled together to reveal the whole genome. The most popular approach for doing this is to map the reads to a preexisting reference genome, with the help of tools like MAQ [48]. This has the advantage that, since all genomes are mapped to the same reference, they are automatically aligned. Alternatively, *de novo* assembly can be used to join the reads together into large genomic regions called contigs, for example using Velvet [49]. An alignment can then be generated either with the aid of suitable bioinformatics software, such as Mauve [50], or by searching for the sequence of individual genes within the genomes and performing gene-by-gene alignment, for example using BIGSdb [51].

3.3 Reconstructing Ancestral Relationships

The array of existing methodological approaches designed to reconstruct ancestral relationships between bacterial isolates is vast and continues to expand. No single method has emerged as the universal "Gold Standard" within this domain. Nor should we expect one to do so. Fundamentally, the balance of strengths and limitations inherent in each approach—and, hence, the most appropriate method for inferring genetic ancestry in a given analysis—depends on the sample being analyzed.

Below, we present a description of the contending available methods. We aim to provide an objective introduction to each class of approach, and an overview of the steps required to carry out the most prominent methodological members of the following families: phylogenetic approaches, including standard methods and methods accounting for recombination, and non-phylogenetic approaches, namely model-based inference methods and model-free dimension reduction techniques.

3.4 Phylogenetic Methods Ignoring Recombination

When attempting the reconstruction of ancestral relationships between bacterial genomes, phylogenetic methods are the most obvious choice. Phylogenetic trees provide detailed representations of population structure at all levels; and, whether describing ancestral relationships on an evolutionary timescale or linking individuals genealogically, the interpretation of phylogenetic trees remains pleasingly intuitive.

Among the older and more commonly encountered phylogenetic methods are those that ignore recombination. These methods assume that the evolutionary history of all loci in the genomes of sampled isolates can be adequately described by a single (clonal) genealogy. *See* **Note 1** for a discussion of when to use standard phylogenetic methods. Table 2 compares the features of standard phylogenetic methods and can serve as a guide for selecting the best approach given the dataset in question and the goals of the analysis.

3.4.1 Distance-Based Methods

Aim: Identify the tree that results from progressive agglomerative clustering of similar individuals.

Approach:

1. Select a measure of distance between pairs of individuals.
2. Compute the distance matrix, D, composed of the distances between all pairs of sampled individuals.
3. Cluster together the two *least* genetically distant sequences.
4. Update D to reflect the grouping in (3).
5. Repeat **steps 3** and **4** until all sequences have been clustered together.

Implementations:

An array of distance-based methods exist, each relying on a unique criteria to identify the clustering order, including Complete-Linkage [57], Single-Linkage [52] and Average-Linkage Agglomerative Clustering [58], Weighted—and Unweighted Pair Group Method with Arithmetic Mean (WPGMA [58] and UPGMA [52]), Neighbour-Joining (NJ) [53].

Table 2
Comparing phylogenetic methods that ignore recombination

	Distance-based		Maximum-parsimony	Maximum-likelihood	Bayesian
Accounts for recombination	★		★	★	★
Fast	★★★★★		★★★	★★	★
Scalable[1]	★★★★★		★★★	★	★★
Flexible[2]	★★		★	★★★	★★★★★
Makes few assumptions	★★★★		★★★★★	★★	★
Allows heterogeneous evolutionary rates[3]	Other	(BIO)NJ [22]	★	★★★★★	★★★★★
	★	★★★★★			
Estimates evolutionary rates	★		★	★★★★★	★★★★★
Measure of uncertainty for tree provided	★		★	★	★★★★★
Topological accuracy (0% recombination)[4]	UPGMA [52]	NJ [53]	Parsimony [27]	ML [54]	BEAST [33]
	★★	★★★	★★★	★★★★★	★★★★★
Topological accuracy (1% recombination)[4]	UPGMA [52]	NJ [53]	Parsimony [27]	ML [54]	BEAST [33]
	★	★★	(–)	★★★★	★★★★

A comparison of the four classes of standard phylogenetic method (as discussed in Subheadings 3.1–3.4) is provided. The strengths and limitations of these approaches are examined within a five-star evaluation rubric. Bear in mind the following definitions for terms annotated within Table 2: (1) Computational efficiency not affected by dataset size; (2) Incorporates users' decisions, prior information; (3) Consistent with a model of evolution; (4) Based on data from [55, 56]

The most popular of these methods is the NJ approach [53] and its extensions (e.g., BIONJ [22], FastME [59]). By contrast to the linkage procedures, which assume a molecular clock [60], the NJ algorithm accounts for heterogeneous evolutionary rates. Consequently, linkage procedures such as UPGMA output rooted ultrametric trees where the distance from the root to any leaf is identical (Fig. 1a) whereas NJ outputs unrooted non-ultrametric trees (Fig. 1b) (*see* **Note 2**). Distance-based methods run in polynomial time, enabling rapid analyses even for large datasets (e.g., $N = 1{,}000$) [61].

Applications:

Many studies use NJ as a first approach to show relationships between bacterial pathogen genomes, before more complex methods are applied, because it is easy to apply and has well-known properties [12, 62].

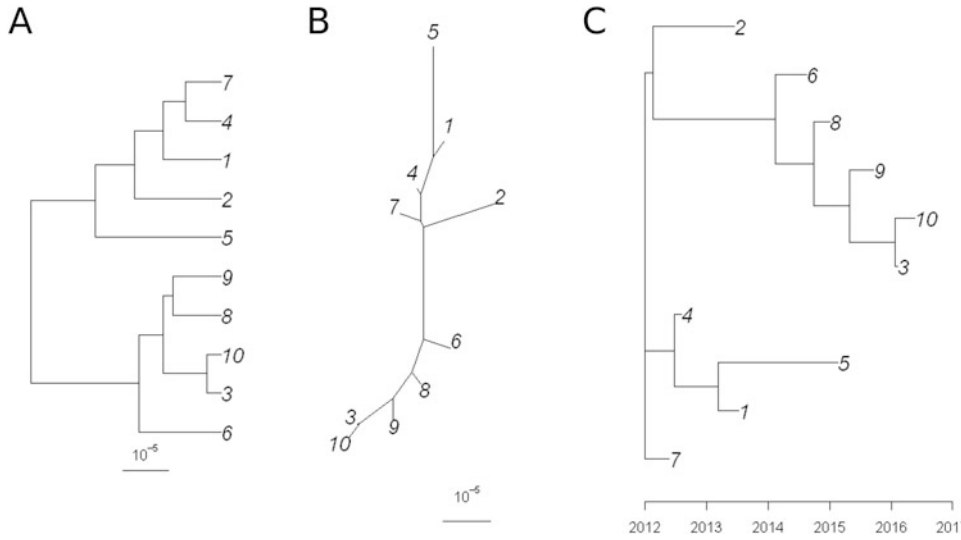

Fig. 1 Typical output for three standard phylogenetic methods ($N = 10$). (**a**) UPGMA outputs a rooted, ultrametric tree. The line segment at the bottom of the figure provides a scale for branch lengths in the tree, measured in units of nucleotide substitutions per site. Note that evolution is inferred to occur at a constant rate throughout the tree (assumes a molecular clock). **(b)** *NJ* outputs a star-like, non-ultrametric tree. An unrooted representation is recommended for NJ trees (*see* **Note 2**). Here, the tree inferred by NJ suggests that the molecular clock hypothesis has been violated (compare evolutionary rates for nodes 1 and 5). In such cases, NJ enables more accurate phylogenetic inference than UPGMA, which is not robust to this violation. A comparison of Fig. 1a, b shows how the bottom-up agglomerative clustering procedure of UPGMA preferentially clusters isolates on short branches, resulting in the subsequent misplacement of long branches within the topology. **(c)** *BEAST* outputs rooted, non-ultrametric trees. Like the NJ approach, Bayesian methods can make accurate inferences despite variable evolutionary rates. Among its numerous parameters and possibilities, however, the ability to reliably estimate dated trees on a timescale has been a major component of the rapid popularization of software like BEAST [33]

3.4.2 Maximum-Parsimony Methods

Aim: Identify the tree that requires the smallest number of substitutions on branches to explain the data ("parsimony cost").

Approach:

1. Select an initial tree topology (*see* **Note 3**).
2. Compute parsimony cost.
3. Apply a random modification to the tree.
4. Compute new parsimony cost.
5. Accept new tree if new parsimony cost is lower than previous; else, keep previous tree.
6. Repeat **steps 3–5** until no further improvements can be found.

Implementations:

The dnapars algorithm in PHYLIP [24] is among the most popular implementations, though a large number of alternatives exist (*see* Table 1).

Applications:

While this class of phylogenetic methods is less frequently cited in the bacterial genomics literature, examples of its successful application can be found, especially for the study of closely related genomes within genetically monomorphic pathogens such *as M. tuberculosis* lineage Beijing [63], *Y. pestis* [64, 65], and *S. enterica* serovar Agona [66].

3.4.3 Maximum-Likelihood Methods

Aim: Simultaneously estimate a phylogenetic tree and evolutionary model parameters, selecting those that achieve the highest probability of observing the genomic data (*see* **Note 4**) [67].

Approach:

1. Select an initial tree and parameters of the model of sequence evolution.
2. Compute likelihood.
3. Propose changes to the tree and parameters.
4. Compute new likelihood.
5. Accept the proposed changes if the new likelihood is higher than the previous one; else, reject the changes.
6. Repeat **steps 3–5** until no further improvements can be found.

Implementations:

Among the most popular maximum-likelihood methods for bacterial pathogen genome analysis are PhyML [26], RAxML [27], GARLI [28], and FastTree [29, 30].

Applications:

Maximum-likelihood methods are the most popular approach to reconstruct phylogenies from alignments of whole genomes of bacterial pathogens, with many high profile studies using them for example in *Vibrio cholerae* [68], *Staphylococcus aureus* [69], or *Chlamydia trachomatis* [70].

3.4.4 Bayesian Methods

Aim: Simultaneously estimate a phylogenetic tree and evolutionary model parameters, selecting a sample of trees from the posterior probability distribution (*see* **Notes 4** and **5**).

Approach:

Use a Monte-Carlo Markov Chain (MCMC) to sample from the posterior distribution:

1. Select an initial location in the parameter space (defined by tree topology, branch lengths, and parameters of the model of sequence evolution).
2. Propose changes to the parameters according to a proposal distribution.
3. Compute the Metropolis-Hastings ratio [71, 72], R, between locations 1 and 2.
4. If $R > 1$, adopt the proposed changes. If $R \leq 1$, reject them.
5. Repeat **steps 2–4** until convergence is achieved (*see* **Note 6**).

Implementations:

Standard Bayesian methods include those offered by MrBayes [32], BEAST [33], and BEAST2 [34].

Applications:

In bacterial population genomics, the Bayesian method BEAST is a popular method of reconstructing a timed phylogeny, where leaves are aligned with their known sampling dates and the age of ancestors is estimated (Fig. 1c). Such timed phylogenies are more useful than standard phylogenies to draw inferences about the epidemiology of the pathogen under study [73].

3.5 Phylogenetic Methods Accounting for Recombination

While their asexual, haploid, and clonal nature renders bacterial populations amenable to phylogenetic reconstruction, the propensity of some species and lineages to undergo homologous recombination prevents us from relying solely on standard phylogenetic approaches. A description of recombination as it pertains to phylogenetic inference can be found in **Note 7**, and a discussion of when to use a phylogenetic method that accounts for recombination in **Note 8**.

3.5.1 ClonalFrameML

Aim: Reconstruct the clonal genealogy, while accounting for recombination and identifying the location of recombinant regions.

Approach:

1. Construct an initial maximum-likelihood tree.
2. Reconstruct ancestral sequences using maximum-likelihood [74].
3. Estimate the recombination parameters (rate, length of events, and average donor/recipient distance), location of recombination evens for each branch and branch lengths of the clonal genealogy via Baum-Welch Expectation-Maximisation (EM) algorithm.
4. Estimate uncertainty using a bootstrapping procedure (*see* Subheading 3.5).

Implementations:

ClonalFrame [35, 36] is one of the most frequently used phylogenetic approaches that explicitly models and accounts for recombination. Capable of handling hundreds of genomes, ClonalFrameML [36] is gradually replacing the original ClonalFrame [35] which works well for MLST data or very few genomes.

Applications:

ClonalFrame [35, 36] was applied in its initial incarnation [35] to *E. coli* [75] and *C. trachomatis* [76, 77]. ClonalFrameML [36] has been used in *Campylobacter* [78], *S. pneumoniae* [79], and *M. tuberculosis* [80].

3.5.2 Gubbins

Aim: Reconstruct the clonal genealogy, finding and excluding regions of likely recombination

Approach:

1. Construct initial maximum-likelihood tree.
2. Reconstruct ancestral sequences using maximum-likelihood (FastML [31]).
3. Identify putative recombinant regions (i.e., clusters of substitutions unlikely to have arisen through point mutation) using a sliding window scan.
4. Remove putative recombinant sites.
5. Iterate through **steps 1–4** until convergence occurs.

Implementations:

In contrast with ClonalFrameML [36], Gubbins [37] *excludes*—rather than accounts for—recombinant regions when reconstructing the clonal genealogy. Moreover, Gubbins [37] delimits

recombinant regions only in the sampled genomes (focusing on outcomes at the terminal nodes of the genealogy), whereas ClonalFrameML [36] identifies recombinant regions in both sampled and un-sampled genomes (focusing on processes between internal and terminal nodes). As Fig. 2 illustrates, an upstream recombination event will be represented once on an internal genome by ClonalFrameML and twice on the two terminal recipient genomes by Gubbins.

Applications:

Gubbins [37] has been used many times to examine the population structure and dynamics of *S. pneumoniae* [81–85], the pathogen for which it was initially designed [8], as well as for analyses of *Chlamydia trachomatis* [70] and *Listeria monocytogenes* [86].

3.6 Model-Based Non-phylogenetic Methods

Non-phylogenetic methods—whether model-based or model-free—attempt to cluster individuals into genetically related or similar populations. Many do not, however, attempt to model the relationships between these populations nor the individuals within each cluster [87]. *See* **Note 9** on when to use a non-phylogenetic method.

All of the clustering methods described below can be used to identify the number of subpopulations, K, in a sample. However, it is better to think of the aim of clustering methods as finding the most *useful* K, rather than some hidden "true" K (*see* **Note 10**). Model-based non-phylogenetic methods attempt to remove some of the subjectivity inherent in this problem by relying on an explicit population genetics model and a set of stated assumptions.

3.6.1 The STRUCTURE Model

Aim: Assign each locus in the sampled genomes to one of K ancestral populations of origin (*see* **Note 11** on assumptions and choosing K).

Approach:

In the linkage version of the original STRUCTURE algorithm [88, 89], a Bayesian MCMC algorithm is used to jointly estimate the following quantities:

1. For each locus of each sequence, the probabilities of derivation from each of the K ancestral populations, accounting for the fact that neighboring loci are more likely to be inherited from the same ancestral population.
2. For each locus and each of the K ancestral populations, the population allele frequencies.
3. Additional global parameters, such as the average length of fragments inherited from an ancestral population.

The results can then be visualized with programs like DISTRUCT [90] or STRUCTURE PLOT [91] to display the most likely ancestral population at each locus (as in [92], representation in Fig. 3) or the ancestry proportions of each individual (as in ref. [93]).

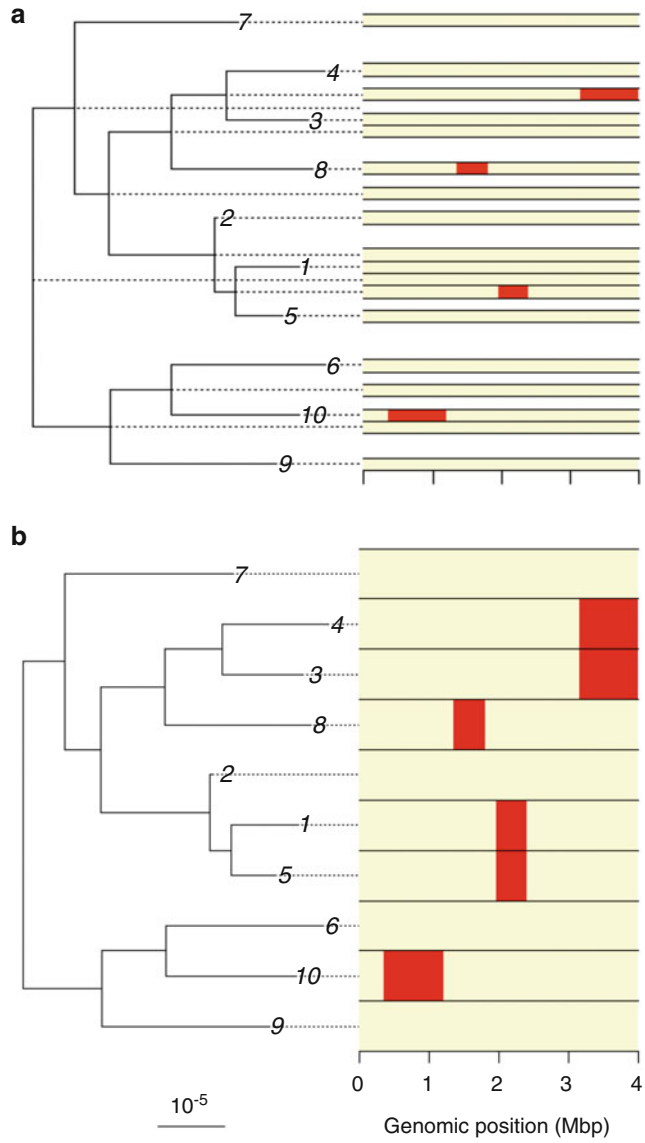

Fig. 2 Typical output for two phylogenetic methods that account for recombination ($N = 10$). The output from (**a**) ClonalFrameML and (**b**) Gubbins can be summarized by two components: the inferred clonal genealogy (*left*) and a representation of the inferred genomic locations of recombination (*right*). Both (**a**) ClonalFrameML and (**b**) Gubbins return rooted, non-ultrametric trees. A scale for the branch lengths of these trees is provided at the bottom of each *left-hand panel*. On the *right-hand side*, the two methods employ similar means to represent recombination events, using colored regions to represent recombinant loci occurring at positions in the genome indicated by the scale that runs along the *x*-axis. Genomes are represented in rows in line with corresponding nodes in the tree at *left*. A key difference, however, exists between the *right-hand panels* demarcating the recombinant loci inferred by each method. In (**a**), ClonalFrameML represents all nodes, both internal and terminal, with a genome and indicates recombinant loci on the genome first affected by recombination (but not its ancestors). In (**b**), Gubbins represents only terminal nodes, which serve as a record of the recombinant loci accumulated by its ancestors in the genealogy. In (**b**), two pairs of terminal nodes in the inferred genealogy, 4 + 6 and 1 + 5, contain matching recombination signatures in the accompanying alignment by Gubbins. In (**a**), no recombinant loci are indicated in the genomes of any of these nodes; instead, the loci appear in the genome of their common ancestors

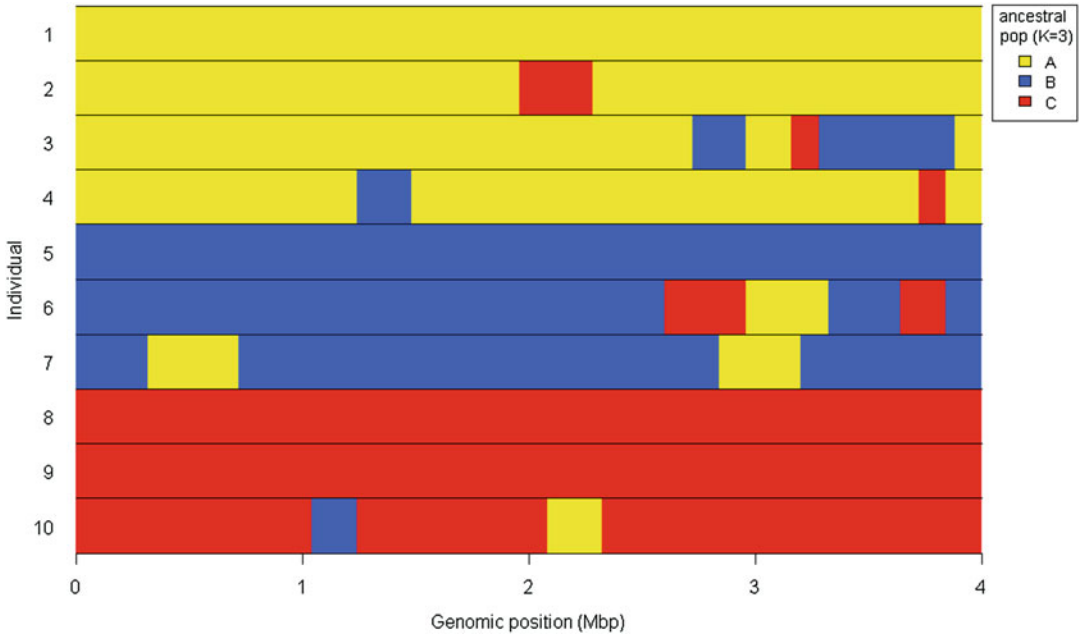

Fig. 3 Typical output for the model-based non-phylogenetic method STRUCTURE ($N = 10$; $K = 3$). This figure provides a visual summary of STRUCTURE output attained by applying the linkage model to a sample of ten bacterial isolates. The STRUCTURE linkage model assigns—to each locus in each genome—a set of ancestry proportions, which indicate the probability that the locus in question was inherited from each of K ancestral populations. Graphical representations of this sort of output can be generated with DISTRUCT [90] or STRUCTURE PLOT [91]. Within the figure, individual genomes are represented in rows and linked blocks of loci are represented in columns whose genomic positions are indicated along the x-axis. The colours of loci within each genome correspond to the K ancestral populations stated in the inset legend. Although the ancestry proportions inferred by STRUCTURE could be depicted for each site in theory, interpretability and utility often favor the depiction of only the most likely ancestral population for each locus. Given this representation, it can be observed that all three of the K ancestral populations are well represented and that clusters of sampled isolates can be readily identified on the basis of this ancestral inference

Implementations:

STRUCTURE [88, 89] is one of the older and better-known model-based methods. However, it was initially designed for multilocus sequence type (MLST) data and is unable to deal with the large amounts of genomic data typical of modern analyses. BAPS [40], BratNextGen [41], and ADMIXTURE [42] accomplish similar results in less time by replacing the Bayesian MCMC used in STRUCTURE with faster alternatives.

Applications:

STRUCTURE has been used to identify the distinct ancestral origins of pathogenic and commensal *Escherichia coli* isolates [93], to detect asymmetric patterns of gene flow between *Campylobacter coli* and *jejuni* sequence types [94], and to infer speciation in

Salmonella enterica [92]. Applications of other model-based methods include BAPS in *Streptococcus pneumoniae* [82] and BratNextGen in *Staphylococcus aureus* [95].

3.6.2 FineStructure

Aim: Identify the sets of sampled individuals that belong to the same "population."

Approach:

1. Consider one individual in the sample to be a "recipient" whose genome is entirely composed of segments of DNA copied from other "donor" individuals in the sample.
2. For all sections of the genome, identify the donor individuals, i.e., the set of sampled individuals most genetically similar in this region.
3. Repeat **steps 1** and **2** for all individuals in the sample, treating each in turn as the "recipient" and all others as putative "donor."
4. Create a coancestry matrix from the results of this copying model, summarizing the number of genome fragments being copied between all pairs of sampled individuals across the genome.
5. Determine the membership and the number (K) of populations in the sample, based on the principle that two members of the same population should have similar coancestry patterns.

Implementations:

FineStructure [43] differs from the STRUCTURE model in that genomes copy from contemporaneous genomes rather than ancestral populations. This enables much faster inference for large datasets. A modified version called orderedPainting has been implemented specifically with the aim of identifying recombination hotspots in bacterial whole genomes [44].

Applications:

FineStructure was originally created for the analysis of human genomic data, but has since proved useful to reconstruct the ancestry of highly recombinant bacterial pathogens such as *H. pylori* [96] and *Vibrio parahaemolyticus* [97]. Preliminary results from these bacterial applications of FineStructure suggest that it may be better-suited to detecting finer population structures than the other non-phylogenetic methods [98].

3.7 Model-Free Non-phylogenetic Methods

Model-free non-phylogenetic methods rely on multivariate dimension reduction techniques to identify genetic clusters based on shared variation. These procedures are not based on any explicit population genetics model and make few assumptions (*see* **Note 12**). They run quickly even for large datasets and the performance of most is not

affected by correlations in the dataset (i.e., extent of LD). The most generic approach is to use a Principal Component Analysis (PCA) with k-means clustering, as detailed below.

3.7.1 Principal Component Analysis

Aim: Summarize genetic sequence data into a set of linearly uncorrelated principal components (PCs) of decreasing overall variance, positioning all sampled individuals along these major axes of variation.

Approach:

1. Consider each of p genetic variables in a p-dimensional space.
2. Compute the covariance matrix of the dataset.
3. Identify the first PC—a weighted linear combination of the initial variables whose squared coefficients sum to one—which contains the greatest variance.
4. Identify the linearly uncorrelated PC that contains the next-largest variance.
5. Repeat **step 4** until all variance in the original dataset is summarized in the reduced model.
6. Run k-means clustering on the PC data at varying K (number of clusters), and identify the K that best fits the data using the Bayesian Information Criterion (BIC) or alternatives (*see* **Note 13**).
7. Visualize results by plotting individuals along the most significant PCs (*see* Fig. 4) (*see* **Note 14**).

Implementations:

All relevant multivariate methods are available in the R statistical software [99] packages *adegenet* [100, 101] and *ade4* [45]. While PCA [102–105] is the most well-known dimension reduction method, alternative approaches include the closely related Multi-Dimensional Scaling [106] and Singular Value Decomposition [107] methods, as well as Principal Co-ordinate Analysis [108], Discriminant Analysis [109], and many more. Jombart [110] disentangles thirteen of these multivariate methods and sheds light on their place in genetic data analysis. One essential addition to this list is the Discriminant Analysis of Principal Components (DAPC) [46]. Owing to the ability of DAPC to hone in on the variation that discriminates between subpopulation groups—as opposed to the more general focus of PCA on overall variation, including both between- and within-group variance—the utility of DAPC may surpass that of PCA in the context of population genetics.

Applications:

PCA has been used to identify populations of related *Campylobacter* isolates [111], and examine the composition of oral microbial communities [112], and DAPC has been employed to describe the population structure of *H. pylori* [113].

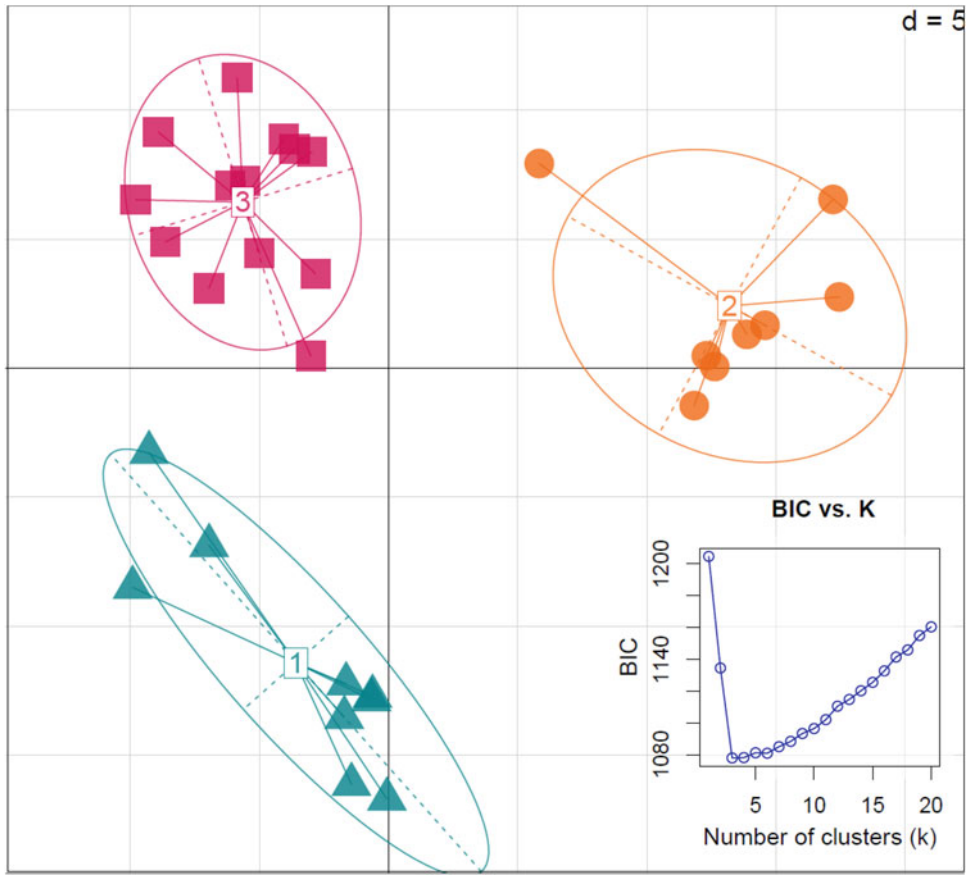

Fig. 4 Typical output for the model-free non-phylogenetic method PCA ($N = 30$; $K = 3$). This figure contains a two-dimensional representation of the output of a two-step k-means + PCA procedure applied to a dataset containing 30 bacterial isolates. The (optional) *inset* plot at the *bottom right* displays the BIC curve used to select the K that best fits the data (*see* **Note 13**). A distinct optimal (minimum) BIC value is achieved at $K = 3$, after which point BIC values begin to climb again. The individual composition of the three population clusters is defined by k-means clustering with $K = 3$. In the main plotting area, all 30 individuals are projected onto the first two PCs (the most significant axes of variation). Each datapoint represents a bacterial isolate. The shape and color of these datapoints distinguish isolates by population (k-means cluster). Each population is accompanied by an ellipse whose area corresponds to its variance. Because PCA maximizes overall variation, PCA plots capture the variance that exists both between clusters and within them. If DAPC were used instead of PCA, the within-group component of overall variance would be minimized and the resulting plot would show tighter clusters

3.8 Estimating Uncertainty

Bayesian phylogenetic methods and model-based non-phylogenetic methods are accompanied by natural probabilistic assessments of the confidence users can have in the clustering estimates obtained, because they generate a sample of trees from the posterior (*see* **Note 5** on Bayesian output). Estimating uncertainty for standard phylogenetic methods, however, requires a separate procedure to be performed.

3.8.1 Bootstrapping

Aim: Assign a probability of occurrence to the topological features of a phylogenetic tree to quantify the reliability of estimates made by standard phylogenetic methods (from Subheadings 3.1–3.3 only).

Approach:

1. Resample the alignment columns (i.e., generate a fake dataset in which each alignment column is sampled at random with replacement from the real original dataset).
2. Recompute the phylogenetic tree.
3. Repeat **steps 1** and **2** many times, for example 1000 times.
4. Compute the bootstrap support of each node in the original tree, i.e., the proportion of times that the same node occurs in trees computed in **step 2**.
5. Represent support on the tree and optionally collapse nodes with low confidence.

Implementations:

The nonparametric bootstrap was developed by Efron [114]; however, the first-order approximation devised by Felsenstein [115] is the most common implementation, available in many of the aforementioned phylogenetic software.

3.8.2 Approximate Likelihood-Ratio Test

The bootstrapping approach requires spending at least two or three orders of magnitude longer to generate confidence support values than it takes to build a tree. When working with hundreds of whole bacterial genomes, this can be prohibitively time consuming as it means that the process of phylogenetic estimation can take many hours or days. A much faster alternative (but also less accurate) is to use an approximate likelihood-ratio test (aLRT) [116] as implemented, for example, in PhyML [26].

4 Notes

1. *When to use a standard phylogenetic method:* In modeling bacterial population structure, standard phylogenetic methods are most useful for highly clonal organisms that undergo minimal recombination (Table 3), for example, *Mycobacterium tuberculosis* [117]. When recombination is more frequent, some authors have suggested that by removing recombinant regions, the clonal frame [118] can be revealed using standard phylogenetic methods [64, 119, 120]. However, recent evaluation of this hypothesis suggests that this removal can, in fact, intensify the distortive effect that recombination has on the tree [55].

Table 3
Optimal methods and example species at varying recombination rates

Typical evolution	Optimal method	Example of applications
Completely clonal	Phylogenetic methods ignoring recombination	*Mycobacterium tuberculosis* [117], *Leptospira interrogans* [121]
Low rate of recombination	Phylogenetic methods accounting for recombination	*Escherichia coli* [75], *Staphylococcus aureus* [121], *Chlamydia trachomatis* [70, 76], *Clostridium difficile* [122], individual lineages of *Campylobacter jejuni* [94], and *Streptococcus pneumoniae* [123]
High rate of recombination	Phylogeny-independent approaches	*Helicobacter pylori* [124], *Neisseria meningitidis* [121], species-wide datasets of *Campylobacter jejuni* [94], and *Streptococcus pneumoniae* [8]

2. *Rooted versus unrooted trees*: The root of a phylogenetic tree should represent the most recent common ancestor (MRCA) of all nodes in the tree. Any phylogenetic tree can be represented as rooted (e.g., Fig.5c) by choosing an arbitrary point on the tree to be the root. When the location of the root is unknown, however, it is recommended that trees be left unrooted (e.g., Fig.5a). This representation reduces the likelihood that an arbitrarily selected root (for example, the midpoint (e.g., Fig.5b) will be inferred to be the most recent common ancestor when, in fact, this information is not known. If a rooted representation is desired, the root can be accurately determined by using an outgroup (usually an individual from a separate-but-related species or clade). Isolates within the original phylogenetic tree will be more similar to each other than to the outgroup. Hence, by identifying the internal node to which the outgroup is affixed, one inherently selects a reasonable common ancestor for the original tree.
3. *Initial trees and tree spaces:* All methods that search the space of possible trees, i.e., all standard phylogenetic methods except the distance-based, begin by selecting some "initial tree topology." In principle, this initial tree can be selected at random [26]. In practice, however, it is best to identify a reasonable starting tree topology with a fast approach (e.g., NJ [53]). The space of all possible trees is distributed unevenly and unpredictably. Starting with a reasonable initial tree ensures that the method will improve upon a tree that could otherwise be obtained by faster methods and reduces the risk of entrapment by suboptimal local maxima or minima [26]. Note that this risk is increased for larger sample sizes and parameter sets, which add complexity to the search space [125].

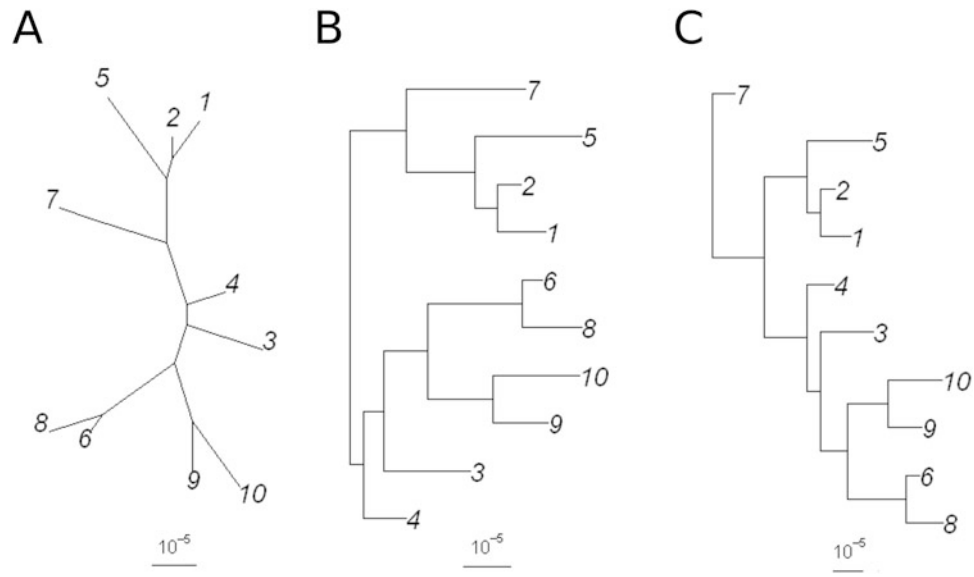

Fig. 5 A comparison of rooted and unrooted trees. The purpose of this figure is to examine the ways in which rooting a phylogenetic tree can affect inferences made about that tree. All three panels (**a, b, c**) contain the same phylogenetic tree; the only source of variation is the placement of the root. (**a**) An unrooted star-like tree (similar to the output of NJ in Fig. 1b) is the most reliable representation for a phylogenetic tree whose root is unknown. This configuration discourages readers from making the potentially unjustified assumption that any root truly represents the MRCA. (**b**) The phylogeny from panel (**a**) has been rooted at the midpoint. Notwithstanding its aesthetic benefit, midpoint rooting in this instance remains unjustified. An incautious observer might infer from this tree that the age of node 7 is similar to that of node 6 or 9. Given the arbitrary placement of the root, no such evidence to support this claim is actually presented. (**c**) The phylogeny from panel (**a**) has been rooted at the division between node 7 and the rest of the tree. The identification of this division as the true MRCA can be obtained by (i) Bayesian phylogenetic methods (*see* Subheading 3.1, **step 4**), or (ii) using an outgroup (*see* **Note 2**).

4. *Joint versus marginal estimation:* Both ML and Bayesian phylogenetic methods search parameter spaces describing possible tree and parameter values. Within the ML framework, a given tree topology is evaluated with reference only to the highest peak of the likelihood function. ML methods ask, "When all other parameters are set to optimize the likelihood of the tree topology at hand, what is the maximum joint likelihood that can be achieved?" [67]. Within a Bayesian framework, by contrast, the posterior probability distribution (a function of the likelihood and prior probability distributions) associated with a given tree topology is assessed more holistically. Bayesian methods ask, "Considering the marginal effects of all possible parameter values on the posterior probability of this tree topology, what volume under this (multidimensional) distribution is achieved?" [67].
5. *Interpreting the output of Bayesian phylogenetic methods:* By contrast to the distance-based, parsimony, and ML approaches to

traditional phylogenetic inference, each of which outputs a single "best" tree, the Bayesian Markov chain Monte Carlo (MCMC) approach described in Subheading 3.1, **step 4** returns a whole set of sampled trees—one for each sampled iteration of the MCMC [67]. Users may wish to summarize all of the information contained in the sample of trees drawn from the posterior. One way this can be achieved is by combining the sample of trees into a single graph to get a qualitative visual assessment of support for elements of the topology, for example, using DensiTree [126]. Alternatively, a single tree may also be desired. This is commonly done by finding a single representative tree and annotating its branches with uncertainty figures for the sample using, for example, TreeAnnotator in BEAST [33].

6. *Convergence:* In theory, Bayesian MCMC is guaranteed to converge toward the correct posterior distribution. In practice, however, convergence can take a long time and full exploration of the posterior distribution, also known as "mixing," can be difficult, particularly when this distribution is multimodal. The convergence of all parameters being estimated should be assessed to ensure that the desired stationary distribution has been reached. If the Markov chain has undergone a sufficient number of iterations, the mean and variance of parameter estimates will achieve a constant state of equilibrium.

7. *Recombination:* Recombination in bacterial populations involves the import of a short contiguous fragment of DNA from a donor to a recipient isolate via virus-mediated conjugation, transformation (uptake from the environment), or contact-mediated conjugation [127].

   Failing to adequately account for recombination when constructing a phylogeny can obscure the true clonal relationships between isolates [128–130]. Even very low levels of recombination can cause traditional phylogenetic methods (Subheading 3.1, Table 2) to produce trees that are topologically inaccurate [130] and/or have distorted branch lengths [55, 128]. Altogether, the evidence suggests that where recombination is present but unaccounted for, the conclusions drawn from phylogenetic inference should be questioned [55, 131].

   Different bacterial species have characteristic rates of recombination [121, 123]. However, as recombination rates vary within, as well as between, species [62, 94, 121, 123, 132–134], it is better to measure the rate of recombination in a given study sample than to rely on species-specific rates. Recombination rates can be quantified by the phylogenetic congruence between loci [135], or the extent of genome-wide linkage disequilibrium via the four-gamete test [136], D' measure [137], or r-squared measure [138]. Alternatively, more sophisticated model-based approaches can be used to infer recombination rates [41, 44, 139].

8. *When to use a phylogenetic method that accounts for recombination*: Where recombination is present at such a rate that standard phylogenetic methods (Subheading 3.1) become unreliable, but no so extensive as to completely obscure the clonal genealogy, phylogenetic methods that account for recombination [35–37] can be recommended (Table 3). These methods allow users to retain the information contained in a phylogenetic tree (as opposed to the lower-resolution clustering approaches in Subheading 3.3–4) while avoiding the errors that can arise from the application of standard phylogenetic methods to populations undergoing recombination.
9. *When to use a non-phylogenetic method:* Non-phylogenetic methods are recommended when recombination occurs to such an extent that no phylogenetic method can be expected to reliably identify the clonal genealogy (Table 3). If recombination is minimal or moderate, then a phylogenetic approach will allow for a much more detailed representation of the ancestral relationships between isolates. Where extensive recombination renders all phylogenetic methods unreliable, however, cluster-based and dimension-reduction approaches provide valuable alternatives. It is also important to keep the purpose of the analysis in mind. In some cases, the identification of accurate clusters may be sufficient, for example, to stratify an analysis by subpopulation.
10. *Useful K versus "true" K:* The number of clusters, K, is simply a parameter being used to represent the observed reality. There is no such thing as a "true K." Admixture, overlap, clines, and hierarchical structures may obfuscate the clear-cut clusters for which we are searching. Consider, for example, a hierarchical population structure in which three meta-populations each contain two subpopulations. If it is more useful for the analysis to group individuals into as many distinct clusters as possible, select $K = 6$. Equally, if a lower resolution will suffice, $K = 3$ may be preferred.
11. *STRUCTURE linkage model:* The STRUCTURE linkage model is based on the following assumptions:

    STRUCTURE requires the user to specify K, the number of ancestral populations, *before* running the analysis. Unless prior information is available to guide your choice, K can be estimated by performing multiple runs of STRUCTURE at different values of K and selecting the K associated with the highest log probability of the data [140]. Another popular approach is to use a peak in the second order rate of change of the log probability of the data between increasing values of K [141]. Note that STRUCTURE becomes impracticably inefficient around $K = 10$ [43].

1. A set of *K* ancestral populations existed some time ago, each of which is defined by population-specific allele frequencies at each locus [88].
2. The genomes of individuals in the sample are the product of admixture events that mixed the *K* populations.
3. The genomes of sampled individuals are composed of linked blocks of alleles inherited from ancestors. Within these inherited chromosomal chunks, the states of alleles are inter-dependent (as opposed to independent individual sites) [89].

12. *Comparing model-based and model-free non-phylogenetic methods:* Among the non-phylogenetic methods, model-based approaches allow users to make inferences about the relationships among isolates within an explicit population genetics model. Parametric frameworks allow for the incorporation of prior information about the population and its evolution, while stated assumptions make inherent biases clear. Results generated in model-based frameworks are often favored for the ease with which biological interpretations can be made.

    Model-free approaches work within a more exploratory framework. Sequence data is analyzed on its own merits without the incorporation of prior information or additional model parameters that may be equally difficult to justify and test. Model-free approaches are usually more computationally efficient and more easily scaled to large datasets.

13. *Defining groups with K-means clustering:* K-means clustering [142, 143] can be used to identify the *K* that best fits the data, according to some criteria. Such criteria include the Bayesian Information Criterion (BIC), Akaike Information Criterion (AIC), or the adjusted R^2, among which BIC is recommended for use in genetic data [144–146]. The group membership of individuals for the *K* selected is identified during the clustering process.

    Note that because it assigns each individual to a single cluster, k-means clustering is not designed to identify admixture. When admixture is expected, fuzzy c-means clustering [147, 148] and alternative algorithms [149] can allow individuals to have a degree of belonging to multiple clusters.

14. *Visualizing the results of PCA:* Visualizing the results is an important final step in the PCA procedure (Subheading 3.4.1). Plots (as in Fig. 4) allow for an examination of the relationships between clusters and the identification of more nuanced patterns (e.g., Clines, hierarchical clustering) that are not captured by population identification, for example, with k-means clustering. For example, when individuals are plotted along the PCs of PCA, a continuum of individuals may suggest a cline [150]. The position of individuals along this cline may indicate the admixture proportions of two source populations at its extremes [151].

References

1. Didelot X, Bowden R, Wilson DJ et al (2012) Transforming clinical microbiology with bacterial genome sequencing. Nat Rev Genet 13:601–612
2. Loman NJ, Pallen MJ (2015) Twenty years of bacterial genome sequencing. Nat Rev Microbiol 13:787–794
3. World Health Organisation (2015) World health statistics. Global health indicators: cause-specific mortality and morbidity.
4. Kiechle FL, Zhang X, Holland-Staley CA (2004) The -omics era and its impact. Arch Pathol Lab Med 128:1337–1345
5. Lowder BV, Guinane CM, Ben Zakour NL et al (2009) Recent human-to-poultry host jump, adaptation, and pandemic spread of Staphylococcus aureus. Proc Natl Acad Sci U S A 106:19545–19550
6. Guinane CM, Ben Zakour NL, Tormo-Mas MA et al (2010) Evolutionary genomics of Staphylococcus aureus reveals insights into the origin and molecular basis of ruminant host adaptation. Genome Biol Evol 2:454–466
7. Holden MTG, Hsu L-Y, Kurt K et al (2013) A genomic portrait of the emergence, evolution, and global spread of a methicillin-resistant Staphylococcus aureus pandemic. Genome Res 23:653–664
8. Croucher NJ, Harris SR, Fraser C et al (2011) Rapid pneumococcal evolution in response to clinical interventions. Science 331:430–434
9. Charlesworth J, Eyre-Walker A (2006) The rate of adaptive evolution in enteric bacteria. Mol Biol Evol 23:1348–1356
10. Batut B, Knibbe C, Marais G, Daubin V (2014) Reductive genome evolution at both ends of the bacterial population size spectrum. Nat Rev Microbiol 12:841–850
11. Achtman M (2004) Chapter 2: age, descent and genetic diversity within Yersinia pestis. In: Carniel E, Joseph Hinnesbusch B (eds) Yersinia: molecular and cellular biology, 1st edn. Taylor & Francis, Norfolk, UK, pp 17–29
12. Sheppard SK, Didelot X, Meric G et al (2013) Genome-wide association study identifies vitamin B5 biosynthesis as a host specificity factor in Campylobacter. Proc Natl Acad Sci U S A 110:11923–11927
13. Alam MT, Petit RA 3rd, Crispell EK et al (2014) Dissecting vancomycin-intermediate resistance in staphylococcus aureus using genome-wide association. Genome Biol Evol 6:1174–1185
14. Didelot X, Gardy J, Colijn C (2014) Bayesian inference of infectious disease transmission from whole-genome sequence data. Mol Biol Evol 31:1869–1879
15. Price AL, Zaitlen NA, Reich D, Patterson N (2010) New approaches to population stratification in genome-wide association studies. Nat Rev Genet 11:459–463
16. Kwok RBH (2011) Phylogeny, genealogy and the Linnaean hierarchy: a logical analysis. J Math Biol 63:73–108
17. Lefort V, Desper R, Gascuel O (2015) FastME 2.0: a comprehensive, accurate, and fast distance-based phylogeny inference program. Mol Biol Evol 32:2798–2800
18. Murtagh F (2015) R: Hierarchical Clustering. https://stat.ethz.ch/R-manual/R-devel/library/stats/html/hclust.html. Accessed 27 Jul 2015
19. Suzuki R, Shimodaira H (2006) Pvclust: an R package for assessing the uncertainty in hierarchical clustering. Bioinformatics 22:1540–1542
20. Popescu A-A, Huber KT, Paradis E (2012) ape 3.0: new tools for distance-based phylogenetics and evolutionary analysis in R. Bioinformatics 28:1536–1537
21. Schliep KP (2011) phangorn: phylogenetic analysis in R. Bioinformatics 27:592–593
22. Gascuel O (1997) BIONJ: an improved version of the NJ algorithm based on a simple model of sequence data. Mol Biol Evol 14:685–695
23. Tamura K, Peterson D, Peterson N et al (2011) MEGA5: molecular evolutionary genetics analysis using maximum likelihood, evolutionary distance, and maximum parsimony methods. Mol Biol Evol 28:2731–2739
24. Felsenstein J (1989) PHYLIP - phylogeny inference package (Version 3.2). Cladistics 5:164–166
25. Wilgenbusch JC and Swofford D (2003) Inferring Evolutionary Trees with PAUP*. Current Protocols in Bioinformatics. 00:6.4: 6.4.1–6.4.28
26. Guindon S, Dufayard J-F, Lefort V et al (2010) New algorithms and methods to estimate maximum-likelihood phylogenies: assessing the performance of PhyML 3.0. Syst Biol 59:307–321
27. Stamatakis A (2006) RAxML-VI-HPC: maximum likelihood-based phylogenetic analyses with thousands of taxa and mixed models. Bioinformatics 22:2688–2690

28. Zwickl DJ (2006) Genetic algorithm approaches for the phylogenetic analysis of large biological sequence datasets under the maximum likelihood criterion. Ph. D. dissertation, The University of Texas at Austin
29. Price MN, Dehal PS, Arkin AP (2009) FastTree: computing large minimum evolution trees with profiles instead of a distance matrix. Mol Biol Evol 26:1641–1650
30. Price MN, Dehal PS, Arkin AP (2010) FastTree 2--approximately maximum-likelihood trees for large alignments. PLoS One 5:e9490
31. Ashkenazy H, Penn O, Doron-Faigenboim A et al (2012) FastML: a web server for probabilistic reconstruction of ancestral sequences. Nucleic Acids Res 40:W580–W584
32. Ronquist F, Teslenko M, van der Mark P et al (2012) MrBayes 3.2: efficient Bayesian phylogenetic inference and model choice across a large model space. Syst Biol 61:539–542
33. Drummond AJ, Rambaut A (2007) BEAST: Bayesian evolutionary analysis by sampling trees. BMC Evol Biol 7:214
34. Bouckaert R, Heled J, Kühnert D et al (2014) BEAST 2: a software platform for Bayesian evolutionary analysis. PLoS Comput Biol 10:e1003537
35. Didelot X, Falush D (2007) Inference of bacterial microevolution using multilocus sequence data. Genetics 175:1251–1266
36. Didelot X, Wilson DJ (2015) ClonalFrameML: efficient inference of recombination in whole bacterial genomes. PLoS Comput Biol 11:e1004041
37. Croucher NJ, Page AJ, Connor TR et al (2015) Rapid phylogenetic analysis of large samples of recombinant bacterial whole genome sequences using Gubbins. Nucleic Acids Res 43:e15
38. Pritchard JK, Stephens M, Rosenberg NA, Donnelly P (2000) Association mapping in structured populations. Am J Hum Genet 67:170–181
39. Pritchard JK, Wen W, Falush D (2003) Documentation for structure software: version 2
40. Tang J, Hanage WP, Fraser C, Corander J (2009) Identifying currents in the gene pool for bacterial populations using an integrative approach. PLoS Comput Biol 5:e1000455
41. Marttinen P, Hanage WP, Croucher NJ et al (2012) Detection of recombination events in bacterial genomes from large population samples. Nucleic Acids Res 40:e6
42. Alexander DH, Novembre J, Lange K (2009) Fast model-based estimation of ancestry in unrelated individuals. Genome Res 19:1655–1664
43. Lawson DJ, Hellenthal G, Myers S, Falush D (2012) Inference of population structure using dense haplotype data. PLoS Genet 8:e1002453
44. Yahara K, Didelot X, Ansari MA et al (2014) Efficient inference of recombination hot regions in bacterial genomes. Mol Biol Evol 31:1593–1605
45. Dray S, Dufour AB (2007) The ade4 package: implementing the duality diagram for ecologists. J Stat Softw 22:1–20
46. Jombart T, Devillard S, Balloux F (2010) Discriminant analysis of principal components: a new method for the analysis of genetically structured populations. BMC Genet 11:94
47. Dunitz MI, Lang JM, Jospin G et al (2015) Swabs to genomes: a comprehensive workflow. PeerJ 3:e960
48. Li H, Ruan J, Durbin R (2008) Mapping short DNA sequencing reads and calling variants using mapping quality scores. Genome Res 18:1851–1858
49. Zerbino DR, Birney E (2008) Velvet: algorithms for de novo short read assembly using de Bruijn graphs. Genome Res 18:821–829
50. Darling AE, Mau B, Perna NT (2010) ProgressiveMauve: multiple genome alignment with gene gain, loss and rearrangement. PLoS One 5:e11147
51. Jolley KA, Maiden MCJ (2010) BIGSdb: Scalable analysis of bacterial genome variation at the population level. BMC Bioinformatics 11:595
52. Legendre P, Legendre LFJ (1983) Developments in environmental modelling, vol 24, 2nd edn, Numerical ecology. Elsevier, Amsterdam
53. Saitou N, Nei M (1987) The neighbor-joining method: a new method for reconstructing phylogenetic trees. Mol Biol Evol 4:406–425
54. Felsenstein J (1981) Evolutionary trees from DNA sequences: a maximum likelihood approach. J Mol Evol 17:368–376
55. Hedge J, Wilson DJ (2014) Bacterial phylogenetic reconstruction from whole genomes is robust to recombination but demographic inference is not. MBio 5:e02158
56. Bogdanowicz D, Giaro K, Wróbel B (2012) TreeCmp: comparison of trees in polynomial time. Evol Bioinform Online 8:475
57. Sørensen T (1948) A method of establishing groups of equal amplitude in plant sociology based on similarity of species and its application

to analyses of the vegetation on Danish commons. Kongelige Danske Videnskabernes Selskabs Biologiske Skrifter 5:1–34

58. Sneath PHA, Sokal RR, Freeman WH (1975) Numerical taxonomy. The principles and practice of numerical classification. Syst Zool 24:263–268
59. Gascuel O, Steel M (2006) Neighbor-joining revealed. Mol Biol Evol 23:1997–2000
60. Zuckerland E, Pauling LB (1962) Molecular disease, evolution, and genetic heterogeneity. In: Kasha M, Pullman B (eds) Horizons in biochemistry. Academic Press, New York, pp 189–225
61. Wang L-S, Warnow T, Moret BME et al (2006) Distance-based genome rearrangement phylogeny. J Mol Evol 63:473–483
62. Sheppard SK, Didelot X, Jolley KA et al (2013) Progressive genome-wide introgression in agricultural Campylobacter coli. Mol Ecol 22:1051–1064
63. Merker M, Blin C, Mona S et al (2015) Evolutionary history and global spread of the Mycobacterium tuberculosis Beijing lineage. Nat Genet 47:242–249
64. Morelli G, Song Y, Mazzoni CJ et al (2010) Yersinia pestis genome sequencing identifies patterns of global phylogenetic diversity. Nat Genet 42:1140–1143
65. Cui Y, Yu C, Yan Y et al (2013) Historical variations in mutation rate in an epidemic pathogen, Yersinia pestis. Proc Natl Acad Sci U S A 110:577–582
66. Zhou Z, McCann A, Litrup E et al (2013) Neutral genomic microevolution of a recently emerged pathogen, Salmonella enterica serovar Agona. PLoS Genet 9:e1003471
67. Holder M, Lewis PO (2003) Phylogeny estimation: traditional and Bayesian approaches. Nat Rev Genet 4:275–284
68. Mutreja A, Kim DW, Thomson NR et al (2011) Evidence for several waves of global transmission in the seventh cholera pandemic. Nature 477:462–465
69. Harris SR, Feil EJ, Holden MTG et al (2010) Evolution of MRSA during hospital transmission and intercontinental spread. Science 327:469–474
70. Harris SR, Clarke IN, Seth-Smith HMB et al (2012) Whole-genome analysis of diverse Chlamydia trachomatis strains identifies phylogenetic relationships masked by current clinical typing. Nat Genet 44(413–9):S1
71. Metropolis N, Rosenbluth AW, Rosenbluth MN et al (1953) Equation of state calculations by fast computing machines. J Chem Phys 21:1087–1092
72. Hastings WK (1970) Monte Carlo sampling methods using Markov chains and their applications. Biometrika 57:97–109
73. Biek R, Pybus OG, Lloyd-Smith JO, Didelot X (2015) Measurably evolving pathogens in the genomic era. Trends Ecol Evol 30:306–313
74. Pupko T, Pe'er I, Shamir R, Graur D (2000) A fast algorithm for joint reconstruction of ancestral amino acid sequences. Mol Biol Evol 17:890–896
75. Didelot X, Meric G, Falush D, Darling A (2012) Impact of homologous and non-homologous recombination in the genomic evolution of Escherichia coli. BMC Genomics 13:256
76. Joseph SJ, Didelot X, Gandhi K et al (2011) Interplay of recombination and selection in the genomes of Chlamydia trachomatis. Biol Direct 6:28
77. Joseph SJ, Didelot X, Rothschild J et al (2012) Population genomics of Chlamydia trachomatis: insights on drift, selection, recombination, and population structure. Mol Biol Evol 29:3933–3946
78. Dearlove BL, Cody AJ, Pascoe B et al (2015) Rapid host switching in generalist Campylobacter strains erodes the signal for tracing human infections. ISME J 10:721–729. doi:10.1038/ismej.2015.149
79. van Tonder AJ, Bray JE, Roalfe L et al (2015) Genomics reveals the worldwide distribution of multidrug-resistant serotype 6E pneumococci. J Clin Microbiol 53:2271–2285
80. Walker TM, Kohl TA, Omar SV et al (2015) Whole-genome sequencing for prediction of Mycobacterium tuberculosis drug susceptibility and resistance: a retrospective cohort study. Lancet Infect Dis 15:1193–1202
81. Croucher NJ, Finkelstein JA, Pelton SI et al (2015) Population genomic datasets describing the post-vaccine evolutionary epidemiology of Streptococcus pneumoniae. Sci Data 2:150058
82. Chewapreecha C, Harris SR, Croucher NJ et al (2014) Dense genomic sampling identifies highways of pneumococcal recombination. Nat Genet 46:305–309
83. Cornick JE, Chaguza C, Harris SR et al (2015) Region-specific diversification of the highly virulent serotype 1 Streptococcus pneumoniae. Microbial Genomics 1:10. doi: 10.1099/mgen.0.000027
84. Kamng'ona AW, Hinds J, Bar-Zeev N et al (2015) High multiple carriage and emergence of Streptococcus pneumoniae vaccine serotype variants in Malawian children. BMC Infect Dis 15:234

85. Turner CE, Abbott J, Lamagni T et al (2015) Emergence of a new highly successful acapsular group A Streptococcus clade of genotype emm89 in the United Kingdom. MBio 6:e00622
86. Stasiewicz MJ, Oliver HF, Wiedmann M, den Bakker HC (2015) Whole-genome sequencing allows for improved identification of persistent listeria monocytogenes in food-associated environments. Appl Environ Microbiol 81:6024–6037
87. Robinson DA, Feil EJ, Falush D (2010) Bacterial population genetics in infectious disease. Wiley-Blackwell, Malden, MA
88. Pritchard JK, Stephens M, Donnelly P (2000) Inference of population structure using multilocus genotype data. Genetics 155:945–959
89. Falush D, Stephens M, Pritchard JK (2003) Inference of population structure using multilocus genotype data: linked loci and correlated allele frequencies. Genetics 164:1567–1587
90. Rosenberg NA (2004) distruct: a program for the graphical display of population structure. Mol Ecol Notes 4:137–138
91. Ramasamy RK, Ramasamy S, Bindroo BB, Naik VG (2014) STRUCTURE PLOT: a program for drawing elegant STRUCTURE bar plots in user friendly interface. SpringerPlus 3:431
92. Falush D, Torpdahl M, Didelot X et al (2006) Mismatch induced speciation in Salmonella: model and data. Philos Trans R Soc Lond B Biol Sci 361:2045–2053
93. Wirth T, Falush D, Lan R et al (2006) Sex and virulence in Escherichia coli: an evolutionary perspective. Mol Microbiol 60:1136–1151
94. Sheppard SK, McCarthy ND, Falush D, Maiden MCJ (2008) Convergence of Campylobacter species: implications for bacterial evolution. Science 320:237–239
95. Castillo-Ramírez S, Corander J, Marttinen P et al (2012) Phylogeographic variation in recombination rates within a global clone of methicillin-resistant Staphylococcus aureus. Genome Biol 13:R126
96. Yahara K, Furuta Y, Oshima K et al (2013) Chromosome painting in silico in a bacterial species reveals fine population structure. Mol Biol Evol 30:1454–1464
97. Cui Y, Yang X, Didelot X et al (2015) Epidemic clones, oceanic gene pools and eco-LD in the free living marine pathogen Vibrio parahaemolyticus. Mol Biol Evol 32:1396–1410. doi:10.1093/molbev/msv009
98. Lawson DJ, Falush D (2012) Population identification using genetic data. Annu Rev Genomics Hum Genet 13:337–361
99. R Core Development Team (2013) The R project for statistical computing. In: R: a language and environment for statistical computing. http://www.r-project.org/. Accessed 1 Feb 2015
100. Jombart T (2008) adegenet: a R package for the multivariate analysis of genetic markers. Bioinformatics 24:1403–1405
101. Jombart T, Ahmed I (2011) adegenet 1.3-1: new tools for the analysis of genome-wide SNP data. Bioinformatics 27:3070–3071
102. Pearson K (1901) On lines and planes of closest fit to systems of points in space. Philosophical Magazine Series 6 2:559–572
103. Cavalli-Sforza LL (1966) Population structure and human evolution. Proc R Soc Lond B Biol Sci 164:362–379
104. Patterson N, Price AL, Reich D (2006) Population structure and eigenanalysis. PLoS Genet 2:e190
105. Paschou P, Ziv E, Burchard EG et al (2007) PCA-correlated SNPs for structure identification in worldwide human populations. PLoS Genet 3:1672–1686
106. Lessa EP (1990) Multidimensional analysis of geographic genetic structure. Syst Biol 39:242–252
107. Alter O, Brown PO, Botstein D (2000) Singular value decomposition for genome-wide expression data processing and modeling. Proc Natl Acad Sci U S A 97:10101–10106
108. Sanchez-Mazas A, Langaney A (1988) Common genetic pools between human populations. Hum Genet 78:161–166
109. Smouse PE, Spielman RS, Park MH (1982) Multiple-locus allocation of individuals to groups as a function of the genetic variation within and differences among human populations. Am Nat 119:445–463
110. Jombart T, Pontier D, Dufour A-B (2009) Genetic markers in the playground of multivariate analysis. Heredity 102:330–341
111. Lefébure T, Bitar PDP, Suzuki H, Stanhope MJ (2010) Evolutionary dynamics of complete Campylobacter pan-genomes and the bacterial species concept. Genome Biol Evol 2:646–655
112. Bolivar I, Whiteson K, Stadelmann B et al (2012) Bacterial diversity in oral samples of children in niger with acute noma, acute necrotizing gingivitis, and healthy controls. PLoS Negl Trop Dis 6:e1556
113. Montano V, Didelot X, Foll M et al (2015) Worldwide population structure, long term

demography, and local adaptation of helicobacter pylori. Genetics 200:947–963. doi:10.1534/genetics.115.176404

114. Efron B (1979) Bootstrap methods: another look at the Jackknife. Ann Statist 7:1–26
115. Felsenstein J (1985) Confidence limits on phylogenies: an approach using the bootstrap. Evolution 39:783–791. doi:10.2307/2408678
116. Anisimova M, Gascuel O (2006) Approximate likelihood-ratio test for branches: a fast, accurate, and powerful alternative. Syst Biol 55:539–552
117. Comas I, Coscolla M, Luo T et al (2013) Out-of-Africa migration and Neolithic coexpansion of Mycobacterium tuberculosis with modern humans. Nat Genet 45:1176–1182
118. Milkman R, Bridges MM (1990) Molecular evolution of the Escherichia coli chromosome. III clonal frames. Genetics 126:505–517
119. Dress AWM, Flamm C, Fritzsch G et al (2008) Noisy: identification of problematic columns in multiple sequence alignments. Algorithms Mol Biol 3:7
120. Hornstra HM, Priestley RA, Georgia SM et al (2011) Rapid typing of Coxiella burnetii. PLoS One 6:e26201
121. Vos M, Didelot X (2008) A comparison of homologous recombination rates in bacteria and archaea. ISME J 3:199–208
122. Didelot X, Eyre DW, Cule M et al (2012) Microevolutionary analysis of Clostridium difficile genomes to investigate transmission. Genome Biol 13:R118
123. Feil EJ, Holmes EC, Bessen DE et al (2001) Recombination within natural populations of pathogenic bacteria: short-term empirical estimates and long-term phylogenetic consequences. Proc Natl Acad Sci U S A 98:182–187
124. Kennemann L, Didelot X, Aebischer T et al (2011) Helicobacter pylori genome evolution during human infection. Proc Natl Acad Sci U S A 108:5033–5038
125. Albright E, Hessel J, Hiranuma N et al (2014) A comparative analysis of popular phylogenetic reconstruction algorithms. In: Proceedings of the Midwest Instruction and Computing Symposium (MICS)
126. Bouckaert RR (2010) DensiTree: making sense of sets of phylogenetic trees. Bioinformatics 26:1372–1373
127. Ochman H, Lawrence JG, Groisman EA (2000) Lateral gene transfer and the nature of bacterial innovation. Nature 405:299–304
128. Schierup MH, Hein J (2000) Consequences of recombination on traditional phylogenetic analysis. Genetics 156:879–891
129. Schierup MH, Hein J (2000) Recombination and the molecular clock. Mol Biol Evol 17:1578–1579
130. Posada D, Crandall KA (2002) The effect of recombination on the accuracy of phylogeny estimation. J Mol Evol 54:396–402
131. Rannala B, Yang Z (2008) Phylogenetic inference using whole genomes. Annu Rev Genomics Hum Genet 9:217–231
132. Everitt RG, Didelot X, Batty EM et al (2014) Mobile elements drive recombination hotspots in the core genome of Staphylococcus aureus. Nat Commun 5:3956
133. Mostowy R, Croucher NJ, Hanage WP et al (2014) Heterogeneity in the frequency and characteristics of homologous recombination in pneumococcal evolution. PLoS Genet 10:e1004300
134. Namouchi A, Didelot X, Schöck U et al (2012) After the bottleneck: genome-wide diversification of the Mycobacterium tuberculosis complex by mutation, recombination, and natural selection. Genome Res 22:721–734
135. Dykhuizen DE, Green L (1991) Recombination in Escherichia coli and the definition of biological species. J Bacteriol 173:7257–7268
136. Hudson RR, Kaplan NL (1985) Statistical properties of the number of recombination events in the history of a sample of DNA sequences. Genetics 111:147–164
137. Lewontin RC (1964) The interaction of selection and linkage. I general considerations; heterotic models. Genetics 49:49–67
138. Hill WG, Robertson A (1968) Linkage disequilibrium in finite populations. Theor Appl Genet 38:226–231
139. Didelot X, Lawson D, Darling A, Falush D (2010) Inference of homologous recombination in bacteria using whole-genome sequences. Genetics 186:1435–1449
140. Waples RS, Gaggiotti O (2006) What is a population? An empirical evaluation of some genetic methods for identifying the number of gene pools and their degree of connectivity. Mol Ecol 15:1419–1439
141. Evanno G, Regnaut S, Goudet J (2005) Detecting the number of clusters of individuals using the software STRUCTURE: a simulation study. Mol Ecol 14:2611–2620
142. Hartigan JA, Wong MA (1979) Algorithm AS 136: A K-means clustering algorithm. J R Stat Soc Ser C Appl Stat 28:100–108
143. MacQueen J (1967) Some methods for classification and analysis of multivariate observations. In: Cao J, Mao K, Cambria E et al (eds) Proceedings of ELM-2014 Volume 1: Algorithms and theories. Springer International Publishing, pp 281–297

144. Fraley C, Raftery AE (1998) How many clusters? Which clustering method? Answers via model-based cluster analysis. Comput J 41:578–588
145. Lee C, Abdool A, Huang C-H (2009) PCA-based population structure inference with generic clustering algorithms. BMC Bioinformatics 10(Suppl 1):S73
146. Zhu X, Zhang S, Zhao H, Cooper RS (2002) Association mapping, using a mixture model for complex traits. Genet Epidemiol 23:181–196
147. Bezdek JC (1981) Pattern recognition with fuzzy objective function algorithms. Plenum Press, New York
148. Kaufman L, Rousseeuw PJ (1990) Finding groups in data: an introduction to cluster analysis. Wiley, New York
149. Fraley C, Raferty AE (2002) Model-based clustering, discriminant analysis, and density estimation. J Am Stat Assoc 97:611–631
150. Lawson DJ (2013) Populations in statistical genetic modelling and inference. arXiv [q-bio.PE]
151. McVean G (2009) A genealogical interpretation of principal components analysis. PLoS Genet 5:e1000686

Part IV

Bacterial Imaging Approaches and Related Techniques

Chapter 9

Making Fluorescent Streptococci and Enterococci for Live Imaging

Sarah Shabayek and Barbara Spellerberg

Abstract

Since the discovery of the green fluorescent protein (GFP) from the jellyfish *Aequorea victoria*, outstanding fluorescent labeling tools with numerous applications in vastly different areas of life sciences have been developed. To optimize GFP for diverse life science applications, a large variety of GFP derivatives with different environmental characteristics have been generated by mutagenesis. The enhanced green fluorescent protein (EGFP) is a well-known GFP derivative with highly increased fluorescence intensity compared to the GFP wild-type molecule. Further optimization strategies include numerous GFP derivatives with blue- and yellow-shifted fluorescence and increased pH-stability. The methods reported herein describe in detail the construction of customized fluorescent GFP reporter plasmids where the fluorescence gene is expressed under the control of a certain bacterial promoter of interest. Special attention is given to the GFP derivatives EGFP and Sirius. We explain how to generate EGFP/Sirius expressing streptococci and how to employ recombinantly labeled streptococci in different downstream fluorescent applications.

Key words Fluorescence labeling, Streptococci, Green fluorescent protein, GFP, EGFP, Sirius

1 Introduction

In 2008, the Nobel Prize in chemistry was awarded to Osamu Shimomura, Roger Tsien, and Martin Chalfie for their groundbreaking discovery of the green fluorescent protein (GFP) from the jellyfish *Aequorea victoria* [1]. It has since been developed into an outstanding fluorescent labeling tool with innumerable applications in vastly different areas of life sciences. GFP has been widely used for clonal tagging or as a reporter for specific gene expression in both bacteria and higher eukaryotic organisms [1–3]. Among the advantages of GFP is being more sensitive than other reporter genes and requiring no extraneous substrates or cofactors for its detection [2, 3]. Autocatalytic formation of the fluorophore in combination with the advantages of fluorescence for advanced microscopy and image analysis has driven the rapid development of innovative methods for in situ investigations of complex biological scenarios.

Pontus Nordenfelt and Mattias Collin (eds.), *Bacterial Pathogenesis: Methods and Protocols*, Methods in Molecular Biology, vol. 1535, DOI 10.1007/978-1-4939-6673-8_9,

To optimize GFP for diverse life science applications, numerous GFP derivatives with blue- and yellow-shifted fluorescence were generated by mutagenesis [1, 4]. The enhanced green fluorescent protein (EGFP) for instance displays greatly increased fluorescence intensity compared to the GFP wild-type molecule [5]. EGFP is a stable F64L-S65T GFP variant with an excitation peak at 488 nm and an emission peak at 509 nm [4]. A major advantage of GFP and its derivatives is the lack of causing harmful effects on living cells [2, 6, 7]. Disadvantages include properties such as a narrow range of pH stability hampering its use in some applications. Alkaline as well as acidic conditions cause drastic reductions in the fluorescence intensity [8, 9]. These obstacles are overcome by Sirius, a GFP variant that possesses an ultramarine-shifted fluorescence with increased photostability and pH-insensitivity. With an excitation peak at 355 nm and an emission peak at 424 nm it represents the shortest emission wavelength among fluorescent proteins reported to date [10]. The most noteworthy feature of Sirius is its fluorescence stability in a wide range of proton concentrations (pH 3–9), which renders it highly suitable for fluorescence imaging in acidic environments [10].

Based on the *Escherichia coli*-streptococcal shuttle plasmid pAT28 [11], we have previously examined the induction of the streptococcal C5a peptidase gene (*scpB*) in an EGFP-pAT28 derivative designated pBSU409 where *egfp* gene is expressed under the control of the *scpB* promoter [12]. Utilizing the same vector backbone we were able to monitor the expression pattern of the streptococcal streptolysin S gene (*sag*) of *Streptococcus anginosus* by inducing *egfp* gene expression under the control of the *sag* promoter [13]. Furthermore, our laboratory reported the construction of a novel EGFP-pAT28 derivative with the ability to propagate in various bacterial species from different genera. The plasmid carries a promoterless copy of *egfp* gene under the control of the CAMP-factor gene (*cfb*) promoter of *Streptococcus agalactiae* and was designated pBSU101 [14]. We have successfully demonstrated the suitability of this construct for high efficiency fluorescence labeling in many different gram positive bacterial species such as *Streptococcus pyogenes*, *Streptococcus agalactiae*, *Streptococcus dysgalactiae* subsp. *equisimilis*, *Enterococcus faecalis*, *Enterococcus faecium*, *Streptococcus mutans*, *Streptococcus anginosus*, and *Staphylococcus aureus*. In addition, in a recent investigation on acid dependent genes we were able to assemble a new construct, a Sirius-pAT28 shuttle vector where the *sirius* gene is expressed under the control of the *cfb* promoter mentioned above and this vector was designated pBSU836 (Shabayek et al, manuscript in revision). We were able to successfully apply the *sirius*-based vector in various downstream fluorescence applications at low pH.

The methods described herein include in detail the construction of customized fluorescent GFP-pAT28 derivative reporter plasmids where the fluorescence gene is expressed under the control of a certain bacterial promoter of interest. We explain how to

produce EGFP/Sirius expressing streptococci and how to manipulate recombinant labeled streptococci in different downstream fluorescent applications such as clonal tagging or monitoring gene expression using fluorescence microscopy and fluorescence activated cell sorting (FACS) respectively. A general outline for the methods is illustrated in Fig. 1. Based on the choice of vector and

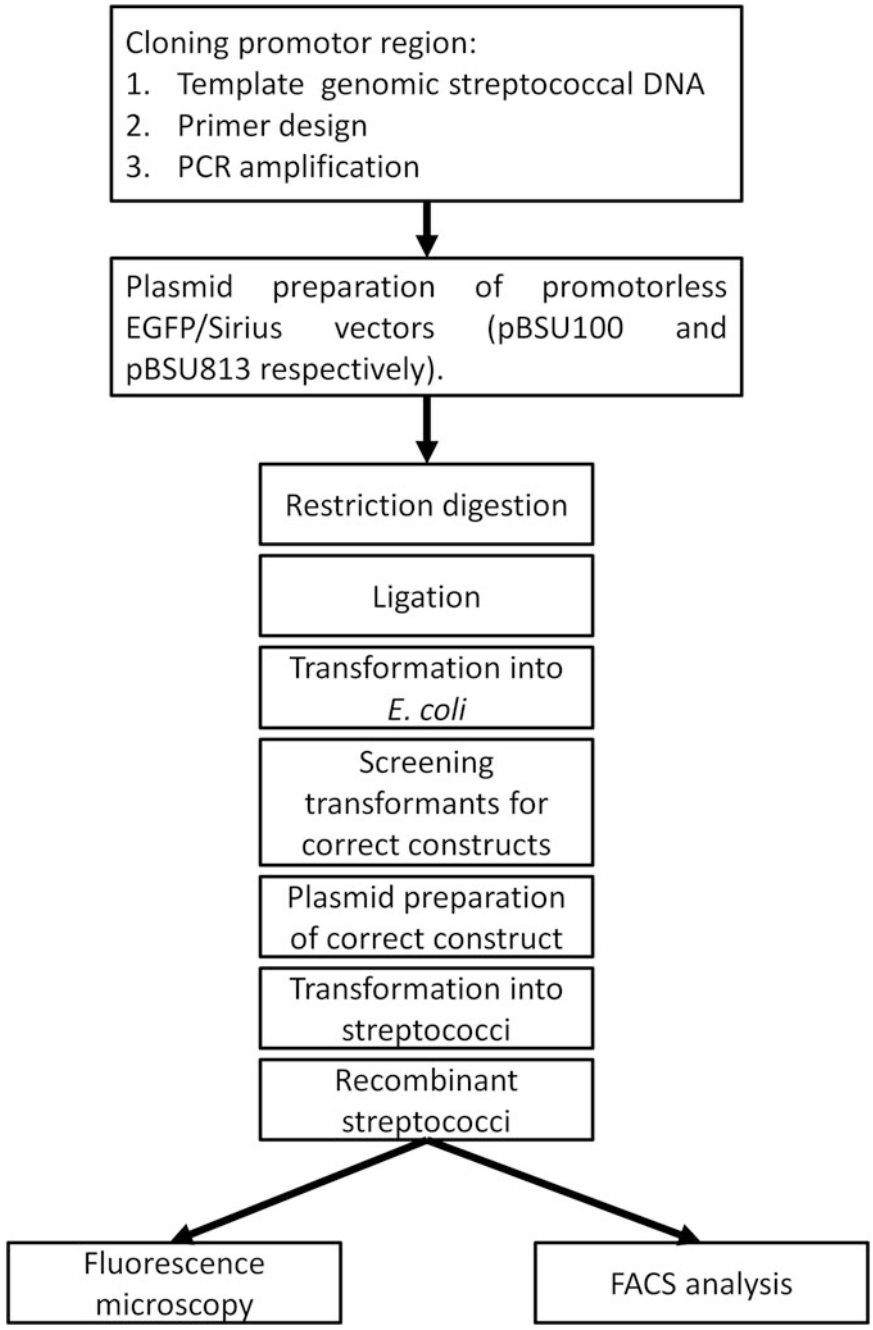

Fig. 1 Methods outline

the GFP variant used, these methods can be easily modified to create suitable fluorescent labeling tools for a wide variety of different bacteria and applications.

2 Materials

2.1 Bacterial Strains

1. *See* Table 1.

2.2 Plasmids

1. *See* Table 2.

2.3 Culture Media

1. THY broth: Todd-Hewitt broth, 0.5 % yeast extract.
2. THY agar: THY broth, 1.5 % agar.

Table 1
Bacterial strains

Strain	Description	Source or reference
Escherichia coli DH5α	*endA1 hsdR17 supE44 ΔlacU169(φ80lacZDM15) recA1 gyrA96 thi-1 relA1*	Boehringer
Streptococcus agalactiae BSU6	wild-type serotype Ia, similar to *Streptococcus agalactiae* A909	Ulm collection
Streptococcus mutans BSU269	DSM 20523	DSMZ collection
Streptococcus anginosus BSU485	Clinical isolate	Ulm collection
Enterococcus faecalis BSU386	Clinical isolate	Ulm collection
Enterococcus faecium BSU385	Clinical isolate	Ulm collection

Table 2
Plasmids

Plasmid	Description	Source or reference
pBSU100	pAT28 derivative carrying *egfp*	Aymanns et al. (2011) [14]
pBSU101	pAT28 derivative carrying *egfp* under the control of *cfb* promoter	Aymanns et al. (2011) [14]
pBSU813	pAT28 derivative carrying *sirius*	Shabayek et al., manuscript in preparation
pBSU836	pAT28 derivative carrying *sirius* under the control of *cfb* promoter	Shabayek et al., manuscript in preparation

3. Luria Bertani broth (LB): 1% NaCl, 1% peptone, 0.5% yeast extract.
4. LB agar: LB broth, 1.5% agar.

2.4 Antibiotics

1. Spectinomycin.

2.5 Genomic DNA Isolation from Streptococcal Wild-Type Strains

1. A genomic DNA extraction kit: QIAmp DNA Mini, QIAGEN or GenElute Bacterial Genomic DNA, Sigma.
2. 50 mg/ml lysozyme.
3. 5000 U/ml mutanolysin.
4. 20 mg/ml proteinase K.
5. TE buffer: 10 mM Tris, 1 mM EDTA, pH 7.5.
6. TES buffer: 50 mM Tris, 5 mM EDTA, 50 mM NaCl, pH 8.15.
7. Tris buffer: 10 mM Tris, pH 7.5.
8. 10% SDS.
9. Saturated NaCl solution.
10. Phenol–chloroform mixture 1:1.
11. Cold 100% ethanol.
12. Clean tissue paper.
13. 1.5 ml Eppendorf tubes.
14. Falcon tubes.
15. Thermal block or water bath.
16. Vortex, microcentrifuge.
17. Falcon centrifuge.
18. CO_2 incubator or candle jar.

2.6 Primers and Primer Design

1. Primer pair flanking the Multiple Cloning Site (MCS) in pBSU100/pBSU813 derivatives (*see* Table 3).
2. Primer pAT28-sirius reverse (*see* Table 3) to sequence the region upstream the *sirius* gene in a pBSU813 derivative.

Table 3
Primers

Primer	Sequence	Target
pat28-2	5′- CTCTTCGCTATTACGCCAGCT -3′	Region flanking the multiple cloning site in pAT28 derivatives
pat28-3	5′- GTTGTGTGGAATTGTGAGCGG -3′	Region flanking the multiple cloning site in pAT28 derivatives
Pat28-sirius reverse	5′- CCAGCTCGACCAGGATGGGC -3′	Sequencing region upstream the Sirius gene in pAT28 reporter plasmids

3. Primers to amplify the promoter region of interest, access to the online bacterial genome data bases.

2.7 Restriction Digestion

1. Restriction enzymes compatible with the MCS upstream the *egfp* gene in pBSU100 (*Bam*HI, *Eco*RI, *Sac*I, *Kpn*I, *Sma*I, *Xma*I).
2. Restriction enzymes compatible with the MCS upstream the *sirius* gene in pBSU813 (*Bam*HI, *Xba*I, *Sal*I, *Pst*I, *Sph*I, *Hind*III).
3. DNA purification kit (QIAGEN).

2.8 Determination of DNA Concentration

1. Fluorometric determination using Quant-iT assay kit (Thermo Fisher Scientific) and the Qubit fluorometer (Thermo Fisher Scientific). Alternatively, a spectrophotometer adjusted to 260 nm can be used.

2.9 Ligation Reaction

1. Rapid DNA Ligase kit (Affymetrix).

2.10 Polymerase Chain Reaction (PCR)

1. Taq DNA polymerase kit (Roche).
2. PCR tubes, Thermocycler (Biometra).
3. PCR and gel cleanup kit (MACHEREY-NAGEL).

2.11 Sequencing Reaction

1. Sequencing kit (ABI PRISM Dye terminator cycle sequencing kit).
2. Sequencing columns (Genaxxon bioscience).
3. Sequencer (ABI 373 automated DNA sequencer, Applied Biosystems).

2.12 Transformation of E. coli

1. $CaCl_2$ solution: 0.1 M, cold and sterilized.
2. Crushed ice, LB broth.
3. LB agar supplemented with 100 μg/ml spectinomycin.
4. 1.5 ml Eppendorf tubes.
5. Falcon tubes.
6. Microcentrifuge.
7. Falcon tube centrifuge.
8. Vortex.
9. Thermal block or water bath.
10. Shaking incubator.

2.13 Transformation of Streptococci by Electroporation

1. 10% glycerol (cold and sterilized).
2. 20% glycerol (cold and sterilized).
3. THY broth with 10% glycerol.
4. THY agar supplemented with 120 μg/ml spectinomycin.

5. 1 mm electroporation cuvette.
6. Gene pulser apparatus (Bio-Rad).
7. Sterilized glass beads.
8. 1.5 ml Eppendorf tubes.
9. Falcon tubes.
10. Microcentrifuge.
11. Falcon tube centrifuge.
12. Vortex.
13. Thermal block.
14. CO_2 incubator or candle jar.

2.14 Plasmid Extraction from Recombinant E. coli Carrying pBSU100/pBSU813 or Their Derivatives

1. LB broth supplemented with 100 μg/ml spectinomycin.
2. Plasmid extraction kit (QIAprep Spin Miniprep kit, QIAGEN).
3. 1.5 ml Eppendorf tubes.
4. Falcon tubes.
5. Microcentrifuge.
6. Falcon tube centrifuge.
7. Vortex.
8. Shaking incubator.

2.15 Plasmid Extraction from Recombinant Streptococci Carrying pBSU100/pBSU813 or Their Derivatives

1. THY broth supplemented with 120 μg/ml spectinomycin.
2. Micro-glass beads (150–212 μm).
3. Ribolyser tubes (Sarstedt AG & Co., Nümbrecht, Germany).
4. Ribolyser (FastPrep FB120, BIO 101, Inc., Vista, CA, USA).
5. Plasmid extraction kit (QIAprep Spin Miniprep,QIAGEN).
6. 1.5 ml Eppendorf tubes.
7. Falcon tubes.
8. Microcentrifuge.
9. Falcon tube centrifuge.
10. Vortex.
11. CO_2 incubator or candle jar.

2.16 Fluorescence Microscopy

1. Fluorescence microscope with GFP and DAPI filter sets.
2. PBS or DPBS.
3. Microscopical slides.
4. Coverslips.
5. Falcon tubes.
6. Falcon tube centrifuge.
7. Vortex.

2.17 Fluorescence Activated Cell Sorting (FACS)

1. FACS machine (BD LSRFortessa™) supplied with: (1) 488 nm blue laser and a bandpass filter 530/30 for detecting EGFP expressing bacteria, (2) UV laser 355 nm and a bandpass filter 450/50 for detecting Sirius expressing bacteria.
2. Phosphate buffer saline (PBS) or Dulbecco's Phosphate buffer saline (DPBS).
3. FACS tubes.
4. Crushed ice.
5. Falcon tubes.
6. Falcon centrifuge.
7. Vortex.

2.18 The THP-1 Cell Line

1. THP-1 (ATCC TIB-202) human monocyte cell line is maintained in THP-1 medium.
2. THP-1 medium: RPMI 1640 medium, 2 mM L-Glutamine, 0.05 mM 2- mercaptoethanol, 10% fetal bovine serum, 100 U/ml penicillin, 100 μg/ml streptomycin, 10 mM HEPES. Cells are grown at a density of $2–4 \times 10^5$ cells/ml at 37 °C in a humidified atmosphere containing 5% CO_2. Cells should be subcultured when concentration reaches 8×10^6 cells/ml. Medium renewal is done every 2–3 days.
3. THP-1 medium containing 10 ng/ml Phorbol 12-myristate 13-acetate (PMA). To differentiate THP-1 cells into macrophages, cells are cultured for 24 h at 37 °C in a humidified atmosphere containing 5% CO_2 in THP-1 medium containing 10 ng/ml PMA.

2.19 Fixation and FACS Analysis of Fluorescent THP-1 Cells

1. 4% paraformaldehyde: prepare by adding 4 g to 50 ml distilled water in a suitable glass container on a hot stir plate adjusted to 60 °C, add NaOH solution dropwise until obtaining a clear solution, cool down, add 50 ml 2× PBS, and filter-sterilize with a 0.22 μm filter membrane.
2. FACS buffer: 1× PBS, 1% bovine serum albumin, 0.01% NaN_3, 1% human serum or heat-inactivated plasma.

3 Methods

3.1 Cloning of Promoter Region

3.1.1 Genomic DNA Isolation from Streptococci (Template DNA for Promoter)

Genomic DNA isolation can be done by using a commercially available genomic DNA extraction kit (QIAmp DNA Mini, QIAGEN, or GenElute Bacterial Genomic DNA, Sigma). Alternatively, genomic DNA can be isolated with the following protocol (all centrifugation steps are done in a microcentrifuge unless otherwise indicated):

1. Prepare fresh 5 ml overnight cultures of wild-type streptococcal strains in THY broth at 37 °C, 5% CO_2.
2. Pellet bacteria by centrifugation for 10 min at ≥4000 × *g* in a Falcon tube centrifuge or at 7700 × *g* in a microcentrifuge.
3. Resuspend the bacterial pellet in 1 ml TE buffer and centrifuge for 1 min at 7700 × *g*. Discard the supernatant.
4. Resuspend the pellet in 300 µl TES buffer.
5. Add 4 µl lysozyme (50 mg/ml), and 10 µl mutanolysin (5000 U/ml). Incubate for 2 h at 37 °C.
6. Add 22 µl 10% SDS and 15 µl proteinase K (20 mg/ml). Incubate for 2 h at 55 °C.
7. Add 100 µl saturated NaCl solution. Centrifuge for 10 min at 17,000 × *g*. Transfer the supernatant into a new Eppendorf tube.
8. Add equal volume of phenol–chloroform mixture 1:1 and mix by inverting the tubes up and down. Centrifuge for 4 min at 17,000× *g*.
9. Transfer the upper phase into a new Eppendorf tube and complete the rest volume with cold 100% ethanol. Mix gently by inverting the tube up and down.
10. Centrifuge for 5 min at 17,000 × *g*. Discard the supernatant. Let DNA pellet dry on a clean tissue paper.
11. Resuspend the dried pellet in 100 µl Tris buffer. Sore at 4 °C for short-term or at −20 °C for longer term storage.

3.1.2 Primer Design of Specific Promoter Region of Interest

1. Identify the correct sequence of the promoter region of interest (usually 500 bp upstream the gene under test) using The Kyoto Encyclopedia of Genes and Genomes (http://www.kegg.jp/) and the NCBI server (http://www.ncbi.nlm.nih.gov/).
2. Design a primer pair to amplify the selected promoter region including the ATG start codon of the corresponding gene. Make sure that the triplet nucleotide order for the region following the start codon is maintained when designing the primers in order to ensure correct N-terminal translational fusions of the promoter 3′-end and the fluorescence gene 5′-end with no translational shifts.
3. Design primers in a way to add suitable restriction sites to the cloned promoter region in order to facilitate directional cloning. These restriction sites should be compatible with those available in the MCS upstream the fluorescence gene. In case of using the promoterless EGFP-pAT28 reporter plasmid pBSU100 the available restriction sites are *Bam*HI, *Eco*RI, *Sac*I, *Kp*nI,*Sma*I, *Xma*I (Fig. 2). In case of using the promoterless Sirius-pAT28 reporter plasmid pBSU813 the available restriction sites are *Bam*HI, *Xba*I, *Sal*I, *Pst*I, *Sph*I, *Hind*III (Fig. 3).

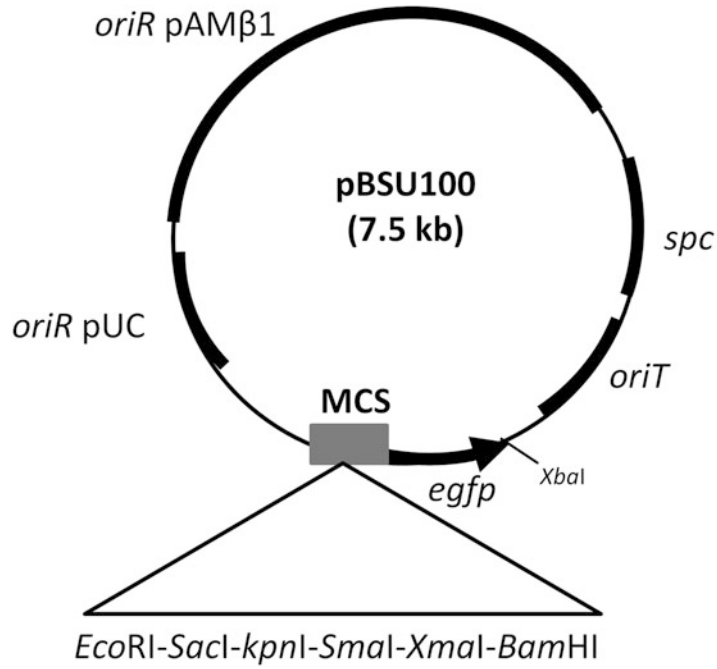

Fig. 2 Schematic diagram of the promoter-less *egfp*-pAT28 vector (pBSU100) showing the multiple cloning site upstream of the *egfp* fluorescence gene

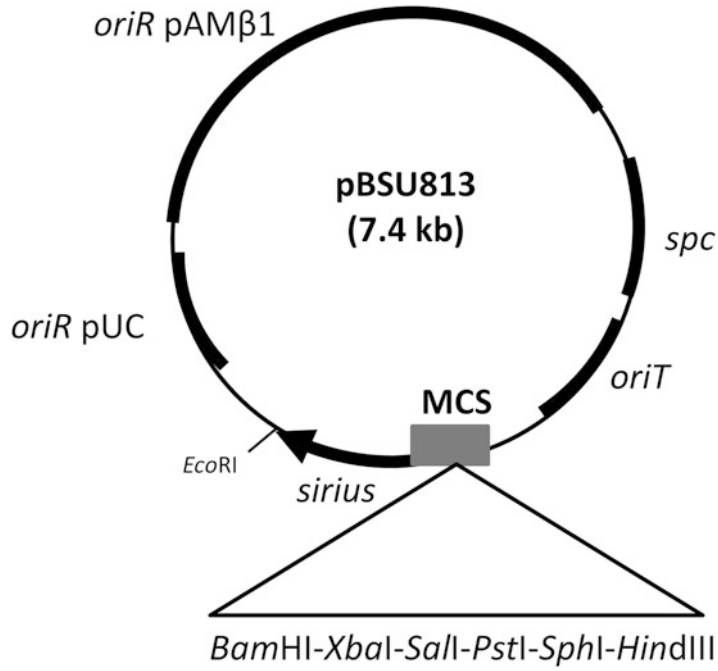

Fig. 3 Schematic diagram of the promoter-less *sirius*-pAT28 vector (pBSU813) showing multiple cloning site upstream of the *sirius* fluorescence gene

3.1.3 PCR Amplification of the Promoter Region

1. Using the wild-type genomic streptococcal DNA as a template (*see* Subheading 3.1.1), perform a PCR reaction with *Taq* polymerase according to the manufacturer's protocol (Roche, Mannheim, Germany), with 35 cycles of amplification steps of 1 min at 94 °C, 1 min at 55 °C, and 1–3 min at 72 °C depending on product size.
2. To confirm correct amplicon size, run PCR products on 1–2% agarose gel along with a proper DNA ladder (*see* **Note 1**).
3. Perform a PCR cleanup of the PCR product to remove salts, enzymes, etc. from the enzymatic reaction using a PCR cleanup kit.
4. Determine the DNA concentration of the amplified promoter using the Quant-iT assay kit and the Qubit fluorometer. Alternatively, DNA concentration can be determined by reading the absorbance at 260 nm in a spectrophotometer.
5. Use immediately or store at −20 °C until use.

3.2 Plasmid Preparation of pBSU100 and pBSU813 from E. coli BSU100/BSU813 (recombinant E. coli hosts carrying promoterless pAT28 derivatives of egfp and sirius fluorescence genes respectively)

1. Prepare fresh overnight cultures of the corresponding *E. coli* strain in LB broth supplemented with 100 μg/ml spectinomycin at 37 °C in a shaking incubator.
2. Pellet 1–5 ml bacteria overnight culture by centrifugation for 10 min at 4000 × *g* in a Falcon centrifuge or for 3 min at 7700 × *g* in a microcentrifuge.
3. Proceed with the plasmid preparation using a commercial plasmid extraction kit (QIAprep Spin Miniprep, QIAGEN).
4. Use immediately or store at 4 °C until use.

3.3 Restriction Digestion and Purification of Digested DNA

1. In case of constructing an EGFP reporter plasmid, perform a restriction digestion for the amplified promoter region (*see* Subheading 3.1.3) and pBSU100 (*see* Subheading 3.2) using the same restriction enzymes. In case the desired construct is a Sirius reporter plasmid, then restriction digestion is done for the amplified promoter region (*see* Subheading 3.1.3) and pBSU813 (*see* Subheading 3.2) using the same restriction enzymes.
2. Run restriction reaction as indicated by the manufacturer (Roche), mostly at 37 °C for 1–4 h in a thermocycler or a thermal block (*see* **Note 2**).
3. Make sure to select a proper buffer, which is compatible with the restriction enzymes used.
4. Digest up to 1 μg DNA per reaction.

5. Perform a DNA cleanup for the digested products using a DNA cleanup kit (Mini Elute reaction cleanup, QIAGEN).
6. Determine the DNA concentration of the restricted products using the Quant-iT Assay kit and the Qubit fluorometer or by reading the absorbance at 260 nm in a spectrophotometer.
7. Use immediately or store at −20 °C until use.

3.4 Ligation of the Digested Products Using a Rapid Ligation Kit as Follows

1. Thaw ligation reaction buffer, mix thoroughly and keep on ice.
2. Mix 50–100 ng of vector DNA (purified restricted pBSU100/pBSU813, *see* Subheading 3.3) with a fourfold molar excess of insert DNA (the purified restricted promoter region, *see* Subheading 3.3). Size of pBSU100 is equal to 7.5 kb and that of pBSU813 is 7.4 kb.
3. Bring volume to x μl with nuclease free water.
4. Add y μl of ligation buffer, and mix by pipetting.
5. Add z μl T4 DNA ligase, mix gently.
6. Incubate at room temperature for 10 min. Then place on ice.
7. Transform immediately into *E. coli* DH5α or store at −20 °C until use.

3.5 Transformation of New Recombinant Constructs into E. coli DH5α

In order to increase the plasmid copy number and maintain a permanent source for newly constructed vectors it is recommended to transform the new vectors into a suitable *E. coli* host such as *E. coli* DH5α. Transformation protocol is done as follows:

1. Prepare 5 ml fresh overnight cultures of *E. coli* DH5α in LB broth at 37 °C in a shaking incubator.
2. Transfer 1 ml overnight culture into 50 ml LB broth. Incubate for 2 h at 37 °C in a shaking incubator.
3. Centrifuge for 10 min at 4000 × *g* in a Falcon centrifuge adjusted to 4 °C. Discard the supernatant.
4. Resuspend the pellet in 25 ml 0.1 M $CaCl_2$ (cold and sterilized). Place on ice for 30 min.
5. Centrifuge for 10 min at 4000 × *g* in a Falcon tube centrifuge adjusted to 4 °C. Discard the supernatant.
6. Resuspend the pellet in 5 ml 0.1 M $CaCl_2$ (cold and sterilized).
7. Use immediately or store on ice at 4 °C until use (maximum storage 18 h). Now competent cells are ready to use.
8. On ice, mix 10 μl of ligation mixture (*see* Subheading 3.6) with 200 μl competent cells in prechilled Eppendorf tubes (*see* **Note 3**). An aliquot of competent cells to which no DNA is added should be included as a negative control. Positive controls are prepared by adding a known amount of a standard plasmid DNA to an aliquot of competent cells.

9. Incubate on ice for 30 min then at 42 °C for 2 min, and finally on ice for 3 min.
10. Add 800 µl LB broth and incubate for 1 h at 37 °C.
11. Centrifuge for 1 min at 20,000 × *g*. Resuspend in 100 µl of supernatant and discard the rest.
12. Using sterilized glass beads spread the resuspended cells on LB agar supplemented with 100 µg/ml spectinomycin.
13. Incubate overnight at 37 °C. Transformed colonies should appear on the next day. No bacterial colonies should appear on the negative control plates.

3.6 Screening Transformed E. coli Colonies for the Presence of Correct Recombinant Plasmids

1. Perform a plasmid preparation of recombinant *E. coli* (*see* Subheading 3.2).
2. Screen the prepared plasmids for the correct construct by visualization on 0.8–1% agarose (*see* **Note 1**) gel in comparison to the parent plasmid. Afterwards selected plasmids undergo a restriction digestion to test the presence of the correct insert. Additionally, perform PCR and sequencing of selected plasmids using primers flanking the whole insertion site shown in Table 3 (*see* **Note 4**).
3. Recombinant *E. coli* strains harboring the correct constructs can be stored at −80 °C.

3.7 Transformation of Recombinant Plasmid Constructs into Streptococci by Electroporation (All Steps Done on Ice)

1. Prepare fresh 5 ml overnight cultures of wild-type streptococci in THY broth at 37 °C, 5% CO_2.
2. For *S. agalactiae*, inoculate 100 ml THY broth with 2 ml overnight culture, incubate at 37 °C, 5% CO_2 until reaching an OD of 0.4 at 600 nm. For other streptococci, inoculate 5 ml THY broth with 150 µl overnight culture, incubate at 37 °C, 5% CO_2 for 6–8 h then transfer 2 ml into 100 ml THY broth and incubate overnight at 37 °C, 5% CO_2.
3. Centrifuge for 10 min at 4000 × *g* for *S. agalactiae* and 5000 × *g* for other streptococci in a Falcon tube centrifuge at 4 °C. Discard the supernatant.
4. Resuspend the pellet in 100 ml 10% glycerol (cold and sterilized).
5. Centrifuge for 10 min at 4000 × *g* for *S. agalactiae* and 5000 × *g* for other streptococci in a Falcon tube centrifuge at 4 °C. Discard the supernatant.
6. Resuspend the pellet in 50 ml 10% glycerol (cold and sterilized). Repeat **step 5**.
7. Resuspend the pellet in 25 ml 10% glycerol (cold and sterilized). Repeat **step 5**.

8. Resuspend the pellet in 12.5 ml 10% glycerol (cold and sterilized). Repeat **step 5**.
9. Resuspend in the pellet in 1 ml 10% glycerol (cold and sterilized). Transfer into a sterilized 1.5 ml Eppendorf tube. Centrifuge for 5 min at 20,000×*g* in a microcentrifuge at 4 °C. Discard the supernatant.
10. Resuspend the pellet in 1 volume 20% glycerol (cold and sterilized) (*see* **Note 5**). Now streptococcal competent cells are ready to use. On ice, divide the competent cells into 25 µl aliquots.
11. Mix 25 µl competent cells with 25 µl 10% glycerol (cold and sterilized) and 1 µg DNA (new recombinant plasmid isolated from *E. coli*, *see* Subheading 3.6).
12. Transfer into 1 mm electroporation cuvette.
13. Expose to a single electric pulse with a gene pulser apparatus (2 kV, 25 µF, 10 Ω) (*see* **Note 5**).
14. Add 1 ml pre-warmed THY broth (or Todd-Hewitt broth with 10% glycerol).
15. Transfer to 1.5 ml Eppendorf tube and incubate for 1.5–2 h at 37 °C.
16. Centrifuge for 1 min at 20,000×*g*. Resuspend in 100 µl of supernatant and discard the rest.
17. Using sterilized glass beads spread the resuspended cells on THY agar supplemented with 120 µg/ml spectinomycin. Incubate overnight at 37 °C, 5% CO_2.
18. On the next day check the plates for colonies of recombinant streptococci.

3.8 Plasmid Preparation from Recombinant Streptococci Carrying pBSU100/pBSU813 or Their Derivatives

1. Prepare fresh 10 ml overnight cultures of recombinant streptococci (from Subheading 3.7) in THY broth supplemented with 120 µg/ml spectinomycin at 37 °C, 5% CO_2.
2. Pellet bacteria by centrifugation for 10 min at 4000–5000×*g* in a Falcon tube centrifuge.
3. Discard the supernatant and resuspend the pellet in 1 ml 1×PBS or 0.9% NaCl. Transfer into a 1.5 ml Eppendorf tube and centrifuge for 5 min at 20,000×*g*. Discard the supernatant.
4. Resuspend the pellet in 350 µl P1 buffer (QIAprep Spin Miniprep kit, QIAGEN).
5. Transfer into ribolyser tubes filled with glass beads (150–212 µm) to the 250 µl level mark.
6. Ribolyse four times at speed 6.0, for 20 s.
7. Centrifuge for 5 min at 20,000×*g*.

8. Transfer the supernatant (approximately 250 µl) into a 1.5 ml Eppendorf tube.
9. Add 250 µl P2 buffer and proceed with the manufacturer's protocol.
10. Isolated plasmids are used immediately or stored at 4 °C until use.

3.9 Confirm Success of Electroporation

Recombinant plasmids from recombinant streptococci (prepared in Subheading 3.10) are checked for the correct construction (*see* Subheading 3.8). Recombinant streptococcal strains are then stored at −80 °C.

3.10 Fluorescence Microscopy

3.10.1 Fluorescence Microscopy of EGFP/Sirius Expressing Streptococci (Harboring pBSU101/pBSU836 Respectively or Derivatives of pBSU100/pBSU813)

1. Prepare fresh 10 ml overnight cultures of recombinant streptococci in THY broth supplemented with 120 µg/ml spectinomycin at 37 °C, 5 % CO_2 (*see* **Note 6**).
2. Pellet bacteria by centrifugation for 10 min at 4000–5000 × *g* in a falcon centrifuge at 4 °C. Discard the supernatant.
3. Resuspend the pellet in 10 ml PBS. Centrifuge for 10 min at 4000–5000 × *g* in a Falcon centrifuge at 4 °C. Discard the supernatant.
4. Resuspend in 1 ml PBS. Spot 10 µl on a clean microscopic slide. Cover with a clear coverslip.
5. Examine under fluorescence microscope (Zeiss Axioskop-2® fluorescence microscope fitted with an Axiocam HR camera and Axiovison software version 4.8) in a darkened room. Use GFP filter set for recombinant streptococci carrying EGFP reporter plasmids and DAPI filter set for strains carrying the Sirius reporter plasmids.

3.10.2 Fluorescence Microscopy of EGFP-Expressing Streptococci in THP-1 Cells

1. Seed an amount of 0.5×10^6 THP-1 cells cultured in THP-1 medium with antibiotics into 12-well tissue culture plate containing sterilized coverslips.
2. Allow for monocytic THP-1 differentiation into macrophages by adding 10 ng/ml PMA to the culture medium. Incubate overnight at 37 °C, 5 % CO2. Differentiated macrophages will become adherent to the coverslips present at the bottom of the well.
3. On the next day, wash adherent THP-1 cells three times with pre-warmed THP-1 medium without antibiotics or 1× PBS.
4. Using fresh overnight bacterial cultures or bacterial cells grown to mid-logarithmic phase (washed once in 1× PBS and resuspended in THP-1 medium without antibiotics) infect differentiated THP-1 macrophages with EGFP-expressing streptococci at a multiplicity of infection (MOI) 1:1 and 10:1. Incubate at 37 °C, 5 % CO_2 for 1 h (MOIs and incubation times should be optimized according to the purpose of the experiment and streptococcal species used).

5. At the end of the incubation time wash infected THP-1 macrophages three times with pre-warmed 1× PBS followed by fixation with freshly prepared 4% formaldehyde for 20 min.
6. Wash once with 1× PBS. The coverslips with adherent THP-1 infected macrophages are removed and allowed to air-dry.
7. Perform staining with Evans Blue (1: 400 dilution in 1× PBS) for 30 min in the dark.
8. Wash once with 1× PBS. The coverslips are air-dried again in the dark.
9. To mount the cells on a microscopic glass slide, add one drop of a suitable mounting medium (VECTASHIELD) with an anti-fade reagent supplemented with/without DAPI stain.
10. Use immediately or store in the dark at 4 °C until use.
11. Visualize intracellular EGFP-expressing bacteria within THP-1 macrophages by a fluorescence microscope (Zeiss Axioskop-2® fluorescence microscope fitted with an Axiocam HR camera and Axiovison software version 4.8) using GFP filter set.

3.11 Fluorescence Activated Cell Sorting (FACS)

3.11.1 Promoter Analysis Using FACS

Activity pattern of the cloned promoter of interest can be analyzed using recombinant streptococcal stains carrying EGFP/Sirius reporter plasmids where EGFP/Sirius is expressed under the control of that promoter. Promoter fluorescence activity is determined by FACS as follows:

1. Harvest fresh cultures of recombinant streptococci in THY broth supplemented with 120 μg/ml spectinomycin (bacteria should be grown at suitable induction conditions for the promoter under investigation, *see* **Note 6**) by centrifugation for 10 min at 4000–5000 × *g* in a Falcon tube centrifuge at 4 °C. Discard the supernatant.
2. Wash once by resuspending in equal volume of PBS. Centrifuge for 10 min at 4000 × *g* in a Falcon tube centrifuge at 4 °C. Discard the supernatant.
3. Resuspend in 1 ml PBS and keep on ice.
4. Analyze by FACS (BD LSRFortessa™) using a 488 nm blue laser and a bandpass filter 530/30 for EGFP recombinant reporter plasmids. Sirius recombinant plasmids are examined using a UV laser 355 nm and a bandpass filter 450/50.
5. Adjust the bacterial suspensions in order to keep an acquisition flow rate at 150–250 events/s.
6. Determine background fluorescence for EGFP and Sirius expressing bacteria by using recombinant streptococcal strains harboring the promoterless *egfp/sirius* plasmids pBSU100 and pBSU813 respectively.
7. Determine relative fluorescence intensity for 10,000 events.

8. Further analysis of generated FACS files can be done using Flow Jo software (FlowJo Enterprise).

3.11.2 FACS Analysis for EGFP/Sirius Expressing Bacteria (Harboring pBSU101/pBSU836 Respectively)

The fluorescent vectors pBSU101/pBSU836 harbor EGFP/Sirius which are expressed under the control of the *cfb* promoter of *S. agalactiae*. These vectors can be used for fluorescence labeling of *S. agalactiae* and other streptococcal species. Streptococcal stains harboring pBSU101/pBSU836 can be analyzed by FACS as described under Subheading 3.11.1

3.11.3 FACS Analysis for Fluorescent THP-1 Macrophages Infected with EGFP-Expressing Streptococci

1. Seed an amount of 1×10^6 THP-1 cells cultured in THP-1 medium into 6-well tissue culture plate.
2. Allow for monocytic THP-1 differentiation into macrophages by adding 10 ng/ml PMA to the culture medium. Incubate overnight at 37 °C, 5% CO2. Differentiated macrophages will become adherent to the coverslips present at the bottom of the well.
3. On the next day, wash adherent THP-1 cells three times with pre-warmed THP-1 medium without antibiotics or 1× PBS. Add equal volume of THP-1 medium without antibiotics.
4. Using fresh overnight bacterial cultures or bacterial cells grown to mid-logarithmic phase (washed once in 1× PBS and resuspended in THP-1 medium without antibiotics) infect differentiated THP-1 macrophages with EGFP-expressing streptococci at a multiplicity of infection 1:1, 10:1. Incubate infected macrophages at 37 °C, 5% CO_2 for 1 h (MOIs and incubation times should be optimized according to the purpose of the experiment and streptococcal species used).
5. At the end of the incubation time, wash three times with pre-warmed 1× PBS then scrap adherent THP-1 macrophages with sterile cell scrapers.
6. Harvest by centrifugation at 2000 × *g* for 10 min. Discard the supernatant.
7. Resuspend in 1 ml FACS buffer. Centrifuge at 2000 × *g* for 10 min. Discard the supernatant.
8. Resuspend the cell pellet in 750 μl FACS buffer and fix the cells by adding 250 μl freshly prepared 4% formaldehyde solution.
9. Use immediately or store at 4 °C in the dark until use.
10. Percentage of fluorescent THP-1 macrophages infected with EGFP-expressing bacteria is analyzed by FACS (BD LSRFortessa™) using a 488 nm blue laser and a bandpass filter 530/30.
11. Use uninfected THP-1 cells as a negative control for background fluorescence.
12. Further analysis for generated FACS files can be done using Flow Jo software.

4 Notes

1. Agarose concentration: 1–2 % agarose has a good resolution for small fragments less than 500 bp. However, 0.8 % agarose has a good resolution for large DNA fragments 5–10 kb.
2. Ensure that the volume of the restriction enzyme does not exceed more than 10 % of the total reaction volume otherwise the glycerol in which the enzyme is supplied may inhibit digestion.
3. Transforming DNA should be added in a volume not exceeding 5 % of that of the competent cells.
4. In case that pBSU100 is used as a vector backbone then PCR amplification of the insertion site can also be achieved using the forward promoter primer and the pAT-2 primer (Table 3). However, in case pBSU813 is the vector backbone then the pAT-3 primer (Table 3) coupled with the forward promoter primer may be used for the insertion site amplification. In each case the amplified region includes both the fluorescence gene and the promoter.
5. Please keep in mind, for streptococci the preparation of competent cells and applied electric pulse are species and strain dependent and may need further optimization. The given conditions are optimized for *S. agalactiae* and have been found to give good results with other streptococcal species.
6. Always adjust the culture conditions according to the purpose of the experiment (adding certain supplements, pH adjustments, using different culture medium, etc.)

References

1. Chudakov DM, Matz MV, Lukyanov S, Lukyanov KA (2010) Fluorescent proteins and their applications in imaging living cells and tissues. Physiol Rev 90(3):1103–1163. doi:10.1152/physrev.00038.2009
2. Chalfie M, Tu Y, Euskirchen G, Ward WW, Prasher DC (1994) Green fluorescent protein as a marker for gene expression. Science 263(5148):802–805
3. Zimmer M (2002) Green fluorescent protein (GFP): applications, structure, and related photophysical behavior. Chem Rev 102(3):759–781
4. Tsien RY (1998) The green fluorescent protein. Annu Rev Biochem 67:509–544. doi:10.1146/annurev.biochem.67.1.509
5. Cormack BP, Valdivia RH, Falkow S (1996) FACS-optimized mutants of the green fluorescent protein (GFP). Gene 173((1 Spec No)):33–38
6. Bokman SH, Ward WW (1981) Renaturation of Aequorea green-fluorescent protein. Biochem Biophys Res Commun 101(4):1372–1380
7. Cody CW, Prasher DC, Westler WM, Prendergast FG, Ward WW (1993) Chemical structure of the hexapeptide chromophore of the Aequorea green-fluorescent protein. Biochemistry 32(5):1212–1218
8. Hansen MC, Palmer RJ Jr, Udsen C, White DC, Molin S (2001) Assessment of GFP fluorescence in cells of Streptococcus gordonii under conditions of low pH and low oxygen concentration. Microbiology 147(Pt 5): V1383–1391
9. Smith CB, Anderson JE, Fischer RL, Webb SR (2002) Stability of green fluorescent protein using luminescence spectroscopy: is GFP applicable to field analysis of contaminants? Environ Pollut 120(3):517–520

10. Tomosugi W, Matsuda T, Tani T, Nemoto T, Kotera I, Saito K, Horikawa K, Nagai T (2009) An ultramarine fluorescent protein with increased photostability and pH insensitivity. Nat Methods 6(5):351–353. doi:10.1038/nmeth.1317
11. Trieu-Cuot P, Carlier C, Poyart-Salmeron C, Courvalin P (1990) A pair of mobilizable shuttle vectors conferring resistance to spectinomycin for molecular cloning in Escherichia coli and in gram-positive bacteria. Nucleic Acids Res 18(14):4296
12. Gleich-Theurer U, Aymanns S, Haas G, Mauerer S, Vogt J, Spellerberg B (2009) Human serum induces streptococcal c5a peptidase expression. Infect Immun 77(9):3817–3825. doi:10.1128/iai.00826-08
13. Asam D, Mauerer S, Spellerberg B (2015) Streptolysin S of Streptococcus anginosus exhibits broad-range hemolytic activity. Med Microbiol Immunol 204(2):227–237. doi:10.1007/s00430-014-0363-0
14. Aymanns S, Mauerer S, van Zandbergen G, Wolz C, Spellerberg B (2011) High-level fluorescence labeling of gram-positive pathogens. PLoS One 6(6):e19822. doi:10.1371/journal.pone.0019822

Chapter 10

Computer Vision-Based Image Analysis of Bacteria

Jonas Danielsen and Pontus Nordenfelt

Abstract

Microscopy is an essential tool for studying bacteria, but is today mostly used in a qualitative or possibly semi-quantitative manner often involving time-consuming manual analysis. It also makes it difficult to assess the importance of individual bacterial phenotypes, especially when there are only subtle differences in features such as shape, size, or signal intensity, which is typically very difficult for the human eye to discern. With computer vision-based image analysis — where computer algorithms interpret image data — it is possible to achieve an objective and reproducible quantification of images in an automated fashion. Besides being a much more efficient and consistent way to analyze images, this can also reveal important information that was previously hard to extract with traditional methods. Here, we present basic concepts of automated image processing, segmentation and analysis that can be relatively easy implemented for use with bacterial research.

Key words Image segmentation, Object recognition, Region properties, MATLAB, ImageJ

1 Introduction

In bacterial research, images of bacteria are still mostly analyzed and interpreted through methods reliant on continuous manual input. The main disadvantages of this are related to our human nature, with the risk of subjectivity and reproducibility — especially after long sessions—as well as the fact that it takes up a significant amount of time. These issues are especially apparent when there are hundreds, if not thousands, of images to analyze [1]. The recent revolution in fluorescent microscopy with computer-controlled microscopes that can acquire images at high speed in multiple dimensions, including channels, time, and space only adds to the complexity of image analysis — in many cases making quantitative manual analysis an impossible task. An alternative way of identifying bacteria and analyzing them is to use computer algorithms instead; this subfield of artificial intelligence is called computer vision. Computer vision has the advantage of being automated, objective, and completely reproducible; this approach also has the added benefit of "seeing" data that is typically not detectable by a human operator [1]. While this method is

Pontus Nordenfelt and Mattias Collin (eds.), *Bacterial Pathogenesis: Methods and Protocols*, Methods in Molecular Biology, vol. 1535, DOI 10.1007/978-1-4939-6673-8_10,

currently commonly used in other fields of application, such as facial recognition [2], optical character recognition for scanning documents [3], medical imaging [4], and automatic cell counters [5–7], there is a distinct lack of general approaches within bacterial pathogenesis research. Examples found [8–11] pertaining computer vision are generally restricted to one specific study or a group of studies and in overall computer vision seems currently to be an under-developed field in bacterial pathogenesis research. Besides the obvious benefits for accurate quantification and detailed analysis, one of the most interesting applications of automatic image analysis is the possibility to identify a single bacterium and track its movements reliably over time in information dense movies. Here, we present the basic concepts of computer vision with a focus on explaining principal methods and their uses, in an effort to give a starting point for interested scientists.

2 Materials

ImageJ (NIH) and MATLAB (Mathworks) are two of the most commonly used software packages for computer vision analysis. ImageJ is open source and much of its functionality comes from user-designed plugins. MATLAB has several toolboxes that expand the functionality and include many optimized algorithms for computer vision. We have listed some useful ImageJ plugins and MATLAB toolboxes.

2.1 ImageJ (See Note 1)

1. Otsu Thresholding.
2. Watershed Transformation.
3. Multi Thresholder.
4. Cell Counter.
5. Hough Circles.
6. Bio-Formats.

2.2 MATLAB (See Note 2)

1. Image Processing Toolbox.
2. Computer Vision System Toolbox.
3. Fuzzy Logic Toolbox.
4. Signal Processing Toolbox.
5. Bio-Formats Toolbox (*see* **Note 3**).

3 Methods

3.1 Basic Program Design

A flowchart for a basic bacterial image analysis software (*see* **Note 4**) is shown in Fig. 1. The software in question is broken up into major sections, which in turn consists of smaller and more specific modules. The initial step, input, is composed of simply loading the raw

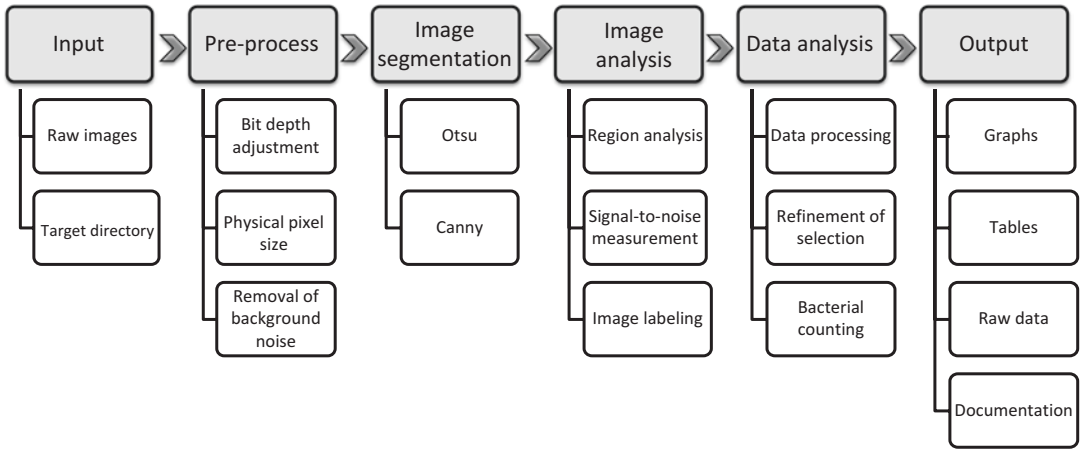

Fig. 1 Flowchart for a basic bacterial image analysis software

image into the software, and defining the directory the results will be deposited in. The preprocessing step is used for preparing the image for segmentation by cleaning up noise, reducing background and extracting important information about the raw image (often designated metadata) that can be used at later stages. It is also here that any global adjustments to the data is done (*see* **Notes 5** and **6**). The third step, image segmentation, is where the preprocessed image is turned into a binary mask. In relation to this chapter, a mask is considered a binary image consisting of only 1s and 0s, and the 1s correspond to regions defined as objects and the 0s as regions defined as background. Image segmentation is also the step that often needs to be optimized the most to achieve good results from the image analysis. The generated mask works by functioning as a filter in the image analysis step and the analysis is performed on the same preprocessed image as the mask was generated from. This means that the software can divide analyzed areas of the preprocessed image that corresponds to the regions that are composed of 0s and 1s in the mask. Different analysis modules can be present in the same software as can be seen in Fig. 1 and each will generate its own data output. The generated data in the previous step is then analyzed, structured, and refined in the data analysis step. Examples of analyses are counting the numbers of bacteria found, calculating bacterial area based on μm/pixel, and calculating the eccentricity of bacteria. Refinement of selection is essential to ensure that only relevant data is analyzed, that different groups of bacteria are separated, and outliers can be identified. The goal of the data analysis step is to present the relevant data in an understandable and useable form. The final step, output, involves converting the refined data into tables and graphs to present the results of the analysis. Another important function of the output is to generate all the data from each step and store it in a structured system. This allows the data and the whole process to be reexamined without having to rerun

the entire process. Most importantly, together with the program code, this provides documentation on exactly what was done, on what it was done, when it was done, and how it was done.

3.2 Principal Methods

Segmentation is a common step in image analysis and consists of separating objects from the background in an image. This is based on identifying features, such as pixel intensity, and using that to divide the pixels into non-overlapping regions [12]. For the purpose of this chapter the aim of the segmentation is to acquire a binary image that is typically called a mask. The mask is then used for defining the regions the software should analyze, and this step is therefore critical for performing image analysis with any reliability. The four major groups of grayscale segmentation methods that will be examined here are the following; thresholding, edge detection, active contour, and watershed transformation.

Threshold-based segmentation functions by using a threshold value to separate objects from the background. Bi-level thresholding results in pixels being divided into two classes, objects and background, and requires the use of only one threshold value. Using multiple thresholds allows multiple classes or groups of pixels to be identified, and this method goes under the name of multilevel thresholding [12].

Edge detection defines edges based on discontinuities in intensity between pixels [13]. This can be done due to the general assumption that it will correspond to discontinuities in depth, properties, illumination, or surface orientation [14]. One common problem with edge detection is fragmentation, which is where the edges are not completely connected to each other, but instead consists of multiple fragments. A second issue is the presence of false edges which can be considered the equivalent of false positives concerning detection [14].

Active contour segmentation uses a malleable spline, or snake, to adhere to object contours. Snakes utilize algorithms that minimizes the energy present when the snake has localized and molded itself to a feature [15]. The strengths of active contouring are: tracking objects in motion, it is autonomous and adaptive, sensitivity is scalable through Gaussian smoothing, and that the snake's behavior is intuitive. A disadvantage of this method is that there is a risk that matching the major feature will result in a lower energy compared to matching minor details, and therefore it may miss those. Further issues are that the accuracy of the method is directly proportional to the computational time and there exists a tendency to remain stuck in local minima states [15].

Watershed transformation is easiest illustrated by imagining a topographical relief, with pixel intensity seen as depth. This means that the higher the pixel's intensity is, the deeper it is located. The first step is the placement of markers in objects and the background. The second and final step is to "flood" the image, using the markers as the sources of "water." A "dam" is created every time distinct catchment basins' water would come into contact

with each other. This results in a segmented image where each marker should be in its own separate region. The major issue with this method is the high risk of over-segmentation (*see* **Note 7**) [16]. Watershed transformation is useful as a secondary segmentation method, where it can be used to separate merged regions from each other and in that way achieve a better mask.

Otsu's method is a threshold segmentation variant. The algorithm calculates the threshold by minimizing the intra-class variance and maximizing the inter-class variance between the pixel classes. This generates a so called "optimal threshold," which both removes the need to manually enter the threshold value but more importantly maximizing the separability of bacteria and background. However, this method requires the pixel intensity distribution to be following a bimodal histogram and therefore cannot reliably be used on multi-class images [17]. Fortunately, Otsu's method is easily adapted to be able to calculate multiple thresholds which allow it to segment these multi-class images. This modified method generally goes under the name of Multi Otsu [18]. However, it is rather inefficient and time-consuming [19] (*see* **Note 8**).

Canny edge detector is another commonly used segmentation method (*see* **Note 9**), which as an edge detector functions by identifying edges based on difference in intensity between pixels. This is done through five different steps of computation. First a Gaussian filter is applied to negate background noise followed by identifying the gradients of intensity, suppressing non-maxima, finding potential edges by identifying the gradients of intensity, and finally by suppressing weak edges through hysteresis [13]. One of the advantages with Canny is how sensitive the method is at detecting edges, but it is less robust than Otsu and has a tendency to over-segment, especially when exposed to Gaussian background noise.

Otsu's optimal threshold can replace Canny's own calculated high threshold value (*see* **Note 10**) and this improves the segmentation results from the Canny edge detector [20].

3.2.1 Refinement of Bacterial Selection

One of the most essential aspects of image analysis is to properly screen and select, based on the research aim, the data that should be analyzed. Enhancing data selection is important due to the fact that the software will be non-discriminatory without explicit directions, for example it would treat artifact signals as equally important as bacterial signals. This enhancement of data can be based on multiple parameters, some which are detailed in Table 1 along with in what scenarios certain parameters would be preferred. This has the additional advantage of allowing the analysis of different signals from a single image. For instance, separating two different species of bacteria can be achieved by comparing their eccentricity if there is a significant difference in shape between the bacterial species. In comparison, an area based separation would not perform nearly as well if the species had a similar size, despite any differences in shape. The opposite is seen in removal

Table 1
Bacterial selection measurements easily attainable with MATLAB and their potential applications for refinement

Measurement	Good for
Signal-to-noise	Eliminating weakly fluorescent bacteria and artifacts. Evaluating image and segmentation quality (*see* **Note 13**)
Area	Eliminating artifacts that significantly differ in size Calculating number of bacteria based on average size, when working with clustering bacteria
Eccentricity	Separating different bacterial species
Mean intensity	Eliminating weakly fluorescent bacteria and artifacts
Centroid	Labeling and identifying bacteria
Weighted Centroid	Combine with Centroid to generate a vector for spatial correlation of molecular activity (*see* **Note 14**)
STD/SEM pixel intensity	Separating homogenously fluorescent bacteria from heterogeneously fluorescent bacteria
Perimeter	Component for calculating the length of the medial axis of rod shaped bacteria (*see* **Note 15**)
Color	Separating bacteria based on different fluorescence markers

of artifacts—a task area-based separation excels at—while eccentricity separation will be lacking (*see* **Notes 11** and **12**). This is due to artifacts having a random shape, and there is a smaller potential span of measurement compared to area. Another way of isolating bacteria behaving differently would be to utilize the standard deviation of pixel intensity, and separate the population into groups depending on how homogenous the fluorescence appears.

3.3 Results: Segmentation Example

Figure 2 illustrates the process of a bacterial analysis using a software whose structure is based on the flowchart in Fig. 1. From the initial raw dual channel image of GFP (channel 1) and mCherry (channel 2) marked fluorescent bacteria we analyzed the 20% brightest and dimmest bacteria in channel 1. The original microscopy image with both channels is shown in Fig. 2a. Figure 2b, c also contains the segmented masks of channel 1 by Otsu segmentation and Canny segmentation using Otsu threshold value respectively. The difference in segmentation between Canny and Otsu is illustrated through visually comparing their masks, and by automatically counting the amount of bacteria each method found. In addition, the numbers of segmented bacteria are compared to the manually counted bacteria to test the validity of the segmentation methods and the results of this test are shown in the table *All Objects* in Fig. 2d. The results are presented as the percent of all

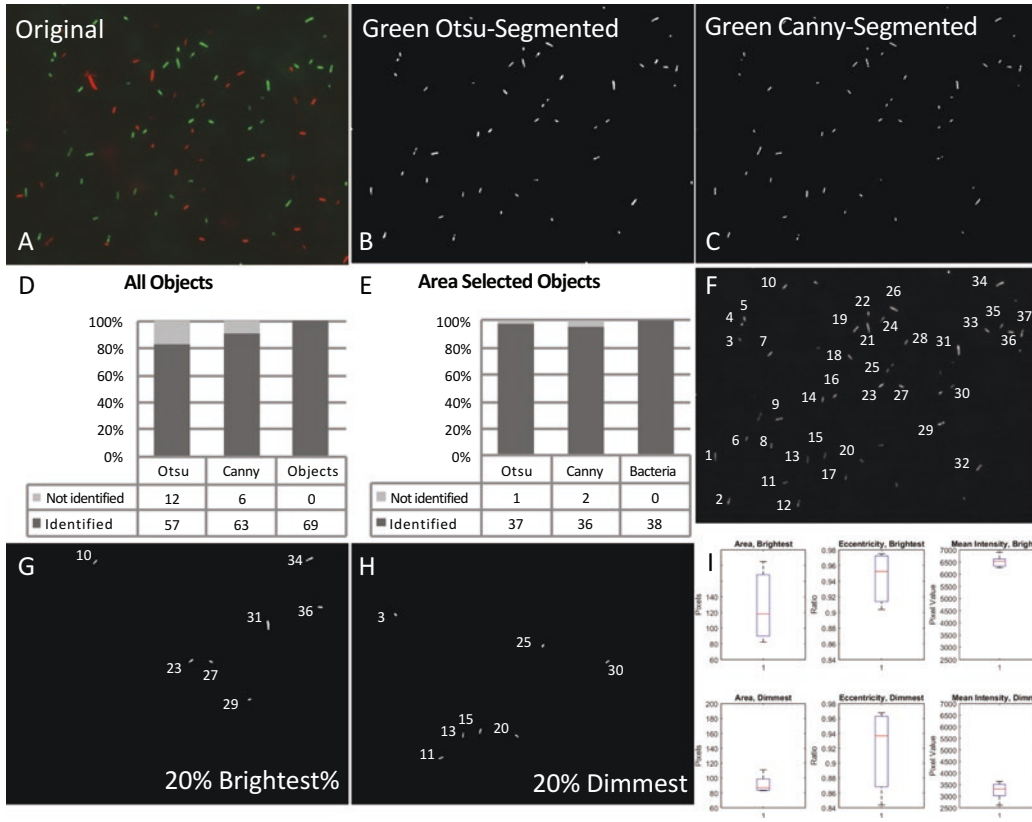

Fig. 2 Application of automated image analysis. (**a**) Raw dual channel microscopy image. (**b**) Mask generated from channel 1/green channel in (**a**) using Otsu segmentation. (**c**) Mask generated from channel 1/green channel in (**a**) using Canny segmentation. (**d**) Validity testing of Otsu and Canny segmentation by comparing the ratio of identified objects, in (**b**) and (**c**) respectively, with the total amount of objects present in channel 1/green channel from (**a**). (**e**) Validity testing of the area based selection refinement method for identifying bacteria of interest applied on the Otsu and Canny segmented masks compared with the manually selected bacteria in channel 1/green channel from (**a**). (**f**) Channel 1/green channel raw image where each bacterium identified using an area based selection on (**b**) has been individually labeled. (**g**) Mask containing the 20 % brightest bacteria isolated from the area based bacterial selection in (**f**). (**h**) Mask containing the 20 % dimmest bacteria isolated from the area based bacterial selection in (**f**). (**i**) Comparison between the 20 % brightest (**g**) and 20 % dimmest bacteria (**h**) in area, eccentricity, and mean intensity

the manually counted objects found by each method. As can be seen Otsu identifies 57 out of 69 (83 %) objects while Canny manages to identify 63 out of 69 (91 %) objects present in the image (*see* **Note 16**). This does not necessarily mean that every object we found actually corresponds to bacteria, nor does it mean that this is the type of bacteria we are interested in studying (*see* **Note 17**). The next step is the refinement of bacterial selection and in this case an area based selection (*see* **Notes 18** and **19**) was applied to enhance the identification of bacteria generated from the both the Otsu and the Canny segmentation. As before, the amount of

bacteria the method found was counted and compared to the manually counted bacteria of interest, and this is shown in the table *Area Selected Objects* of Fig. 2e. In this scenario it allows us to avoid analyzing outliers, artifacts, vertically positioned bacteria, and the initial formation of new dividing bacteria**.** The image (Fig. 2f) which numbers selected bacteria in the original image is the result of labeling the bacteria identified by the area based selection applied on the Otsu segmentation from Fig. 2b. Further data selection can be used to specify targets even more and in this scenario we compare the most fluorescent and the least fluorescent bacteria based on mean intensity (*see* **Note 20**). Figure 2g, h shows the resulting selection of the 20% brightest and the 20% dimmest from the area selected Otsu mask. Finally, the regions we identified have been analyzed and compared and the resulting graph is shown in Fig. 2i (*see* **Note 21**). As can be seen in Fig. 2i the areas are quite different between the brightest and the dimmest bacteria, while the eccentricity does not differ nearly as much. Such differences would be very hard to find by manual analysis, and can provide a source for both generating new hypothesis as well as testing existing ones.

4 Notes

1. Fiji (Fiji is just ImageJ), is an alternative version of ImageJ that comes bundled with many useful plugins for image processing and computer vision-based methods.
2. Many universities and research institutions (especially those that have Engineering or Science faculties) have group licenses for MATLAB.
3. Bio-Formats is a standardized and open format for reading and writing microscopy image data and metadata. It is developed by Open Microscopy Environment (OME).
4. A good software is built to fulfill one clearly defined goal or function. It should also be separated into manageable modules or minor software, to facility debugging, adding minor functions, modifications, and understanding.
5. One typical problem that can occur is that the bit depth of the image is misclassified by the computer. This is when the bit depth is considered to be higher or lower than it actually is. The result of this is that all intensity values will be too low or too high. One example of this happening is taking images with a 12 bit camera and opening them in MATLAB where they will be considered 16 bit images. This makes the image either extremely dark or bright, and segmentation is unlikely to succeed without adjusting the bit depth. In MATLAB this can be done by mul-

tiplying every pixel value with **VALUE** = $2^{(\text{wrong bit depth-real bit depth})}$, or as in the example, $2^{(16-12)} = 2^4$.

```
image=floor (image.*/VALUE);
```

A second possible method is by performing a bit shift on the image with difference in bit depth used as value. In this example, 12 – 16 = –4 = VALUE.

```
image=bitshift (image,VALUE);
```

6. Occasionally the image metadata does not contain the μm/pixel information, or the data could be wrong. This can be remedied when using the Bio-Formats toolbox in MATLAB by assigning the correct values.

```
pixelSize=ome.units.quantity.Length(java.
lang.Double(.VALUE), ome.units.UNITS.
MICROM);
YOURMETADATA.setPixelsPhysicalSizeX(pixel
Size, 0); (Exchange X for Y for setting Y
value)
```

7. Over-segmentation is a common problem when using watershed transformation, but it can sometimes be solved by defining a height threshold in the segmentation code. Done in MATLAB by adding the "imhim" function directly before the watershed function:

```
Image2=imhim (Image1, VALUE);
L=watershed (Image2);
```

A value of 20 is considered to be the threshold for suppressing shallow minima. Higher values will result in suppression of less shallow minima.

8. Two more efficient multilevel Otsu thresholding methods are: NM-PSO-Otsu [21], and Two-Stage Multithreshold Otsu [22].
9. Edge detection/Canny cannot be used on its own to segment an image since it only results in lines, and not a complete mask. It requires the assistance of morphological closing, filling, and opening operations to arrive at a complete mask. The structuring element chosen for these morphological operations should be as similar in shape as possible to the bacteria you are analyzing. Adjusting the structuring elements and their size through trial and error is often required to get good results.
10. The lower threshold should be set as the Otsu threshold value divided by 2. This is possible since the low threshold will always be half that of the high threshold in the original automatic Canny calculation [20].
11. Objects 1/10 of the mean size can generally be considered artifacts and can therefore in many cases be discarded [7].
12. Eccentricity is measured from 0 to 1, with 0 being a circle and 1 corresponding to a line.

13. Signal-to-noise is calculated by first removing the initial mask generated from the original image. Then the mean of the resulting image — which ideally should only consist of background pixels — is calculated and converted to double precision. The standard deviation of the background is calculated as well. Lastly the background mean is subtracted from every region's mean intensity value before being divided by the standard deviation. The following code has been adapted for use in MATLAB.

```
backgroundValues=ORIGINAL(~MASK);
backgroundMean=mean (backgroundValues(:));
backgroundValues=double (backgroundValues);
backgroundSTD=std (backgroundValues);
Signal-to-noise=(Region -backgroundValues)/
backgroundSTD;
```

14. Weighted centroid calculates the center of the region based on location and intensity values. In comparison the standard centroid calculation results in a center of mass. These two disparate markers can be used to calculate a vector between them in the bacteria. This vector can then be used for spatial correlation of molecular activity.
15. The medial axis length can be calculated with the following formula (Eq. 1):

$$\text{Length} = \frac{\text{Perimeter} + \sqrt{\left(\text{Perimeter}^2 - 16 \times \text{Area}\right)}}{4} \qquad (1)$$

16. As can be seen here, different segmentation methods will not generate the exact same results, due to approaching the information in the image differently. This makes choosing your segmentation method based on your images extremely important, and this will often require a trial and error approach. One advantage of using self-written software for this is the ability to run any sort of different segmentation methods in parallel and then comparing the results.
17. All objects are not bacteria, or the type of bacteria that we are interested in studying. This is a typical problem when you have more than one bacterial strain in your culture. A second scenario would be when you have an uneven fluorescence marker production and you only want to study bacteria over a certain fluorescence threshold.
18. In this case the MATLAB function bwareaopen was used for the area based selection. For this function you simply specify the pixel area and everything below that threshold will be removed.

19. Generally, you cannot use the same selection values on different segmentation methods and expect equal results, due to the difference in the mask generated. In this case different pixel areas were used for selection depending on the segmentation method.
20. The MATLAB function `bwpropfilt` was used on the "MeanIntensity" value parameter of `regionprops` to select the 20 % brightest and dimmest regions. This works by specifying which value it should select from, the number of objects, and if it should select the largest or smallest objects.
21. The MATLAB functions `regionprops` and `boxplot` was used for analyzing the regions and generating the graphs respectively.

Acknowledgments

This work was supported by the Crafoord Foundation, the Swedish Research Council, the Swedish Society of Medicine, and the O.E. and Edla Johansson Foundation.

References

1. Danuser G (2011) Computer vision in cell biology. Cell 147(5):973–978. doi:10.1016/j.cell.2011.11.001
2. Sinha P, Balas B, Otrovsky Y, Russel R (2006) Face recognition by humans: nineteen results all computer vision researchers should know about. Proc IEEE 94(11):1948–1962. doi:10.1109/JPROC.2006.884093
3. Smith R (2009) Hybrid page layout analysis via tab-stop detection. Paper presented at the Proceedings of the 10th international conference on document analysis and recognition, Barcelona
4. Computer Vision in Medical Imaging (2014), vol 2. Computer Vision
5. Lojk J, Sajn L, Cibej U, Pavlin M (2014) Automatic cell counter for cell viability estimation. Paper presented at the 37th International Convention on Information and Communication Technology, Electronics and Microelectronics (MIPRO), Opatija
6. Farnoush A (1977) The application of an image analyzing computer (Quantimet 720) for quantitation of biological structures—the automatic counting of mast cells. Microsc Acta 80(1):43–47
7. Selinummi J, Seppälä J, Yli-Harja O, Puhakka JA (2005) Software for quantification of labeled bacteria from digital microscope images by automated image analysis. BioTechniques 39(6):859–863. doi:10.2144/000112018
8. Forero MG, Crisóbal G, Sroubek F (2004) Identification of tuberculosis bacteria based on shape and color. Real-Time Imaging 10(4):251–262. doi:10.1016/j.rti.2004.05.007
9. Forero MG, Crisóbal G, Alvarez-Borrego J (2006) Automatic identification of *Mycobacterium tuberculosis* by Gaussian mixture models. J Microsc 223(2):120–132. doi:10.1111/j.1365-2818.2006.01610.x
10. Vallotton P, Sun C, Wang D, Turnbull L, Ranganathan P (2009) Segmentation and tracking individual *Pseudomonas aeruginosa* bacteria in dense populations of motile cells. Paper presented at the Image and vision computing New Zealand, 24th International Conference, Wellington
11. Jung CR, Scharcanski J (2005) Robust watershed segmentation using wavelets. Image Vis Comput 23(7):661–669. doi:10.1016/j.imavis.2005.03.001
12. Mahmoudi L, El Zaart A (2012) A survey of entropy image thresholding techniques. Paper presented at the 2012 2nd International conference on advances in computational tools for engineering applications (ACTEA), Beirut
13. Canny J (1986) A computational approach to edge detection. IEEE Trans Pattern Anal Mach Intell 8(6):679–698. doi:10.1109/TPAMI.1986.4767851
14. Lindeberg T (1998) Edge detection and ridge detection with automatic scale selection. Int J Comput Vis 30(1):117–154. doi:10.1023/A:1008097225773

15. Kass M, Witkin A, Tersopoulos D (1988) Snakes: active contour models. Int J Comput Vis 1(4):321–331. doi:10.1007/BF00133570
16. Meyer F (1994) Topographic distance and watershed lines. Signal Process 38(1):113–125. doi:10.1016/0165-1684(94)90060-4
17. Otsu N (1979) A threshold selection method from gray-level histograms. IEEE Trans Syst Man Cybern 9(1):62–66. doi:10.1109/TSMC.1979.4310076
18. Ping-Sung L, Tse-Sheng C, Pau-Choo C (2001) A fast algorithm for multilevel thresholding. J Inf Sci Eng 17:713–727
19. Zhang Y, Wu L (2011) Optimal multi-level thresholding based on maximum Tsallis entropy via an artificial bee colony approach. Entropy 13(4):841–859. doi:10.3390/e13040841
20. Fang M, Yue G, QingCang Y The study on an application of Otsu method in Canny operator. In: Proceedings of the 2009 International Symposium on Information Processing, Huangshan, P. R. China, 21–23 August 2009. p 109–112
21. Zahara E, Fan S-KS, Tsai D-M (2005) Optimal multi-thresholding using a hybrid optimization approach. Pattern Recognit Lett 26:1082–1095. doi:10.1016/j.patrec.2004.10.003
22. Huang D-Y, Wang C-H (2009) Optimal multi-level thresholding using a two-stage Otsu optimization approach. Pattern Recognit Lett 30:275–284. doi:10.1016/j.patrec.2008.10.003

Chapter 11

Assessing Vacuolar Escape of *Listeria Monocytogenes*

Juan J. Quereda, Martin Sachse, Damien Balestrino, Théodore Grenier, Jennifer Fredlund, Anne Danckaert, Nathalie Aulner, Spencer Shorte, Jost Enninga, Pascale Cossart, and Javier Pizarro-Cerdá

Abstract

Listeria monocytogenes is a bacterial pathogen which invades and multiplies within non-professional phagocytes. Signaling cascades involved in cellular entry have been extensively analyzed, but the events leading to vacuolar escape remain less clear. In this chapter, we detail a microscopy FRET-based assay which allows quantitatively measuring *L. monocytogenes* infection and escape from its internalization vacuole, as well as a correlative light/electron microscopy method to investigate the morphological features of the vacuolar compartments containing *L. monocytogenes*.

Key words *Listeria monocytogenes*, Phagocytosis, Vacuole, Listeriolysin O, Phospholipases, CCF4, Förster resonance energy transfer (FRET) microscopy, Correlative light/electron microcopy (CLEM)

1 Introduction

The gram-positive bacterium *Listeria monocytogenes* is a facultative intracellular pathogen responsible for listeriosis, a food-borne disease characterized by meningitis in newborns, abortion in pregnant women and septicemia in immunocompromised individuals [1]. For more than 50 years, *Listeria* has been used as major model in infection biology to investigate the interplay between immune cellular responses to control bacterial intracellular pathogens [2] and the role of bacterial virulence factors in subverting host cell functions [3]. *Listeria* internalization within non-phagocytic epithelial cells has been particularly well studied [4, 5]. Interaction of the bacterial surface proteins internalin (InlA) and InlB with their respective host cell receptors E-cadherin and Met triggers the recruitment of a clathrin-based machinery [6, 7] which controls in turn actin recruitment and membrane remodeling at bacterial internalization foci [8]. Modulation of phosphoinositide metabolism cooperates with the actin cytoskeleton to favor [9] or to restrict [10] *Listeria* entry within host cells [11].

Pontus Nordenfelt and Mattias Collin (eds.), *Bacterial Pathogenesis: Methods and Protocols*, Methods in Molecular Biology, vol. 1535, DOI 10.1007/978-1-4939-6673-8_11,

Following cell invasion, *Listeria* is located within a membrane-bound compartment that is ruptured to allow bacterial cytoplasmic access. Listeriolysin O (LLO), a pore-forming toxin encoded by the gene *hly* and responsible for the hemolytic activity that was very early associated to virulent *Listeria* strains [12], has been referred as a major actor in disrupting the bacterial vacuole [13, 14]. Two other bacterial virulence factors, PlcA and PlcB, are phosphatidylinositol-specific and broad range phospholipases respectively which also participate in vacuolar destabilization [15, 16]. However, how these bacterial virulence factors specifically contribute to *Listeria* vacuolar escape is not fully understood. For example, inactivation of LLO in J774 cells completely abrogates bacterial translocation to the cytoplasm [14, 17] but in human epithelial HeLa, HEp-2, and Henle 407 cells, the broad range phospholipase PlcB can rescue a Δ*hly* mutant, suggesting that host factors also contribute to the stability of the bacterial vacuole. Indeed, it has been demonstrated in murine macrophages that the gamma-interferon-inducible lysosomal thiol reductase (GILT) and the cystic fibrosis transmembrane conductance regulator (CFTR) enhance the oligomerization and the lytic activity of LLO to facilitate vacuolar rupture [18, 19] while inducible renitence limits vacuolar disruption by restoring the integrity of endolysosomal membranes [20].

Listeria vacuolar escape in epithelial cells has been studied recently by our team [21]. In this present article, we present two complementary approaches to address this topic: we describe first a detailed protocol for a Förster resonance energy transfer (FRET) microscopy assay which measures bacterial cytoplasmic translocation by monitoring the fluorescence of the β-lactamase-sensitive FRET probe CCF4 (this molecule emits photons at 535 nm when intact, but fluoresces at 450 nm when cleaved) (Fig. 1). The use of an engineered *Listeria* strain expressing a surface β-lactamase allows the identification of vacuolar escape by cleavage of the CCF4 molecule via the surface enzymatic activity. This approach has been successfully used with the bacterial pathogen *Shigella flexneri* to screen multiplexed small interfering (si)RNA libraries for the discovery of cellular factors regulating bacterial cytoplasmic translocation in HeLa cells [22]. We also present a correlative light/electron microscopy (CLEM) method in which we use green fluorescence protein (GFP)-expressing bacteria in conjunction to actin fluorescent staining to assess the localization of internalized bacteria that do not form actin tails: further characterization of these specific bacteria using transmission electron microscopy allows to investigate in detail their subcellular environment, and to analyze their potential association to membrane-bound compartments.

These two methodological strategies are therefore complementary and can be coupled to identify and characterize novel cellular host factors modulating *Listeria* translocation to the cytoplasmic

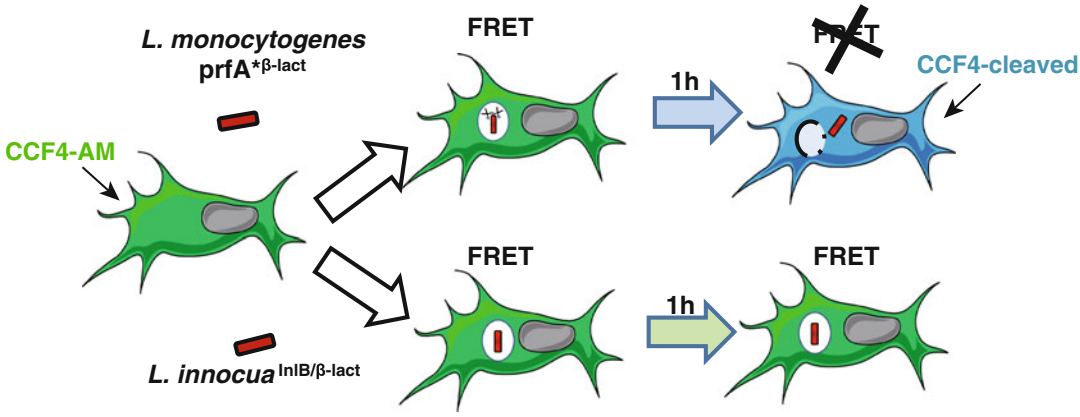

Fig. 1 FRET-based assay principle for tracking vacuolar rupture. CCF4-AM diffuses through the plasma membrane into the cytoplasm where it is modified by cell esterases to form CCF4. CCF4 is trapped in the cytoplasm emitting photons at 535 nm when intact, but fluorescing at 450 nm when cleaved. *L. monocytogenes* encoding a surface β-lactamase enters into cells, escape from its vacuolar compartments and cleaves the CCF4 probe whilst *L. innocua*^{inlB} encoding a surface β-lactamase is able to enter into cells but remain trapped inside vacuoles

space: the FRET-based microscopy assay is suited to perform high-throughput screens of drug or siRNA libraries targeting host factors, in order to first identify host candidate molecules which may control vacuolar membrane stability (in this chapter, this assay is coupled to a microscopical test to differentiate extracellular from total bacterial populations, which allows to determine whether failure in vacuolar escape could be explained by inhibition of bacterial entry or vacuolar rupture [21]). The CLEM assay can then be employed to investigate in finer detail the contribution of specific host candidate molecules to the enhancement or inhibition of *Listeria* vacuolar escape, through a morphological analysis of the structure of membranes and intracellular organelles that may interact with the bacterial-containing compartments prior to vacuolar rupture.

2 Materials

Vacuolar escape assays were performed in HeLa cells, which have been commonly used as a model to understand the intracellular lifestyle of *Listeria* [23, 24] and which are dependent on the InlB-invasion pathway. HeLa cells are grown in the absence of antibiotics to avoid potential endocytosis that could kill intracellular bacteria. To increase cellular invasion and therefore the statistical power of the microscopy-based assay described in this chapter, we employ a *L. monocytogenes* EGDe PrfA* strain which contains a Gly145Ser point mutation in the transcriptional regulator PrfA, increasing expression of virulence factors [25]. To express

β-lactamase at the bacterial cell surface, we engineered a fusion protein containing the signal peptide of InlA at the N terminal part of the chimera (to direct the protein to the bacterial cell wall), the β-lactamase gene (codon usage optimized for *Listeria*) and the LPXTG motif of InlA at the 3′ end of the construct (to anchor the protein to the bacterial cell wall through sortase A). This synthetic gene is under the control of the Hyper-SPO1 constitutive promoter (pHyper) fused to the *hly* 5′-untranslated region to enhance expression of the gene construct [21] and was electroporated into *L. monocytogenes* EGDe PrfA* strain as well as in our negative control *L. innocua* ^{InlB} (synthetic strain containing InlB attached to the cell wall to allow invasion of this nonpathogenic *Listeria* species).

2.1 FRET-Based Microscopy Assay for Vacuolar Escape Quantification

1. Cell preservation medium: 50% Dulbecco's Modified Eagle Medium (DMEM), 40% heat inactivated fetal calf serum (FCS), 10% DMSO.
2. HeLa cell clone CCL2 (American Type Cell Collection): kept in frozen stocks in cell preservation medium in liquid nitrogen.
3. Standard cell culture medium: DMEM supplemented with 10% heat inactivated FCS.
4. Lipofectamine RNAiMax (Thermo Fisher).
5. (Optional) siRNAs (*see* Subheading 3).
6. HEPES buffer: 120 mM NaCl, 7 mM KCl, 1.8 mM $CaCl_2$, 0.8 mM $MgCl_2$, 5 mM glucose, 25 mM HEPES at pH 7.3.
7. Probenecid (Sigma).
8. CCF4-AM (LiveBlazer Loading Kit, Invitrogen).
9. Solution B: 100 mg/ml Pluronic-F127 surfactant in DMSO/0.1% acetic acid provided along the CCF4-AM LiveBlazer Loading Kit by Invitrogen. Keep at room temperature.
10. Dulbecco's phosphate-buffered saline (DPBS) without calcium and magnesium to rinse chelators from the culture before cell dissociation and used also to prepare dilutions of antibodies.
11. Trypsin–EDTA solution.
12. A BHI agar plate with *L. monocytogenes* EGDe PrfA*$^{β\text{-lact}}$ colonies.
13. A BHI agar plate with *L. innocua*$^{β\text{-lact/InlB}}$ colonies.
14. *Listeria* culture medium: brain-heart infusion (BHI) as liquid medium or in agar plates. Chloramphenicol was used at a final concentration of 7 μg/ml to maintain the pPl2 plasmid encoding the β-lactamase and erythromycin 5 μg/ml was used to maintain the pP1 plasmid encoding the InlB in *L. innocua*.

15. Dark 96-well cell culture plates for cell microscopy.
16. Distilled water.
17. Fixation solution: DPBS, 4% paraformaldehyde (PFA) 1 mM probenecid.
18. DPBS supplemented with 1% bovine serum albumin (BSA).
19. DPBS supplemented with 1% BSA and 0.1% Triton X-100.
20. Anti-*L. monocytogenes* and anti-*L. innocua* polyclonal rabbit antibodies (*see* **Note 1**).
21. Fluorescently labeled secondary antibodies. Goat anti-rabbit Alexa 647 and goat anti-rabbit Alexa 488 (Life Technologies).
22. Dye DRAQ5 (eBioscience) and Hoechst (Thermo Fisher) to stain cell nuclei and DNA (bacteria and host).
23. Automated confocal microscope Opera QEHS (PerkinElmer Technologies) (*see* **Note 2**).
24. Multichannel pipette.
25. 50 ml reagent reservoir.

2.2 CLEM Assay for Ultrastructural Analysis

1. MatTek petri dishes with gridded coverslip (P35G-2-14-C-GRID).
2. Standard cell culture medium: DMEM, 10% heat-inactivated fetal calf serum.
3. Infection cell culture medium: DMEM, 1% heat-inactivated fetal calf serum.
4. HeLa cell clone CCL2 (American Type Cell Collection): kept in frozen stocks in cell preservation medium in liquid nitrogen.
5. Brain-heart infusion agar plate.
6. *L. monocytogenes* strain EGDe PrfA*-green fluorescent protein (GFP).
7. Gentamicin solution.
8. Fixation solution 1: PHEM buffer, 4% PFA.
9. Anti-*L. monocytogenes* primary antibodies (*see* **Note 1**).
10. DAPI or Hoechst, 1 mg/ml.
11. Fluorescently labeled secondary antibodies (anti-rabbit Alexa Fluor 647 antibodies).
12. Fluorescently labeled phalloidin (Alexa Fluor 546).
13. Phosphate-buffered solution (PBS) supplemented with 1% BSA.
14. Microscope equipped with fluorescence/white light lamps and 20×/100× objectives.
15. Fixation solution 2: PHEM buffer, 2.5% glutaraldehyde.
16. Pen and nail polish.

17. 0.1 M cacodylate buffer.
18. 1% osmium tetroxide solution in H_2O.
19. 70% ethanol supplemented with 1.2% uranyl acetate.
20. Distilled H_2O.
21. Series of graded ethanol: 50, 75, 95, and 100% ethanol.
22. EPON resin.
23. Gelatine capsules.
24. Razor blades.
25. Scalpel.
26. Glass slides.
27. Incubator at 60 °C.
28. Matches.
29. Reynold's lead citrate.
30. 80–120 kV transmission electron microscope equipped with a CCD camera.
31. Diamond knife.
32. Carbon-coated grids.
33. 4% uranyl acetate in H_2O.

3 Methods

The FRET-based microscopy assay for vacuolar escape is divided in two parts: in the first part (Subheading 3.1.1) cells are preloaded with the CCF4 dye and are subsequently infected with *Listeria* for 1 h. Afterwards, nuclei are stained with the DRAQ5 probe and the cells are imaged in an automated confocal microscope to identify the ratio of the 450 nm versus the 535 nm signals, which allows estimating the number of cells in which bacteria are trapped in vacuoles versus those that translocate to the cytoplasm. In the second part (Subheading 3.1.2) of the assay, extracellular and total *Listeria* are differentially labeled to estimate the number of bacteria which reached the intracellular space. The CLEM protocol is also divided in two parts: in the first part (Subheading 3.2.1) mammalian cells are infected with *Listeria* and labeled to detect extracellular bacteria, nuclei, the actin cytoskeleton and events of interest (intracellular bacteria not associated with actin) and finally imaged on a fluorescence microscope. In the second part (Subheading 3.2.2) of the assay, cells are embedded in a resin, the events of interest are located, the resin is trimmed and contrasted, and finally the cells are viewed on a transmission electron microscope.

As mentioned in the introduction, this FRET-based assay is suited to screen drug or siRNA libraries and in the protocol we present below, we describe a methodology which includes cellular transfection with siRNAs in a 96-well plate format. However, this protocol can be used without siRNAs and can be downscaled to a 24-well plate format if required. In the same manner, the CLEM assay that we present here in the absence of siRNA transfection, can be coupled to siRNA treatment to monitor the specific phenotype of targets identified in the FRET-based assay.

3.1 FRET-Based Microscopy Assay for Vacuolar Escape Quantification

3.1.1 CCF4 Loading, Listeria Infection, and FRET Measurements

1. Perform the siRNA transfection of HeLa cells 72 h before the infection for efficient knock down of gene expression (*see* **Note 3**). For each well mix 1 µl of the siRNA under study (diluted at 2 µM) with 9.0 µl of DMEM without serum and mix gently (*see* **Note 4**). Mix gently 0.1 µl of Lipofectamine RNAiMax with 9.9 µl of DMEM and wait for 5 min. Combine the diluted siRNA with the diluted Lipofectamine, mix gently and incubate 30 min at room temperature. Add these 20 µl of siRNA/lipofectamine to one well of the 96-well plate black microscopy plate (Fig. 2) and plate 6000 HeLa cells in a volume of 80 µl (*see* **Note 5**), avoiding the use of wells in the borders of the plate (columns 1 and 12, rows A and H) (*see* **Note 6**). After distribution of the cells with multichannel pipette, allow the cells to settle down for 15 min at room temperature (*see* **Note 7**).
2. Incubate the plate at 37 °C in a humidified 10% CO_2-containing atmosphere incubator (*see* **Note 8**).
3. The day before the infection prepare a liquid culture of *L. monocytogenes* EGDe PrfA*$^{\beta\text{-lact}}$ (include chloramphenicol) and *L. innocua*$^{\beta\text{-lact/InlB}}$ (include chloramphenicol and erythromycin) by inoculating a bacterial colony from the agar plate to 5 ml of BHI liquid medium supplemented with the required antibiotics. Allow the culture to grow during 18 h at 37 °C in a shaker (180 rpm).
4. The day of infection remove the cell culture medium and wash the cells with 100 µl DPBS per well. Remove the DPBS (*see* **Note 9**).
5. Load the cells with CCF4-AM. Prepare the CCF4-AM loading mix for a final volume of 25 µl per well containing 1 mM probenecid, 1.0 µM CCF4-AM and 1.25 µl of loading solution B in EM buffer (*see* **Note 10**). Allow cells to load with CCF4-AM for 150 min at room temperature in the dark.
6. Prepare bacteria for infection. Spin 0.5 ml of the overnight *Listeria* cultures at 5500 × *g* for 3 min using a tabletop centrifuge and remove the supernatant (containing LLO which is cytolytic). Resuspend the pellet in 1 ml of DPBS. Repeat the washing steps to a total of four washes. After the last wash, resuspend bacteria in 1 ml of DPBS.

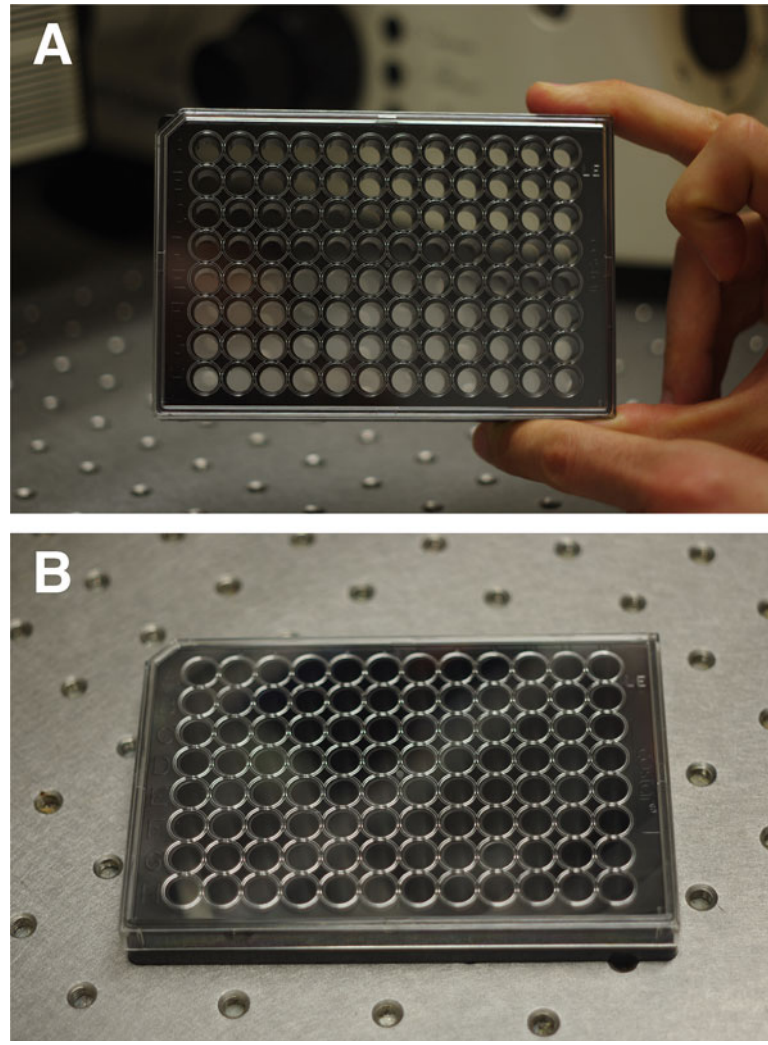

Fig. 2 96-well dark microscopy plate. (**a**) Frontal and (**b**) Side view of plates used for the FRET-based microscopy assay, which should be dark to preserve the fluorescence signals throughout the experiment. In this particular case, a Costar plate is depicted

7. Estimate the number of bacteria by reading the bacterial optical density at 600 nm (for *Listeria* spp., OD = 1 is equivalent of 1×10^9 bacteria/ml). Prepare the inoculum by adding the necessary volume of the bacteria suspension to a final volume of 100 μl of EM buffer/1 mM probenecid per well (*see* **Note 11**).
8. After 150 min of incubation discard the CCF4-AM loading solution from the 96-well plate and wash the HeLa cells once with 150 μl PBS/1 mM probenecid (*see* **Note 12**).
9. Discard the PBS/1 mM probenecid and add 100 μl of the inoculum in EM buffer/1 mM probenecid to each well.

10. Centrifuge the 96-well plate at 210×*g* during 3 min at room temperature to synchronize the infection.
11. Switch the plate to an incubator with a humidified 10% CO_2 atmosphere at 37 °C for 1 h to allow *L. monocytogenes* EGDe PrfA*$^{\beta\text{-lact}}$ and *L. innocua*$^{\beta\text{-lact/InlB}}$ invade cells.
12. Remove the plate from the incubator and wash cells with 150 µl PBS/1 mM probenecid.
13. Discard the DPBS/1 mM probenecid and fix with 50 µl PFA 4%/1 mM probenecid for 10 min in the dark (*see* **Note 13**).
14. Eliminate the PFA 4%/1 mM probenecid and wash the plate with 150 µl DPBS.
15. Remove the DPBS and add 30 µl of 10 µM nuclei dye DRAQ5. Incubate during 30 min in the dark.
16. Discard the DRAQ5 solution and wash with 150 µl DPBS.
17. Eliminate the DPBS and leave samples in 100 µl of new DPBS.
18. Acquisition of fixed samples is performed using the automated spinning disk confocal microscope Opera QEHS (PerkinElmer Technologies). The following sequence is used: firstly, CCF4 (excitation/emission [ex/em] 405/535 and 405/450 nm on two separate cameras) and secondly, DRAQ5 (ex/em 640/690). 23 fields, correspond roughly to 6000 cells, are acquired per well using a 10× air objective (numerical aperture: 0.4). Recorded images (Fig. 3) are transferred to a Columbus database (PerkinElmer Technologies) for storage, management and analysis (*see* **Note 14**).
19. Feature extraction was performed for each individual cell by using integrated Columbus building block routines (*see* **Note 14**). In

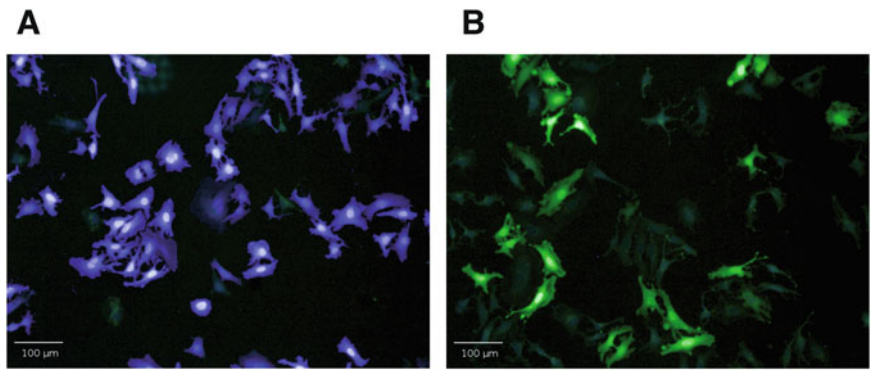

Fig. 3 Assessment of *L. monocytogenes* vacuolar escape using a FRET-based microscopical assay. HeLa cells were loaded with CCF4-AM and infected with *L. monocytogenes* EGDe PrfA*$^{\beta\text{-lact}}$ (**a**) or *L. innocua*$^{\beta\text{-lact/InlB}}$ (**b**) strains for 1 h. Images were obtained using a confocal microscope OPERA QEHS with a 10× objective. Pictures were obtained after merging the following channels: 535 nm (*green*, intact CCF4 probe) and 450 nm (*blue*, cleaved CCF4) (Bar: 100 µm)

brief, cells were segmented using the DRAQ5 channel by first detecting nuclei and then expanding into the cytoplasm for robust single cell identification.

20. The FRET 450/535 ratio is calculated for each cell and a mean ratio is calculated per well.
21. Statistical analysis of the results is performed using the strictly standardized mean difference (SSMD) statistical tests for quality control (QC), hit selection and validation [22].
22. If the experiment is not continued immediately (*see* Subheading 3.1.2), keep the plate at 4 °C for not more than 24 h (*see* **Note 15**).

3.1.2 Differential Staining of Extracellular and Total Listeria Populations

1. Continuing with samples from Subheading 3.1.1, discard the DPBS contained in the wells of the plate.
2. Add 100 µl of new DPBS and discard it again.
3. Extracellular *Listeria* spp. are labeled with a primary polyclonal rabbit anti-*L. monocytogenes* or anti *L. innocua* serum (*see* **Note 1**). Prepare this primary antibody solution by diluting the antibodies 1:500 in DPBS supplemented with 1 % serum albumin. Add 30 µl of primary antibody to each well.
4. Incubate for 30 min at room temperature to label extracellular *Listeria*.
5. Discard the primary antibody solution and wash four times with 100 µl of DPBS supplemented with 1 % serum albumin.
6. Dilute the secondary goat anti-rabbit Alexa 647 1:200 in DPBS supplemented with 1 % serum albumin, and add 30 µl to each well.
7. Incubate for 30 min at room temperature in the dark to avoid degradation of the fluorescent probe.
8. Discard the secondary antibody solution and wash four times with 100 µl of DPBS supplemented with 1 % serum albumin.
9. Cells are permeabilized using 100 µl of 0.1 % Triton X-100 for 4 min at room temperature in the dark.
10. Discard the Triton X-100 solution and wash one time with 100 µl of DPBS supplemented with 1 % serum albumin.
11. Intracellular (and extracellular) *Listeria* spp. are labeled with a primary polyclonal rabbit anti-*L. monocytogenes* or anti *L. innocua* serum. Prepare this primary antibody solution by diluting the antibodies 1:500 in DPBS supplemented with 1 % serum albumin. Add 30 µl of primary antibody to each well.
12. Incubate for 30 min at room temperature in the dark to label total *Listeria* populations.
13. Discard the primary antibody solution and wash four times with 100 µl of DPBS supplemented with 1 % serum albumin.

14. Dilute the secondary goat anti-rabbit Alexa 488 1:200 in DPBS supplemented with 1% serum albumin containing Hoechst diluted 1:1000. Add 30 µl to each well.
15. Incubate for 30 min at room temperature in the dark to avoid degradation of the fluorescent dyes.
16. Discard the secondary antibody solution and wash four times with 100 µl of DPBS. Keep the cells in 100 µl of DPBS at 4 °C in the dark until acquisition.
17. Acquisition of fixed samples is performed 4 days after the immunofluorescence (*see* **Note 16**) using the automated spinning disk confocal microscope Opera QEHS (PerkinElmer Technologies) (*see* **Note 2**). The following sequence is used: extracellular bacteria labeled with Alexa 647 and Alexa 488 secondary antibodies (ex/em 640/690), and intracellular bacteria labeled only with an Alexa 488 secondary antibody (ex/em 488/540) and Hoechst 33342 (ex/em 405/450). 23 fields, corresponding roughly to 6000 cells, are acquired per well using a 10× air objective (numerical aperture: 0.4). Recorded images (Fig. 4) are transferred to a database for storage, management and analysis.
18. The number of intracellular bacteria per cell was measured using Columbus analyzing building block routines (*see* **Note 14**).
19. Statistical analysis of the results is performed using the strictly standardized mean difference (SSMD) statistical tests for quality control (QC), hit selection and validation [22].
20. Classify each hit by cross-examination of the two screening results, i.e., a hit selected in the two assays defines a "bacteria entry hit," a hit in the FRET assay but not in the "intra/extra bacteria" assay corresponds to a "vacuolar rupture hit".

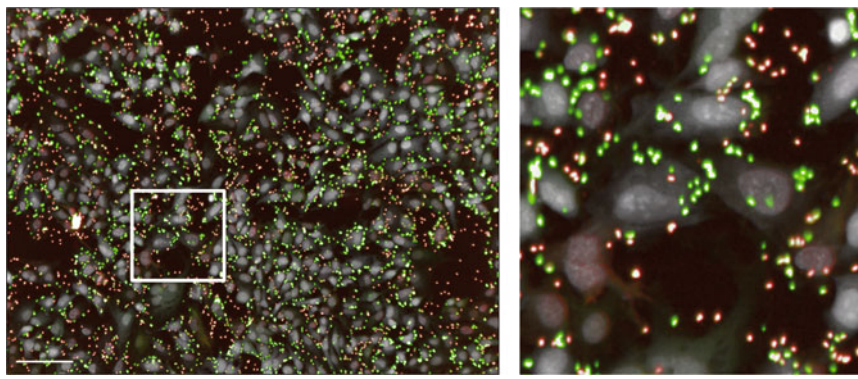

Fig. 4 Immunofluorescence staining to differentiate extracellular versus total *L. monocytogenes*. HeLa cells previously loaded with CCF4-AM and assessed for vacuolar escape were subjected to immunofluorescence. Extracellular bacteria were marked with a secondary goat anti-rabbit Alexa 647 (*red*) and total (extracellular and intracellular) bacteria were marked with a secondary goat anti-rabbit Alexa 488 (*green*) after cell permeabilization with 0.1% triton X-100. Nuclei were stained with Hoechst (*grey*). Intracellular and extracellular bacteria are labeled respectively in *green* and *red* (Bar: 100 µm)

3.2 CLEM Assay of Intracellular Listeria Populations

3.2.1 Listeria Infection and Immunofluorescence

1. HeLa cells and *L. monocytogenes* EGDe.PrfA*-GFP are grown as described in **steps 3–7** of Subheading 3.1.1 of the FRET-based vacuolar escape analysis protocol (bacterial agar plates and liquid medium should be supplemented with 5 μg/ml of erythromycin to select for GFP-expressing clones).
2. Prepare HeLa cells for the experiment using similar procedures as the ones described in **steps 1–3** of Subheading 3.1.1, plating cells in MatTek petri dishes (instead of dark microscopy 96-well plates) (Fig. 5) (*see* **Note 17**).
3. Infect cells as described in Subheading 3.1.1, **steps 6–10**, using infection medium (DMEM 1% FCS).
4. Transfer the MatTek petri dishes to an incubator with a humidified 10% CO_2 atmosphere at 37 °C, and let the bacteria enter the cells for 1 h.
5. Aspirate the infection medium, wash cells twice with 2 ml of pre-warmed cell culture medium supplemented with 40 μg/ml gentamicin and replace with 2 ml of the same gentamicin-containing medium.
6. Transfer the MatTek petri dishes back to the incubator, and keep them at 37 °C in the humidified 10% CO_2 atmosphere for another 4 h (*see* **Note 18**).
7. Aspirate the gentamicin-containing medium, wash cells twice with 2 ml of pre-warmed standard cell culture medium.
8. Adjust medium level to 1 ml, and fix cells by adding 1 ml of the 4% PFA/PHEM buffer fixation solution (final PFA concentration: 2%) for 10 min (*see* **Note 19**).
9. Replace the fixation solution by 1 ml of 4% PFA/PHEM buffer fixation solution and fix for another 20 min at room temperature.
10. Remove the fixative, wash the cells three times with 2 ml of PBS supplemented with 1% bovine serum albumin.
11. Prepare the primary antibody solution by diluting the rabbit-derived anti-*L. monocytogenes* antibody (*see* **Note 1**) 1:500 in DPBS supplemented with 1% bovine serum albumin, and add 500 μl of primary antibody per dish (only in the center area).
12. Incubate for 20 min at room temperature to label extracellular *L. monocytogenes*.
13. Discard the primary antibody solution and wash four times with 2 ml of DPBS supplemented with 1% bovine serum albumin.
14. Dilute the secondary Alexa Fluor 647-coupled anti-rabbit antibody (1:200), the DAPI solution (1:1000) and the Alexa Fluor 546-coupled phalloidin in PBS supplemented with 1% bovine serum albumin.

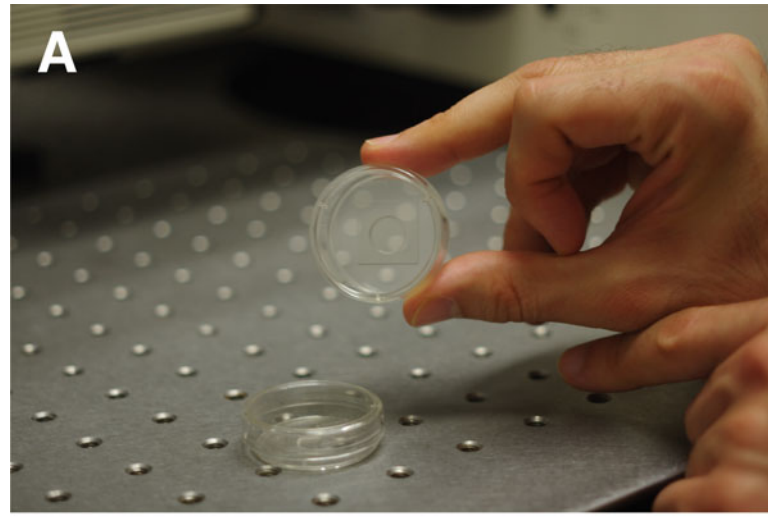

B

0A	1A	2A	3A	4A	5A	6A	7A	8A	9A	AA	BA	CA	DA	EA	FA	GA	HA	IA	JA
0B	1B	2B	3B	4B	5B	6B	7B	8B	9B	AB	BB	CB	DB	EB	FB	GB	HB	IB	JB
0C	1C	2C	3C	4C	5C	6C	7C	8C	9C	AC	BC	CC	DC	EC	FC	GC	HC	IC	JC
0D	1D	2D	3D	4D	5D	6D	7D	8D	9D	AD	BD	CD	DD	ED	FD	GD	HD	ID	JD
0E	1E	2E	3E	4E	5E	6E	7E	8E	9E	AE	BE	CE	DE	EE	FE	GE	HE	IE	JE
0F	1F	2F	3F	4F	5F	6F	7F	8F	9F	AF	BF	CF	DF	EF	FF	GF	HF	IF	JF
0G	1G	2G	3G	4G	5G	6G	7G	8G	9G	AG	BG	CG	DG	EG	FG	GG	HG	IG	JG
0H	1H	2H	3H	4H	5H	6H	7H	8H	9H	AH	BH	CH	DH	EH	FH	GH	HH	IH	JH
0I	1I	2I	3I	4I	5I	6I	7I	8I	9I	AI	BI	CI	DI	EI	FI	GI	HI	II	JI
0J	1J	2J	3J	4J	5J	6J	7J	8J	9J	AJ	BJ	CJ	DJ	EJ	FJ	GJ	HJ	IJ	JJ
0K	1K	2K	3K	4K	5K	6K	7K	8K	9K	AK	BK	CK	DK	EK	FK	GK	HK	IK	JK
0L	1L	2L	3L	4L	5L	6L	7L	8L	9L	AL	BL	CL	DL	EL	FL	GL	HL	IL	JL
0M	1M	2M	3M	4M	5M	6M	7M	8M	9M	AM	BM	CM	DM	EM	FM	GM	HM	IM	JM
0N	1N	2N	3N	4N	5N	6N	7N	8N	9N	AN	BN	CN	DN	EN	FN	GN	HN	IN	JN
0O	1O	2O	3O	4O	5O	6O	7O	8O	9O	AO	BO	CO	DO	EO	FO	GO	HO	IO	JO
0P	1P	2P	3P	4P	5P	6P	7P	8P	9P	AP	BP	CP	DP	EP	FP	GP	HP	IP	JP
0Q	1Q	2Q	3Q	4Q	5Q	6Q	7Q	8Q	9Q	AQ	BQ	CQ	DQ	EQ	FQ	GQ	HQ	IQ	JQ
0R	1R	2R	3R	4R	5R	6R	7R	8R	9R	AR	BR	CR	DR	ER	FR	GR	HR	IR	JR
0S	1S	2S	3S	4S	5S	6S	7S	8S	9S	AS	BS	CS	DS	ES	FS	GS	HS	IS	JS
0T	1T	2T	3T	4T	5T	6T	7T	8T	9T	AT	BT	CT	DT	ET	FT	GT	HT	IT	JT
0U	1U	2U	3U	4U	5U	6U	7U	8U	9U	AU	BU	CU	DU	EU	FU	GU	HU	IU	JU
0V	1V	2V	3V	4V	5V	6V	7V	8V	9V	AV	BV	CV	DV	EV	FV	GV	HV	IV	JV
0W	1W	2W	3W	4W	5W	6W	7W	8W	9W	AW	BW	CW	DW	EW	FW	GW	HW	IW	JW
0X	1X	2X	3X	4X	5X	6X	7X	8X	9X	AX	BX	CX	DX	EX	FX	GX	HX	IX	JX
0Y	1Y	2Y	3Y	4Y	5Y	6Y	7Y	8Y	9Y	AY	BY	CY	DY	EY	FY	GY	HY	IY	JY
0Z	1Z	2Z	3Z	4Z	5Z	6Z	7Z	8Z	9Z	AZ	BZ	CZ	DZ	EZ	FZ	GZ	HZ	IZ	JZ

Fig. 5 MatTek 35 mm dish. (**a**) Frontal and side views of a MatTek 35 mm dish, with a glass coverslip that includes a photo-etched grid. (**b**) Scheme of the grid photo-etched on the glass coverslip

15. Add 500 µl of this secondary probe solution to each dish (use only the center area) (*see* **Note 20**).
16. Incubate for 30 min at room temperature in the dark to protect the fluorescent antibody.
17. Discard the secondary probe solution and wash four times with 2 ml of DPBS supplemented with 1% bovine serum albumin.
18. Perform imaging in an inverted microscopy using fluorescence and a 100× objective to identify cells in which GFP-positive bacteria are not detected by the secondary Alexa Fluor 647-coupled antibody and in which actin comet tails are not detected by the Alexa Fluor 546-coupled phalloidin.
19. Locate the position of the cells of interest in the grid by imaging with white light and a 20× objective (*see* **Note 21**).

3.2.2 Sample Processing for Electron Transmission Microscopy

1. Fix the cells a second time by adding 1 ml of the PHEM buffer/glutaraldehyde fixation solution for 20 min.
2. Wash the samples three times for 5 min with PHEM buffer to remove the glutaraldehyde.
3. When the glutaraldehyde is removed, mark the areas with the cells of interest with a pen and nail polish (*see* **Note 22**).
4. Post-fix the samples for 45 min with 1% OsO_4 in the dark.
5. Wash the samples three times for 5 min with H_2O.
6. Incubate the samples 5 min with the 25% ethanol solution.
7. Incubate the samples 5 min with the 50% ethanol solution.
8. Incubate the samples 20 min with the 70% ethanol solution supplemented with 1.2% uranyl acetate.
9. Prepare the EPON solution according to the manufacturer's instructions (*see* **Note 23**).
10. Incubate the samples 5 min with the 75% ethanol solution.
11. Incubate the samples two times for 10 min each time with the 95% ethanol solution.
12. Finally incubate the samples three times for 6 min each time with the 100% ethanol solution.
13. Put a drop of the mixed EPON solution on a glass slide.
14. Remove carefully the coverslip from the petri dish with a scalpel and put it on top of the EPON drop with the cells facing up.
15. Put a drop of EPON on the cells and incubate for at least 6 h at room temperature.
16. Fill a capsule of gelatin with EPON and place it in such a way that the mark with the cells of interest is located at the center (Fig. 6).

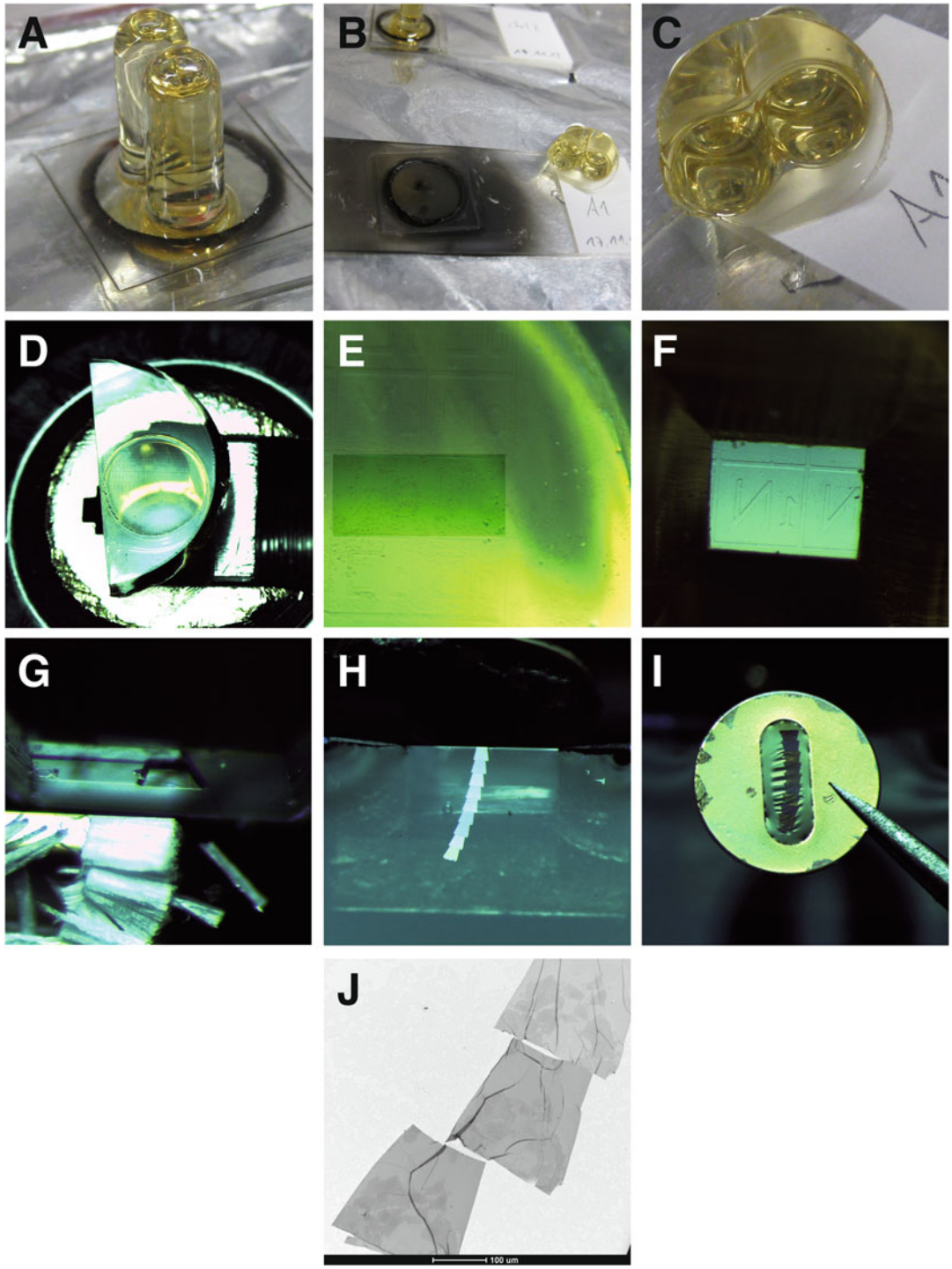

Fig. 6 Sample preparation for transmission electron microscopy. (**a**) The gridded coverslip with the cells/events of interest is removed from the dish and flat-embedded in Epon. (**b**) After polymerization, Epon is removed from the coverslip by heating the glass slide with a match. (**c**) Close-up of the flat-embedded sample after coverslip removal. (**d**) The Epon is cut to separate the two gelatine capsules and one is mounted on the sample holder of the microtome. (**e**) Close-up of the region of interest before trimming. (**f**) Rough trimming of the area of interest before trimming the trapezoid. (**g**) Trapezoid-shape sample after trimming. Note that only the area above the top of the 1 remains from the square 1N. (**h**) Cut thin sections floating on the water in the boat of the knife. (**i**) Thin sections on a slot grid. (**j**) Low magnification of the thin sections on the slot grid after contrasting

17. Incubate overnight at room temperature and then polymerize the samples for 48 h at 60 °C.
18. After the polymerization, the EPON is removed from the coverslip by heating the glass slide with a match.
19. The area of interest is trimmed with a trimming diamond or a razor blade (*see* **Note 24**).
20. Thin sections (70 mm nominal thickness) are prepared and picked up with slot grids.
21. Stain the sections with 4% uranyl acetate and Reynold's lead citrate.
22. Observe the samples in a transmission electron microscope operated between 80 and 120 kV (*see* **Note 25**).

4 Notes

1. In our experiments, we use homemade rabbit polyclonal antibodies against *L. monocytogenes* and *L. innocua*. There are many commercial monoclonal and polyclonal antibodies that can be used to specifically recognize *L. monocytogenes*, and there are several commercial polyclonal antibodies that recognize several *Listeria* spp. and therefore can be used to recognize both *L. monocytogenes* and *L. innocua*. When using these primary antibodies, special attention should be taken concerning the species in which they are produced, in order to choose the right secondary antibodies.
2. We present in this document results generated using an automated confocal microscopy. However, a non-automated widefield microscopy equipped with a motorized stage can be also used. The only special requirement is the right combination of filters to detect FRET: excitation is performed at 405 nm (Semrock, FF01-387/11-25) and emission detected via 450 nm (Semrock, FF02-447/60-25) and 535 nm (Semrock, FF01-520/35-25) filters.
3. If the aim of the experiment does not require transfection of siRNAs (for example, for the analysis of the specific contribution of bacterial proteins in vacuolar escape), HeLa cells can be seeded into the 96-well plate 15–24 h before infection [26].
4. Positive controls of siRNA transfection and gene knock-down are strongly suggested. We suggest the use of siRNAs targeting the Kinesin Family Member 11 (Kif11) that arrest cells in mitosis, leading to reduced cell numbers exhibiting a "rounded-up" phenotype.
5. We typically use quadruplicates for each siRNA in order to obtain statistically significant results, but the number of well rep-

licates per siRNA is flexible. We recommend preparing four consecutive wells in the same column for each siRNA. It is important to check the number of cells per well the day of infection in order to test if the siRNAs under study cause cell death.

6. The wells in the borders of the plate (columns 1 and 12, rows A and H) are not used in order to avoid interferences due to evaporation. We therefore fill these wells with culture medium that will serve as evaporation and temperature buffer for inner wells.
7. The position of the wells in a plate can cause artifacts. Some possibilities to avoid these artifacts include: (1) Allow cells to settle down for 15 min at room temperature (2) Maintain the plates in the incubator on aluminum blocks to ensure equal distribution of the temperature across the plate (3) Seal the plates with Parafilm to prevent evaporation and (4) Distribute randomly the control wells as well the rest of the siRNA under study.
8. Take always the plate by the lateral edges. Do not touch the bottom of the plate with your fingers to avoid smearing which may affect image acquisition.
9. Remove the liquid from the wells by inverting the plate gently but efficiently. This technique avoids detachment of cells from the well. Always settle the different reagents in the well very carefully by letting the liquid fall slowly through the wall of the wells, otherwise cells will detach from the bottom.
10. Pipet slowly to avoid bubble formation and inconsistency in the distribution of the CCF4-AM loading solution.
11. We normally use a *L. monocytogenes* PrfA* strain and a multiplicity of infection (MOI) of 10. Using a higher MOI (i.e., 20) does increase the statistical power of the assay but could cause undesirable cytotoxic effects by virulence factors secreted by this bacterium. It could be recommendable to increase the MOI if a non-PrfA* strain is used.
12. The continuous use of probenecid is critical to avoid leakage of the CCF4 out of the cells.
13. PFA is toxic and must be handled in an appropriate fume hood. After cell fixation PFA should be disposed of correctly in a sealed container.
14. For this chapter, we used the Columbus database (PerkinElmer Technologies) for image storage, management and analysis. However, any storage device or database including the Open Microscopy Environment repository OMERO (http://www.openmicroscopy.org/site/products/omero) can be used instead. For image analysis, open resources including ImageJ ((http://imagej.nih.gov/ij/), FIJI (http://fiji.sc/Fiji), Icy (http://icy.bioimageanalysis.org/), and CellProfiler (http://cellprofiler.org/) are also excellent solutions.

15. PFA-fixed cells get permeabilized after 24 h. For this reason, the differential immuno-staining of total versus extracellular bacteria should be performed before 24 h post PFA fixation.
16. To avoid an interference signal from the CCF4 probe, the cells are kept at 4 °C during 4 days to allow the passive leakage of the probe from the cell cytoplasm.
17. MatTek petri dishes contain a grid on the coverslip as indicated in Fig. 5. The characters and numbers illustrated in the grid are photo-etched into the coverslip and therefore leave an imprint on the EPON resin that will be used to embed the cells, allowing locating them during the resin trimming. If the coverslip is mounted upside-down, no imprint will be left on the EPON and it will not be possible to locate the cells. Therefore, verify that the MatTek petri dishes have a grid in the right orientation: the characters and letters are not inverted when looking at the dish on a standard white light microscope.
18. In this assay, GFP bacteria of interest will be located by the absence of extracellular staining, and by the absence of actin staining. We would need therefore to infect cells long enough (at least 4 h) to allow for actin polymerization in those bacteria that escape their vacuolar containing compartment.
19. Mixing the fixation solution with the medium containing the cells is a gentler way of fixing them, allowing to better preserve their morphological features.
20. Use only the central area of the dish to avoid the use of large volumes of antibodies or secondary probes).
21. To locate at least two independent events within a MatTek dish, it is recommended to choose cells which are not close to each other and which are located preferentially in separate areas of the grid (for example, one event may be located in the area with numbers and characters while the other event may be located in the area which contain only characters).
22. The cell of interest can be localized on a basic, inverted light microscope that has phase contrast. A 4× objective gives sufficient space to mark with a pen the area on the grid from underneath the coverslip. Since most markers dissolve in Epon resin, we recommend to put on the mark a fine drop of nail polish.
23. The hardness of the Epon mixture depends on the ratio of the hardeners in the mixture. We recommend to use a hard formula, which facilitates easier detachment of the coverslip.
24. It is important to have the area to be sectioned as small as possible. In addition, the orientation of the sample/cell of interest

in the trimmed area should be noted: this helps to get orientated when the sections are observed.

25. Since the protocol does not include fiducial markers, the correlation between the light microscopy image of a whole cell and the EM image of a thin section needs to be done manually by eye. It is important to know the orientation of the cell of interest and the neighbors within the trimmed trapeze. We recommend to start the observation not with the first grid, which contains the sections of the cells close to the coverslip, but rather with a grid that that contains sections where they cells are cut in the medium of their nucleus. At low/intermediate magnification the nuclei are clearly recognizable as large organelles (Fig. 7). Their pattern can be correlated to the Hoechst/DAPI staining in immunofluorescence. Once the cell of interest is found in the section, the other sections/grids are screened to find the bacteria/events of interest. Dehydration at room temperature is fast but induces artifacts to membranes. In case the membrane of the bacteria containing vacuole is not clearly visible or not perpendicular to the surface of the section, we use the presence of ribosomes or other cytoplasmic material as criteria to judge the state of vacuole (Fig. 8).

Acknowledgments

We thank Servier Medical Art (http://www.servier.com/Powerpoint-image-bank) for providing drawings used in Fig. 1. Work in the laboratory of P.C. is supported by the Institut Pasteur (Unité des Interactions Bactéries-Cellules), the Institut National de la Santé et de la Recherche Médicale (Unité 604), the Institut National de la Recherche Agronomique (Unité Sous Contrat 2020), the Fondation Les Mousquetaires, and an European Research Council Advanced Grant (BacEpiCell 670823). The Imagopole is part of the FranceBioImaging infrastructure supported by the French National Research Agency (ANR-10-INSB-04-01, "Investments for the Future") and is grateful to supports by Conseil de la Region Ile-de-France (program Sesame 2007, project Imagopole to S.S.) and from the Fondation Française pour la Recherche Médicale (FRM, Programme Grands Equipements to N.A.). J.E. is supported by the Institut Pasteur (PTR-460), by the Institut Pasteur Carnot-MIE program and by a European Research Council Starting Grant (RuptEffects 261166).

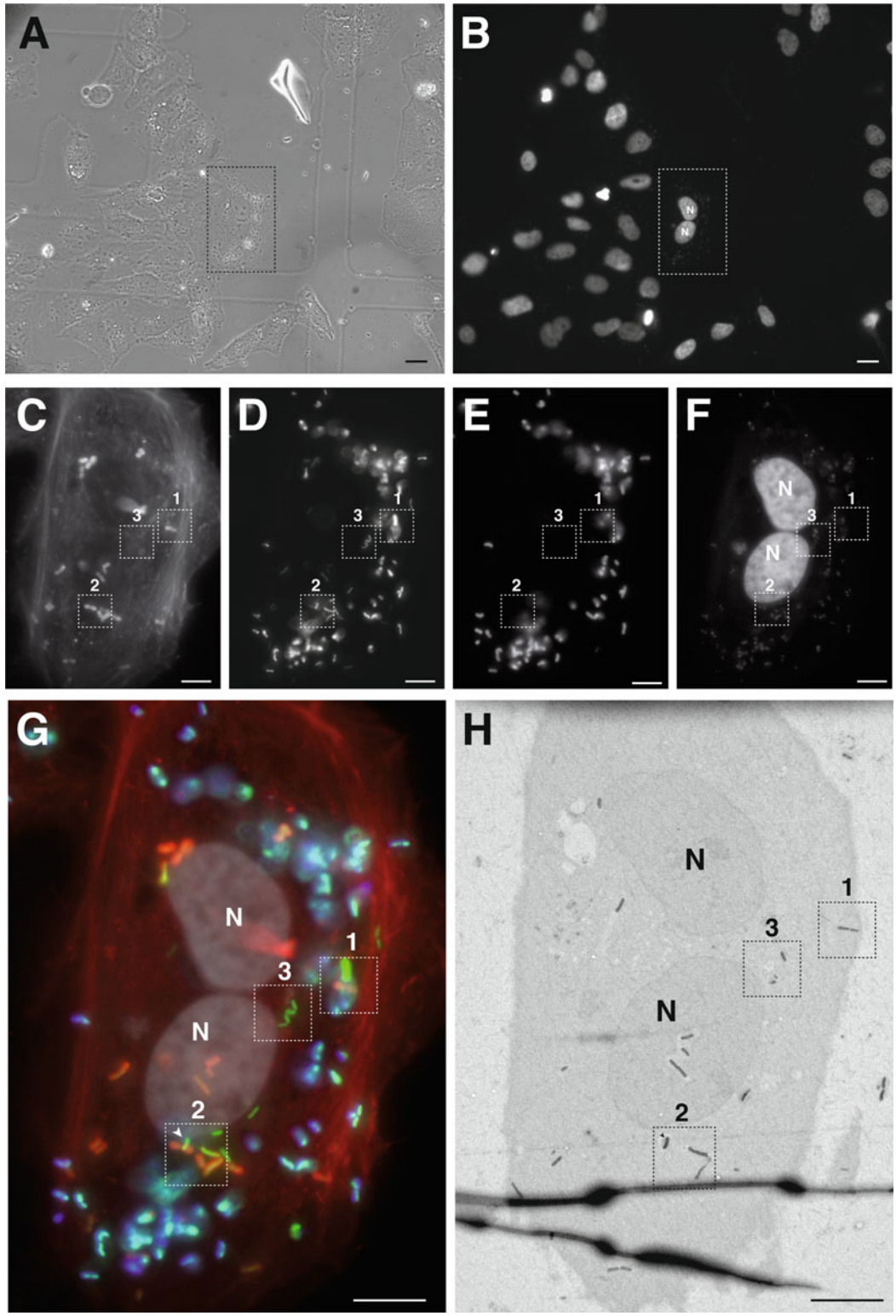

Fig. 7 CLEM of HeLa cells infected with *L. monocytogenes* GFP. (**a**) Low magnification (40×) of a monolayer of HeLa cells growing on a MatTek dish. The cell of interest (*dashed box*) is located at the left lower corner of the eN square (tilted −80 °C in the image) (Bar: 10 μm). (**b**) DAPI staining of the same monolayer of HeLa cells depicted in (**a**). (N: nuclei). (**c**) Actin staining at high magnification (63×) of the cell of interest located in the *dashed box* in (**a**) and (**b**). The *dashed boxes* labeled *1*, *2*, and *3* represent three individual groups of bacteria

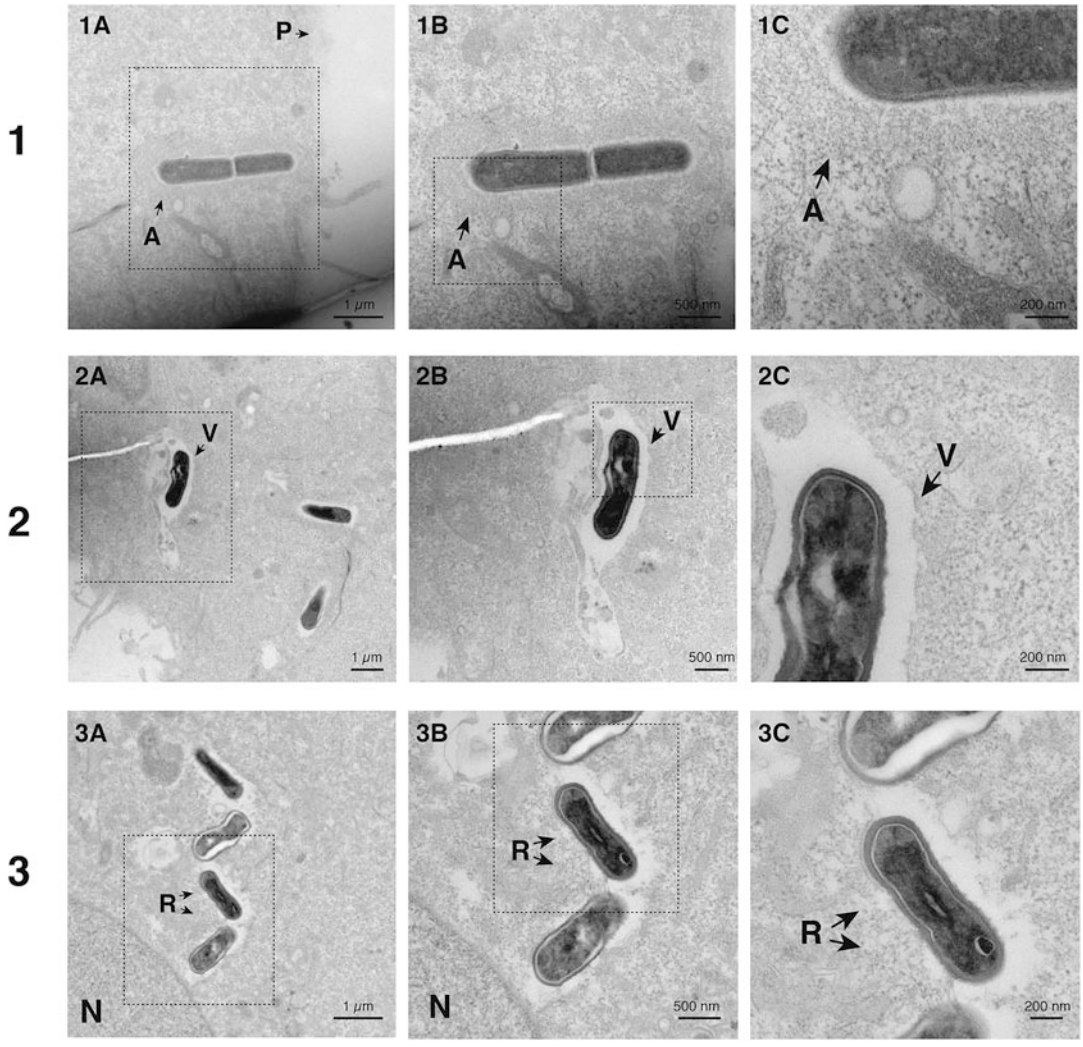

Fig. 8 Transmission electron microscopy of HeLa cells infected with *L. monocytogenes* GFP. (*1)* Overview of the dividing bacterium shown in Fig. 7, dashed box 1. The bacterium is in close proximity to the plasma membrane (*P*). At higher magnification (*1b*) it is shown the polymerized actin (*a*) around the bacteria. The *dashed box* in *1b* shows a zoom of the dense structure of the actin network (*a*), which excludes bigger material from the cytoplasm such as ribosomes. (*2*) Overview of the bacterium shown with an *arrowhead* in Fig. 7h, g, *dashed box* 2. The bacterium is present in a vacuole (*V*). Panel (*2c*) presents a zoom of an area of the vacuole where its limiting membrane (*arrow*) is perpendicular to the section and clearly visible. (*3*) Group of bacteria shown in Fig. 7, dashed box 3 devoid of actin label. In contrast to (*1*) the bacteria are present in the cytoplasm and there is no coat of polymerized actin visible. Instead, bacteria are surrounded by cytoplasm and ribosomes (*R*) can be seen in close vicinity to the bacteria. Scale Bars: 1 μm (*1a*, *2a*, and *3a*), 500 nm (*1b*, *2b*, and *3b*), and 200 μm (*1c*, *2c*, and *3c*)

Fig. 7 (continued) that will be observed in detail by electron microscopy (Fig. 8). Actin polymerizing bacteria can be clearly observed in groups 1 and 2 (Bar: 10 μm). (**d**) Same area as in (**c**) displaying the *L. monocytogenes* GFP signal (Bar: 10 μm). (**e**) Same area as in (**c**) displaying the antibody labeling against extracellular *L. monocytogenes* (Bar: 10 μm). (**f**) DAPI staining of the same area as in (**c**). (**g**) Merge of images from (**c**) to (**f**): actin is displayed in *red*, *L. monocytogenes* GFP are shown in *green*, extracellular *L. monocytogenes* are displayed in *blue* and DAPI staining is shown in *white* (Bar: 10 μm). (**h**) Transmission electron micrograph of the cell observed in (**g**). (Bar: 10 μm). In the *dashed box 2*, the bacterium pointed with a *white arrowhead* (**g**) and a *black arrowhead* (**h**) is present in a vacuole (Fig. 8)

J.P.C. is supported by the Institut Pasteur (PTR-460 and PTR-521) and by the French National Research Agency (ANR-15-CE15-0017). P.C. and J.E. acknowledge the LabEx consortium IBEID. P.C. is a Howard Hughes Medical Institute Senior International Research Scholar.

References

1. de Noordhout CM, Devleesschauwer B, Angulo F et al (2014) The global burden of listeriosis: a systematic review and meta-analysis. Lancet Infect Dis 14:1073–1082
2. Mackaness GB (1962) Cellular resistance to infection. J Exp Med 116:381–406
3. Cossart P (2011) Illuminating the landscape of host-pathogen interactions with the bacterium *Listeria monocytogenes*. Proc Natl Acad Sci U S A 108:19484–19491. doi:10.1073/pnas.1112371108
4. Pizarro-Cerdá J, Kühbacher A, Cossart P (2012) Entry of *Listeria monocytogenes* in mammalian epithelial cells: an updated view. Cold Spring Harb Perspect Med 2:a010009. doi:10.1101/cshperspect.a010009
5. Kühbacher A, Emmenlauer M, Rämö P et al (2015) Genome-wide siRNA screen identifies complementary signaling pathways involved in Listeria infection and reveals different actin nucleation mechanisms during Listeria cell invasion and actin comet tail formation. MBio 6:e00598–15. doi:10.1128/mBio.00598-15
6. Bonazzi M, Kühbacher A, Toledo-Arana A et al (2012) A common clathrin-mediated machinery co-ordinates cell–cell adhesion and bacterial internalization. Traffic 13:1653–1666. doi:10.1111/tra.12009
7. Pizarro-Cerdá J, Bonazzi M, Cossart P (2010) Clathrin-mediated endocytosis: what works for small, also works for big. Bioessays 32:496–504. doi:10.1002/bies.200900172
8. Pizarro-Cerdá J, Cossart P (2009) *Listeria monocytogenes* membrane trafficking and lifestyle: the exception or the rule? Annu Rev Cell Dev Biol 25:649–670. doi:10.1146/annurev.cellbio.042308.113331
9. Ireton K, Payrastre B, Chap H et al (1996) A role for phosphoinositide 3-kinase in bacterial invasion. Science 274:780–782
10. Kühbacher A, Dambournet D, Echard A et al (2012) Phosphatidylinositol 5-phosphatase oculocerebrorenal syndrome of Lowe protein (OCRL) controls actin dynamics during early steps of *Listeria monocytogenes* infection. J Biol Chem 287:13128–13136. doi:10.1074/jbc.M111.315788
11. Pizarro-Cerdá J, Kühbacher A, Cossart P (2014) Phosphoinositides and host-pathogen interactions. Biochim Biophys Acta 1851:911–918. doi:10.1016/j.bbalip.2014.09.011
12. Seastone CV (1935) Pathogenic organisms of the genus *Listerella*. J Exp Med 62:203–212
13. Gaillard JL, Berche P, Mounier J et al (1987) In vitro model of penetration and intracellular growth of *Listeria monocytogenes* in the human enterocyte-like cell line Caco-2. Infect Immun 55:2822–2829
14. Henry R, Shaughnessy L, Loessner MJ et al (2006) Cytolysin-dependent delay of vacuole maturation in macrophages infected with *Listeria monocytogenes*. Cell Microbiol 8:107–119.doi:10.1111/j.1462-5822.2005.00604.x
15. Mengaud J, Braun-Breton C, Cossart P (1991) Identification of phosphatidylinositol-specific phospholipase C activity in *Listeria monocytogenes*: a novel type of virulence factor? Mol Microbiol 5:367–372
16. Vázquez-Boland JA, Kocks C, Dramsi S et al (1992) Nucleotide sequence of the lecithinase operon of *Listeria monocytogenes* and possible role of lecithinase in cell-to-cell spread. Infect Immun 60:219–230
17. Barry RA, Bouwer HG, Portnoy DA, Hinrichs DJ (1992) Pathogenicity and immunogenicity of *Listeria monocytogenes* small-plaque mutants defective for intracellular growth and cell-to-cell spread. Infect Immun 60:1625–1632
18. Singh R, Jamieson A, Cresswell P (2008) GILT is a critical host factor for *Listeria monocytogenes* infection. Nature 455:1244–1247. doi:10.1038/nature07344
19. Radtke AL, Anderson KL, Davis MJ et al (2011) *Listeria monocytogenes* exploits cystic fibrosis transmembrane conductance regulator (CFTR) to escape the phagosome. Proc Natl Acad Sci U S A 108:1633–1638. doi:10.1073/pnas.1013262108
20. Davis MJ, Gregorka B, Gestwicki JE, Swanson JA (2012) Inducible renitence limits *Listeria monocytogenes* escape from vacuoles in macrophages. J Immunol 189:4488–4495. doi:10.4049/jimmunol.1103158

21. Quereda JJ, Pizarro-Cerdá J, Balestrino D et al (2015) A dual microscopy-based assay to assess *Listeria monocytogenes* cellular entry and vacuolar escape. Appl Environ Microbiol 82(1):211–217. doi:10.1128/AEM.02302-15
22. Mellouk N, Weiner A, Aulner N et al (2014) Shigella subverts the host recycling compartment to rupture its vacuole. Cell Host Microbe 16:517–530. doi:10.1016/j.chom.2014.09.005
23. Mostowy S, Janel S, Forestier C et al (2011) A role for Septins in the interaction between the *Listeria monocytogenes* invasion protein InlB and the met receptor. Biophys J 100:1949–1959. doi:10.1016/j.bpj.2011.02.040
24. Quereda JJ, Pucciarelli MG (2014) Deletion of the membrane protein Lmo0412 increases the virulence of *Listeria monocytogenes*. Microbes Infect 16:623–632. doi:10.1016/j.micinf.2014.07.002
25. Ripio MT, Domínguez-Bernal G, Lara M et al (1997) A Gly145Ser substitution in the transcriptional activator PrfA causes constitutive overexpression of virulence factors in *Listeria monocytogenes*. J Bacteriol 179:1533–1540
26. Kühbacher A, Cossart P, Pizarro-Cerdá J (2014) Internalization assays for Listeria monocytogenes. In: Methods in molecular biology. Springer New York, New York, NY, pp 167–178

Chapter 12

Immobilization Techniques of Bacteria for Live Super-resolution Imaging Using Structured Illumination Microscopy

Amy L. Bottomley*, Lynne Turnbull*, Cynthia B. Whitchurch, and Elizabeth J. Harry

Abstract

Advancements in optical microscopy technology have allowed huge progression in the ability to understand protein structure and dynamics in live bacterial cells using fluorescence microscopy. Paramount to high-quality microscopy is good sample preparation to avoid bacterial cell movement that can result in motion blur during image acquisition. Here, we describe two techniques of sample preparation that reduce unwanted cell movement and are suitable for application to a number of bacterial species and imaging methods.

Key words Bacterial slide preparation, Agarose pads, GelGro slabs, Super-resolution microscopy, Fast three-dimensional structured illumination microscopy

1 Introduction

Although advances in microscopy technology have aided researchers in improving image resolution, the key to high-quality microscopy is good sample preparation. One critical aspect of this for live cell imaging is the reduction of unwanted movement of the cells that can cause motion blur during image acquisition. The major causes of movement arise from Brownian motion or via motility appendages on the bacterial cell surface such as flagella or pili. To overcome this, the liquid interface between the coverslip and imaging surface can be reduced, imaging can be conducted at lower temperatures, or motility mutants can be utilized. However, these conditions may not reflect those encountered by bacteria in their environmental niche and may affect protein structure and dynamics, thus affecting data interpretation. Here we describe two techniques, utilizing agarose pads and gellan gum slabs, for the

Amy L. Bottomley and Lynne Turnbull are the joint first authors.

Pontus Nordenfelt and Mattias Collin (eds.), *Bacterial Pathogenesis: Methods and Protocols*, Methods in Molecular Biology, vol. 1535, DOI 10.1007/978-1-4939-6673-8_12, © Springer Science+Business Media New York 2017

preparation of bacteria for live imaging that reduce unwanted motion whilst preserving bacterial shape and function. These techniques have been adapted from earlier methods used in conventional microscopy [1–4] and are also suitable for widefield conventional or confocal fluorescent live imaging of bacterial cells.

Several super-resolution fluorescent imaging techniques have been developed in the past decade. These techniques have enabled at least a doubling of the lateral resolution obtained by conventional light microscopy by manipulating the illumination and/or analysis of the emitted light to overcome the diffraction barrier and create genuine increases in apparent resolution. There are three main types of super-resolution optical microscopy currently used; single molecule localization microscopy (SMLM; including techniques such as photoactivated localization microscopy (PALM) and stochastic optical reconstruction microscopy (STORM)), stimulated emission depletion microscopy (STED), and structured illumination microscopy (SIM). Advances in all three of these techniques allow for three dimensional imaging and imaging of live specimens. However, SIM has advantages over the other two methods of allowing higher temporal image acquisition with a lower photon budget than either SMLM or STED [5]. SIM can be implemented in 2D, 3D, or total internal reflection fluorescence (TIRF) modes and can use widefield, nonlinear, or lattice lightsheet illumination [5–8]. Importantly, each of these super-resolution imaging modes require longer image acquisition periods than conventional imaging modes making it imperative that cell movement is limited to avoid image blur. In this chapter, we describe two methods for supporting bacterial cells for live imaging using 3D-structured illumination microscopy (3D-SIM) realized using a DeltaVision OMX Blaze platform (linear SIM). This platform was selected as it provides improvement in lateral and axial resolution (110 and 280 nm, respectively) and a temporal resolution of one frame per second for a 1 μm volume. However, as stated above, these samples could be imaged using other conventional microscopy platforms.

2 Materials

Prepare all solutions using ultrapure water (prepared by purifying deionized water to attain a sensitivity of 18 MΩ/cm at 25 °C) and analytical grade reagents. Chemicals specific to these protocols are listed below. All media should be autoclaved (121 °C, 15 psi, 20 min) before storage. Prepare and store all reagents at room temperature (unless indicated otherwise).

2.1 Bacterial Growth Media for Preparation of Bacteria for Imaging on Agarose Pads

1. *L* broth: 10 g tryptone, 5 g NaCl, 5 g yeast extract, 1 L water.
2. Tryptic soy broth (TSB): 37 g tryptic soy broth powder, 1 L water.

3. Luria–Bertani (LB) broth: 10 g tryptone, 10 g NaCl, 5 g yeast extract, 1 L water.

2.2 Agarose Pads

1. 2% electrophoresis-grade agarose dissolved in 1× growth medium (i.e., 0.2 g agarose and 10 mL growth medium).
2. 25 mL conical flask (*see* **Note 1**).
3. 65 µL adhesive frame and plastic coverslips (Gene Frame, Thermo Fisher Scientific).
4. Microscope slides (75 × 25 mm).
5. Coverslips (22 × 22 mm), 170 µm thick (#1.5) (*see* **Note 2**).
6. 200 µL pipette and pipette tips.
7. Microwave.
8. Humidified chamber: plastic or glass container with lid containing dampened (using sterile water) paper towel in base.
9. Forceps, metal.
10. Microscope slide sealant or nail polish.

2.3 GelGro Slabs

1. Gellan gum media (GG): 0.8 g gellan gum (*see* **Note 3**), 0.4 g tryptone, 0.2 g yeast extract, 0.2 g NaCl, 0.1 g $MgSO_4 \cdot 7H_2O$, 100 mL water (*see* **Note 4**). The method described below is used for *Pseudomonas aeruginosa*. However, we have also applied this method to *Myxococcus xanthus, Staphylococcus aureus*, non-typeable *Haemophilus influenzae, Acinetobacter baumannii, Shewanella oneidensis, Proteus mirabilis, Escherichia coli, Citrobacter rodentium,* and *Mycoplasma hypopnemoniae*. As a general rule, the GG slab is prepared with 10–40% dilution of the normal nutrient media concentration used for solidified plate culturing of that bacteria. For example for *S. aureus*, use 10% strength TSB in place of the tryptone, yeast extract, and salt when preparing the GG slabs. The 0.1 g $MgSO_4 \cdot 7H_2O$ must be maintained as it is necessary for the gellan gum to solidify. Care must be taken to ensure that the prepared slabs do not autofluoresce (*see* **Note 5**).
2. Dry heating block set to 65 °C with holder for 50 mL tubes or a dry heating bath containing metal beads set to 65 °C (*see* **Note 6**).
3. Heated slide preparation stage set to 65 °C (*see* **Note 7**).
4. Large petri plates (145 mm diameter), sterile.
5. 50 mL disposable plastic tubes, sterile.
6. 5 mL disposable plastic tubes, sterile.
7. Forceps, metal.
8. Microscope slides (75 × 25 mm).
9. Coverslips (22 × 40 mm), 170 µm thick (#1.5) (*see* **Note 2**).
10. Spatula, fine.
11. Disposable plastic inoculation loops, 10 µL.

12. Tissues (*see* **Note 8**).
13. Lint free cleaning tissues (Kimwipes).
14. Paraffin film (Parafilm).
15. Humidified chamber: Plastic or glass lunchbox/container with lid containing paper towel in base dampened with sterile water sized to hold large petri dish.

3 Methods

3.1 Imaging Bacteria on Agarose Pads

Appropriate concentration of antibiotics and inducers should be added to room temperature media for strains that express fluorescent fusion proteins under inducible control.

3.1.1 Growing of Bacterial Cultures

1. *L* broth: Weigh 10 g tryptone, 5 g NaCl and 5 g yeast extract and add to a 1 L measuring cylinder or beaker. Add water to a volume of 1 L and dissolve using a magnetic stirrer. Transfer media to a screw-capped glass bottle and autoclave to sterilize. Ensure the media has cooled to room temperature after autoclaving before using for bacterial growth (*see* **Note 9**).
2. TSB: Weigh 37 g tryptic soy broth powder and prepare as described for *L* broth.
3. LB broth: Weigh 10 g tryptone, 10 g NaCl and 5 g yeast extract and prepare as described for *L* broth.

3.1.2 Preparation of Bacterial Cells for Imaging

1. Inoculate 5 mL of appropriate growth medium with a single colony of bacterial strain in a 50 mL sterile tube and grow overnight with shaking (250 rpm) at 37 °C. For *Bacillus subtilis*, use *L* Broth, for *S. aureus*, use TSB and for *E. coli* and *Acinetobacter* spp., use LB broth.
2. Measure A_{600} (absorbance at 600 nm) of overnight culture using a spectrophotometer (*see* **Note 10**).
3. Calculate the volume of overnight culture needed to inoculate 5 mL of fresh growth medium to a starting A_{600} of 0.05. Add this volume to 5 mL of fresh growth medium in a 50 mL sterile tube and grow at 37 °C with shaking (250 rpm) until mid-exponential phase of growth is reached ($A_{600} \sim 0.4$).
4. Harvest a 1 mL aliquot of the sample and centrifuge at 5900 × *g* for 30 s. Remove the supernatant and resuspend the cell pellet in 200 μL fresh medium. If required, cells can be labeled with fluorescent counterstains at this step (*see* **Note 11**).

3.1.3 Preparation of Agarose Pads

1. Attach an adhesive frame to the center of a standard glass microscope slide by removing the thin polyester backing sheet (not the sheet that has the center square removed) and applying the exposed adhesive surface of the frame to the surface of the cover-

slip. Leave the thick polyester sheet attached to the frame to prevent the plastic coverslip adhering in the subsequent steps.

2. Heat the prepared microscope slides in the microwave for 30–60 s prior to dissolving the agarose, and allow slides to continue heating in the microwave during the next step. Heating the slide ensures the agarose does not set immediately when pipetted onto the slide surface, allowing sufficient time for the plastic coverslip to be added. Use appropriate care when handling as the glass slide will be hot.
3. Dissolve agarose using a microwave in short (10–20 s) bursts with intermittent mixing and constant observation to avoid overheating and bubbling of agarose. If inducer is required for expression of fusion proteins during time-lapse microscopy, allow the dissolved agarose to cool slightly (able to touch with hand) before adding the appropriate concentration of inducer.
4. Immediately pipette 65 μL into the adhesive frame using a 200 μL pipette and tip. Pipette the melted agarose slowly as the solution is viscous and large amounts of air can sucked into the tip, resulting in an inaccurate volume which will affect the thickness of the agarose pad.
5. Immediately place a plastic coverslip (supplied with GeneFrames) on top to create a flat surface. Working quickly is paramount to ensure a flat agarose pad is prepared, so arrange the coverslips to allow easy access e.g., line coverslips along edge of microfuge rack so they can be quickly placed on surface of microscope slide to create an agarose pad. If preparing several slides, place each coverslip on top of the agarose immediately as each pad is pipetted onto the glass. Inclusion of air bubbles within the pad does not affect the use of the microscope slide as they can be avoided during image acquisition.
6. Leave the agarose pad to set at room temperature for 5–10 min (*see* **Note 12**).

3.1.4 Applying Sample to Pre-prepared Pad

1. Remove plastic coverslip from pad and allow condensation to evaporate for 1–2 min at room temperature.
2. Take 2.5 μL of concentrated bacterial sample (Subheading 3.1.2) and pipette onto a pre-prepared pad. Spread the sample evenly along the surface of the pad by either gentle movement of the slide to allow the sample to spread by surface tension, or by using the long edge of a 200 μL pipette tip. Allow to dry at room temperature for 5 min in darkness, but ensuring that the pad does not completely dry out.
3. Carefully lift the prepared agarose pad by the edge using forceps or a sterile pipette tip and flip the pad onto a clean glass No 1.5 coverslip so that the pad is now inverted, i.e., so that the bacterial cells are sandwiched between the glass and the agarose pad (*see* **Note 13**).

4. Place a standard glass microscope centrally onto the coverslip and inverted pad. Turn the slide over so that the coverslip is now on the top facing upwards and seal the coverslip using microscope slide sealant or nail polish.
5. The resulting bacteria can be visualized by phase-contrast microscopy, conventional widefield, confocal, or super-resolution 3D-SIM. Series of time-lapse images can also be captured (*see* **Note 14**).

3.2 Imaging Bacteria on GelGro Slabs

3.2.1 Preparation of GG Slabs

1. Weigh out each component of GG except the gellan gum and add to water in a beaker containing a magnetic stirring bar.
2. Heat the medium with stirring on a magnetic stirring/heating block.
3. Gradually add the gellan gum in small amounts with stirring to prevent clumps forming. Heat the medium to boiling while stirring to dissolve.
4. Once the mixture turns clear, autoclave for 20 min at 121 °C, 15 psi (*see* **Note 15**).
5. Remove sterile GG from autoclave and decant into 50 mL tubes that have been preheated to 65 °C either in a dry block heater or in the metal beads of a 65 °C dry bath. Allow to cool to 65 °C. Gellan gum will set below 60 °C, so care must be taken to keep temperature of GG above 65 °C. All procedures should be done as quickly as possible to avoid GG setting in tubes. Care should also be taken to minimize water loss by steam or condensation and by minimizing the time that lids are removed from containers (*see* **Note 16**).
6. Preheat the slide preparation stage to 65 °C, and ensure it is level (*see* **Note 17**).
7. Preheat 5 mL tubes to 65 °C in the heating block or dry bath.
8. Preheat a large petri plate on the 65 °C slide preparation stage.
9. Flame-sterilize four microscope slides by holding each slide with a pair of forceps, dipping the slide into a glass beaker containing 96% ethanol, touching the corner of the slide to the edge of beaker to drain off most of the ethanol and passing the slide through the flame of a Bunsen burner to burn the remaining ethanol. Align each slide side by side inside the petri plate using sterile forceps. Push the slides tightly together so that the long edge of one slide is touching the wall of the petri plate and allow to preheat to 65 °C.
10. Decant 5 mL of GG into the pre-warmed 5 mL tube. Return the 5 mL tube to heating block or dry bath to maintain temperature. If using any fluorescent dyes for staining the bacteria, they should be added at this stage. Vortex the dye into the GG quickly before returning the tube to the heating block (*see* **Note 18**).

11. Remove lid of petri plate and rest on bench so that you have two free hands.
12. Remove 5 mL tube with GG from heating block and pour GG over all four slides. Gently tilt the petri dish from side to side so that the GG covers all surfaces of the slides. Try to get an even coverage of GG on the four slides but not let the GG pour off the edges of the slides. Some GG may leak between the slides and settle between the slides and the bottom of the petri plate; this is acceptable.
13. Allow GG to settle, replace lid and move petri plate carefully from the warm stage to a cool, level area and allow GG to set for 30 min. If you wish to proceed immediately, go to **step 18**.
14. To store prepared slides, fold a tissue in half and in half again until you have a small wad approximately 1×4 cm in size. You will need two per petri plate. Wet the tissues with sterile water until the tissues are full but not quite dripping and place at empty ends of the petri dish. Do not let free water run into the base of the petri plate. Be careful not to let the tissues touch the slides.
15. Holding the petri plate level, seal the lid to the base using parafin film and transfer to a 4 °C refrigerator until required (*see* **Note 19**). These slabs will last for up to a week.
16. When required, remove the pre-poured slides from 4 °C.
17. Remove the two tissues from each end of the plate and keep aside aseptically.
18. Flame-sterilize a fine spatula and use to gently score the GG between each slide and separate slides a little using the spatula.
19. Place open large petri plate (lid removed) in a Type 1 or Type 2 Biohazard Cabinet for approximately 20 min to dry slides (use the same cabinet each time for consistency, *see* **Note 20**).
20. Remove petri plate from cabinet and remove excess GG from under the slides. To do this, slowly lift out each slide using a spatula and wipe the back of each slide with a lint free cleaning tissue (Kimwipes). Also wipe out the petri plate. Replace slides into the large petri plate.
21. Using the edge of a flame-sterilized fine spatula, gently score around the edge of each slide. Remove excess GG by lifting gently away with the flat edge of the spatula. Trim 1–2 mm from the long edges of the slide, 5–10 mm from the clear short edges to prevent contact of the GG with the microscope stage and all of the frosted section so that slide can be adequately labeled.

3.2.2 Applying Bacterial Sample to the Prepared GG Slabs

1. For each bacterial strain, you will need a freshly grown culture on solid media (*see* **Note 21**). For example, for *P. aeruginosa*, you will need an overnight streak plate grown on *L* broth solidified with 1.5% agar (*see* **Note 22**).

2. With a plastic inoculation loop take a small portion of the bacterial streak and lightly streak onto the center of the GG slide, creating a small inoculation Z-shaped streak of 10 mm long and 4–5 mm wide. Take care not to rip or dent the GG.
3. Using 96 % ethanol, flame-sterilize a 22 × 40 mm coverslip and allow to cool. Placing one short edge of coverslip onto the GG, slowly lower coverslip onto the GG at an angle using either sterilized metal forceps or spatula, trying to minimize bubble formation between the coverslip and the GG (*see* **Note 23**).
4. Place slides back into petri dish along with damp tissues, being careful not to let the tissues touch the slides (to prevent excess moisture being introduced under the coverslip).
5. Incubate at 37 °C for at least 1 h, until required for microscopic analysis. The resulting bacteria can be visualized by phase-contrast microscopy, conventional widefield, confocal, or super-resolution 3D-SIM. Series of time-lapse images can also be captured.

3.3 Preparation of the Microscope and Image Acquisition

1. We recommend using the following imaging platforms to perform fast 3D-SIM (f3D-SIM) on the samples prepared. The samples can be imaged live using a DeltaVision V3 or V4 OMX Blaze Imaging System or a DeltaVision OMX SR Imaging System (GE Healthcare). The following steps should be taken although the specific details of how to operate each system will vary. For detailed instructions for use of OMX Blaze, please refer to ref. 9.
2. For live cell imaging, ensure a heated stage is present and an objective-heating collar is attached to the objective.
3. Turn on the objective and stage heaters at least 4 h prior to imaging, slowly increasing the temperature to the desired setting at a maximum rate of 5 °C/h. Turn on the system at least 1 h prior to imaging to allow stabilization of the system and excitation source (lasers). Load any dish stage inserts onto the heated stage to preheat.
4. Careful attention to refractive index mismatch during acquisition must be maintained. 3D-SIM is a method that is very sensitive to changes in refractive index through the sample. At the beginning of your acquisition process, check for spherical aberration and if necessary, change the immersion oil used. This is done be carefully removing the old immersion oil from the coverslip with a cotton-tipped stick dipped in 96–100 % ethanol. The immersion oil must also be cleaned from the objective. We recommend a starting immersion oil of 1.518 for imaging agarose or GG slabs at 37 °C. However, this will need to be empirically tested for each sample and experiment.

3.4 Checking Data Quality for f3D-SIM Acquisition

1. To check image acquisition parameters check that there has not been more than a 10% decrease in signal intensity through the z-stack by noting the maximum intensity value at the beginning of acquisition and the corresponding value at the end of acquisition. If there has been this level of photobleaching, move to a new area of the slide and lower the excitation input energy (i.e., exposure time and neutral density filter settings).
2. If there has been more than this level of photobleaching in the first time point of a time-series, the data through the time series will be of insufficient quality for analysis and the time series acquisition should be stopped. This can be checked during time-series capture.
3. At the end of the acquisition of the time series, open the resulting raw image file and ascertain the decrease in maximum signal intensity from the beginning of the time series to the final image. Discard any time points where there has been more than 30% photobleaching.
4. Raw image files can now be reconstructed [10, 11] and analyzed using appropriate methods (for example, *see* ref. 1).

4 Notes

1. We find that using a conical flask is preferable to a glass beaker as it reduces evaporation during microwaving, making the agarose easier to pipette when dissolved.
2. We have found that some batches of slides and coverslips can be covered in debris. If this happens, we recommend cleaning the slides with a toothbrush and powder cleaner such as Ajax and rinsing well with deionized water. Coverslips can be cleaned also with a powder cleaner by rubbing gently between thumb and forefinger, taking great care not the crack the coverslip or cut the operator.
3. Gellan gum is available under the trade names Gel-Gro, Gelzan, and Gelrite. Gellan gum is optically clearer than agar and agarose as a setting agent and does not autofluoresce. This reduces background for fluorescence microscopy and enables the addition of fluorescent dyes to the GG or to use bacteria expressing fluorescent proteins for the assay.
4. It is advisable to set aside a stock of bottles that are only used for making GG media. Results will be more reproducible if you minimize the possibility of chemical contamination into the bottles.
5. Autofluorescence can be caused by the presence of media components in the slabs or the setting agent itself, resulting in unwanted uniform background fluorescence in the sample. To

check for this, image a prepared slab without the addition of bacterial cells using the filters appropriate for your fluorophore. If autofluorescence is higher than your signal fluorescence, optimization of the slab components and/or fluorophores used should be performed to improve the signal-to-noise ratio.

6. We do not recommend the use of water baths for this method. We have found that the need for rapid movements during this method can lead to contamination. Dry heating is best. Dry block heaters are routinely used in many molecular biology labs and users will only need to obtain inserts for larger tubes (e.g., 50 mL centrifuge tubes). For a dry bath, use a standard water bath and fill with metal beads instead of water.
7. We use a heated slide preparation stage for this step. It is the best option if you have access to one. These are routinely used in pathology labs. However, you can also use a dry block heater with the blocks turned upside down to maximize the heating surface. It is very important that you can control the temperature so we do not recommend a normal heating plate unless it has a temperature control feature.
8. We have found that occasionally tissues can be a source of contamination. If you are experiencing contamination in your assay, make a batch of wet tissues, autoclave and keep aseptically until needed.
9. Aliquot media in 100 mL bottles to avoid contamination from repeated opening of bottle.
10. To ensure the reading lies within the linear range of absorbance, dilute the overnight culture 1:10 (100 μL culture and 900 μL medium) in a 1 mL spectroscopy cuvette before reading.
11. For cell membrane staining, add 1 μL of 0.25 mg/mL FM4-64 (Thermo Fisher Scientific; dissolved in DMSO) to 1 mL culture in a microfuge tube. Incubate cells at growth temperature for 10–30 min. For cells in the exponential phase of growth, 10 min incubation is sufficient, but for later stages of growth (late exponential) a longer incubation time is required; this should be optimized by the user. Wash cells twice with fresh medium by centrifugation at $5900 \times g$ for 30 s, then remove supernatant and resuspend the cell pellet in 200 μL fresh medium. To stain nucleoids, add DAPI (Thermo Fisher Scientific; 20 μg/mL in H_2O) to a final concentration of 0.2 μg/mL (i.e., add 2–200 μL of sample). Incubate at room temperature for 10 min in darkness and wash cells as described for membrane staining. Excitation/emission maxima for FM4-64 is 515/640 nm, and for DAPI is 358/461. Keep the sample wrapped in foil to avoid photo bleaching of fluorescence.

12. Agarose pads can be prepared and slides stored at 4 °C 1–2 h before use, but longer storage will result in the agarose pad drying out. Store slides in a humidified chamber to protect from evaporation during storage. Before use, place the slide at room temperature for 15 min.
13. Samples should be prepared on the coverslip rather than the glass slide to keep the distance between the objective and the sample to a minimum. The focal distance of most high NA objectives is less than 200 μm. Additionally, the refractive index of the sample changes with z-depth. To ensure minimal spherical aberration, it is important to place the sample as close to the coverslip as possible. This is best achieved by preparing the cells on the coverslip rather than on the glass slide.
14. It is recommended that the user establishes a "fitness measurement" for their bacterial species, as exposure to different solidifying agents used for microscopy may affect bacterial growth and thus data interpretation. Examples of fitness measurements are to visualize cell length extension and cell division events to establish growth rate via phase contrast microscopy after desired fluorescence image acquisition (suitable for *B. subtilis* and *S. aureus*), or to test motility of bacteria after fluorescence microscopy (suitable for *P. aeruginosa*) as we have observed that motility is lost if bacterial cells are under stressed conditions.
15. It is important to visually inspect the boiling solution and to make sure that there are no small lumps in the solution. These will interfere with the gellan gum setting.
16. The GG solution can be used immediately (after cooling to 65 °C) or it can be allowed to set, stored at room temperature, then melted later when required. When melting GG, use a microwave set to low power and monitor the solution to make sure it does not boil over. Make sure the solution is completely melted before using, as any small lumps will affect the ability to form flat surfaces for microscopy. Again take care when handling the heated solution.
17. Ensure the surface is level by using a spirit level. This is important or the slides will have an uneven surface and this makes microscopic inspection very difficult.
18. A number of dyes may be added to the GG slabs when imaging the bacteria. We have used DNA dyes such as TOTO-1, TOTO-3, ethidium homodimer, and Sytox Orange, membrane dyes such as those from the FM family (FM1-43, FM4-64) or the Di family (DiI, DiL, DiO), calcofluor white, and cell tracking dyes such as CellTracker Orange. Different dyes work better with different bacteria. This needs to be optimized for each bacterial species or strain. Care must be taken to ensure

that the dye is not toxic to the bacteria by confirmation using an appropriate fitness test for the bacterial species. We recommend using the manufacturer's preparation instructions and concentrations as a starting point for using each dye.

19. The slides may be stored for up to one week at 4 °C before use. We recommend making all slides needed for 1 week from one batch of molten GG and discarding the disused portion. Slides containing fluorescent dyes must be wrapped in foil to prevent dye bleaching.
20. Drying times will vary between different cabinets and will need to be optimized. 15 min drying is a good starting point, but it is useful to come to recognize how much drying a particular set of slides needs through tactile and visual senses. If the conditions are too moist, it is possible that the bacteria will swarm or swim. Slides that have been dried the right amount will have a slightly matte sheen over the surface of the GG and will be slightly tacky to handle.
21. We do not recommend using liquid overnight cultures for inoculation as flagellated strains will swim or swarm if too much liquid is deposited in the stab site.
22. For example *M. xanthus* would be used from a 2–3 day plate cultured on CYE solidified with 1.5 % agar, *S. aureus* from an overnight plate cultured in TSB solidified with 1.5 % agar, nontypeable *H. influenzae* from an overnight plate cultured on BHI with hemin and NADH solidified with 1.5 % agar.
23. If the cover slip is too warm, not only will the bacteria be killed, moisture will be trapped due to condensation between the coverslip and the GG. It doesn't matter if there are a small number of bubbles trapped under the coverslip, as some will go away during incubation. You can use areas away from the bubbles for observation. The lowering of the coverslip step is the most difficult and you will get better with practice.

References

1. Strauss MP et al (2012) 3D-SIM super resolution microscopy reveals a bead-like arrangement for FtsZ and the division machinery: implications for triggering cytokinesis. PLoS Biol 10(9):e1001389
2. Glaser P et al (1997) Dynamic, mitotic-like behavior of a bacterial protein required for accurate chromosome partitioning. Genes Dev 11(9):1160–1168
3. Turnbull L, Whitchurch CB (2014) Motility assay: twitching motility. Methods Mol Biol 1149:73–86
4. Semmler ABT, Whitchurch CB, Mattick JS (1999) A re-examination of twitching motility in *Pseudomonas aeruginosa*. Microbiology 145:2863–2873
5. Li D et al (2015) ADVANCED IMAGING. Extended-resolution structured illumination imaging of endocytic and cytoskeletal dynamics. Science 349(6251):aab3500
6. Gustafsson MG (2000) Surpassing the lateral resolution limit by a factor of two using structured illumination microscopy. J Microsc 198(Pt 2):82–87

7. Gustafsson MG (2005) Nonlinear structured-illumination microscopy: wide-field fluorescence imaging with theoretically unlimited resolution. Proc Natl Acad Sci U S A 102(37):13081–13086
8. Rego EH et al (2012) Nonlinear structured-illumination microscopy with a photoswitchable protein reveals cellular structures at 50-nm resolution. Proc Natl Acad Sci U S A 109(3):E135–E143
9. Turnbull L et al (2014) Super-resolution imaging of the cytokinetic Z ring in live bacteria using fast 3D-Structured Illumination Microscopy (f3D-SIM). J Vis Exp 29(91):51469
10. Schermelleh L et al (2008) Subdiffraction multicolor imaging of the nuclear periphery with 3D structured illumination microscopy. Science 320(5881):1332–1336
11. Gustafsson MG et al (2008) Three-dimensional resolution doubling in wide-field fluorescence microscopy by structured illumination. Biophys J 94(12):4957–4970

Chapter 13

Negative Staining and Transmission Electron Microscopy of Bacterial Surface Structures

Matthias Mörgelin

Abstract

Negative staining is an essential and versatile staining technique in transmission electron microscopy that can be employed for visualizing bacterial cell morphology, size, and surface architecture at high resolution. Bacteria are usually transferred by passive electrostatic adsorption from suspensions in physiological saline onto suitable hydrophilic support films on electron microscopic grids. There they are contrasted, or "stained," by heavy metal ions in solution such as tungsten, uranyl, molybdate, or vanadate compounds. Here, I describe how to visualize the interaction between the bacterial M1 protein and complement factors C1q and C3 on the surface of group A streptococcus by negative staining with uranyl formate on carbon support films. The methodology should be generally applicable to the study of a large number of other bacteria-protein interactions.

Key words Negative staining, Transmission electron microscopy, Bacteria, Adsorption, Carbon film, Contrast, Immunostaining, Protein interactions

1 Introduction

The advantages of negative staining include the use of aqueous bacterial and protein samples, which are contrasted by the heavy metal ions in solution without the necessity of air drying prior to electron microscopic preparation. This feature introduces a tremendous technical advantage with respect to particle resolution. Negative staining with uranyl formate employs the use of uranyl ions at low pH, and due to electrostatic repulsion between the stain and the bacterial surface, the uranyl ions will not penetrate the bacterial surface. Thus, the results yield clear bacterial cells and supramolecular assemblies on the bacterial surface with a dark background (Fig. 1). At the same time, uranyl formate acts as a mild fixing agent and thus pretreatment of bacteria by chemical fixation or heat is not required.

Bacteria, typically some 2×10^7 particles/ml, are transferred by passive electrostatic adsorption to thin carbon support films [1] on

Pontus Nordenfelt and Mattias Collin (eds.), *Bacterial Pathogenesis: Methods and Protocols*, Methods in Molecular Biology, vol. 1535, DOI 10.1007/978-1-4939-6673-8_13,

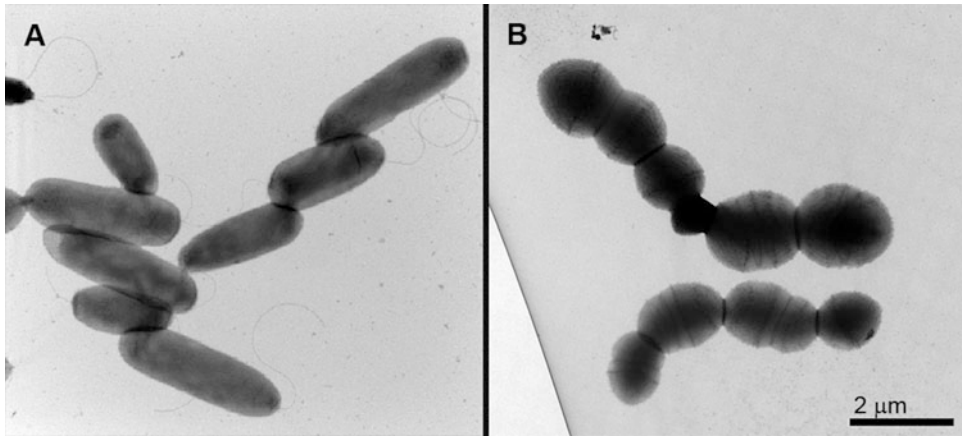

Fig. 1 Negative staining with uranyl formate on carbon support films of gram-negative rods, e.g., *Escherichia coli* (**a**), and gram-positive cocci, e.g., *Streptococcus pyogenes* (**b**). Bacteria are adsorbed on the surface of carbon support films from aqueous suspensions containing typically 10^7 cfu/ml and subsequently stained with 0.75 % uranyl formate solutions

150–400 mesh electron microscopic copper grids [2–4]. The carbon films are hydrophobic in nature and thus, prior to the experiment, have to be rendered hydrophilic by glow discharge at low pressure in a specially designed glow discharge unit [5]. This procedure improves adsorption of particles by several orders of magnitude.

Subsequent to the initial adsorption step, bacteria are briefly washed with water to remove excess particles, and then negatively stained with a 0.75 % uranyl formate solution [6, 7]. Between these different steps the electron microscopic grid with the adsorbed sample is not allowed to air-dry. This staining procedure reveals more ultrastructural details than any other positive or negative staining method employed ([Fig. 2] (for ref. *see* [8]). Therefore, uranyl formate is also the heavy metal ion of choice in cryo-negative staining, electron spectroscopy, and single particle analysis (for ref. *see* [9]).

In combination with negative staining, immunogold labeling provides significant advantages in highly sensitive and unequivocal detection of individual proteins on the bacterial surface. Moreover, the use of antibodies labeled with colloidal gold of different sizes allows the reliable colocalization of ligands such as C1q and C3 bound to bacterial surface constituents such as M1 protein ([Fig. 3] for refs. *see* [10, 11]).

Thus, we can obtain both structural and functional information by the combination of negative staining and transmission electron microscopy and immunogold techniques.

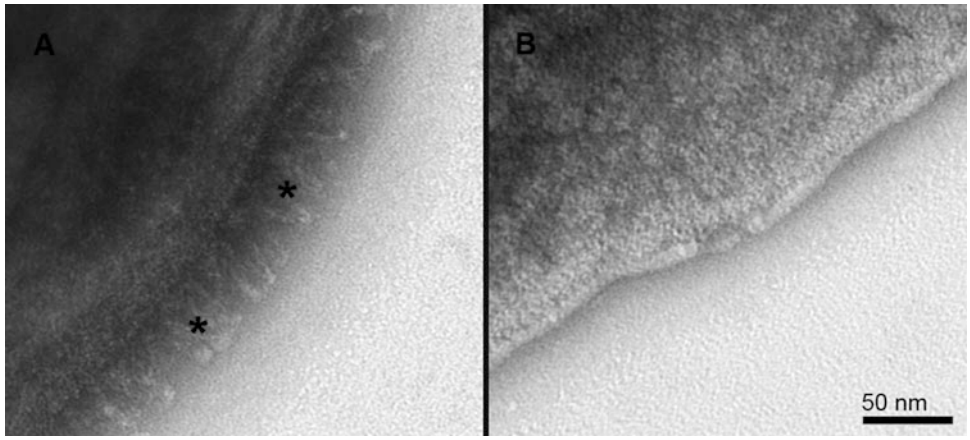

Fig. 2 Negative staining reveals structural details of the streptococcal surface at high resolution. (**a**) *Streptococcus pyogenes* wild-type bacteria with tightly packed molecular assemblies of M1 protein and protein H at their surface (*asterisks*). (**b**) in contrast, isogenic mutants lacking these surface structures reveal a smooth surface appearance

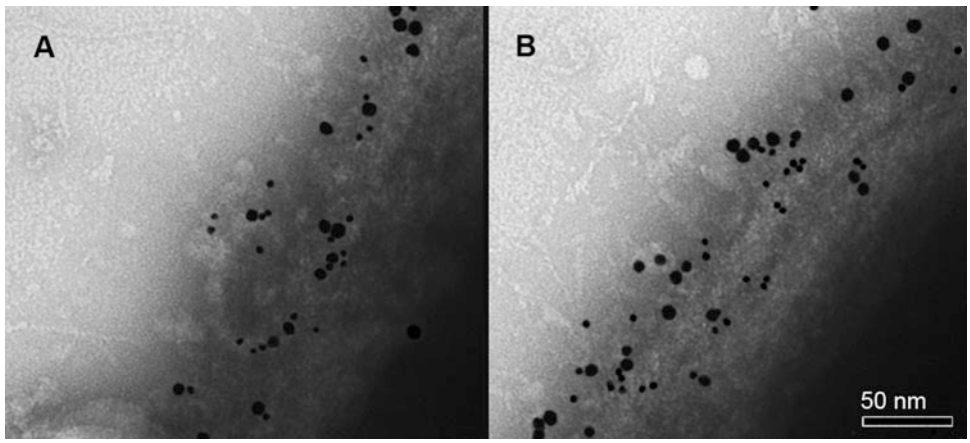

Fig. 3 Immunolabeling of supramolecular assembly on the streptococcal surface and identification of individual components by immunogold technique. (**a**) C1q (10 nm gold) binds to M1 protein (5 nm gold), (**b**) C3 (10 nm gold) is found in complex with M1 protein (5 nm gold) on the bacterial surface

2 Materials

All solutions are prepared with sterile and ultrapure water (purify deionized water to attain a sensitivity of 10 MΩ/cm at 25 °C). Reagents are puriss p.a. grade and stored at room temperature unless indicated otherwise.

2.1 Bacterial Strains

1. *Streptococcus pyogenes* strain AP1 (40/58) of serotype M1 (*see* **Note 1**) is from the World Health Organization Collaborating Centre for Reference and Research on Streptococci, Prague, Czech Republic. Store in glycerol stocks at –80 °C.
2. Todd-Hewitt Broth.
3. 10 mM Tris–HCl solution containing 5 mM glucose (referred to as Tris-glucose, *see* **Note 2**).

2.2 Negative Staining Components

1. Ultra-pure water.
2. For 0.75% uranyl formate in ultra-pure water: weigh 37.5 mg uranyl formate powder (to 5 ml water) in 5 ml plastic Falcon tubes (*see* **Note 3**).
3. Wrap with aluminum foil. Store at 4 °C.
4. Double sticky tape.

2.3 Carbon Coated Grids

1. Mica discs.
2. Carbon thread.
3. 150–400 mesh electron microscopy copper grids (Electron Microscopy Sciences, Hatfield, PA, USA). Store at room temperature.
4. High vacuum coating device (Leica Microsystems, Wetzlar, Germany).

2.4 Glow Discharge Unit

1. Plastic vacuum chamber.
2. Plastic desiccator.
3. Vacuum pump.
4. Vacuum leak detector (Tesla coil).
5. High-voltage power supply.

2.5 Antigens and Conjugates

1. Purified human plasma from local blood donors.
2. Mouse monoclonal anti-C1q and anti-C3 antibodies from Abcam, Cambridge, UK. Store at 4 °C.
3. Colloidal gold of defined sizes is prepared by reduction of a CCl_4 solution with sodium citrate or sodium thiocyanate under routine conditions [10] (*see* **Note 4**).

3 Methods

All experimental procedures are carried out at room temperature unless otherwise specified.

3.1 Bacterial Culture Conditions

1. Grow bacteria to mid-logarithmic phase in Todd-Hewitt broth (THB, Difco, Detroit, DI, USA) and incubate at 37 °C in a humid atmosphere with 5% CO_2 (*see* **Note 5**).

2. Wash bacteria and resuspend in Tris-glucose to obtain a suspension of 2×10^7 cfu/ml (*see* **Note 6**).

3.2 Carbon Coated Electron Microscopy Grids

1. Freshly cleave mica discs and put onto the rotating stage of a carbon coating device with a double-sticky tape (*see* **Note 7**).
2. Evaporate a 5 nm carbon film under rotation onto the mica surface from a carbon source (carbon rod or carbon thread) in a high vacuum ($\leq 10^{-6}$ bar) (*see* **Note 8**).
3. Float off the carbon film on the mica disc by emerging the disc in ultra-pure water in a specially designed plastic trough (*see* **Note 9**).
4. Pick up the floating carbon film by electron microscopy copper grids from below and air dry (*see* **Note 10**).

3.3 Incubation with Antigens and Conjugates

1. Incubate 100 µl of the bacterial solution with purified C1q or C3 at a concentration of 2–5 µM for 30 min.
2. Wash bacteria with Tris-glucose and resuspend the bacterial pellet in the same buffer.
3. Incubate the specimens with gold-conjugated antibodies against M1 protein (5 nm gold), either in combination with anti-C1q (10 nm gold) or C3 (10 nm gold), for 1 h at room temperature.
4. After a final wash with 10 mM Tris–HCl containing 5 mM glucose, subject the specimens to negative staining (*see* **Note 11**).

3.4 Negative Staining

1. Pipet rows of drops of: 1× TBS, 1× bacterial solution, 2× water, 2× uranyl formate, and 1× water onto a Parafilm sheet (*see* **Note 12**).
2. The grids are rendered hydrophilic glow discharge for 30 s in a specially designed glow discharge device as described above.
3. Absorb, wash, and stain specimens by subsequently touching the surface of the different drops for 30–60 s each (*see* **Note 13**).
4. After the final washing step with water, remove the water by blotting the grid on a filter paper surface and air-dry the grids.

3.5 Transmission Electron Microscopy

1. Examine negatively stained specimens in a Philips/FEI CM 100 TWIN transmission electron microscope operated at 60 kV accelerating voltage.
2. Record images with a side-mounted Olympus Veleta camera with a resolution of 2048×2048 pixels (2 k×2 K) and the ITEM acquisitions software (*see* **Note 14**).
3. If necessary, adjust contrast and brightness in Photoshop.

4 Notes

1. This method works with any kind of bacteria and there are no limitations. Eukaryotic cells such as Candida etc. work equally well provided they adsorb to the carbon support film. In case of adsorption problems, purified cell homogenates or membrane preparations can be used instead which adsorb easier to hydrophilic carbon films than whole cells.
2. Any kind of buffer can be used instead of Tris-glucose. However, culture media containing proteins or other particles should be avoided as they would yield a high particle background on electron micrographs. Phosphate-containing buffers should also be avoided as they tend to form precipitates with uranyl formate during the staining process. Conveniently, bacteria are transferred into a particle- and phosphate-free physiological saline in a final washing step.
3. For your convenience, prepare a rack with some 50 tubes containing uranyl formate powder on stock. It will take less time than weighing 37.5 mg uranyl formate powder each time you prepare the solution.
4. Purified and characterized colloidal gold particles of defined sizes can also be purchased from Electron Microscopy Sciences, Hatfield, PA, USA, or other providers. Store at 4 °C. Observe that protein conjugates with colloidal gold must not be stored frozen as freezing releases the gold particle from the conjugate by electrostatic discharge.
5. Alternatively, bacteria from any time point of a given growth curve may be used. There are no limitations as long as the particles adsorb to the carbon support film.
6. 2×10^7 cfu/ml turned out to yield good particle densities on electron microscopic grids, which facilitates observation and statistical evaluation. However, up to 10× more or 10× less bacteria can also be applied if necessary. As different bacteria strains vary somewhat in surface charge densities, it is recommended to test their adsorption properties before applying valuable reagents such as ligands or antibodies.
7. Mica discs should be freshly cleaved immediately before use as the cleaved faces are ultra-clean and do not add contaminating particles to electron micrographs.
8. The carbon film thickness is carefully controlled by either evaporating a piece of carbon thread of defined length, or by means of a swing quartz-based thickness measuring device routinely provided with the high vacuum coating unit.
9. Carbon films detach easier from the mica discs if they are allowed to maturate overnight after coating.

10. Alternatively, ready-to-use electron microscopy grids can be purchased from Electron Microscopy Sciences, Hatfield, PA, USA, or other providers. Store in a dry and dust-free environment at room temperature, e.g., in a standard 10 cm polystyrene Petri dish with a filter paper sheet.
11. The specimens are now ready for transmission electron microscopy. Store in a specially designed grid box and protect from moisture, light, and dust. We store our grid boxes in a standard glass desiccator.
12. The uranyl formate solution is stored in a 5 ml Falcon tube wrapped in aluminum foil to protect from light. The reagent is stable for 1 day and has to be freshly prepared each time before use.
13. The grid surface is not allowed to dry between individual drops as this will compromise the resolution of specimen fine structure and details.
14. The camera and image acquisition software are integrated parts of any particular electron microscope and may vary between different instruments. The use of the above-specified camera and software is thus not mandatory.

References

1. Valentine RC, Shapiro BM, Stadtman ER (1968) Regulation of glutamine synthetase. XII electron microscopy of the enzyme from Escherichia coli. Biochemistry 7:2143–2152
2. Grupe M (1974) Method for the preparation of reproducible carbon- and platinum steam-layer-strengths on electron microscopy grid slides. Z Med Labortech 15:296–301
3. Pegg-Feige K, Doane FW (1983) Effect of specimen support film in solid phase immuno-electron microscopy. J Virol Methods 7:315–319
4. Smith CA, Seegan GW (1984) The pleated sheet: an unusual negative-staining method for transmission electron microscopy of biological macromolecules. J Ultrastruct Res 89:111–122
5. Aebi U, Pollard TD (1987) A glow discharge unit to render electron microscope grids and other surfaces hydrophilic. J Electron Microsc Tech 7:29–33
6. Leberman R (1965) Use of uranyl formate as a negative stain. J Mol Biol 13:606
7. Knight DP (1975) Negative staining of rat tail tendon collagen fibrils with uranyl formate. Tissue Cell 7:651–654
8. Bremer A, Henn C, Häner M, Aebi U, Isenberg G (1992) Has negative staining still a place in biomolecular electron microscopy? Ultramicroscopy 46:85–111
9. Cheng Y, Grigorieff N, Penczek PA, Walz T (2015) A primer to single-particle cryo-electron microscopy. Cell 161:438–449
10. Roth J, Zuber C, Komminoth P, Sara T, Li WP, Heitz PU (1996) Applications of immunogold and lectin-gold labeling in tumor research and diagnosis. Histochem Cell Biol 106:131–148
11. Baschong W, Wrigley NG (1990) Small colloidal gold conjugated to Fab fragments or to immunoglobulin G as high-resolution labels for electron microscopy: a technical overview. J Electron Microsc Tech 14:313–323

Chapter 14

Detection of Intracellular Proteins by High-Resolution Immunofluorescence Microscopy in *Streptococcus pyogenes*

Assaf Raz

Abstract

Immunofluorescence microscopy is an invaluable tool for the study of biological processes at the cellular level. While the localization of surface-exposed antigens can easily be determined using fluorescent antibodies, localization of intracellular antigens requires permeabilization of the bacterial cell wall and membrane. Here, we describe an immunofluorescence protocol tailored specifically for *Streptococcus pyogenes*, applying the phage lysin PlyC for cell wall permeabilization. This protocol allows a high level of morphological preservation, suitable for high-resolution microscopy. With slight modification, this protocol could also be used for other Gram-positive pathogens.

Key words Immunofluorescence, Microscopy, *Streptococcus pyogenes*, Gram positive, Fluorescent, Antibody, Deconvolution

1 Introduction

The image resolution attainable by fluorescence microscopy has dramatically increased in recent years, greatly facilitating the study of bacterial physiology at the subcellular level [1, 2]. Two important approaches for protein localization are immunofluorescence and fluorescent protein fusion; each has specific advantages and disadvantages. In immunofluorescence, the localization pattern of native cellular proteins is determined through the use of fluorescent antibodies that are specific for a protein of interest. This method does not require genetic manipulation of the target organism, making it particularly useful in bacteria for which the genetic tools are not fully developed. Nevertheless, since antibodies cannot traverse the bacterial cell wall and membrane [3], localization of intracellular antigens requires fixation and permeabilization of the bacteria, procedures that may harm their cellular morphology.

In contrast to immunofluorescence, fluorescent proteins such as green fluorescent protein (GFP) can be fused to a target protein

Pontus Nordenfelt and Mattias Collin (eds.), *Bacterial Pathogenesis: Methods and Protocols*, Methods in Molecular Biology, vol. 1535, DOI 10.1007/978-1-4939-6673-8_14,

and expressed from the genome or a plasmid. The fusion protein can be imaged in live cells without the need for fixation or permeabilization, and this allows tracking of the protein in real time [4, 5]. This technique has been instrumental in elucidating the molecular mechanisms controlling cell division [6]. Despite the advantages this method offers, fusion of a bulky fluorescent protein (28 kDa in the case of GFP) could alter the function and distribution of the protein being studied. A fusion protein may not interact with all of the native protein's binding partners, or may not display the native expression pattern. Additionally, there are some inherent problems associated with certain fluorescent proteins, including the tendency to form multimers, the requirement for oxygen to become fluorescent, a lag time between the protein's synthesis and the time it becomes fluorescent, and the failure to fold correctly following secretion through the Sec apparatus; some of these issues have been addressed in later generations of fluorescent proteins [4]. The advantages and disadvantages offered by immunofluorescence and fluorescent proteins are therefore complementary in many ways, and the choice of the method largely depends on the question being studied, and the tools available for the specific bacterium.

There are a few critical points that should be considered when initiating an immunofluorescence study. First, it is crucial that the antibodies used are specific for the target protein, and do not recognize any other cellular targets. For this reason, monoclonal antibodies are often preferable. When polyclonal antibodies are used, pre-immune serum should be used as control. Additionally, polyclonal antibodies could be affinity-purified using an immobilized target antigen, and/or adsorbed on a mutant strain that does not express the target protein. Whenever possible, a mutant strain lacking the target protein should also be used as a control in the microscopy experiment, to verify the specificity of the antibodies. In cases where a fluorescent conjugate is used, controls must also be included to rule out nonspecific interactions between these antibodies and the target organism. Incubating the cells with nonimmune serum from an animal similar to that used to produce the fluorescent conjugates can often block such nonspecific interactions. If antibodies specific to the target protein are not available, the target protein can be fused to a small epitope tag (~10 amino acids), for which commercial antibodies are available. Although the small size of epitope tags makes them less likely to interfere with the normal function of the target protein (compared to the much larger fluorescent proteins), caution should still be taken in the interpretation of the results.

A second critical point involves the fixation and permeabilization procedures. These procedures must be specifically calibrated to ensure the preservation of cellular morphology, without harming the target epitopes. Fixation is typically performed using crosslinking agents such as paraformaldehyde and glutaraldehyde, which

covalently links cellular components. This preserves the morphology of the cells and prevents the movement of cellular components during sample preparation and labeling. While extended fixation generally leads to better cellular morphology, it may also harm target epitopes, requiring careful calibration.

When targeting intracellular antigens, permeabilization of the membrane (typically using methanol) must precede the permeabilization of the cell wall. This is because the high osmotic pressure within bacteria could lead to membrane bulging and gross deformation of cellular morphology during cell wall permeabilization, unless the cellular osmotic pressure is first equalized to that of the environment. The cell wall is permeabilized using a cell wall hydrolase, which breaks specific bonds within the peptidoglycan. The cell wall of many nonpathogenic bacteria such as *Escherichia coli* and *Bacillus subtilis* can be permeabilized with lysozyme [7]; however, *Streptococcus pyogenes* (like several other pathogens) is resistant to lysozyme [8, 9]. Phage lysins are cell wall hydrolases produced by bacteriophages to release progeny phage during the late stages of the lytic cycle. In recent years, several such phage lysins have been cloned and recombinantly expressed as potential anti-infective agents [10]. Specifically, PlyC is highly effective in degrading the cell wall of *S. pyogenes* [11], and is ideal for immunofluorescence [12]. In this chapter, we will review the specific conditions and consideration for immunofluorescence studies in *S. pyogenes*. For sample fluorescence images obtained using this method see the following references [12–14]. The procedure described here may also be useful for other gram-positive pathogens with some modifications.

2 Materials

Prepare all solution with milli-Q water (or water of equivalently high purity), and analytical grade reagents.

1. Microscope slides.
2. Microscope cover glass 18 × 18-1.5 (Fisher Scientific) for routine experiments, or No.1.5H 170 ± 5 μm thickness 18 × 18 mm (Zeiss) for high-resolution imaging (*see* **Note 1**).
3. Poly-L-lysine solution, 0.1% w/v (Sigma).
4. 16% paraformaldehyde. Add 16 g paraformaldehyde (Sigma) to 80 ml milli-Q water in a capped bottle. Add 1 ml 1 N NaOH and place in a 65 °C water bath with occasional shaking until the paraformaldehyde is dissolved. Bring to a final volume of 100 ml with milli-Q water. Filter to remove any remaining paraformaldehyde particles, prepare 1 ml single-use aliquots, and freeze at −20 °C.
5. Glutaraldehyde solution, 50% (Sigma).

6. Phosphate buffer 1 M pH 7.4.
7. Phosphate buffered saline pH 7.4 (PBS).
8. Methanol.
9. PlyC, prepared according to Nelson et al. [11], diluted to 3 U/ml in PBS.
10. Antibody dilution buffer: PBS containing 2% bovine serum albumin (Sigma) and 1% gelatin from cold water fish skin (Sigma) (*see* **Note 2**).
11. Blocking buffer: antibody dilution buffer supplemented with 10% nonimmune serum from an animal similar to that used to produce the fluorescent conjugates (where applicable).
12. Primary antibodies, fluorescent conjugates, and fluorescent dyes according to the experimental design (*see* **Note 3**).
13. Mounting medium: 50% glycerol, 0.1% p-phenylenediamine (Sigma) in PBS pH 8.0. Dissolve 0.1 g p-phenylenediamine in 50 ml PBS 2× pH 8.0. Add 50 ml glycerol and mix. Aliquot and store at −80 °C. A working aliquot may be kept at −20 °C for several days but should be discarded when its color darkens (*see* **Note 4**).
14. 10 cm petri dishes.
15. Kimwipes (Kimberly-Clark).
16. An aspirator connected to a trap flask.
17. A wash bottle with PBS (*see* **Note 5**).
18. A dull-edged razor blade and flat-faced tweezers for slide manipulation.
19. A 1 L beaker wrapped with aluminum foil or a similar container.
20. Nail polish (to seal prepared slides) (*see* **Note 6**).
21. A fluorescence microscope: a wide field or an image restoration microscope equipped with an oil immersion 100× objective with a high numerical aperture.

3 Methods

All procedures should be carried out at room temperature unless otherwise noted. Once the cells are attached to the slide, make sure a humid environment is maintained throughout all incubation steps. The cells must never be allowed to dry.

3.1 Slides Preparation

1. Label a corner of a 18 × 18 mm cover glass with the slide number using a black permanent marker. Small additional marks can be made on the back of the slide to help locating the cells (*see* **Note 7**).

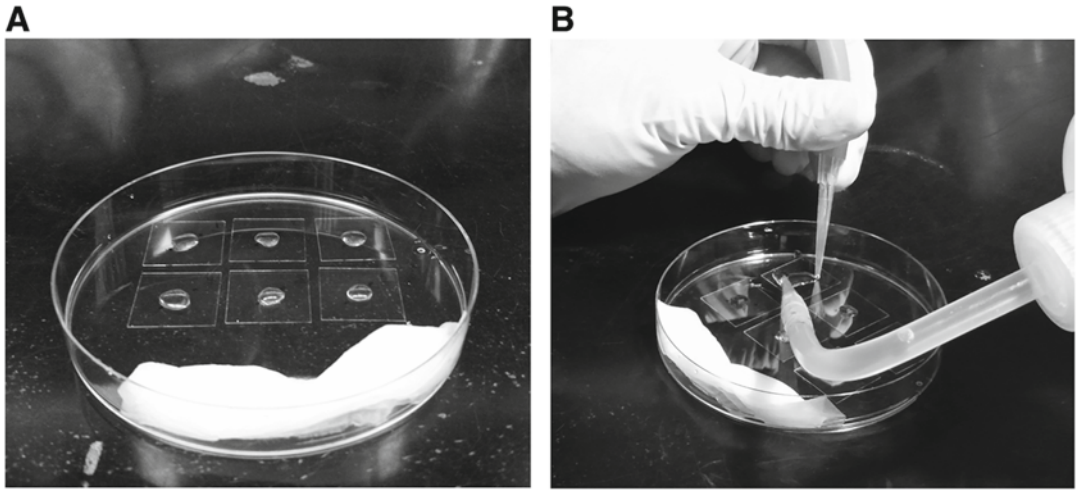

Fig. 1 (**a**) A typical arrangement of cover slides in a petri dish; a wet kimwipe is placed away from the slides to maintain humidity. Only the center of the slide (where a drop of poly-L-lysine is seen) is used for placement of the cells and labeling reagents. (**b**) Efficient washing of multiple slides is facilitated by the simultaneous use of a wash bottle and an aspirator (*see* **Note 10**). Note that a stream of PBS should not be directed toward the cells (particularly following permeabilization)

2. Place up to 6–7 slides in a 10 cm petri dish (Fig. 1a).
3. Place a wet folded kimwipe in each plate (away from the slides) to maintain humidity.
4. Place a 20 µl drop of 0.1% poly-L-lysine at the center of each slide for about 10 min.
5. Wash the slide with milli-Q water and dry.
6. Cover the petri dishes with a lid to protect the slides from dust.

3.2 Fixation of Cells and Attachment to the Slides

1. For each sample to be fixed, prepare a labeled microfuge tube containing 40 µl 1 M phosphate buffer pH 7.4.
2. When the bacteria are ready, add 1.5 µl glutaraldehyde 50% to a 1 ml aliquot of paraformaldehyde 16%. Add 200 µl of the mix to each fixation tube containing phosphate buffer, and then add 1 ml of culture and mix. Unused paraformaldehyde/glutaraldehyde mix may be stored on ice for a few hours (*see* **Note 8**).
3. Incubate at room temperature for 15 min, and on ice for 30 min.
4. Centrifuge for 2 min at 6000 RCF, and wash the pellet with 1 ml PBS.
5. Centrifuge for 2 min at 6000 RCF, and resuspend the pellet in 200–1000 µl PBS (*see* **Note 9**).
6. Place a drop of 10 µl washed cells on each slide for 10–20 min.
7. Aspirate gently and wash with PBS to remove unbound cells (Fig. 1b) (*see* **Note 10**).

3.3 Permeabilization of the Cells

Perform these steps only if intracellular antigens are targeted.

1. Aspirate PBS, and **slowly** dip the slide in ice-cold methanol for 10 s. Then, **slowly** dip in PBS for a few seconds, and return the slide to the dish. Add a drop of PBS to the cells to prevent drying (*see* **Note 11**).
2. Aspirate PBS and place a 10 μl drop of 3 U/ml PlyC in PBS on the cells for 10 min at room temperature (*see* **Note 12**) (Fig. 2).
3. Wash the cells gently with PBS.

3.4 Labeling Procedure

1. Aspirate PBS and add 20 μl of blocking buffer to each slide. Incubate for 10 min.
2. Wash the slides with PBS.
3. Aspirate, and add 10 μl primary antibodies, diluted in antibody dilution buffer. Incubate for 1 h at room temperature in a humidified chamber (*see* **Note 13**).
4. Wash three times with PBS.
5. Aspirate, and add 10 μl fluorescent conjugates (and any additional fluorescent dye, such as DAPI), diluted in antibody dilution buffer. Incubate for 1 h at room temperature in a humidified chamber.
6. Wash three times with PBS.
7. Aspirate, and add 4.5 μl mounting medium.
8. Flip the cover glass onto a glass slide using a dull-edged razor blade.
9. Seal the slides with nail polish (*see* **Note 6**).

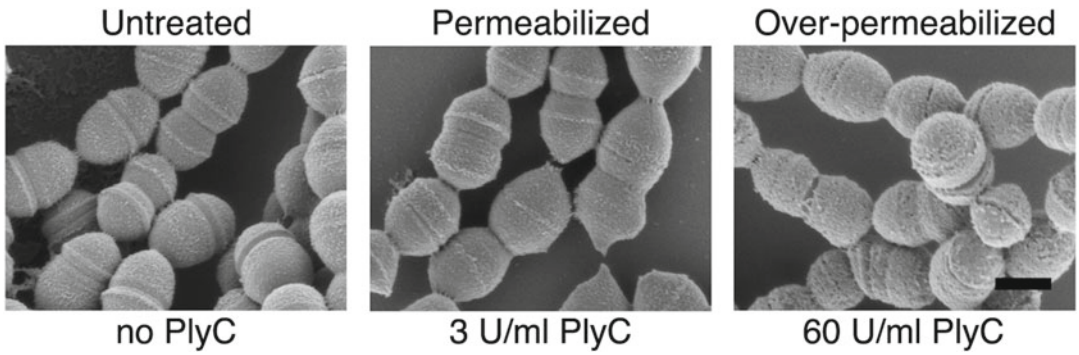

Fig. 2 Scanning electron microscopy images of permeabilized and control cells. The morphology of permeabilized cells (treated with 3 U/ml PlyC, representing the lowest concentration that results in permeabilization of 100 % of the cells) is only slightly different from untreated cells. Signs of morphological deterioration are visible in cells treated with 60 U/ml PlyC, underscoring the need for careful calibration of the permeabilization conditions. The scale bar represents 500 nm

10. Keep the slides at 4 °C, but allow them to reach room temperature before imaging (to avoid drift during high-resolution imaging). For best results, image within a few days.

3.5 Imaging

The imaging procedure may vary according to the microscope available. Imaging would typically require a microscope equipped with a 100× oil immersion objective with a high numerical aperture. We have used this procedure with a standard wide field fluorescence microscope, a high-resolution DeltaVision image restoration microscope (Applied Precision / GE Healthcare), and a super-resolution DeltaVision OMX Blaze 3D Structured Illumination Microscopy (3D-SIM) system (Applied Precision/GE Healthcare). For image restoration microscopy we typically capture Z-stacks images at 0.15 μm intervals, and deconvolve images using SoftWoRx (Applied Precision/GE Healthcare). Slides prepared in this manner, however, should be compatible with a variety of microscopy procedures.

4 Notes

1. While a cover glass with different dimensions can be used, thickness no. 1.5 should always be used. To reduce background signal, slides could be acid-washed prior to the beginning of the procedure. Slides are placed in a beaker containing 1N hydrochloric acid and left on a shaker at a slow speed for 1 h. The slides are then washed several times with milli-Q water until the pH is neutral, washed once with ethanol, and air-dried. While this procedure is not generally needed for routine microscopy, it may help reduce background fluorescence in cases where a grainy nonuniform signal is observed on the surface of the slide.
2. Gelatin provides additional blocking but may be omitted in many cases.
3. When more than one protein is detected using primary antibodies that were produced in different animals, use fluorescent conjugates that have been cross-adsorbed to prevent reaction with antibodies from the other species. Alternatively, primary antibodies could be directly conjugated to a fluorophore using kits available from several manufacturers. While this simplifies the microscopy procedure, the signal obtained using this method is often not as strong as that obtained using a combination of a primary antibody and a secondary fluorescent conjugate, due to the signal amplification obtained using this method. In choosing fluorophores, make sure the excitation/emission spectra of the various fluorophores used do not overlap. Prefer fluorophores that are less susceptible to photobleaching (for example, Alexa Fluor 488 as opposed to FITC).

4. Mounting media should be selected according to the specific application. For 3D imaging, mounting media that remains liquid (typically glycerol-based) should be used, since mounting media that hardens causes flattening of the sample. The type of anti-fade agent used in the mounting media (if any) should be selected to fit to the fluorophore used. An incompatible anti-fade agent may not prevent, or even increase photobleaching, and could lead to nonspecific background. Mounting media could be purchased commercially, or be prepared in the lab. An additional useful mounting medium is the nPG (n-propyl gallate) medium: 9 ml glycerol, 1 ml 0.2 M Tris–HCL pH 8.0, 0.05 g n-propyl gallate. Heat to 60 °C for about 15 min until dissolved. Store aliquots at −80 °C.
5. For improved control over the flow of PBS, remove the inner tube from the wash bottle and attach a 200 μl pipette tip to the nozzle (this can be cut to the desired opening size).
6. Colored nail polish should be avoided as some pigments may cause nonspecific background. A quick-drying, transparent nail polish with glitter is ideal, as it allows easy detection of areas not properly sealed without the use of pigments.
7. A black Sharpie marker works well, but colored markers should be avoided as they may introduce pigments that cause background fluorescence.
8. If an aliquot of 16% paraformaldehyde appears cloudy following defrosting, place it in a 65 °C water bath until it clears. The concentration of paraformaldehyde and glutaraldehyde, and the fixation time should be calibrated for the specific application. Higher fixative concentration and prolonged fixation time lead to better preservation of cellular morphology, but may harm certain target epitopes. Fixation with paraformaldehyde is generally quite gentle, but may still damage the target epitopes at high concentration or a prolonged fixation time. Glutaraldehyde is a harsher fixative, and higher concentrations often lead to a loss of epitope binding.
9. The ideal amount of PBS used to resuspend the cells differs between strains. The final cell density should be adjusted empirically so that an even monolayer of cells is formed on the slide. *S. pyogenes* strains with a large amount of M protein on their surface tend to aggregate during fixation. In these cases, resuspend the cells in about a fifth of the initial culture volume, and allow clumps to settle for a few minutes before adding cells from the upper portion of the tube to the slides.
10. To preserve cellular morphology, wash steps must be done gently (particularly following permeabilization of the cells). Add PBS to an area adjacent to the cells, and aspirate from the opposite side. Do not allow drops of PBS to hit the sample, do not point a stream of PBS directly at the cells, and do not aspi-

rate from the area containing the cells. The aspirator should be fitted with a 200 μl tip, cut to the appropriate opening size. For small experiments, a 1 ml pipette can be used to apply PBS. For larger experiment however, a wash bottle from which the inner tube has been removed is more appropriate. For efficient processing of a large number of slides, hold a wash bottle in one hand (controlling the flow of buffer by the angle the bottle is held), and an aspirator in the other.

11. Fill two 30 ml beakers or 50 ml conical tubes to the brim with methanol and PBS, and place them in an ice bucket. Just before dipping a slide in methanol, aspirate the PBS until it is almost, but not completely dry. Pick up the slide using a flat-faced forceps (grinding one of the sides of the forceps to a sharp edge may ease this). While holding the slide by the labeled corner, dip it into the methanol at a 45° angle, slowly enough for PBS beads to form, and run up the slide (do not dip the labeled part). After 10 s in the methanol, slowly remove the slide, and slowly dip it into the PBS beaker.

12. In large experiments, removing the PBS and adding PlyC to the all the samples may take a few minutes. Start measuring the 10 min incubation period the moment PlyC is added to the first slide. Following this incubation period, wash the slides at the same order, to ensure that each slide is exposed to PlyC for the same amount of time. In large experiments, the PlyC permeabilization step may be performed on half the slides at a time, to ensure accurate incubation time.

    The correct concentration of PlyC should be determined empirically by serially diluting each new PlyC stock. An antibody directed at a cytoplasmic antigen should be used during calibration experiments to monitor complete permeabilization of the cells. The integrity of cell wall material should be monitored using fluorescently labeled wheat germ agglutinin (WGA). To obtain the best cellular morphology, use the lowest PlyC concentration that results in permeabilization of 100% of the cells.

    Presence of M protein on the cell wall is critical for the preservation of its integrity. M protein is a wall-anchored coiled-coil protein that forms a cross-linked mesh during fixation, and this prevents the dissociation of cell wall fragments following treatment with PlyC [12]. In the absence of M protein, the permeabilization procedure would lead to the formation of spheroplasts.

    Lysozyme and mutanolysin are not good substitutes for PlyC. In our hands, 1 mg/ml lysozyme did not permeabilize the cell wall of *S. pyogenes* even after hour-long incubation, in agreement with the observed resistance of this organism to lysozyme [8, 9]. Prolonged incubation with 1000 U/ml

mutanolysin resulted in permeabilization of a large proportion of the cells but also caused a considerable deterioration in cellular morphology.

13. During hour-long incubations, stack the petri dished and place a wet paper towel on the top of the stack, then cover with a 1 L beaker wrapped in aluminum foil, or a similar light-resistant container.

Acknowledgments

I thank Vincent A. Fischetti for his support and insight. I thank Eleana Sphicas from the Rockefeller University Electron Microscopy Resource Center for the capturing of EM images. I thank Alison North from the Rockefeller University Bio-Imaging Resource Center for her advice. This work was supported by U.S. Public Health Service Grant AI11822 to Vincent A. Fischetti.

References

1. Tuson HH, Biteen JS (2015) Unveiling the inner workings of live bacteria using super-resolution microscopy. Anal Chem 87(1):42–63
2. Sanderson MJ, Smith I, Parker I, Bootman MD (2014) Fluorescence microscopy. Cold Spring Harb Protoc 2014(10):pdb top071795
3. Demchick P, Koch AL (1996) The permeability of the wall fabric of *Escherichia coli* and *Bacillus subtilis*. J Bacteriol 178(3):768–773
4. Shaner NC, Patterson GH, Davidson MW (2007) Advances in fluorescent protein technology. J Cell Sci 120(Pt 24):4247–4260
5. Enterina JR, Wu L, Campbell RE (2015) Emerging fluorescent protein technologies. Curr Opin Chem Biol 27:10–17
6. Yao Z, Carballido-Lopez R (2014) Fluorescence imaging for bacterial cell biology: from localization to dynamics, from ensembles to single molecules. Annu Rev Microbiol 68:459–476
7. Levin PA (2002) 6 Light microscopy techniques for bacterial cell biology. In: Philippe S, Arturo Z (eds) Methods in Microbiology, Vol 31, Academic Press, pp 115–132
8. Krause RM, McCarty M (1961) Studies on the chemical structure of the streptococcal cell wall. I. The identification of a mucopeptide in the cell walls of groups A and A-variant streptococci. J Exp Med 114:127–140
9. Gallis HA, Miller SE, Wheat RW (1976) Degradation of 14C-labeled streptococcal cell walls by egg white lysozyme and lysosomal enzymes. Infect Immun 13(5):1459–1466
10. Pastagia M, Schuch R, Fischetti VA, Huang DB (2013) Lysins: the arrival of pathogen-directed anti-infectives. J Med Microbiol 62(Pt 10):1506–1516
11. Nelson D, Schuch R, Chahales P, Zhu S, Fischetti VA (2006) PlyC: a multimeric bacteriophage lysin. Proc Natl Acad Sci U S A 103(28):10765–10770
12. Raz A, Fischetti VA (2008) Sortase A localizes to distinct foci on the *Streptococcus pyogenes* membrane. Proc Natl Acad Sci U S A 105(47):18549–18554
13. Raz A, Talay SR, Fischetti VA (2012) Cellular aspects of the distinct M protein and SfbI anchoring pathways in *Streptococcus pyogenes*. Mol Microbiol 84(4):631–647
14. Raz A et al (2015) *Streptococcus pyogenes* sortase mutants are highly susceptible to killing by host factors due to aberrant envelope physiology. PLoS One 10(10):e0140784

Chapter 15

Antibody Guided Molecular Imaging of Infective Endocarditis

Kenneth L. Pinkston, Peng Gao, Kavindra V. Singh, Ali Azhdarinia, Barbara E. Murray, Eva M. Sevick-Muraca, and Barrett R. Harvey

Abstract

In this protocol, we describe the application of using a high affinity monoclonal antibody generated against the major pilin protein component of the pilin structure of *Enterococcus faecalis* as a PET imaging agent for enterococcal endocarditis detection. The anti-pilin -mAb 64Cu conjugate was able to specifically label enterococcal endocarditis vegetation in vivo in a rodent endocarditis model. By targeting pili, a covalently linked surface antigen extending from the bacterial surface, we provided evidence that gram-positive pilin represent a logical surface antigen to define or target an infectious agent for molecularly guided imaging. Our goal in providing a detailed protocol of our efforts is to enable others to build upon this methodology to answer pertinent translational and basic research questions in the pursuit of diagnosis and treatment of infective endocarditis.

Key words Monoclonal antibody, Gram-positive pathogen, PET imaging, Endocarditis, Enterococcus, Pili, Antigen, LPXTG anchored, In vivo, Bacterial infection

1 Introduction

Over a century ago, German Nobel Laureate Paul Ehrlich described the "Magische Kugel," or "Magic Bullet" theory in which an agent carrying a payload is precisely targeted to an invader in the human body. Acting as a missile seeking a surface marker on the target, the magic bullet could potentially destroy countless diseases, including infectious disease and cancer. The dawn of monoclonal antibody technology and antibody engineering has made Ehrlich's dream a reality in cancer therapy with the clinical use of antibodies and antibody drug conjugates (ADCs). However, despite a clear clinical need, and despite antibodies being an obvious (natural) means of targeting infectious disease, there has been limited success in efforts using antibodies or antibody fragments to diagnose or target

Pontus Nordenfelt and Mattias Collin (eds.), *Bacterial Pathogenesis: Methods and Protocols*, Methods in Molecular Biology, vol. 1535, DOI 10.1007/978-1-4939-6673-8_15,

established in vivo infection. Obstacles in the execution of this objective have included successful identification of bacterial target antigens actively expressed during infection, affinity, and specificity of anti-target antibodies, and the ability of antibody to infiltrate the microenvironment of existing infection to interact with surface antigen.

Our team recently described a molecular imaging study identifying a specific site of enterococcal infection by using a single monoclonal antibody to a defined bacterial surface antigen. This demonstration forms the basis for a number of different avenues of discovery including (1) a model for developing targeted therapeutic strategies including antibody drug conjugates (ADC), (2) an imaging diagnostic for in vivo assessment of existing infection, or (3) providing tools to improve our understanding of bacterial pathogenesis and the accessibility of specific surface antigens. Given that the pilin target represents a class of antigens on gram-positive pathogens anchored by a common LPXTG motif to the peptidoglycan matrix and that the rodent infective endocarditis model utilized has been modified for use with many other gram-positive pathogens [1–4], the opportunity exists for extending and developing these procedures using specific antibodies to other LPXTG anchored targets to suit other Gram-positive infections. Furthermore, because diagnostic imaging is possible under microdosing conditions in which the chance for adverse events is extremely limited, translation of a combinational diagnostic/therapy into humans may be accelerated.

In contrast to a polyclonal preparation that can have batch to batch variation, a mAb is a defined entity, targeting a specific epitope and thus providing a unique opportunity for specific recombinant engineering of agent. While engineering recombinant antibodies for optimized binding affinity and Fc function has become standard practice in the development of antibody therapeutics [5, 6], these practices are not regularly implemented in the development of imaging diagnostics. Recent publications have demonstrated the importance of both affinity [7] and Fc modification [8] in molecular imaging performance using near-infrared fluorescence as well as PET imaging. Deglycosylation of a mAb, for example, can have significant impact on Fc/FcγR interactions, and thus reduce nonspecific binding via this interaction, to improve the accuracy for molecular imaging.

In this chapter, we will provide protocols describing (1) monoclonal antibody characterization, (2) antibody modifications/labeling of imaging agent, (3) application within a rat endocarditis model for diagnostic imaging, and (4) evaluation and analysis of imaging results.

2 Materials

2.1 Flow Cytometry

1. PBS: Potassium phosphate monobasic (KH_2PO_4) 1.44 g/l. Sodium chloride (NaCl) 9.00 g/l, sodium phosphate dibasic (Na_2HPO_4-$7H_2O$) 0.795 g/l, pH 7.4.
2. Bovine serum albumin, Cohn fraction V.
3. 15 ml culture tubes with lid.
4. 125 ml Erlenmeyer flask.
5. Brain Heart Infusion (BHI) powder.
6. 1.5 ml Eppendorf micro centrifuge tubes.
7. Phycoerythrin (PE) conjugated Goat Anti-Mouse IgG (Fc).
8. BD FACS Calibur flow cytometer (BD Bioscience, CA) or equivalent.

2.2 Immunogold Electron Microscopy

1. Formvar carbon-coated Copper grids, 200 mesh (Electron Microscopy Sciences).
2. Wash buffer: 1% BSA in 1× PBS.
3. Blocking buffer: 0.1% Gelatin in 1× PBS.
4. Primary antibody solution: murine monoclonal antibody against specific target in PBS at 1 μg/ml.
5. Gold-labeled secondary antibody solution: 12 nm gold-conjugated donkey anti-mouse IgG (1:20) (Jackson ImmunoResearch Laboratories).
6. Staining solution: 1% uranyl acetate in H_2O.

2.3 EndoS Treatment

1. Recombinant EndoS enzyme (IgGZero , GENOVIS AB).

2.4 Antibody Labeling

1. Unmodified mAb against surface antigen and isotype matched control.
2. Reaction buffer: 0.1 M sodium phosphate buffer (pH 8.3).
3. 1,4,7,10-Tetraazacyclododecane-N,N',N'',N'''-tetraacetic acid (DOTA) mono-N-hydroxysuccinimide ester (DOTA-NHS).
4. Zeba desalting spin columns.
5. Radiolabeling buffer: 0.1 N sodium acetate buffer (pH 6).
6. $^{64}CuCl_2$.
7. Nonradioactive $CuCl_2$.
8. Whatman chromatography paper.
9. Glass thin-layer chromatography (TLC) chamber.
10. TLC eluent: 0.1 M ammonium acetate buffer (pH 6) containing 50 mM EDTA.
11. Radio-TLC scanner (Eckert & Ziegler Radiopharma).

12. DOTA-conjugated mAb.
13. Quenching solution: 10 mM ethylenediaminetetraacetic acid (EDTA).
14. Radio-high-performance liquid chromatography.
15. TSK gel G3000SW (5 μm) size exclusion HPLC column.
16. HPLC mobile phase: 90% buffer A (0.1 M sodium phosphate buffer [pH 7.3]) and 10% buffer B (CH_3CN) (isocratic).

2.5 Potency ELISA

1. PBS: Potassium Phosphate monobasic (KH_2PO_4) 1.44 g/l. Sodium chloride (NaCl) 9.00 g/l, Sodium phosphate dibasic (Na_2HPO_4-$7H_2O$) 0.795 g/l, pH 7.4.
2. PBST: PBS, 0.05% Tween-20.
3. BLOTTO: PBST, 5% Non-Fat Dry Milk.
4. mAb treated and untreated as described in Subheadings 3.3 and 3.4.
5. Horse Radish Peroxidase (HRP) Goat anti-mouse IgG (Fc).
6. TMB substrate: 3,3′,5,5′-tetramethylbenzidine (TMB) substrate.
7. TMB color stop reagent: H_2SO_4, 2 N.
8. ELISA plate reader capable of OD450 nm determination.
9. ELISA plate washer or 8–12 channel manual well washer.

3 Methods

The use of hybridoma technology and subsequent screening techniques for the isolation of high affinity mAb panels against specific antigens has been described for decades. Identification of the antipilin mAb utilized in this protocol has been detailed elsewhere [9]. Here, we describe our expanded techniques to confirm that the selected mAb does in fact bind robustly to the natively displayed antigen on the surface of the cell and maintains this activity upon modifications, prior to proceeding with in vivo imaging models.

3.1 Flow Cytometry

1. Overnight-cultured *E. faecalis* OG1RF cells are inoculated into a 125 ml Erlenmeyer flask containing 20 ml Brain Heart Infusion (BHI) broth to a starting optical density at 600 nm (OD_{600}) of 0.05 and harvested at approximately mid-log phase (*see* **Note 1**).
2. Sample aliquots equivalent to an optical density at 600 nm (OD_{600}) of 0.2 are harvested into 1.5 ml micro-centrifuge tubes and spun at 10,000 × *g* for 1.5 min., media removed and cells washed twice with 1.0 ml phosphate-buffered saline containing 2% Bovine Serum Albumin (PBS-BSA).

3. After final spin, cell pellets are resuspended with 100 µl of PBS-BSA containing 5 µg/ml anti-EbpC mAb 69 and incubated for 1 h at room temperature (25 °C).
4. Wash cells three times with PBS-BSA, followed by the addition of 100 µl of a 1:100 dilution of PE -conjugated Goat Anti-Mouse IgG (Fc) in PBS-BSA, and incubate for 30 min at room temperature (25 °C).
5. Wash cells three times with PBS-BSA before fixing with 1 ml 1 % paraformaldehyde in PBS-BSA. Analyze with a BD FACS Calibur flow cytometer (BD Bioscience, CA).

3.2 Electron Microscopy Confirmation of Surface Labeling

1. Overnight-cultured *E. faecalis* OG1RF cells are inoculated into 20 ml brain heart infusion (BHI) broth at a starting optical density at 600 nm (OD_{600}) of 0.05 and harvested at mid-log phase or approximately $OD_{600} = 0.6$. (*see* **Note 1**).
2. One OD_{600} equivalent of cells are washed once with 0.1 M NaCl before being resuspended in 1 ml phosphate-buffered saline (PBS).
3. Eight microliters of cells from the above step are pipetted onto the coated side of the carbon-coated copper grid, and allowed to sit for 1 min.
4. Grid is washed three times in 500 µl of wash buffer before placing the grid to the top of the blocking buffer droplet. Grid is incubated at R.T. for 1 h.
5. After blocking, the grid is washed once with wash buffer before placing it into the primary antibody solution droplet of 200 µl. Incubate at R.T. for 1 h.
6. Rinse the grid three times with wash buffer before placing it into the secondary antibody solution droplet of 200 µl. Incubate at R.T. for 1 h.
7. After incubation, the grid is rinsed five times with ddH_2O. Pipette 7 µL of 1 % uranyl acetate on the top of the grid to stain for 1 min.
8. Samples are viewed using a JEOL 1400 transmission electron microscope (Fig. 1).

3.3 Antibody Modification and Labeling

Conjugation

1. Buffer exchange the required amount of the antibody (typically 1–5 mg) into 500 µl 0.1 M sodium phosphate buffer (pH 8.3).
2. Add a 20-fold molar excess of 1,4,7,10-Tetraazacyclododecane-*N*,*N*′,*N*″ *N*‴-tetraacetic acid (DOTA) mono-N-hydroxysuccinimide ester (DOTA-NHS) to the antibody solution and react at 4 °C for 4 h. End-over-end mixing at 4 °C may be used if conjugation yields are lower than expected.

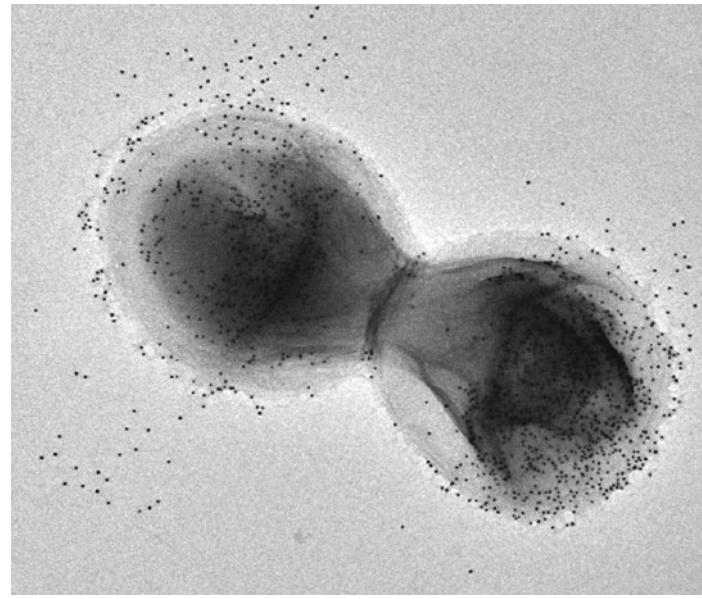

Fig. 1 Electron microscopy detection of EbpC pilin subunits on and extending from cell surface

3. Load the reaction mixture onto a Zeba desalting spin column and collect the purified immunoconjugate in PBS.
4. Aliquot the immunoconjugate and store at −80 °C until needed.

Chelator quantification

1. To calculate the average number of chelates per antibody, buffer exchange 300 pmol of immunoconjugate into 0.1 N sodium acetate buffer (pH 6).
2. Add a tenfold excess of carrier added $^{64}CuCl_2$ and incubate at 40 °C for 1 h.
3. Spot the radioactive mixture on a paper chromatography strip and develop in a glass chamber using a running buffer consisting of 0.1 M ammonium acetate buffer (pH 6) containing 50 mM EDTA.
4. The radiochemical yield of the reaction is determined using a radio-thin-layer chromatography scanner.

Radiolabeling

1. Buffer exchange 100 μg of immunoconjugate into 0.1 N sodium acetate buffer (pH 6) and add the required volume of radioactive solution.
2. Incubate the reaction at 40 °C for 1 h.

3. Quench the reaction with 3 μl of 10 mM EDTA.
4. Load the reaction mixture onto a Zeba desalting spin column and collect the purified radiotracer in PBS.
5. Determine radiochemical purity by radio-high-performance liquid chromatography with a TSK gel G3000SW (5 μm) column and a mobile phase of 90% buffer A (0.1 M sodium phosphate buffer [pH 7.3]) and 10% buffer B (CH_3CN) (isocratic) at a flow rate of 1 ml/min.

3.4 mAb Deglycosylation

To broadly disrupt FcγR / IgG Fc interactions to minimize off-target binding of the mAbs for imaging, we have previously deglycosylated the IgG Fc domain with the endoglycosidase EndoS which removes most of the N-glycan moiety from Asn^{297} of the Fc domain (*see* **Note 2**).

1. Recombinant EndoS enzyme is added to the target mAbs (unlabeled or labeled) solution (0.1–1 μg/ml in PBS) at 1 unit/μg of mAb.
2. Each reaction is incubated at 37 °C for 1 h and used directly for imaging without further purification (*see* **Note 3**).
3. Purified EndoS treated and untreated mAbs are accessed by SDS Page for molecular weight decrease of the heavy chain. Briefly, 5 μg samples are diluted with SDS sample buffer containing 2-mercaptoethanol and boiled at 95 °C for 8 min before separation in Tris-glycine gel containing 12% polyacrylamide. Proteins are stained with 1% Coomassie Blue.

3.5 Anti-EbpC Potency ELISA

1. Coating target material. Prepare recombinant antigen coating material in PBS at 0.5 μg/ml. Apply 50 μl/well to high bind ELISA plate, cover and store in a humid chamber overnight at 4 °C.
2. Nonspecific blocking. Remove coating solution by sharply inverting and flicking material into sink followed by blotting plate onto an absorbent paper towel. Dispense 200 μl/well of BLOTTO. Cover and store in a humid chamber for 1 h at room temperature (RT).
3. Application of treated and untreated mAb. Dilute both unlabeled and DOTA labeled (mock radiolabeled) mAbs in BLOTTO diluent to 10 μg/ml and serially dilute to represent maximal and minimal binding (e.g., 10–0.001 μg/ml). Number of dilutions needed is empirically determined. Wash ELISA plate three times with PBST and add 50 μl/well diluted mAb. Cover and store in a humid chamber for 1 h RT (*see* **Note 4**).
4. Application of secondary detection antibody. Dilute HRP labeled secondary antibody 1:5000 into BLOTTO diluent. Wash the

ELISA plate three times with PBST and add 50 µl/well diluted secondary antibody. Cover and store in a humid chamber for 1 h RT (*see* **Note 5**).

5. Visualization of bound secondary antibody. Freshly prepare TMB substrate. Wash ELISA plate three times with PBST and add 100 µl/well HRP substrate. Cover and store in a humid chamber for 15–30 min at RT.
6. Color development and absorbance determinations. Add 50 µl/well H2SO4, 2 N reagent and measure optical density (OD) at 450 nm using an ELISA plate reader. Plot absorbance values on Y-axis vs concentrations on X-axis. Compare treated and untreated mAb values. See the example figure below (Fig. 2).

3.6 Rat Endocarditis Model

This model is part of a protocol approved by the Animal Welfare Committee, University of Texas Health Science Center at Houston, Houston, TX, USA.

3.7 Animal Acclimatization

Animals are acclimatized (Sprague–Dawley rats, ~200 g) for ≥72 h prior to any manipulation.

3.8 Surgery Preparations

1. Catheters (PE10; inside and outside diameters, 0.28 and 0.61 mm, respectively) are gas sterilized and surgical instruments are autoclaved.

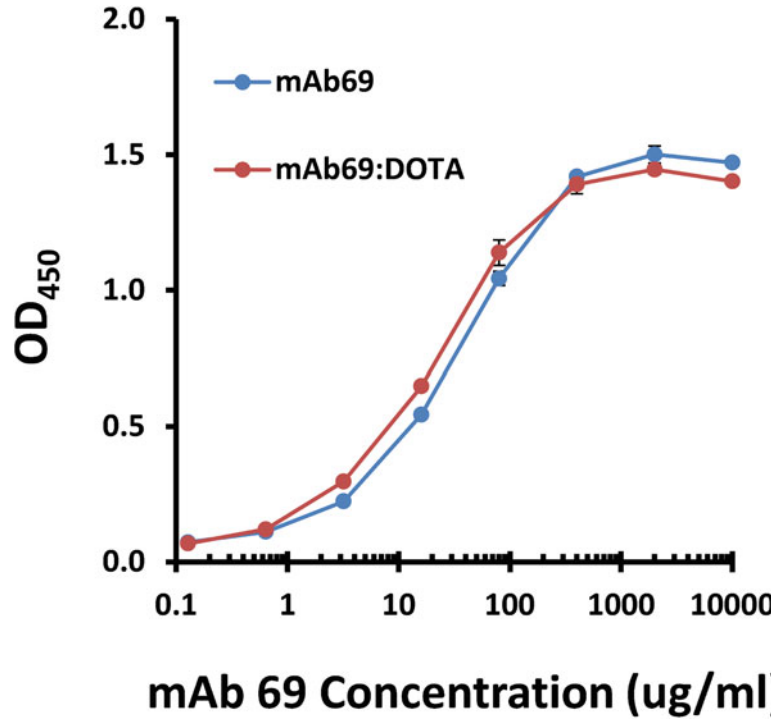

Fig. 2 Primary binding ELISA to confirm that addition of DOTA and conditions utilized for radiolabeling have minimal effect on binding affinity of mAb

2. Surface sterilize surgery station using 70% alcohol spray and instrument trays and a dry glass bead sterilizer Germinator 500 (Braintree Scientific) for instrument sterilization in between surgeries (*see* **Note 6**).

3.9 Presurgery Preparation of Rats

1. Place rat singly in an anesthetic chamber and expose to isoflurane (2.5–4%) mixed with oxygen until effective.
2. Remove anesthetized rat from the chamber and place onto a surgical table in the dorsal position and place its nose into the nose cone to supply anesthesia (*see* **Note 7**).

3.10 Catheter Placement

1. Gently wipe the surgical area using 70% alcohol. Inject Marcaine (0.25%, <1 ml/kg) around the site of surgery area.
2. Place two rolled sterile 4×4 gauze under neck to slightly hyperextend for better exposure. Make a 1.5–2 cm ventral cervical skin incision right of the midline of the neck using a sterile scalpel.

3.11 Carotid Artery (Left) Catheterization

1. Using scissors, dissect the omohyoid muscle longitudinally to slightly expose the left carotid artery and carefully isolate a 4–5 mm section of the vessel. Make sure to separate the vagus nerve (white color) completely from the artery using forceps.
2. Using 4–0 SOFSILK suture, loosely tie the caudal end of the vessel, tie off the cranial end, and place a bulldog clamp caudally above the loosely tied suture to prevent the blood flow following the incision. Using Vannas scissors (8 cm), make an incision in the vessel between the two ligatures. Insert the arterial catheter and advance to ~4 cm across the aortic valve into the left ventricle using forceps.
3. When the catheter is inside the vessel, assure proper positioning by feeling the resistance and vigorous pulsation of the line, indicating the catheter is in the heart. Tie the loose caudal ligature around the inserted catheter in vessel to secure in place.
4. Inoculum preparation. Grow *E. faecalis* bacteria at 37 °C for ~14 h, gentle shaking in brain heart infusion broth (Sigma) plus 40% horse serum (BHIS) for inoculum preparation. Harvest the cells at 10,000×*g* for 10 min and suspend them in prechilled, sterile, 0.9% saline until ready for inoculation. Determine the bacterial OD_{600} and CFU/ml count each time (*see* **Note 8**).
5. Animal Inoculation. Fifteen minutes after catheter placement, administer $\geq 1 \times 10^7$ CFU/rat of *E. faecalis* (mixed in chilled 0.9% saline) to 2 of 3 groups. To group (1), administer radiolabeled mAb 69 against EbpC and for group (2) a radiolabeled non-Ebp control mAb that demonstrates no reactivity to *E. faecalis* surface antigens. For group (3), administer each agent to catheterized but noninfected rat to serve as control

for binding to the catheter or the site of catheter damage. Immediately after bacteria inoculation, heat seal the catheter using a glue gun containing preinserted glue stick, let the glue solidify and then move the sealed catheter underneath the surrounding tissue/skin and close the surgical wound with non-absorbable sutures.

3.12 Post-Surgery Animal Care

1. Immediately after catheterization, bacteria inoculation, and suturing the incision site, remove anesthesia and move animal to recover in a chamber connected with uninterrupted oxygen flow.
2. Wait until the animal regains full consciousness and begin grooming and eating solid food pellets available in a recovery chamber.
3. Return the animal to its cage once it is able to move around. Observe daily.

3.13 Euthanasia

1. After the imaging process, euthanize rats by CO_2 inhalation in a chamber connected with CO_2 flow.
2. After euthanasia, remove hearts aseptically from each animal and place in a sterile petri dish for further examination/manipulation. Further tissue manipulation should be carried out in a biosafety hood.
3. Excise aortic valve containing vegetation using sterile forceps and scissor and place the excised tissue in pre-weighed sterile Eppendorf tubes. Weigh the tubes again to determine the weight of aortic valve containing vegetation.
4. Transfer the tissue in a sterile glass homogenizer tube, and homogenize (manually or using automated system) in 1 ml of sterile 0.9% saline.
5. Prepare serial dilutions of tissue homogenate and plate in entirety (~1 ml each) onto Enterococcosel agar (Difco Laboratories) supplemented with desired antibiotic for the selection of inoculated *E. faecalis* strain.
6. Rats with sterile cultures of undiluted vegetation homogenates (~1 ml) should be considered to have had no induction of endocarditis. The CFU/g of tissue can be calculated based on recovered colonies/dilution.

3.14 Imaging and Image Analysis

1. Injection of imaging agent. Under 1% isoflurane anesthesia, tail vein injection of rats with and without endocarditis infection is injected with 40 μg of radiolabeled mAb in 0.5 ml of solution. The dose represents between 5 and 8 MBq of radioactivity, which is measured at the time of injection. Animals are allowed to recover and returned to housing.
2. μPET/CT imaging. Approximately 24 h after imaging agent administration, rats are anesthetized with 1% isoflurane anesthesia. Animals are then imaged using an ungated protocol

with deadtime and decay correlation performed during data acquisition. A total of approximately one million counts are registered. In our studies a Siemens mPET/CT Inveon scanner was employed.

3. Imaging Analysis and Quantification of %ID/g. Using Inveon and Workplace software normalization, attenuation, and scatter correction are performed and a 3D reconstruction algorithm such as (3D-OSEM or 3D MAP) is used to reconstruct images. An updated calibration curve is used to convert photon counts into kBq/cc, again using scanner and processing software. From the reconstructed image, a region of interest (ROI) is selected that corresponds to the infection site. The total activity in the ROI is divided by the decay-corrected activity injected in the animal (as measured at the time of injection in **step 1**) to determine the %ID/g associated with the targeted agent in the infection site.
4. The values of %ID/g can be later correlated to the CFU measured after animal sacrifice, determined in Subheading 3.6.

4 Notes

1. Surface display of some bacterial antigens is growth phase dependent [10]. It is thus important to evaluate different growth phases in vitro to maximize labeling, with the caveat that this may not always accurately reflect in vivo, surface expression conditions.
2. The effect of deglycosylation on antibody interaction with various immune cells expressing FcγRs will depend on the isotype of the mAb used. Deglycosylation of murine IgG2a, or human IgG1 Fc that binds strongly to their respective FcγRIs, significantly decreases affinity of this interaction. The benefit of EndoS treatment of other subtypes may not be as significant, and must be determined individually. In addition, recent work has demonstrated that complete Fc deglycosylation, by recombinant modification or through PNGase F treatment, could be even more effective in preventing unwanted Fc/FcγR interactions [11].
3. It is important to determine the stabilities of the mAbs (especially labeled mAbs) under this experimental procedure. In our experience, the affinity of the mAb to target antigen did not change before and after DOTA labeling as monitored by ELISA.
4. Experiments involving in vivo imaging should include an isotype matched control mAb manufactured in a similar fashion as test mAb. For these experiments an isotype matched control (murine IgG1) was used (data not shown). Care must be taken to assure treatment of all mAbs (control and test) does not

significantly affect protein binding and overall integrity, which in some cases could lead to uninterpretable or misleading data. Additional test to consider includes SDS-PAGE or size exclusion chromatography under native conditions.

5. For these experiments a secondary polyclonal anti-IgG (Fc) antibody was used. Additional reagents to consider would include anti-Light chain (e.g., kappa chain) or anti-F(ab′)2. This would be considered if antibody fragments are to be used or if the antibody Fc region is non-accessible. Other considerations would be to directly label mAb (intact or fragments) with either biotin or HRP. Many commercially available kits of this type are readily available.
6. Surgeons should wear a cap and sterile gown when there are surgical procedures with increased risk for clinical infection. Such cases are when (1) the animal is immunosuppressed, (2) a substantial incision is made and underlying tissues are exposed, (3) the surgical site is exposed for a prolonged period of time, (4) there is significant tissue injury, and/or (5) if biohazardous agents are being used. Surgeons should wash their hands with a disinfectant scrub and dry their hands prior to gloving. Sterile surgeon's gloves must be used. Once gloved, care must be taken to only touch the sterile operative field and equipment.
7. Adequate depth of general anesthesia has been achieved when the animal (1) is breathing regularly and effectively (has pink ears and mucous membranes), (2) does not withdraw its foot when its toes are pinched, and (3) does not blink when the eye or eyelid is touched. Anesthetic gas vaporizer calibration should be performed as recommended by the manufacturer of the anesthetic machine. The interval recommended for servicing by the manufacturer varies with the model but most require calibration checks annually.
8. BHIS grown cells clump and it is important to vortex them vigorously prior to OD_{600} determination of serial dilution preparations for CFU/ml count.

References

1. Lerche CJ et al (2015) Low efficacy of tobramycin in experimental Staphylococcus aureus endocarditis. Eur J Clin Microbiol Infect Dis 34(12):2349–2357
2. Hanses F et al (2014) Staphylococcus aureus gene expression in a rat model of infective endocarditis. Genome Med 6(10):93
3. Jung CJ et al (2009) Streptococcus mutans autolysin AtlA is a fibronectin-binding protein and contributes to bacterial survival in the bloodstream and virulence for infective endocarditis. Mol Microbiol 74(4):888–902
4. Entenza JM et al (2005) Therapeutic effects of bacteriophage Cpl-1 lysin against Streptococcus pneumoniae endocarditis in rats. Antimicrob Agents Chemother 49(11):4789–4792
5. Strohl WR (2009) Optimization of Fc-mediated effector functions of monoclonal antibodies. Curr Opin Biotechnol 20(6):685–691

6. Cao Y et al (2012) Single-chain antibody-based immunotoxins targeting Her2/neu: design optimization and impact of affinity on antitumor efficacy and off-target toxicity. Mol Cancer Ther 11(1):143–153
7. Hall MA et al (2012) Comparison of mAbs targeting epithelial cell adhesion molecule for the detection of prostate cancer lymph node metastases with multimodal contrast agents: quantitative small-animal PET/CT and NIRF. J Nucl Med 53(9):1427–1437
8. Gao P et al (2015) Deglycosylation of mAb by EndoS for improved molecular imaging. Mol Imaging Biol 17(2):195–203
9. Gao P et al (2010) Enterococcus faecalis rnjB is required for pilin gene expression and biofilm formation. J Bacteriol 192(20):5489–5498
10. Pinkston KL et al (2011) The Fsr quorum-sensing system of Enterococcus faecalis modulates surface display of the collagen-binding MSCRAMM Ace through regulation of gelE. J Bacteriol 193(17):4317–4325
11. Kao D et al (2015) A Monosaccharide residue is sufficient to maintain mouse and human IgG subclass activity and directs IgG effector functions to cellular Fc receptors. Cell Rep 13(11):2376–2385

Part V

Models for Studying Bacterial Pathogenesis

Chapter 16

The Zebrafish as a Model for Human Bacterial Infections

Melody N. Neely

Abstract

The development of the zebrafish (*Danio rerio*) infectious disease model has provided new insights and information into pathogenesis. Many of these new discoveries would not have been possible using a typical mammalian model. The advantages of using this model are many and in the last 15 years the model has been exploited for the analysis of many different pathogens. Here, we describe in detail how to perform a bacterial infection using either the adult zebrafish or zebrafish larvae using microinjection. Multiple methods of analysis are described that can be used to address specific questions pertaining to disease progression and the interactions with the immune system.

Key words Zebrafish, Infection, Histology, Streptococcus infection, Microinjection, Animal model, Pathogenesis

1 Introduction

Animal models have been hugely instrumental in providing new information about infectious disease mechanisms and the specific virulence genes required. In addition, many mechanisms of how the host immune system responds to the invading pathogens have been elucidated. Previously, mammalian model hosts from nonhuman primates to mammalian rodent models have successfully filled this role. However, many animal models are too expensive, too difficult to maintain, or, most importantly, do not reliably mimic the disease characteristics or clinical syndromes that are observed during human infections. Unfortunately, there is no perfect model organism for analysis of every human pathogen or for addressing every virulence question. This dilemma has spurred the development of new model hosts for analysis of infectious disease. Which model works best for a particular pathogen needs to be determined experimentally.

In the past 15 years, zebrafish have become a tremendously popular model for the study of infectious diseases, with *Mycobacterium* (*see* refs. [1–7] for review and citations within) and *Streptococcus* [8–14] being the first pathogens to be analyzed in

Pontus Nordenfelt and Mattias Collin (eds.), *Bacterial Pathogenesis: Methods and Protocols*, Methods in Molecular Biology, vol. 1535, DOI 10.1007/978-1-4939-6673-8_16,

this model. Importantly, the disease characteristics observed in the zebrafish from infection with these pathogens closely mimic those observed in human infections. There are many reasons for using the zebrafish, including their small size, low cost, easy maintenance, prolific breeding capacity resulting in large numbers of progeny and ex vivo embryo development. Furthermore, there is high conservation between human and zebrafish immune systems, which includes both innate and adaptive immunity, which is not found in smaller invertebrate systems [15–21]. This allows us to directly address host-pathogen interactions that occur during infections that can be related directly to human disease.

Multiple life stages have been utilized in the zebrafish model to ask specific questions relating to the immune response. While the innate immune system is active within 24 h postfertilization in zebrafish, the adaptive immune system is not completely developed until 3–4 weeks later [14, 18, 22]. This difference in immunity development can be exploited to determine important differences that are required by the immune system for fighting specific infections. In addition, the transparency of the zebrafish larvae for the first week of life allows visualization of bacterial dissemination during an infection using labeled bacteria in real time in a live organism. The use of zebrafish larvae that have fluorescence-expressing immune cells [23, 24] provides another layer of unique information by allowing visualization of direct interactions between the immune system and bacteria in real time [9, 24–29].

Detailed below are protocols for infecting adult zebrafish and zebrafish larvae using streptococcal pathogens. We describe the culture growth conditions and a detailed setup for adult infections and multiple techniques for analyzing infection over time. Bacterial dissemination allows analysis of the ability of the organism to spread to other tissues, which is particularly useful when comparing the wild-type strain to an avirulent mutant strain. Cytospin preparations allow the visualization of the interactions of the bacteria with specific cells of the immune system. Histological preparations of whole infected fish allow observation of the bacteria in various organs, as well as the infiltration of host immune cells and any tissue damage that may have occurred. The protocols for infection of zebrafish larvae include the breeding of embryos and complete setup for microinjections. One of the major advantages in doing larval infections is the optical transparency of the larvae at this stage, allowing visualization of labeled bacteria in a live animal in real time using fluorescence microscopy. Measuring total colonization is a useful technique to determine the overall fitness of a bacterial mutant compared to the wild-type strain in vivo. While the wild-type strain will multiply over time, eventually ending in death of the larvae, the mutant strains may actually be cleared or will show much lower colonization than the wild-type strain. This provides a great deal of information on what genes are required for growth/persistence in vivo.

2 Materials

All reagents should be made with ultrapure double distilled water (ddH_2O) unless stated otherwise. Store all reagents at room temperature unless stated otherwise.

1. Infection water: reverse osmosis treated water (RO water) with 60 mg/l Instant Ocean aquarium salts. Autoclave.
2. Todd-Hewitt Yeast Broth (THY B): 30 g Todd Hewitt media, 1 g yeast extract. Bring to 1 l with ddH_2O. Stir until completely dissolved. Pour 100 ml into 125 ml bottles. Autoclave.
3. Todd-Hewitt Yeast Agar (THY A): 30 g Todd Hewitt media, 1 g yeast extract, 14 g high quality agar. Bring to 1 l with ddH_2O. Autoclave. Cool and add appropriate antibiotics and pour into petri dishes.
4. Tricaine (3-amino benzoic acidethylester): For stock solution, add 97.9 ml of ddH_2O to 400 mg Tricaine powder and 2.1 ml 1 M Tris–base (pH 9). Adjust to pH ~7. Filter sterilize and store a 4 °C. To use as an anesthetic (168 μg/ml), add 4.2 ml Tricaine stock solution to 95.8 ml infection water. Place in a 250 ml glass beaker.

   To use for euthanization (336 μg/ml), add 8.4 ml Triciane stock solution to 91.6 ml infection water (*see* **Note 1**).
5. Dissecting board: we use a 13″ × 11″ high-density polyethylene board (Richard-Allan Scientific).
6. Petri dishes, sterile (100 mm × 15 mm).
7. 70% ethanol in a washing/dispensing bottle.
8. 6.25 in. hemostat.
9. Padded gauze tape (*see* **Note 2**).
10. 400 ml glass beakers.
11. Colored masking tape.
12. Plastic inserts from pipet tip boxes to use as “lids.”
13. Disposable 3/10 cc U-100 ultrafine insulin syringe with a 0.5 in., 29-gauge needle (Becton Dicknson).
14. Portable fish tank (we use 11″ plastic mouse cages with a perforated lid).
15. Disposable plastic spoons.
16. Styrofoam board (*see* **Note 3**).
17. Sterile dissecting scissors, scalpel, forceps.
18. Microcentrifuge tubes.
19. Mini pellet pestle homogenizer (Kimble Kontes Pellet Pestle cordless homogenizer).
20. Sterile pellet pestles to fit 1.5 ml microcentrifuge tubes.

21. Sterile phosphate buffered saline (PBS).
22. 26-gauge needles.
23. 1 ml syringes.
24. Single CytoSep cytology funnels (Simport Scientific).
25. Acid-alcohol wash for slides: 8 ml concentrated HCl added to 1 l 70% ETOH. Slides should be washed in acid-alcohol solution for at least 1 h. Rinse in ddH_2O three times at 5 min each rinse.
26. Glass microscope slides.
27. PROTOCOL Hema 3 staining set (Fisher).
28. Dietrich Fixative: 150 ml 95% ETOH, 10 ml glacial acetic acid, 185 ml 37% formaldehyde, 155 ml water.
29. 100% ethanol for histology.
30. Clearify Clearing Agent (American MasterTech).
31. Histosette II tissue cassette (15-182-701A).
32. Histo Base mold 37 × 24 × 5 mm (15-182-505E).
33. Surgipath Tissue infiltration medium.
34. Surgipath Formula R paraffin.
35. Dawn dish detergent.
36. Hematoxylin.
37. Eosin.
38. Permount mounting medium.
39. Zebrafish breeding tank.
40. 0.1% Methylene Blue: 1.0 g Methylene Blue, 1 l ddH_2O. Mix well.
41. Embryo water: RO treated water, 60 mg/l Instant Ocean, 200 μl/l methylene blue.
42. Dumont fine tip tweezers (we use either #55 or #4).
43. 10% Phenol red.
44. Three inch thinwall glass capillary tubes, size 1.00 OD/0.75 ID (Item # TW100-3, World Precision Instruments).
45. Microloader pipet tips (Eppendorf # 5242 956.003).
46. Calibration millimeter glass slide.
47. 3% methylcellulose: Add 3 g of methyl cellulose to 50 ml water that has been heated to ~80 °C. Stir with magnetic stir bar until all methylcellulose is wetted. Add 50 ml of cold water and place at 4 °C at least 3 h with stirring or overnight. Let sit at 4 °C (without stirring) until all bubbles dissipate and solution becomes translucent. Store at 4 °C and warm to room temperature before using.
48. Microscope slides with a concave well.

3 Methods

These methods detail performing infections with *Streptococcus pyogenes*, but can be adapted to any bacteria. The methods assume that you have adult zebrafish available from a breeding facility. Methods for breeding, rearing, and maintaining a zebrafish facility have been published previously [30].

3.1 Adult Zebrafish Infections

3.1.1 Preparing Cultures for Adult Zebrafish Infections

1. Set up cultures in 10 ml THY B with appropriate antibiotics in a 15 ml conical tube sealed with a screw cap and incubate at 37 °C overnight without shaking.
2. Next morning dilute overnight cultures 1:100 into fresh THY B with appropriate antibiotics and incubate as described above.
3. Grow at 37 °C to mid-log phase. For *S. pyogenes* this is $OD_{600} \sim 0.300$ (1×10^8 cfu/ml). Grow all cultures so that final OD_{600} is over 0.300, but not over 0.600 (*see* **Note 1**).
4. Adjust all cultures to the same OD_{600} by dilution in 1 ml media in a micro-centrifuge tube (*see* **Note 2**).
5. Make dilutions from this tube for the appropriate concentrations(s) for injection in labeled 1 ml tubes and put on ice. Keep in mind that you will be injecting only 10 μl into the fish, meaning that a 10 μl injection of a culture of 1×10^8 cfu/ml will result in a 1×10^6 cfu injection.
6. Make serial dilutions of all cultures for subsequent plating on a THY agar (THY A) + antibiotic plate to confirm the actual injection dose. Incubate the streptococcus plates either in a 37 °C CO_2 incubator overnight or use a GASPAK jar with the appropriate GAS pak media in a 37 °C air incubator.

3.1.2 Setting Up for Injections

1. Using ETOH squeeze bottle, clean dissection board. Fill the bottom of a sterile petri dish (larger half) with infection water and place on one corner of the board.
2. Place two petri dish lids (side by side) right side up on board and cover with Kim-wipe and wet lightly with infection water.
3. Wrap teeth of a hemostat with gauze tape and wet by dipping in water-filled petri dish. Position wrapped hemostat on petri dishes with the jaws slightly open so that it creates a padded "cradle" to hold anesthetized fish (*see* Fig. 1).
4. Freshly prepare two Tricaine solutions in 250 ml glass beakers, one for anesthetizing (168 μg/ml) and one for euthanizing (336 μg/ml) and place next to injection stage setup (*see* **Note 3**).
5. Place ~225 ml infection water into 400 ml beakers and label appropriately (strain, dose, injection route, date) with masking tape. Set up as many beakers as there are infection conditions being sure to include both a positive control (WT strain, dose)

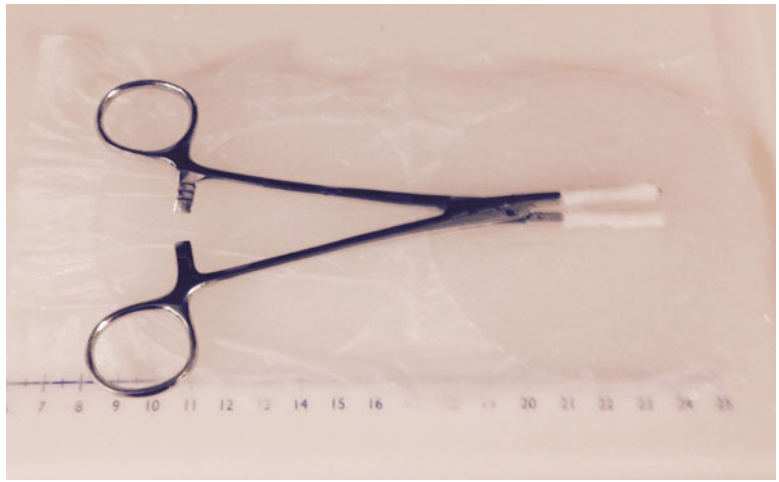

Fig. 1 Injection stage for adult zebrafish. Hemostat with padded-gauze tape wrapped around teeth of the jaws to make a "cradle" for holding the anesthetized adult zebrafish. The hemostat is placed on top of two petri dish lids with a wet kim wipe on top

and a negative control (sterile media injection). Tape one side of a perforated top (we use pipet tip box inserts) over the beaker to prevent fish from jumping out (*see* **Note 4**) (Fig. 2).

6. Use a separate syringe for each dilution and strain. Fill syringes by pulling up from the micro-centrifuge tube of the correct dose, label syringe, and set aside. Do not recap syringes. You can use the needle caps to place under the syringe to prop up the needle so that it does not touch the board and remains sterile (*see* **Note 5**).

3.1.3 Retrieving Fish for Infections

1. Fish should not be fed within 24 h of injection. Fish should also not be fed during the course of the infection (*see* **Note 6**).
2. Fill portable tanks with water directly from the tank from which the fish will be taken (Fig. 3).
3. For adult fish injections, we use fish that are 6–9 months old. All fish should be the same age, preferably born on the same day or within a few days of each other. Remove the correct number of fish from the fish facility and take to the lab for experiments no earlier than 1 h before injections are to commence (*see* **Note 7**).
4. Place portable tank with fish in a 28 °C glass front incubator in laboratory until ready to inject to maintain water temperature and decrease stress on fish.
5. Once fish leave the fish facility, they should not be returned. Therefore, only take the number of fish you will need for the entire experiment.

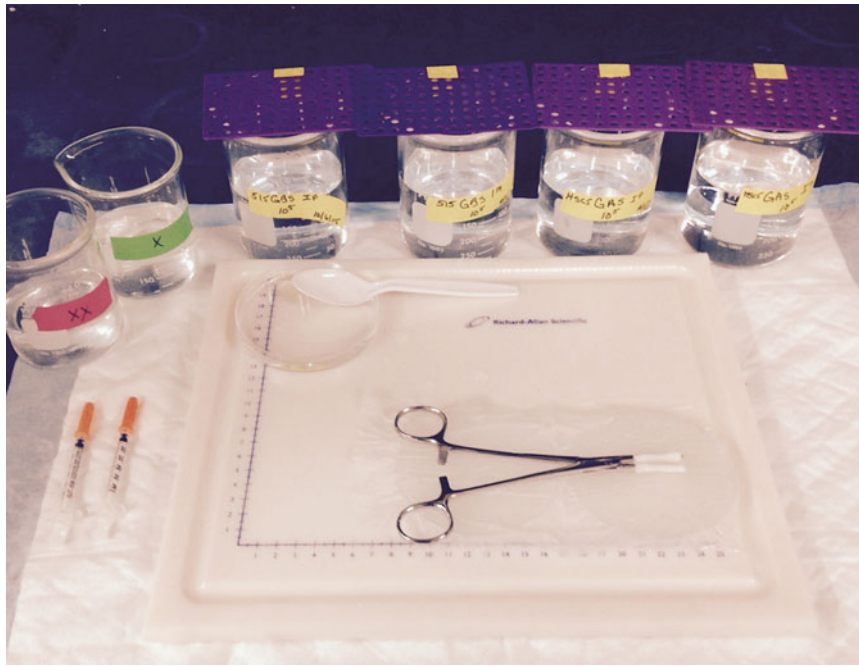

Fig. 2 Assembled materials for injection of adult zebrafish. Setup for injecting adult zebrafish includes labeled beakers with lids filled with infection water for injected zebrafish, an anesthetizing dose of Tricaine and a euthanizing dose of Tricaine, syringes, plastic spoon for handling anesthetized zebrafish, petri dish of water for rinsing zebrafish and injection stage with hemostat

3.1.4 Injection of Adult Zebrafish

1. Using a small fish net, capture 3–4 zebrafish from the portable fish tank and gently place into the beaker holding 168 μg/ml of Tricaine (anesthetizing dose). Keep fish in Tricaine solution for a maximum of 3 min. A fish is anesthetized when it is laying on its side and gill movement stops (*see* **Note 8**).
2. After a fish is anesthetized, use a plastic spoon to remove from the Tricaine solution and briefly dip in the petri dish with injection water before placing on the "cradle" of the hemostat. This washes off any residual Tricaine and allows faster recovery postinjection (refer to Fig. 2).
3. Intraperitoneal (IP) injection involves injecting into the intraperitoneal space on the ventral side of the fish. To do this, position the anesthetized fish upside down on the "cradle" of the hemostat with the head pointing toward the hemostat hinge.
4. Inject directly between and slightly behind (toward the tail) the anal fins, being careful to keep the needle horizontal so as to not pierce any organs (*see* **Note 9**).
5. The needle is inserted into the peritoneal cavity and held in place using the right hand. The syringe plunger is then depressed with the left hand, so that the fingers are not in the

Fig. 3 Portable fish tank. Fish are retrieved from the fish facility and taken to the laboratory for injections using a portable tank with lid. A small net will be needed for removing fish from the tank and placing into anesthesia

vicinity of the needle when the culture is injected into the fish. This procedure minimizes the possibility of accidental needle stick of lab personnel.

6. Intramuscular (IM) injection involves injection directly into the dorsal muscle. To do this, set the anesthetized fish on the hemostat "cradle" dorsal side up with the head of the fish pointing toward the hinge of the hemostat.
7. Locate the dorsal fin on the top of the fish and place the needle directly below (~1/8″) and slightly forward of the dorsal fin. Angle the needle so that it goes toward the front of the fish at an approximately 45° angle. This allows injection only into the thick region of muscle and not into the spinal cord area. Inject very slowly and leave the needle in place for a second or two after injection to avoid leakage from the injection site (*see* **Note 10**).
8. Immediately after injection, using the plastic spoon, gently place the injected fish into the appropriately labeled beaker and close the lid.
9. Check on the injected fish after 30–60 s to make sure that the fish has recovered from the anesthesia and is swimming normally. If the fish does not recover within 2 min or is swimming erratically, the fish should be removed and euthanized by placing in the 336 μg/ml Tricaine beaker.

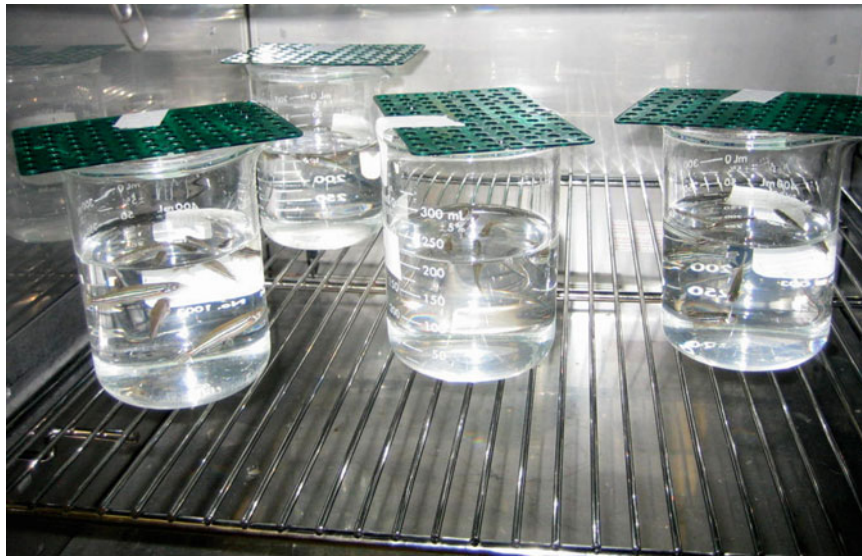

Fig. 4 Incubation of injected zebrafish. Once injected zebrafish have recovered in the labeled glass beakers, they are placed in a glass front incubator at ~28 °C for observation

10. A typical injection will have six zebrafish per beaker (all replicates of the same treatment, i.e., same dose, strain, injection method). The only exception would be the negative control (media only injection) in which we only use four fish per beaker. We repeat this entire setup three times on different days for a total of 18 fish per dose/strain.
11. After all the fish in a beaker have recovered, place the covered beaker in a glass front incubator at 27°–28 °C for observation (*see* **Note 11**) (Fig. 4).
12. Place disposable needle in a sharps container. Do not recap needle.

3.1.5 Methods for Analysis of Adult Zebrafish Infection

Dissemination

1. To determine the spread of infection at specific time points postinfection, euthanize fish by placing in 336 μg/ml Tricaine for 25 min (*see* **Note 12**).
2. Set up microcentrifuge tubes with 200 μl sterile PBS and label appropriately. Typically, the spleen, heart, and brain are removed for analysis.
3. Use a small piece of styrofoam board (~2″ × 2″) and sterile dissecting pins. Wipe styrofoam with 70% ETOH. Have a 250 ml beaker with 95% ETOH and a Bunsen burner available nearby. Place the euthanized zebrafish on the styrofoam with the ventral side facing up. Place one pin through the lower jaw into the board and a second pin through the tissue adjacent to the tail. Using a sterile scalpel, make a shallow incision from the gills to the anal fins. Using sterile dissecting scissors, cut through the gill cartilage being careful not to pierce the heart. Make four

cuts with the scissors perpendicular to the original incision at the top and the bottom of the incision, creating a sideways "H." Pin open the incision by placing pins in the two flaps that you created with the scissors. One can easily visualize the spleen (bright red) and heart (directly between the gills) once the cavity has been opened. Aseptically remove organs with sterile forceps and immediately place into 200 µl PBS in a microcentrifuge tube and place on ice. Place the utensils into the beaker with ETOH.

4. To remove the brain, turn the dissected fish over and replace pins into the jaw cartilage and the tail section from the dorsal side. Use a cotton swab dipped in ETOH to swab the top of the fish head. Remove the scalpel from the ETOH and briefly pass through the Bunsen burner. Place the blade of the scalpel at the base of the head. You should feel a small hard ridge. By hooking the scalpel under this ridge and scraping/lifting forward (toward the mouth) one can expose the brain cavity. Using the forceps that have been in ETOH and passed through the Bunsen burner, carefully pull out the brain tissue and place into 200 µl PBS and place on ice (*see* **Note 13**).
5. Disassociate the tissue using a hand-held homogenizer and a sterile disposable pestle in the microcentrifuge tube.
6. The homogenate is then vortexed and centrifuged and the supernatant is serially diluted and plated on selective media to determine the concentration of bacteria per organ at a specific time point postinjection (*see* **Note 14**).

Cytospin Preparations

1. Euthanize fish by placing in 340 µg/ml Tricaine for 25 min.
2. Dissect desired organs and place in 200 µl of PBS in a microcentrifuge tube as described above for dissemination.
3. For spleens, hearts and brains, vortex briefly, then pass through a 26-gauge needle on a 1 ml syringe.
4. Dilute to 600 µl with PBS.
5. Use 300 µl for the cytospin funnel and 100 µl for serial dilution and plating on selective media.
6. Label microscope slides with tissue sample and place with an empty cytospin funnel in the special clips in the Shandon Cytospin centrifuge. Then place 300 µl into the appropriate funnel while they are in the centrifuge. This keeps the tissue sample from spilling or smearing the slide while placing it in the centrifuge.
7. Set the Shandon Cytospin Centrifuge at 700 RPM for 3 min.
8. Carefully remove funnel and slide from the centrifuge, being careful to not smear the sample on the slide.

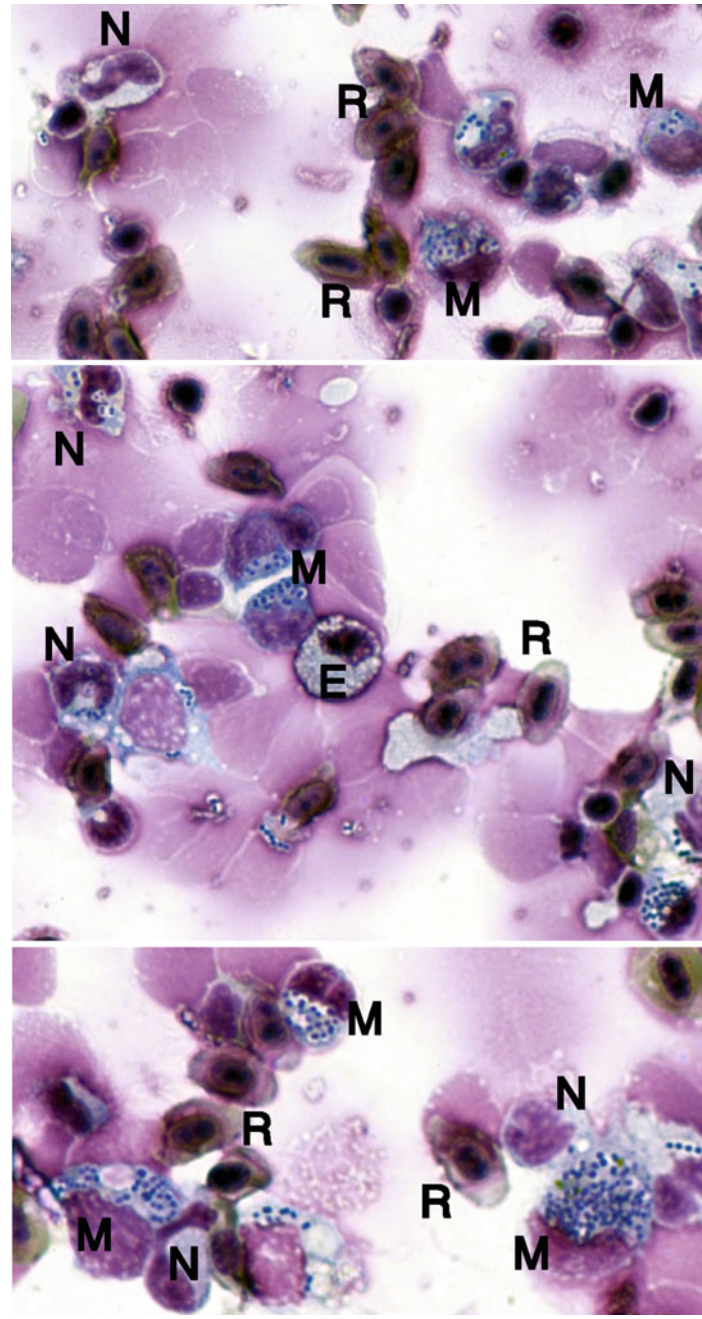

Fig. 5 Micrographs of stained cytospin preparations. Cytospins are from homogenized spleens at 3 h post IM injection of *Streptococcus iniae*. E = eosinophil, M = macrophage, N = neutrophil, R = red blood cell

9. Immediately stain the slides using a modified Wright-Giemsa staining method. We use the PROTOCOL Hema-3 set, which is a 30 s, 3-step technique. Allow slides to dry, mount a cover slip with Permount media, and then view under light microscopy (*see* **Note 15**) (Fig. 5).

Histology—Fixation and Paraffin Embedding

1. Euthanize infected zebrafish as above. Using a sterile scalpel, remove the tail end of fish just behind the anal fins and discard. Immediately place fish body in 10 ml Dietrich's fixative in a 15 ml plug-seal screw cap centrifuge tube and place on a rocker for 24–48 h.
2. Drain fixative and add 50% ETOH for 1 h.
3. Drain and add 70% ETOH for 1 h.
4. Drain and add 95% ETOH for 1 h.
5. Drain and add fresh 95% ETOH for 1 h.
6. Drain and add 100% ETOH for at least 2 h.
7. Drain and add Clearify (Master Tech) overnight (*see* **Note 16**).
8. Drain. Put fish body into a labeled plastic histology tissue cassette. Add to 60 °C paraffin. Incubate in a 60°–64 °C water bath for at least 1 h. We use Surgipath Tissue infiltration medium for this step.
9. Change paraffin and incubate in 60°–64 °C water bath at least overnight (over the weekend is best).
10. Place fish in metal base mold with the head pointing to the right side so that the injection site (left side of fish) will be toward the outside of the block (which is now the bottom of the base mold). Place the cassette over the fish with the label on the right side (same side as head). Place the cassette on a 60 °C heat block to keep warm. Add melted 60 °C paraffin until the cassette is covered. Gently remove base and cassette to an ice block to cool. We use Surgipath Formula R paraffin at this step. Do not use infiltration medium for this step.
11. Before sectioning, remove cassette from the metal base. This will expose the side to be sectioned. Soak the paraffin block in water with dish detergent (we use Dawn) to hydrate for 20 min.
12. Remove sections to shallow container with cold water.
13. Cut block at 10 microns until reaching the region of interest, then section at 2–5 microns. Float paraffin ribbon in a 50°–55 °C water bath with gelatin added to the surface.
14. Dip acid-alcohol washed slide under section in the water bath and slowly pick up. Allow slide to dry.

Histology—Deparaffinization and Staining

1. Place slide in Clearify for 15 min.
2. Place in fresh Clearify for another 15 min.
3. Place in 100% ETOH for 2 min.
4. Repeat **step 3**.
5. Place in 95% ETOH for 2 min.
6. Place in 70% ETOH for 2 min.

7. Place in 50% ETOH for 2 min.
8. Place in 30% ETOH for 2 min.
9. Place in PBS for 5 min.
10. Place in hematoxylin for 6 min (*see* **Note 17**).
11. Pass through slowly running tap water 3–5 times.
12. Place in distilled water for 2 min.
13. Dip slide into 80% ETOH 10–15 times.
14. Place in Eosin for 1 min.
15. Dip slide in 95% ETOH 10–15 times.
16. Using fresh 95% ETOH, repeat **step 15**.
17. Dip slide in 100% ETOH 10–15 times.
18. Using fresh 100% ETOH, repeat **step 17**.
19. Place in Clearify for 1 min.
20. Place in fresh Clearify for 1 min.
21. Leave slide in fresh Clearify until ready to be cover slipped. Cover slip with Permount (*see* Fig. 6).

3.2 Zebrafish Larvae Infections

3.2.1 Breeding of Zebrafish Larvae for Infections

1. We use yolk sac injections to analyze overall infection, dissemination, and host immune interactions in zebrafish larvae. We also use otic vesicle injections to visualize interactions with specific immune cells of the host. An excellent reference for otic vesicle injections can be found at [31].
2. For yolk sac injections, we use larvae that are 48 h postfertilization (hpf).
3. To breed zebrafish, late in the day, set up breeding pairs in small breeding tanks. These tanks have a smaller tank with a perforated bottom set into a larger tank. A clear plexi-glass divider placed in the middle of the tank separates the male and female adult fish. Place these tanks with the adult fish in the dark by covering with a cardboard box or plastic cover.
4. Next morning, expose the tanks to light and remove dividers between male and female fish. The fish should start breeding within 20–30 min.
5. After approximately 2–3 h, remove adult fish by pulling out the top tank and place the adult zebrafish back into aquariums. The embryos will have fallen through the perforated bottom into the second larger tank. Gently collect embryos by pouring into a fine metal mesh strainer. Rinse embryos in the strainer very gently using a squeeze bottle with embryo water.
6. Place embryos into a plastic petri dish in embryo water and immediately examine under a dissecting scope. Remove any nonfertilized eggs and debris left by adult fish (nonfertilized embryos will be opaque as opposed to transparent). Petri

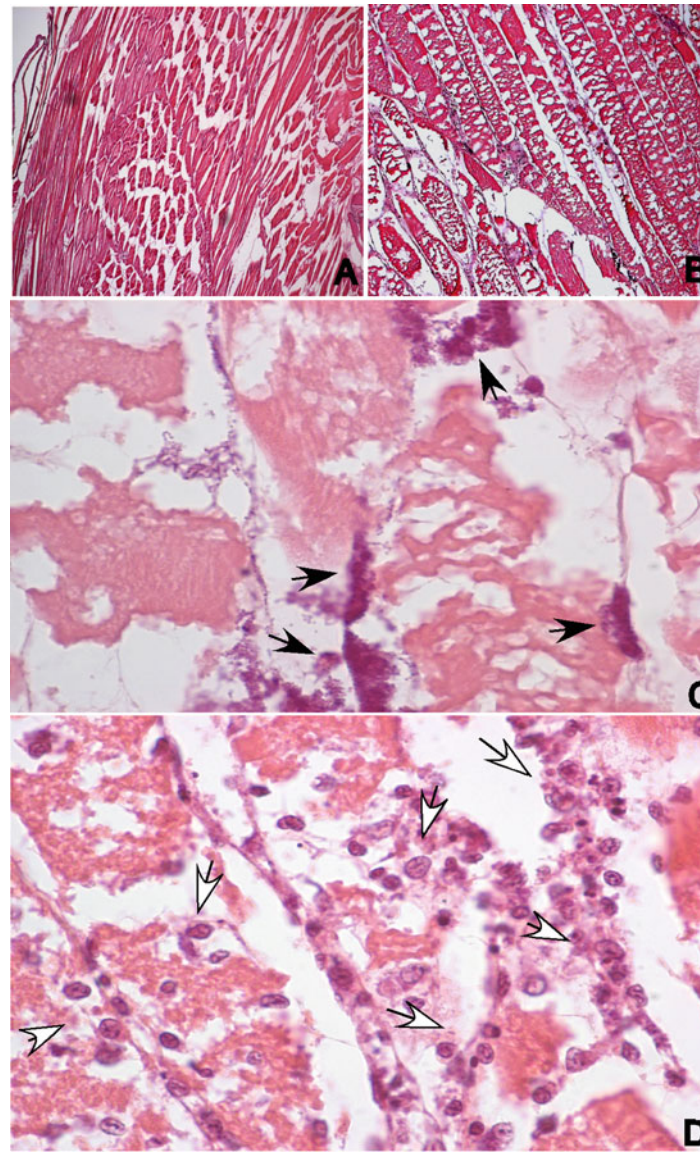

Fig. 6 Micrographs of hematoxylin and eosin stained dorsal muscle tissue. (**a**) Normal dorsal skeletal muscle tissue of a zebrafish (200×). (**b**) Dorsal muscle tissue of a zebrafish 24 h post IM injection with *Streptococcus pyogenes* strain HSC5. Notice necrotic tissue and large aggregates of bacteria (*purple*) following fascial planes (200×). (**c**) 1000× magnification of (**b**). *Black arrowheads* point to aggregates of bacteria. Note absence of inflammatory cells. (**d**) 1000× magnification of dorsal muscle tissue from a zebrafish 24 h post IM injection with an avirulent mutant strain of *S. pyogenes* strain HSC5. *White arrowheads* point to many infiltrated inflammatory cells. Note a lack of bacterial aggregates compared to (**c**)

dishes containing embryos are kept at 27°–28 °C in a glass front incubator and checked periodically to remove any dead embryos or embryos that show evidence of fungus.

3.2.2 Preparing Bacteria for Infections

1. Grow bacteria as described above for adult zebrafish infections.
2. Make dilutions of bacteria for injections, keeping in mind that you will be injecting 1–2 nl. The doses we typically use are 10, 100, and 1000 cfu. This means for a 100 cfu injection, you will need a culture of 1×10^8 cfu/ml. For streptococcus, we have found that the bacteria will survive better on ice if the dilutions are made in THY B instead of PBS. A tube with sterile THY B will also need to be set up for injection of your negative controls.
3. Add Phenol red to all cultures at a final concentration of 0.1 % to aid in visualizing injections. Place cultures on ice (*see* **Note 18**).

3.2.3 Preparing for Microinjections

1. To make a stage for the injection, use a petri dish containing a layer of 1.5 % high-melt agarose (25–30 ml) made up in embryo water. Allow agarose to solidify. Add embryo water to cover the top of the agarose and store at 4 °C. Approximately an hour before injection setup, remove plate from the cold, pour off liquid, and allow it to warm to room temperature.
2. For yolk sac injections, you will want to use 48–50 hpf larvae. At this stage most will still be within the chorion and will need to be dechorinated before injection (*see* **Note 19**). This is best done in the morning to allow recovery of the embryos before injection. Using two fine tipped dissecting tweezers and observing under the dissecting scope, pinch the chorion with one set of forceps, being careful not to catch any of the larval body. Then carefully bring the other forceps next to the area of the chorion that is being held and gently grab the chorion and pull open. Usually, the larvae will wiggle enough to break free of the torn chorion. Dechorinate enough larvae for the entire experiment, including controls. Place dechorinated larvae back into the incubator until time for injection.
3. Pull needles using 3 in. thinwall glass capillaries size 1.00 OD/0.75 ID using a micropipette puller device. We use a Narishige PE-21 with the settings of: Main magnet = 41.0, Sub-magnet = 38.5, Heat = 78.2 (*see* **Note 20**).
4. Briefly vortex culture and use a microloader pipet tip to slowly pull up ~3 μl. Gently insert the pipet tip into the back end of the capillary needle up to the region where the needle starts to narrow. Slowly expel the culture into the needle drawing the tip out as it fills the capillary tube (*see* **Note 21**).
5. Place the needle on a glass slide with a black marker line drawn perpendicularly across the slide. Visualizing under high power

of the dissecting scope, locate the tip of the needle on the black line. Using forceps or a clean razor blade, break off the tip by scraping against the very end of the needle (*see* **Note 22**).

6. Place the needle into the needle holder of the microinjection apparatus. We use WPI PV830 Pneumatic PicoPump attached to a nitrogen tank. Turn on nitrogen tank and PicoPump. We start with the settings at period = 25 ms, eject pressure = 14 psi, hold pressure = 1–3 psi. These can be adjusted based on your needle size and desired volume.
7. You will want to calibrate the injection volume to make sure you are injecting the correct amount. To do this, use a glass calibration slide that has 1 mm divided into 100 units. Add a drop of mineral oil to the slide and place the tip of the needle in the oil without touching the glass below. Hit the foot pedal once. You should get a hanging drop in the oil that makes a sphere. Do not let the drop flatten out on the bottom of the slide. You should aim for a diameter of your drop to be approximately 0.10–0.14 mm (volume of a sphere = $4/3\Pi r^3$). By adjusting the ejection pressure or ejection period, you can change the volume. This should be repeated every time you use a new needle.
8. Put approximately 60 larvae in a petri dish with Tricaine solution. We have found that the larvae are more resistant to the anesthesia than the adult fish. Therefore, we use 200 μg/ml for anesthesia of the larvae. We have found that the larvae can be left in this concentration for at least an hour and recover quite well from this dose. Allow ~15 min after placing the larvae in the Tricaine to become anesthetized (*see* **Note 23**).
9. Remove all embryo water from the injection plate (plate made in #1 above). Place a small amount of 3% methylcellulose on one area of the plate about the size of a dime using a transfer pipet. Then spread out the small mound to about the size of a quarter, making sure not to make it too thick. This is where you will place the anesthetized larvae for injection.

3.2.4 Microinjections of Zebrafish Larvae

1. Pipet 10–12 larvae into the small mound of methylcellulose on the injection plate that you have set up using a transfer pipet. Take care not to transfer too much liquid with the embryos that would dilute out the methylcellulose (*see* **Note 24**). Using a microloader pipet tip and looking through the dissecting scope, gently arrange the larvae in the methylcellulose with their yolk sacs facing to the right (if you are right-handed) or the side from which the injection needle will be used.
2. Gently insert the needle through the methylcellulose into the yolk sac of the larvae. The methylcellulose will keep the larvae from moving or rolling over. The injection should be in the lower half of the yolk sac to avoid the duct of Cuvier that is just below the heart. Make sure that the needle does not extend out

to the other side or into the spinal column. The needle only needs to pierce the yolk sac. Press the injection pedal once and you should observe a small dot of red showing the injection of the phenol red/culture mixture in the yolk sac (*see* **Note 25**).

3. Remove the needle and move on to the next larvae until all of the larvae on the injection plate have been injected.
4. To remove the injected larvae, hold the injection plate over a petri dish 1/3 full of embryo water and with a squeeze bottle of embryo water, gently wash the larvae off the injection plate into the petri dish. This step will help to remove any traces of the methylcellulose.
5. Using a transfer pipet, carefully move the injected larvae from the rinse water in the petri dish into the well of a 6-well plate. Label this well with the strain, dose, and number of injected larvae (*see* **Note 26**). Typically, we do 20 larvae per strain/dose/well, plus 10 larvae injected with sterile media as a negative control. This is usually repeated once on a different day for a total of 40 larvae per strain/dose total.
6. To determine the exact dose of the injection, take 5 of the injected larvae and place them individually into 100 μl of PBS in a microcentrifuge tube. These are immediately homogenized and the entire 100 μl is plated on agar plates with selection and incubated overnight to determine the average injection dose per embryo. For the 1000 cfu injected larvae, place into 1 ml PBS and plate 100 μl. This should be repeated every time a new needle is used.

3.3 Analysis of Zebrafish Larvae Infections

3.3.1 Fluorescence Microscopy

1. Bacteria can be fluorescently labeled after growth using cell tracker dyes (Invitrogen) or you can use a strain of bacteria that is expressing fluorescence endogenously from a bacterial promoter. The second method will provide clues as to the expression of a particular gene in vivo in comparison to in vitro. Since zebrafish have autofluorescence in the green region, it is best to use another fluor for labeling. As a control, one should always take a picture of a noninfected fish under fluorescence to determine the regions of the larvae that naturally fluoresce.
2. After injecting the fluorescently labeled bacteria, at specific time points postinjection, place several larvae in Tricaine solution. After 15 min, carefully transfer larvae from Tricaine to the well of a concave microscope slide. Leave just enough Tricaine liquid to cover the larvae and then add a cover slip. Observe under a fluorescent microscope using the proper filter for the fluorescence being observed.
3. To aid the observer in the orientation of the fish and areas of dissemination of the bacteria, it is best to take a photo using bright field microscopy and then, without moving the fish,

switch to the appropriate fluorescence filter to see only the areas that contain the bacteria. These two figures can be merged later to get a good visual of the areas of dissemination.

3.3.2 Time to Death

1. To determine overall time to death, periodically check wells of injected embryos. Most larvae will be easily determined to be dead just by observation of larvae under the dissecting microscope.
2. Remove any dead larvae and make a tally of how many have died per well (*see* **Note 27**). Replace in embryo water that is removed or has evaporated. Approximately 1.5 ml of embryo water per well should be maintained.
3. By 72 h postinjection, most of the fish that are going to die will have died and the experiment should be terminated and the rest of the population euthanized by placing in 400 μg/ml of Tricaine for 20–30 min.

3.3.3 Total Colonization

1. At specific time points, euthanize larvae by placing in 400 μg/ml Tricaine for 20–30 min.
2. Place larvae into 100 μl PBS and homogenize with a Pellet Pestle homogenizer.
3. Depending on dose, do serial dilutions or plate the 100 μl directly onto an agar plate with appropriate selection. You should do at least six larvae per strain/dose/time point to get an accurate indication of colonization. This should be repeated twice more on different days for a total of 18. As with all animal studies, data can vary from animal to animal.

4 Notes

1. If the culture grows past OD600 = 0.600, it is best to stop the experiment and start over the next day. The culture must be in log phase to cause a successful infection. We have found this to be true for most pathogens we have analyzed in the zebrafish model.
2. Divide 0.300 (the desired OD_{600}) by the actual OD_{600} of the culture to determine how many milliliters of culture to place in the microcentrifuge tube. Example: Desired $OD_{600} = 0.300$. Actual OD_{600} of culture = 0.435. 0.300/0.435 = 0.6897. Place 690 μl (0.6897 ml) into a microcentrifuge tube and add 310 μl of sterile media to bring the culture to $OD_{600} = 0.300$.
3. For easy reference we put green tape on one beaker with one "X" marked on it for the anesthetizing dose and red tape on the other beaker with two "X"s on it for the euthanizing dose (*see* Fig. 2).

4. Use different colored masking tape for different strains so they can be easily distinguished in the incubator. Also, place tape that identifies the strain/dose on the same side of the beaker that has the white volume markings. This provides a clear area in which to view the fish through the beaker while they are in the incubator (the opposite side of the beaker from the tape).
5. Before filling the syringe, briefly vortex culture tube. Place needle into the culture and draw up a small amount and then expel back into tube. This will prime the syringe. Then draw up the desired amount into the syringe very slowly being careful not to introduce bubbles. When finished filling the syringe, hold with needle up and tap the side of the syringe to get any possible bubbles to float to the tip then expel a very small amount back into the tube to remove any bubbles or empty space at the tip.
6. We have found that fish that have been fed do not recover well from the anesthesia. In addition, feeding during the infection reduces water quality and introduces an additional variable for which it is hard to control, e.g., how much an individual fish eats compared to the other fish.
7. Sizes of zebrafish can vary greatly between 6 and 9 months of age. Using fish of different sizes will affect the results because of the difference in ratio of dose to milligram of fish tissue.
8. The same fish net should not be used for handling infected and noninfected fish. Label a fish net that is only to be used for infected fish. Use only clean fishnets on noninfected fish. Fishnets can be cleaned by soaking in 10% bleach for 30 min, rinsing well and then allowing to dry.
9. Once you pierce the skin on the ventral side of the fish, gently lift the syringe slightly to see that the needle is only inserted under the skin and not inserted into any internal organs.
10. Do not insert the needle too far as this will cause too much tissue damage. Inserting until the bevel of the needle is just covered is sufficient. In order to observe this, make sure that the bevel of the needle is pointing up when you insert the needle into the fish.
11. Sick or dead fish should be removed from the beaker as soon as possible. Water quality diminishes very quickly after a fish dies and starts to decompose. If a fish appears to be in distress or showing signs of pain or discomfort, they should be removed from the beaker and euthanized by placing in 336 μg/ml Triciane. Sick fish will swim at the top of the water and show little to no startle response. Unusual swimming behavior such as flipping upside down or jerky movements also indicate pain or distress. Using a glass front incubator provides easier observation of the experiment without having to open and close a door, which would contribute to stress on the fish. In addition,

being located in a central location of the main lab is preferable so that fish can be observed often.

12. This technique allows you to determine the spread of infection to different organs at specific time points. This is especially helpful in comparison of mutant strain dissemination to wild-type dissemination to identify genes that are required for colonization of a particular tissue.
13. If you plan to dissect the brain, always remove after dissecting the heart. This will help to ensure that none of the bacteria that are in the bloodstream contaminate the brain tissue during removal, resulting in elevated numbers being enumerated in the brain tissue homogenates.
14. Serial dilutions will have to be determined experimentally. The spleen typically has the highest concentration of bacteria. For wild-type *Streptococcus iniae* we would typically see 10^5 cfu in the spleen and 10^4 cfu in the brain at 24 h postinjection.
15. Depending on the preparation, some regions of the slide will be too dense to observe individual cells. If this is the case, move to the outer region of the preparation to visualize individual cells. You can also increase the dilution of the homogenate.
16. Clearify is a nonhazardous, nonflammable, and noncarcinogenic substitute for Xylene solutions that are typically used in fixation processes.
17. Hematoxylin needs to be freshly filtered using filter paper. After depariffinization, slides may also be stained with antibody instead of hematoxylin and eosin.
18. Try not to keep cultures on ice for too long. We have found with streptococcus that viability goes down the longer the cultures are kept on ice. It is better to do fewer injections per day to minimize the time kept on ice. A preliminary test for bacterial viability after various periods on ice is advisable for a particular pathogen.
19. The chorion is a clear membrane surrounding the embryo providing protection during early development. Most zebrafish embryos will "hatch" out of their chorion between 30 and 40 hpf.
20. The needles will play a major role in your success in microinjection. The needle tip needs to be strong enough to pierce the yolk sac without bending, but small enough to cause minimal damage to the larvae.
21. Do not worry if there are gaps in the liquid inside the needle. The pressure from the injector will take care of this.
22. The opening of the tip should be ~10 μm as determined using the millimeter scale glass slide.

23. Anesthetizing the larvae at this age is mainly to keep them from moving during the injection process and therefore, minimizing damage to the fish. Fish at this age do not have fully developed nervous systems and therefore the treatments could not produce discomfort because the neural centers mediating pain sensation are still undeveloped.
24. After pulling up 10–12 larvae into the transfer pipet from the Tricaine solution, hold the pipet vertically until all of the larvae fall to the pipet tip by gravity. This allows you to pipet just the larvae with minimal transfer of liquid.
25. If you see red dye spreading out into the spinal column or the heart, discard embryo as this indicates you have pierced beyond the yolk sac.
26. Remember to count the larvae as they are placed into the well of the 6-well plate. It is much easier to count while they are anesthetized than when they are swimming around.
27. By having an initial tally of all injected larvae in a well, you can easily count only those that have died without having to count all of the larvae in the well. Since healthy larvae will be rapidly swimming around the well, it is vastly easier to count those that are dead. In some cases, you will want to move to the highest power of the dissecting scope to determine if a particular larva is still alive by observing the beating of the heart. In addition, if the heartbeat is greatly slowed or malformed, it is best to euthanize. These fish will eventually die and contaminate the rest of the well as they deteriorate.

References

1. Deng W, Tang X, Hou M, Li C, Xie J (2011) New insights into the pathogenesis of tuberculosis revealed by *Mycobacterium marinum*: the zebrafish model from the systems biology perspective. Crit Rev Eukaryot Gene Expr 21(4):337–345
2. Krishnan N, Robertson BD, Thwaites G (2010) The mechanisms and consequences of the extrapulmonary dissemination of *Mycobacterium tuberculosis*. Tuberculosis (Edinb) 90(6):361–366
3. Lesley R, Ramakrishnan L (2008) Insights into early mycobacterial pathogenesis from the zebrafish. Curr Opin Microbiol 11(3):277–283
4. Meijer AH, Spaink HP (2011) Host-pathogen interactions made transparent with the zebrafish model. Curr Drug Targets 12(7):1000–1017
5. Pozos TC, Ramakrishnan L (2004) New models for the study of *Mycobacterium*-host interactions. Curr Opin Immunol 16(4):499–505
6. Ramakrishnan L (2013) Looking within the zebrafish to understand the tuberculous granuloma. Adv Exp Med Biol 783:251–266
7. Tobin DM, Ramakrishnan L (2008) Comparative pathogenesis of M*ycobacterium marinum* and Mycobacterium tuberculosis. Cell Microbiol 10(5):1027–1039
8. Allen JP, Neely MN (2011) The *Streptococcus iniae* transcriptional regulator CpsY is required for protection from neutrophil-mediated killing and proper growth in vitro. Infect Immun 79(11):4638–4648
9. Harvie EA, Green JM, Neely MN, Huttenlocher A (2013) Innate immune response to *Streptococcus iniae* infection in zebrafish larvae. Infect Immun 81(1):110–121
10. Locke JB, Aziz RK, Vicknair MR, Nizet V, Buchanan JT (2008) *Streptococcus iniae* M-like protein contributes to virulence in fish and is a

target for live attenuated vaccine development. PLoS One 3(7):e2824

11. Lowe BA, Miller JD, Neely MN (2007) Analysis of the polysaccharide capsule of the systemic pathogen *Streptococcus iniae* and its implications in virulence. Infect Immun 75(3):1255–1264
12. Miller JD, Neely MN (2005) Large-scale screen highlights the importance of capsule for virulence in the zoonotic pathogen *Streptococcus iniae*. Infect Immun 73(2): 921–934
13. Neely M, Pfeifer J, Caparon MG (2002) Streptococcus-zebrafish model of bacterial pathogenesis. Infect Immun 70(7):3904–3914
14. Phelps HA, Neely MN (2005) Evolution of the zebrafish model: from development to immunity and infectious disease. Zebrafish 2(2):87–103
15. Meijer AH, Gabby Krens SF, Medina Rodriguez IA, He S, Bitter W, Ewa Snaar-Jagalska B, Spaink HP (2004) Expression analysis of the Toll-like receptor and TIR domain adaptor families of zebrafish. Mol Immunol 40(11):773–783
16. Murayama E, Kissa K, Zapata A, Mordelet E, Briolat V, Lin HF, Handin RI, Herbomel P (2006) Tracing hematopoietic precursor migration to successive hematopoietic organs during zebrafish development. Immunity 25(6):963–975
17. Stein C, Caccamo M, Laird G, Leptin M (2007) Conservation and divergence of gene families encoding components of innate immune response systems in zebrafish. Genome Biol 8(11):R251
18. Sullivan C, Kim CH (2008) Zebrafish as a model for infectious disease and immune function. Fish Shellfish Immunol 25(4):341–350
19. Traver D, Herbomel P, Patton EE, Murphey RD, Yoder JA, Litman GW, Catic A, Amemiya CT, Zon LI, Trede NS (2003) The zebrafish as a model organism to study development of the immune system. Adv Immunol 81:253–330
20. Trede NS, Langenau DM, Traver D, Look AT, Zon LI (2004) The use of zebrafish to understand immunity. Immunity 20(4):367–379
21. Yoder JA (2004) Investigating the morphology, function and genetics of cytotoxic cells in bony fish. Comp Biochem Physiol C Toxicol Pharmacol 138(3):271–280
22. Meeker ND, Trede NS (2008) Immunology and zebrafish: spawning new models of human disease. Dev Comp Immunol 32(7):745–757
23. Lawson ND, Weinstein BM (2002) In vivo imaging of embryonic vascular development using transgenic zebrafish. Dev Biol 248(2):307–318
24. Mathias JR, Perrin BJ, Liu TX, Kanki J, Look AT, Huttenlocher A (2006) Resolution of inflammation by retrograde chemotaxis of neutrophils in transgenic zebrafish. J Leukoc Biol 80(6):1281–1288
25. Clay H, Davis JM, Beery D, Huttenlocher A, Lyons SE, Ramakrishnan L (2007) Dichotomous role of the macrophage in early *Mycobacterium marinum* infection of the zebrafish. Cell Host Microbe 2(1):29–39
26. Redd MJ, Kelly G, Dunn G, Way M, Martin P (2006) Imaging macrophage chemotaxis in vivo: studies of microtubule function in zebrafish wound inflammation. Cell Motil Cytoskeleton 63(7):415–422
27. Renshaw SA, Loynes CA, Trushell DM, Elworthy S, Ingham PW, Whyte MK (2006) A transgenic zebrafish model of neutrophilic inflammation. Blood 108(13):3976–3978
28. van der Sar AM, Musters RJ, van Eeden FJ, Appelmelk BJ, Vandenbroucke-Grauls CM, Bitter W (2003) Zebrafish embryos as a model host for the real time analysis of *Salmonella typhimurium* infections. Cell Microbiol 5(9):601–611
29. Ward AC, McPhee DO, Condron MM, Varma S, Cody SH, Onnebo SM, Paw BH, Zon LI, Lieschke GJ (2003) The zebrafish spi1 promoter drives myeloid-specific expression in stable transgenic fish. Blood 102(9):3238–3240
30. Phelps HA, Runft DL, Neely MN (2009) Adult zebrafish model of streptococcal infection. Curr Protoc Microbiol Chapter 9:9D.1
31. Harvie EA, Huttenlocher A (2015) Non-invasive imaging of the innate immune response in a zebrafish larval model of Streptococcus iniae infection. J Vis Exp. 2015 Apr 21;(98). doi:10.3791/52788. PMID:25938624

Chapter 17

Determining Platelet Activation and Aggregation in Response to Bacteria

Oonagh Shannon

Abstract

Many pathogenic bacteria have been reported to interact with human platelets to mediate platelet activation and aggregation. The importance of these interactions to the immune response or pathogenesis of bacterial infection has not been clarified. It may therefore be valuable to assess platelet responses mediated by diverse strains of bacteria. Here, I describe a method to study platelet integrin activation and granule release using flow cytometry, and a complementary method to study platelet aggregation using a dedicated platelet aggregometer. The combination of these methods represents a rapid and cost-effective strategy to provide mechanistic insight on the type of platelet response mediated by the bacteria.

Key words Platelets, Bacteria, Coagulation, Flow cytometry, Streptococci

1 Introduction

Platelets patrol the vessels and maintain haemostasis. Platelets rapidly become activated in response to endothelial damage, activation of the coagulation cascade, and generation of soluble platelet agonists. Platelets may also contribute to the immune response to infection [1]. Platelet activation and aggregation has been reported to occur in response to some bacterial species or to released bacterial products [2, 3]. Direct binding of bacteria to the platelet surface has been reported but also indirect binding via a protein bridge that binds to both platelets and bacteria. For many bacterial species investigated, plasma Immunoglobulin (IgG) and the platelet Fc receptor participate in the generation of platelet activation in susceptible donors [4–8]. It is not clear whether the ability of platelets to respond to bacterial pathogens may contribute to the immune response to infection or the pathogenesis of infection mediated by distinct pathogens. It is therefore of interest to determine platelet activation in response to distinct bacterial

Pontus Nordenfelt and Mattias Collin (eds.), *Bacterial Pathogenesis: Methods and Protocols*, Methods in Molecular Biology, vol. 1535, DOI 10.1007/978-1-4939-6673-8_17,

species and strains. Diverse platelet function tests are available, which take advantage of the biochemical changes that occur in platelets upon activation. This includes surface mobilization and activation of integrins, surface mobilization and release of granule proteins, binding of plasma ligands, platelet-platelet aggregation, and platelet-leukocyte aggregation [9]. Herein, I present a combination of methods that can be used to assess distinct aspects of platelet activation in response to bacteria.

1. Flow cytometry is a powerful approach to simultaneously determine multiple aspects of platelet activation by combining three or more monoclonal antibodies. The platelet population is identified using an antibody against CD42a, the activation status of CD41/CD61 (GPIIb/IIIa) integrin complex is determined using an antibody specific for an activation-dependent conformational change (PAC-1.FITC), and mobilization of the alpha granules is determined using an antibody against CD62P. Both parameters are low or absent on platelets prior to activation.
2. Platelet aggregation can be monitored using specialized equipment to determine turbidometric platelet aggregometry, such as the ChronoLog aggregometer.

2 Materials

2.1 Blood Preparation

1. Vacutainer citrate tubes (BD Biosciences).
2. 15 ml round bottomed plastic tubes (Falcon).
3. Centrifuge with swing-out rotor.

2.2 Flow Cytometry

1. PBS buffer pH 7.4 filtered through a 0.2 μm filter.
2. 100 μM of adenosine diphosphate (ADP) from Sigma Aldrich.
3. Mouse antihuman CD42a PerCP (BD Biosciences, clone Beb 1, IgG1).
4. Mouse antihuman GPIIb/IIIa - PAC-1.FITC (BD Biosciences, clone SP-2, IgM).
5. Mouse antihuman CD62P.PE (BD Biosciences, clone AK-4, IgG1).
6. Isotype control antibodies (BD Biosciences).
7. 0.5% formaldehyde in PBS.

2.3 Platelet Aggregation

1. Platelet aggregometer (ChronoLog Corp).
2. Glass assay tubes and stirbars (ChronoLog Corp).
3. 1 mg/ml Collagen (ChronoLog Corp).

3 Methods

3.1 Isolation of Platelets

1. Collect blood from healthy volunteers by venipuncture into a citrate vacutainer. Discard the first tube to limit artefactual platelet activation and save the subsequent tubes (*see* **Note 1**).
2. Carefully transfer the whole blood to 15 ml plastic tubes and spin at 150 g for 10 min, with no brake set on the centrifuge.
3. Carefully remove the upper Platelet Rich Plasma (PRP) and transfer to a clean tube (*see* **Note 2**).
4. Spin the remaining blood once again at 2000 × *g*.
5. Remove the upper Platelet Poor Plasma (PPP).

3.2 Preparation of Bacteria

1. Grow the bacteria to early exponential phase or stationary phase in the appropriate growth medium for the bacterial species.
2. Pellet the bacteria by centrifugation at 2000 × *g*, 10 min.
3. Resuspend the bacteria pellet in 1 ml of PBS.
4. Transfer the bacteria to a microcentrifuge tube and wash twice with PBS.
5. Adjust the final bacterial concentration to approximately 2×10^6/μl.

3.3 Flow Cytometry of Platelet Activation in Platelet Rich Plasma

1. Add 10 μl of PRP to 40 μl PBS in each microcentrifuge tube.
2. Add the platelet agonist to be investigated to each tube, as illustrated in Table 1 (*see* **Note 3**).
3. Incubate the tubes at room temperature for 15 min.
4. Add 5 μl of each flourochrome-conjugated antibody according to Table 1.
5. Incubate at room temperature for 15 min.
6. Fix the samples by addition of 500 μl of 0.5% formaldehyde in PBS.
7. Run the samples on a flow cytometer with logarithmic acquisition settings.
8. Adjust the settings for threshold to exclude small debris determined by size exclusion on a plot of Forward Scatter (FSC) versus Side Scatter (SSC).
9. Adjust the sample flow rate to ≤2500 events per second and dilute the sample with additional PBS if necessary.
10. Adjust the compensation between the fluorescent channels (FL-1, FL-2, and FL-3) using the single-stained samples.
11. Set the background fluorescence for each antibody using the isotype controls.

Table 1
Experimental plan for three-color flow cytometry of platelet activation in response to bacteria

Tube	Agonist	FL1 FITC	FL2 PE	FL3 PerCP	Purpose of sample
1	Buffer				Control for autofluorescence
2	ADP (10 μM	PAC-1			Single stain for compensation
3	ADP (10 μM)		CD62		Single stain for compensation
4	ADP (10 μM)			CD42a	Single stain for compensation
5	Buffer	PAC-1	CD62	CD42a	Control for background activation
6	ADP (10 μM)	PAC-1	CD62	CD42a	Control for platelet activation
7	Bacteria (1×10^5/μl)	PAC-1	CD62	CD42a	Test for platelet activation
8	Buffer		IgG1	IgG1	Isotype control for nonspecific binding
9	ADP (10 μM)		IgG1	IgG1	Isotype control for nonspecific binding
10	Bacteria (1×10^5/μl)		IgG1	IgG1	Isotype control for nonspecific binding

12. Identify the platelet population as CD42-positive events and determine the Median Fluorescence Intensity (MFI) of binding of PAC-1 antibody and anti CD62P for each agonist investigated (Fig. 1).

3.4 Platelet Aggregation in Platelet Rich Plasma

1. When the Chrono-Log aggregometer achieves the working temperature of 37 °C, place 450 μl of PPP in a Chrono-Log glass assay tube and place in the reference well.
2. Take 450 μl of PRP to a Chrono-Log glass assay tube and pre-incubate for 5 min in the incubation well.
3. Move the sample to the test well and add a stirbar.
4. Start the aggregation trace in the software and adjust the baseline to 0 light transmission in the PRP test well as compared with 100% light transmission in the PPP reference sample.
5. When the trace has stabilized add an agonist;
   (a) 2 μl of collagen 1 mg/ml.
   (b) 20 μl of bacteria 2×10^6/μl (*see* **Note 4**).
6. The software plots the aggregation trace live as the light transmission increases when platelet aggregates form. On addition of collagen, aggregation occurs within 30–60 s.
7. On addition of bacteria it can take 1–20 min for aggregation to occur (Fig. 2). Record the time to initiation of aggregation and stop the test when the aggregation trace has stabilized or after 20 min if no aggregation has occurred (*see* **Note 5**).

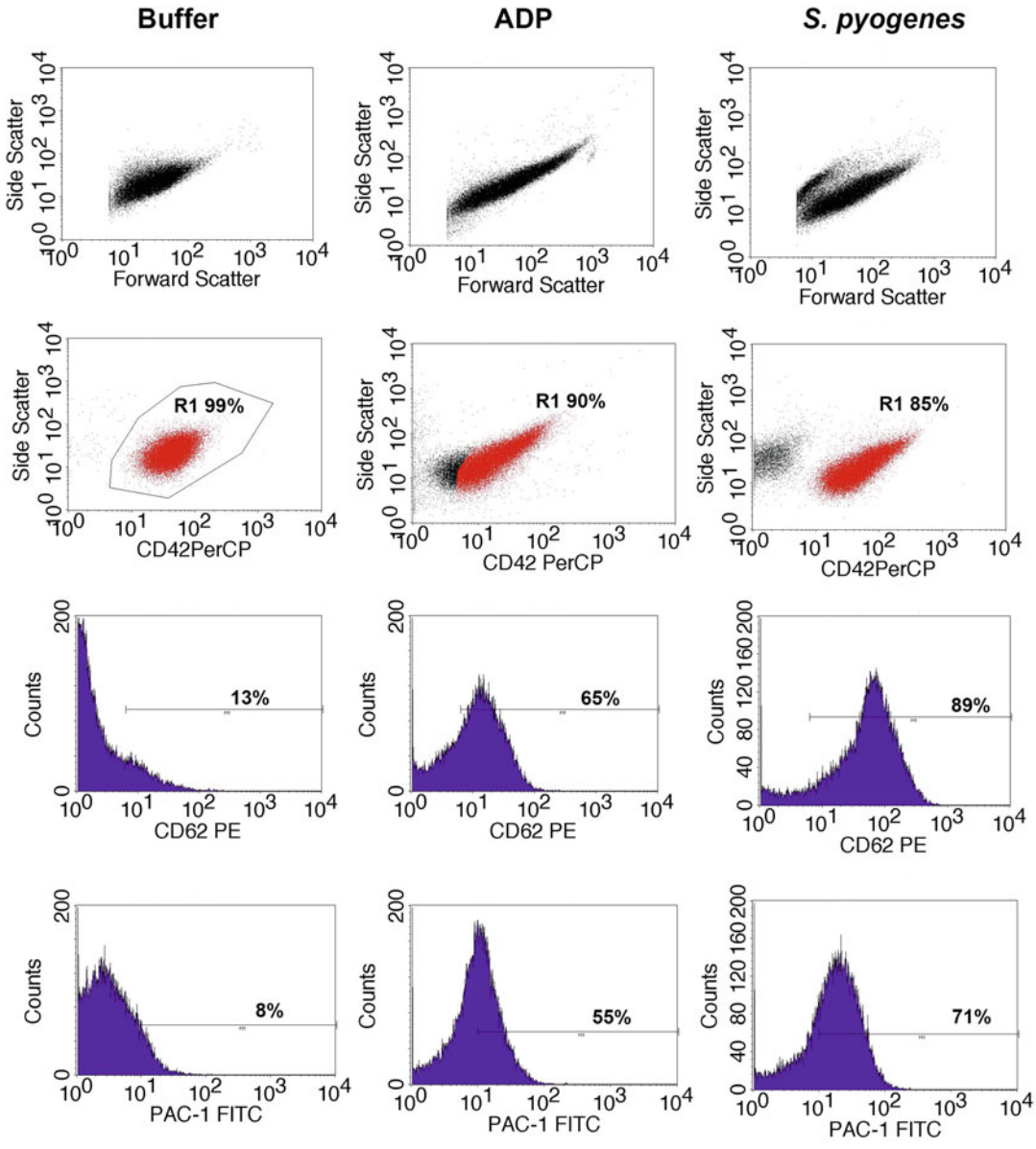

Fig. 1 Determination of platelet activation using flow cytometry. Buffer (*left column*), ADP (*middle column*), or washed Streptococcus pyogenes bacteria (*right column*) were added to PRP and incubated with monoclonal antibodies prior to fixation and acquisition of data on a BD Accuri flow cytometer. The relative size (*forward scatter*) and complexity (*side scatter*) of the population was assessed. Platelets were specifically identified and gated in R1 (*red*) as CD42PerCP positive events. Platelet activation within this gated population was determination using histograms of the relative fluorescent intensity of CD62P-PE and PAC-1-FITC respectively. The percentage positive cells for each antibody was determined using isotype control antibodies to demonstrate background

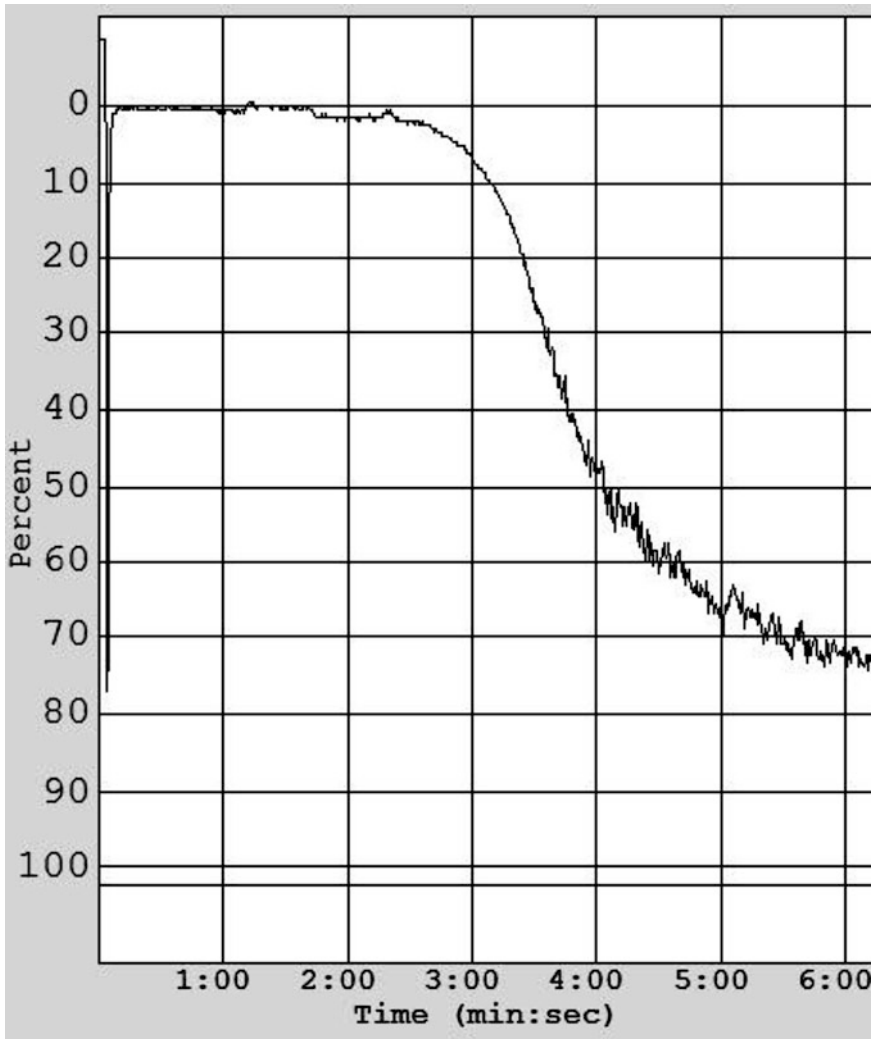

Fig. 2 Platelet aggregation determined using a Chrono-log aggregometer. Washed Streptococcus pyogenes bacteria was added to PRP at time = 0 and aggregation was monitored over time. Aggregation began to occur within 2-3 minutes and by 6 minutes 80% aggregation had occurred and the curve planed out

4 Notes

1. The healthy blood donor should not have taken antiplatelet medication for 10 days prior to blood collection. Citrate is an anticoagulant of choice for platelet studies since it is a weak calcium chelator and facilitates subsequent studies of calcium-dependent integrin activation.
2. Five mls of citrated blood will typically yield between 1 and 2 mls of PRP. Platelets in PRP should be used within 2–4 h.

3. Other positive control agonists for platelet activation can be used such as TRAP-6, thrombin, or collagen. For the bacteria agonist it is recommended to perform a dose–response experiment with titrated concentrations of washed bacteria since the optimal concentration of bacteria reported to mediate platelet activation varies according to bacterial species and donor. Addition of 10 µl of Streptococcus pyogenes AP1 strain adjusted to 5×105 /µl mediates platelet activation in donors tested at our institution (Fig. 1).
4. For the bacteria agonist it is recommended to perform a dose–response experiment with titrated concentrations of washed bacteria since the optimal concentration of bacteria reported to mediate platelet activation varies according to bacterial species and donor. Addition of 20 µl of *Streptococcus pyogenes* AP1 strain adjusted to 2×10^6 /µl mediates platelet aggregation in donors tested at our institution (Fig. 2).
5. PRP used for aggregation studies can be centrifuged at $2000 \times g$ for 10 min and the supernatant recovered for subsequent determination of platelet released products such as, serotonin, thromboxane, CD62P, CD40L, and Platelet factor 4 by commercial enzyme-linked-immunosorbent-assays (ELISAs).

References

1. Semple JW, Freedman J (2010) Platelets and innate immunity. Cell Mol Life Sci 67:499–511
2. Kerrigan SW (2015) The expanding field of platelet-bacterial interconnections. Platelets 26:293–301
3. Shannon O (2015) Platelet interaction with bacterial toxins and secreted products. Platelets 26:1–7
4. Sjöbring U, Ringdahl U, Ruggeri ZM (2002) Induction of platelet thrombi by bacteria and antibodies. Blood 100:4470–4477
5. Kerrigan SW, Clarke N, Loughman A et al (2008) Molecular basis for Staphylococcus aureus-mediated platelet aggregate formation under arterial shear in vitro. Arterioscler Thromb Vasc Biol 28:335–340
6. Shannon O, Mörgelin M, Rasmussen M (2010) Platelet activation and biofilm formation by Aerococcus urinae, an endocarditis-causing pathogen. Infect Immun 78:4268–4275
7. Svensson L, Baumgarten M, Mörgelin M, Shannon O (2014) Platelet activation by Streptococcus pyogenes leads to entrapment in platelet aggregates, from which bacteria subsequently escape. Infect Immun 82:4307–4314
8. Svensson L, Frick I-M, Shannon O (2016) Group G streptococci mediate fibrinogen-dependent platelet aggregation leading to transient entrapment in platelet aggregates. Microbiology 162:117–126
9. Michelson AD (2009) Methods for the measurement of platelet function. Am J Cardiol 103:20A–26A

Chapter 18

Killing Bacteria with Cytotoxic Effector Proteins of Human Killer Immune Cells: Granzymes, Granulysin, and Perforin

Diego López León, Isabelle Fellay, Pierre-Yves Mantel, and Michael Walch

Abstract

Bacterial pathogens represent a constant threat to human health that was exacerbated in recent years by a dramatic increase of strains resistant to last resort antibiotics. The immune system of higher vertebrates generally evolved several efficient innate and adaptive mechanisms to fight ubiquitous bacterial pathogens. Among those mechanisms, immune proteases were recognized to contribute essentially to antibacterial immune defense. The effector serine proteases of the adaptive immune system, the granzymes, exert potent antimicrobial activity when they are delivered into the bacterial cytosol by prokaryotic membrane disrupting proteins, such as granulysin.

In this chapter, we are detailing experimental protocols to study the synergistic cytotoxic effects of human granzymes and granulysin on extracellular as well as on intracellular bacterial pathogens in vitro. In addition, we provide a simple and fast-forward method to biochemically purify native cytotoxic effector molecules necessary to perform this kind of investigations.

Key words Cell-mediated cytotoxicity, Antibacterial activity, Immune serine proteases, Granzymes, Granulysin

1 Introduction

When cytotoxic T lymphocytes (CTL) or natural killer (NK) cells recognize cells infected with intracellular pathogens, they release their cytotoxic granule content to eliminate the target cells and the intracellular pathogen [1]. Cytotoxicity is mediated by granule effector proteases, the granzymes (Gzms), delivered into the host cell cytosol by the pore-forming protein perforin (PFN) [2]. Cytotoxic granules of humans and some other mammals, but not rodents, contain another pore-forming protein, termed granulysin (GNLY) [3]. GNLY belongs to the saposin-like protein family (SAPLIP) that is characterized by its affinity to a variety of lipids [4]. Recombinant GNLY was found to efficiently disrupt prokaryotic (but not eukaryotic) membranes [5] and to kill bacteria, parasites, and fungi in vitro [6].

Pontus Nordenfelt and Mattias Collin (eds.), *Bacterial Pathogenesis: Methods and Protocols*, Methods in Molecular Biology, vol. 1535, DOI 10.1007/978-1-4939-6673-8_18,

The Gzms are a group of homologous serine proteases localized in specialized lysosomes of CTL and NK cells, together with GNLY and PFN [7]. There are five Gzms in humans (GzmA, B, H, K, and M), and ten Gzms in mice (GzmA—G, K, M, and N). The best established function of the Gzms, in particular of GzmA and GzmB, is the induction of apoptosis when delivered into the target cells by PFN [8, 9]. More recent work additionally demonstrated extracellular roles of the Gzms affecting immune regulation and inflammation, independently of PFN [10, 11]. Importantly, the scope of cells that are highly susceptible to the Gzms was recently widened from mammalian cells to bacteria [12, 13] and even to certain unicellular parasites [14, 15].

We recently discovered that—analogous to PFN delivery of the Gzms into mammalian cells—GNLY in, per se, sublytic concentrations allowed entry of Gzms into bacteria [12] and certain unicellular parasites [15], where these enzymes proteolytically attacked subunits of the bacterial respiratory chain complex I, as well as radical oxygen species (ROS) degrading enzymes, increasing intracellular lethal ROS levels to rapidly execute microbial death. Human CTL killed intracellular pathogens in a serine protease-dependent mechanism even before significant host cell death occurred. Importantly, mice transgenically expressing human GNLY were more resistant to infection with *Listeria monocytogenes, Toxoplasma gondii*, *and Trypanosoma cruzi* than their wild-type litter mates. Thus, CTL eliminate intracellular microbial pathogens in a Gzm and GNLY-dependent process.

These recent discoveries opened up a whole new playground for Gzm researchers. Therefore, detailed protocols of how to investigate the synergistic effects of the Gzms and GNLY to kill microbial pathogens will significantly ease the way for these future studies.

2 Materials

2.1 Killing Extracellular Bacteria

1. *E. coli*, *Listeria*, *Salmonella*, *Staphylococci*, or whatever bacterial strain is available (*see* **Note 1**).
2. Bacterial culture media (lysogeny broth, LB; brain heart infusion, BHI) and corresponding agar plates.
3. Assay buffer: 20 mM Tris–Base, 10 mM NaCl, pH = 8 (*see* **Note 2**).
4. Purified GNLY and GzmB stock solutions, for their purification *see* Subheading 3. Lysozyme and various antibiotics as positive controls.
5. A 37 °C shaking incubator for bacterial plates and liquid cultures.
6. Flat-bottomed 96-well plates.

7. A heat controlled microplate reader that allows kinetic readings with discontinuous shaking.

2.2 Killing Intracellular Bacteria

1. HeLa cells or any available cell line, which can be infected with pathogenic bacteria, grown in DMEM + 10% fetal bovine serum (FBS) without antibiotics in six-well plates.
2. Trypsin/EDTA solution (Sigma).
3. Facultative intracellular bacteria, such as *Listeria, Salmonella,* or *Shigella*.
4. 10 mg/ml gentamycin solution (Sigma).
5. Cell buffer: 4 mM $CaCl_2$, 0.4% BSA in Hank's balanced salt solution (HBSS).
6. HBSS.
7. Gzm, GNLY, and PFN stock solutions.
8. Bacterial liquid medium and agar plates (*see* **Note 1**).
9. A humidified cell culture incubator and a bacterial shaking incubator.

2.3 Purification of Native GzmB and GNLY from YT Indy Cells

1. YT Indy cells (human NK cell line [16]).
2. 175 cm^2 tissue culture flasks, preferably multilayer flasks.
3. Complete medium: RPMI1640 + tissue culture supplement (100 U/ml penicillin G, 100 µg/ml streptomycin sulfate, 6 mM Hepes-free acid, 1.6 mM L-glutamine, 50 µM β-mercaptoethanol) + 10% FBS).
4. HBSS.
5. Relaxation buffer: 10 mM PIPES, 0.1 M KCl, 3.5 mM $MgCl_2$, 1 mM ATP, 1.25 mM EGTA, 0.05% BSA, pH 6.8, prepare fresh, put on ice.
6. Phenyl buffer A: 50 mM Tris-Base, 2 M NaCl, pH 7.2, filtered.
7. S column binding buffer A: 50 mM bisTris, 50 mM NaCl, pH 5.8, filtered.
8. S column elution buffer B: 50 mM bisTris, 1 M NaCl, pH 5.8, filtered.
9. Nitrogen cavitation bomb (Equilabo).
10. HiTrap Phenyl FF 1 ml (GE Healthcare).
11. HiTrap SP FF 1 ml (GE Healthcare).
12. Colorimetric assay buffer: 50 mM Tris-Base, pH 7.5 + 0.2 mM N-Ac-IEPD-pNA (Sigma).
13. Centricon, 10 + 30 kDa MWCO (Millipore).

3 Methods

3.1 Killing Extracellular Bacteria

The following protocol describes the basic method of how to treat bacteria in suspension to investigate the synergistic effects of the two cytotoxic effector molecules GNLY and GzmB. Our standard readout is colony forming unit assays (CFU). As alternative readout we outline a method to measure bacterial growth. For continuative protocols of how to assess bacterial membrane integrity, radical oxygen species generation, or intracellular protein substrate cleavage, we refer to [12, 15].

3.1.1 Colony Forming Unit Assays

1. Dilute an overnight bacterial culture 1:50 in fresh medium and grow bacteria to mid-log phase ($OD_{600nm} = 0.5$ equaling $\sim 2 \times 10^8$/ml viable bacteria in LB and other rich media) in a shaking incubator at 37 °C.
2. Wash bacteria three times, by spinning at $15{,}000 \times g$ for 1 min and resuspending in 1 ml assay buffer. Dilute to 5×10^5 bacteria/ml.
3. Prepare dilutions of GNLY (between 1 and 0.06 μM) ± 0.05–0.2 μM GzmB in 20 μl of assay buffer. Use buffer and GzmB only as negative controls. Antibiotics or lysozyme (Sigma) may serve as positive control.
4. Add 20 μl of bacterial dilutions to each reaction and incubate for 5–60 min at 37 °C. Assay buffer only serves as no-bacteria control.
5. Add 200 μl of medium to each reaction and prepare tenfold dilutions from each reaction.
6. Plate 50 μl of the dilutions on appropriate agar plates and incubate at 37 °C overnight.
7. Count colonies manually or with an adequate imager and colony counting software. Calculate the percent lysis using the following equation: $\%\ \text{specific lysis} = CFU_{\text{test-treated}}/CFU_{\text{buffer-treated}} \times 100$ (Fig. 1a).

3.1.2 Bacterial Growth

1. To measure bacterial growth, prepare serial dilutions of effector molecules in 20 μl of assay buffer in flat-bottomed 96-well plates. Include positive (lysozyme) and negative (buffer, Gzm only) controls.
2. Add 20 μl of washed and prediluted bacteria as above to each well and incubate for 15 min at 37 °C.
3. Add 200 μl medium to each well.
4. Put plate in a heat controlled plate reader and measure OD_{600nm} every 10 min for 12 h with discontinuous shaking at 37 °C. The bactericidal effect of the treatment shifts grows curves to the right (*see* **Note 3** and Fig. 1b).

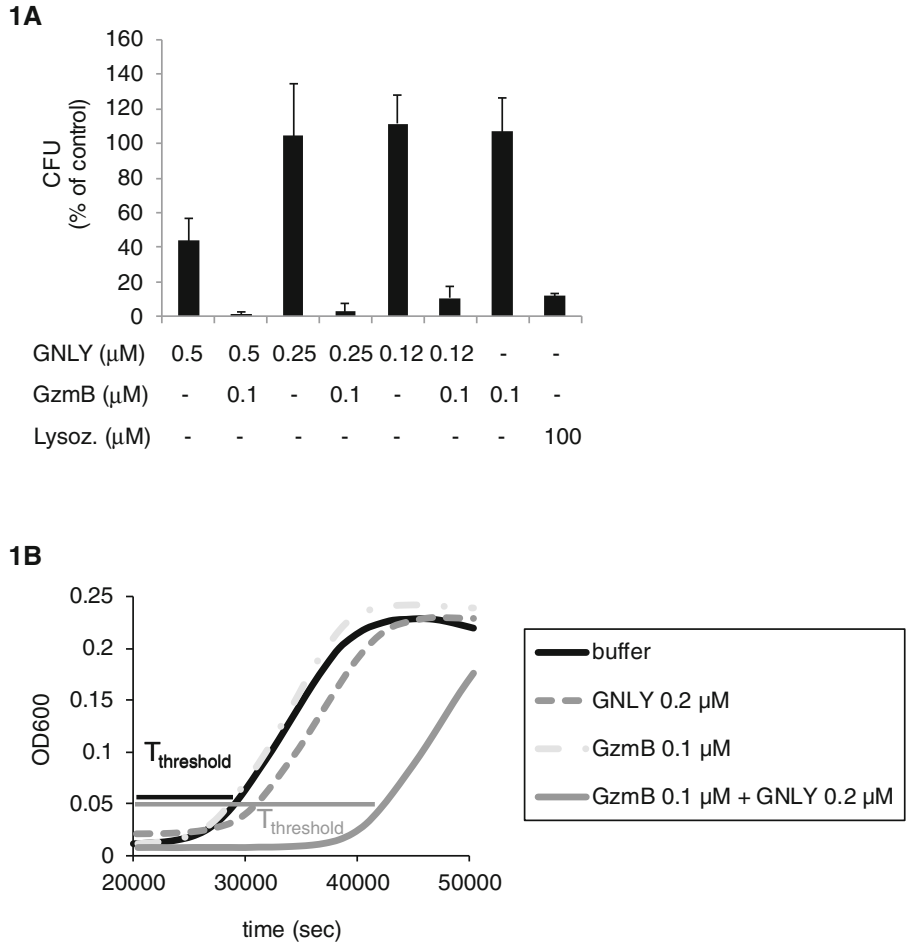

Fig. 1 Killing extracellular bacteria with GzmB and GNLY. *Listeria monocytogenes* were treated with the indicated concentrations of GzmB, GNLY, and lysozyme (Lysoz.) for 15 min at 37 °C and bacterial viability was assessed in CFU assays (**a**) or by recording bacterial growth curves (**b**). Mean and standard deviation of a representative experiment is presented in **a**. The times for bacterial growth curves to reach a threshold OD ($T_{threshold}$) for untreated in comparison to GzmB/GNLY-treated bacteria are indicated in **b**

3.2 Killing Intracellular Bacteria

The following outlines the protocol of a standard loading experiment to determine which combinations and concentrations of the three major cytotoxic effector molecules (PFN, Gzm, and GNLY) in a time-dependent manner efficiently lyse intracellular bacteria and the host cell.

1. Infect HeLa cells with virulent, facultative intracellular bacteria, such as *Listeria* or *Salmonella*, for 1 h at 37 °C at a multiplicity of infection of 10.
2. Remove uninfected bacteria by washing with PBS and treating with 20 μg/ml gentamycin in culture medium for 60 min at 37 °C.

3. Wash with PBS and detach infected HeLa cells by gentle trypsinization.
4. Wash with PBS and resuspend cells in cell buffer at a density of 10^6 cells/ml.
5. Prepare dilutions of GNLY (between 1 and 0.25 μM) ± GzmB (between 1 and 0.25 μM) ± sublytic PFN (*see* **Note 4**) in 25 μl HBSS.
6. Add 25 μl of the cell suspension to the effector molecule dilutions and incubate for various times (15 min to 4 h) at 37 °C.
7. To determine bacterial viability, add 200 μl of ice cold water for hypotonic host cell lysis and incubate on ice for 15 min. Prepare tenfold dilutions of every reaction in an appropriate bacterial medium and plate 50 μl on agar plates. Incubate overnight at 37 °C.
8. Count colonies and calculate percentage bacteriolysis as above.
9. In parallel experiments, host cell viability can be assessed by annexin V/propidium iodide staining and flow cytometry or related methods as described [17].

3.3 Purification of Native GNLY, GzmB from YT Indy Cells

Here, we present an improved adaption of a protocol that we published recently [17]. By avoiding one column in the purification procedure, we are proposing a fast-forward method that reliably generates highly active, native GzmB and GNLY from the human NK cell line YT Indy. For the purification of PFN from YT Indy cells we refer to the published method of Froelich et al. [18].

1. Grow YT Indy cells in complete medium to about 3×10^9 (*see* **Note 5**).
2. Collect expanded cells by centrifugation, 500 × *g* for 10 min at 4 °C, and wash cells twice in ice-cold HBSS.
3. Resuspend cells at 10^8 cells/ml in ice cold relaxation buffer (in a conical 50-ml tube).
4. Disrupt cells in a nitrogen cavitation bomb at 35 bar at 4 °C for 15 min, stirring at 150 rpm with a small stir bar in the tube.
5. Centrifuge at 400 × *g* for 7 min at 4 °C and transfer post nuclear supernatant (PNS) to new 50-ml tube. Wash nuclear pellet twice (or until PNS is clear). Combine the PNS.
6. Centrifuge PNS at 15,000 × *g* for 15 min at 4 °C to yield the granule pellet.
7. Extract the granule pellet by mixing with phenyl buffer A for 60 min at 4 °C (2 ml per 10^9 cells), vortex occasionally, and freeze at −80 °C. Perform a total of three freeze-thaw cycles.
8. Centrifuge the extract at 15,000 × *g* for 10 min at 4 °C, and then pass supernatant through a 0.45-μm syringe filter.

9. Attach a phenyl column to a suitable FPLC system and equilibrate the column with ten column volumes (CV) of phenyl buffer A. Apply the cleared supernatant at 1 ml/min to the phenyl column and wash with phenyl buffer A until UV baseline. Important: as positively charged Gzms and GNLY do not bind to the phenyl column, it is crucial to collect flow-through (FT) and complete wash volume.
10. Elute and wash the phenyl column with ddH_2O (*see* **Note 6**).
11. Concentrate FT and wash from phenyl column by ultrafiltration (10 kDa MWCO, to a volume of about 0.5 ml). During the concentration procedure, attach the S column to the FPLC system and equilibrate with 10 CV of S buffer A.
12. Dilute the concentrated FT and wash from the phenyl column 20-fold in S column buffer A and apply this sample at 1 ml/min to the S column. Wash with S buffer A until UV baseline is reached.
13. Elute with a linear gradient (0–100% S buffer B) of 20 ml length, followed by 10 ml S buffer B at a flow rate of 1 ml/min. Collect 1-ml fractions (*see* **Note 7**).
14. Run 10 µl of fractions 11–24 on SDS-PAGE (using 15%) for Coomassie blue staining (Fig. 2a).
15. Lay 4 µl of fractions 11–30, as well as of the cleared granule lysate as positive control and S buffer B as negative control in a flat-bottomed 96-well plate and add 100 µl of colorimetric assay buffer. Incubate for 10 min at 37 °C and record absorbance at 405 nm in a microplate reader (Fig. 2b) [19].
16. Concentrate all fractions that contain GzmB activity and appear as bands (*see* Fig. 2a) of about 30 kDa (=GzmB). Fractions that show double bands of about 15 and 10 kDa (=GNLY) on the gel and are free of GzmB activity are separately concentrated by ultrafiltration (10 kDa MWCO).

4 Notes

1. When working with pathogenic bacteria ensure that appropriate biosafety measures and institutional authorizations are in place. The choice of the medium is strain specific, though most common bacteria grow in LB. To better preserve virulence, *Listeria* and *Staphylococci* should be expanded in BHI.
2. GNLY activity under in vitro settings is inhibited by NaCl in concentrations higher than 50 mM [20]; therefore, low salt assay buffers are indicated.
3. To quantify the changes in bacterial growth under different treatment conditions, measure the time until the growth curves

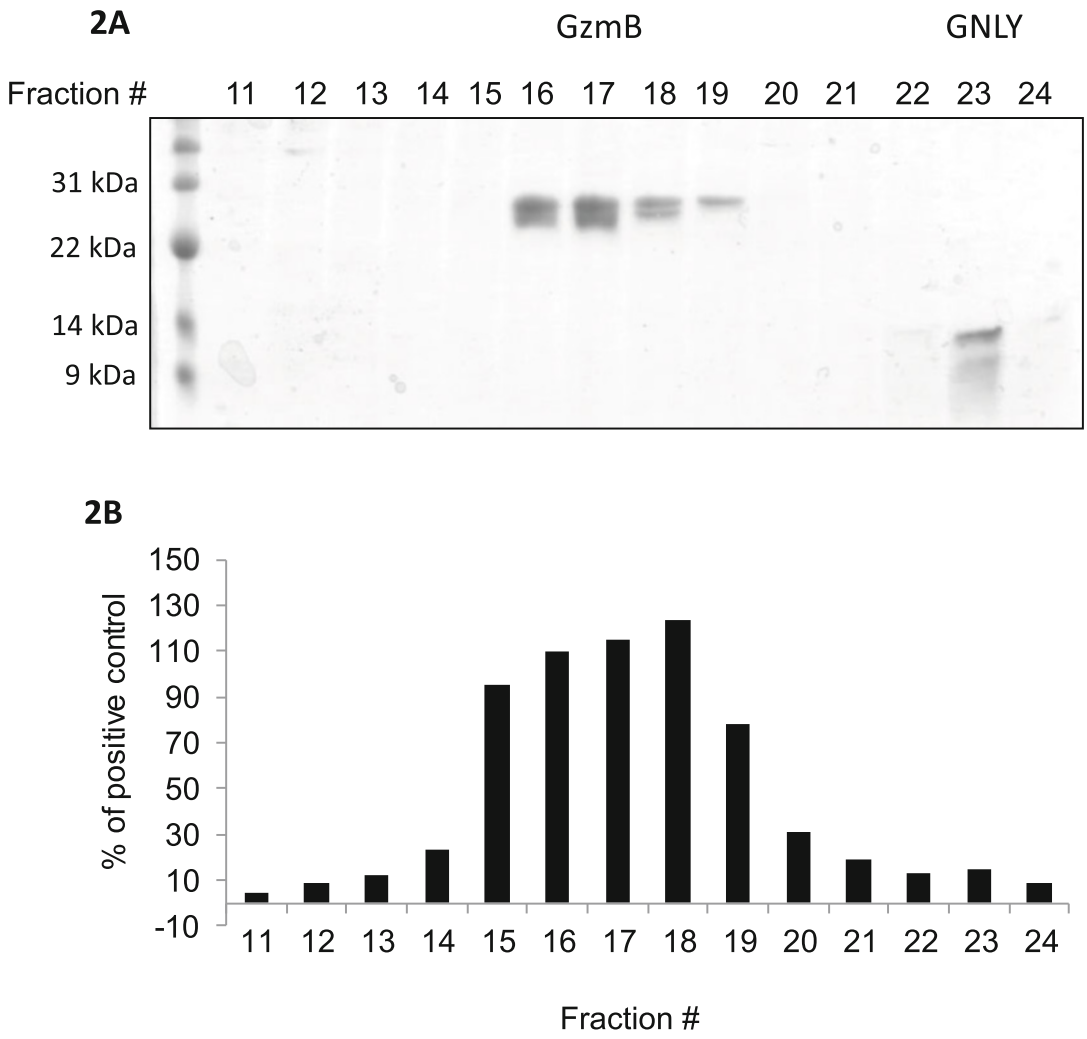

Fig. 2 Purification of native GzmB and GNLY from YT Indy cells. Elution fractions from the S column during the linear NaCl gradient were subjected to SDS-PAGE and subsequent Coomassie blue staining (**a**) and to colorimetric assay indicating GzmB activity (**b**)

reach an OD_{600nm} of 0.05 ($T_{threshold}$). The ratio of ($T_{threshold}$ (untreated)/$T_{threshold}$ (treated)) indicates the change in bacterial growth. To reduce interexperimental variations, correct $T_{threshold}$ times by subtracting the time for untreated control cultures to reach an OD_{600} increase of 0.005 (*see* Fig. 1b).

4. The concentration of sublytic PFN of every purification batch has to be carefully determined by titration beforehand by propidium iodide staining for flow cytometry according to [17]. A sublytic dose is considered to lyse less than 15% of treated cells.

5. The human NK cell line, YT Indy [16], expresses high levels of PFN, GzmB, and GNLY. It completely lacks tryptase (GzmA and GzmK) activity and is therefore well suited for the single purification of GzmB. The cell line grows very slowly at a density over 0.5×10^6/ml. Therefore, we recommended growing the cells in multilayer flasks and splitting at a 1:4-ratio every third day of culture.
6. In theory, PFN binds to the phenyl column and can be found in the elution fractions. However, in our hands eluted PFN displayed little to no lytic activity. We therefore recommend simply washing the column with water and discarding the eluate. For the purification of PFN from YT Indy cells, the published protocol of Froelich et al. [18] is reliable and efficient.
7. GzmB elutes at about 750 mM NaCl and GNLY at over 900 mM NaCl. By using a 1 ml column (SP HiTrap) and a linear gradient of 20 ml length, the two effector molecules elute completely separated (*see* Fig. 2a).

Acknowledgments

This work was supported by grants from the Novartis Foundation for Medical-Biological Research, from the Research Pool and Fund of the University of Fribourg, as well as from the Gottfried and Julia Bangerter-Rhyner foundation (to M.W. and P.Y.M.). We thank Luis Filgueira at the University of Fribourg and Denis Martinvalet at the University of Geneva for helpful discussions. We also acknowledge the contributions of Judy Lieberman and Farokh Dotiwala at Harvard Medical School to the design and establishment of the outlined methods.

References

1. Russell JH, Ley TJ (2002) Lymphocyte-mediated cytotoxicity. Annu Rev Immunol 20:323–370
2. Thiery J, Keefe D, Boulant S, Boucrot E, Walch M, Martinvalet D, Goping IS, Bleackley RC, Kirchhausen T, Lieberman J (2011) Perforin pores in the endosomal membrane trigger the release of endocytosed granzyme B into the cytosol of target cells. Nat Immunol 12(8):770–777
3. Krensky AM, Clayberger C (2009) Biology and clinical relevance of granulysin. Tissue Antigens 73(3):193–198
4. Vaccaro AM, Salvioli R, Tatti M, Ciaffoni F (1999) Saposins and their interaction with lipids. Neurochem Res 24(2):307–314
5. Barman H, Walch M, Latinovic-Golic S, Dumrese C, Dolder M, Groscurth P, Ziegler U (2006) Cholesterol in negatively charged lipid bilayers modulates the effect of the antimicrobial protein granulysin. J Membr Biol 212(1):29–39
6. Stenger S, Hanson DA, Teitelbaum R, Dewan P, Niazi KR, Froelich CJ, Ganz T, Thoma-Uszynski S, Melian A, Bogdan C, Porcelli SA, Bloom BR, Krensky AM, Modlin RL (1998) An antimicrobial activity of cytolytic T cells mediated by granulysin. Science 282(5386):121–125
7. Chowdhury D, Lieberman J (2008) Death by a thousand cuts: granzyme pathways of programmed cell death. Annu Rev Immunol 26:389–420

8. Martinvalet D, Dykxhoorn DM, Ferrini R, Lieberman J (2008) Granzyme A cleaves a mitochondrial complex I protein to initiate caspase-independent cell death. Cell 133(4):681–692
9. Heusel JW, Wesselschmidt RL, Shresta S, Russell JH, Ley TJ (1994) Cytotoxic lymphocytes require granzyme B for the rapid induction of DNA fragmentation and apoptosis in allogeneic target cells. Cell 76(6):977–987
10. Hiebert PR, Granville DJ (2012) Granzyme B in injury, inflammation, and repair. Trends Mol Med 18(12):732–741
11. Afonina IS, Cullen SP, Martin SJ (2010) Cytotoxic and non-cytotoxic roles of the CTL/NK protease granzyme B. Immunol Rev 235(1):105–116
12. Walch M, Dotiwala F, Mulik S, Thiery J, Kirchhausen T, Clayberger C, Krensky AM, Martinvalet D, Lieberman J (2014) Cytotoxic cells kill intracellular bacteria through granulysin-mediated delivery of granzymes. Cell 157(6):1309–1323
13. Lee WY, Sanz MJ, Wong CH, Hardy PO, Salman-Dilgimen A, Moriarty TJ, Chaconas G, Marques A, Krawetz R, Mody CH, Kubes P (2014) Invariant natural killer T cells act as an extravascular cytotoxic barrier for joint-invading Lyme Borrelia. Proc Natl Acad Sci U S A 111(38):13936–13941
14. Kapelski S, de Almeida M, Fischer R, Barth S, Fendel R (2014) Antimalarial activity of granzyme B and its targeted delivery by a granzyme B-scFv fusion protein. Antimicrob Agents Chemother 59(1):669–672
15. Dotiwala F, Mulik S, Barbosa RP, Ansara JA, Burleigh B, Walch M, Gazzinelli RT, Lieberman J (2016) Killer lymphocytes use granulysin, perforin and granzymes to kill intracellular parasites. Nat Med 22:210–216
16. Su B, Bochan MR, Hanna WL, Froelich CJ, Brahmi Z (1994) Human granzyme B is essential for DNA fragmentation of susceptible target cells. Eur J Immunol 24(9):2073–2080
17. Thiery J, Walch M, Jensen DK, Martinvalet D, Lieberman J (2010) Isolation of cytotoxic T cell and NK granules and purification of their effector proteins. Curr Protoc Cell Biol 3:Unit 3 37
18. Froelich CJ, Turbov J, Hanna W (1996) Human perforin: rapid enrichment by immobilized metal affinity chromatography (IMAC) for whole cell cytotoxicity assays. Biochem Biophys Res Commun 229(1):44–49
19. Dotiwala F, Fellay I, Filgueira L, Martinvalet D, Lieberman J, Walch M (2015) A high yield and cost-efficient expression system of human granzymes in mammalian cells. J Vis Exp 100, e52911
20. Ernst WA, Thoma-Uszynski S, Teitelbaum R, Ko C, Hanson DA, Clayberger C, Krensky AM, Leippe M, Bloom BR, Ganz T, Modlin RL (2000) Granulysin, a T cell product, kills bacteria by altering membrane permeability. J Immunol 165(12):7102–7108

Chapter 19

In Vitro and In Vivo Biofilm Formation by Pathogenic Streptococci

Yashuan Chao, Caroline Bergenfelz, and Anders P. Håkansson

Abstract

This manuscript presents novel approaches to grow and evaluate Streptococcal biofilm formation using the human respiratory pathogen *Streptococcus pneumoniae* (the pneumococcus) as the main model organism on biological surfaces in vitro and in vivo. Most biofilm models are based on growth on abiotic surfaces, which is relevant for many pathogens whose growth on surfaces or medical devices is a major cause of disease transmission and infections, especially in hospital environments. However, most infections with commensal organisms require biofilm formation on biological surfaces in the host at the site of colonization or infection. In vitro model systems incorporating biological components from the host and taking into account the host environment of the infectious site are not well described.

In a series of publications, we have shown that *S. pneumoniae* form complex biofilms in the nasopharynx of mice and have devised methodology to evaluate the biofilm structure and function in this environment. We have also been able to recapitulate this biofilm phenotype in vitro by incorporating crucial factors associated with the host environment. Although the protocols presented in this manuscript are focused on *S. pneumoniae*, the same methodology can and has been used for other Streptococcal species that form biofilms on mucosal surfaces.

Key words Biofilm, *Streptococcus pneumoniae*, Streptococci, Epithelium, Mucosa, Nasopharynx, Colonization, Respiratory tract, Virulence

1 Introduction

Just like eukaryotic cells associate into tissues and organ structures, bacteria have been shown to form biofilms in nature, often containing bacteria with specialized functions benefiting the community [1, 2]. Biofilms are aggregations of microbes, usually polymicrobial, encased in and held together by a self-produced polymeric matrix. The biofilm structure and the distinct metabolism and gene expression profile of biofilm bacteria provide advantages for biofilm persistence in the host niche through increased resistance to environmental and host challenges [3–5]. It is estimated that 65–80% of infections are associated with

Pontus Nordenfelt and Mattias Collin (eds.), *Bacterial Pathogenesis: Methods and Protocols*, Methods in Molecular Biology, vol. 1535, DOI 10.1007/978-1-4939-6673-8_19,

microbial biofilms [1, 3] that either directly cause disease or act as a dormant reservoir of pathogenic organisms [6–8]. Biofilm formation on surfaces in hospital settings is also a major cause of bacterial spread [9, 10].

S. pneumoniae effectively colonizes the mucosal surface of the nasopharynx (NP). To remain in the harsh nasopharyngeal environment, it has been suggested that pneumococci form biofilms in vivo, as it is more difficult to eradicate colonization than infection [11, 12]. Work from our laboratory has confirmed these two observations in a colonization model in mice [13]. Pneumococcal biofilms have been detected in vivo during otitis media and chronic sinusitis [14–17] where they act as a reservoir for the release of pathogenic organisms [8] and constitute the main life form during colonization of the NP [13, 18–21].

In vitro modeling has shown a role for various virulence factors in biofilm formation [22–25], as well as an altered virulence gene expression leading to a decreased virulence of biofilm bacteria in vivo [26–28]. However, until recently, in vitro studies did not take the host environment, the only environment the pneumococcus colonizes, into consideration.

The methods described here were developed to mimic the biofilm formation in the NP environment [13, 21]. Pneumococcal biofilms were formed on respiratory epithelial cells, providing a relevant interaction with host tissue and at a lower temperature consistent with the NP environment in humans and mice [29]. Furthermore, biofilm growth was ameliorated when grown over at least 48 h in nutrient-limiting media, consistent with the high bacterial density and nutritional starvation typical of biofilms in general [30]. Using this setup, we obtained dense and well-structured biofilms encased in extracellular matrix with high tolerance to antibiotic treatment with most pneumococcal isolates tested, a phenotype not seen with biofilms grown on glass or plastic surfaces (Fig. 1; [13]). Furthermore, strains that showed higher propensity for colonization in animal models made in vitro biofilms with higher bacterial burden and a more intricate structure than more invasive strains [31].

Besides being a useful surrogate in vitro model for pneumococcal colonization, this model has been further used to verify that the biofilm colonization environment is responsible for the high levels of genetic recombination observed epidemiologically in pneumococci [32] and can also support natural transformation in group A streptococci [33].

The models described in this manuscript have also been very useful in better understanding the mechanisms involved in the transition from asymptomatic colonization to infection. Using the in vitro biofilm model, infection of the live epithelial cell substratum with influenza A virus (an epidemiological disease trigger; [34–36]) or treatment with virus-induced host factors caused active release of

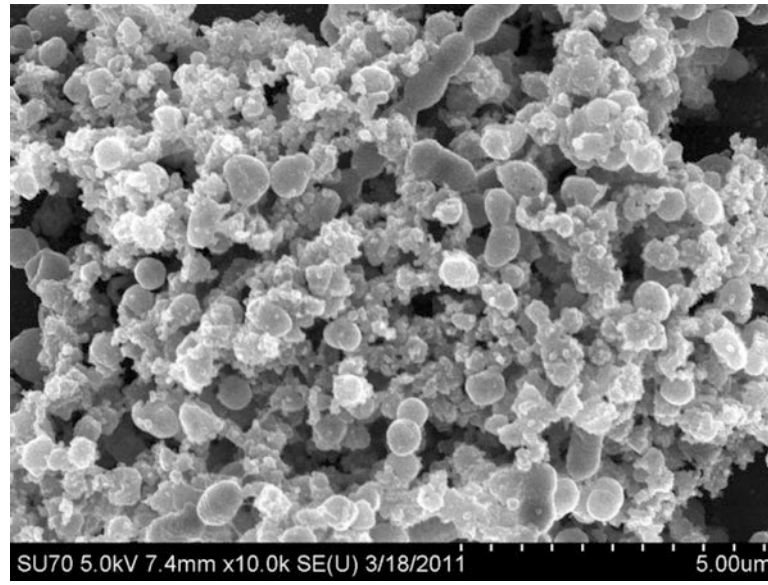

Fig. 1 A pneumococcal biofilm in high magnification in the early phase of biofilm formation (24 h). The image shows aggregation and organization of bacteria (diplococci) into clusters with empty spaces that will become pores and the formation of extracellular matrix encasing the bacteria. The matrix will end up holding the biofilm together and protecting it from the host environment

bacteria from the biofilm. These biofilm-dispersed bacteria were more virulent in models of pneumonia and sepsis than either biofilm bacteria or bacteria grown in broth [37], and were associated with a defined change in gene transcription that can be used to test and verify the biofilm phenotype using RNA-sequencing or quantitative reverse-transcriptase PCR (qRT-PCR; [38]).

These observations suggest that growth of biofilms under the conditions described in this manuscript could serve as a surrogate model for studies related to the colonization state of pneumococci and other Streptococcal species as well as a model to study the mechanisms of transition to disease.

2 Materials

2.1 Preparation of Bacterial Strains

1. Pneumococcal strains of interest.
2. Bacterial growth medium: Todd-Hewitt medium supplemented with 0.5 % yeast extract (THY; BD Bioscience). Ensure that the medium is autoclaved (preferred) or sterile filtered using a 0.45 μm vacuum-filter.

3. Spectrophotometer for measuring optical density at 600 nm (OD_{600}) (*see* **Note 1**).
4. Bacterial freezing solution: Glycerol (80% vol/vol; Sigma) in phosphate buffered saline (PBS, pH 7.2). Autoclaved (*see* **Note 2**).
5. Blood agar plates: Agar plates with 5% sheep blood can be purchased from ThermoFisher or other vendors. Plates can also be made in the lab (*see* **Note 3**).

2.2 Preparation of Epithelial Substratum

1. Cells*:* Epithelial cell lines, such as human mucoepidermoid pulmonary carcinoma cells NCI-H292 (CRL-1849; ATCC) or human lung carcinoma cells A549 (CCL-185; ATCC). (For other cell types that can be used, *see* **Note 4**).
2. Cell culture medium*:* RPMI-1640 medium with the addition of 10% fetal bovine serum (FBS) and 5 mM sodium pyruvate. For comments on other appropriate growth media for these and other cells (*see* **Note 4**).
3. Cell detachment: PBS (pH 7.2) for washing the cell monolayer. Trypsin-solution (Hyclone or other vendors) for detachment of cells.
4. Cell fixation: 4% buffered paraformaldehyde solution (PFA).

2.3 Biofilm Formation In Vitro on Pre-fixed Epithelial Cells

1. 24-well plate with substratum of epithelial cells pre-fixed in PFA.
2. Wash solution: PBS (pH 7.2) to wash away the PFA solution.
3. Frozen stock of bacteria (see section 2.1. above).
4. Chemically defined medium (CDM; 39) supplemented with 1 g/l choline chloride, 0.75 g/l L-cysteine hydrochloride, and 2.5 g/l of sodium bicarbonate. Sterile filter the medium through a 0.45 μm vacuum filter. (For full recipe *see* **Note 5**).

2.4 Biofilm Formation In Vitro on Live Epithelial Cells

1. 24-well plate with live, confluent epithelial cells.
2. Mature pneumococcal biofilms (preformed for 48 h on fixed epithelial cells).
3. Antibiotic-free RPMI-1640 medium (*see* Subheading 2.2, **item 2** above), supplemented with 5 mM sodium pyruvate and 2% FBS.

2.5 Biomass and Antibiotic Resistance of In Vitro Biofilms

1. Gentamicin solution (50 mg/ml; ThermoFisher or other vendors).
2. Blood agar plates (*see* Subheading 2.1, **item 5** above and **Note 3**).

2.6 RNA Isolation and qRT-PCR of In Vitro Biofilms

1. 0.9% NaCl solution in water treated with diethylpyrocarbonate (DEPC; Sigma).
2. RNAprotect (Qiagen).

3. Tris-EDTA-glucose solution: 10 mM Tris–HCl, 1 mM EDTA (pH 8.0), and 25% glucose (wt/vol) in DEPC-treated water.
4. Cell wall-degrading enzymes (Sigma): mutanolysin (5000 U/ml stock in DEPC-treated water), lysozyme (100 mg/ml stock in DEPC-treated water).
5. RNA purification: QiaShredder columns, RNeasy minikit, RNase-free DNase kit, RNase-free DNase I (Qiagen or Sigma).
6. Spectrophotometer with glass cuvettes for UV-readings (*see* **Note 6**).
7. Gel electrophoresis equipment and buffers: Gibco-Agarose (Invitrogen), TAE buffer (4.84 g/l Tris Base, 1.14 ml glacial acetic acid, and 100 ml of 0.5 M EDTA solution at pH 8.0 in water), gel electrophoresis system with power supply.
8. cDNA synthesis: iScript cDNA synthesis kit (Bio-Rad).
9. qRT-PCR: Primer pairs for genes of interest (*see* **Note 7**) and SYBR green supermix (Bio-Rad).

2.7 Biofilm Formation and Determination of Biomass In Vivo

1. Bacterial culture in THY medium.
2. Wash and resuspension buffer: PBS (pH 7.2).
3. 6–8 week old BALB/cByJ mice (*see* **Note 8**).
4. Dissection equipment: forceps, scissors, and homogenization bags.
5. Blood agar plates (*see* Subheading 2.1, **item 5** above, and **Note 3**).

2.8 Scanning Electron Microscopy (SEM)

1. Fixation solution (Sigma): 2.5% glutaraldehyde, 0.075% ruthenium red, 0.075 M lysine acetate in 0.1 M sodium cacodylate buffer (pH 7.2) (*see* **Note 9**).
2. Wash solution: 0.075% ruthenium red in 0.2 M sodium cacodylate buffer (pH 7.2).
3. Ethanol solutions (10, 30, 50, 75, 95, and 100%).
4. Hexamethyldisilazane (HMDS, 100%; Sigma).
5. SEM stubs and sputter coater.

3 Methods

3.1 Biofilm Formation In Vitro

Most pneumococcal strains have the capacity to produce well-structured, functional biofilms on respiratory epithelial cells, but form poor biofilms on abiotic surfaces [13]. The origin of the epithelial substratum appears to be of some importance as cells from the respiratory tract generally provide a better surface for pneumococcal biofilm formation than cells from other parts of the body. As pneumococci grown in broth show considerable toxicity toward live epithelial cells, biofilm formation on live cells requires the prior

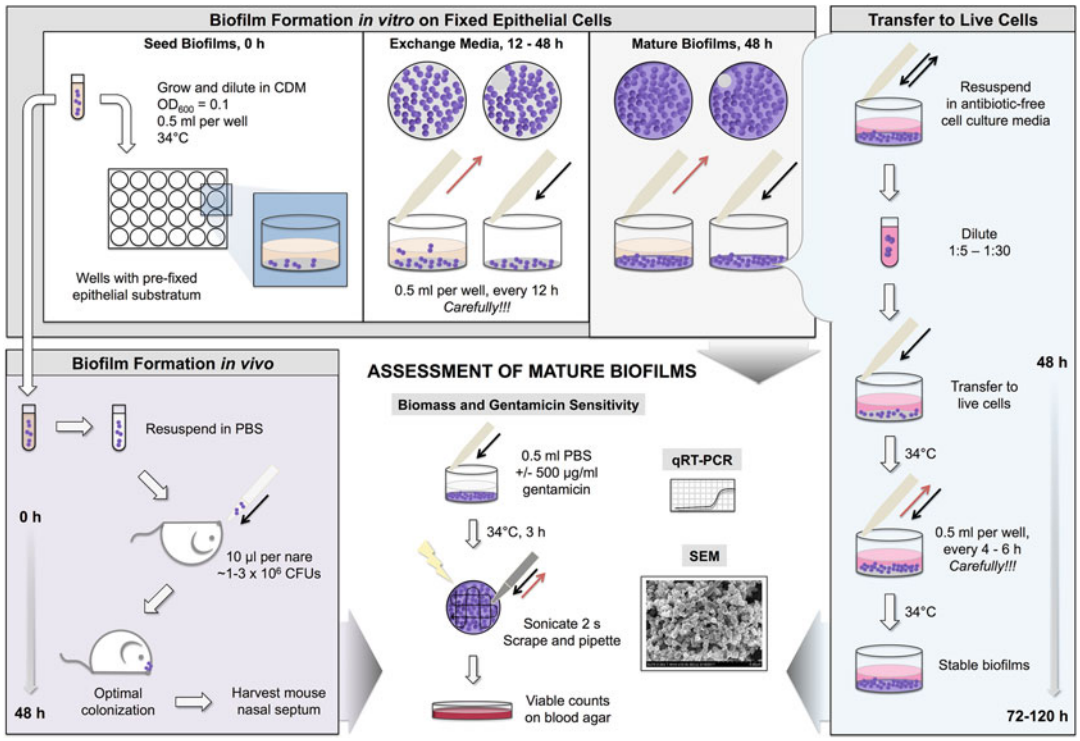

Fig. 2 A cartoon of the methodology presented in this protocol. Biofilm formation in vitro on fixed epithelial cells (Subheading 3.1.3) is shown in the *upper left corner* and transfer of biofilm bacteria to live epithelial cells (Subheading 3.1.4) is shown in the *right section* of the figure. Biofilm colonization in vivo (Subheading 3.2) is shown in the *lower left corner* and ways to assess the biofilm phenotype (Subheading 3.3) are shown in the *lower mid-section* of the cartoon

step of growing biofilms on fixed cells to allow down-regulation of virulence factors before bacteria are transferred to live epithelial cells [37, 38]. For a cartoon of the methodology presented in this paper, *see* Fig. 2.

3.1.1 Preparation of Bacterial Strains

1. Plate pneumococcal strain on blood agar and grow overnight at 37 °C (*see* **Note 10**).
2. Transfer bacteria from the blood agar plate to a 10-ml glass tube (16×100 mm) or a 15-ml conical tube containing 10 ml of THY using an inoculation loop. Tighten the caps and grow statically at 37 °C to an OD_{600} of approximately 0.6 (*see* **Note 11**).
3. Add 2 ml of 80 % glycerol solution (*see* **Note 2**) directly to the culture, mix by pipetting, and then transfer to microcentrifuge cryotubes in 1 ml aliquots.
4. Store aliquots at −80 °C (*see* **Note 12**).

3.1.2 Preparation of Epithelial Substratum

1. Propagate epithelial cell line(s) of choice in cell culture flasks.
2. Detach confluent cell monolayer from flask with trypsin solution, resuspend in 48 ml (T75 flask) fresh cell culture medium,

add 0.5 ml cell suspension per well in 24-well cell culture plates, and grow at 37 °C in 5% CO_2 until near-confluent.

3. Aspirate medium and wash cell substratum three times with 1 ml PBS per well to remove medium residues.
4. The confluent epithelial substratum can now either be (a) fixed by adding 0.5 ml of 4% PFA solution per well for 1 h at room temperature (fixed epithelia can be saved in PFA solution at 4 °C for up to a month, if kept hydrated), or (b) used immediately for biofilm formation on live epithelial substratum (*see* Subheading 3.1.4).

3.1.3 Biofilm Formation on Pre-fixed Epithelial Cells

1. Thaw a frozen stock of pneumococcal strain of interest.
2. Seed 1 ml frozen stock into 9 ml of chemically defined medium (CDM) into 10-ml glass tubes or 15-ml conical tubes and grow statically at 37 °C to an OD_{600} of approximately 0.2 (*see* **Notes 11** and **12**).
3. While the bacteria are growing, wash a 24-well plate containing pre-fixed epithelial substratum three times with 1 ml PBS per well. Allow 10 min between washes.
4. Dilute pneumococci 1:2 in CDM to an OD_{600} of approximately 0.1 and seed 0.5 ml pneumococcal suspension in each well containing fixed cells.
5. Incubate at 34 °C in 5% CO_2 for biofilm formation (*see* **Note 13**), carefully exchanging the supernatant with 0.5 ml fresh CDM approximately every 12 h (*see* **Note 14**). Avoid disturbing the biofilm as much as possible (*see* **Note 15**).
6. Grow biofilms for appropriate times, but for at least 48 h (*see* **Note 14**).

3.1.4 Biofilm Formation In Vitro on Live Epithelial Cells

1. Wash live, confluent epithelial cells (*see* Subheading 3.1.2, **step 4**) three times in 1 ml PBS per well (*see* **Note 16**).
2. Carefully remove the supernatant from 48-h biofilms formed on fixed epithelial cells.
3. Add 0.5 ml fresh antibiotic-free cell culture medium (prewarmed to 34 °C) and gently resuspend the biofilm by pipetting (*see* **Note 17**).
4. Dilute the bacterial biofilm from one well 1:5–1:30 in fresh antibiotic-free cell culture medium and add 0.5 ml per well to live, confluent epithelial cells.
5. Incubate at 34 °C in 5% CO_2, carefully exchanging the antibiotic-free cell culture medium frequently, preferably every 4–6 h for pneumococci (*see* **Note 18**).

6. A new biofilm will form within 24 h and the epithelial cells should be viable up to 72 h after transfer (*see* **Note 19**).

3.2 Biofilm Formation In Vivo: Colonization of the Nasopharynx of Mice

S. pneumoniae effectively colonizes the mucosal surface of the NP beginning within the first few weeks or months of life [39]. To remain in the harsh NP environment, pneumococci form biofilms in vivo that can be reproduced using the model described below (Fig. 2; [13]).

1. Thaw a frozen stock of the pneumococcal strain of interest (*see* **Note 20**).
2. Pellet the bacteria by centrifugation at 9000 × *g* for 2 min in a microcentrifuge, wash twice by resuspension in PBS followed by centrifugation, and resuspend the pellet in PBS to original volume.
3. Pipet 10 µl of bacterial suspension (approximately 1–3 × 10^6 CFUs) into each nare of non-anesthetized 6–8 week old BALB/cByJ mice (*see* **Notes 8** and **21**) and monitor mice for 48 h, at which point optimal colonization has occurred.

3.3 Assessment of Biofilms

Biofilm formation in vitro can be assessed in various ways to ensure an appropriate phenotype (*see* Fig. 2). Biofilms typically produce specific structures that can most effectively be observed by scanning electron microscopy [13]. This structural phenotype with matrix formation, together with an increased population of cells with a lowered metabolic rate, so-called persister cells [40], makes biofilms highly insensitive to antimicrobial agents and host response mechanisms [2]. The phenotypic change of the biofilm bacteria is associated with a dramatic transcriptional decrease in expression of genes associated with metabolism and virulence factors, with an increase in expression of genes associated with adherence to surfaces, quorum sensing, and competence [38, 41, 42]. This section describes methods to evaluate these biofilm features.

3.3.1 Determination of Biomass and Antibiotic Resistance In Vitro

1. Pipet off media from a biofilm (*see* Subheading 3.1) and treat in 0.5 ml PBS with or without 500 µg/ml gentamicin for 3 h at 34 °C in 5 % CO_2 (*see* **Note 22**).
2. Float the 24-well plate in a water bath sonicator and sonicate for 2 s to loosen all biofilm cells and disperse aggregates (*see* **Note 23**).
3. Scrape or pipet the bacteria from the bottom of the well and further disrupt the biofilm bacteria by pipetting up and down (*see* **Note 23**).
4. Determine total viable colony forming units (CFUs) per biofilm for initial biomass and antibiotic resistance by plating 100 µl of tenfold dilutions of the biofilm samples on blood agar plates, incubate at 37 °C overnight, and count plates containing 20–200 colonies to determine the CFU per ml.

3.3.2 Determination of Biomass In Vivo

1. Colonize mice as presented in Subheading 3.2 above.
2. Euthanize mice colonized with pneumococci (*see* Subheading 3.2 above) according to your approved animal use protocol (IACUC protocol).
3. First completely remove the skin from the skull and nose of the mouse using forceps and dissection scissors to remove fur.
4. Using dissection scissors, cut the maxillary bone on each side followed by an incision through the frontal skull bone just above the nasal bone.
5. Place forceps in the latter incision and slowly separate the nasal bone from the frontal bone by pushing the forceps on the nasal bone while holding the rest of the skull firmly in place. This reveals the nasal concha containing the nasal septum.
6. Carefully harvest the tissue attached to the ethmoid bone (medial bone in the concha) with forceps to keep the mucosal tissue intact.
7. Place tissue in a homogenization bag with 1 ml of PBS and homogenize the tissue.
8. Determine total CFUs per tissue by plate counts on blood agar (*see* Subheading 3.3.1, **step 4**).

3.3.3 RNA Isolation and Performance of qRT-PCR

1. For isolation of RNA from in vitro biofilms, sonicate and resuspend 48-h biofilms in PBS. For isolation of in vivo biofilms, use homogenized tissue suspension from Subheading 3.3.2. In both cases pellet bacteria by centrifugation at 9000 × *g* for 2 min at 4 °C in a microcentrifuge.
2. Resuspend pellets in 0.5 ml 0.9% NaCl, add 1 ml RNAprotect, and incubate for 5 min at room temperature.
3. Pellet bacteria by centrifugation at 9000 × *g* for 2 min in a microcentrifuge. Remove and discard supernatant by pipetting without disturbing the pellet. (The pellet can be stored at −80 °C at this time for later RNA purification or can be directly isolated as indicated in **step 4**).
4. Resuspend the preserved RNA pellet in 500 µl TE + 25% glucose.
5. Add 20 µl 100 mg/ml lysozyme and 10 µl of 5000 U/ml mutanolysin to break up the cell wall. Incubate at 37 °C in a water bath for 15 min.
6. Isolate RNA using Qiashredder columns and the RNeasy mini-kit according to the manufacturer's instructions. DNase I treatment can be performed on column during RNA isolation (Qiagen) or in solution after RNA isolation (Sigma).
7. Verify the RNA purity by measuring the 260/280 nm absorbance ratio in a spectrophotometer and assure that the ratio is above 2 (*see* **Note 6**).

8. Verify the RNA integrity by separating the RNA in a 1% agarose gel, by gel electrophoresis (*see* **Note 24**).
9. For qRT-PCR analysis of the RNA, reverse transcribe the RNA using the Bio-Rad iScript cDNA synthesis kit according to the manufacturer's instructions.
10. qRT-PCR: cDNA amplification is quantified using a Bio-Rad iCycler or similar instrument according to the manufacturer's instructions in the presence of SYBR green supermix and primers for *comD* (competence), *licD2* (cell wall synthesis), and *gyrA* (housekeeping gene) (*see* **Note 7**).

3.3.4 Scanning Electron Microscopy of In Vitro and In Vivo Biofilms

1. Fix biofilms grown in vitro on epithelial cells grown on round coverslips (*see* Subheading 3.1.3) or excised tissue from in vivo colonization in SEM fixation solution for 1 h at room temperature, changing the solution once during the process (*see* **Note 25**).
2. Wash in vitro or in vivo samples in wash solution three times, 15 min each time, at room temperature without shaking.
3. Dehydrate the samples with increasing graded series of ethanol solutions at room temperature for 15 min per concentration.
4. Exchange samples into enough 100% HMDS to coat the samples and allow to air dry in chemical hood. Repeat addition and evaporation of HMDS once.
5. Mount samples onto stubs and analyze morphology of biofilms and surrounding structures using scanning electron microscopy (*see* **Note 26**).

4 Notes

1. The $OD_{600\ nm}$ can be followed in different ways. We recommend using the glass tubes together with a Spectronic™ Spectrophotometer that has a compartment for test tubes. Alternatively, the OD of the culture can be measured in any regular spectrophotometer with a sterile cuvette (1 cm path length).
2. 80% glycerol solution has decreased viscosity that facilitates pipetting.
3. To make blood agar plates, mix Tryptic Soy Broth, Bacto-agar (5 g/l) (BD Biosciences) and water, then autoclave. Once cooled, add 5% sheep blood and pour approximately 10 ml of blood agar in each Petri dish and let it solidify at room temperature.
4. Other cell lines, such as Detroit 562 (CCL-138; ATCC) pharyngeal carcinoma cells and Calu-3 (HTB-55; ATCC) lung adenocarcinoma cells are also suitable. Additionally, primary

bronchial epithelial cells commercially available from Lonza (NHBE) or ATCC (PCS-300-010) can also be used with their recommended media.

5. CDM recipe [43]: Make a powder consisting of 10 g/l glucose, 4.5 g/l sodium acetate $3H_2O$, 3.195 g/l sodium phosphate monobasic H_2O, 7.35 g/l sodium phosphate dibasic, anhydrous, 1 g/l potassium phosphate monobasic, 0.2 g/l potassium phosphate dibasic, 0.7 g/l magnesium sulfate $7H_2O$, 0.005 g/l manganese sulfate anhydrous, 0.005 g/l ferrous sulfate $7H_2O$, 0.001 g/l ferric nitrate $9H_2O$, 0.005 g/l calcium chloride anhydrous, 0.1 g/l each of DL-alanine, L-arginine, L-aspartic acid, L-glutamic acid, glycine, L-histidine, hydroxy-L-proline, L-isoleucine, L-leucine, L-lysine, L-methionine, L-phenylalanine, L-proline, L-serine, L-tryptophan, L-tyrosine, and L-valine, 0.5 g/l L-cysteine, 0.05 g/l L-cystine 2HC1, 0.2 g/l each of L-glutamine and L-threonine, 0.02 g/l each of adenine, guanine HCI, and uracil, 0.0002 g/l each of PABA and biotin, 0.0008 g/l folic acid, 0.01 g/l niacinamide, 0.0025 g/l B-NAD, 0.002 g/l D-Ca pantothenate, 0.001 g/l each of pyridoxal HCl and pyridoxamine 2HC1, 0.002 g/l riboflavin, 0.001 g/l thiamine HCl, 0.0001 g/l cyanocobalamin, 2.5 g/l sodium bicarbonate. This powder is stable at 4 °C for several months. Resuspend 27.12 g of powder per liter deionized water and add 1 g/l choline chloride, 0.75 g/l L-cysteine HCl and add an additional 2.5 g/l of sodium bicarbonate to freshly made medium.
6. RNA purity (absorbance ratio 260/280 nm) is most commonly measured using special spectrophotometers, such as the Nanodrop One (Thermo Scientific) or special inserts to plate readers, but can also be measured in glass cuvettes in any spectrophotometer.
7. As biofilm down-regulate genes associated with cell toxicity and virulence and up-regulate colonization factors, the pneumococcal biofilm phenotype can be verified by qRT-PCR. Primers for *comD* (forward: 5′-GGTTCGTATCATGAGCGTTT and reverse: 5′-CCTGAAGGAGTCATCGTCAT) and *licD2* (forward: 5′-ACGAGCAGTTCACGGTGATAGCAA and reverse: 5′-ATCCCTTCCTTACCGATCCCAACT) that are up-regulated in biofilms were used. The cDNA amplification using these primer pairs was compared with the gene *gyrA* that was stably expressed in all populations in the RNA-seq analysis [38] (forward: 5′-ATGGTCTCAAAGCGCTGAAT and reverse: 5′-TGGCGATACGACTCATACCA). Broth-grown bacteria served as a control as *comD* and *licD2* are down-regulated in these bacteria [38].
8. Colonization experiments with pneumococci have also been successful in C57BL/6 inbred mice and CD-1 outbred mice.

9. To retain polysaccharide matrix during SEM preparation, L-lysine and ruthenium red are added to the buffers as described by Hammerschmidt et al. [44].
10. Pneumococci are sensitive to optochin and will show a growth inhibition zone around an optochin disc (Sigma) placed on a blood agar plate after overnight growth. This is done to distinguish pneumococci from other viridans streptococci.
11. As pneumococci are facultative anaerobes, incubate without shaking and with the tubes capped. Avoid exceeding OD_{600} of 0.6 (mid-logarithmic phase corresponding to approximately 3×10^8 CFU/ml) as pneumococci undergo autolysis at higher ODs.
12. Preparation of frozen stocks is recommended as liquid cultures seeded from pneumococci grown on blood agar plates grow slowly. Moreover, frozen stocks enable (a) seeding biofilms earlier in the day and (b) providing more reproducibility.
13. The temperature of 34 °C is chosen as this is the temperature of the NP environment [29] and also improves biofilm formation compared to 37 °C [13, 37].
14. The medium is of great importance for biofilm formation. Biofilms do not form well in nutrient-rich media (such as THY and Brain Heart Infusion) [13, 32]. Seed the bacteria as early as possible during the day to enable change of the medium later the same day. Changing medium regularly is of great importance to prevent the pneumococci from undergoing autolysis and will ensure that the biofilm remains stable for up to a week. Pneumococci generally form robust biofilms by 48 h with change of media every 12 h. However, depending on species and strain of bacteria, growth time and frequency of media change may vary.
15. This is the most critical step of the procedure. During the first 24 h, the biofilms are delicate and must be handled gently when removing and replacing the media. *Do not use a vacuum aspirator*. A 10-ml serological pipette induces less shear force and works better than a 1-ml pipette tip in this regard.
16. This wash step is to remove traces of antibiotics from the cell culture medium.
17. Avoid pipetting or vortexing the biofilm too vigorously as the biofilm will reform faster if aggregates are present. This can be verified in a microscope.
18. Change medium carefully as the biofilms are delicate during the process of reformation (*see* **Notes 15** and **17**). Changing medium frequently is important for the viability of the epithelial cells as the nutrients are rapidly consumed. Using pre-warmed

medium (34 °C) is recommended for keeping the temperature constant.

19. Planktonic, broth-grown pneumococci induce epithelial cell death within 12 h of exposure [37]. Based on the down-regulation of virulence factors, biofilm bacteria are less toxic to live epithelial cells. The time required to reform a mature biofilm on live cells varies between species and strains, but usually takes between 24 and 48 h.
20. Frozen stocks are advantageous for these experiments as aliquots have been made and the exact concentration of bacteria in CFU/ml will be known.
21. Pipetting into the nare is most easily done by holding the mouse firmly upside down and pipetting the bacterial suspension slowly.
22. The biomass of a mature biofilm should be in the range of 1×10^7–3×10^8 CFU/ml. Antibiotic tolerance to gentamicin indicates a structurally intact and functional biofilm, and a robust biofilm will tolerate gentamicin exposure well (generally less than 1 log10 decrease is seen compared with an untreated biofilm). Gentamicin is used as it penetrates biofilms poorly [45, 46]. The concentration used may vary depending on strain. Thus use a concentration that reduced the viability of planktonic organisms in broth of the strain used 6 log10. For *S. pneumoniae* 500 μg/ml used over the incubation time mentioned is most often appropriate. Penicillin G can be used instead of gentamicin at a concentration of 1 μg/ml for pneumococci, which is the concentration that will reduce the bacterial burden 6 log10 of a planktonic culture [13].
23. Sonication will loosen the biofilm aggregates. However, do not sonicate longer than 2 s as the bacteria may lyse. Use the pointy end of a 20–200 μl pipette tip and scrape the bottom of the 24-well plate from top to bottom and left to right. Pipette the suspension up and down vigorously, without introducing bubbles, to further disrupt the biofilm bacteria. It is important to disrupt the biofilm bacteria into single cells for accurate viable plate counts. Verify in microscope before plating.
24. Separation of RNA by gel electrophoresis should provide two distinct bands representing rRNA as well as a high molecular weight smear of mRNA. A low molecular weight smear indicates degraded RNA that will not work well in the qRT-PCR reaction.
25. For SEM analyses, grow epithelial cells on round coverslips placed into a 24-well plate. Once confluent, fix the epithelial substratum as described in Subheading 3.1.2.
26. If charging occurs when imaging the biofilms, the samples can be sputter coated, e.g., chromium coated.

References

1. Costerton JW, Stewart PS, Greenberg EP (1999) Bacterial biofilms: a common cause of persistent infections. Science 284:1318–1322
2. Fux CA, Stoodley P, Hall-Stoodley L, Costerton JW (2003) Bacterial biofilms: a diagnostic and therapeutic challenge. Expert Rev Anti Infect Ther 1:667–683
3. Wolcott RD, Ehrlich GD (2008) Biofilms and chronic infections. JAMA 299:2682–2684
4. Domenech M, García E, Prieto A, Moscoso M (2013) Insight into the composition of the intercellular matrix of *Streptococcus pneumoniae* biofilms. Environ Microbiol 15:502–516
5. Hernandez-Jimenez E, Del Campo R, Toledano V, Vallejo-Cremades MT, Munoz A, Largo C, Arnalich F, Garcia-Rio F, Cubillos-Zapata C, Lopez-Collazo E (2013) Biofilm vs. planktonic bacterial mode of growth: which do human macrophages prefer? Biochem Biophys Res Commun 441:947–952
6. Nistico L, Kreft R, Gieseke A, Coticchia JM, Burrows A, Khampang P, Liu Y, Kerschner JE, Post JC, Lonergan S, Sampath R, Hu FZ, Ehrlich GD, Stoodley P, Hall-Stoodley L (2011) An adenoid reservoir for pathogenic biofilm bacteria. J Clin Microbiol 49(4):1411–1420
7. Napimoga MH, Hofling JF, Klein MI, Kamiya RU, Goncalves RB (2005) Transmission, diversity and virulence factors of *Streptococcus mutans* genotypes. J Oral Sci 47:59–64
8. Weimer KE, Armbruster CE, Juneau RA, Hong W, Pang B, Swords WE (2010) Coinfection with *Haemophilus influenzae* promotes pneumococcal biofilm formation during experimental otitis media and impedes the progression of pneumococcal disease. J Infect Dis 202:1068–1075
9. Bloomfield S, Exner M, Flemming HC, Goroncy-Bermes P, Hartemann P, Heeg P, Ilschner C, Krämer I, Merkens W, Oltmanns P, Rotter M, Rutala WA, Sonntag HG, Trautmann M (2015) Lesser-known or hidden reservoirs of infection and implications for adequate prevention strategies: where to look and what to look for. GMS Hyg Infect Control 10:Doc04
10. Dettenkofer M, Block C (2005) Hospital disinfection: efficacy and safety issues. Curr Opin Infect Dis 18:320–325
11. Dabernat H, Geslin P, Megraud F, Begue P, Boulesteix J, Dubreuil C, de La Roque F, Trinh A, Scheimberg A (1998) Effects of cefixime or coamoxiclav treatment on nasopharyngeal carriage of *Streptococcus pneumoniae* and *Haemophilus influenzae* in children with acute otitis media. J Antimicrob Chemother 41:253–258
12. Dagan R, Leibovitz E, Greenberg D, Yagupsky P, Fliss DM, Leiberman A (1998) Dynamics of pneumococcal nasopharyngeal colonization during the first days of antibiotic treatment in pediatric patients. Pediatr Infect Dis J 17:880–885
13. Marks LR, Parameswaran GI, Hakansson AP (2012) Pneumococcal interactions with epithelial cells are crucial for optimal biofilm formation and colonization in vitro and in vivo. Infect Immun 80:2744–2760
14. Ehrlich GD, Veeh R, Wang X, Costerton JW, Hayes JD, Hu FZ, Daigle BJ, Ehrlich MD, Post JC (2002) Mucosal biofilm formation on middle-ear mucosa in the chinchilla model of otitis media. JAMA 287:1710–1715
15. Sanderson AR, Leid JG, Hunsaker D (2006) Bacterial biofilms on the sinus mucosa of human subjects with chronic rhinosinusitis. Laryngoscope 116:1121–1126
16. Hall-Stoodley L, Hu FZ, Gieseke A, Nistico L, Nguyen D, Hayes J, Forbes M, Greenberg DP, Dice B, Burrows A, Wackym PA, Stoodley P, Post JC, Ehrlich GD, Kerschner JE (2006) Direct detection of bacterial biofilms on the middle-ear mucosa of children with chronic otitis media. JAMA 296:202–211
17. Reid SD, Hong W, Dew KE, Winn DR, Pang B, Watt J, Glover DT, Hollingshead SK, Swords WE (2009) *Streptococcus pneumoniae* forms surface-attached communities in the middle ear of experimentally infected chinchillas. J Infect Dis 199:786–794
18. Charalambous BM, Leung MH (2012) Pneumococcal sepsis and nasopharyngeal carriage. Curr Opin Pulm Med 18:222–227
19. Shak JR, Vidal JE, Klugman KP (2013) Influence of bacterial interactions on pneumococcal colonization of the nasopharynx. Trends Microbiol 21:129–135
20. Gilley RP, Orihuela CJ (2014) Pneumococci in biofilms are non-invasive: implications on nasopharyngeal colonization. Front Cell Infect Microbiol 4:163
21. Chao Y, Marks LR, Pettigrew MM, Hakansson AP (2015) *Streptococcus pneumoniae* biofilm formation and dispersion during colonization and disease. Front Cell Infect Microbiol 4:194 (1–16)
22. Allegrucci M, Hu FZ, Shen K, Hayes J, Ehrlich GD, Post JC, Sauer K (2006) Phenotypic characterization of *Streptococcus pneumoniae* biofilm development. J Bacteriol 188:2325–2335
23. Moscoso M, Garcia E, Lopez R (2006) Biofilm formation by *Streptococcus pneumoniae*: role of choline, extracellular DNA, and capsular

polysaccharide in microbial accretion. J Bacteriol 188:7785–7795

24. Munoz-Elias EJ, Marcano J, Camilli A (2008) Isolation of *Streptococcus pneumoniae* biofilm mutants and their characterization during nasopharyngeal colonization. Infect Immun 76:5049–5061
25. Sanchez CJ, Shivshankar P, Stol K, Trakhtenbroit S, Sullam PM, Sauer K, Hermans PW, Orihuela CJ (2010) The pneumococcal serine-rich repeat protein is an intra-species bacterial adhesin that promotes bacterial aggregation in vivo and in biofilms. PLoS Pathog 6:e1001044
26. Yadav MK, Kwon SK, Cho CG, Park SW, Chae SW, Song JJ (2012) Gene expression profile of early in vitro biofilms of *Streptococcus pneumoniae*. Microbiol Immunol 56:621–629
27. Sanchez CJ, Kumar N, Lizcano A, Shivshankar P, Dunning Hotopp JC, Jorgensen JH, Tettelin H, Orihuela CJ (2011) *Streptococcus pneumoniae* in biofilms are unable to cause invasive disease due to altered virulence determinant production. PLoS One 6:e28738
28. Blanchette-Cain K, Hinojosa CA, Akula Suresh Babu R, Lizcano A, Gonzalez-Juarbe N, Munoz-Almagro C, Sanchez CJ, Bergman MA, Orihuela CJ (2013) *Streptococcus pneumoniae* biofilm formation is strain dependent, multifactorial, and associated with reduced invasiveness and immunoreactivity during colonization. MBio 4:e00745–13
29. Keck T, Leiacker R, Riechelmann H, Rettinger G (2000) Temperature profile in the nasal cavity. Laryngoscope 110:651–654
30. Fux CA, Costerton JW, Stewart PS, Stoodley P (2005) Survival strategies of infectious biofilms. Trends Microbiol 13:34–40
31. Lizcano A, Chin T, Sauer K, Tuomanen EI, Orihuela CJ (2010) Early biofilm formation on microtiter plates is not correlated with the invasive disease potential of *Streptococcus pneumoniae*. Microb Pathog 48:124–130
32. Marks LR, Reddinger RM, Hakansson AP (2012) High levels of genetic recombination during nasopharyngeal carriage and biofilm formation in *Streptococcus pneumoniae*. MBio 3:e00200–12
33. Mashburn-Warren L, Morrison DA, Federle MJ (2012) The cryptic competence pathway in *Streptococcus pyogenes* is controlled by a peptide Pheromone. J Bacteriol 194:4589–4600
34. Chonmaitree T, Howie VM, Truant AL (1986) Presence of respiratory viruses in middle ear fluids and nasal wash specimens from children with acute otitis media. Pediatrics 77:698–702
35. Diavatopoulos DA, Short KR, Price JT, Wilksch JJ, Brown LE, Briles DE, Strugnell RA, Wijburg OL (2010) Influenza A virus facilitates *Streptococcus pneumoniae* transmission and disease. FASEB J 24(6):1789–1798
36. Pettigrew MM, Gent JF, Pyles RB, Miller AL, Nokso-Koivisto J, Chonmaitree T (2011) Viral-bacterial interactions and risk of acute otitis media complicating upper respiratory tract infection. J Clin Microbiol 49:3750–3755
37. Marks LR, Davidson BA, Knight PR, Hakansson AP (2013) Interkingdom signaling induces *Streptococcus pneumoniae* biofilm dispersion and transition from asymptomatic colonization to disease. MBio 4:e00438–13
38. Pettigrew MM, Marks LR, Kong Y, Gent JF, Roche-Hakansson H, Hakansson AP (2014) Dynamic changes in the *Streptococcus pneumoniae* transcriptome during transition from biofilm formation to invasive disease upon influenza A virus infection. Infect Immun 82:4607–4619
39. Kadioglu A, Weiser JN, Paton JC, Andrew PW (2008) The role of *Streptococcus pneumoniae* virulence factors in host respiratory colonization and disease. Nat Rev Microbiol 6:288–301
40. Lewis K (2010) Persister cells. Annu Rev Microbiol 64:357–372
41. Oggioni MR, Trappetti C, Kadioglu A, Cassone M, Iannelli F, Ricci S, Andrew PW, Pozzi G (2006) Switch from planktonic to sessile life: a major event in pneumococcal pathogenesis. Mol Microbiol 61:1196–1210
42. Vidal JE, Howery KE, Ludewick HP, Nava P, Klugman KP (2013) Quorum-sensing systems LuxS/autoinducer 2 and Com regulate *Streptococcus pneumoniae* biofilms in a bioreactor with living cultures of human respiratory cells. Infect Immun 81:1341–1353
43. van de Rijn I, Kessler RE (1980) Growth characteristics of group A streptococci in a new chemically defined medium. Infect Immun 27:444–448
44. Hammerschmidt S, Wolff S, Hocke A, Rosseau S, Muller E, Rohde M (2005) Illustration of pneumococcal polysaccharide capsule during adherence and invasion of epithelial cells. Infect Immun 73:4653–4667
45. Carmen JC, Nelson JL, Beckstead BL, Runyan CM, Robison RA, Schaalje GB, Pitt WG (2004) Ultrasonic-enhanced gentamicin transport through colony biofilms of *Pseudomonas aeruginosa* and *Escherichia coli*. J Infect Chemother 10:193–199
46. Abdi-Ali A, Mohammadi-Mehr M, Agha Alaei Y (2006) Bactericidal activity of various antibiotics against biofilm-producing *Pseudomonas aeruginosa*. Int J Antimicrob Agents 27:196–200

Chapter 20

Murine *Mycobacterium marinum* Infection as a Model for Tuberculosis

Julia Lienard and Fredric Carlsson

Abstract

Mycobacteria are a major human health problem globally. Regarding tuberculosis the situation is worsened by the poor efficacy of current vaccine regimens and by emergence of drug-resistant strains (Manjelievskaia J et al, Trans R Soc Trop Med Hyg 110: 110, 2016; Pereira et al., Lancet Infect Dis 12:300–306, 2012; http://www.who.int/tb/publications/global_report/en/) undermining both disease-prevention and available treatments. Thus, increased basic understanding of mycobacterial—and particularly *Mycobacterium tuberculosis*—virulence strategies and pathogenesis is of great importance. To this end several in vivo infection models are available (Guirado and Schlesinger, Front Immunol 4:98, 2013; Leung et al., Eur J Immunol 43:2246–2254, 2013; Patel et al., J Lab Physicians 3:75–79, 2011; van Leeuwen et al., Cold Spring Harb Perspect Med 5:a018580, 2015). While these models all have their merits they also exhibit limitations, and none perfectly mimics all aspects of human tuberculosis. Thus, there is a need for multiple models that may complement each other, ultimately allowing us to gain true insight into the pathogenesis of mycobacterial infections.

Here, we describe a recently developed mouse model of *Mycobacterium marinum* infection that allows kinetic and quantitative studies of disease progression in live animals [8]. Notably, this model exhibits features of human tuberculosis not replicated in *M. tuberculosis* infected mice, and may provide an important complement to the field. For example, granulomas in the *M. marinum* model develop central caseating necrosis (Carlsson et al., PLoS Pathog 6:e1000895, 2010), a hallmark of granulomas in human tuberculosis normally not replicated in murine *M. tuberculosis* infection. Moreover, while tuberculosis is heterogeneous and presents with a continuum of active and latent disease, *M. tuberculosis* infected mice essentially lack this dynamic range and do not replicate latency (Guirado and Schlesinger, Front Immunol 4:98, 2013; Patel et al., J Lab Physicians 3(2):75–79, 2011). In contrast, *M. marinum* infected mice may naturally develop latency, as suggested by reduced inflammation and healing of the diseased tissue while low numbers of bacteria persist in granulomatous lesions (Carlsson et al., PLoS Pathog 6:e1000895, 2010). Thus, infection with *M. marinum* may offer a unique murine model for studying granuloma formation as well as latency—and possibly also for studies of disease-reactivation. In addition to the in vivo model, we describe infection of bone marrow-derived murine macrophages, an in vitro platform enabling detailed mechanistic studies of host-pathogen interactions occurring in the principal host target cell for pathogenic mycobacteria.

Key words Tuberculosis, *Mycobacterium marinum*, Mouse model, Bone marrow-derived macrophages, Granuloma formation, Caseating necrosis, Latency, Chronicity, Host-pathogen interactions

Pontus Nordenfelt and Mattias Collin (eds.), *Bacterial Pathogenesis: Methods and Protocols*, Methods in Molecular Biology, vol. 1535, DOI 10.1007/978-1-4939-6673-8_20,

1 Introduction

It is estimated that one third of the world's population is infected with *M. tuberculosis*, a human pathogen responsible for ~1.5 million deaths annually [3]. To facilitate fundamental studies into *M. tuberculosis* pathogenesis and virulence mechanisms, safer and experimentally more amenable mycobacterial species may be used as models. Among these, the closely related *M. marinum* is emerging as a particularly relevant system [9–11]. *M. marinum* is a natural pathogen of fish and amphibians where it causes disease with many features of tuberculosis [12]. It is also able to infect immunocompetent humans and induce formation of dermal granulomas pathologically very similar to those formed in tuberculosis patients [12, 13]. Thus, *M. marinum* is a virulent mycobacterium, which shares virulence factors as well as mechanisms of inducing and maintaining infection with *M. tuberculosis* [14]. This situation gives *M. marinum* an advantage to study mycobacterial pathogenesis compared to, for example, the attenuated *Mycobacterium bovis* Bacille Calmette-Guérin (BCG) strain, which lacks critical virulence determinants. Importantly, however, *M. marinum* is generally unable to produce systemic infection in humans, presumably due to its low optimal growth temperature (~32 °C), and poses a reduced risk for laboratory personnel compared to *M. tuberculosis*, allowing work to be carried out in BSL-2 facilities. Moreover, *M. marinum* replicates significantly faster than *M. tuberculosis*, and there are genetic tools available enabling relatively rapid genetic screens and construction of targeted knockout strains.

Here, we describe an in vivo mouse model of *M. marinum* infection as well as infection of bone marrow-derived macrophages in vitro. The latter provides an experimentally tractable platform for molecular studies of the host-pathogen interactions occurring between mycobacteria and macrophages, which represent the primary growth niche for both *M. tuberculosis* and *M. marinum* in vivo [9, 12]. The in vivo model is based on intravenous injection of bacteria via the tail vein. Upon injection *M. marinum* is seeded systemically, but is unable to colonize internal organs productively while it successfully establishes and maintains colonization in the cooler areas of the mouse, primarily the tail [8, 15]. Tropism for the tail is likely due to the low optimal growth temperature of the bacteria and the cooler environment provided in this tissue, and not merely a consequence of inoculation at the site of injection; indeed, intracardiac injection of *M. marinum* similarly produces infection primarily in the tail [8]. *M. marinum* shows growth during the first 3 weeks of infection, after which bacterial numbers are significantly reduced and subsequently maintained at a low level for extended periods of time—a feature that might be explained by onset of adaptive immunity [8], which is typically initiated ~20 days

postinfection in *M. tuberculosis* infected mice [16, 17]. In accordance with its tissue tropism *M. marinum* cause disease in the tail. Visible lesions appear in the tail ~1 week postinfection, and over the course of the first 3–4 weeks of infection the lesions increase in size and become more numerous (*see* Fig. 1). Notably, however, the lesions regress and eventually heal following the decreased bacterial load observed after 3 weeks. Importantly, determination of the accumulated length of all visible lesions in individual tails allows for quantitative and longitudinal studies of disease progression in live mice [8, 15]. Moreover, *M. marinum* infection causes erosion of tail vertebrae, a trait that can be quantitated by measuring bone volume using micro-computed tomography (micro-CT), and represents an indirect readout of inflammation [8]. Thus, two different quantitative traits, visible tail lesions and bone volume, may be used to measure disease and inflammation during infection. Our protocol will describe the infection procedure, analysis of bacterial growth as well as aforementioned traits. Additional procedures that will be described include how the tail is prepared for

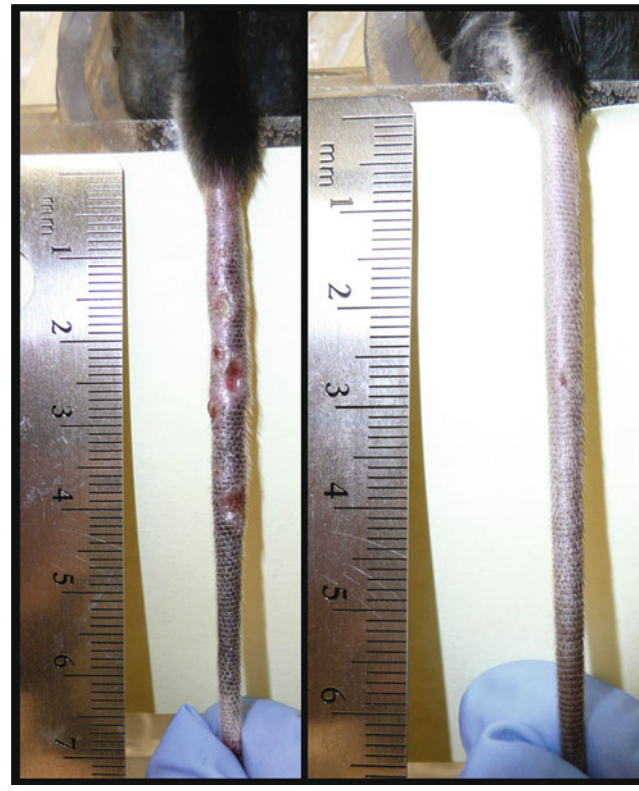

Fig. 1 Analyses of visible tail lesions 20 days postinfection. C57BL/6 mice infected with wild-type *M. marinum* (*left* picture) and an isogenic ESX-1-deficient (ΔRD1) mutant (*right* picture) unable to produce disease in infected animals

immunohistochemistry analysis as well as how tail tissue is prepared for analysis of cytokines and protein content in general using, for example, ELISA and Western blot.

2 Materials

1. Albumin-Dextrose-Catalase (ADC) enrichment: 5% bovine albumin fraction V, 2% dextrose, 0.003% catalase, distilled H_2O. Filter-sterilize.
2. Amikacin.
3. Biopulverizer.
4. Bone marrow-derived macrophage medium (BMM): RPMI, 5% 3 T3-CSF-cell conditioned medium, 5% heat-inactivated fetal calf serum, 2 mM L-Glutamine.
5. Fibronectin-coated glass cover slips (22 or 15 mm in diameter; 0.13–0.16 mm in thickness).
6. Freezing medium: Heat-inactivated fetal calf serum supplemented with 5% DMSO. Filter-sterilize.
7. Hemacytometer.
8. Immunocal (Decal Chemical Corp).
9. Lysis buffer: 150 mM sodium chloride, 1.0% NP-40, 50 mM Tris base (pH 8.0), protease inhibitor cocktail. Depending on the experiment, phosphatase inhibitor cocktail can also be added.
10. Micro-computed tomography (micro-CT) scanner.
11. Mowiol (for 50 ml): 6 g glycerol, 2.4 g Mowiol, 6 ml distilled H_2O, 12 ml 0.2 M Tris (pH 8.5). *See* **Note 1** for preparation.
12. Oleic acid-Albumin-Dextrose-Catalase (OADC) enrichment: 0.06% oleic acid, 5% bovine albumin fraction V, 2% dextrose, 0.003% catalase, 0.85% sodium chloride, distilled H_2O. Filter-sterilize.
13. Paraformaldehyde 4% (for 100 ml): 4 g paraformaldehyde to 100 ml PBS, 1N NaOH. *See* **Note 2** for preparation.
14. Tissue homogenizer (providing ≥70 W output power) with ~105 × 10 mm saw tooth adaptors.
15. Trypsin-EDTA solution: Hank's balanced salt solution with phenol red, 2.5 g/l porcine trypsin, 0.2 g/l EDTA.
16. Square petri dishes (100 × 15 mm) with a grid forming 6 by 6 squares.
17. 3T3 medium: DMEM, 10% heat-inactivated fetal calf serum, 2 mM l-Glutamine.
18. 7H9 (composition per liter): 4.7 g Middlebrook 7H9 powder (2.5 g disodium phosphate, 1.0 g monopotassium phosphate, 0.5 g l-glutamic acid, 0.5 g ammonium sulfate, 0.1 g sodium

citrate, 0.05 g magnesium sulfate, 0.04 g ferric ammonium citrate, 2.0 mg Mycobactin J, 1.0 mg copper sulfate, 1.0 mg pyridoxine, 1.0 mg zinc sulfate, 0.5 mg biotin, 0.5 mg calcium chloride), 2 ml glycerol, 0.5 g tween 80, 100 ml ADC, distilled H_2O (to 1 l). Filter-sterilize.

19. 7H10 agar (composition per liter): 19.47 g Middlebrook 7H10 powder (15 g agar, 1.5 g disodium phosphate, 1.5 g monopotassium phosphate, 0.5 g ammonium sulfate, 0.5 g l-glutamic acid, 0.4 g sodium citrate, 0.04 g ferric ammonium citrate, 0.025 g magnesium sulfate, 1.0 mg zinc sulfate, 1.0 mg copper sulfate, 1.0 mg pyridoxine hydrochloride, 0.5 mg biotin, 0.5 mg calcium chloride, 0.25 mg malachite green), 5 ml glycerol, distilled H_2O (to 900 ml). Sterilize by autoclaving 20 min. 100 ml pre-warmed OADC is added after autoclavation when the solution is around 50 °C.
20. 26G1/2 needles.

3 Methods

3.1 Mouse Infection Model

3.1.1 Preparation of *M. marinum* for Infection

1. Grow *M. marinum* in 25 ml 7H9 broth to logarithmic growth phase ($OD_{600} = 0.7 \pm 0.2$) at 30 °C under slow shaking conditions (about 100 rpm).
2. Collect culture by centrifugation ($2500 \times g$, 10 min) and wash twice in PBS (final resuspension should be done in 9 ml to obtain an appropriate bacterial concentration).
3. Pass the suspension through a 26G1/2 needle three times to disrupt bacterial aggregates ("shoot" the suspension against the wall of a 15 ml conical to ensure efficient disruption of aggregates).
4. Pellet remaining bacterial aggregates by two separate centrifugation steps ($450 \times g$, 1 min), where the supernatants—enriched for single cell bacteria—are transferred to new tubes. Subsequently, the bacterial suspensions may be analyzed by light microscopy to confirm the absence of bacterial aggregates.
5. Determine the bacterial concentration by counting cells in a hemacytometer, using a ≥60× objective. Dilute the suspension in PBS to a final concentration of 5×10^7 bacteria/ml. Place the bacteria on ice until infection of mice.
6. To determine the actual inoculum used, perform a serial dilution (five times tenfold dilution steps) in PBS and plate on dry 7H10 agar plates for calculation of colony forming units (CFUs) per ml. For simplicity, use square petri dishes with a grid. Drop 10 μl from each dilution into squares, let dry and place in 30 °C incubator. Of note, plates may be placed in a sealed plastic back to avoid drying.

3.1.2 Tail Vein Injection

1. Heat the tail of the mouse (female C57BL/6, 12 weeks of age; *see* **Note 3**) by heat lamp or warm water to dilate the tail vein.
2. Place the mice in a constrainer and inject 200 μl of your bacterial suspension (make sure the suspension is at room temperature at the time of injection), thus infecting with 1×10^7 bacteria/mouse. Place the injection site similarly in all mice at ~3 cm from the tail base. To enable longitudinal analysis of disease progression in individual animals, it is recommended that each mouse be individually labeled.

3.1.3 Measurement of Visible Tail Lesions

1. At regular intervals (for example, three times per week), place animals in a constrainer and measure the length (broadest width) of each individual visible lesion with a ruler. Of note, the first lesions typically appear at ~7 days postinfection.
2. Calculate the accumulated length of all lesions in individual tails.

3.1.4 Measurement of Bone Erosion

1. Sacrifice the mice and sever the tails at the tail base. Place the tails in 10% formalin and put at 4 °C until micro-CT analysis.
2. For each mouse, scan three corresponding vertebrae at or near the site of injection. Segment the bone by applying an appropriate threshold (~0.7 gHA/cc) to the 3D image data sets. Measure the mean bone volume within the segmented bone for each vertebrae, and calculate the mean bone volume for each animal. Of note, we have used an ex vivo micro-CT scanner (microCT 40 from SCANCO Medical, Switzerland) at 12 μm isotropic voxel size, 1000 projections/rotation, 300 ms integration time, 70 keV photon energy, and 114 μA current [8].

3.1.5 Analysis of Bacterial Growth

1. Sacrifice the mice and sever the tails at the tail base. Place tails in 50 ml conicals and put on ice.
2. Determine the weight of each individual tail, and cut into ~2–5 mm pieces using scissors or a racer blade.
3. Homogenize each tail in 3 ml DMEM supplemented with 0.1% Triton X-100 using a homogenizer akin to the AHS200 homogenizer system (from VWR), with 10×105 mm saw tooth adaptors.
4. Perform serial dilutions in PBS and plate on 7H10 agar plates as described above (*see* Subheading 3.1.1), and place in 30 °C incubator.
5. Count CFUs and determine the bacterial load as CFUs/g tissue.

3.1.6 Preparation of Tail Tissue for Analyses of Cytokines and Protein Content

1. Sacrifice the mice and sever the tails at the tail base. Immediately place the tails in bags and put on dry ice. At this point the tails can be transferred to −80 °C for storage until proceeding with the protocol.

2. Freeze the tails in liquid nitrogen and pulverize in a similarly chilled biopulverizer.
3. Transfer the powder to a 1.5 ml tube, and resuspend in ≤1 ml PBS supplemented with protease inhibitors. Incubate on ice for 1.5 h, with shaking.
4. Pellet debris by two consecutive centrifugations (20, 000 × *g*, 20 min at 4 °C), where the supernatants are transferred to new 1.5 ml tubes.
5. Analyze samples for the desired cytokine and protein using, for example, ELISA or Western blot.
6. Samples can be stored at −80 °C. Avoid repeated freeze-thawing.

3.1.7 Preparation of Tails for Immunohistochemistry

1. Sacrifice the mice and sever the tails at the tail base. Place the tails in 10% formalin. At this point the tails can be kept at 4 °C until proceeding with the protocol.
2. Decalcify the tails in, for example, Immunocal (Decal Chemical Corp) for 48 h.
3. For each tail, generate five transverse 3 μm sections (at or near the initial injection site), which include soft tissue as well as coccygeal vertebrae.
4. Stain sections with hematoxylin and eosin, or with relevant antibodies for immunohistochemical evaluation, using standard procedures.

3.2 Bone Marrow-Derived Mouse Macrophage Infection Model

3T3-CSF is a fibroblast cell line that produces murine M-CSF, which is subsequently used for the generation and culture of bone marrow-derived macrophages.

3.2.1 Production of M-CSF from 3T3-CSF Cells

1. Grow the 3T3-CSF cells in 3 T3 medium until confluency (3–4 days) in a tissue culture-treated 175 cm^2 flask, at 37 °C with 5% CO_2.
2. Remove medium and wash once with PBS to remove traces of serum.
3. Add 5 ml of Trypsin-EDTA solution and incubate 2–5 min at 37 °C. Detach cells by scraping and subsequently add 30 ml 3T3 medium to inactivate Trypsin.
4. Transfer to a 50 ml conical and collect cells by centrifugation (250 g, 5 min).
5. Resuspend in 30 ml 3T3 medium. Divide into six new tissue culture-treated 175 cm^2 flasks and adjust final volume to 35 ml with 3T3 medium.
6. Incubate until confluency and then change the 3 T3 medium (35 ml).

7. Incubate for 4–5 days, and harvest medium containing M-CSF (3T3-CSF cell-conditioned medium). Filter-sterilize and prepare 50 ml aliquots. Of note, new 3T3 medium (35 ml) can be added on the same cells and the medium can be collected another two rounds.
8. Store M-CSF aliquots at −80 °C.

3.2.2 Generation of Bone Marrow-Derived Macrophages

1. Sacrifice the mouse and briefly soak the animal in 70% ethanol to prevent subsequent contamination of the femurs.
2. Pin down the animal and dissect and clean the femurs from tissues using a scalpel and scissors.
3. Place femurs in 50 ml conicals containing 5 ml BMM (supplemented with 100 units/ml Penicillin and 100 μg/ml Streptomycin), and put on ice for at least 15 min.
4. Under sterile conditions, open the femurs by cutting at the tip of the joints on both ends of the bone using a razor blade.
5. Using a syringe, flush the bone marrow from each bone with 5 ml cold BMM into a 15 ml conical.
6. Pellet/remove tissue debris by centrifugation (60 × *g*, 1 min at 4 °C).
7. Transfer the supernatant into a new 15 ml conical and subsequently collect cells by centrifugation (250 × *g*, 10 min at 4 °C).
8. Resuspend cells in 6 ml cold BMM. Divide cells into 6–8 non-tissue culture treated petri dishes (150 × 15 mm) in a total volume of 30 ml BMM per plate.
9. Incubate at 37 °C with 5% CO_2.
10. On day 4, add 10 ml of BMM into each plate.
11. On day 7, the bone marrow-derived macrophages are harvested (*see* **Note 4**).

3.2.3 Freezing or Seeding of Bone Marrow-Derived Macrophages

On day 7 after generation of bone marrow-derived macrophages, cells can be seeded for infection or frozen for long-term storage.

1. Aspirate supernatant from the plate on which the macrophages are growing, and add 7 ml cold PBS to each plate.
2. Keep on ice for 5 min.
3. Detach cells by gently using a cell scraper.
4. Transfer the cells into a 50 ml conical. Collect remaining cells by washing the plate with 7 ml cold PBS, which is transferred into the same conical.
5. Take out an aliquot and stain with Trypan blue. Determine the viable cell count using a hemacytometer.
6. Collect cells by centrifugation (250 × *g*, 10 min at 4 °C).

Point 7–9 below relates to freezing of cells. Jump to point 10 for how to seed cells for infection.

7. Discard the supernatant and resuspend cells to a final concentration of 10^7 viable cells/ml in cold freezing medium.
8. Dispense aliquots of cells in sterile cryogenic storage vials, and place vials in a cool cell chamber, which is subsequently placed at −80 °C overnight.
9. For long-term storage, transfer frozen cells to −150 °C or liquid nitrogen.
10. Discard the supernatant and resuspend cells in BMM to a final concentration that will give you the appropriate number of live cells per well (*see* Table 1 and **Note 5**).
11. Dispense the appropriate volume of cells (*see* Table 1) to each well, and incubate overnight (37 °C with 5 % CO_2).

3.2.4 Thawing of Frozen Bone Marrow-Derived Macrophages

1. Quickly thaw 1 vial of BMDMs (<1 min) in a 37 °C water bath.
2. Promptly transfer cells into a 15 ml conical containing 10 ml BMM, so as to dilute the DMSO present in the freezing medium.
3. Collect cells by centrifugation (250 × *g*, 5 min).
4. Discard the supernatant and resuspend cells in 5 ml BMM.
5. Dispense the cells in a non-tissue culture treated petri dish (150 × 15 mm) containing 25 ml BMM.
6. Incubate at 37 °C with 5 % CO_2 overnight.
7. Seed cells for infection (*see* Subheading 3.2.3).

Table 1
Recommended numbers of bone marrow-derived macrophages to be seeded for infection in different plate formats (*see* Note 5), as well as the appropriate volume to be used

Plate format	Numbers of macrophages to be seeded per well	Seeding volume per well	Volume of bacterial inoculum	Volume of 1/3 BMM with Amikacin	Final volume of BMM
96-well	0.05×10^6	100 µl	100 µl	150 µl	200 µl
48-well	0.125×10^6	250 µl	250 µl	250 µl	250 µl
24-well	0.25×10^6	500 µl	500 µl	500 µl	500 µl
12-well	0.5×10^6	1 ml	1 ml	1 ml	1 ml
6-well	1×10^6	2 ml	2 ml	2 ml	2 ml

3.2.5 Preparation of M. marinum for Infection of Bone Marrow-Derived Macrophages

1. *M. marinum* is grown and prepared essentially as described above (*see* Subheading 3.1.1) However, 1/3 BMM (i.e., BMM diluted 1–3 with RPMI) is used instead of PBS. Moreover, the final concentration is adjusted according to the desired multiplicity of infection (MOI; *see* **Note 6**).

3.2.6 Infection of Bone Marrow-Derived Macrophages with M. marinum

1. Remove BMM from cells, seeded the day before as described above (*see* Subheading 3.2.3.).
2. Add the bacterial suspension (*see* Table 1 for volume) prepared as described above (*see* Subheading 3.2.5).
3. Incubate at 32 °C with 5% CO_2 for 2 h. Of note, from this point on all incubations are performed at 32 °C due to the low optimal growth temperature of *M. marinum*.
4. During the 2 h incubation, perform serial dilutions of the inoculum and plate on 7H10 agar plates as described above (*see* Subheading 3.1.1) to determine the actual bacterial concentration in the inoculum. Based on this information the *de facto* MOI of the infection can be established.
5. Remove supernatant and add 1/3 BMM supplemented with 200 μg/ml (final concentration) Amikacin to kill off extracellular bacteria (*see* Table 1 for volume).
6. Incubate at 32 °C with 5% CO_2 for 2 h.
7. Remove supernatant and wash the cells twice with 1/3 BMM to remove remaining extracellular bacteria and traces of Amikacin.
8. Add the final volume of BMM (*see* Table 1 for volume), and incubate infected cells at 32 °C with 5% CO_2 until further analysis.

3.2.7 Analysis of Intracellular Growth in Bone Marrow-Derived Macrophages

For analysis of intracellular growth we generally perform the infection in a 96-well format.

1. At the desired time points postinfection, add Triton X-100 at a final concentration of 0.1%. Incubate for 10 min at room temperature to lyse the cells and release intracellular bacteria.
2. Perform a serial dilution (five times tenfold dilution steps) in PBS and plate on dry 7H10 agar plates for calculation of CFUs/ml. Use square petri dishes (100 × 15 mm) with a grid (forming 6 by 6 squares). Drop 10 μl from each dilution into squares, let dry and place in 30 °C incubator.

3.2.8 Collection of Infection Supernatants for Analysis of Cytokine/Protein Output

1. Collect supernatants from the infections, and uninfected controls, at the desired time point postinfection, and transfer to a 1.5 ml tube kept on ice.
2. Pellet cellular debris and bacteria by centrifugation (4000 × *g*, 10 min at 4 °C).

3. Transfer supernatant to a new tube on ice.
4. Analyze cytokine/protein content by, for example, ELISA or Western blot.
5. Supernatants can be stored at −80 °C. Avoid repeated freeze-thawing.

3.2.9 Preparation of Cell Lysates for Western Blot Analysis

For analysis with Western blot we generally perform the infection in 6- or 12-well formats to obtain a sufficient amount of material.

1. At the desired time points, place the plate on ice and remove supernatants. Add cold lysis buffer (300 or 150 µl per well for experiments performed in 6- or 12-well plates, respectively) to the wells. Of note, supernatant can be centrifuged (250 × *g*, 5 min at 4 °C) to pellet and recover detached cells; similarly lyse the pellet and transfer to the corresponding well.
2. Incubate the plate on ice 2–3 min.
3. Scrape each well with the tip of a pipette and transfer the lysates to a 1.5 ml tube kept on ice.
4. Agitate the tubes by rotation at 4 °C for 30 min.
5. Pellet cellular debris by centrifugation (13,400 × *g*, 20 min at 4 °C).
6. Collect the supernatant and store at −80 °C until analysis. Avoid repeated freeze-thawing.

3.2.10 Preparation of Cells for Immunofluorescence Microscopy Analysis

For microscopy analysis we generally perform the infections in 6- or 12-well formats, where the cells are seeded onto fibronectin-coated cover slips, which allow for firm adhesion. Figure 2 illustrates the ability of *M. marinum* to generate actin-tails in the cytosol of infected macrophages, thus generating motile force that promotes spread [18, 19].

1. Place sterile glass coverslips in the bottom of a non-tissue culture treated 6- or 12-well plate; use 22 or 15 mm diameter coverslips, respectively.
2. Coat glass coverslips with PBS containing 10 µg/ml fibronectin. Add enough solution to cover the entire surface of the coverslips.
3. Incubate for 30–45 min at room temperature.
4. Aspirate the solution and rinse the cover slips twice with PBS or BMM.
5. Cells can be immediately seeded onto the fibronectin-coated cover slips. We generally seed 4×10^5 and 2×10^5 cells onto 22 and 15 mm diameter coverslips, respectively.
6. Proceed with the infection as described above (*see* Subheading 3.2.6).

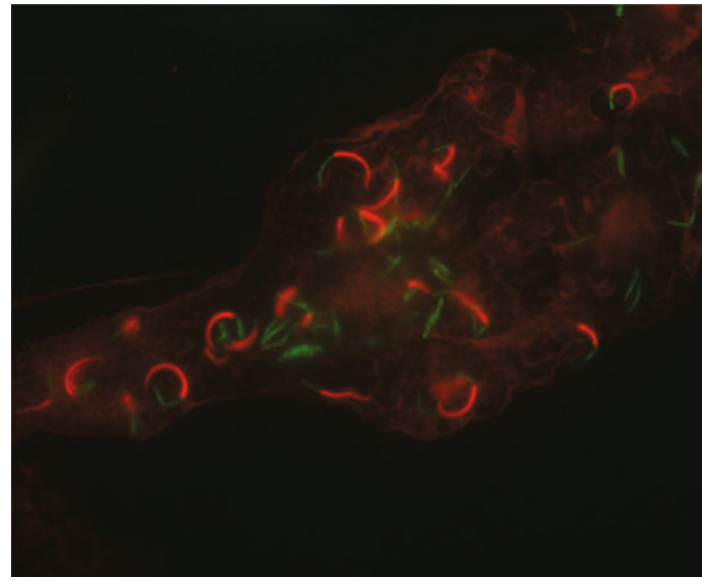

Fig. 2 Image of a bone marrow-derived macrophage 24 h postinfection with GFP-expressing *M. marinum*. Cells were stained with Phalloidin-594, which binds to actin filaments and visualizes *M. marinum*-induced actin-tail formation (originally described by Stamm et al. 2003 [18])

7. After the desired time point postinfection, wash cells on coverslips once with pre-warmed PBS.
8. Incubate with 4% paraformaldehyde (room temperature, 20 min) to fix cells.
9. Wash once with pre-warmed or room temperatured PBS.
10. Incubate with PBS supplemented with 0.1% Triton X-100 (room temperature, 4 min) to permeabilize cells. Of note, to avoid cell lysis it is important to not incubate longer than 4 min.
11. Wash once with PBS.
12. Incubate with PBS supplemented with 1% Bovine serum albumin (BSA; room temperature, 1 h) to block cells. Alternatively, this incubation can be performed overnight at 4 °C.
13. Perform the staining using reagents/antibodies diluted in PBS with 1% BSA. For most reagents/antibodies, incubation for 40–60 min at room temperature is sufficient. Importantly, the appropriate dilution for each reagent/antibody, as well as the appropriate concentration of BSA (or other means of blocking), needs to be experimentally optimized using appropriate controls.
14. Wash three times with PBS.
15. Perform the secondary staining using appropriate antibodies (diluted in PBS with 1% BSA).

16. Wash twice with PBS, followed by one rinse with distilled H_20.
17. Mount in mowiol using 10 or 15 μl per 15 and 22 mm diameter coverslips, respectively. Place the mowiol on a glass slide, and carefully put the coverslip on the drop upside down (such that the cells are embedded in mowiol).
18. Let dry in the dark at room temperature.
19. Store at 4 °C until analysis.

4 Notes

1. Mowiol is prepared as follows: mix glycerol and mowiol and then add distilled H_2O. Leave stirring 2 h at room temperature. Add Tris and incubate 10 min at 50–60 °C to dissolve the solids. Repeat as necessary. Centrifuge (5000×*g*, 15 min) to remove undissolved material. Collect the supernatant and make 1 ml aliquots. These can be stored at −20 °C for up to 1 year.
2. 4% Paraformaldehyde is prepared as follows: Add 4 g paraformaldehyde to 100 ml PBS. To help dissolve the paraformaldehyde add eight drops of 1N NaOH, put in a 65 °C water bath and agitate at regular intervals until completely dissolved. Filter-sterilize the solution and store aliquots at −20 °C. Once thawed, it can be kept for 1 week at 4 °C.
3. We have titrated the inoculum in different mouse strains, and found that 1×10^6 –1×10^7 bacteria/animal is appropriate for female C57BL/6 mice (12 weeks of age). At these concentrations the mice develop local disease in the tail without apparent systemic effects. Titration may be needed, especially if using other mouse strains. For example, we have found that BALB/C mice a much more sensitive to infection, and develop a more aggressive tail disease associated with weight loss when infected with similar numbers of bacteria. For BALB/C mice, infection in the range of 1×10^5 bacteria/animal is more appropriate (unpublished observations).
4. When generating bone marrow-derived macrophages it is our experience that the fetal calf serum used is of critical importance. For example, a fraction of intracellular *M. marinum* normally induces actin tail formation at one polar end of the bacteria [18]. However, this feature is dependent on the sera used to generate the macrophages, for unknown reasons (unpublished observation). While most sera support outgrowth of macrophages that do allow actin tail formation, we always test batches to confirm that they do before buying.
5. Table 1 indicates the standard number of bone marrow-derived macrophages that are seeded for infection using different plate formats. It should be noted, however, that these numbers

might need to be adapted depending on the readout used. For example, in our experience we need to seed less cells when performing infections for microscopy analyses (*see* Subheading 3.2.10), to prevents the cells from becoming too confluent for appropriate visualization.

6. Appropriate MOI for different analyses may need to be optimized for each laboratory (since macrophages generated with different sera etc. may be more or less sensitive to infection). We typically use a low MOI (0.1–1) for analyses of intracellular growth over 96 h. For cytokine analysis or microscopy analysis at 24 h postinfection we typically use MOI = 5, which generates robust cytokine output but a very low degree of cell death at earlier time points postinfection. In our hands an MOI of 10 or higher cause significant host cell death already at 24 h postinfection.

Acknowledgments

Work in the Carlsson laboratory is supported by the Swedish Research Council, the Knut and Alice Wallenberg Foundation, as well as the foundations of Crafoord, Gyllenstiernska Krapperup, Emil and Wera Cornell, Clas Groschinsky, Alfred Österlund, the Swedish Society of Clinical Microbiology, and the Royal Physiographic Society in Lund.

References

1. Manjelievskaia J, Erck D, Piracha S, Schrager L (2016) Drug-resistant TB: deadly, costly and in need of a vaccine. Trans R Soc Trop Med Hyg 110(3):186–191
2. Pereira SM et al (2012) Effectiveness and cost-effectiveness of first BCG vaccination against tuberculosis in school-age children without previous tuberculin test (BCG-REVAC trial): a cluster-randomised trial. Lancet Infect Dis 12(4):300–306
3. http://www.who.int/tb/publications/global_report/en/
4. Guirado E, Schlesinger LS (2013) Modeling the Mycobacterium tuberculosis Granuloma - the critical battlefield in host immunity and disease. Front Immunol 4:98
5. Leung C et al (2013) Infectious diseases in humanized mice. Eur J Immunol 43(9):2246–2254
6. Patel K, Jhamb SS, Singh PP (2011) Models of latent tuberculosis: their salient features, limitations, and development. J Lab Physicians 3(2):75–79
7. van Leeuwen LM, van der Sar AM, Bitter W (2015) Animal models of tuberculosis: zebrafish. Cold Spring Harb Perspect Med 5(3):a018580
8. Carlsson F et al (2010) Host-detrimental role of Esx-1-mediated inflammasome activation in mycobacterial infection. PLoS Pathog 6(5):e1000895
9. Cambier CJ, Falkow S, Ramakrishnan L (2014) Host evasion and exploitation schemes of mycobacterium tuberculosis. Cell 159(7):1497–1509
10. Stinear TP et al (2008) Insights from the complete genome sequence of mycobacterium marinum on the evolution of mycobacterium tuberculosis. Genome Res 18(5):729–741
11. Stamm LM, Brown EJ (2004) Mycobacterium marinum: the generalization and specialization of a pathogenic mycobacterium. Microbes Infect 6(15):1418–1428
12. Cosma CL, Sherman DR, Ramakrishnan L (2003) The secret lives of the pathogenic mycobacteria. Annu Rev Microbiol 57:641–676

13. Travis WD, Travis LB, Roberts GD, Su DW, Weiland LW (1985) The histopathologic spectrum in mycobacterium marinum infection. Arch Pathol Lab Med 109(12):1109–1113
14. Tobin DM, Ramakrishnan L (2008) Comparative pathogenesis of mycobacterium marinum and mycobacterium tuberculosis. Cell Microbiol 10(5):1027–1039
15. Watkins BY et al (2012) Mycobacterium marinum SecA2 promotes stable granulomas and induces tumor necrosis factor alpha in vivo. Infect Immun 80(10):3512–3520
16. Shaler CR, Horvath C, Lai R, Xing Z (2012) Understanding delayed T-cell priming, lung recruitment, and airway luminal T-cell responses in host defense against pulmonary tuberculosis. Clin Dev Immunol 2012:628293
17. Urdahl KB, Shafiani S, Ernst JD (2011) Initiation and regulation of T-cell responses in tuberculosis. Mucosal Immunol 4(3):288–293
18. Stamm LM et al (2003) Mycobacterium marinum escapes from phagosomes and is propelled by actin-based motility. J Exp Med 198(9):1361–1368
19. Stamm LM et al (2005) Role of the WASP family proteins for Mycobacterium marinum actin tail formation. Proc Natl Acad Sci U S A 102(41):14837–14842

Part VI

Methods Exploiting Bacterial Immune Evasion

Chapter 21

Generating and Purifying Fab Fragments from Human and Mouse IgG Using the Bacterial Enzymes IdeS, SpeB and Kgp

Jonathan Sjögren, Linda Andersson, Malin Mejàre, and Fredrik Olsson

Abstract

Fab fragments are valuable research tools in various areas of science including applications in imaging, binding studies, removal of Fc-mediated effector functions, mass spectrometry, infection biology, and many others. The enzymatic tools for the generation of Fab fragments have been discovered through basic research within the field of molecular bacterial pathogenesis. Today, these enzymes are widely applied as research tools and in this chapter, we describe methodologies based on bacterial enzymes to generate Fab fragments from both human and mouse IgG. For all human IgG subclasses, the IdeS enzyme from *Streptococcus pyogenes* has been applied to generate F(ab′)2 fragments that subsequently can be reduced under mild conditions to generate a homogenous pool of Fab′ fragments. The enzyme Kgp from *Porphyromonas gingivalis* has been applied to generate intact Fab fragments from human IgG1 and the Fab fragments can be purified using a CH1-specific affinity resin. The SpeB protease, also from *S. pyogenes*, is able to digest mouse IgGs and has been applied to digest antibodies and Fab fragments can be purified on light chain affinity resins. In this chapter, we describe methodologies that can be used to obtain Fab fragments from human and mouse IgG using bacterial proteases.

Key words Fab fragments, F(ab′)2, Bacterial protease, IdeS, Gingipain K, Kgp, SpeB, Analytical methods, Affinity purification

1 Introduction

Antibodies are essential tools in many areas of research and the generation of specific antigen binding (Fab) fragments without the Fc fragment is sometimes required. An intact antibody has an overall mass of around 150,000 Da and consists of two heavy (50 kDa) and two light (25 kDa) chains. Di-sulfide bridges in the hinge region of the antibody hold the heavy chains together. For human IgG the number of inter-chain disulfide bridges range from 2 in IgG1 and IgG4, 4 in IgG2, and 11 in IgG3 [1]. The fragment of antigen binding (Fab) consists of the variable domain of the light and heavy chains and the CH1 domain of the heavy chain

Pontus Nordenfelt and Mattias Collin (eds.), *Bacterial Pathogenesis: Methods and Protocols*, Methods in Molecular Biology, vol. 1535, DOI 10.1007/978-1-4939-6673-8_21,

and the constant region of the light chain. The Fab fragment of the antibody interacts with the antigen, whereas the Fc domain (fragment crystallizable) directs the immune effector functions.

The discovery and characterization of bacterial enzymes with immunomodulatory activities has been an integral part of basic research within bacterial pathogenesis and infection medicine. Molecular studies within the field of infection biology have led to the discovery of a number of enzymes with unique activities [2–4]. The overall goal has been a deeper understanding of the virulence mechanisms of bacteria as means for therapeutic intervention [5]. However, the specific activities of bacterial enzymes have allowed several enzymes to be applied as biotechnology tools within the biopharmaceutical industry. For instance, bacterial enzymes with proteolytic activity on IgG have spurred applications in therapeutic antibody characterization, as specific tools for imaging, and as tools for generating specific antibody fragments. In this paper, we will focus on three proteases with distinct activity on IgG, namely IdeS, Kgp, and SpeB and the methodologies for the generation of Fab fragments [6–8].

The immunoglobulin degrading enzymes from *Streptococcus pyogenes*, IdeS, is a cysteine protease with specific digestion of IgG at a single site in the hinge region generating F(ab′)2 and Fc/2 fragments [6]. The specific digestion site of IdeS on human IgG (…CPAPELLG / GPSVF…) is identical for all human subclasses, including IgG2 (…CPAPPVA / GPSVF…). The enzyme is active at pH ranging from 5.1 to 7.6, has a temperature optimum at 37 °C, and can be inactivated using iodoacetate or iodacetamine [9]. The specificity and robustness of IdeS have led to multiple applications within analytical characterization of therapeutic antibody products, studying quality attributes such as glycosylation, oxidation, deamidation using mass spectrometry workflows [10–13]. The specificity of IdeS is also the key in the therapeutic exploration of this enzyme as a biotherapeutic drug for antibody mediated transplantation rejection or antibody driven autoimmune disease [14, 15]. In this paper, we describe the use of IdeS to generate a homogenous pool of Fab fragments, using affinity purification and mild reduction of the F(ab′)2 fragment.

Kgp is a cysteine protease produced by the anaerobe human pathogen *Porphyromonas gingivalis* that causes periodontitis, an inflammatory disease, which destroys the gums [16]. Kgp is implicated in the virulence of this organism, responsible for colonization and evasion of the immune response. The enzyme specifically digests proteins C-terminal to lysine residues. Proteins are hydrolyzed strictly after lysine residues but only if the lysine bond is exposed and there are no secondary structure restrictions. Of the human IgG subclasses only human IgG1 will be digested into intact Fab and Fc fragments, as the heavy chain of human IgG1 is cleaved in the upper hinge at a single site, …EPKSCDK/THTCPPCP… [17]. Kgp also digests human IgG3 but the CH2 domain is further

degraded whereas human IgG2 and IgG4 are not hydrolyzed. The hinge region of human IgG2 contains four cysteines, which probably makes it more rigid and not susceptible to digestion by Kgp. Furthermore, the hinge regions of IgG2 and IgG4 are shorter by three amino acid residues as compared to IgG1. The Kgp enzyme depends on the presence of reducing agents to be active. Mild reducing conditions, i.e., 2 mM cysteine, will yield intact Fab fragments of human IgG1. Catalysis may require a catalytic triad, Cys477-His444-Asp388 rather than the cysteine-histidine dyad normally found in cysteine proteases [18]. The pH optimum of Kgp is at pH 8.0–8.5, but it is active at neutral pH and slightly below that. Kgp is irreversible inhibited by thiol blocking agents such iodacetamide. The best irreversible inhibitor is Z-Phe-Lys-2,4,6-trimehylbenzoyloxymethylketone and KYT-36 is the most potent reversible inhibitor [19]. Pure and intact Fab fragments can be obtained by digestion of human IgG1 with Kgp and subsequent purification of the Fab fragments with CaptureSelect™ IgG-CH1 affinity matrix. This resin recognizes the CH1 domain of human IgG antibodies independent of the light-chain isotype and source material. Due to its unique selectivity for the CH1 domain, no co-purification of free light-chain contaminants will occur.

SpeB is probably the oldest known proteolytic enzyme from *S. pyogenes*. Although the methodology was rudimental, the characterization of a papain like enzyme, dependent on reductive environment and inhibition by iodoacetic acid, performed by Elliot et al in 1945 still remains accurate [20]. The proteolytic activity has since been studied on a number of substrates, IgG being one of them [8, 21]. SpeB has activity in the hinge region of human IgG but it has been debated whether this activity has a role in the virulence of *S. pyogenes*. The SpeB digestion site on human IgG1 has been denoted to be similar to that of IdeS (…CPAPELLG/GPSVF…) but N-terminal sequencing of the Fc fragment and our own data show digestion above the hinge (…KTHT/CPPCPAP…) [8, 22]. The activity of SpeB on human IgG requires reducing conditions, a state considered nonphysiological, and thus, it is believed that the digestion of IgG does not occur in vivo [23]. Still, by adding reducing agents such as dithiothreitol (DTT), mercaptoethanol, or L-cysteine, the enzyme has proven a valuable research tool for specific digestion of antibodies. SpeB is capable of digesting IgG, IgA, IgD, IgM, and IgE from humans, and also immunoglobulins from other species including murine antibodies [8, 22, 24–26]. In early monoclonal antibody discovery the murine and rat models remain frequently used and tools are needed to characterize these antibodies, for this reason SpeB has been applied to specifically digest antibodies for characterization. The primary digestion site on mouse IgG1 occurs below the hinge (…CKPCIC/TVPEVS…) although unpublished data has indicated that further digestion may occur in the upper hinge region …CKPC/IC/TVPEVS… and …DCG/CKPC/IC/TV…, generating Fab fragments. The reason for this

effect may be unspecific digestion by the enzyme and/or thiol disulfide interchange, as the concentration of cysteine impacts the digestion [27]. The enzyme could be applied in a workflow to generate Fab fragments from a mouse IgG1 antibody utilizing the upper hinge digestion. In this paper, we demonstrate for the first time the use of SpeB and a kappa-specific affinity resin for generating and purifying Fab fragments from murine IgG1.

2 Materials

2.1 IdeS Digestion, Purification, and Mild Reduction

1. IdeS enzyme and purification kit: FragIT™ Kit (cat# A0-FR6-050, Genovis AB).
2. IgG of choice, in a physiological buffer with pH ranging from 6.0 to 8.0 and in a concentration of 1–10 mg/mL.
3. Fc specific CaptureSelect™ affinity purification column (supplied in the FragIT™ Kit) available as a resin from Thermo Fisher (cat# 191285505).
4. Mercaptoethylamine-HCl (2-MEA).
5. Materials to run a SDS-PAGE gel.

2.2 Kgp Digestion and Purification of Fab Fragments

1. Kgp enzyme and purification resin: GingisKHAN™ Fab Kit (cat# B0-GFK-020, Genovis AB).
2. CH1 specific CaptureSelect™ affinity resin (supplied in the GingisKHAN™ Fab Kit) available in a resin format from Thermo Fisher (cat# 194320005).
3. Human IgG1 of choice in 100 mM Tris pH 8.
4. Materials to run a SDS-PAGE gel.

2.3 SpeB Digestion of Murine IgGs

1. SpeB enzyme and purification resin: FabULOUS Fab Kit (cat# A2-PU2-020, Genovis AB).
2. CaptureSelect™ LC-kappa resin (supplied in FabULOUS Fab Kit) available in a resin format from Thermo Fisher (cat#1913150).
3. Murine IgG1 of choice in PBS/TBS at neutral pH.
4. Materials to run a SDS-PAGE gel.

3 Methods

3.1 Generation of Fab Fragments Using IdeS

1. Prepare the human antibody (subclass 1–4) at 5 mg/mL in digestion buffer (*see* **Note 1**).
2. Equilibrate the column with 2 × 300 µl digestion buffer. Centrifuge at 200 × *g* for 1 min.

3. Add the antibody to the FragIT™ column. Cap the column and incubate at room temperature with end-over-end mixing for 15 min.
4. Collect the F(ab′)2 and Fc antibody fragments by centrifugation at 200 × *g* for 1 min. For maximum recovery, add 100 µl digestion buffer and centrifuge at 200 × *g* for 1 min, repeat once and centrifuge at 1000 × *g* for 1 min in the final centrifugation step.
5. Equilibrate the CaptureSelect™ column with 2 × 300 µl binding buffer. Centrifuge at 200 × *g* for 1 min. Add the eluted antibody fragments from **step 3**.
6. Cap the column and incubate with end-over-end mixing for 30 min at room temperature.
7. Collect the F(ab′)2 fragments by centrifugation at 200 × *g* for 1 min. For maximum recovery add 100 µl digestion buffer and centrifuge at 200 × *g* for 1 min. Repeat once and centrifuge at 1000 × *g* for 1 min in the final centrifugation step. The Fc fragments can be eluted if desired.
8. The eluted F(ab′)2 fragments can now be separated into Fab fragments using mild reduction of the hinge thiols.
9. Prepare 500 mM 2-MEA in 50 mM phosphate, 150 mM NaCl, 5 mM EDTA, pH 7.2.
10. Add 2-MEA to the F(ab′)2 fragments with a final concentration of 50 mM and incubate at 37 °C for 90 min.
11. The solution now contains Fab fragments and 2-MEA. To remove the 2-MEA a desalting column can be used for rapid and convenient processing (*see* **Note 2**).
12. Digestion and separation efficiency can be visualized by separation on a SDS-PAGE (Fig. 1).

3.2 Generation and Purification of Fab Fragments from Human IgG1 Using Kgp

1. Prepare the human IgG1 antibody in 100 mM Tris, pH 8 (*see* **Note 3**).
2. Reconstitute GingisKHAN™ in 200 µL double distilled H_2O to a concentration of 10 units/µl. Reconstitute GingisKHAN™ Reducing Agent in 50 µl double distilled H_2O and keep on ice. Use the same day as prepared, it cannot be stored (*see* **Note 4**).
3. Add 1 unit GingisKHAN™/ 1 µg human IgG1. Add GingisKHAN™ Reducing Agent to the reaction mixture. Add 1/10 v/v to yield 2 mM cysteine in reaction.
4. Incubate for 1–2 h in digestion buffer at 37 °C (*see* **Note 5**).
5. Equilibrate the CaptureSelect™ column with 2 × 300 µl binding buffer. Centrifuge at 200 × *g* for 1 min. Add the GingisKHAN™ digested sample from **step 3**.
6. Cap the column and incubate by end-over-end mixing for 30 min at room temperature.

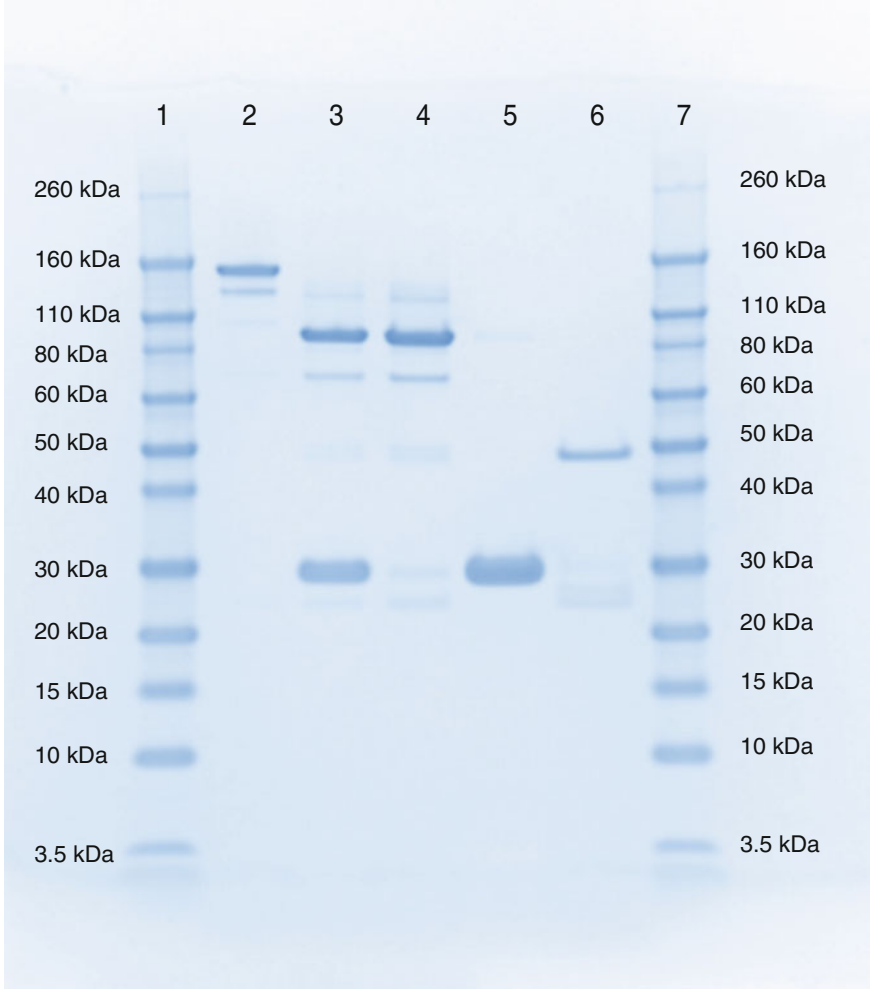

Fig. 1 SDS-PAGE analysis of trastuzumab (Herceptin®, human IgG1) digested with IdeS and the resulting F(ab′2) fragments purified using CaptureSelect™ Fc affinity resin (FragIT™ Kit). Further, the F(ab′)2 fragments were reduced using mild reduction to obtain Fab fragments. Lane 1 and 7: MW marker, lane 2: Intact IgG, lane 3: F(ab′)2 and Fc after FragIT digestion column, lane 4: Flow-through of F(ab′)2 fragments, lane 5: Eluted Fc fragments, lane 6: Fab fragments after mild reduction of F(ab′)2

7. Elute the Fc fragments by centrifugation at 200 × *g* for 1 min. For maximum recovery add 100 µl binding buffer and centrifuge at 200 × *g* for 1 min. Repeat once and centrifuge at 1000 × *g* for 1 min in the final centrifugation step.
8. Wash the CaptureSelect™ column with 2 × 300 µl binding buffer, centrifuge at 200 × g for 1 min.
9. Add 25 µl neutralizing buffer (0.1 volume) to each collection tube. Add 250 µl 0.1 M Glycine, pH 3.0 to each spin column, seal the columns, and invert manually a couple of times.
10. Immediately, transfer the CaptureSelect™ CH1 column to the collection tube (containing 25 µl neutralizing buffer) and

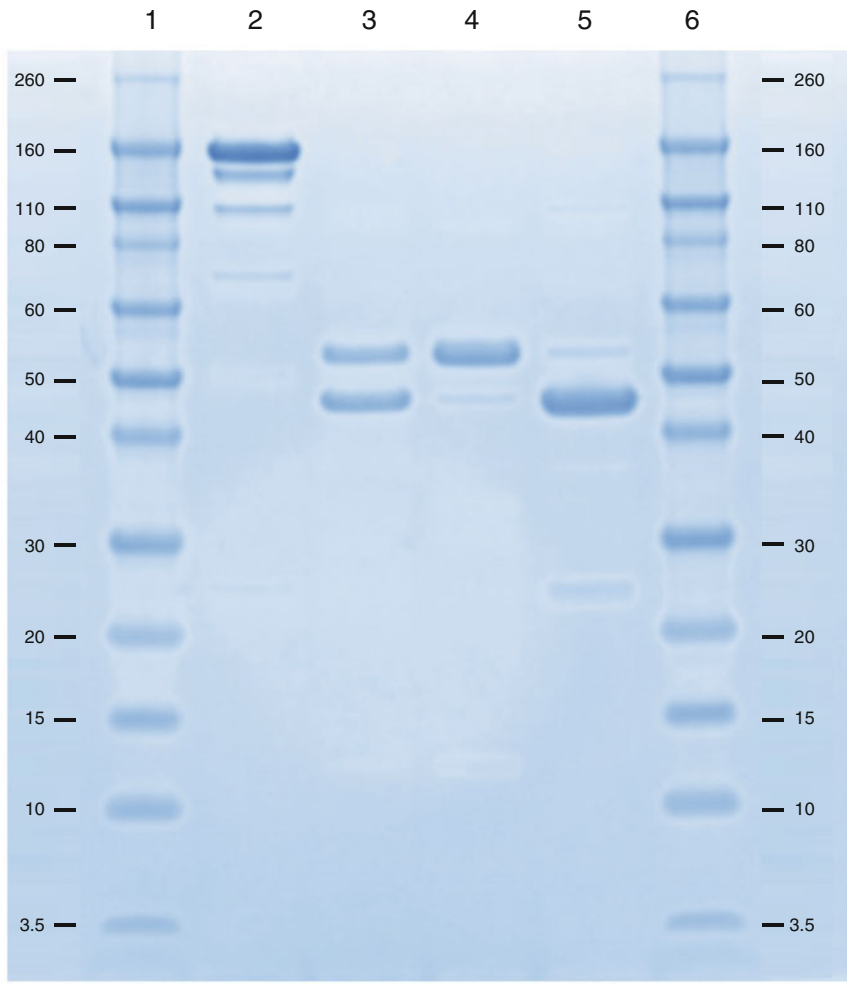

Fig. 2 SDS-PAGE analysis of purified Fab fragments from trastuzumab (Herceptin®) using Kgp digestion and purification of Fab fragments on CaptureSelect™ CH1 affinity resin (GingisKHAN™ Fab Kit). Lane 1 and 6: MW marker, lane 2: Intact human IgG1, lane 3: Fab and Fc fragments after Kgp digestion, lane 4: Flow-through Fc fragments and Kgp enzyme, lane 5: Eluted Fab fragments

collect the Fab fragments by centrifugation at 200 × *g* for 1 min. For maximum recovery repeat **steps 8** and **9** and centrifuge at 1000 × *g* for 1 min.

11. Separate the produced Fab fragments on a SDS-PAGE gel as a control (Fig. 2).

3.3 SpeB Digestion for Generation of Fab Fragments from Mouse IgG1

1. Prepare the mouse IgG1 in PBS or TBS.
2. Reconstitute FabULOUS® in 50 µl double distilled water to a concentration of 40 units/µl.
3. Add 1 unit FabULOUS®/1 µg IgG. Add cysteine to the reaction mixture to a final concentration of 30-50mM cysteine in the reaction (*see* **Note 6**).
4. Incubate the enzymatic reaction for 1 h at 37 °C.

5. Purification of the Fab fragments. Equilibrate the CaptureSelect™ LC kappa column (*see* **Note 7**) with 2 × 300 µl PBS or TBS (*see* **step 1**). Centrifuge at 200 × *g* for 1 min. Add the FabULOUS digested sample from **step 3**.
6. Cap the column and incubate by end-over-end mixing for 30 min at room temperature.
7. Elute the Fc fragments by centrifugation at 200 × *g* for 1 min. For maximum recovery add 100 µl binding buffer and centrifuge at 200 × *g* for 1 min. Repeat once and centrifuge at 1000 × *g* for 1 min in the final centrifugation step.
8. Wash the CaptureSelect™ LC-kappa column with 2 × 300 µl binding buffer, centrifuge at 200 × *g* for 1 min.
9. Add 25 µl neutralizing buffer (0.1 volume) to each collection tube. Add 250 µl 0.1 M Glycine, pH 3.0 to each spin column, seal the columns and invert manually a couple of times.
10. Immediately, transfer the CaptureSelect™ LC-kappa column to the collection tube (containing 25 µl neutralizing buffer) and collect the Fab fragments by centrifugation at 200 × *g* for 1 min. For maximum recovery repeat **steps 8** and **9** and centrifuge at 1000 × *g* for 1 min.
11. Analyze the produced Fab fragments on a SDS-PAGE gel as a control (Fig. 3, *see* **Note 5**).

4 Notes

1. IdeS is active in a range of physiological buffers including phosphate buffered saline (PBS) pH 6.0–8.0, Tris buffer pH 7.0–8.0, MES buffer pH 5.5–6.5, HEPES buffer 7.0–8.0, ammonium bicarbonate buffer pH 6.0–7.0, sodium acetate buffer pH 6.0, and common antibody formulation buffers. Digestion buffer in the protocol refers to any of the above-mentioned buffers.
2. For F(ab′)2 fragments that have been reduced using 2-MEA it is sometimes necessary to remove the 2-MEA using desalting. From our experience, using desalting columns from GE Healthcare (NAP 5, NAP 10, NAP 25) and similar G25 Sephadex™ columns have proven effective in removing the 2-MEA.
3. The digestion efficiency of GingisKHAN™ may be negatively affected by the presence of salts. A recommendation is to keep the salt concentration in the reaction below 75 mM NaCl.
4. The GingisKHAN™ reducing agent contains 20 mM cysteine. The cysteine concentration in the reaction is 2 mM cysteine. This will allow the enzyme to be catalytically active, while it

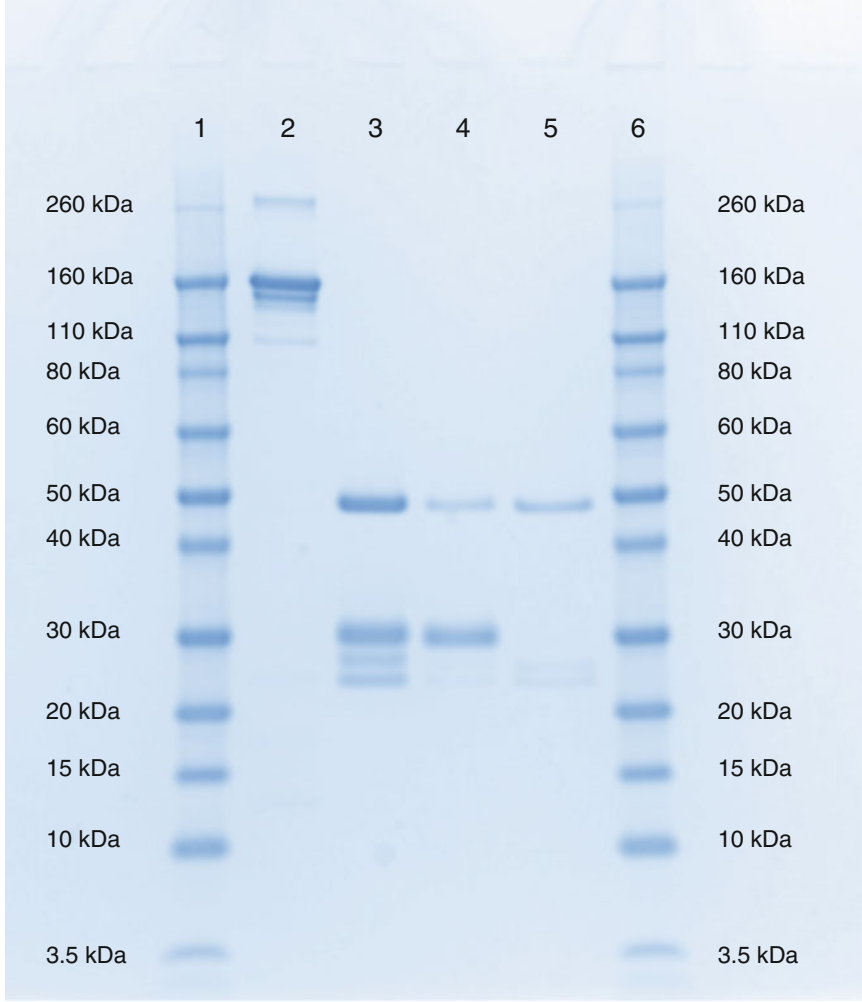

Fig. 3 SDS-PAGE analysis of Fab fragments from a mouse IgG1 antibody digested with SpeB and purified using CaptureSelect™ LC kappa affinity resin (FabULOUS Fab Kit). Lane 1 and 6: MW marker, lane 2: Intact mouse IgG1, lane 3: Fab and Fc fragments after SpeB digestion, lane 4: Flow-through Fc fragments and SpeB enzyme, lane 5: Purified Fab fragments

retains the disulfide bridges between the heavy and light chains. Also note that upon reconstitution the GingisKHAN™ reducing agent may appear cloudy. This does not affect the performance of the enzyme but make sure to mix the reducing agent properly prior addition to the enzymatic reaction.

5. To achieve optimal digestion efficiency, the incubation time may need to be optimized for individual antibodies.
6. Prepare cysteine and make sure it is at neutral pH. Cysteine neutral solution needs to be freshly prepared and used the same day as prepared. Care must be taken so that the cysteine

solution is at neutral pH and does not lower the pH of the digestion buffer. Prepare a stock solution of 1 M cysteine in double distilled water (90 µl aliquots may be stored at –20 °C). To neutralize the cysteine solution thaw one vial and add 10 µl 8 M NaOH to the 90 µl cysteine solution. This gives 100 µl of 0.9 M pH neutral cysteine solution ready to use. Note! Use freshly prepared (within 6h), it cannot be stored.

7. About 95 % of all mouse IgG1 has a kappa light chain. It is also possible to separate light chains of lambda type by using CaptureSelect™ LC-lambda (cat#19432305, Thermo Fisher).

References

1. Liu H, May K (2012) Disulfide bond structures of IgG molecules: structural variations, chemical modifications and possible impacts to stability and biological function. MAbs 4:17–23
2. Sjögren J, Collin M (2014) Bacterial glycosidases in pathogenesis and glycoengineering. Future Microbiol 9:1039–1051
3. Collin M, Olsén A (2003) Extracellular enzymes with immunomodulating activities: variations on a theme in *Streptococcus pyogenes*. Infect Immun 71:2983–2992
4. Walker MJ, Barnett TC, Mcarthur JD et al (2014) Disease manifestations and pathogenic mechanisms of group a Streptococcus. Clin Microbiol Rev 27:264–301
5. Nizet V (2007) Understanding how leading bacterial pathogens subvert innate immunity to reveal novel therapeutic targets. J Allergy Clin Immunol 120:13
6. von Pawel-Rammingen U, Johansson BP, Björck L (2002) IdeS, a novel streptococcal cysteine proteinase with unique specificity for immunoglobulin G. EMBO J 21:1607–1615
7. Abe N, Kadowaki T, Okamoto K et al (1998) Biochemical and functional properties of lysine-specific cysteine proteinase (Lys-gingipain) as a virulence factor of Porphyromonas gingivalis in periodontal disease. J Biochem 123:305–312
8. Collin M, Olsén A (2001) Effect of SpeB and EndoS from *Streptococcus pyogenes* on human immunoglobulins. Infect Immun 69:7187–7189
9. Vincents B, von Pawel-Rammingen U, Björck L et al (2004) Enzymatic characterization of the streptococcal endopeptidase, IdeS, reveals that it is a cysteine protease with strict specificity for IgG cleavage due to exosite binding. Biochemistry 43:15540–15549
10. Sjögren J, Olsson F, Beck A (2016) Rapid and improved characterization of therapeutic antibodies and antibody related products using IdeS digestion and subunit analysis, The Analyst 141(11):3114–3125
11. An Y, Zhang Y, Mueller H-M et al (2014) A new tool for monoclonal antibody analysis: application of IdeS proteolysis in IgG domain-specific characterization. MAbs 6:879–893
12. Beck A, Debaene F, Diemer H et al (2015) Cutting-edge mass spectrometry characterization of originator, biosimilar and biobetter antibodies. J Mass Spectrom 50:285–297
13. Beck A, Terral G, Debaene F et al (2016) Cutting-edge mass spectrometry methods for the multi-level structural characterization of antibody-drug conjugates. Expert Rev Proteomics 13:157–183
14. Johansson BP, Shannon O, Björck L (2008) IdeS: a bacterial proteolytic enzyme with therapeutic potential. PLoS One 3:e1692
15. Winstedt L, Järnum S, Nordahl EA et al (2015) Complete removal of extracellular IgG antibodies in a randomized dose-escalation phase I study with the bacterial enzyme IdeS - a novel therapeutic opportunity. PLoS One 10:e0132011
16. Mysak J, Podzimek S, Sommerova P et al (2014) Porphyromonas gingivalis: major periodontopathic pathogen overview. J Immunol Res 2014:1–8
17. Vincents B, Guentsch A, Kostolowska D et al (2011) Cleavage of IgG1 and IgG3 by gingipain K from *Porphyromonas gingivalis* may compromise host defense in progressive periodontitis. FASEB J 25:3741–3750
18. de Diego I, Veillard F, Sztukowska MN et al (2014) Structure and mechanism of cysteine peptidase gingipain K (Kgp), a major virulence factor of *Porphyromonas gingivalis* in periodontitis. J Biol Chem 289:32291–32302
19. Shen A, Bogyo M (2012) Chapter 523 Gingipain K, Elsevier Ltd. Handbook of Proteolytic Enzymes, (2012) 2337-2344. doi:10.1016/B978-0-12-382219-2.00521-4

20. Elliott SD (1945) A proteolytic enzyme produced by group A streptococci with special reference to its effect on the type-specific m antigen. J Exp Med 81:573–592
21. Elliott SD (1950) The crystallization and serological differentiation of a streptococcal proteinase and its precursor. J Exp Med 92:201–218
22. Olsson F, Norgren M, Mejare M et al (2013) Initial characterization of a recombinantly modified SpeB from *Streptococcus pyogenes* for antibody subunit domain generation. Poster presented at CASSS Mass Spectrometry Conference, Boston, MA, USA
23. Persson H, Vindebro R, von Pawel-Rammingen U (2013) The streptococcal cysteine protease SpeB is not a natural immunoglobulin-cleaving enzyme. Infect Immun 81:2236–2241
24. Collin M, Svensson MD, Sjöholm AG et al (2002) EndoS and SpeB from *Streptococcus pyogenes* inhibit immunoglobulin-mediated opsonophagocytosis. Infect Immun 70:6646–6651
25. Nelson DC, Garbe J, Collin M (2011) Cysteine proteinase SpeB from *Streptococcus pyogenes* - a potent modifier of immunologically important host and bacterial proteins. Biol Chem 392:1077–1088
26. Eriksson A, Norgren M (2003) Cleavage of antigen-bound immunoglobulin G by SpeB contributes to streptococcal persistence in opsonizing blood. Infect Immun 71:211–217
27. Singh R, Whitesides GM (1993) Thiol—disulfide interchange. In: Patai S, Rappoport Z (eds) Sulphur-containing functional groups (1993). John Wiley & Sons, Inc., Chichester, UK

Chapter 22

Measuring Antibody Orientation at the Bacterial Surface

Oonagh Shannon and Pontus Nordenfelt

Abstract

Many bacteria have the ability to interact with antibodies as a means to circumvent the immune response. This includes binding to the Fc portion of antibodies, effectively reversing the antibody orientation and thus decreasing the Fc-mediated immune signaling. Since antibody orientation at the bacterial surface has been shown to be important in human disease, it is valuable to be able to assess how antibodies are interacting with bacterial pathogens. Here, we describe a method to measure the proportion of human IgG that are bound via their Fc or Fabs to a bacterial surface. This is achieved by treating antibody-coated bacteria with the bacterial enzyme IdeS – which will cleave IgG into Fc and Fab fragments – and subsequently detect remaining fragments with fluorescent Fabs. The method is easy and fast, and the principle is most likely also applicable to other systems where distinguishing between antibody Fc and Fab binding is important.

Key words IgG, Bacteria, Flow cytometry, IgG-binding proteins, IdeS

1 Introduction

The correct binding of antibodies – or opsonization – is essential for an efficient immune response, whether it be initiating the complement system or triggering phagocytosis. The biological importance is demonstrated not only by the large number of bacterial pathogens that have IgG-binding proteins, or the many different types of IgG-interacting bacterial proteins, but also by the fact that this is an example of convergent evolution [1]. Protein G [2] from Group G streptococcus, protein A [3] from *Staphylococcus aureus*, and protein H [4] from *Streptococcus pyogenes* have very little in common structurally, but have very similar biological function [1]. The resulting bacterial Fc-binding is dependent on both the competing affinities of antibody Fabs and bacterial surface proteins as well as the local antibody concentrations [5]. A more detailed characterization of when and where antibodies are correctly oriented, i.e., binding in an opsonizing manner, will likely give us a better understanding of the pathogenesis of different bacteria in humans [6].

Pontus Nordenfelt and Mattias Collin (eds.), *Bacterial Pathogenesis: Methods and Protocols*, Methods in Molecular Biology, vol. 1535, DOI 10.1007/978-1-4939-6673-8_22,

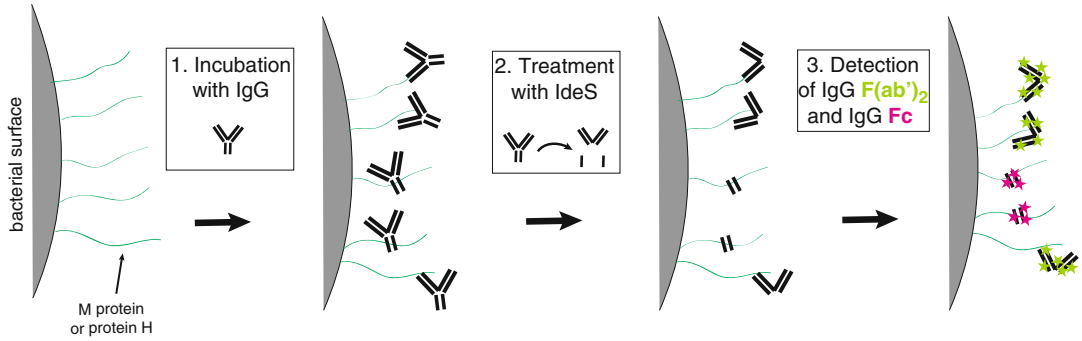

Fig. 1 IgG orientation assay. Bacteria are preincubated with IgG, washed and treated with IdeS, a proteinase of S. pyogenes which specifically cleaves IgG in the lower hinge region generating two half Fc fragments and one F(ab)′$_2$ fragment. Each sample is measured before and after IdeS treatment to determine which fragments of the bound IgG antibodies that remains at the bacterial surface following proteolytic cleavage. IgG fragments are identified and measured by flow cytometry with fluorescently labeled Fab fragments raised against human IgGFc or IgGFab fragments. Note: This is merely an illustration and both IgGFc and IgGFab are detected in the far red channel, using parallel samples and not simultaneously in the same sample

The IgG orientation method presented here (Fig. 1) is based on the assay used in a previous study on antibody orientation on Gram-positive bacteria [5]. Bacteria are first coated with antibodies, either in complex environments such as blood plasma or saliva, or in pure antibody solutions (*see* **Note 1**). After washing, they are then treated with the bacterial IgG-degrading enzyme IdeS [7]. This enzymatic cleavage is highly efficient and specific for the hinge region of IgG, resulting in either F(ab)$_2$′ or Fc fragments remaining on the bacterial surface. By splitting each sample before addition of IdeS, the Fab and Fc signal can be quantified using flow cytometry (Fig. 2), and thereby the proportion of Fab or Fc binding can be measured.

2 Materials

In this chapter, we are specifically describing the protocol for the *S. pyogenes* AP1 strain, so all media and other bacteria-specific reagents will need to be exchanged to match the particular bacteria being studied.

2.1 Bacteria and Antibody Reagents

1. Na-medium: 5.6 mM glucose, 127 mM NaCl, 10.8 mM KCl, 2.4 mM KH_2PO_4, 1.6 mM $MgSO_4$, 10 mM Hepes, and 1.8 mM $CaCl_2$; pH adjusted to 7.4 with NaOH (*see* **Note 2**).
2. IgG solution, monoclonal IgG for Fc-binding control and polyclonal IgG for opsonization (*see* **Note 3**).
3. 10 μg/μl IdeS (*see* **Note 4**).

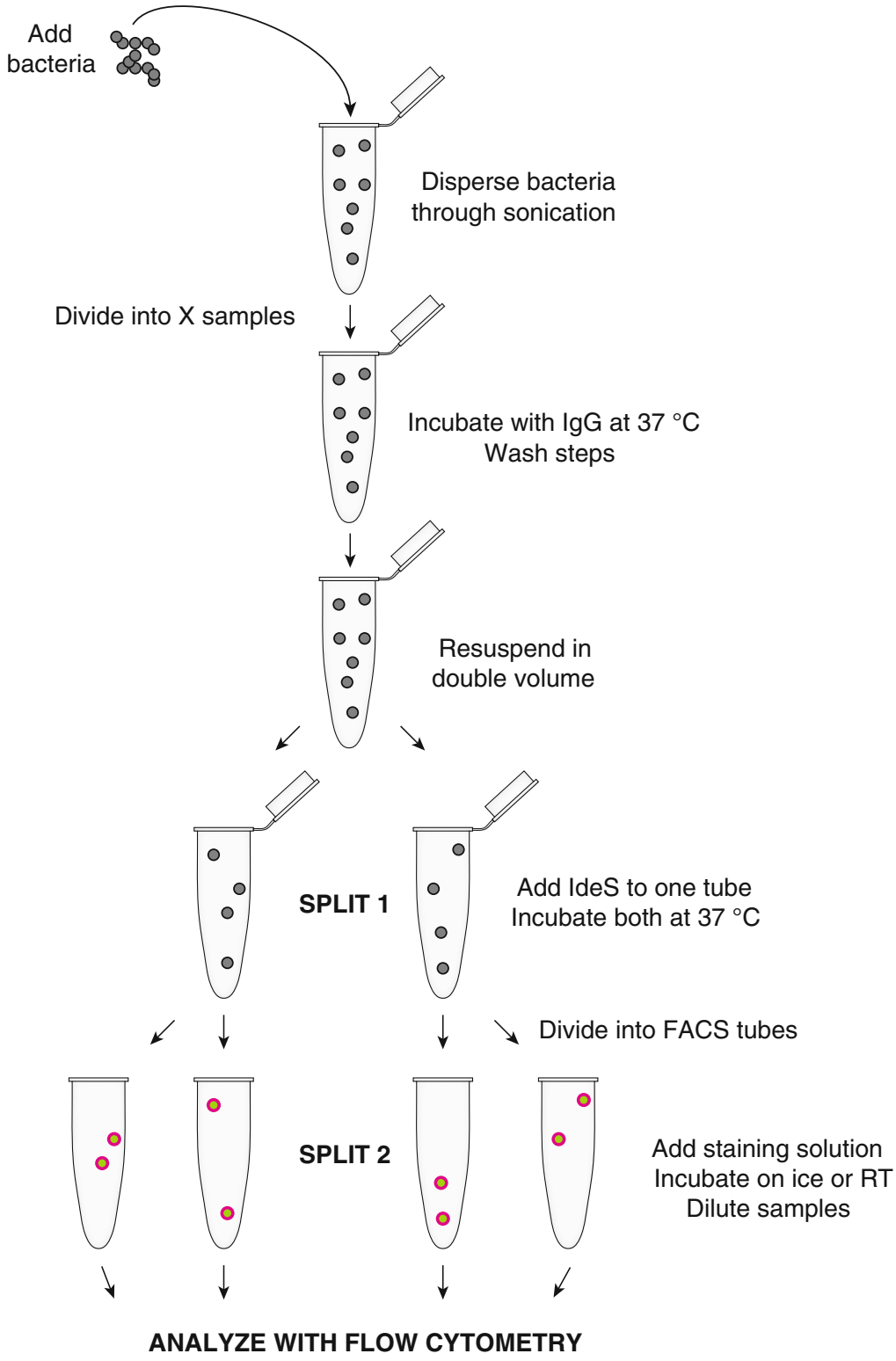

Fig. 2 Sample handling. Outline of the sample handling for the IgG orientation assay. The number of tubes will be multiplied by X conditions

4. Bacteria, heat-killed or live *S. pyogenes* AP1.
5. Microcentrifuge tube centrifuge with swing-out rotor (*see* **Note 5**).
6. Microcentrifuge sonicator (VialTweeter, Hielscher).
7. CountBright counting beads (Invitrogen).
8. Low-binding microcentrifuge tubes (Costar).

2.2 Antibodies and Fluorescent Dyes for Flow Cytometry

1. Goat Fab anti-human Fab DyLight 649 (Jackson, *see* **Note 6**). 1:50 stock concentration.
2. Goat Fab anti-human Fc DyLight 649 (Jackson). 1:50 stock concentration.
3. Syto9 (Invitrogen). 1:800 stock concentration.

3 Methods

The assay is divided into the following parts: Initial preparation of the bacteria; separating bacterial aggregates and binding of bacteria; enzymatic cleavage of bound antibodies into Fab and Fc fragments; labeling of bacteria and remaining antibody fragments; and finally analysis using a flow cytometer (*see* also Fig. 1). A general overview of the sample handling is illustrated in Fig. 2.

3.1 Preparation of Bacteria

1. Grow bacteria to early exponential phase (*see* **Note 7**).
2. Wash three times with cold PBS (2000×*g*, 10 min, angle rotor).
3. Resuspend in Na-medium and place on ice.

3.2 Sonication and Opsonization

1. Adjust the concentration of bacteria to 10 million per 100 µl by diluting with Na-medium. The samples should be in low-binding microcentrifuge tubes.
2. Place samples in the middle position on microcentrifuge sonicator and sonicate using 100% amplitude and a 0.5 cycle for 1 min (*see* **Note 8**).
3. Take 100 µl nonaggregated bacteria and combine with IgG solution and Na-medium for a total volume of 200 µl (*see* **Note 9**).
4. Incubate for 30 min at 37 °C under shaking (500 rpm) conditions.
5. Wash twice with 500 µl Na-medium (3000×*g*, 5 min, swing-out rotor, soft deceleration).
6. Resuspend in 450 µl Na-medium.

3.3 Enzymatic Cleavage of Bound Antibodies

1. Divide the bacteria into two new tubes with 200 µl in each. *See* SPLIT 1 in Fig. 2.
2. Add 1 µl IdeS to one of the tubes (end concentration 50 ng/ml) (*see* **Note 10**).

3. Incubate for 2 h at 37 °C.
4. Centrifuge and resuspend in 200 µl Na-medium.

3.4 Label Bacteria and Antibody Fragments

1. Divide the bacteria into two flow cytometry tubes with 100 µl in each. *See* SPLIT 2 in Fig. 2.
2. Add 100 µl staining solution (end concentration 1:1600 Syto9, and 1:100 anti-human Fab) (*see* **Note 11**).
3. Incubate at room temperature for 30 min in the dark.
4. Add 500 µl Na-medium (*see* **Note 12**).
5. Continue with analysis in flow cytometer.

3.5 Analysis with Flow Cytometer

1. Set the flow cytometer to logarithmic scale.
2. Adjust the side scatter threshold to exclude small debris but include single bacteria.
3. Prepare a sample for volumetric calibration and background fluorescence by taking 100 µl non-opsonized bacteria (from Subheading 3.2**, step 2**), 100 µl staining solution, 50 µl Countbright beads and 500 µl Na-medium (*see* **Note 13**).
4. Set forward and side scatter gate on bacteria.
5. Analyze the fluorescence in the FL-1 (green, bacterial DNA) and FL-4 (far red, IgGFc or IgGFab) channels.
6. The Fab and Fc signal combined is set to 100% and the volumetric calibration (using CountBright) is used to compensate for potential absolute bacterial concentration differences between the different samples (*see* **Note 14**).
7. Figure 3 shows example of results with monoclonal IgG and IVIG (pooled human IgG from thousands of individuals).

4 Notes

1. Monoclonal IgG not targeting bacterial epitopes works well as a control for bacterial Fc-binding.
2. Other buffered media, such as PBS, also works well.
3. The compatibility of the bacterial IgG-binding proteins with the species for the source of antibody needs to be considered.
4. IdeS can be purchased under the name FABricator from Genovis.
5. Angle rotor can work but will typically result in larger losses during each step.
6. These secondary antibody fragments need to be Fabs to avoid binding by IgGFc-binding bacterial proteins. If studying IgGFab-binding proteins such as protein L (binds light chain

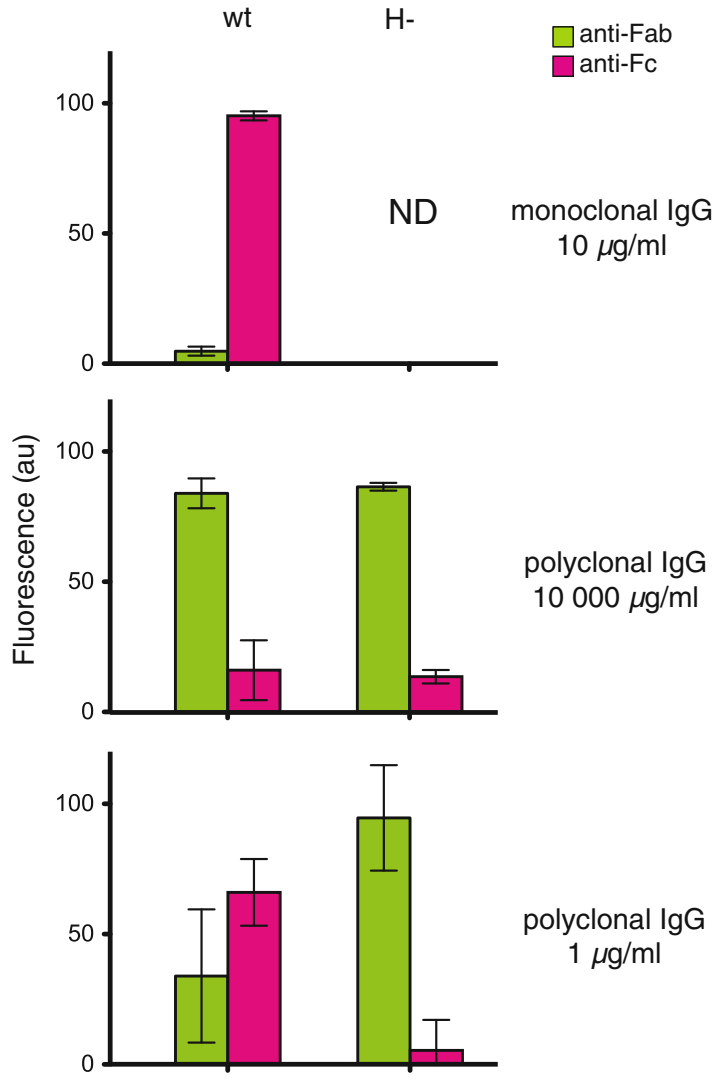

Fig. 3 IgG orientation with monoclonal and polyclonal IgG. Example of data from analysis of wild-type S. pyogenes and protein H mutant. The bacteria were pre-incubated with monoclonal IgG or polyclonal IgG at different concentrations and treated with IdeS. The remaining IgG fragments at the bacterial surface were measured using flow cytometry as outlined in this chapter. Values are mean ± SEM of three independent experiments. For monoclonal IgG, no bound antibodies were detected at the surface of protein H mutant bacteria

of IgG [8]), this needs to be taken into consideration when interpreting the results.

7. The expression of many virulence factors is dependent on the growth phase.
8. The *S. pyogenes* AP1 strain aggregates strongly and this is a necessary step for later quantitative analysis and to reduce clogging of flow cytometer tubing. For other species, sonication

might not be needed at all, or can be done using water bath sonication instead, although the latter is difficult to achieve in a reproducible manner.

9. Small (0.65 ml) low-binding microcentrifuge tubes are recommended to minimize potential losses.
10. Lower concentrations will most likely also work well due to the efficiency of the enzyme.
11. The specific concentrations can be titrated to find an optimal signal to noise.
12. This dilution is to avoid an additional wash step and has been tested empirically to work well enough in most cases. If signal to noise is low, a wash step can be introduced or alter the Fab concentrations and incubation times.
13. The bacteria should ideally be included in the staining step (*see* Subheading 3.4, **step 2**) and then the beads can be added afterward.
14. This is particularly important if different bacteria with different adhesion characteristics are to be compared, as this will typically result in variation in the amount of bacteria lost in each centrifugation step.

Acknowledgments

This work was supported by the Crafoord Foundation, the Swedish Research Council, and the Swedish Society of Medicine.

References

1. Frick IM, Wikström M, Forsén S, Drakenberg T, Gomi H, Sjöbring U, Björck L (1992) Convergent evolution among immunoglobulin G-binding bacterial proteins. Proc Natl Acad Sci U S A 89(18):8532–8536
2. Björck L, Kronvall G (1984) Purification and some properties of streptococcal protein G, a novel IgG-binding reagent. J Immunol 133(2): 969–974
3. Forsgren A, Sjöquist J (1966) Protein A from *S. aureus*. I. Pseudo-immune reaction with human gamma-globulin. J Immunol 97(6):822–827
4. Akesson P, Cooney J, Kishimoto F, Björck L (1990) Protein H--a novel IgG binding bacterial protein. Mol Immunol 27(6):523–531
5. Nordenfelt P, Waldemarson S, Linder A, Mörgelin M, Karlsson C, Malmström J, Björck L (2012) Antibody orientation at bacterial surfaces is related to invasive infection. J Exp Med 209(13):2367–2381. doi:10.1084/jem.20120325
6. Lood R, Waldetoft KW, Nordenfelt P (2015) Localization-triggered bacterial pathogenesis. Future Microbiol 10(10):1659–1668. doi:10.2217/fmb.15.89
7. von Pawel-Rammingen U, Johansson BP, Björck L (2002) IdeS, a novel streptococcal cysteine proteinase with unique specificity for immunoglobulin G. EMBO J 21(7):1607–1615. doi:10.1093/emboj/21.7.1607
8. Björck L (1988) Protein L. A novel bacterial cell wall protein with affinity for Ig L chains. J Immunol 140(4):1194–1197

Chapter 23

Toward Clinical use of the IgG Specific Enzymes IdeS and EndoS against Antibody-Mediated Diseases

Mattias Collin and Lars Björck

Abstract

The endoglycosidase EndoS and the protease IdeS from the human pathogen *Streptococcus pyogenes* are immunomodulating enzymes hydrolyzing human IgG. IdeS cleaves IgG in the lower hinge region, while EndoS hydrolyzes the conserved N-linked glycan in the Fc region. Both enzymes are remarkably specific for human IgG that after hydrolysis loses most of its effector functions, such as binding to leukocytes and complement activation, all contributing to bacterial evasion of adaptive immunity. However, taken out of their infectious context, we and others have shown that IdeS and EndoS can alleviate autoimmune disease in a number of animal models of antibody-mediated disorders. In this chapter, we will briefly describe the discovery and characterization of these unique enzymes, present the findings from a number of animal models of autoimmunity where the enzymes have been tested, and outline the ongoing clinical testing of IdeS. Furthermore, we will discuss the rationale for further development of IdeS and EndoS into novel pharmaceuticals against diseases where IgG antibodies contribute to the pathology, including, but not restricted to, chronic and acute autoimmunity, transplant rejection, and antidrug antibody reactions.

Key words Immunoglobulins, Proteases, Glycosylation, Glycan hydrolysis, Immune evasion, Autoimmunity, Transplant rejection

1 Introduction

During evolution microbes inhabiting the human body have developed a plethora of means to survive, and unsuccessful genotypes and phenotypes have been outcompeted. As a result of this evolutionary process, microbes still around have become the true experts of our physiology and especially our immune defenses. Characterization of the microbial components involved in immune evasion is essential to understand the interplay between the microbe and the human host in a healthy and diseased state. Another intriguing aspect of microbial immunomodulation is that such mechanisms could be exploited for other purposes such as suppression of autoimmunity, or to alleviate other adverse immune reactions such as transplant rejection or antidrug antibody reactions. Such

Pontus Nordenfelt and Mattias Collin (eds.), *Bacterial Pathogenesis: Methods and Protocols*, Methods in Molecular Biology, vol. 1535, DOI 10.1007/978-1-4939-6673-8_23,

pathogen-derived immunomodulating molecules from viruses, bacteria, fungi, and parasites have been evaluated as experimental therapeutics against both innate and acquired immunity-mediated conditions [1–6]. In this chapter, we will introduce two immunomodulating enzymes from the human pathogen *Streptococcus pyogenes*, IdeS and EndoS, which both are specific for human IgG, but have distinct modes of action. We will present evidence from a number of animal models of autoimmunity supporting that these two enzymes could represent novel types of therapies against antibody-mediated diseases (summarized in Table 1). Furthermore, we will also discuss the ongoing clinical testing of IdeS against transplant rejection and the future development of both enzymes as drugs against acute and chronic antibody-mediated diseases.

2 Antibody-Hydrolyzing Enzymes from Bacteria

2.1 The IgG Protease IdeS

The strictly human pathogen *S. pyogenes* is a well-characterized example of a bacterial pathogen that expresses a whole array of immunomodulating proteins, both surface associated and secreted (for a review *see* ref. [7]). Immunoglobulins are key molecules in the adaptive immune response, and it is therefore not a surprise that bacteria that successfully colonize or infect human have developed multiple mechanisms to evade recognition and killing mediated by antibodies. A very important group of immune evasion proteins in Gram-positive bacteria are the cell-wall anchored immunoglobulin binding proteins [8]. A completely different mechanism is enzymatic hydrolysis of antibodies by bacterial secreted enzymes. One very well studied group of enzymes are the IgA proteases, which can be found in a number of mucosal colonizing/infecting bacteria such as *Streptococcus pneumoniae*, *Neisseria meningitidis*, *Neisseria gonorrhoeae*, *Streptococcus mitis*, *Streptococcus mutans*, *Haemophilus influenzae*, and *Prevotella*. These proteases are highly specific for the hinge region of IgA and hydrolysis leads to elimination of Fc-mediated effector functions (for a review *see* ref. [9]). Proteases with similar specificity for IgG were until quite recently not known; however, a number of bacterial broad spectrum proteases including the major secreted protein from *S. pyogenes*, SpeB, have been reported to also hydrolyze/degrade IgG, but the physiological relevance can, in many cases, be questioned [9–11]. In contrast, in the same bacterium, *S. pyogenes*, an additional secreted cysteine proteinase, with extreme specificity for human IgG has been identified. This enzyme, IdeS, hydrolyzes all subclasses of human IgG below the disulfide bridge in the hinge region and thereby generates $F(ab')_2$ and monomeric Fc fragments (1/2 Fc) [12]. The unique specificity of IdeS for IgG is its most noteworthy property, and is explained by the fact that IdeS has to bind to the Fc region of IgG before cleavage can occur; the specificity relies on this initial protein-protein interaction [13]. From a bacterial point of view this of course serves an important purpose;

Table 1
EndoS/IdeS in animal models of autoimmunity

Disease model	Enzyme	Effects seen	Refs
Healthy rabbits	EndoS/IdeS	Complete hydrolysis of IgG pool, antibody response against EndoS/IdeS, no apparent negative health effects	[34, 35]
Immune thrombocytopenic purpura (ITP) in mice	EndoS/IdeS	Pretreatment of IgG and direct injection of IdeS/EndoS rescued mice from lethal disease. EndoS pretreatment of IgG inhibited platelet depletion in a subclass-dependent manner	[34, 35, 37]
Collagen—and collagen antibody induced arthritis in mice (CIA, CAIA)	EndoS/IdeS	Pretreatment of IgG with EndoS inhibited induction of arthritis and gave milder arthritis than untreated IgG. IdeS hydrolyzed IgG in vivo, reduced severity, and delayed onset of arthritis	[36, 38]
Lupus-prone mice	EndoS	No activity on development of autoantibodies. Two injections of EndoS significantly prolonged life and reduced disease severity.	[37]
Serum transfer arthritis in mice	EndoS	Pretreatment of K/BxN serum with EndoS decreased joint swelling, inhibited cellular infiltration, and improved the clinical score	[37]
Goodpasture's disease in mice	EndoS/IdeS	Both enzymes inhibited proteinuria, IdeS hydrolyzed anti-GBM antibodies and inhibited complement deposition in the kidney	[43]
ANCA-mediated vasculitis in mice	EndoS	Pretreatment of anti-MPO antibodies reduced kidney dysfunction and glomerular crescent formation. Early direct treatment with EndoS reduced kidney damage and dysfunction	[44]
Experimental autoimmune encephalomyelitis (EAE) in mice	EndoS	Systemically administered EndoS significantly improves the clinical score and inhibits demyelinization	[50]
Neuromyelitis optica	EndoS/IdeS	EndoS pretreatment of anti-AQP4 inhibits disease and treated antibodies blocks demyelinization. IdeS cleaves anti-AQP4 IgG in vivo and alleviates NMO	[53, 54]
Epidermolysis bullosa acquisita (EBA) in mice (auto immune blistering disease)	EndoS	Pretreatment of anti-Col7 antibodies inhibited development of disease, direct EndoS treatment alleviates disease in both passively and actively immunized mice	[59]

bacteria are protected from IgG-mediated opsonophagocytosis [14, 15]. Interestingly, IdeS not only hydrolyzes soluble IgG, but also IgG being part of the B-cell receptor (BCR), thereby blocking antigen binding to the BCR which may further enhance the immunosuppressive effect [16]. True homologs to IdeS have also been identified in animal isolates of the *Streptococcus equi* subspecies *equi*

and *zooepidemicus* [17]. Besides the therapeutic potential of IdeS, further outlined below, the enzyme has been successfully developed into an excellent tool to analyze IgG for research purposes, and for the development of IgG-based pharmaceuticals (see Chapter 21 in this volume).

2.2 The IgG Glycan Hydrolase EndoS

Most human proteins are posttranslationally modified with carbohydrate structures (glycans) and the immune system is no exception [18]. Among the antibodies, IgG is the "simplest" glycoprotein with one complex *N*-linked glycan on Asn297 on each heavy chain in the Fc fragment. Minor changes in this glycan have major effects on the effector functions of IgG, including altered binding to Fc-receptors on leukocytes and activation of the complement system. It is therefore not surprising that bacteria have evolved enzymes that can modify these glycans on IgG. Glycan hydrolases from bacteria have been extensively used as glycoprotein mapping and modification tools. These are, for instance, a family of enzymes ($EndoF_{1-3}$ and PNGaseF) from the opportunistic pathogen *Elizabethkingia meningoseptica* with activity on *N*-linked glycans on glycoproteins [19–21]. However, it is not until quite recently the focus has turned toward enzymes with activity on the glycoprotein IgG. The endoglycosidase EndoS from *S. pyogenes* was the first IgG-specific glycan hydrolase to be described [22]. In contrast to many other characterized endoglycosidases that are not protein specific, EndoS only hydrolyzes native and fully folded IgG or Fc, suggesting protein-protein interactions in addition to glycan recognition [23, 24]. True EndoS homologs have also been found in *S. equi* subsp. *equi*, and closely related enzymes have been identified in animal isolates of *Streptococcus dysgalactiae* subsp. *dysgalatictiae* [25, 26]. EndoS hydrolysis of IgG in vitro leads to increased bacterial survival due to reduced phagocytosis and complement activation [27], but in a nonimmune state EndoS does not contribute to virulence in mice [28]. However, analysis of the IgG glycosylation state in patients with mild and severe *S. pyogenes* infections indicates that IgG glycan hydrolysis does occur, especially in the most severe cases of infections such as severe sepsis or septic shock (Naegeli et al., in preparation). In addition to the evaluation of EndoS as a novel pharmaceutical, the enzyme and the variant EndoS2 are already well-established glycan mapping and antibody modification tools [29, 30].

3 Experimental Treatment with IgG—Hydrolyzing Enzymes

3.1 Antibody-Mediated Autoimmunity and Transplant Rejection

Autoimmune diseases constitute an enormous health burden by affecting approximately 5 % of the human population (NIH Autoimmune Coordinating Committee 2002), and by being a leading cause of death among young and middle-aged women in the industrialized world [31]. Autoimmune diseases are

characterized by an immune system that has turned against our own bodies in one or several ways. Many of the diseases are very complex in nature and involve both cellular and antibody-mediated destruction of cells and tissues. However, autoantibodies, primarily of the IgG isotype, are involved in the pathological process of many of the diseases [32]. This is also the case for rejection of transplanted organs, where antibodies directed against the transplant play an important role [33]. Therefore, enzymes like IdeS and EndoS that hydrolyze IgG with a high degree of specificity present themselves as a potential novel type of pharmaceuticals against IgG-driven pathological conditions. However, there have been many obstacles that needed to be overcome before venturing into specific disease models. One important aspect is in vivo activity and specificity to avoid off target and adverse effects. This was addressed early on for both IdeS and EndoS, where both enzymes proved to be very efficient and well tolerated in healthy rabbits and could be administered repeatedly without any obvious adverse effects [34, 35].

3.2 Models of Rheumatic Diseases

Based on the very efficient and specific IgG proteolysis and IgG glycan hydrolysis by IdeS and EndoS, respectively, we were stimulated to elucidate if these enzymes could be used to treat antibody-mediated immunological diseases including autoimmunity. This was made possible through a series of in-house studies, but most importantly very fruitful collaborations with experts within the field of autoimmunity. The first model in which both EndoS and IdeS were tested was a mouse models of collagen antibody induced (CAIA) and collagen induced arthritis (CIA) that was performed as a collaboration with Rikard Holmdahl's group (presently at Karolinska Institute). Here, it was clearly shown that EndoS pre-treatment of arthritogenic antibodies against collagen type II generated less immune complexes and inhibited the development of arthritis in CAIA mice [36]. This was later confirmed in a serum transfer model of arthritis [37]. For IdeS it was shown that IgG was hydrolyzed in vivo in mice, and that early treatment could reduce the severity of arthritis. Furthermore, IdeS treatment delayed the onset and reduced the severity of CIA [38]. These proof-of-concept studies indicated that both enzymes indeed could inhibit antibody-mediated pathology and stimulated further development.

3.3 Models of Autoimmunity of the Blood

Autoimmunity of the blood in many ways presents itself as an ideal situation for testing enzymatic antibody hydrolysis, since the pathology largely takes place in a very accessible compartment, the blood stream. We therefore first turned to a fairly simple mouse model of autoimmune depletion of platelets, immune thrombocytopenic purpura (ITP), based on rabbit antibodies against mouse platelets. ITP is a quite common isolated condition, or as a part of

other autoimmune diseases [39, 40]. In the process, we also tested IdeS and EndoS activity in healthy rabbits which demonstrated that the enzymes were efficient and could be administered several times in the same animal [34, 35]. For EndoS, we could show that pretreatment of rabbit anti-platelet antibodies abolished pathogenicity, and for both EndoS and IdeS we could show that direct treatment could rescue mice even at a very late stage of the disease with severe lack of platelets and signs of subcutaneous bleeding [34]. For EndoS we could, in collaboration with Falk Nimmerjahn's group (University of Erlangen), subsequently confirm these findings in another model of ITP, based on mouse monoclonal antibodies against platelets, even though there were some IgG subclass differences [37].

Autoimmune destruction of erythrocytes (autoimmune hemolysis or anemia) can also be an isolated disease, or be a component of systemic autoimmune diseases such as Systemic Lupus Erythematosus (SLE) [41]. In collaboration with the groups of Martin L Olsson and Shozo Izui (Lund University and University of Geneva), we could show that EndoS treatment of human anti-RhD antibodies, or rabbit antihuman erythrocyte antibodies efficiently inhibited in vitro hemolysis. In a mouse model using mouse monoclonals against erythrocytes, EndoS could also reduce hemolysis, classical complement activation, and erythrocyte phagocytosis in the liver [42]. These studies clearly indicated that both EndoS and IdeS are very efficient in suppressing antibody-mediated experimental disease of the blood, suggesting that the enzymes might be very useful in human autoimmune anemia and bleeding disorders.

3.4 Models of Autoimmune Vessel and Kidney Diseases

Antibody-mediated disease affecting the kidney is fairly common, in isolated form or as a component of systemic autoimmune diseases such as SLE, Goodpasture's disease, and vasculitis. In collaboration with the groups of Peter Heeringa (University of Groningen), Thomas Hellmark (Lund University), Mårten Segelmark (presently Linköping University), and Mohamed R Daha (University of Leiden), we have addressed the effect of both EndoS and IdeS in mouse models of Goodpasture's disease and ANCA(anti-neutrophil cytoplasmic autoantibodies)-mediated vasculitis. In the model of Goodpasture's disease it was shown that both enzymes could inhibit the severe proteinuria, and IdeS cleaved the anti-GBM (glomerular basement membrane) IgG antibodies and thereby inhibited complement deposition in the kidney [43]. In the ANCA-mediated vasculitis model, EndoS pretreatment of anti-MPO (myeloperoxidase) IgG reduced the signs of kidney dysfunction (hematuria, leukocyturia, albuminuria), and both neutrophil migration and crescent formation in the glomeruli were inhibited. Furthermore, early, but not late, direct treatment with EndoS reduced kidney damage and dysfunction [44]. Taken

together, these studies show that both enzymes could potentially be used in autoimmune kidney diseases, but IdeS clearly stands out as the more efficient option under these conditions.

3.5 Models of Systemic and Spontaneous Autoimmunity

Most of the hitherto described autoimmune disease models rely on passive transfer of pathogenic antibodies, and might not fully reflect the complexity of a naturally developing autoimmune disease. We therefore turned to a mouse model of SLE, where BXSB mice spontaneously develop a disease with an autoantibody profile, disease progression, and pathology that closely resembles the human disease [45]. In this model EndoS treatment at weeks 18 and 26 could significantly prolong the life of the BXSB mice, in fact to the same extent as when the common γ-chain is knocked out in this background [37, 46]. This suggests that EndoS inhibits most of the IgG/FcγR-mediated pathology seen in this disease model, and that it had a long-term effect that was somewhat surprising. Furthermore, in this model we could also establish a very low therapeutic dose (10 μg/mouse) that only gave a week IgM, and no detectable IgG, response against the enzyme. In collaboration with Anders Bengtsson's group (Lund University) we recently substantiated the therapeutic potential of EndoS in SLE by showing that EndoS ex vivo can block many of the pathogenic properties of immune complexes, such as inhibition of type 1 interferon in plasmacytoid dendritic cells, reduced complement activation, and inhibition of phagocytosis [47]. Taken together, these results show that EndoS has very good short and long-term effects in a chronic autoimmune SLE-like condition. This is very promising for the development of EndoS against more chronic type of autoimmunity, but more studies in vitro and in animal models are needed to understand the mechanisms behind the long-term effects.

3.6 Models of Autoimmunity of the Central Nervous System

Multiple sclerosis (MS) is an autoimmune disease mainly affecting the central nervous system (CNS) by demyelinating neurons. The pathophysiological mechanisms have not been fully elucidated, but B cells and autoantibodies against different myelin proteins have been implicated [48]. Experimental autoimmune encephalomyelitis (EAE) triggered by immunization with myelin, mimics MS fairly well and responds to intravenous immunoglobulin (IVIG) therapy [49]. In collaboration with Patrice Lalive (University of Geneva), we tested EndoS treatment of mice that develop EAE after immunization with myelin oligodendrocyte glycoprotein (MOG). This revealed that systemic administration of EndoS significantly improves the clinical score and inhibits demyelinization in the CNS [50]. Besides strengthening the idea to use EndoS as therapy this also highlighted that B cells and antibodies are important in this particular model of MS, and that EndoS can cross the blood–brain barrier under these conditions.

A condition that is closely related to MS is Neuromyelitis optica (NMO). This disease is driven by autoantibodies against Aquaporin 4 (AQP4) leading to demyelinization in the spinal cord and the optical nerve causing blindness that is a hallmark of this disease [51, 52]. Verkman and colleagues have tested different aspects of both EndoS and IdeS in their model mouse of NMO. Their studies have shown that EndoS pretreated AQP4 pathological antibodies can longer drive disease, and that the treated antibodies can also be used to block demyelinization [53]. When IdeS was tested, the effects were even more clear; IdeS could cleave AQP4 antibodies in vivo and alleviate the NMO in mice [54].

Another severe autoimmune disease of the CNS is Guillain-Barré syndrome where antibodies against gangliosides (glycolipids) develop due to microbial molecular mimicry [55]. The potential of IdeS against this disease has been demonstrated by in vitro hydrolysis of anti-ganglioside antibodies and inhibition of complement activation [56].

A general problem with therapies targeting CNS is how to get the drug through the blood–brain barrier. It is therefore promising that both IdeS and EndoS seem to readily reach the CNS during an ongoing inflammation and inhibit IgG-driven pathology.

3.7 Models of Autoimmune Skin Diseases

Autoimmune blistering (bullous) skin disorders constitute a heterogeneous group of diseases, but for some of them, the pemphigoid diseases, there is a very clear link between autoantibodies against extracellular matrix components in the skin and disease [57]. For several of them there are good mouse models, and particularly for Epidermolysis bullosa acquisita (EBA) where both passive and active experimental autoimmunity against collagen VII (Col7) has provided much information about the development of disease [58]. In collaboration with the groups of Enno Schmidt and Ralf Ludwig (University of Lübeck), we have been able to show that EndoS pretreatment of anti-Col7 inhibited development of disease and that direct treatment with EndoS can alleviate disease in both passively and actively Col7 immunized mice [59]. Furthermore, in collaboration with Frank Petersen's group (Research Center Borstel), we could show that EndoS hydrolysis of anti-Col7 immune complexes leads to diminished Fc-mediated activation of neutrophils [60]. These data suggest that EndoS, when administered systemically, can reach such peripheral tissue as dermis/epidermis and inhibit the pathogenicity of already bound autoantibodies to alleviate antibody-mediated autoimmune skin disease.

4 Toward the Clinic with IgG—Hydrolyzing Enzymes

Given the IgG specificity of both IdeS and EndoS and the positive results from a number of animal models of autoimmune diseases, it is quite logical to initiate a development toward clinical trials. Any experimental researcher attempting to take this path knows how much patience, tenacity, and funding is needed just to take the first few steps toward clinical development. However, we have been fortunate enough to have had a long-standing collaboration with a local pharmaceutical company, Hansa Medical AB (www.hansamedical.com). This company has supported our research without clear economical gains in sight, but with a philosophy that supporting good science within academia with unrestricted grants will ultimately be a good investment. This has now in the case of IdeS turned out to be a fruitful strategy, since clinical trials with this enzyme have been initiated. A Swedish phase I study with IdeS has recently been concluded showing that IgG is rapidly hydrolyzed in vivo in humans and that IdeS was considered safe with no serious adverse effects [61] (http://clinicaltrials.gov/show/NCT01802697). This rapid and transient IdeS removal of IgG is now further developed against antibody-mediated transplant rejections. More specifically, a Swedish phase II study has been initiated in patients who normally cannot be kidney transplanted due to pan-specific antibodies toward HLA. In this trial ten patients have been treated with IdeS prior to kidney transplantation and are currently being monitored (http://clinicaltrials.gov/ct2/show/NCT02224820). This study primarily evaluates safety and tolerability of the IdeS in sensitized kidney transplantation patients, but is also aimed at identifying an IdeS dose that results in anti-HLA antibody levels acceptable for transplantation within 24 h from dosing. Results are expected in the end of 2016. An additional US phase II trial has also been initiated where IdeS is tested in combination with high dose IVIG and anti-CD20 treatment. This study will include 10–20 patients who will be followed for 6 months after transplantation (http://clinicaltrials.gov/ct2/show/NCT02426684).

Given the accumulated scientific evidence that also EndoS can cure or alleviate autoimmune disease in animal models and the successful initial clinical testing with IdeS, we strongly believe that also this enzyme should be developed toward clinical trials. It is too early to say exactly when this will take place, and what the indication will be, but we have great hopes that also EndoS in time could be incorporated in the pharmaceutical arsenal against acute and/or chronic immunological disorders that cause so much suffering worldwide.

Acknowledgments

This work was supported by grants from the Swedish Research Council (projects 2012–1875 and 7480), the Royal Physiographic Society in Lund, the Foundations of Knut and Alice Wallenberg, Åke Wiberg, Alfred Österlund, Gyllenstierna-Krapperup, Torsten Söderberg, Greta and Johan Kock, King Gustaf V`s 80 years fund, the Swedish Society for Medicine, Swedish Governmental Funds for Clinical Research (ALF), and Hansa Medical AB. The funders had no role in the preparation of the manuscript or in the decision to publish.

Conflict of interests: Hansa Medical AB (HMAB) (www.hansamedical.com) holds patents for using EndoS and IdeS as treatment for antibody-mediated diseases. MC and LB are listed as inventors on the EndoS patents, and LB is listed as an inventor on the IdeS patents. MC and LB are scientific consultants for HMAB through their private companies GlycImmun (GI) (www.glycimmun.com) and AB Protiga, respectively. Genovis AB (GAB) (www.genovis.com) holds patents for the biotechnological use of IdeS, EndoS, and EndoS2 where MC is listed as an inventor on the EndoS/EndoS2 patents and LB on the IdeS patents.

References

1. Alcami A, Saraiva M (2009) Chemokine binding proteins encoded by pathogens. Adv Exp Med Biol 666:167–179. doi:10.1007/978-1-4419-1601-3_13
2. Donaldson DS, Williams NA (2009) Bacterial toxins as immunomodulators. Adv Exp Med Biol 666:1–18. doi:10.1007/978-1-4419-1601-3_1
3. Fallon PG, Alcami A (2006) Pathogen-derived immunomodulatory molecules: future immunotherapeutics? Trends Immunol 27:470–476. doi:10.1016/j.it.2006.08.002
4. Jongerius I, Ram S, Rooijakkers S (2009) Bacterial complement escape. Adv Exp Med Biol 666:32–48. doi:10.1007/978-1-4419-1601-3_3
5. Juncadella IJ, Anguita J (2009) The immunosuppressive tick salivary protein, Salp15. Adv Exp Med Biol 666:121–131. doi:10.1007/978-1-4419-1601-3_10
6. Elliott DE, Weinstock JV (2012) Helminth-host immunological interactions: prevention and control of immune-mediated diseases. Ann N Y Acad Sci 1247:83–96. doi:10.1111/j.1749-6632.2011.06292.x
7. Nizet V (2007) Understanding how leading bacterial pathogens subvert innate immunity to reveal novel therapeutic targets. J Allergy Clin Immunol 120:13–22. doi:10.1016/j.jaci.2007.06.005
8. Navarre WW, Schneewind O (1999) Surface proteins of gram-positive bacteria and mechanisms of their targeting to the cell wall envelope. Microbiol Mol Biol Rev 63:174–229
9. Collin M, Kilian M (2013) Bacterial modulation of Fc effector functions. In: Ackerman ME, Nimmerjahn F (eds) Antibody FC: linking adaptive and innate immunity, 1st edn. Academic Press (London), pp 317–332
10. Nelson DC, Garbe J, Collin M (2011) Cysteine proteinase SpeB from *Streptococcus pyogenes* - a potent modifier of immunologically important host and bacterial proteins. Biol Chem 392:1077–1088. doi:10.1515/BC.2011.208
11. Persson H, Vindebro R, von Pawel-Rammingen U (2013) The streptococcal cysteine protease SpeB is not a natural immunoglobulin cleaving enzyme. Infect Immun 81:2236–2241. doi:10.1128/IAI.00168-13
12. von Pawel-Rammingen U, Johansson BP, Björck L (2002) IdeS, a novel streptococcal cysteine proteinase with unique specificity for immunoglobulin G. EMBO J 21:1607–1615. doi:10.1093/emboj/21.7.1607
13. Vincents B, Pawel-Rammingen von U, Björck L, Abrahamson M (2004) Enzymatic charac-

terization of the streptococcal endopeptidase, IdeS, reveals that it is a cysteine protease with strict specificity for IgG cleavage due to exosite binding. Biochemistry 43:15540–15549. doi:10.1021/bi048284d

14. von Pawel-Rammingen U, Johansson BP, Tapper H, Björck L (2002) *Streptococcus pyogenes* and phagocytic killing. Nat Med 8:1044–1045. doi:10.1038/nm1002-1044, author reply 1045–6
15. Söderberg JJ, von Pawel-Rammingen U (2008) The streptococcal protease IdeS modulates bacterial IgGFc binding and generates 1/2Fc fragments with the ability to prime polymorphonuclear leucocytes. Mol Immunol 45:3347–3353. doi:10.1016/j.molimm.2008.04.013
16. Järnum S, Bockermann R, Runström A et al (2015) The bacterial enzyme IdeS cleaves the IgG-type of B cell receptor (BCR), abolishes BCR-mediated cell signaling, and inhibits memory B cell activation. J Immunol 195:5592–5601. doi:10.4049/jimmunol.1501929
17. Lannergård J, Guss B (2006) IdeE, an IgG-endopeptidase of *Streptococcus equi* ssp. *equi*. FEMS Microbiol Lett 262:230–235. doi:10.1111/j.1574-6968.2006.00404.x
18. Rudd P, Elliott T, Cresswell P et al (2001) Glycosylation and the immune system. Science 291:2370–2376
19. Tarentino AL, Quinones G, Schrader WP et al (1992) Multiple endoglycosidase (Endo) F activities expressed by *Flavobacterium meningosepticum*. Endo F1: molecular cloning, primary sequence, and structural relationship to Endo H. J Biol Chem 267:3868–3872
20. Tarentino A, Quinones G, Changchien L, Plummer T (1993) Multiple endoglycosidase F activities expressed by Flavobacterium meningosepticum endoglycosidases F2 and F3. Molecular cloning, primary sequence, and enzyme expression. J Biol Chem 268:9702–9708
21. Tarentino A, Gomez C, Plummer T (1985) Deglycosylation of asparagine-linked glycans by peptide:N-glycosidase F. Biochemistry 24:4665–4671
22. Collin M, Olsén A (2001) EndoS, a novel secreted protein from *Streptococcus pyogenes* with endoglycosidase activity on human IgG. EMBO J 20:3046–3055. doi:10.1093/emboj/20.12.3046
23. Collin M, Olsén A (2001) Effect of SpeB and EndoS from *Streptococcus pyogenes* on human immunoglobulins. Infect Immun 69:7187–7189. doi:10.1128/IAI.69.11.7187-7189.2001
24. Dixon EV, Claridge JK, Harvey DJ et al (2014) Fragments of bacterial endoglycosidase s and immunoglobulin g reveal subdomains of each that contribute to deglycosylation. J Biol Chem 289:13876–13889. doi:10.1074/jbc.M113.532812
25. Flock M, Frykberg L, Sköld M et al (2012) Antiphagocytic function of an IgG glycosyl hydrolase from *Streptococcus equi* subsp. *equi* and its use as a vaccine component. Infect Immun 80:2914–2919. doi:10.1128/IAI.06083-11
26. Shadnezhad A, Naegeli A, Sjögren J et al (2016) EndoSd, an IgG glycan hydrolyzing enzyme in *Streptococcus dysgalactiae* subspecies *dysgalactiae*. Future Microbiol 11:721–736. doi:10.2217/FMB.16.14
27. Collin M, Svensson MD, Sjöholm AG et al (2002) EndoS and SpeB from *Streptococcus pyogenes* inhibit immunoglobulin-mediated opsonophagocytosis. Infect Immun 70:6646–6651. doi:10.1128/IAI.70.12.6646-6651.2002
28. Sjögren J, Okumura CYM, Collin M et al (2011) Study of the IgG endoglycosidase EndoS in group A streptococcal phagocyte resistance and virulence. BMC Microbiol 11:120. doi:10.1186/1471-2180-11-120
29. Sjögren J, Collin M (2014) Bacterial glycosidases in pathogenesis and glycoengineering. Future Microbiol 9:1039–1051. doi:10.2217/fmb.14.71
30. Sjögren J, Cosgrave EFJ, Allhorn M et al (2015) EndoS and EndoS2 hydrolyze Fc-glycans on therapeutic antibodies with different glycoform selectivity and can be used for rapid quantification of high-mannose glycans. Glycobiology 25:1053–1063. doi:10.1093/glycob/cwv047
31. Walsh SJ, Rau LM (2000) Autoimmune diseases: a leading cause of death among young and middle-aged women in the United States. Am J Public Health 90:1463–1466
32. Lim P-L, Zouali M (2006) Pathogenic autoantibodies: emerging insights into tissue injury. Immunol Lett 103:17–26. doi:10.1016/j.imlet.2005.10.023
33. Colvin RB, Smith RN (2005) Antibody-mediated organ-allograft rejection. Nat Rev Immunol 5:807–817. doi:10.1038/nri1702
34. Collin M, Shannon O, Björck L (2008) IgG glycan hydrolysis by a bacterial enzyme as a therapy against autoimmune conditions. Proc Natl Acad Sci U S A 105:4265–4270. doi:10.1073/pnas.0711271105
35. Johansson BP, Shannon O, Björck L (2008) IdeS: a bacterial proteolytic enzyme with therapeutic potential. PLoS One 3:e1692. doi:10.1371/journal.pone.0001692

36. Nandakumar KS, Collin M, Olsén A et al (2007) Endoglycosidase treatment abrogates IgG arthritogenicity: importance of IgG glycosylation in arthritis. Eur J Immunol 37:2973–2982. doi:10.1002/eji.200737581
37. Albert H, Collin M, Dudziak D et al (2008) In vivo enzymatic modulation of IgG glycosylation inhibits autoimmune disease in an IgG subclass-dependent manner. Proc Natl Acad Sci U S A 105:15005–15009. doi:10.1073/pnas.0808248105
38. Nandakumar KS, Johansson BP, Björck L, Holmdahl R (2007) Blocking of experimental arthritis by cleavage of IgG antibodies in vivo. Arthritis Rheum 56:3253–3260. doi:10.1002/art.22930
39. Cines DB, Blanchette VS (2002) Immune thrombocytopenic purpura. N Engl J Med 346:995–1008. doi:10.1056/NEJMra010501
40. McMillan R (1997) Therapy for adults with refractory chronic immune thrombocytopenic purpura. Ann Intern Med 126:307–314
41. Voulgarelis M, Kokori SI, Ioannidis JP et al (2000) Anaemia in systemic lupus erythematosus: aetiological profile and the role of erythropoietin. Ann Rheum Dis 59:217–222. doi:10.1136/ard.59.3.217
42. Allhorn M, Briceño JG, Baudino L et al (2010) The IgG-specific endoglycosidase EndoS inhibits both cellular and complement-mediated autoimmune hemolysis. Blood 115:5080–5088. doi:10.1182/blood-2009-08-239020
43. Yang R, Otten MA, Hellmark T et al (2010) Successful treatment of experimental glomerulonephritis with IdeS and EndoS, IgG-degrading streptococcal enzymes. Nephrol Dial Transplant 25:2479–2486. doi:10.1093/ndt/gfq115
44. van Timmeren MM, van der Veen BS, Stegeman CA et al (2010) IgG glycan hydrolysis attenuates ANCA-mediated glomerulonephritis. J Am Soc Nephrol 21:1103–1114. doi:10.1681/ASN.2009090984
45. Andrews BS, Eisenberg RA, Theofilopoulos AN et al (1978) Spontaneous murine lupus-like syndromes. Clinical and immunopathological manifestations in several strains. J Exp Med 148:1198–1215
46. Lin Q, Xiu Y, Jiang Y et al (2006) Genetic dissection of the effects of stimulatory and inhibitory IgG Fc receptors on murine lupus. J Immunol 177:1646–1654. doi:10.4049/jimmunol.177.3.1646
47. Lood C, Allhorn M, Lood R et al (2012) IgG glycan hydrolysis by endoglycosidase S diminishes the proinflammatory properties of immune complexes from patients with systemic lupus erythematosus: a possible new treatment? Arthritis Rheum 64:2698–2706. doi:10.1002/art.34454
48. Antel J, Baror A (2006) Roles of immunoglobulins and B cells in multiple sclerosis: from pathogenesis to treatment. J Neuroimmunol 180:3–8. doi:10.1016/j.jneuroim.2006.06.032
49. Humle Jorgensen S, Sorensen PS (2005) Intravenous immunoglobulin treatment of multiple sclerosis and its animal model, experimental autoimmune encephalomyelitis. J Neurol Sci 233:61–65. doi:10.1016/j.jns.2005.03.005
50. Benkhoucha M, Molnarfi N, Santiago-Raber M-L et al (2012) IgG glycan hydrolysis by EndoS inhibits experimental autoimmune encephalomyelitis. J Neuroinflammation 9:209. doi:10.1186/1742-2094-9-209
51. Krumbholz M, Meinl E (2014) B cells in MS and NMO: pathogenesis and therapy. Semin Immunopathol 36:339–350. doi:10.1007/s00281-014-0424-x
52. Ratelade J, Verkman AS (2012) Neuromyelitis optica: aquaporin-4 based pathogenesis mechanisms and new therapies. Int J Biochem Cell Biol 44:1519–1530. doi:10.1016/j.biocel.2012.06.013
53. Tradtrantip L, Ratelade J, Zhang H, Verkman AS (2013) Enzymatic deglycosylation converts pathogenic neuromyelitis optica anti-aquaporin-4 immunoglobulin G into therapeutic antibody. Ann Neurol 73:77–85. doi:10.1002/ana.23741
54. Tradtrantip L, Asavapanumas N, Verkman AS (2013) Therapeutic cleavage of anti-aquaporin-4 autoantibody in neuromyelitis optica by an IgG-selective proteinase. Mol Pharmacol 83:1268–1275. doi:10.1124/mol.113.086470
55. Kaida K, Ariga T, Yu RK (2009) Antiganglioside antibodies and their pathophysiological effects on Guillain-Barré syndrome and related disorders--a review. Glycobiology 19:676–692. doi:10.1093/glycob/cwp027
56. Takahashi R, Yuki N (2015) Streptococcal IdeS: therapeutic potential for Guillain-Barré syndrome. Sci Rep 5:10809. doi:10.1038/srep10809
57. Schmidt E, Zillikens D (2013) Pemphigoid diseases. Lancet 381:320–332. doi:10.1016/S0140-6736(12)61140-4
58. Kasperkiewicz M, Sadik CD, Bieber K et al (2016) Epidermolysis bullosa acquisita: from pathophysiology to novel therapeutic options. J Invest Dermatol 136:24–33. doi:10.1038/JID.2015.356

59. Hirose M, Vafia K, Kalies K et al (2012) Enzymatic autoantibody glycan hydrolysis alleviates autoimmunity against type VII collagen. J Autoimmun 39:304–314. doi:10.1016/j.jaut.2012.04.002
60. Yu X, Zheng J, Collin M et al (2014) EndoS reduces the pathogenicity of anti-mCOL7 IgG through reduced binding of immune complexes to neutrophils. PLoS One 9:e85317. doi:10.1371/journal.pone.0085317
61. Winstedt L, Järnum S, Nordahl EA et al (2015) Complete removal of extracellular IgG antibodies in a randomized dose-escalation phase I study with the bacterial enzyme IdeS--a novel therapeutic opportunity. PLoS One 10:e0132011. doi:10.1371/journal.pone.0132011

INDEX

B

Pontus Nordenfelt and Mattias Collin (eds.), *Bacterial Pathogenesis: Methods and Protocols*, Methods in Molecular Biology, vol. 1535, DOI 10.1007/978-1-4939-6673-8, © Springer Science+Business Media New York 2017

C

D

G

H

I

M

P

R

S

T

V